Chemistry of Precious Metals

Dr S.A. COTTON
Uppingham School
Rutland
UK

BLACKIE ACADEMIC & PROFESSIONAL
An Imprint of Chapman & Hall
London · Weinheim · New York · Tokyo · Melbourne · Madras

**Published by Blackie Academic and Professional,
an imprint of Chapman & Hall, 2–6 Boundary Row, London SE1 8HN, UK**

Chapman & Hall, 2–6 Boundary Row, London SE1 8HN, UK

Chapman & Hall GmbH, Pappelallee 3, 69469 Weinheim, Germany

Chapman & Hall USA, 115 Fifth Avenue, New York, NY 10003, USA

Chapman & Hall Japan, ITP-Japan, Kyowa Building, 3F, 2-2-1 Hirakawacho,
Chiyoda-ku, Tokyo 102, Japan

DA Book (Aust.) Pty Ltd, 648 Whitehorse Road, Mitcham 3132, Victoria,
Australia

Chapman & Hall India, R. Seshadri, 32 Second Main Road, CIT East, Madras
600 035, India

First edition 1997

Typeset in 10/12pt Times by Academic & Technical Typesetting, Bristol

Printed in Great Britain by T. J. International Ltd.

ISBN 0 7514 0413 6

A catalogue record for this book is available from the British Library

Library of Congress Catalog Card Number: 97–70446

∞ Printed on acid-free text paper, manufactured in accordance with ANSI/NISO Z39.48-1992 (Permanence of Paper).

Preface

Some 20 years ago, I was privileged to share in writing a book on the descriptive chemistry of the 4d, 5d, 4f and 5f metals that included these eight elements within its compass (S.A. Cotton and F.A. Hart, *The Heavy Transition Elements*, Macmillan, 1975). This volume shares the same aim of covering the descriptive chemistry of silver, gold and the six platinum metals in some detail at a level suitable for advanced undergraduate and postgraduate study.

It does not attempt to be a comprehensive treatise on the chemistry of these metals. It attempts to fill a slot between the general text and the in-depth review or monograph. The organometallic chemistry is confined to σ-bonded compounds in normal oxidation states; compounds with π-bonding ligands are generally excluded. Their inclusion would have increased the length of the book considerably and, moreover, their recent chemistry has been extensively and expertly reviewed in the new *Comprehensive Organometallic Chemistry*, *II*, eds G. Wilkinson, F.G.A. Stone and E.W. Abel, Pergamon, Oxford, 1995.

I have concentrated upon providing information on ‘essential’ binary compounds and complexes of these elements – oxides, halides, aqua complexes, ammines and tertiary phosphine complexes, for example – and highlighting key areas of study rather than giving comprehensive coverage (impossible outside a monograph). It is easy to be seduced by the ‘latest thing’ in research to the detriment of more fundamental, if prosaic, topics (in any case, there are other texts that provide up to the moment coverage of all research developments). There is still a lot of basic research waiting to be done out there and we have all heard the horror stories of students who can produce *ab initio* MO calculations at the drop of a hat yet think that sodium chloride is a green gas. The data are intended to illustrate trends in the chemistry and not to replace it; theories explain facts and not vice versa. I make no apology for this approach; a sound factual understanding is fundamental to any scientific discipline.

My first priority has, therefore, been to try to provide ‘the facts’ (and I hope that I have got (most of) them right) but I have tried to write the book with the needs of the teacher in mind, by providing plenty of bond lengths and also spectroscopic data (mainly vibrational, with a little NMR and ESR) that can be used as a teaching tool by hard-pressed lecturers or tutors who have not time to look up the information themselves.

The bibliography is intended to give key references (particularly to structures), not just to the recent literature (which can be hard to find because they are not yet in compilations) but in some cases to relevant older work (which can also be hard to find because everyone assumes that you know them); it begins for each chapter with a listing of the relevant sections of Gmelin and of the various 'Comprehensive Chemistries' and monographs. I have attempted to follow the literature received up to March 1996.

Some readers may feel that I have been unduly optimistic (or just plain presumptuous) in writing this book, when I am not actually carrying out research on any of these metals. They may well be right, though I would point out that the spectator does get a different view of events on the sports fields to that obtained by the player.

Producing a book like this is impossible without access to the primary literature, for which I am mainly indebted to the Chemistry Department of the University of Cambridge, and to Mrs Cheryl Cook in particular.

Much of the background reading, especially for osmium and gold, as well as work on the bibliography was done in the course of visits to l'Abbaye N-D du Bec-Hellouin; it is again a pleasure to give thanks to Dom Philibert Zobel O.S.B., Abbot of Bec, and to the monastic community for the shelter of their roof and a calm and sympathetic environment.

I should like to take the opportunity to thank all those who have supplied information, answered questions or discussed points with me, including the late Sir Geoffrey Wilkinson; Professors S. Ahrland, K.G. Caulton, F.A. Cotton, W.P. Griffith, D.M.P. Mingos, J.D. Woollins and R.K. Pomeroy; and Drs A.J. Blake, P.R. Raithby, S.D. Robinson and P. Thornton. They are not, of course, responsible for the use I have made of the information.

I am particularly grateful to Dr John Burgess for reading the whole manuscript in (a very rough) draft and making many helpful suggestions for improvement, some of which I have been wise enough to adopt. John has also been an invaluable sounding board for ideas. I must also thank three (anonymous) reviewers for drawing my attention to a number of omissions, mistakes and ambiguities, which I hope have now been resolved.

I should finally like to thank Patricia Morrison for her encouragement in the earlier part of the project and Louise Crawford for patient, sympathetic and accurate typing.

Simon Cotton
Uppingham
December 1996

Abbreviations

acac	acetylacetonate, $CH_3COCHCOCH_3$
Ar	aryl
bipy	bipyridyl (usually 2,2′-bipyridyl)
Bu or Bu^n	*n*-butyl, $CH_3CH_2CH_2CH_2$
Bu^t	*t*-butyl, $(CH_3)_3C$
bz	benzyl
cod	cycloocta-1,5-diene
cy	cyclohexyl, cyclo-C_6H_{11}
cyclam	1,4,8,11-tetraazaacyclotetracane
depe	bis(diethylphosphino)ethane
diars	*o*-phenylenebis(dimethylarsine), $C_6H_4(AsMe_2)_2$
dien	diethylenetriamine, $HN[(CH_2)_2NH_2)]_2$
dimphen	2,9-dimethylphenanthroline
dme	1,2-dimethoxyethane, glyme
DMF	*N*,*N*-dimethylformamide
dmg	dimethylglyoximate
dmpe	bis(dimethylphosphino)ethane
DMSO	dimethylsulphoxide, Me_2SO
dppe	1,2-bis(diphenylphosphino)ethane, $Ph_2(CH_2)_2Ph_2$
dppm	1,2-bis(diphenylphophino)methane, $Ph_2(CH_2)Ph_2$
dppp	1,2-bis(diphenylphosphino)propane, $Ph_2(CH_2)_3Ph_2$
dppz	bis(diphenylphospino)benzene
EDTA	ethylenediamine tetracetate (4-)
en	1,2-diaminoethane, ethylenediamine
equ	2-ethyl-8-quinolinate
Et	ethyl
Et_4dien	*N*,*N*,*N*′,*N*′-tetraethyldiethylenetriamine, $HN[(CH_2)_2NEt_2]_2$
im	imidazole
M-CPBA	*m*-chloroperoxybenzoic acid
Me	methyl
mes	mesityl, 2,4,6-trimethylphenyl
MNTS	*N*-methyl-*N*-nitrosotoluene sulphonamide
ncs	*N*-chlorosuccinamide
np	naphthyl
OEP	octaethylporphyrin
Ph	phenyl
phen	1,10-phenanthroline

PP	2,11-bis(diphenylphosphinomethyl)benzo[c]phenanthrene
Pr	propyl, $CH_3CH_2CH_2$
Pr^i	isopropyl, $(CH_3)_2CH$
py	pyridine, C_5H_5N
py_2CH_2	dipyridiniomethane, $(C_5H_5N)_2CH_2$
pz	pyrazole
tacn	1,4,7-triazacyclononane, [9]aneN_3
terpy	2,2′:6,2″-terpyridyl
thf	tetrahydrofuran
tht	tetrahydrothiophene
TMP	tetramesitylporphyrin
tmpp	tris(2,4,6-trimethoxyphenyl)phosphine
tmu	tetramethylthiourea
TPP	tetraphenylporphyrin
trien	triethylenetetramine, $N[(CH_2)_2NH_2)]_3$
ttcn	1,4,7-trithiacyclononane, $9S_3$
tu	thiourea, $(H_2N)_2CS$
$9S_3$	1,4,7-trithiacyclononane
$10S_3$	1,4,7-trithiacyclodecane
14[ane]N_4	1,4,8,11-tetraazaacyclotetracane, cyclam
$14S_4$	1,4,8,11-tetrathiacyclotetradecane
$18S_6$	1,4,8,11,14,17-hexathiacyclooctadecane

All bond lengths given in ångström units (1 Å = 0.1nm)

Contents

1 Ruthenium and osmium

1.1 Introduction

Ruthenium and osmium are the first pair of 'platinum metals' [1–13]. They exhibit oxidation states up to +8, the highest observed for any element, as in MO_4 (M = Ru, Os) though this requires the use of the most electronegative elements, fluorine and oxygen, for stability. Generally, the +2 and +3 states are the most important, along with +4 for osmium; however, there is a considerable chemistry of the MO_2^{2+} ('osmyl' and 'ruthenyl') and $M{\equiv}N^{3+}$groups, as well as the 'classical' hydride complexes $OsH_6(PR_3)_2$, which also involve osmium(VI).

1.2 The elements and uses

Along with iridium, osmium was discovered in 1803 by Smithson Tennant. He took the insoluble residue from the digestion of platinum ores with aqua regia and heated it with sodium carbonate to give soluble yellow $OsO_4(OH)_2^{2-}$. On acidification, distillable OsO_4 formed. Noting the smell of the (very toxic) tetroxide, Tennant gave the element its name from the Greek *osme* (*οσμη* = smell); he also noted that it stained the skin, prefiguring a future use.

The last of the metals described in this book to be discovered was ruthenium. As with osmium, it was extracted from the aqua regia-insoluble residue from concentrated platinum ores and was first claimed in 1826 by G.W. Osann but definitely characterized by K.K. Klaus (1844), who oxidized the residue with KOH/KNO_3, acidified and distilled off the OsO_4 then reacted the residue with NH_4Cl. (Aqua regia is a 3 : 1 mixture of concentrated HCl/HNO_3 (containing some chlorine).) Thermal decomposition of the resulting $(NH_4)_2RuCl_6$ in an inert atmosphere gave ruthenium, taking its name from *ruthenia*, the Latin name for Russia.

Both of these elements are silver–white lustrous metals with high melting (ruthenium 2310°C, osmium 3900°C) and boiling (3900 and 5510°C, respectively) points. As usual, the 5d metal is much more dense (ruthenium 12.45, osmium 22.59 g cm^{-3}); both adopt hcp structures; osmium is the densest metal known. The metals are unreactive, insoluble in all acids, even aqua regia. Ruthenium tends to form a protective coating of the dioxide and is not attacked by oxygen below 600°C nor by chlorine or fluorine below

300°C. Powdered osmium is slowly attacked by oxygen at room temperature, yielding OsO_4 (though not below 400°C if in bulk). Osmium reacts with fluorine and chlorine at about 100°C. Both metals are attacked by molten alkalis and oxidizing fluxes.

Ruthenium nowadays finds many uses in the electronics industry, particularly for making resistor tracks. It is used as an ingredient in various catalysts and, importantly, in electrode materials, e.g. RuO_2-coated titanium elements in the chloralkali industry. Osmium tetroxide is a very useful organic oxidant and, classically, is used as a tissue stain. Both elements are employed in making certain platinum alloys.

1.2.1 Extraction

Extraction of ruthenium and osmium is done by solvent extraction [1, 2, 5, 14]. Following the traditional route, however, aqua regia-insoluble residues or anode slimes from nickel refining undergo bisulphate oxidation to remove rhodium, then on alkaline fusion ruthenium and osmium are stabilized as Na_2RuO_4 and $Na_2OsO_2(OH)_4$. The ruthenium(VI) can be reduced (alcohol) to RuO_2, which is then converted into $(NH_4)_3RuCl_6$, giving ruthenium metal in a flow of hydrogen at 100°C. Osmium can be precipitated and stored as $K_2OsO_2(OH)_4$ or first converted into OsO_4 (by distillation of the osmate with HNO_3) which is then reduced with hydrogen or turned into $(NH_4)_2OsCl_6$, reduced in the same manner as the ruthenium analogue.

In the solvent-extraction process, the platinum metal concentrate is solubilized in acid using chlorine oxidant. Ruthenium and osmium are separated by turning them into the volatile tetroxides.

1.3 Halides

1.3.1 Ruthenium halides

Ruthenium forms the whole range of trihalides but only fluorides in higher states.

RuF_3 can be made by iodine reduction of RuF_5. It is obtained as a dark brown powder that contains corner-shared RuF_6 octahedra [15]. $RuCl_3$ exists in α- and β-phases:

$$Ru_3(CO)_{12} \xrightarrow[360°C]{Cl_2/N_2} \beta\text{-}RuCl_3 \text{ (brown solid)}$$

$$\beta\text{-}RuCl_3 \xrightarrow[360°C]{Cl_2} \alpha\text{-}RuCl_3 \text{ (black crystals)}$$

The α-form has the α-$TiCl_3$ structure with 6-coordinate ruthenium and a rather long Ru–Ru distance (3.46 Å) compared with the β-form where there are one-dimensional chains, again with octahedrally coordinated ruthenium (Ru–Ru 2.83 Å). The β-form transforms irreversibly to the α-form above 450°C. Both these forms are insoluble in water though β-$RuCl_3$ dissolves in ethanol [16].

Commercial 'ruthenium trichloride' purporting to be $RuCl_3.xH_2O$ is an ill-defined mixture of oxochloro and hydroxychloro species of more than one oxidation state. Obtained by dissolving RuO_4 in hydrochloric acid, it can be purified by repeatedly evaporating to dryness with concentrated HCl. $RuBr_3$ is usually made by brominating the metal while several routes to RuI_3 are open

$$Ru \xrightarrow[450°C,\,20\,atm]{Br_2} RuBr_3$$

$$RuO_4 \xrightarrow{HI\,(aq.)} RuI_3$$

$$Ru(NH_3)_5I_3 \xrightarrow{heat} RuI_3$$

Black–brown $RuBr_3$ has roughly octahedral coordination of ruthenium (Ru–Br 2.46–2.54 Å) with short Ru–Ru contacts (2.73 Å) [17]. Black RuI_3 has a similar structure. Neither is particularly soluble in water.

RuF_4 can be made as a deep pink solid:

$$K_2RuF_6 \xrightarrow{AsF_5/HF} RuF_4$$

It has a VF_4 type puckered sheet structure with 6-coordinated ruthenium; four fluorines bridge, two non-bridging ones are *trans* with the terminal distances shorter as expected (Table 1.1). It is paramagnetic ($\mu_{eff} = 3.04\,\mu_B$ at room temperature).

Green RuF_5, sublimeable *in vacuo* (65°C, 10^{-8} torr (1.33×10^{-6} Pa)) can be made by fluorination

$$Ru \xrightarrow{F_2} RuF_5$$

$$Ru \xrightarrow{BrF_3} BrF_2^+RuF_6^- \xrightarrow{120°C} BrF_3 + RuF_5$$

It melts at 86.5°C and boils at 227°C. The tetrameric structure (Figure 1.1) is one adopted by a number of pentafluorides with *cis*-bridges completing the 6-coordination.

Table 1.1 Bond lengths (Å) in ruthenium fluorides

	Ru–F (terminal)	Ru–F (bridge)
RuF_3	–	1.982
RuF_4	1.82	2.00
RuF_5	1.795–1.824	1.995–2.007
RuF_6	1.824	–

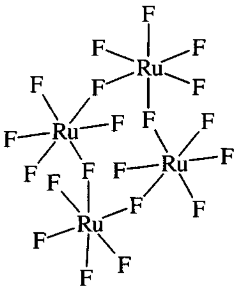

Figure 1.1 The tetrameric structure of RuF_5.

A second, red form has recently been reported; from mass spectral evidence, it may be a trimer. In the gas phase at 120°C, it consists mainly of a trimer (with octahedrally coordinated Ru) [18].

RuF_6 is made by fluorination of RuF_5 under forcing conditions:

$$RuF_5 \xrightarrow[50\,\text{atm},\,230°\text{C}]{F_5} RuF_6$$

It is an extremely moisture-sensitive dark brown solid (m.p. 54°C); bond lengths have been obtained from an EXAFS study [19].

There is some evidence that $RuCl_3$ reacts with chlorine in the gas phase above 400°C to form $RuCl_4$ but $RuCl_4$ has not been authenticated as a solid, neither has RuF_8, which is claimed to exist at low temperatures.

1.3.2 Osmium halides

Unlike ruthenium (and other platinum metals) osmium forms chlorides and bromides in a range of oxidation states [11, 12].

There are no convincing reports of halides in oxidation states below III: early reports of OsI and OsI_2 seem to result from oxide contaminations. Neither is there OsF_3, evidence of the greater stability of the +4 state compared with that of ruthenium.

Dark grey $OsCl_3$ has the 6-coordinate α-$RuCl_3$ structure

$$OsCl_4 \xrightarrow[Cl_2,\,100-500\,\text{torr}]{470°\text{C}} OsCl_3$$

Black $OsBr_3$ and OsI_3 ($\mu = 1.8\,\mu_B$) are also prepared by thermal methods

$$OsBr_4 \xrightarrow[\text{sealed tube}]{300-400°\text{C}} OsBr_3$$

$$(H_3O)_2OsI_6 \xrightarrow[N_2/\text{sealed tube}]{250°\text{C}} OsI_3$$

There is evidence for $OsX_{3.5}$ (X = Cl, Br).

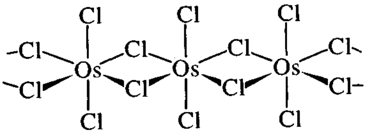

Figure 1.2 The structure adopted by $OsCl_4$.

OsF_4, a yellow–brown solid that distills as a viscous liquid, is made by reduction of solutions of OsF_5

$$OsF_5 \xrightarrow[UV]{H_2/Pt\ gauze} OsF_4$$

It is isomorphous with MF_4 (M = Pd, Pt, Ir, Rh).

Black $OsCl_4$ exists in two forms. A high-temperature form is made by reaction of the elements

$$Os \xrightarrow[700°C]{Cl_2} OsCl_4$$

It has 6-coordinate osmium in a structure (Figure 1.2) regarded as being made from a hexagonally packed array of chlorides with osmiums occupying half the holes in alternate layers; Os–Cl bond lengths are 2.261 Å (terminal) and 2.378 Å (bridge) [20].

The low-temperature form is made using thionyl chloride as the chlorinating agent.

$$OsO_4 \xrightarrow[reflux]{SOCl_2} OsCl_4$$

Black $OsBr_4$ (PtX_4 structure) has 6-coordinate osmium [21]

$$OsCl_4 \xrightarrow[330°C/120\,atm]{Br_2} OsBr_4$$

$$Os \xrightarrow[10\,atm,\ 470°C]{Br_2} OsBr_4$$

A second form can be made by refluxing OsO_4 with ethanolic HBr, then drying the product.

The green–blue pentafluoride (m.p. 70°C, b.p. 226°C) is thermochromic, becoming bright blue at its boiling point (the vapour is colourless). It is synthesized by reducing OsF_6: it has the tetrameric structure adopted by RuF_5 (Os–F = 1.84 Å (terminal) 2.03 Å (bridge)) in the solid state [18c].

$$OsF_6 \xrightarrow[55°C]{I_2/IF_5} OsF_5$$

Like RuF_5, it is mainly a trimer $(OsF_5)_3$ in the gas phase.

In contrast to this, very moisture-sensitive black $OsCl_5$, prepared by chlorinating OsF_6 using BCl_3 as the chlorinating agent, has the dimeric

$ReCl_5$ structure (Os–Cl = 2.24 Å (terminal) 2.42 Å (bridge)). Its magnetic moment is 2.54 μ_B

$$OsF_6 \xrightarrow[RT]{BCl_3} OsCl_5$$

Like several other heavy metals, osmium forms a volatile (bright yellow) hexafluoride (m.p. 33.2°C, b.p. 47°C)

$$Os + 3F_2 \xrightarrow[1\,atm]{250-300°C} OsF_6$$

The solid is polymorphic, with a cubic structure above 1.4°C. A bond length of 1.816 Å has been obtained from EXAFS measurements at 10 K, while vapour phase measurements give Os–F of 1.831 Å [22].

There is uncertainty about the heptafluoride, claimed to be formed as a yellow solid from fluorination under very high pressure

$$Os \xrightarrow[600°C/450\,atm]{F_2} OsF_7$$

Material with the same IR spectrum has been obtained by fluorination of OsO_3F_2 at 180°C (50 atm). OsF_7 is said to decompose at −100°C (1 atm fluorine pressure) [23].

As osmium forms a tetroxide, OsF_8 might possibly exist, especially in view of the existence of the osmium(VIII) oxyfluorides, but MO calculations indicate the Os–F bond would be weaker in the binary fluoride. It is also likely that non-bonding repulsions between eight fluorines would make an octafluoride unstable [23b].

1.3.3 Oxyhalides

Much less is known about ruthenium oxyhalides than about the osmium compounds. The only compound definitely characterized [24] is $RuOF_4$, synthesized by fluorination of RuO_2, condensing the product at −196°C. It loses oxygen slowly at room temperature, rapidly at 70°C.

$$RuO_2 + 2F_2 \xrightarrow{300-400°C} RuOF_4 + \tfrac{1}{2}O_2$$

It has also been made by passing RuF_5 vapour down a hot glass tube:

$$RuF_5 + SiO_2 \longrightarrow RuOF_4 + SiF_4$$

It gives the parent ion in the mass spectrum and has a simple IR spectrum (ν(Ru=O) 1040 cm^{-1} and (ν(Ru–F) 720 cm^{-1}) similar to that of the vapour (1060, 710, 675 cm^{-1}), implying a monomeric structure. Chlorides $RuOCl_2$ and Ru_2OCl_x ($x = 5, 6$) have been claimed; various oxo complexes $Ru_2OX_{10}^{4-}$ are well defined.

Although no OsF_8 has been described, there are oxofluorides in the +8 state.

Table 1.2 Vibrational frequencies[a] for osmium oxyhalides

	State[b]	Vibrational frequencies (cm^{-1})		
		Os=O	Os–F (term)	Os–F (bridge)
cis-OsO_2F_4				
Raman		942, 932	672, 579, 571	
IR		940, 930	675, 588, 570	
OsO_3F_2		954 (947, 942)		
	Matrix	931	646	
$OsOF_5$		960	710, 700, 640	
	Matrix	966.5	713, 638.5	
	Vapour	964	717, 700, 645	
OsO_2F_3		995, 955	720	480–580 (broad)
	Matrix	907	655	
$OsOF_4$		1018	735, 705, 657, 648	529, 423
	Matrix	1079.5	685	
$OsOCl_4$		1028	392 (Os–Cl)	
	Matrix	1032	395	
	Gas	1028	397	

[a] Only IR except for OsO_2F_4; [b] solid unless otherwise stated.

Deep red OsO_2F_4 (m.p. 89°C) has recently been made [25]

$$OsO_4 \xrightarrow[-196°C]{HF/KrF_2} cis\text{-}OsO_2F_4$$

It is thermally stable but instantly hydrolysed in air (like osmium oxyhalides in general); it has a simple vibrational spectrum (ν(Os=O) 940 cm^{-1}; ν(Os–F) 680, 590, 570 cm^{-1}) (Table 1.2) and a *cis*-octahedral structure has been confirmed by an electron diffraction study (Os=O 1.674 Å, Os–F 1.843–1.883 Å).

Several syntheses have been reported for orange–yellow diamagnetic OsO_3F_2 (m.p. 172–173°C) [26]:

$$OsO_4 \xrightarrow[300°C]{F_2} OsO_3F_2$$

$$OsO_4 \xrightarrow[RT]{ClF_3} OsO_3F_2$$

OsO_3F_2 is a monomer in the gas phase, to which a monomeric D_{3h} structure has been assigned. EXAFS and X-ray diffraction measurements show a 6-coordinate solid-state structure with *cis*-fluorine bridges (Figure 1.3) (Os=O 1.678–1.727 Å, Os–F 1.879 Å (terminal), 2.108–2.126 Å (bridge)).

The other possible osmium(VIII) oxyfluoride $OsOF_6$ has so far eluded synthesis and recent *ab initio* MO calculations indicate it is unlikely to exist.

Emerald green $OsOF_5$ (m.p. 59.5°C; b.p. 100.6°C) has an octahedral structure like OsF_6 but is rather less volatile (Os=O 1.74 Å, Os–F 1.72 Å (*trans*) 1.76–1.80 Å (*cis*)) [27]. It is paramagnetic ($\mu_{eff} = 1.47\,\mu_B$ at 298 K) and ESR

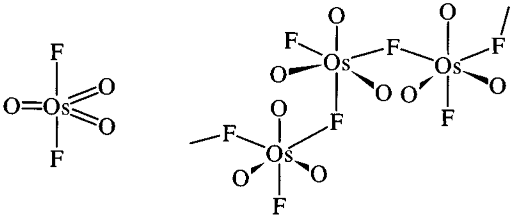

Figure 1.3 The structure of OsO_3F_2 in (a) the gas phase and (b) the solid state.

studies in low-temperature matrices indicate delocalization of the unpaired electron 11.5% from the osmium $5d_{xy}$ orbital to each equational fluorine. Syntheses include

$$OsO_3F_2 \xrightarrow[180^\circ C]{\text{exc. } F_2} OsOF_5$$

On heating a 3 : 1 OsF_6/OsO_4 mixture at 150–200°C, a mixture of $OsOF_5$ and OsO_4 is obtained that can be separated by using the greater volatility of $OsOF_5$.

OsO_2F_3 is a yellow–green solid, disproportionating at 60°C to OsO_3F_2 and $OsOF_4$, from which it may be made:

$$OsOF_4 + OsO_3F_2 \xrightarrow[12\,h]{100^\circ C} 2OsO_2F_3$$

$$OsO_4 + OsF_6 \xrightarrow[17\,h]{150^\circ C} 2OsO_2F_3$$

Matrix isolation studies suggest isolated D_{3h} molecules, but the pure solid has a more complicated IR spectrum indicating both bridging and terminal fluorines [28].

Blue–green $OsOF_4$ (m.p. 80°C) is a byproduct in the synthesis of $OsOF_5$ and can also be made in small quantities by reduction of $OsOF_5$ on a hot tungsten wire. In the gas phase it has a C_{4v} pyramidal structure (Os=O 1.624 Å, Os–F 1.835 Å); crystallography suggests a solid-state structure similar to tetrameric OsF_5; the more complex IR spectrum of the solid is in keeping with this [29].

Oxychlorides are less prolific, apart from the red–brown $OsOCl_4$ (m.p. 32°C). This probably has a molecular structure in the solid state as the IR spectra of the solid, matrix-isolated and gas-phase molecules are very similar, and the volatility is consonant with this [30]. Syntheses include heating osmium in a stream of oxygen/chlorine ('oxychlorination') and by:

$$OsO_4 \xrightarrow{BCl_3} OsOCl_4$$

Table 1.3 Bond lengths in MX_6^{n-} (Å)

n	RuF_6	$RuCl_6$	$RuBr_6$	OsF_6	$OsCl_6$	$OsBr_6$
0	1.824 (EX)			1.816 (EX) 1.831 (ED)		
1	1.845 (EX) 1.85 (X)			1.882 (EX)	2.284 (X) 2.303 (X)	
2	1.916 (EX)	2.29 (X) 2.318 (X)		1.927 (EX)	2.332 (X) 2.336 (X)	~2.5 (X)
3		2.375 (X)	2.514 (X)			

ED, electron diffraction; X, X-ray; EX = EXAFS.

Electron diffraction measurements on the vapour indicate a C_{4v} square pyramidal structure (Os=O 1.663 Å, Os–Cl 2.258 Å; O–Os–Cl 108.3° Cl–Os–Cl 84.4°) with osmium 0.709 Å above the basal plane.

$OsOCl_2$ can be made as dark olive green needles from heating $OsCl_4$ in oxygen [31]. There are also reports of $OsO_{0.5}Cl_3$ (probably Os_2OCl_6) and a corresponding bromide [32].

1.3.4 *Halide complexes*

The complexes of ruthenium and osmium in the same oxidation state are generally similar and are, therefore, treated together; the structural (Table 1.3) and vibrational data (Table 1.4) have been set out in some detail to demonstrate halogen-dependent trends.

No complexes have at present been authenticated in oxidation states greater than +6, whereas oxyhalide complexes exist where the +8 state is known; this parallels trends in the halides and oxyhalides.

Oxidation state +6

Reaction of NOF with OsF_6 produces $NO^+OsF_7^-$, along with some $NO^+OsF_6^-$.

Table 1.4 Vibrational frequencies in MX_6^{n-} species (cm^{-1}) (M = Ru, Os; X = halogen)

n	RuF_6	$RuCl_6$	$RuBr_6$	RuI_6	OsF_6	$OsCl_6$	$OsBr_6$	OsI_6
0	675, 735				731, 720			
1	660, 630				688, 616 (XeF_5^+)	375, 325 (Et_4N)		
2	609, 581	328, 327 (Cs)	209, 248 (K)		608, 547 (Cs)	344, 313 (Cs)	211, 227 (K)	152, 170 (Bu_4N)
3		–, 310 (K)	184, 236 ($PhNH_3^+$)			313, 294 ($Co(en)_3$)	201, 200 ($Co(en)_3$)	144, 140 ($Co(en)_3$)

The first figure given for each species is ν_1 (A_{1g}), the second is ν_3 ($T_{1\mu}$).
Data are for ions in solution except where a counter-ion is indicated.

Oxidation state +5

Fluorination of a mixture of alkali metal halide and an appropriate ruthenium or osmium halide affords cream $MRuF_6$ (M = alkali metal, Ag; $\mu_{eff} = 3.5\text{–}3.8\,\mu_B$) or white $MOsF_6$:

$$RuCl_3 \text{ or } OsF_4 \xrightarrow[BrF_3 \text{ or } F_2]{MCl} MRuF_6 \text{ or } MOsF_6$$

They contain octahedral MF_6^- (Table 1.3) [33]; in $XeF^+RuF_6^-$ the attraction of XeF^+ distorts the octahedron by pulling one fluorine towards it, so that there is one long Ru–F distance of 1.919 Å compared with the others of 1.778–1.835 Å (EXAFS measurements indicate $KRuF_6$ has regular octahedral coordination (Ru–F 1.845 Å)) [19].

Magnetic moments are as expected for d^3 ions. Disproportionation occurs on hydrolysis:

$$MF_6^- \xrightarrow{H_2O} MO_4 + MF_6^{2-}$$

Octahedral $OsCl_6^-$ has been isolated as Ph_4As, Ph_4P and Ph_4N salts (μ_{eff} values of 3.21 and 3.03 μ_B have been reported) [34]:

$$OsCl_5 + Ph_4AsCl \xrightarrow{CCl_3CF_3} Ph_4AsOsCl_6$$

$$Os(CO)_2X_4^- \xrightarrow[120^\circ C]{Cl_2} Et_4NOsCl_6 \qquad (X = Br, I)$$

$OsCl_6^-$ is reduced to $OsCl_6^{2-}$ in contact with most solvents (e.g. CH_2Cl_2); the redox potential for $OsCl_6^-/OsCl_6^{2-}$ is 0.8 V and for $OsBr_6^-/OsBr_6^{2-}$ it is 1.20 V. PbO_2 can be used to form a transient $OsBr_6^-$ ion by oxidizing $OsBr_6^{2-}$; it will also oxidize $OsCl_6^{2-}$ to $OsCl_6^-$.

Cation size can affect bond lengths in $OsCl_6^-$; Os–Cl is 2.284 Å and 2.303 Å in the Ph_4P and Bu_4N salts, respectively. Oxidation, however, has a more significant effect, so that Os–Cl in $(Ph_4P)_2OsCl_6$ is 2.332 Å.

Oxidation state +4

All MX_6^{2-} have been isolated except RuI_6^{2-}. MF_6^{2-} can be made by hydrolysis of MF_6^-, as already mentioned, but other methods are available:

$$RuCl_3 + BaCl_2 \xrightarrow{F_2} BaRuF_6$$

Yellow Na_2RuF_6 has the Na_2SiF_6 structure while M_2RuF_6 adopts the K_2GeF_6 structure (M = K to Cs). EXAFS indicates Ru–F is 1.934 Å in K_2RuF_6 while in K_2OsF_6 Os–F is 1.927 Å [35]. Magnetic moments are as expected for a low spin d^4 ion (K_2RuF_6 2.86 μ_B, Cs_2RuF_6 2.98 μ_B, K_2OsF_6 1.30 μ_B, Cs_2OsF_6 1.50 μ_B); the lower values for the osmium compounds are a consequence of the stronger spin-orbit coupling for the 5d metal.

Various routes are available for the chlorides [36]:

$$\text{Ru or Os} \xrightarrow[\text{MCl}]{\text{Cl}_2} \text{M}_2\text{RuCl}_6 \text{ or } \text{M}_2\text{OsCl}_6$$

$$\text{M}_2\text{RuCl}_5(\text{OH}_2) \xrightarrow[\text{HCl (aq.)}]{\text{Cl}_2} \text{M}_2\text{RuCl}_6$$

$$\text{OsO}_4 \xrightarrow[\text{EtOH}]{\text{conc. HCl/MCl}} \text{M}_2\text{OsCl}_6$$

The last synthesis uses ethanol as the reducing agent. Soluble Na_2OsCl_6 has been used to make the less soluble salts of other alkali metals by metathesis.

Typical colours are red–brown to black (Ru) and orange to dark red (Os). K_2RuCl_6 has the K_2PtCl_6 structure. Magnetic moments for the ruthenium compounds are $2.7–3.0\,\mu_B$; the osmium compounds have substantially lower moments ($1.51\,\mu_B$ for K_2OsCl_6) but on doping into K_2PtCl_6 the moment of $OsCl_6^{2-}$ rises to $2.1\,\mu_B$, 'superexchange' causing a lowered value in the undiluted salts.

Bromides and iodides can be made (except X = I for Ru).

$$\text{RuBr}_5(\text{H}_2\text{O})^{2-} \xrightarrow[\text{Br}_2]{\text{HBr(aq.)}} \text{RuBr}_6^{2-}$$

$$\text{K}_2\text{RuCl}_6 \xrightarrow{\text{Br}_2} \text{K}_2\text{RuBr}_6$$

$$\text{OsO}_4 \xrightarrow[\text{M}^+]{\text{HBr(aq.)}} \text{M}_2\text{OsBr}_6 \qquad (\text{M} = \text{alkali metal})$$

$$\text{OsO}_4 \xrightarrow[\text{M}^+]{\text{HI(aq.)}} \text{M}_2\text{OsI}_6$$

These compounds tend to be black in colour. Magnetic moments of 2.84 and $1.65\,\mu_B$ have been reported for K_2RuBr_6 and K_2OsI_6, respectively.

$OsCl_6^{2-}$ is a useful starting material for the synthesis of a range of osmium complexes (Figure 1.4).

The mixed halide species $OsX_{6-n}Y_n^{2-}$ or $OsX_aY_bZ_c^{2-}$ $(a + b + c = 6)$ have been studied in considerable detail [37].

Reaction of $OsCl_6^{2-}$ with BrF_3 affords stepwise substitution

$$\text{OsCl}_6^{2-} \rightarrow \text{OsCl}_5\text{F}^{2-} \rightarrow cis\text{-OsCl}_4\text{F}_2^{2-} \rightarrow fac\text{-OsCl}_3\text{F}_3^{2-} \rightarrow$$

$$cis\text{-OsCl}_2\text{F}_4^{2-} \rightarrow \text{OsClF}_5^{2-} \rightarrow \text{OsF}_6^{2-}$$

with the stronger *trans*-effect of chloride directing the position of substitution. This can likewise be utilized to synthesize the *trans*- and *mer*-isomers, for example

$$cis\text{-OsCl}_2\text{F}_4^{2-} \xrightarrow{\text{Cl}^-} mer\text{-OsCl}_3\text{F}_3^{2-}$$

The isomer(s) obtained depend on the reaction time; thus reaction of K_2OsCl_6 with BrF_3 at 20°C affords 90% *cis*-$OsF_4Cl_2^{2-}$ after 20 min whereas

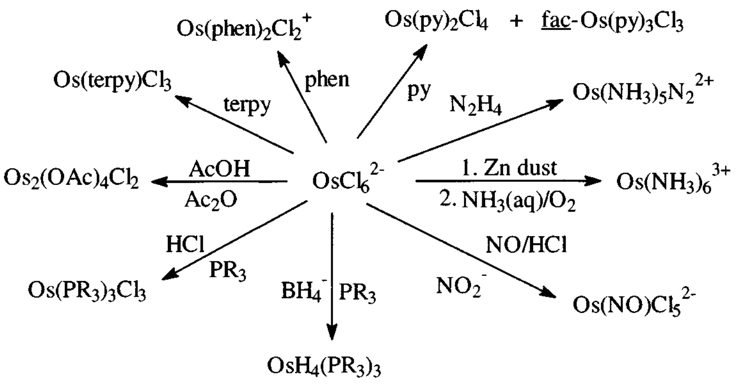

Figure 1.4 Reactions of $OsCl_6^{2-}$.

after 10 h the mixture contains 30% *cis*-$OsF_4Cl_2^{2-}$, 40% OsF_5Cl^{2-} and 30% OsF_6^{2-}. Mixtures can be separated by chromatography or ionophoresis; within this series, the *cis*-isomers are eluted before the *trans* (on diethylaminoethyl cellulose) whereas in ionophoresis, the *trans*-isomers move 3–5% faster.

Such octahedral anions are, of course, amenable to study by vibrational spectroscopy; as the anion symmetry descends from $O_h(MX_6^{2-})$, the number of bands increases as the degeneracy of vibrations is removed. Pairs of isomers can be distinguished; thus for $OsF_2Cl_4^{2-}$, the more symmetric *trans*-isomer (D_{4h}) gives rise to fewer stretching vibrations (5) than the *cis*-isomer (C_{2v}), which has 6. Moreover the centre of symmetry in the *trans*-isomer means there are no IR/Raman coincidences. The Os–F vibrations can be associated with bands in the 490–560 cm^{-1} region and Os–Cl stretching vibrations in the 300–360 cm^{-1} region (Figure 1.5).

Other series of mixed hexahalide complexes have been made. Thus from K_2OsI_6 and concentrated HBr:

$$OsI_6^{2-} \rightarrow OsBrI_5^{2-} \rightarrow cis\text{-}OsBr_2I_4^{2-} \rightarrow fac\text{-}OsBr_3I_3^{2-} \rightarrow$$

$$cis\text{-}OsBr_4I_2^{2-} \rightarrow OsBr_5I^{2-} \rightarrow OsBr_6^{2-}$$

As before the *trans*-isomers can be obtained using $OsBr_6^{2-}$ and concentrated HI; similarly, starting from $OsCl_6^{2-}$ and concentrated HI, the sequence $OsCl_5I^{2-}$, *trans*-$OsCl_4I_2^{2-}$, *mer*-$OsCl_3I_3^{2-}$, *trans*-$OsCl_2I_4^{2-}$, $OsClI_5^{2-}$ and OsI_6^{2-} is obtained. A more drastic synthesis of this type has been achieved by taking mixed crystals K_2OsBr_6/K_2SnCl_6 and using the nuclear process $^{190}Os(n,\gamma)^{191}Os$, when all the mixed species $^{191}OsCl_nBr_{6-n}^{2-}$ were obtained.

Mixed species with three different halogens have been made

$$OsF_5Cl^{2-} \xrightarrow[50°C,\,30\,min]{conc.\ HBr} trans\text{-}OsF_4ClBr^{2-}$$

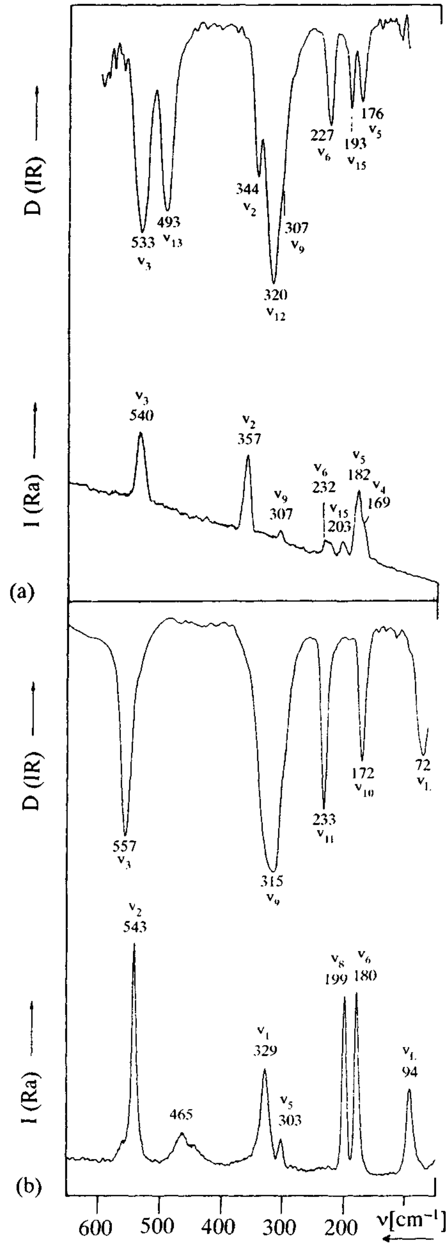

Figure 1.5 The vibrational spectra of the *cis* (a) and *trans* (b) isomers of $[OsCl_2F_4]^{2-}$ in their caesium salts. (Reproduced with permission from *Z. Naturforsch.*, Teil B, 1984, **39**, 1100.)

Table 1.5 Bond lengths (Å) in dipyridinio methane salts

	OsF_5Cl^{2-}	*fac*-$OsF_3Cl_3^{2-}$	*mer*-$OsF_3Cl_3^{2-}$	*cis*-$OsF_2Cl_4^{2-}$	*trans*-$OsF_2Cl_4^{2-}$
Os–F					
trans to F	1.918		1.944		1.926
trans to Cl	1.959	1.948	1.976	1.948	
Os–Cl					
trans to F	2.329	2.320	2.278	2.316	
trans to Cl			2.307	2.338	2.337

The crystal structure of the caesium salt shows Os–F, Os–Cl and Os–Br bonds of 1.94, 2.43 and 2.49 Å, respectively. The complex exhibits strong IR bands at 552, 320 and 222 cm^{-1}, assigned to Os–F, Os–Cl and Os–Br stretching, respectively (compare ν_3 of OsX_6^{2-} at 547 cm^{-1} (F), 313 cm^{-1} (Cl) and 227 cm^{-1} (Br)) [38].

Bond lengths in the dipyridinio methane salts $[(C_5H_5N)_2CH_2][OsF_5Cl]$, *fac*- and *mer*-$[(C_5H_5N)_2CH_2][OsF_3Cl_3]$ and *cis*- and *trans*-$[(C_5H_5)_2CH_2][OsF_2Cl_4]$ show the mutual *trans*-influence of chlorine and fluorine; thus Os–Cl bonds *trans* to fluorine are shorter than those *trans* to chlorine, while Os–F bonds *trans* to chlorine are longer than those *trans* to fluorine (Table 1.5) [38c].

Oxidation state +3

Halide complex ions of ruthenium and osmium in the +3 state are known for all except OsF_6^{3-} [39]. Syntheses include:

$$RuCl_3 \xrightarrow[\text{fuse}]{KHF_2} K_3RuF_6 \qquad (\mu = 1.25\,\mu_B)$$

$$K_2RuCl_5(H_2O) \xrightarrow{HCl(g)} K_3RuCl_6$$

$$RuX_3 \xrightarrow[\text{conc. }HX/N_2]{[C_6H_5NH_3]^+X^-} (C_6H_5NH_3)_3RuX_6 \qquad (\mu = 2.09\,\mu_B,\ X = Br)$$

A general synthesis for the osmium compounds is

$$OsX_6^{2-} \xrightarrow{\text{conc. }HX/N_2} (Coen_3)^{3+}OsX_6 \qquad (X = Cl, Br, I)$$

Magnetic moments reported for the OsX_6^{3-} salts are 1.70, 1.67 and 1.61 μ_B for X = Cl, Br and I, respectively, consonant with the low-spin d^5 configuration.

A number of dinuclear complexes have been synthesized [40]

$$Os_2(OCOMe)_4Cl_2 \xrightarrow[EtOH]{HCl(g)} Os_2Cl_8^{2-}$$

$$Os_2Cl_8^{2-} \xrightarrow[Me_2CO]{NaI} Os_2I_8^{2-}$$

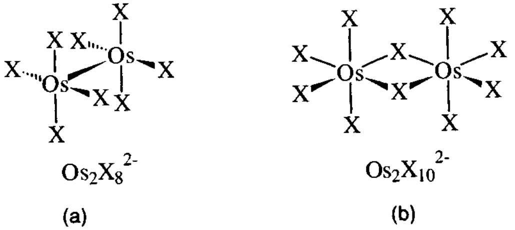

Figure 1.6 The structures of the diosmate ions $Os_2X_8^{2-}$ (a) and $Os_2X_{10}^{2-}$ (b).

Oxidation with halogens gives the decahalogenodiosmate (IV) (2−) ions (Figure 1.6):

$$Os_2X_8^{2-} \xrightarrow[CH_2Cl_2]{X_2} Os_2X_{10}^{2-} \qquad (X = Cl, Br)$$

The short Os–Os bonds in $Os_2X_8^{2-}$ correspond to triple bonds and give rise to stretching vibrations associated with bands around 280 cm^{-1} in the Raman spectrum (Table 1.6).

The $Os_2X_8^{2-}$ ions participate in various redox processes: at 235 K $Os_2Cl_8^{2-}$ undergoes reversible oxidation to $Os_2Cl_8^{n-}$ ($n = 1, 0$), the bromide behaves similarly. At high temperatures, the Os–Os bond is broken and $OsCl_6^-$ is formed. $Os_2Cl_8^{2-}$ can also be cleaved with Bu^{t}NC to form *trans*-$OsCl_4(CNBu^t)_2^-$ [41].

In addition to the doubly bridged $Os_2X_{10}^{2-}$, triply bridged $Os_2Br_9^-$ can be made (Figure 1.7):

$$OsBr_6^{2-} \xrightarrow[40°C]{CF_3CO_2H} Os_2Br_{10}^{2-} \xrightarrow[110°C]{CF_3CO_2H} Os_2Br_9^-$$

It can be reduced electrochemically to $Os_2Br_9^{n-}$ ($n = 2, 3$), with $Os_2Br_{10}^{n-}$ ($n = 3, 4$) similarly accessible. $Rb_3Os_2Br_9$ has Os–Os 2.799 Å [42].

Table 1.6 Characteristics of $Os_2X_8^{2-}$

	Counter-ion	Os–Os (Å)	ν_{sym} (Os–Os) (cm^{-1})
$Os_2Cl_8^{2-}$	Bu_4N	2.182	285
$Os_2Br_8^{2-}$	Bu_4N	2.196	287
$Os_2I_8^{2-}$	$(Ph_3P)_2N$	2.212	270

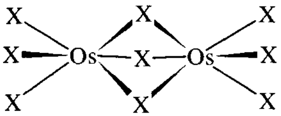

Figure 1.7 The structures of the diosmate ions $Os_2X_9^{3-}$.

In the case of ruthenium, the Ru_2X_9 system with confacial octahedra is important

$$M_2RuCl_5(H_2O) \xrightarrow[\textit{in vacuo}]{250°C} M_3Ru_2Cl_9 \qquad (M = \text{alkali metal})$$

$$RuCl_6^{3-} \xrightarrow{HBr} Ru_2Br_9^{3-}$$

These evidently have some Ru–Ru bonding with Ru–Ru distances of 2.73 and 2.87 Å in $Cs_3Ru_2Cl_9$ and (1-methyl-3-ethylimidazolinium)$_3Ru_2Br_9$, respectively; the magnetic moments of $(Bu_4N)_3Ru_2X_9$ of $0.86\,\mu_B$ (Cl) and $1.18\,\mu_B$ (Br) are lower than expected for low spin d^5 and indicate some metal–metal interaction. $Ru_2X_9^{3-}$ again forms part of a redox-related series $Ru_2X_9^{n-}$ ($n = 1$–4) obtainable in solution by low-temperature electrochemistry [42].

1.3.5 'Ruthenium blues' [43]

It has long been known (Claus, 1846) that reduction (e.g. Zn, H_2 with Pt catalyst) of some ruthenium salts gives a blue solution, which on treatment with HCl or oxidation turns green. Various claims have been made for the species present: $RuCl_4^{2-}$, $Ru_2Cl_3^{2+}$, $Ru_2Cl_4^{+}$ and $Ru_5Cl_{12}^{2-}$. A cluster $(Cl_3Ru(\mu\text{-}Cl)_3Ru(\mu\text{-}Cl)_3RuCl_3)^{4-}$ has been isolated and characterized from such a solution [44]. At present it seems likely that the compound in solution is a cluster, that the ruthenium valency is between 2 and 2.5 and that more than one species is present.

The blue solutions have been found to catalyse alkene isomerization and hydrogenation and have very considerable synthetic utility (Figure 1.8).

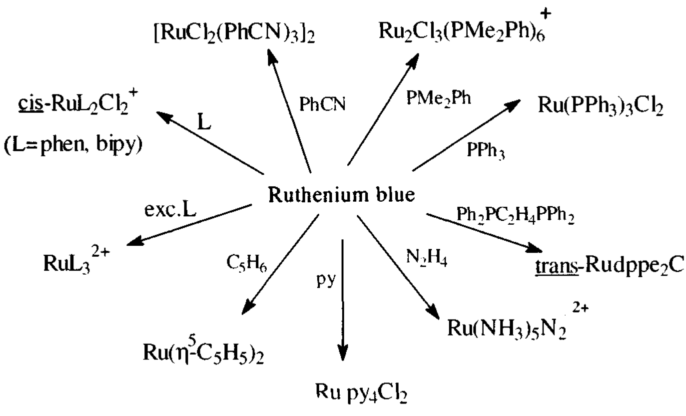

Figure 1.8 Syntheses using 'Ruthenium blue'.

1.3.6 Oxyhalide complexes

Various anionic complexes have been made [26a]:

$$OsO_3F_2 + KF \xrightarrow{\text{heat}} K[OsO_3F_3]$$

$$OsO_4 \xrightarrow{\text{CsF(aq.)}} Cs_2[OsO_4F_2]$$

EXAFS measurements on $KOsO_3F_3$ indicate the presence of *fac*-$OsO_3F_3^-$ with Os=O 1.70 Å, Os–F 1.92 Å; in $Cs_2OsO_4F_2$, *cis*-$OsO_4F_2^{2-}$ has Os=O 1.70 Å and Os–F 2.05 Å.

Reaction of Ph_4PCl with OsO_4 gives $Ph_4P^+OsO_4Cl^-$, the anion having a tbp structure with a very long equatorial Os–Cl bond (2.76 Å) [45].

Both ruthenium and osmium form *trans*-$MO_2X_4^{2-}$ species (X = Cl, Br), for example

$$RuO_4 \xrightarrow[\text{HCl}]{\text{MCl}} M_2RuO_2Cl_4 \qquad (M = Rb, Cs)$$

$$K_2[OsO_2(OH)_4] \xrightarrow{\text{HCl}} K_2OsO_2Cl_4$$

Typical bond lengths are M=O 1.709 Å (Ru) 1.750 Å (Os) and M–Cl 2.388–2.394 Å (Ru) 2.379 Å (Os) in $[(Ph_3P)_2N]RuO_2Cl_4$ and $K_2OsO_2Cl_4$, respectively. Characteristic ν(M=O) bands can be seen in the vibrational spectra owing to both the symmetric and asymmetric stretches: for $OsO_2X_4^{2-}$ the symmetric stretch is at 904 (X = Cl) and 900 (X = Br) cm^{-1}, with corresponding values for the asymmetric stretch of 837 and 842 cm^{-1} (in the potassium salts).

In solution $[(Ph_3P)_2N]_2$ RuO_2Cl_4 loses chloride to form $[(Ph_3P)_2N]$ RuO_2Cl_3, which has a tbp structure with two axial chlorines (Ru–Cl 2.37–2.39 Å); the equatorial bond lengths are 1.66–1.69 Å (Ru–O) and 2.13 Å (Ru–Cl) [46].

The dimeric $M_2OCl_{10}^{4-}$ ions contain linear M–O–M units (Figure 1.9); in $Cs_4Os_2OCl_{10}$ the Os–O–Os stretching vibration is at 852 cm^{-1} in the IR spectrum [47] while its crystal structure reveals Os=O 1.778 Å, Os–Cl 2.367–2.377 Å (*cis* to O) and 2.433 Å (*trans* to O). In $K_4Ru_2OCl_{10}$, Ru=O is 1.801 Å, Ru–Cl is 2.363 (*cis*) and 2.317 Å (*trans*). The shortness of the M–O bridge bonds is explained by the formation of two M–O–M three-centre MOs. Figure 1.10 shows the formation of one of these by overlap of

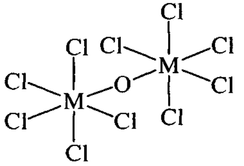

Figure 1.9 The dimeric $[M_2OCl_{10}]^{4-}$ ions (M = Ru, Os).

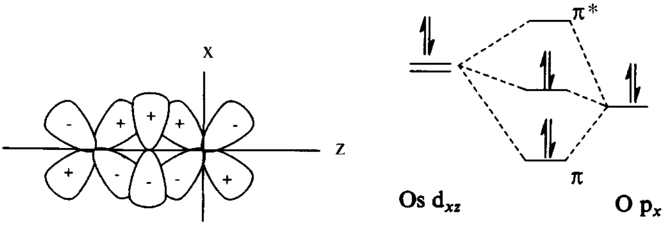

Figure 1.10 The three-centre molecular orbitals in $[Os_2OCl_{10}]^{4-}$.

osmium 5d and oxygen 2p orbitals; each MO contains two osmium electrons and two from the oxygen occupying the bonding and non-bonding MOs. These two MOs account for two of the four electrons belonging to each Os^{4+} ion (d^4); the remaining two occupy the d_{xy} orbital (unused in the MO scheme) explaining the diamagnetism of these M^{IV} compounds.

1.4 Oxides and related anions

The oxides are dominated by the very volatile and toxic tetroxides. Yellow RuO_4 (m.p. 25.4°C, b.p. 40°C) is isomorphous with OsO_4; electron diffraction measurements indicate that it is tetrahedral in the gas phase (Ru–O 1.706 Å) [48a]. It is light sensitive and thermodynamically unstable with respect to RuO_2 (from which, however, it can be made) and can be explosive. Because of the lesser stability of ruthenium(VIII) compared with osmium (VIII), RuO_4 is a stronger oxidizing agent than OsO_4 (and therefore less selective); solutions in CCl_4 are stable [48b]. A convenient synthesis involves periodate oxidation of $RuCl_3$ or RuO_2:

$$RuCl_3 \text{ or } RuO_2 \xrightarrow{NaIO_4} RuO_4$$

RuO_4 reacts with pyridine to form $RuO_3(py)$, probably a dimer $Py_2(O)_2Ru(\mu\text{-}O)_2Ru(O)_2Py_2$, an aerobically assisted oxidant [48c].

RuO_2 can be made by high-temperature oxidation of ruthenium. It has the rutile structure (Ru–O 1.942 Å and 1.984 Å) and forms blue–black crystals [49b].

Recently RuO_3 has been made as a brown solid by photolysis:

$$RuO_4 \xrightarrow[370-440\,\text{nm}]{h\nu} RuO_3$$

In matrices, RuO_2 is bent (149°) while RuO_3 is trigonal planar.

Copper-coloured OsO_2 also has the rutile structure: it can be made from the metal and NO at 650°C.

OsO_4 is obtained on oxidation of any osmium compound or by direct synthesis at 300–800°C from the elements [50]. Its solubility in CCl_4 and volatility make it easy to purify; it forms pale yellow crystals (m.p. 40.46°C, b.p. 131°C). Like RuO_4 it forms tetrahedral molecules with Os–O 1.684–1.710 Å, O–Os–O 106.7–110.7° in the solid state; Os–O 1.711 Å in the gas phase [51]. It is soluble in water as well as in CCl_4 and is very toxic (TLV 2.5 ppm), affecting the eyes. (Its use as a biological stain involves its reaction with tissue.)

Gas-phase vibrational data for OsO_4 are $\nu_1 = 965.2$, $\nu_2 = 333.1$, $\nu_3 = 960.1$ and $\nu_4 = 322.7\,\mathrm{cm}^{-1}$.

Photoelectron spectra have been interpreted with a MO scheme, shown in Figure 1.11 [52].

OsO_4 will add to C=C bonds but will only attack the most reactive aromatic bonds; thus benzene is inert, but it will attack the 9,10 bond in phenanthrene and will convert anthracene to 1,2,3,4-tetrahydroxytetrahydroanthracene. It can be used catalytically in the presence of oxidizing agents such as $NaClO_3$ or H_2O_2 [53].

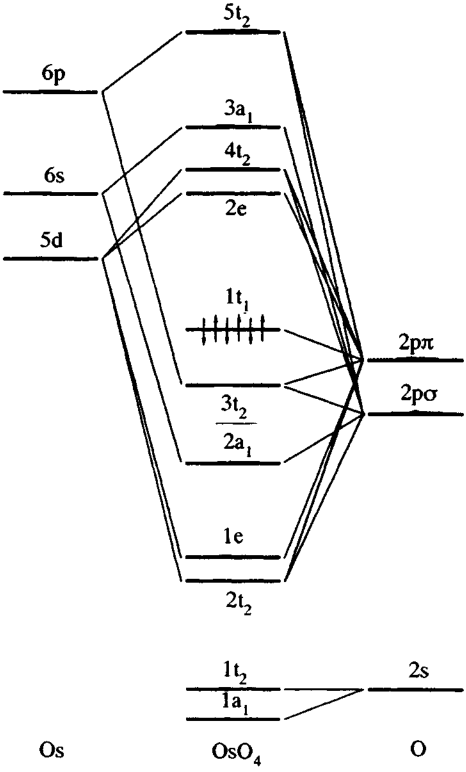

Figure 1.11 A molecular orbital diagram for OsO_4. (Reprinted with permission from *Inorg. Chem.*, 1992, **31**, 1588. Copyright American Chemical Society.)

1.4.1 Anions

Alkalis reduce RuO_4 to RuO_4^-; various salts have been prepared

$$RuCl_3.xH_2O \xrightarrow{NaIO_4} RuO_4 \xrightarrow[K_2CO_3]{Pr_4NOH} Pr_4NRuO_4$$

On heating it decomposes in a similar manner to $KMnO_4$:

$$2KRuO_4 \rightarrow K_2RuO_4 + RuO_2 + O_2$$

The anion in $KRuO_4$ has a slightly flattened tetrahedral structure (Ru–O 1.73 Å). Organic-soluble salts like Pr_4NRuO_4 are selective mild oxidants that will oxidize alcohols to carbonyl compounds but will not affect double bonds [54a]. ESR indicates that RuO_4^- ($g_x = 1.93$; $g_y = 1.98$; $g_z = 2.06$) has a compressed tetrahedral geometry with the electron in d_{z^2} [54b].

RuO_4^{2-}, which is believed to be tetrahedral in solution, is formed from RuO_4 and excess concentrated aqueous KOH, isolable as black crystals of $K_2RuO_4.H_2O$, which is actually $K_2[RuO_3(OH)_2]$. The anion has a tbp structure with axial OH groups (Ru=O 1.741–1.763 Å, Ru–OH 2.028–2.040 Å) [55].

In contrast to ruthenium, osmium exists in alkaline solution as $OsO_4(OH)_2^{2-}$, believed to be *cis* and isolable as crystalline salts:

$$OsO_4 + 2KOH \rightarrow K_2OsO_4(OH)_2$$

Similarly, instead of forming OsO_4^{2-}, reduction of OsO_4 with ethanolic KOH yields $K_2[OsO_2(OH)_4]$.

The osmiamate ion, OsO_3N^-, is isoelectronic with OsO_4. The yellow potassium salt is the most convenient one to prepare; other, less soluble, salts, can be made by metathesis:

$$OsO_4 + NH_3 \xrightarrow{KOH} KOsO_3N$$

The crystallographic study of the potassium salt is complicated by disorder but in $CsOsO_3N$ Os≡N is 1.676 Å and Os=O 1.739–1.741 Å. Assignments of the vibrational spectrum of OsO_3N^- is assisted by isotopic substitution: the higher frequency absorption is shifted significantly on ^{15}N substitution whereas the band just below 900 cm^{-1} is scarcely affected (Table 1.7); conversely the latter band is shifted by some 50 cm^{-1} on replacing ^{16}O by ^{18}O [56].

Nitrido salts are discussed later (section 1.12.2).

Table 1.7 Vibrational data for osmiamate ions (in cm^{-1})

	ν_1 (Os≡N)	ν_2 (Os=O)
OsO_3N^-	1029	898
$OsO_3{}^{15}N^-$	998	896
$K[Os^{18}O_3N]^-$	1024	844

1.5 Other binary compounds

Ruthenium and osmium form no stable binary hydrides, but very recently heating mixtures of the metals with alkaline earth metal hydrides under pressure in a hydrogen atmosphere have been shown to give oxygen- and moisture-sensitive hydrides M_2RuH_6 (M = Mg, Ba), M_2OsH_6 (M = Mg to Ba) and Li_4OsH_6. These contain MH_6^{4-} (K_2PtCl_6 structure) with Ru–D 1.673 and Os–D 1.682 Å in the corresponding deuterides [57]. $LiMg_2RuH_7$ has RuH_6^{2-} with Ru–D 1.704 Å in the deuteride.

The mineral laurite is the mixed sulphide $(Ru,Os)S_2$; this and RuS_2 and OsS_2 have the pyrite structure as does RuQ_2 (Q = Se, Te). These can be made from the reaction of the chalcogen with the metals, while $RuCl_3$ will also react with Se and Te.

MP_2, MAs_2 and MSb_2 all have a compressed form of the marcasite structure, while the carbides MC have trigonal prismatic coordination in the WC structure. Several borides are known: MB_2 has nets of boron atoms. $Ru_{11}B_8$ has branched chains while Ru_7B_3 has isolated borons.

1.6 Aqua ions [58]

Diamagnetic, low-spin d^6 $Ru(H_2O)_6^{2+}$ has been made by reduction of RuO_4 with activated Pb (or Sn) followed by ion-exchange purification. The pink tosylate salt contains octahedral $Ru(H_2O)_6^{2+}$ (Ru–O 2.122 Å); though the solid is air stable, it is readily oxidized in solution by oxygen and ClO_4^-. The hexaqua ions also occur in the red diamagnetic Tutton salts $M_2Ru(H_2O)_6(SO_4)_2$ (M = NH_4, Rb)

$$RuO_4 \xrightarrow[H^+]{Pb/Hg} Ru(H_2O)_6^{2+} \xrightarrow{(NH_4)_2SO_4} (NH_4)_2Ru(H_2O)_6(SO_4)_2$$

Ru $(H_2O)_6(BF_4)_2$ has been isolated but decomposes on standing.

Aerial oxidation of $Ru(H_2O)_6^{2+}$ produces lemon-yellow $Ru(H_2O)_6^{3+}$ (Ru–O 2.029 Å in the tosylate salt)

$$Ru(H_2O)_6^{2+} \rightarrow Ru(H_2O)_6^{3+} + e^- \qquad E^\ominus = -0.205\,V$$

The yellow alum $CsRu(H_2O)_6(SO_4)_2.6H_2O$ has also been synthesized with $\mu_{eff} = 2.20\,\mu_B$ at 300 K; the Ru–O distance is 2.010 Å.

Vibrational spectra of octahedral $Ru(H_2O)_6^{n+}$ ($n = 2$, $\nu_1 = 424\,cm^{-1}$, $\nu_3 = 426\,cm^{-1}$; $n = 3$, $\nu_1 = 532\,cm^{-1}$, $\nu_3 = 529\,cm^{-1}$) have been interpreted in terms of the force constants 1.91 mdyn $Å^{-1}$ ($n = 2$) and 2.98 mdyn $Å^{-1}$ ($n = 3$), showing a stronger bond for the ruthenium(III) species.

The ruthenium(II) aqua ion reacts with nitrogen at room temperature under high pressure (200 bar) forming yellow–brown $[Ru(H_2O)_5N_2]^{2+}$, isolated as a tosylate salt, showing $\nu(N{\equiv}N)$ at 2141 cm^{-1} in its IR spectrum [59].

The ruthenium(IV) aqua ion, best made by electrochemical oxidation of $Ru(H_2O)_6^{2+}$, but also made by the reaction of RuO_4 with $H_2O_2/HClO_4$, is tetranuclear, formulated as $[Ru_4O_6(H_2O)_{12}]^{4+}$, though this may be protonated [60]. FAB mass spectra of a pyrazolylborate complex show Ru_4O_6-containing fragments.

No simple osmium aqua ion has been definitely isolated and characterized, though in alkaline solution (and the solid state) the osmium(VIII) species $OsO_4(OH)_2^{2-}$ is well characterized (sections 1.4.1 and 1.12.1).

Osmium(II) is probably too reducing to exist as $Os(H_2O)_6^{2+}$, but $Os(H_2O)_6^{3+}$ and a polynuclear Os_4^{+}(aq.) species are likely.

1.7 Compounds of ruthenium(0)

Apart from $Ru(CO)_5$ and other carbonyls, there are mixed carbonyl–phosphine species and a few simple phosphine complexes like $Ru(PF_3)_5$ and $Ru[P(OMe)_3]_5$ [61a].

Photochemistry of $Ru(CO)_3(PMe_3)_2$ and the ruthenium(II) compound $Ru(CO)_2(PMe_3)_2H_2$ in low-temperature matrices affords $[Ru(CO)_2(PMe_3)_2\cdots S]$ ($S = Ar$, Xe, CH_4) [61b]. These monomers all have 18-electron tbp structures.

The phosphine complex $Ru(dmpe)_2$ has been studied in matrices [62]. $Ru(diphos)_2$ (diphos = depe, dppe, $(C_2F_5)_2P(CH_2)_2P(C_2F_5)_2$) has similarly been formed by photolysis of $Ru(diphos)_2H_2$ in low-temperature matrices. They probably have square planar structures and undergo oxidative addition with cobalt, C_2H_4 and hydrogen [63].

Additionally a number of nitrosyls such as $Ru(NO)_2(PPh_3)_2$ (section 1.8.5) exist.

1.8 Complexes of ruthenium(II and III)

Because of the relationship between compounds in the adjacent oxidation states +2 and +3, they are grouped together here; the section is subdivided by ligand, concentrating on some classes of complex important in their diversity and in current research interest.

1.8.1 Ammine complexes

Orange $Ru(NH_3)_6^{2+}$ can be obtained by various routes (see Figure 1.12).

As expected for the +2 state of a heavy metal, it is reducing:

$$Ru(NH_3)_6^{2+} \rightarrow Ru(NH_3)_6^{3+} + e^- \qquad E^\ominus = +0.214\,V$$

Historically, the most important ruthenium(II) ammine species is $[Ru(NH_3)_5N_2]^{2+}$, the first stable dinitrogen complex to be isolated (1965). It was initially obtained by refluxing $RuCl_3$ in hydrazine solution (but many

Next Page

Previous Page

The ruthenium(IV) aqua ion, best made by electrochemical oxidation of $Ru(H_2O)_6^{2+}$, but also made by the reaction of RuO_4 with $H_2O_2/HClO_4$, is tetranuclear, formulated as $[Ru_4O_6(H_2O)_{12}]^{4+}$, though this may be protonated [60]. FAB mass spectra of a pyrazolylborate complex show Ru_4O_6-containing fragments.

No simple osmium aqua ion has been definitely isolated and characterized, though in alkaline solution (and the solid state) the osmium(VIII) species $OsO_4(OH)_2^{2-}$ is well characterized (sections 1.4.1 and 1.12.1).

Osmium(II) is probably too reducing to exist as $Os(H_2O)_6^{2+}$, but $Os(H_2O)_6^{3+}$ and a polynuclear Os_4^+(aq.) species are likely.

1.7 Compounds of ruthenium(0)

Apart from $Ru(CO)_5$ and other carbonyls, there are mixed carbonyl–phosphine species and a few simple phosphine complexes like $Ru(PF_3)_5$ and $Ru[P(OMe)_3]_5$ [61a].

Photochemistry of $Ru(CO)_3(PMe_3)_2$ and the ruthenium(II) compound $Ru(CO)_2(PMe_3)_2H_2$ in low-temperature matrices affords $[Ru(CO)_2(PMe_3)_2 \cdots S]$ ($S = Ar, Xe, CH_4$) [61b]. These monomers all have 18-electron tbp structures.

The phosphine complex $Ru(dmpe)_2$ has been studied in matrices [62]. $Ru(diphos)_2$ (diphos = depe, dppe, $(C_2F_5)_2P(CH_2)_2P(C_2F_5)_2$) has similarly been formed by photolysis of $Ru(diphos)_2H_2$ in low-temperature matrices. They probably have square planar structures and undergo oxidative addition with cobalt, C_2H_4 and hydrogen [63].

Additionally a number of nitrosyls such as $Ru(NO)_2(PPh_3)_2$ (section 1.8.5) exist.

1.8 Complexes of ruthenium(II and III)

Because of the relationship between compounds in the adjacent oxidation states +2 and +3, they are grouped together here; the section is subdivided by ligand, concentrating on some classes of complex important in their diversity and in current research interest.

1.8.1 Ammine complexes

Orange $Ru(NH_3)_6^{2+}$ can be obtained by various routes (see Figure 1.12).

As expected for the +2 state of a heavy metal, it is reducing:

$$Ru(NH_3)_6^{2+} \rightarrow Ru(NH_3)_6^{3+} + e^- \qquad E^{\ominus} = +0.214\,V$$

Historically, the most important ruthenium(II) ammine species is $[Ru(NH_3)_5N_2]^{2+}$, the first stable dinitrogen complex to be isolated (1965). It was initially obtained by refluxing $RuCl_3$ in hydrazine solution (but many

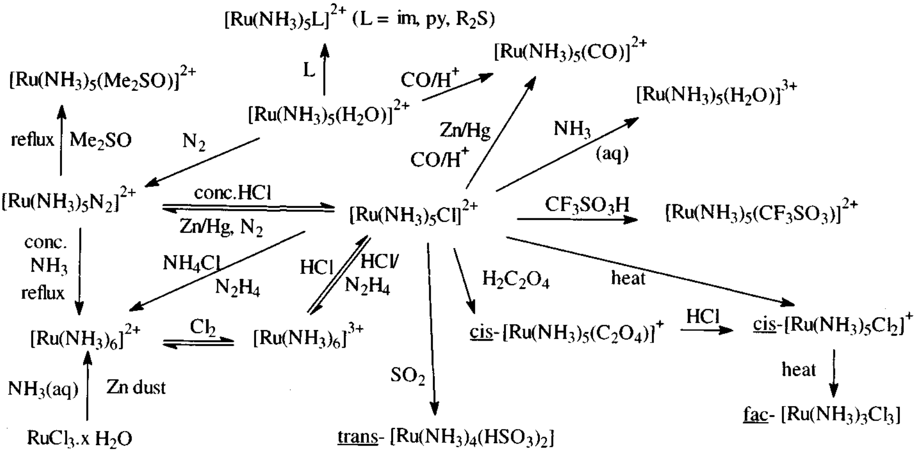

Figure 1.12 Ammine complexes of ruthenium.

other routes are available); it seems that the N_2 ligand may result from the oxidation of coordinated N_2H_4. Another synthesis [64] involves attack by NO on a coordinated NH_3 in $[Ru(NH_3)_6]^{3+}$ (confirmed by using isotopically labelled ^{15}NO), while the reaction of N_2 with $[Ru(NH_3)_5(H_2O)]^{2+}$ is a simple substitution (Figure 1.13).

X-ray diffraction confirms the terminal N_2 geometry, with slight lengthening of the N–N bond (1.12 Å) compared to gaseous N_2 (1.09 Å) with concomitant lengthening shown by the change in $\nu(N{\equiv}N)$ in the IR spectrum (2110 cm^{-1}, compared with 2331 cm^{-1} in nitrogen gas) [65].

The N_2 ligand is displaced by other ligands (e.g. py) and attempted oxidation to $[Ru(NH_3)_5N_2]^{3+}$ results in the loss of N_2.

The colourless paramagnetic $[Ru(NH_3)_6]^{3+}$ is readily synthesized by oxidation of $[Ru(NH_3)_6]^{2+}$. Its magnetic moment is as expected for a low-spin d^5 ion (2.17 μ_B for $Ru(NH_3)_6Br_3$ at 292 K).

The pentammine aqua ion $[Ru(NH_3)_5(H_2O)]^{2+}$, best made by zinc amalgam reduction and aquation of $[Ru(NH_3)_5Cl]^{2+}$, undergoes extensively studied substitution reactions first order in both the ruthenium complex and the incoming ligand (e.g. NH_3, py) and is a convenient source of other

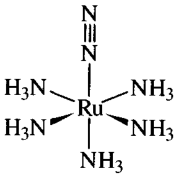

Figure 1.13 $[Ru(NH_3)_5(N_2)]^{2+}$.

pentammines. The corresponding ruthenium(III) species $[Ru(NH_3)_5(H_2O)]^{3+}$ can be made by aquation of $[Ru(NH_3)_5Cl]^{2+}$ or the triflate $[Ru(NH_3)_5(CF_3SO_3)]^{2+}$. Heating solid $[Ru(NH_3)_5(H_2O)]X_3$ gives $[Ru(NH_3)_5X]X_2$ (X = Cl, Br, I, NO_3) [66].

Structures determined include octahedral $Ru(NH_3)_6^{3+}$ in the tetrafluoroborate (Ru–N 2.104 Å) and thiocyanate (2.105–2.113 Å), while in $[Ru(NH_3)_6]BrSO_4$ Ru–N is 2.107 Å. In $[Ru(NH_3)_5Cl]SO_4.4H_2O$, Ru–Cl is 2.374 Å while Ru–N distances fall in the range 2.096–2.113 Å.

Among ruthenium(II) complexes, $Ru(NH_3)_6I_2$ has Ru–N of 2.144 Å; $[Ru(NH_3)_5N_2]^{2+}$ has Ru–N(NH_3) and Ru–N(N_2) 2.11 Å; and $[Ru(NH_3)_5(Me_2SO)]^{2+}$ has Ru–N (*cis*) of 2.169 Å, Ru–N (*trans*) 2.209 Å and Ru–S 2.188 Å. The Ru–N bonds are, therefore, shorter in the ruthenium(III) complexes, as expected on electrostatic grounds [67].

The ESR spectra of $t_{2g}^5Ru(NH_3)_6^{3+}$ on cubic sites in $[Ru(NH_3)_6]BrSO_4$ show an isotropic g value of 1.926 while in $[Ru(NH_3)_6]$ $(NCS)_3$ the g values are 2.357, 1.929 and 1.468 ($g_{av} = 1.918$) in a low symmetry field. The results have been interpreted in a crystal field model with an orbital reduction factor of 0.94 [67].

Binuclear ammine complexes

Two binuclear ammine complexes are of particular interest.

The Creutz–Taube compound (named after its discoverers), $[(NH_3)_5Ru(pyrazine)Ru(NH_3)_5]^{5+}$ is the middle member of a redox-related series, formally containing one ruthenium(II) and one ruthenium(III) (Figure 1.14); the interest lying in whether the two ruthenium centres are identical, whether the valencies are 'trapped' or whether there is partial delocalization.

The mixed-valence ion has an intervalence charge transfer band at 1562 nm not present in the spectra of the +4 and +6 ions. Similar ions have been isolated with other bridging ligands, the choice of which has a big effect on the position and intensity of the charge-transfer band (e.g. L = bipy, 830 nm).

The structural data (Table 1.8) and spectroscopic information indicate that the 5+ ion has considerable delocalization with rapid electron transfer between the two centres ($\sim 10^{12}\,s^{-1}$) [68].

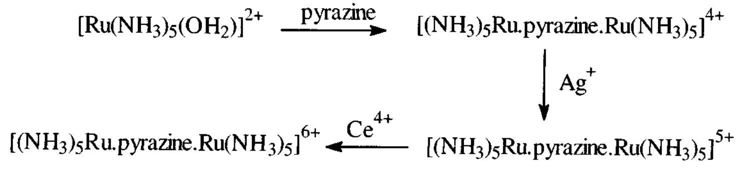

Figure 1.14 Dimeric pyrazine complexes of ruthenium.

Table 1.8 Bond lengths (Å) in $(NH_3)_5RuN$ (pyrazine) $NRu(NH_3)_5^{n+}$

n	4	5	6
$Ru-NH_3$ (*trans*)	2.149	2.134	2.089
$Ru-NH_3$ (*cis*)	2.132	2.111	2.101
$Ru-N$ (pyrazine)	2.013	2.002	2.115

A dimeric dinitrogen complex can be made by several routes, including

$$[Ru(NH_3)_5(H_2O)^{2+}] + [Ru(NH_3)_5N_2]^{2+} \rightarrow$$
$$[(NH_3)_5RuN_2Ru(NH_3)_5]^{4+} + H_2O$$

It has a symmetric eclipsed structure with a linear Ru–N–N–Ru geometry (178.3°) (Figure 1.15).

Because of the symmetric structure, a strong $\nu(N{\equiv}N)$ band is seen in the Raman spectrum at $2100\,cm^{-1}$, but not in the IR spectrum. It can be oxidized to the unstable 5+ ion chemically and to the 6+ ion electrochemically [69].

'Ruthenium red' and 'ruthenium brown'

Air oxidizes ammoniacal ruthenium chloride to a red solution, which on workup gives 'ruthenium red', brown diamagnetic $[Ru_3O_2(NH_3)_{14}]Cl_6$, formally containing two Ru^{3+} and one Ru^{4+}. Oxidation of this (Ce^{4+}, HNO_3) gives $[Ru_3O_2(NH_3)_{14}]^{7+}$, 'ruthenium brown' [70]. These are oxo-bridged species (the IR spectrum of the red shows a band at $805\,cm^{-1}$ owing to Ru–O–Ru stretching, which is shifted to $820\,cm^{-1}$ in 'ruthenium brown'). The structure of the thiosulphate salt of 'ruthenium red' has been determined (Figure 1.16) and confirms the trinuclear Ru–N bonds are eclipsed with the Ru–N bonds at one end but 31° away from the eclipsed position with the Ru–N bonds at the other end, so that the ion is non-centrosymmetric.

Reaction of 'ruthenium red' with ethylenediamine at 45°C yields a red-green analogue with chelating ethylenediamines bound to the central ruthenium $[(NH_3)_5RuORu(en)_2ORu(NH_3)_5]^{6+}$ (Figure 1.17).

Here the $Ru-NH_3$ bonds at each end are eclipsed, with the Ru–N(en) bonds staggered.

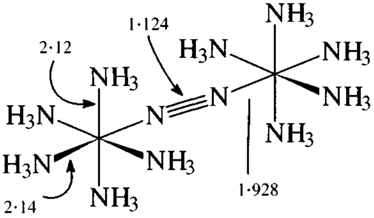

Figure 1.15 Bond lengths in the dimeric ion $[(NH_3)_5RuN_2Ru(NH_3)_5]^{4+}$.

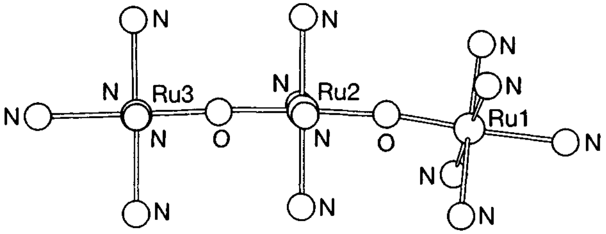

Figure 1.16 The structure of $[Ru_3O_2(NH_3)_{14}]^{6+}$, Ruthenium red. (Reprinted from *Biochim. Biophys. Acta*, **627**, 332, 1980, with kind permission of Elsevier Science – NL, Sara Burgerhartstraat 25, 1055 KV Amsterdam, The Netherlands.)

Complexes of bi- and polydentate ammines

There has been intense study of the complexes of bi- and polydentate ammines since the mid-1970s, driven by interest in the catalytic photodecomposition of water using the excited states of $Ru(bipy)_6^{n+}$ ($n = 2, 3$) and related systems (Figure 1.18) [5, 7, 8, 71].

The most important complexes are tris systems $Ru(L\text{–}L)_3^{2+}$, traditionally prepared by fusing $RuCl_3$ with the molten ligand (L–L, e.g. phen, bipy). The ruthenium(II) compounds can be oxidized to the ruthenium(III) analogues by various chemical oxidizing agents (e.g. Ce^{4+}, PbO_2), though the products are somewhat unstable. X-ray diffraction shows the complexions to have approximately D_3 symmetry (the highest possible for an $M(chelate)_3$ system). Ru–N bond lengths in $[Ru(bipy)_3]^{n+}(PF_6)_n$ are 2.053 Å ($n = 2$) and 2.057 Å ($n = 3$) with N–Ru–N 'bite' angles of *c.* 77°. The relatively short Ru–N bonds, compared with the ammines, suggest some π-bonding [72]. These cations exist in enantionmeric forms, of course; $Ru(bipy)_3^{2+}$ was first resolved by Burstall (1936) and $Ru(bipy)_3^{3+}$ by Dwyer (1949).

The virtual identity of the Ru–N bonds and coordination geometries in the ruthenium(II and III) complexes is noteworthy and accounts for the

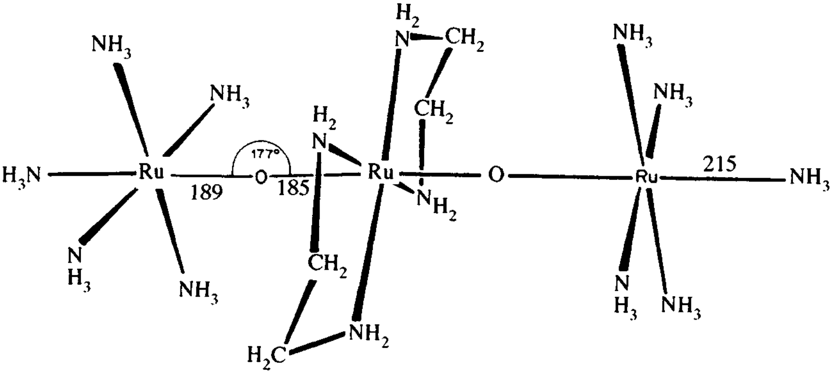

Figure 1.17 The structure of $[Ru_3O_2(en)_2(NH_3)_{10}]^{6+}$. (Reproduced with permission from S.A. Cotton and F.A. Hart, *The Heavy Transition Elements*, Macmillan Press Ltd, 1975, p. 62.)

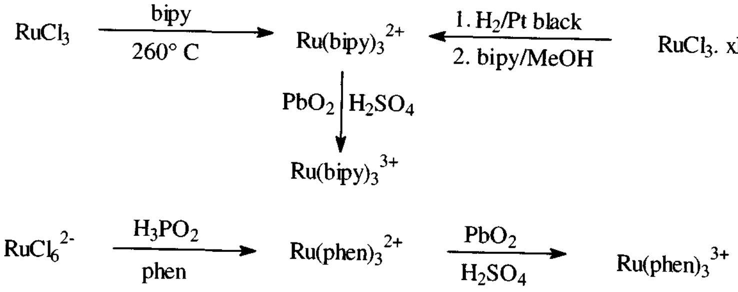

Figure 1.18 Syntheses of ruthenium tris complexes of 1,10-phenanthroline and 2,2′-bipyridyl.

rapidity of the electron exchange.

$$\mathrm{Ru(bipy)_3^{2+} + Ru'(bipy)_3^{3+} \rightarrow Ru(bipy)_3^{3+} + Ru'(bipy)_3^{2+}}$$

for which $K = 4.2 \times 10^8\ \mathrm{M^{-1}\ s^{-1}}$ as virtually no molecular reorganization is needed on electron transfer [72b].

Mixed complexes $[\mathrm{Ru(bipy)_2L}](\mathrm{ClO_4})_2$ (L = phen, 5-methyl(phen)) have virtually identical Ru–N (phen) and Ru–N (bipy) distances.

The UV–visible spectrum of $\mathrm{Ru(bipy)_3^{2+}}$ has a strong absorption at 454 nm ($E = 14\,600$) owing to a $t_{2g} \rightarrow \pi^*$ charge-transfer transition. This triplet-state excited complex $^*\mathrm{Ru(bipy)_3^{2+}}$ can lose an electron by luminescence or by donating it to a suitable acceptor (quencher) producing ground-state $\mathrm{Ru(bipy)_3^{3+}}$, a very strongly oxidizing species

$$\mathrm{Ru(bipy)_3^{3+} + e^- \rightarrow Ru(bipy)_3^{2+}} \qquad E^\ominus = +1.26\,\mathrm{V}$$

capable of oxidizing water or $\mathrm{OH^-}$ to $\mathrm{O_2}$ (it may be germane to this that hydrated $\mathrm{Ru(L{-}L)_3^{3+}}$ salts are less stable than the anhydrous salts in general).

The emission can also be quenched by electron donors causing reduction of the ruthenium complex ion.

Although $\mathrm{Ru(bipy)_3^{2+}}$ alone will not split water into hydrogen and oxygen, it has been accomplished with $\mathrm{Ru(bipy)_3^{2+}}$ using various catalysts or radical carriers. Perhaps the most studied system for the photoreduction of water involves using methyl viologen as the quencher, EDTA as an electron donor (decomposed in the reaction) and colloidal platinum as a redox catalyst (Figure 1.19).

Systems for the photo-oxidation of water have used $\mathrm{Ru(bipy)_3^{2+}}$ with $[\mathrm{Co(NH_3)_5Cl}]^{2+}$ as the electron donor and $\mathrm{RuO_2}$ as catalyst.

Besides the tris ruthenium complexes, other complexes can be made (Figure 1.20), while ethylenediamine (en) complexes exist:

$$\mathrm{RuCl_3} \xrightarrow[\text{Zn dust}]{\text{en}} \mathrm{Ru(en)_3^{2+}ZnCl_4^{2-}} \xrightarrow{\mathrm{Ag^+}} \mathrm{Ru(en)_3^{3+}}$$

The optical isomers can be resolved again, for example with one enantiomer of $\mathrm{Rh(C_2O_4)_3^{3+}}$ [73]. Again there is a contraction in Ru–N on passing from

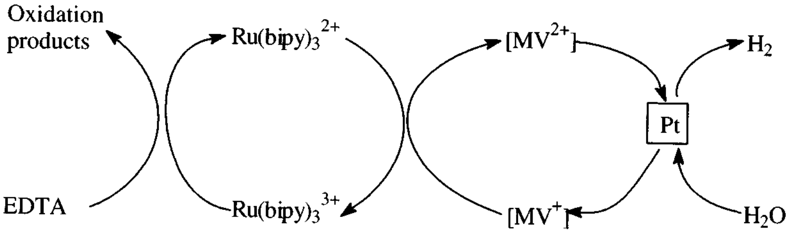

Figure 1.19 Cycles involved in a ruthenium-based system for the reduction of water.

the 2+ ion (2.132 Å) to the 3+ ion (2.11 Å) [74]

$$Ru(C_2O_4)_3^{3-} \xrightarrow[2.\,HCl]{1.\,en} cis\text{-}[Ru(en)_2Cl_2]^+$$

$$\xrightarrow[\text{ethyleneglycol}]{60°C,\ 1\ min} trans\text{-}[Ru(en)_2Cl_2]^+$$

$$RuCl_5(H_2O)^{2-} \xrightarrow{en} trans\text{-}[Ru(en)_2Cl_2]^+$$

The *trans*-dichloro complex can be converted into an unusual complex with bound azide and dinitrogen (Figure 1.21) with linear Ru—N≡N, as in other dinitrogen complexes (ν(N≡N) 2103 cm^{-1}) [75].

The *cis*-isomer can also be obtained (ν(N≡N) 2130 cm^{-1}, $\nu(N_3)$ 2050 cm^{-1}). On oxidation it loses both azide and dinitrogen

$$cis\text{-}[Ru(en)_2(N_2)(N_3)]^+ \xrightarrow{Ce^{4+}} 2.5\,mol\,N_2$$

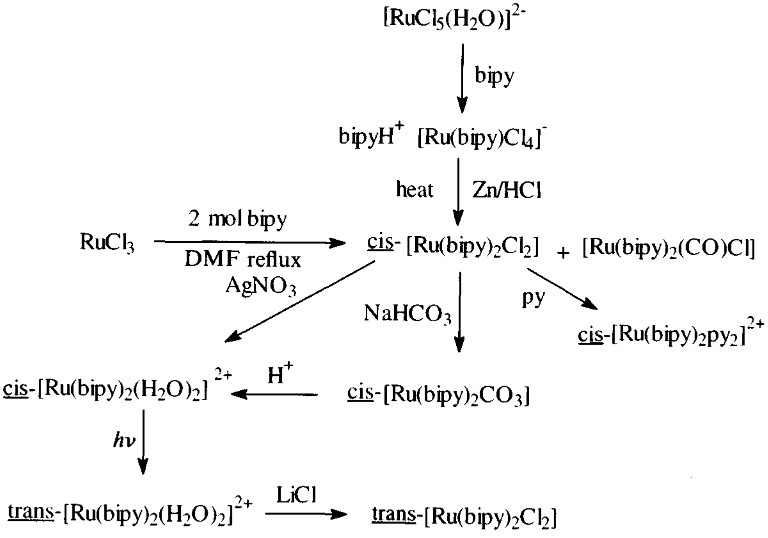

Figure 1.20 Syntheses of ruthenium 2,2′-bipyridyl complexes.

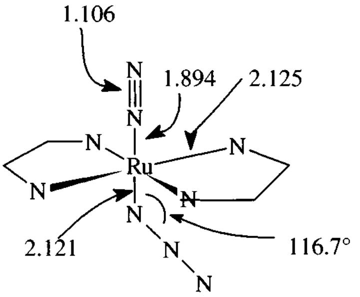

Figure 1.21 Bond lengths in $[Ru(en)_2(N_2)(N_3)]^+$.

The terdentate ligand terpyridyl affords a range of complexes: fusion of $RuCl_3$ with terpy gives $Ru(terpy)_2^{2+}$, while refluxing $RuCl_3$ with an ethanolic solution of the ligand yields $RuCl_3$(terpy). Both of these are doubtless 6-coordinate. Ruthenium bis(terpyridine) complexes are also attracting attention as photosensitizers [76].

mer-[Ru(terpy)Cl_3] is an active cystostatic agent in leukaemia cells, forming interstrand cross-links in DNA [77].

1.8.2 Tertiary phosphine complexes

Tertiary phosphine complexes have been studied intensively since the 1960s. The bulk of the work has been with phosphines, but corresponding arsine complexes are broadly similar.

The reactions of monodentate phosphines have been studied in most depth [58b]. The products of the reaction of a tertiary phosphine with $RuCl_3$ depends on both the phosphine concerned (size and reducing power) and upon the reaction conditions (Figure 1.22).

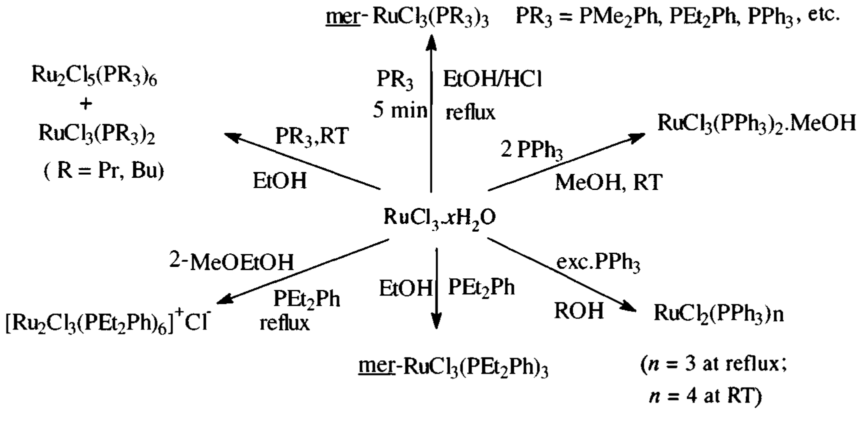

Figure 1.22 Syntheses of tertiary phosphine complexes of ruthenium.

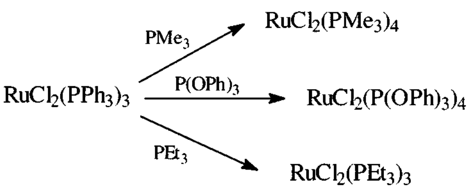

Figure 1.23 Syntheses of complexes of other tertiary phosphines by metathesis of $RuCl_2(PPh_3)_3$.

Initial reaction of $RuCl_3.xH_2O$ with the tertiary phosphine in ethanol/concentrated HCl leads to *mer*-$RuCl_3(PR_3)_3$ or $[RuCl_3(PR_3)_2]$. (Omission of the HCl can lead to faster reduction and the formation of carbonyl complexes, particularly in solvents like 2-methoxyethanol.) Extended reaction times or using excess phosphine lead to reduction to $[Ru_2Cl_3(PR_3)_6]Cl$ or mixed-valence complexes, $Ru_2Cl_5(PR_3)_6$ being typical. Triphenylphosphine, the most studied phosphine (on account of its ease of handling as an air-stable solid) is atypical in forming monomers $RuCl_2(PPh_3)_3$, which are conveniently metathesized into $RuCl_2(PR_3)_n$ with other tertiary phosphines in hexane (use of ethanol or dichloromethane and refluxing leads to the ionic dimer $Ru_2Cl_3(PR_3)_6^+Cl^-$) (Figure 1.23). Alkyl phosphines in general tend to be weaker complexing agents and are more strongly reducing.

$RuCl_2(PPh_3)_3$ has been studied in considerable detail [79]. Synthetic routes to it and some of its reactions are shown in Figure 1.24. It is important as a source of $RuHCl(PPh_3)_3$, a very active hydrogenation catalyst specific for alk-1-enes. Unlike $RhCl(PPh_3)_3$, it is not active in hydroformylation. $RuCl_2(PPh_3)_3$ has a distorted square pyramidal structure (Figure 1.25) with ruthenium in some 0.45 Å above the basal plane [80]. The sixth co-ordination position is blocked by an *ortho*-hydrogen from a phenyl ring (Ru–H 2.59 Å). $RuCl_2(PPh_3)_4$ is probably $RuCl_2(PPh_3)_3PPh_3$ since NMR shows that the fourth phosphine is certainly not bound in solution; the

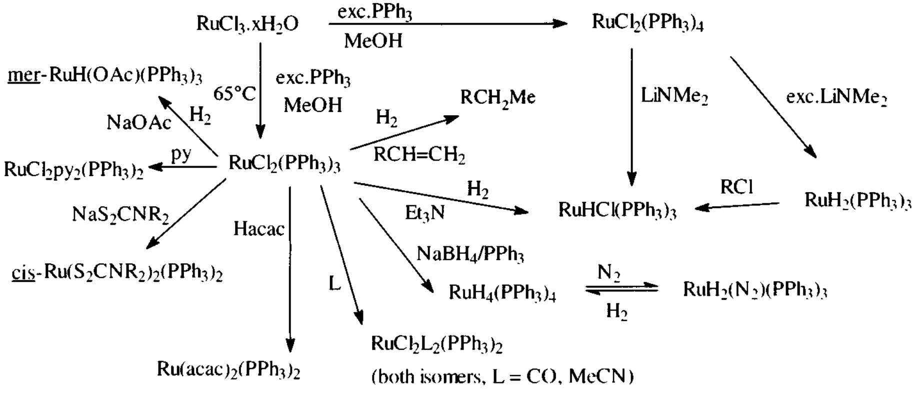

Figure 1.24 Reactions of $RuCl_2(PPh_3)_3$.

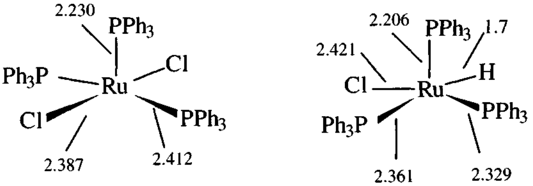

Figure 1.25 A comparison of bond lengths in the complexes $RuCl_2(PPh_3)_3$ and $RuHCl(PPh_3)_3$.

non-existence of the 18-electron 6-coordinate complex is probably a result of steric repulsion between the tertiary phosphine ligands, while 16-electron $RuCl_2(PPh_3)_3$ dissociates in solution affording dimeric $[Cl(PPh_3)_2Ru(\mu\text{-}Cl)_2Ru(PPh_3)_2Cl]$ (NMR evidence at low temperatures). $RuCl_2(SbPh_3)_4$ does exist (X-ray [81]).

Therefore, one reaction frequently observed involves displacement of a tertiary phosphine, either wholly (e.g. PMe_3 in hexane to form $RuCl_2(PMe_3)_4$) or partly (e.g. with pyridine $RuCl_2py_2(PPh_3)_2$ being formed); both are 18-electron species. The former reaction is a very convenient way of making monomeric alkyl phosphine complexes of ruthenium(II) as already noted [78]. Reactions with nitriles and CO are solvent and temperature dependent, with *cis*- and *trans*-isomers of $RuCl_2L_2(PPh_3)_2$ obtained depending upon conditions.

A second type of reaction of $RuCl_2(PPh_3)_3$ involves substitution of the chloride ligands; this can be achieved using hydride, to give $RuH_2(PPh_3)_4$ (via $RuHCl(PPh_3)_3$), and other representative ligands such as dithiocarbamates and diketonates. As mentioned above, $RuCl_2(PPh_3)_3$ is a hydrogenation catalyst [82] (doubtless $RuHCl(PPh_3)_3$ is the active species (Figure 1.26)) where initially a π-alkene complex is formed, followed by hydride transfer [82] to give an alkyl.

$RuHCl(PPh_3)_3$ itself has a distorted square pyramidal structure (Figure 1.25) but the hydride ligand has less steric effect and the structure has been described as a capped tetrahedron (Ru–P 1.7 Å, Ru–Cl 2.421 Å, Ru–P 2.206–2.329 Å; ν(Ru–H) 2020 cm^{-1}) [83]. The Ru–Cl stretching frequency in the IR spectrum of $RuHCl(PPh_3)_3$ is at 282 cm^{-1}, compared with 315 cm^{-1} in $RuCl_2(PPh_3)_3$, the weakening reflecting the *trans*-influence of hydride.

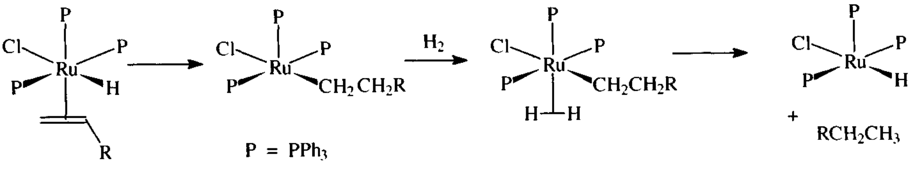

Figure 1.26 Abbreviated mechanism for the catalytic hydrogenation of a terminal alkene using $RuHCl(PPh_3)_3$.

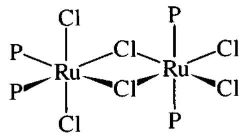

$Ru_2Cl_6(PBu_3)_4$

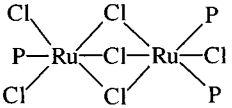

$Ru_2Cl_6(PBu_3)_3$

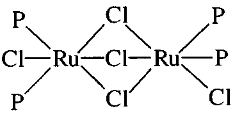

$Ru_2Cl_5(PBu_3)_4$
(brown form)

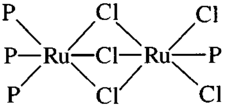

$Ru_2Cl_5(PBu_3)_4$
(green form)

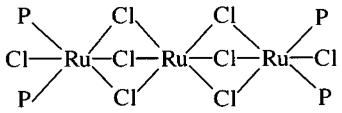

$Ru_3Cl_8(PBu_3)_4$

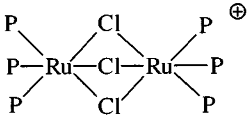

$Ru_2Cl_3(PBu_3)_6^+$

Figure 1.27 Ruthenium complexes of tributylphosphine ($P = PBu^n_3$).

Tributylphosphine complexes have been investigated in detail [84] and have revealed a bewildering variety of complexes. Reaction of $RuCl_3$ with tributylphosphine on brief reflux in ethanol/concentrated HCl gives monomeric *mer*-$RuCl_3(PBu_3)_3$. Otherwise di- and trimeric species are obtained. Reaction with the phosphine in ethanol at room temperature affords two kinds of diruthenium(III, III) dimers: edge-shared $Ru_2Cl_6(PBu_3)_4$ and face-shared $Ru_2Cl_6(PBu_3)_3$ (Figure 1.27).

The former has a long Ru–Ru distance (3.733 Å) while in the latter the rutheniums are drawn closer (3.176 Å). In addition, reduction yields two isomers of $Ru_2Cl_5(PBu_3)_4$ and $Ru_3Cl_8(PBu_3)_4$, as well as the 'ionic' $Ru_3Cl_6(PBu_3)_6^+[RuCl_4(PBu_3)_2]^-$, all of which contain both ruthenium(II) and ruthenium(III). The classic diruthenium(II, III) cation $[Ru_2Cl_3(PBu_3)_6]^+$ has also been isolated.

In general, the dimers have three chlorine bridges, and $Ru_3Cl_8(PBu_3)_4$ resembles the mixed-valence chloro complex $Ru_3Cl_{12}^{4-}$. A similar, but less extensively studied, pattern of behaviour has been found with other alkyl phosphines.

The mixed valence compounds only have one unpaired electron per dimer unit. Their Ru–Ru distances vary from 2.854 Å in $Ru_3Cl_8(PBu_3)_4$ through 3.115 Å in brown $Ru_2Cl_5(PBu_3)_4$ to 3.279 Å in green $Ru_2Cl_5(PBu_3)_4$ with a move to 'trapped' valences. In the $Ru_2Cl_6(PR_3)_4$ dimers, the two ruthenium sites behave independently; the ESR spectrum of $Ru_2Cl_6(PEt_3)_4$ gives separate signals, one characterized by $g_\perp = 2.49$ and $g_\parallel = 1.65$, the second having $g_1 = 2.31$, $g_2 = 2.06$, $g_3 = 1.80$ (Figure 1.28).

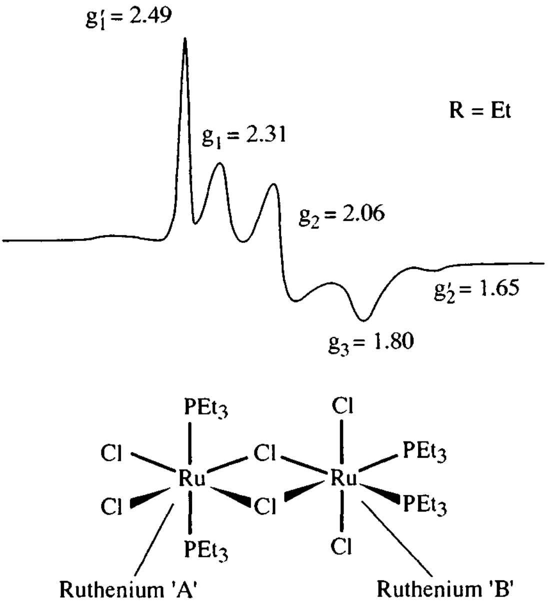

Figure 1.28 ESR spectra of $Ru_2Cl_6(PEt_3)_4$. (Reprinted with permission from *Inorg. Chem.*, 1991, **30**, 4393. Copyright (1991) American Chemical Society.)

The axial resonance is assigned to ruthenium 'A' with its D_{4h} local symmetry (compare $g_{\perp} = 2.51$, $g_{\parallel} = 1.64$ in *trans*-$RuCl_4(PEt_3)_2^-$) while the 'rhombic' signal is assigned to ruthenium 'B', where the 'local' symmetry is D_{2h} and three different components of the g-tensor are expected.

Complexes of bidentate phosphines

The bidentate phosphine complexes were among the earliest ruthenium phosphine complexes to be made [85]; often displacement is a convenient route:

$$Ru_2Cl_3(PR_3)_6^+ \xrightarrow{\text{diphos}} cis\text{-}RuCl_2(\text{diphos})_2$$

$$\xrightarrow[\text{THF}]{\text{LiAlH}_4} trans\text{-}RuHCl(\text{diphos})_2$$

$$\xrightarrow[\text{C}_6\text{H}_6]{\text{LiAlH}_4} trans\text{-}RuH_2(\text{diphos})_2$$

$$RuCl_3.xH_2O \xrightarrow[\text{EtOH}]{\text{diphos}} trans\text{-}RuCl_2(\text{diphos})_2$$

$$\xrightarrow{\text{liq. K}} cis\text{-}RuH_2(\text{diphos})_2$$

$$RuCl_2(PPh_3)_3 \xrightarrow[\text{Me}_2\text{CO}]{\text{diphos}} trans\text{-}RuCl_2(\text{diphos})_2$$

(Diphos typically is $Ph_2PCH_2CH_2PPh_2$.)

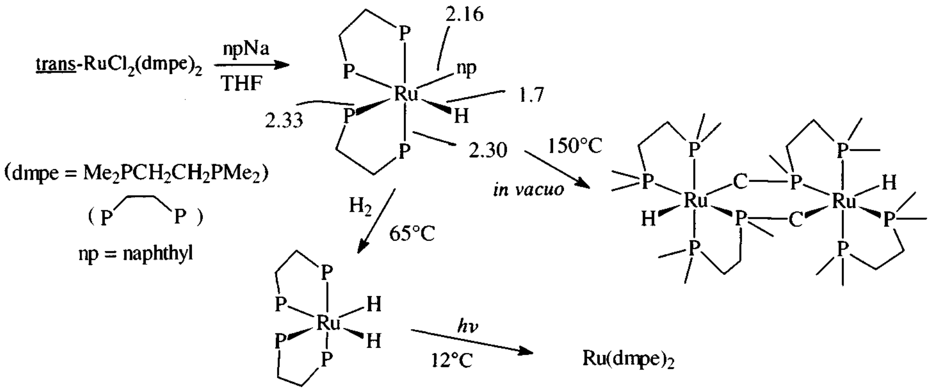

Figure 1.29 Synthesis of ruthenium complexes of the chelating ligand bis(dimethylphosphino)-ethane (dmpe).

The halide groups can be replaced by other substituents like hydride or alkyl [86]. When the naphthyl (np) RuHnp(dmpe)$_2$ is heated, the ligand undergoes an internal metallation to afford a dimer [87] (it was originally believed to be a monomer), though Ru(dmpe)$_2$ has been isolated by photolysis of its dihydride, in matrixes at 12 K (Figure 1.29) [88].

Five coordination is not unknown (Figure 1.30) [89].

Hydridophosphine complexes

All the compounds of the type $RuH_2(PR_3)_4$ seem to be classical hydrides

$$RuCl_3.xH_2O \xrightarrow[NaBH_4/EtOH]{PPh_3} trans\text{-}RuH_2(PPh_3)_4$$

$$Ru_2(PMePh_2)_6Cl_3^+ \xrightarrow[H_2(PMePh)_2]{N_2H_2} cis\text{-}RuH_2(PMePh_2)_4$$

Both *cis*- and *trans*-structures are possible: $RuH_2(PMe_3)_4$ is *cis* (Ru–H 1.507, 1.659 Å, Ru–P 2.276–2.306 Å) [90] while spectra show that $RuH_2(PF_3)_4$ and others have this configuration. $RuH_2[PPh(OEt)_2]_4$ is definitely *trans* (X-ray) with Ru–H 1.6 Å, Ru–P 2.272 Å. Many diphosphines form dihydrides. Ru(dmpe)$_2$H$_2$ has been a useful starting material for the synthesis of thiolate complexes [91] such as *trans*-Ru(SPh)$_2$(dmpe)$_2$.

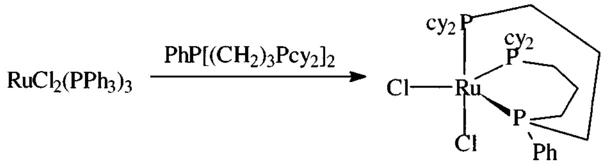

Figure 1.30 A 5-coordinate complex of a tridentate phosphine.

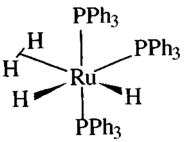

Figure 1.31 The probable structure of $RuH_4(PPh_3)_3$.

Many of the $RuH_4(PR_3)_3$ and $RuH_6(PR_3)_2$ systems have, however, η^2-dihydrogen groups. Therefore, $RuH_4(PPh_3)_3$ prepared by:

$$RuCl_2(PPh_3)_3 \xrightarrow[C_6H_6/MeOH]{NaBH_4} RuH_4(PPh_3)_3$$

is believed to have the structure shown in Figure 1.31, like $Fe(H)_2(\eta^2\text{-}H_2)(PEtPh_2)_3$ (confirmed by neutron diffraction) while the osmium analogues are 'classical' hydrides.

MO calculations on $MH_4(PPh_3)_3$ indicate that the dihydrogen complex is most stable for iron and ruthenium, while the osmium compound is a classical hydride, owing to relativistic effects [92]. The IR spectrum of $RuH_4(PPh_3)_3$ shows an Ru–H absorption at $1950\,cm^{-1}$ (shifting to $1400\,cm^{-1}$ on deuteration): no $Ru\text{–}H_2$ absorption was seen and a low-frequency NMR resonance was seen at approximately 7.1 ppm. Relaxation time measurements, however, indicate a short t_1 (38 ms) characteristic of η^2-bound hydrogen [93]. The dihydrogen ligand is displaced by N_2, forming $Ru(H)_2N_2(PPh_3)_3$ and, reversibly, by PPh_3 to form $RuH_2(PPh_3)_4$. $RuH_6(Pcy_3)_2$ is similarly $Ru(H)_2(H_2)_2(Pcy_3)_2$.

Cationic hydrides have been important in studying dihydrogen complexes [94]

$$trans\text{-}RuHCl(depe)_2 \xrightarrow[NaBPh_4/Me_2CO]{H_2\,(1\,atm)} trans\text{-}RuH(H_2)(depe)_2^+\,BPh_4^-$$

(depe = $Et_2PC_2H_4PEt_2$). In this reaction, the labile chloride is displaced. Protonation can be employed:

$$MH_2(PR_3)_4 \xrightarrow{HBF_4/Et_2O} [MH(H_2)(PR_3)_4]^+$$

(PR = $P(OEt)_3$, $PPh(OEt)_2$, etc.; M = Fe, Ru, Os).

Study of the high-field resonances in the ^1H NMR spectrum at 220 K of $RuH(H_2)(depe)_2^+$ shows a broad singlet (−6.4 ppm) owing to bound H_2 with a very short t_1 (11 ms) and a resonance with a much longer relaxation time (270 ms) at −11.3 ppm associated with the terminal hydride. A large H–D coupling constant is another way to show the presence of a $\eta^2\text{-}H_2$ ligand: J(H–D) is 32 Hz in $RuD(HD)(depe)_2$ compared with 43.2 Hz in HD gas, showing the persistence of the H–D bond.

A few anionic hydrides exist, the best characterized being $RuH_3(PPh_3)_3^-$

$$RuHCl(PPh_3)_3 \xrightarrow{2\,mol\,KBHBu^s_3} RuH_3(PPh_3)_3^-$$

The crystal structure of the K(18-crown-6) salt shows a *fac*-octahedral structure (Ru–H 1.59–1.71 Å, Ru–P 2.312–2.331 Å) with a large distortion from regular octahedral geometry (H–Ru–H 70–88°; P–Ru–P 102–111°) owing to the disparate steric demands of the hydride and tertiary phosphine ligands [95].

In general, ruthenium forms more dihydrogen complexes than osmium. When a hydrogen molecule joins to a metal, there is a balance between the energy lost when the H–H bond is broken and the energy gained in forming M–H bonds; osmium forms stronger 'classical' M–H bonds so is less likely to form dihydrogen complexes [93].

1.8.3 Carboxylate complexes

Ruthenium forms four significant families of carboxylate complexes.

Class 1

Refluxing $RuCl_3.xH_2O$ with ethanoic acid/ethanoic anhydride mixtures, particularly in the presence of LiCl, gives a green solution and crystals of the dimeric $Ru_2(OAc)_4Cl$, an unusual 'mixed-valence' compound with a 'lantern' structure (Figure 1.32) where the dimer units are linked into continuous chains by axial bridging chlorides (the bridges are sometimes kinked, sometimes linear) [96].

The complexes are 1 : 1 electrolytes in solution. Other such complexes can be made by a similar route or by halide (or carboxylate) exchange. The first monomeric system $Ru_2Cl(O_2C.C_4H_4N)_4$ (thf), where the ruthenium at one end of the 'lantern' is bound to a thf and the other to a chloride, has recently been made [97]. $[Ru_2Cl(O_2CBu^t)_4(H_2O)]$ and $[Ru_2Cl(O_2CPr^i)_4(thf)]$ are also monomeric [98].

These mixed-valence compounds have magnetic moments around $4\,\mu_B$, indicating an $S = 3/2$ (quartet) ground state, in keeping with their ESR spectra, which resemble those of Cr^{3+} compounds with a big zero-field splitting ($g_\perp = 4$, $g = 2$) [99].

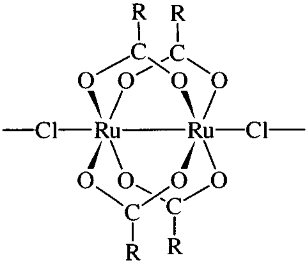

Figure 1.32 The 'lantern' structure adopted by $Ru_2(OAc)_4Cl$ and other similar compounds.

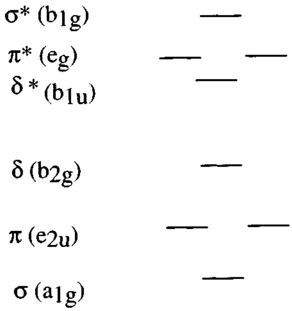

Figure 1.33 A possible orbital sequence for dinuclear ruthenium carboxylates.

The analogous diruthenium(II, II) compounds can be made starting from the blue solution of reduced $RuCl_3$ in ethanol (section 1.3.5) on extended refluxing with sodium acetate, whereupon the solvate $Ru_2(OAc)_4(MeOH)_2$ separates. This loses methanol readily on drying; the resulting anhydrous acetate will form weak adducts $Ru_2(OAc)_4L_2$ (L, e.g. H_2O, thf). These are all paramagnetic with two unpaired electrons [100].

A bonding scheme for the dinuclear carboxylates can be constructed as follows [101]. Assuming the Ru–Ru axis to be the z axis, each ruthenium uses its 5_{px}, 5_{py}, 5s and $4d_{x^2-y^2}$ orbitals to form four σ-bonds to the carboxylate oxygens (lying along the x and y axes). The $4d_{z^2}$ orbitals from each ruthenium form an Ru–Ru σ-bond, d_{xz} and d_{yz} overlap to form two Ru–Ru π-bonds and the d_{xy} orbitals form a σ-bond, shown in an energy level diagram like Figure 1.33. (The p_z orbitals are available to bond to the ligands bridging dimers or in terminal positions.)

In $Ru_2(OAc)_4Cl$, one ruthenium(II) supplies six electrons, the ruthenium(III) five electrons, giving rise to a $\sigma^2\pi^4\delta^2\pi^{*2}\delta^{*1}$ configuration (provided δ^* and π^* are close enough together) with three unpaired electrons. A diruthenium(II,II) dimer would have the configuration $\sigma^2\pi^4\delta^2\pi^{*3}\delta^{*1}$ with two unpaired electrons. (It should be recognized that the ordering of the orbitals can be changed by altering the terminal/bridging ligands.)

Apart from carboxylates, other groups such as carbonate and triazenate (R–NNN–R; R = Ph, p-tolyl, etc.) can fulfil the role of bridging ligands in the 'lantern' [102].

$$Ru_2(Oac)_4Cl \xrightarrow[\text{(aq.)}]{Na_2CO_3} Na_3[Ru_2(CO_3)_4].6H_2O$$

Class 2

The green solution mentioned in class 1 resulting from the reaction of $RuCl_3$ with $RCOOH/(RCO)_2O$ mixtures contains a trinuclear species with an $Ru_3O(OAc)_6$ core. Refluxing $RuCl_3$ with ethanoic acid and sodium acetate

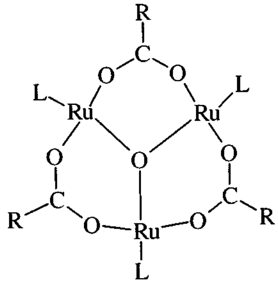

Figure 1.34 The structure of trinuclear oxo-centred ruthenium carboxylates. For clarity, only one of each pair of bridging carboxylates is shown.

in ethanol gives the complex $[Ru_3O(OAc)_6(H_2O)_3]OAc$ in which all the ruthenium is present in the +3 state (Figure 1.34).

This is paramagnetic (one unpaired electron: $\mu = 1.77\,\mu_B$). A similar benzoate $[Ru_3O(OCOPh)_6py_3]PF_6$ has been characterized by X-ray diffraction (the central Ru–O distance is short, at 1.935 Å). The structure of $[Ru_3O(OAc)_6(H_2O)_3]ClO_4$ is similar [103].

The aqua ion $[Ru_3O(OAc)_6(H_2O)_3]^+$ undergoes a one-electron reduction to form the pale green neutral species; either of these reacts with PPh_3 to form the neutral diamagnetic complex $Ru_3O(OAc)_6(PPh_3)_3$ (which cannot be oxidized) that formally contains one ruthenium(II) and two ruthenium(III) centres [104]. The neutral aqua complex will undergo a further two-electron reduction to give a yellow air-sensitive species thought to be $Ru_3(OAc)_6(H_2O)_3$, a ruthenium molecule lacking the central oxygen.

The bonding in these Ru_3O carboxylates can be explained by the usual MO scheme for these systems. A σ-bonding framework involves using six orbitals from each ruthenium (one s, three p, two d) to form bonds to the central O, four carboxylate oxygens and the terminal ligand (PPh_3H_2O, etc.).

There are, therefore, three unused d orbitals per ruthenium one of which is used to form a π-bond with an unused oxygen p orbital (it has already used the 2s and 2p orbitals in the σ-bonds to the three rutheniums).

Complexes $[Ru_3O(OAc)_6L_3]^{n+}$ ($L = H_2O$, PPh_3) have been found to be catalysts for the oxidation of primary and secondary alcohols to aldehydes and ketones under fairly mild conditions (65°C, 3 atm O_2) with high catalytic turnovers [104].

Class 3

Dinuclear complexes with an oxo-bridge have latterly achieved better characterization. When $Ru_3O(OAc)_6(PPh_3)_3$ is reduced by hydrogen on heating, a dinuclear species is obtained that on oxidative workup affords diamagnetic oxo-bridged $[Ru_2O(OAc)_4(PPh_3)_2]$ (Figure 1.35) [104c, 105].

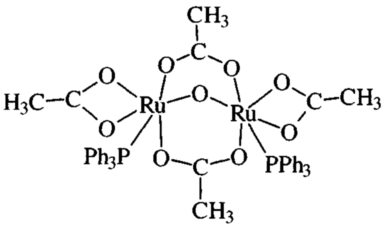

Figure 1.35 The structure of the oxo-bridged dimer $Ru_2O(OAc)_4(PPh_3)_2$.

Class 4

Some important mononuclear complexes exist such as *mer*-$RuH(OAc)(PPh_3)_3$, a very efficient catalyst for the selective hydrogenation of alk-1-enes (Figure 1.36).

It has 6-coordination with a chelating acetate [106] and may be converted (reversibly) into $Ru(OAc)_2(PPh_3)_3$, which has the *fac*-configuration with one monodentate and one bidentate acetate. It is fluxional at room temperature but at −70°C the phosphines are non-equivalent on the NMR timescale [107].

1.8.4 Sulphide and sulphoxide complexes

Sulphide and sulphoxide complexes have been extensively studied since *cis*-$RuCl_2(DMSO)_4$ (DMSO, dimethyl sulphoxide, $(Me)_2SO$) was found to have anti-tumour properties and to be a precessor for radiosensitizing agents. Such complexes can act as catalysts for the oxidation of sulphides with molecular oxygen.

The best characterized complexes are those of ruthenium(II); it is likely that several reports of ruthenium(III) complexes have, until very recently,

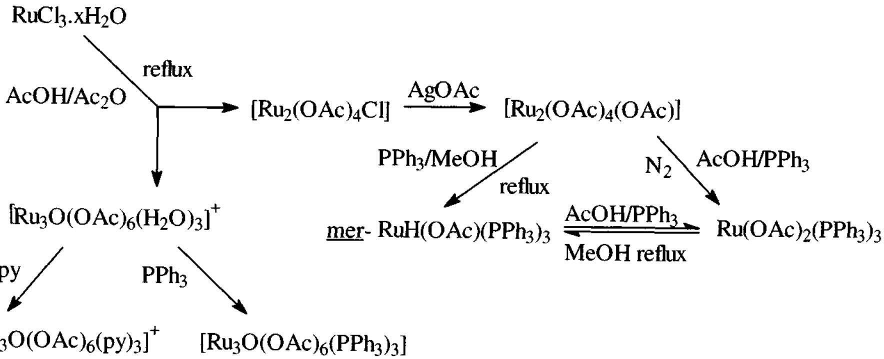

Figure 1.36 Syntheses of ruthenium carboxylate complexes.

been inaccurately describing either ruthenium(II) complexes or ruthenium(III) sulphide complexes formed by redox reaction.

Apart from DMSO complexes, others including those with tetramethylene sulphoxide have been increasingly examined, but the account here focuses on DMSO.

The best understood compounds are *cis*- and *trans*-$RuX_2(DMSO)_4$ (X = Cl, Br). The *trans*-isomers are thermodynamically less stable and isomerize in DMSO solution to the *cis*-isomer, with first-order kinetics, probably via a dissociative mechanism. The reverse process, *cis* to *trans*, is catalysed by light. Syntheses for these and other DMSO complexes are shown in Figure 1.37 [108].

DMSO is an ambidentate ligand, capable of coordinating via either S or O. The *cis*-isomers have three S-bound and one O-bound ligand while in the *trans*-isomers all are S-bonded; IR spectra show the presence of both S- and O-bound DMSO in the *cis*-isomers with absorption owing to $\nu(S{-}O)$ around $1100\,cm^{-1}$ (S-bonded) and $930\,cm^{-1}$ (O-bonded), while the *trans*-isomers only have $\nu(S{-}O)$ around $1100\,cm^{-1}$ (Figure 1.38).

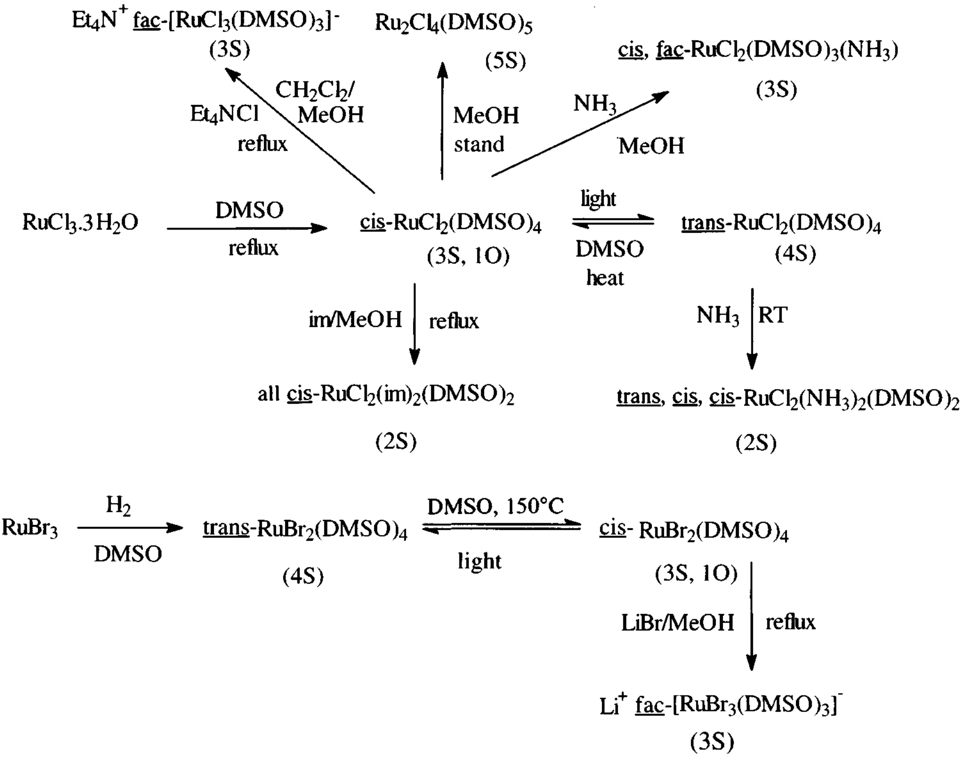

Figure 1.37 Syntheses of ruthenium complexes of dimethylsulphoxide (DMSO).

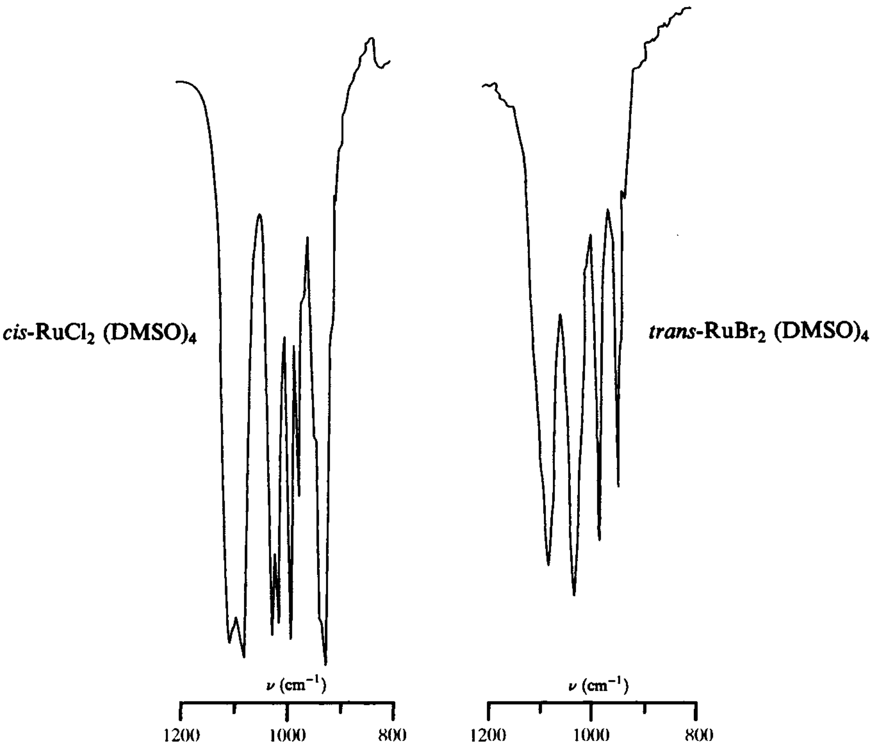

Figure 1.38 IR spectra of DMSO complexes of ruthenium. (Reprinted with permission from *Inorg. Chem.*, 1984, **23**, 157. Copyright (1984) American Chemical Society.)

Ru–S bond lengths in the *cis*- and *trans*-isomers (Figure 1.39) indicate an order of *trans*-influence O < Cl < Br < S.

The O-bonded DMSO ligand in the *cis*-isomers is rather more labile than the S-bonded DMSO and, therefore, it can be replaced by NH_3 or imidazole [109]. Some syntheses using *cis*-$RuCl_2(DMSO)_4$ are shown in Figure 1.40.

When *cis*-$RuCl_2(DMSO)_4$ is stirred in methanol containing traces of water (to catalyse the formation of intermediate aqua species) $Ru_2Cl_4(DMSO)_5$ is formed; this has the unsymmetrical structure $(DMSO)_2ClRu(\mu\text{-}Cl)_3Ru(DMSO)_3$ based on face-sharing octahedra [110].

Ruthenium(III) sulphoxide complexes were less well authenticated until recently [111]; some syntheses are found in Figure 1.41.

Again both S- and O-bonded sulphoxides are found. *mer*-$[RuCl_3(Ph_2SO)_3]$ has one S-bonded sulphoxide and two O-bonded sulphoxides (one *trans* to Cl, one *trans* to S) [112]. The imidazole-substituted complexes are being studied as possible radiosensitizers and for anti-tumour activity.

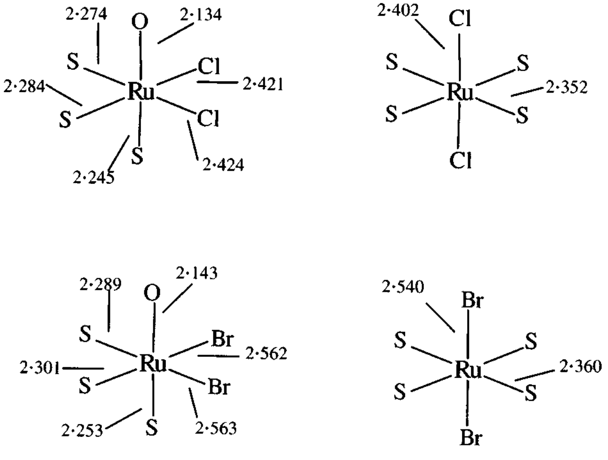

Figure 1.39 Bond lengths in the coordination spheres of *cis*- and *trans*-$[RuX_2(DMSO)_4]$ (X = Cl, Br).

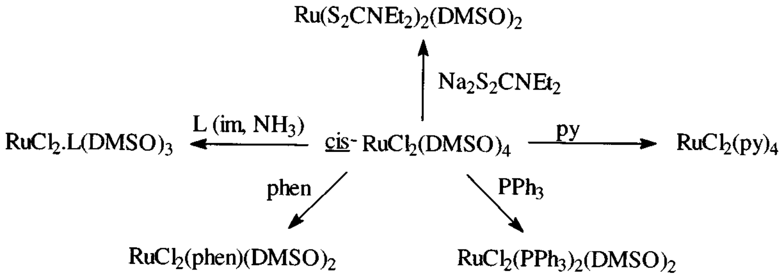

Figure 1.40 Syntheses using $RuCl_2(DMSO)_4$.

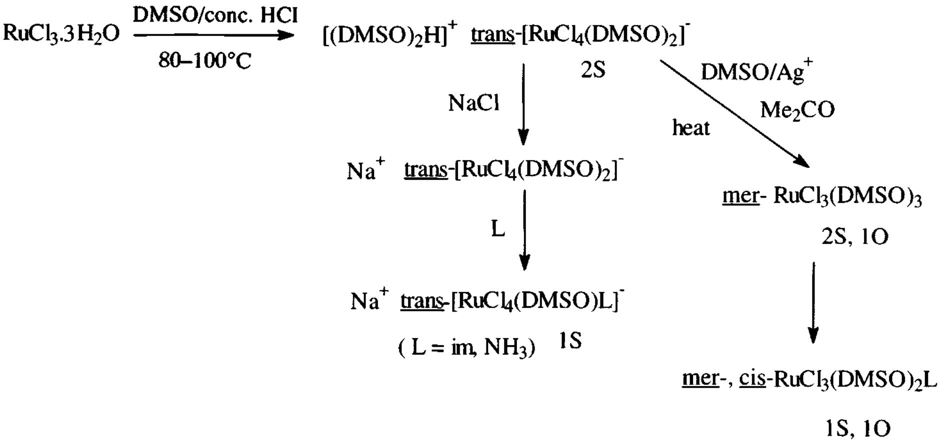

Figure 1.41 Ruthenium(III) sulphoxide complexes.

Carbonyl derivatives of ruthenium sulphoxide complexes have been made [113].

$$cis\text{-}RuCl_2(DMSO)_4 \xrightarrow[MeOH]{CO} RuCl_2(CO)_n(DMSO)_{4-n} \qquad (n = 1,2,3)$$

$$mer\text{-}RuCl_3(DMSO)_3 \xrightarrow[CH_2Cl_2]{CO} mer\text{-}RuCl_3(DMSO)_2(CO)$$

$RuCl_3(DMSO)_3$ reacts with sulphides to form mixed sulphide/sulphoxide complexes that are catalysts for oxidation of thioethers to sulphoxides [114a]:

$$mer\text{-}RuCl_3(DMSO)_3 \xrightarrow{p\text{-}MeC_6H_4SMe} mer\text{-}RuCl_3(DMSO)_2(p\text{-}MeC_6H_4SMe)$$

Alkyl sulphide complexes can be synthesized from $RuCl_3$ and R_2S in ethanol at reflux [114b,c]:

$$RuCl_3.xH_2O \xrightarrow[EtOH]{R_2S} mer\text{-}RuCl_3(R_2S)_3$$

($R_2S = Me_2S$, PhSMe, PhSBu, etc.).

Another method involves refluxing acidified solutions of $RuCl_3$ in dimethylsulphoxide for extended periods

$$RuCl_3.xH_2O \xrightarrow[\text{conc. HCl, reflux}]{DMSO} mer\text{-}RuCl_3(Me_2S)_3$$

The structure of the last has been confirmed by X-ray diffraction.

1.8.5 Nitrosyl complexes

Ruthenium probably forms more nitrosyl complexes [115] than any other metal. Many are octahedral $Ru(NO)X_5$ systems, where X_5 can represent a combination of neutral and anionic ligands; these contain a linear (or very nearly) Ru–NO grouping and are regarded as complexes of ruthenium(II). They are often referred to as $\{Ru(NO)\}^6$ systems.

Two types of NO coordination to ruthenium are known: linear Ru–N–O ~180° and bent, Ru–N–O ~120°. Since NO^+ is isoelectronic with CO, linear Ru–N–O bonding is generally treated as coordination of NO^+, with bent coordination corresponding to NO^-; thus, in the former an electron has initially been donated from NO to Ru, as well as the donation of the lone pair, whereas in the latter an electron is donated from the ruthenium to NO (making it NO^-) followed by donation of the lone pair from N. Though an oversimplification, this view allows a rationale of metal–nitrogen bond lengths, as with the $Ru\text{–}NO^+$ model π-donation is important and a shorter Ru–NO bond is predicted – and, in fact, observed.

Diagnosing the mode of NO coordination, without resort to crystallographic study, can potentially be achieved using the position of ν(N–O) in the IR spectrum. Removing the π^*-electron from NO forming NO^+ strengthens the N–O bond, reflected in a change in ν(N–O) from 1877 cm^{-1} (NO) to 2200–2300 cm^{-1} (NO^+ salts). Coordination as NO^+ would involve stronger back-bonding than with NO^-, so that a higher frequency is expected for a linear arrangement; in fact a considerable overlap region exists. ^{15}N NMR spectra have, however, been utilized diagnostically, as bent nitrosyls give rise to resonances at much higher frequency.

A preparative entry to the area of nitrosyls is possible with the oligomeric $Ru(NO)X_3$ [116] (X = halogen) (Figure 1.42).

This will add halide ions or tertiary phosphines to give octahedral $Ru(NO)X_5^{2-}$ or $Ru(NO)X_3(PR_3)_2$, respectively, all of these having the linear Ru–N–O geometries characteristic of $\{Ru(NO)\}^6$ systems. The preference for octahedral coordination is such that in $Ru(NO)(S_2CNEt_2)_3$, one dithiocarbamate ligand is monodentate (Figure 1.43) [117].

The NO ligand can be supplied by nitric oxide itself, but there are many other sources such as nitrite, nitrate or nitric acid, nitrosonium salts or *N*-methyl-*N*-nitrosotoluene-*p*-sulphonamide (MNTS). The introduction of a nitrosyl group into a ruthenium complex is an ever-present possibility.

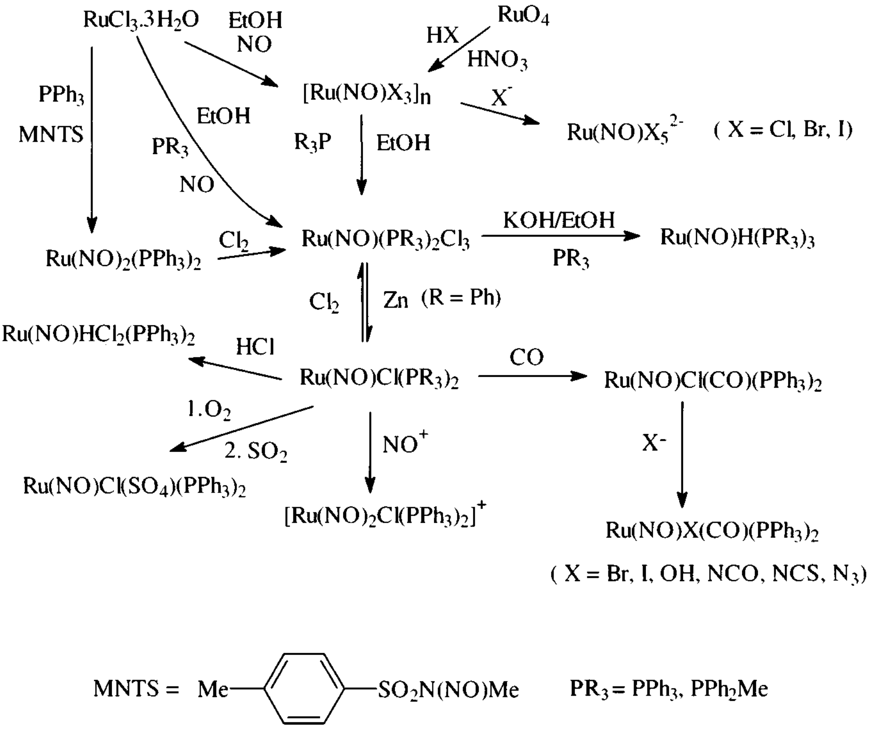

Figure 1.42 Syntheses of ruthenium nitrosyl complexes.

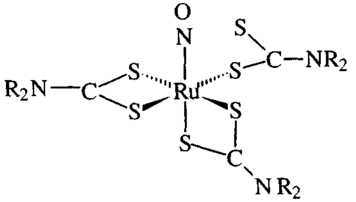

Figure 1.43 The 6-coordinate nitrosyl $Ru(NO)(S_2CNEt_2)_3$.

Cases are known where electrophilic attack occurs at nitrite [118]

$$RuCl(NO_2)(bipy)_2 + 2H^+ \rightarrow RuCl(NO)(bipy)_2^{2+} + H_2O$$

The NO ligand is usually regarded as a good σ-donor and, therefore, electrophilic, so that the above reaction can be reversed by nucleophilic attack

$$RuCl(NO)L_2^{2+} + 2OH^- \rightarrow RuCl(NO_2)L_2 + H_2O \qquad (L = \text{bipy or diars})$$

Complexes of chelating ligands like ethylenediamine (en) and diethylenetriamine (dien) can be made [119]:

$$[RuX_5(NO)]^{2-} \xrightarrow[\text{pH 6 heat}]{\text{1. en 2. HCl}} mer\text{-}RuX_3(en)NO \qquad (X = Cl, Br, I)$$

Some of the *fac*-isomer was obtained for X = Cl.

Three isomers of [Ru(NO)Cl $(2equ)_2$] (2equ = 2-ethyl-8-quinolinate) have been isolated in the solid state; they interconvert in DMSO solution above 100°C (NMR) [120].

Table 1.9 summarizes structural data for a number of ruthenium nitrosyl complexes, along with IR data [121, 122].

Recent study of the $[Ru(NO)X_5]^{2-}$ species (X = halogen, CN) shows that in general the Ru–X bond *trans* to nitrosyl is slightly longer than the *cis*-Ru–X bond (Table 1.10) [121].

Study of the nitrosyls $Ru(NO)X_3(PR_3)_2$ shows that their photochemical behaviour depends on the tertiary phosphine (Figure 1.44).

Where X is phenyl, the result of irradiation (sunlight, mercury lamp) is the formation of $Ru(NO)X_3(PPh_3)(OPPh_3)$ (X = Cl, Br); in the case of the diethylphenylphosphine complex, irradiation causes isomerization to the *cis,mer*-isomer. The *trans,mer*-isomer is the usual synthetic product, but in the case of dimethylphenylphosphine the *fac*-isomer was obtained using short reaction times; it isomerized to the usual *mer,trans*-isomer on heating [123].

$Ru(NO)(PPh_3)_2Cl_3$ gives rise to two interesting $\{Ru(NO)\}^8$ complexes. $Ru(NO)Cl(PPh_3)_2$, similar to Vaska's compound, $Ir(CO)Cl(PPh_3)_2$, undergoes rather similar addition reactions (compare section 2.10.2) [124]. Addition of NO^+ yields $[Ru(NO)_2Cl(PPh_3)_2]^+$, which like the analogous adduct $[Ir(NO)Cl(CO)(PPh_3)_2]^+$ has a bent metal–nitrosyl linkage (Figure 1.45) [125].

Table 1.9 Ruthenium nitrosyl complexes: structural and IR data

Complex	ν (NO) (cm^{-1})	M–N–O (°)	M–N (Å)	
$Na_2[Ru(OH)(NO_2)_4(NO)]^{2-}$	1907	179	1.764	
$[Ru(NH_3)_5NO]Cl_3$	1903	173	1.776	
$K_2[RuCl_5(NO)]$	1887	175	1.759	(neut diff.)
$RuCl(NO)(PPh_3)_2^+$	1845	180	1.74	
$RuH(NO)(PPh_3)_3$	1640	176	1.792	
trans-$[Ru(OH)(NO)(bipy)_2](ClO_4)_2$	1890	175	1.771	
$[Ru(NO)Cl(bipy)_2]^+$	1912	170	1.751	
$Ru(NO)Cl_3(PPh_3)_2$	1848	180	1.737	
$Ru(NO)Cl_3(PMePh_2)_2$	1855	176	1.744	
$Ru(NO)(S_2CNEt_2)_3$	1803	170	1.72	
$[RuCl(NO)_2(PPh_3)_2]^+PF_6^-$	1845, 1687	178, 138	1.743, 1.853	
$Ru(NO)_2(PPh_3)_2$	1665, 1615	178, 171	1.762, 1.776	
$Ru(OH)(NO)_2(PPh_3)_2^+BF_4^-$	1870, 1665	–	–	
$K_2[RuBr_5(NO)]$	1880	–	1.739	
$K_2[RuI_5(NO)]$	1844	–	1.716	
$K_2[RuF_5(NO)]$	1873	–	1.72	
$K_2[Ru(CN)_5(NO)]$	1915	–	1.733	
mer-$[RuCl_3(en)NO]$	1860	174	1.727	
$Ru(NO)Cl_3(AsPh_3)_2$	1869	180	1.729	

Table 1.10 Bond lengths in $Ru(NO)X_5^{2-}$ (Å)

X	F	Cl	Br	I	CN
Ru–N	1.72	1.738	1.739	1.716	1.733
Ru–X (*cis*)	1.958	2.370	2.517	2.719	2.059
Ru–X (*trans*)	1.91	2.362	2.513	2.726	2.051

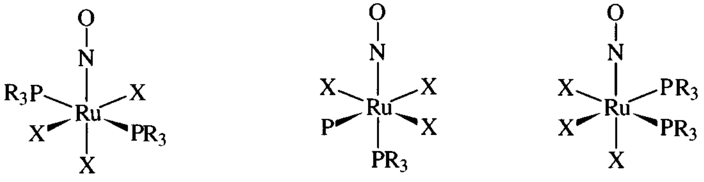

trans, mer cis, mer fac

Figure 1.44 The three isomers of $Ru(NO)(PR_3)_2X_3$.

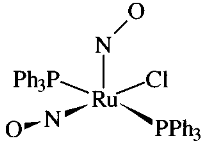

Figure 1.45 The structure of $[Ru(NO)_2Cl(PPh_3)_2]^+$ showing different modes of nitrosyl coordination.

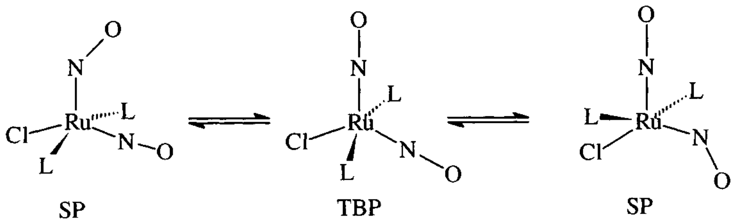

Figure 1.46 A scrambling mechanism envisaged for the interconversion of the metal–nitrosyl linkages in $[Ru(NO)_2Cl(PPh_3)_2]^+$.

Synthesis of this compound from a ^{15}N labelled source revealed that the ^{14}N and ^{15}N were equally distributed between the apical bent nitrosyl (NO^-) and equatorial linear nitrosyl (NO^+):

$$Ru(^{15}NO)Cl(PPh_3)_2 + {}^{14}NOPF_6 \rightarrow [Ru(^{15}NO)(^{14}NO)Cl(PPh_3)_2]^+PF_6^-$$

A scrambling mechanism between them involved a tbp intermediate (Figure 1.46).

$Ru(NO)_2(PPh_3)_2$ has a similar electronic structure to the $[M(NO)_2(PPh_3)_2]^+$ (M = Rh, Ir) ions and like them has a pseudo tetrahedral structure with linear Ru–N–O [126]. It also resembles them in its oxidative addition reactions (Figure 1.47).

The reaction with CO to afford CO_2 and N_2O is particularly interesting in view of the use of platinum metal compounds in automobile cataytic converters.

The nitrosyls $RuH(NO)(PR_3)_3$ are 5-coordinate with trigonal bipyramidal structures and linear Ru–N–O geometries; the hydride and nitrosyl ligands occupy the apical positions (for $RuH(NO)(PPh_3)_3$, ν(Ru–H) 1970 cm^{-1}, ν(N–O) 1640 cm^{-1}; ^{1}H NMR, $\delta = +6.6$ ppm for the hydride resonance). The high-field NMR line is a quartet showing coupling with three equivalent phosphines, which would not be possible in a square pyramidal

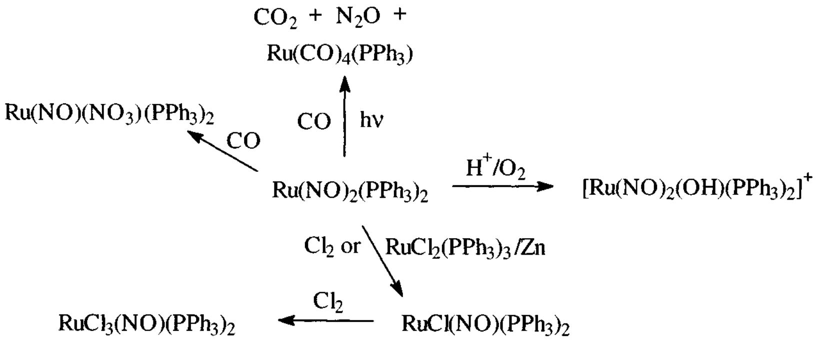

Figure 1.47 Reactions of $Ru(NO)_2(PPh_3)_2$.

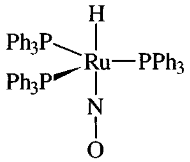

Figure 1.48 The trigonal bipyramidal structure of $RuH(NO)(PPh_3)_3$.

structure; therefore, the structure could be predicted spectroscopically before confirmatory crystallographic evidence was available (Figure 1.48) [127].

Thionitrosyls

A few thionitrosyl complexes have been synthesized. MO calculations suggest that NS is a superior σ-donor and π-acceptor to NO [128]. Syntheses include

$$RuCl_2(PPh_3)_3 + NSCl \rightarrow RuCl_3(NS)(PPh_3)_2$$

(In this compound ν(N–S) occurs at 1295–1310 cm^{-1} compared with ν(N–O) at 1875 cm^{-1} in $RuCl_3(NO)(PPh_3)_2$)

$$RuCl_3.xH_2O \xrightarrow[\text{2. } Ph_4PCl \text{ 3. recrystallize}]{\text{1. } S_3N_3Cl_3} (Ph_4P)[RuCl_4(NS)(OH_2)]$$

The structure of this compound shows a roughly linear thionitrosyl linkage (Ru–N–S 171°) with a rather short Ru–N bond (1.729 Å).

1.8.6 Porphyrin complexes

Porphyrin complexes have been the most intensively studied macrocyclic complexes of these metals [129]. They are formed in a wide range of oxidation states (II–VI) and they are, therefore, treated together under this heading, though most of the chemistry for ruthenium lies in the II–IV states. Octaethylporphyrin (OEP) complexes are typical.

Entry into the series involves metallating the porphyrin; this can be done by passing CO through a boiling solution of $Ru_3(CO)_{12}$ or $RuCl_3$ with the porphyrin in ethanoic acid. The initial product is the 6-coordinate Ru(OEP)(CO)(solvent), but the solvent molecule (e.g. EtOH) is easy displaced by other Lewis bases (and by a second molecule of CO if the solution is saturated with CO). Most of the dicarbonyls lose one CO molecule easily on standing but $Ru(OEP)(CO)_2$ is stable *in vacuo* for some hours; the CO can be displaced, particularly on heating, to afford 6-coordinate $Ru(OEP)L_2$ (L, e.g. py, PR_3). $Ru(OEP)py_2$ desolvates *in vacuo* at 210°C to a dimer $[RuOEP]_2$ with a Ru–Ru distance of 2.408 Å, regarded as a double bond; this compound is useful synthetically. While halogen oxidation of $Ru(OEP)(PR_3)_2$ proceeds only as far as ruthenium(III) in $Ru(OEP)(PR_3)X$, the unsolvated dimer is oxidized to the ruthenium(IV) state in paramagnetic $Ru(OEP)X_2$ (X = Cl, Br). These can be used to make the stable diphenyl $Ru(OEP)Ph_2$,

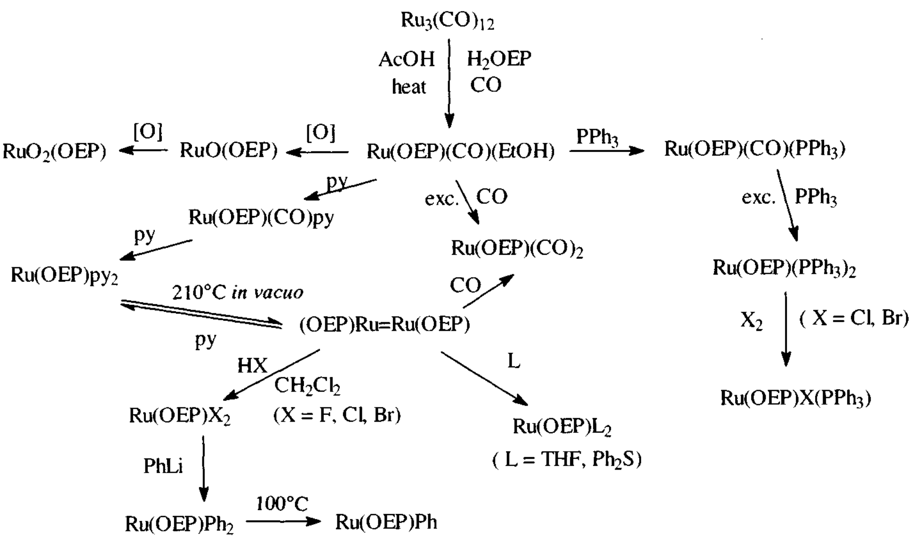

Figure 1.49 Octaethylporphyrin (OEP) complexes of ruthenium.

which on heating in solution undergoes smooth thermolysis to Ru(OEP)Ph. The Ru–Ru bond in the dimer can also be cleaved (e.g. by py, R_2S) retaining the ruthenium(II) oxidation state (Figure 1.49).

Structural data on ruthenium porphyrins shows that the Ru–N (porphyrin) distance is relatively unaffected by changing the oxidation state, as expected for a metal atom inside a fairly rigid macrocyclic ring (Table 1.11).

High oxidation states are accessible: a *t*-butylimide of ruthenium(VI) can be made by oxidative deprotonation

$$\mathrm{Ru(TPP)(Bu^tNH_2)_2} \xrightarrow[\mathrm{CH_2Cl_2}]{\mathrm{Br_2}} \mathrm{RuO(TPP)(NBu^t)}$$

$$\mathrm{Ru(OEP)(CO)(MeOH)} \xrightarrow{\text{M-CPBA}} \mathrm{RuO(OEP)}$$

$$\xrightarrow{\text{exc. M-CPBA}} \mathrm{RuO_2(OEP)}$$

(M-CPBA = *m*-chloroperoxybenzoic acid).

Table 1.11 Structural data for complexes Ru(OEP)(X)(Y) (in Å)

Oxidation state	X	Y	Ru–N (porphyrin)	Ru–X	Ru–Y
II	py	py	2.046–2.048	2.100	2.100
II	PPh_3	PPh_3	2.044–2.057	2.438	2.438
II	CO	H_2O	2.051	1.783	2.253
III	PPh_3	Br	2.025–2.047	2.415	2.552
III	Ph	–	2.007–2.048	2.005	–

Water-soluble ruthenium phthalocyanines show promise as photodynamic cancer therapy agents [129b].

1.8.7 EDTA complexes

A considerable number of EDTA complexes of ruthenium have been synthesized [130–132]; there has been interest in their catalytic potential while several compounds have had their structures determined. Synthetic routes relating to these compounds are shown in Figure 1.50.

In all the compounds of known structure, ruthenium is 6-coordinate; therefore, in complexes like Ru(EDTAH)(H_2O) [131], the acid is pentadentate, with a free carboxylate group; likewise, in K[Ru($EDTAH_2$)Cl_2] and [Ru($EDTAH_2$)(dppm)] two of the carboxylates are protonated, so it is tetradentate.

The structure of the aqua complex (Figure 1.51), which is an active intermediate in some catalytic systems, shows the Ru–OH_2 distance to be some 0.1 Å longer than in the ruthenium(III) hexaqua ion, indicating a possible reason for its lability; the water molecule also lies in a fairly exposed position, away from the bulk of the EDTA group.

The ruthenium(III) complex is oxidized to a paramagnetic ruthenium(V) species, RuO(EDTA): ($\mu = 1.98\,\mu_B$; ν(Ru=O) 890 cm^{-1}) by NaOCl or

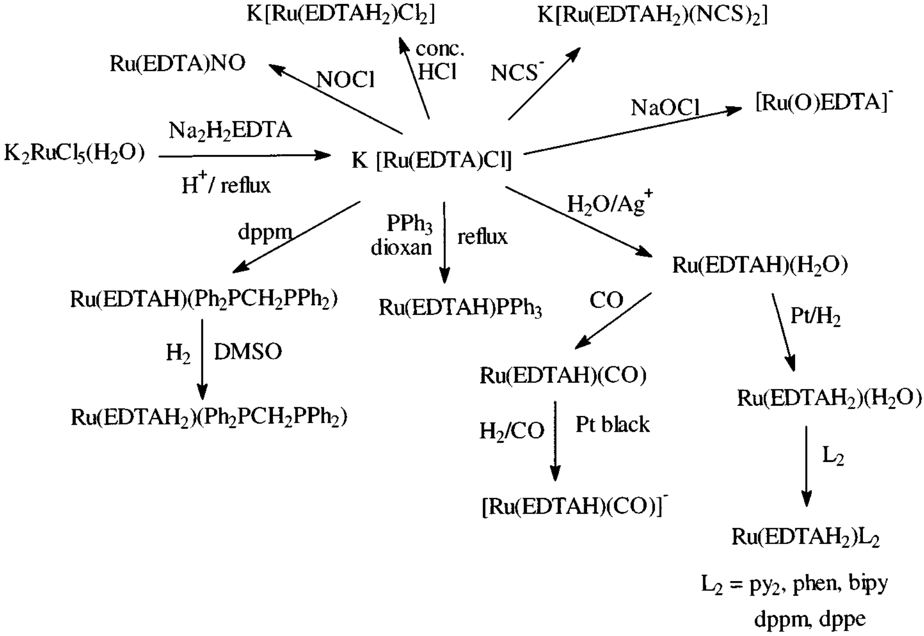

Figure 1.50 Ruthenium complexes of EDTA.

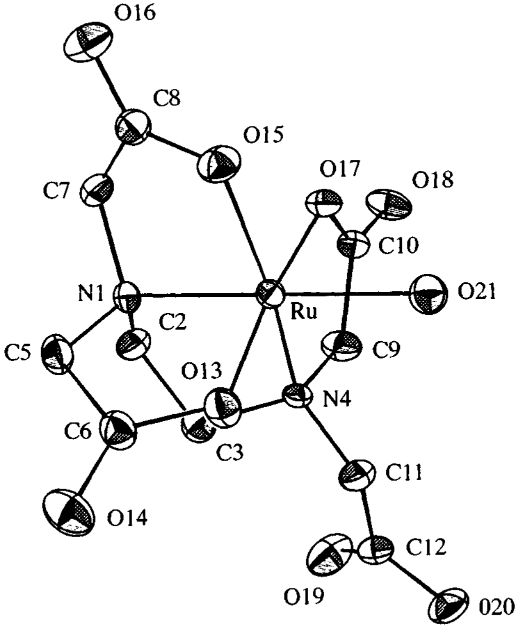

Figure 1.51 The structure of [Ru(EDTA-H)(H_2O)]. (Reproduced with permission from the *Indian J. Chem., Sect. A*, 1992, 206.)

iodosylbenzene. This compound catalyses epoxidation of alkenes and oxidation of phosphines.

The carbonyl complex $[Ru(EDTAH)(CO)]^-$ has been reported to be a very good catalyst for reactions like hydroformylation of alkenes, carbonylation of ammonia and ammines as well as a very active catalyst for the water gas shift reaction. The nitrosyl [Ru(EDTA)(NO)] is an oxygen-transfer agent for the oxidation of hex-1-ene to hexan-2-one, and cyclohexane to the corresponding epoxide.

Bond lengths for a number of the ruthenium EDTA complexes are given in Table 1.12.

Table 1.12 Bond lengths in $[Ru(EDTAH)L]^{n-}$ systems (Å)

	L				
	H_2O	PPh_3	NO	Cl	CO
n	–	–	–	–	1
Oxidation state of Ru	+3	+3	+3	+3	+2
Ru–N (*trans*-L)	2.035	2.070	2.095	2.043	2.119
Ru–N (*cis*-L)	2.49	2.126	2.115	2.114	2.119
Ru–O (*trans*-O)	1.986, 2.062	1.983, 2.050	2.018, 2.021	2.007	2.063, 2.099
Ru–O (*trans*-N)	2.004	1.996	2.010	2.067	2.064
Ru–L	2.137	2.363	1.728	2.358	1.843

They demonstrate the sensitivity of the Ru–N bond length to the *trans*-donor atom and also how when a multidentate ligand is involved bond lengths do not necessarily shorten on increasing the oxidation state.

1.8.8 Other complexes of ruthenium

Ruthenium, in its 'normal' oxidation states of II and III, forms a wide range of complexes with most available donor atoms, of which a representative selection are mentioned below.

The structures of $[Ru(HCONMe_2)_6](CF_3SO_3)_x$ ($x = 2, 3$) show a contraction in Ru–O distance from 2.088 Å to 2.02 Å on passing from the +2 to the +3 oxidation state [133a].

There is a wide range of diketonates, such as $Ru(acac)_3$, with octahedral coordination [133b] (they do not seem, however, to be oxidized to the +4 state; this is possible with osmium); similarly several salts of the tris(oxalato) complex $Ru(C_2O_4)_3^{3-}$ have been isolated.

Complexes of pyridine and substituted pyridines, mainly in the +2 state, have been made [134]:

$$Ru(H_2O)_6^{2+} \xrightarrow{\text{exc. py}} Rupy_6^{2+} \quad \text{(octahedral, Ru–N 2.10–2.14 A)}$$

$$RuCl_6^{2-} \xrightarrow[\text{reflux}]{\text{py}} Rupy_4Cl_2 \xrightarrow{NO_2^-} Rupy_4(NO_2)_2$$

$$Ru(C_2O_4)_3^{3-} \xrightarrow[\text{2. Zn/Hg}]{\text{1. py, reflux}} Rupy_4C_2O_4$$

$$\xrightarrow{HCl} cis\text{-}Rupy_4Cl_2 \xrightarrow[\text{recryst.}]{\text{py}} trans\text{-}Rupy_4Cl_2$$

The reaction of the (necessarily) *cis*-oxalato complex with HCl in the last example, ensures the *cis*-configuration for the chloro complex: on recrystallization, the thermodynamically more stable *trans*-isomer forms. *trans*-$Rupy_4Cl_2$ has Ru–N 2.079 Å and Ru–Cl 2.405 Å. An imidazole complex (imH) *trans*-$[RuCl_4(im)_2]$ shows promise as a tumour inhibitor and is currently undergoing preclinical trials [135].

$$RuCl_3.xH_2O \xrightarrow[\text{2. im/HCl(aq.), warm}]{\text{1. HCl(aq.)/EtOH reflux}} (imH)[RuCl_4(im)_2]$$

Many ruthenium complexes with nitrile ligands also feature tertiary phosphines, but simpler complexes can be synthesized [136]

$$RuCl_3.xH_2O \xrightarrow[80°C]{PhCN} mer\text{-}RuCl_3(PhCN)_3$$

$$RuCl_5^{3-} \xrightarrow{PhCN} Bu_4N\ trans\text{-}[RuCl_4(PhCN)_2]$$

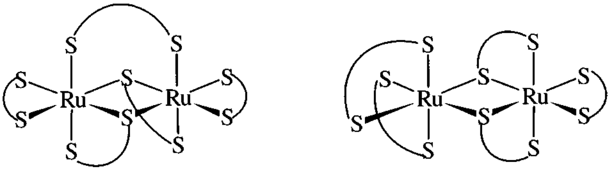

Figure 1.52 Isometric forms of $Ru_2(S_2CNEt_2)_5$.

The structures of both these complexes, typical of ruthenium(III) nitriles, were confirmed by X-ray diffraction; ruthenium(II) nitriles are also possible:

$$RuCl_3 \xrightarrow[\text{RCN}]{\text{H}_2/\text{Adams catalyst}} trans\text{-}RuCl_2(RCN)_4$$

Many ruthenium dithiocarbamates have been synthesized. The ruthenium(III) compounds can be made by standard methods [137]

$$RuCl_3 \xrightarrow{\text{NaS}_2\text{CNEt}_2} Ru(S_2CNEt_2)_3$$

This compound has an octahedral coordination sphere slightly distorted towards a trigonal prism. Oxidation by air leads to $Ru_2(S_2CNEt_2)_5$ which exists in two isomeric forms (Figure 1.52) [138].

In contrast, photolytic oxidation of $Ru(S_2CNR_2)_3$ in $CHCl_3$ or CH_2Cl_2 affords pentagonal bipyramidal $Ru(S_2CNR_2)_3Cl$ (apical Cl and S) and iodine gives $Ru(S_2CNR_2)_3I$, again 7-coordinate. Chloroform solutions of $Ru(S_2CNR_2)_3$ react with NO to form $Ru(NO)(S_2CNR_2)_3$ (section 1.8.5), which has 6-coordinate ruthenium with one monodentate dithiocarbamate.

1.9 Complexes of ruthenium(IV)

Compounds containing ruthenium(IV) such as the dithiocarbamates $Ru(S_2CNR_2)_3Cl$ (section 1.8.6) and the porphyrin complexes (section 1.8.6) were mentioned above. Certain phosphine complexes $RuH_4(PR_3)_3$ are best regarded as ruthenium(II) compounds: $Ru(H)_2(\eta^2\text{-}H_2)(PR_3)_3$ (section 1.8.2).

Some unusual ruthenium(IV) thiolates have been made [139]

$$Ru(MeCN)_2Cl_4^- \xrightarrow[\text{MeCN}]{\text{LiSR, RSSR}} Ru(SR)_4(MeCN)$$

($R = 2,4,6\text{-}Pr^i_3C_6H_2, 2,3,5,6\text{-}Me_4C_6H$).

They doubtless owe their stability to the bulk of the aryl thiolate ligand; they have tbp structures with equatorial nitrile that can be displaced by CO to give rare carbonyls of a metal in the +4 oxidation state.

Another, and less surprising, example of ruthenium(IV) lies in the oxo complexes with macrocycles like 14-TMC (Figure 1.53).

Next Page

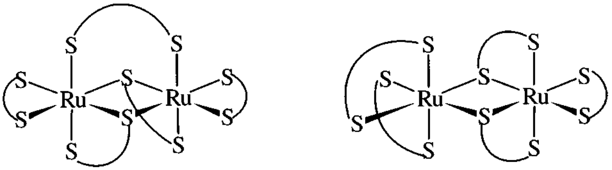

Figure 1.52 Isometric forms of $Ru_2(S_2CNEt_2)_5$.

The structures of both these complexes, typical of ruthenium(III) nitriles, were confirmed by X-ray diffraction; ruthenium(II) nitriles are also possible:

$$RuCl_3 \xrightarrow[\text{RCN}]{H_2/\text{Adams catalyst}} \textit{trans}\text{-}RuCl_2(RCN)_4$$

Many ruthenium dithiocarbamates have been synthesized. The ruthenium(III) compounds can be made by standard methods [137]

$$RuCl_3 \xrightarrow{NaS_2CNEt_2} Ru(S_2CNEt_2)_3$$

This compound has an octahedral coordination sphere slightly distorted towards a trigonal prism. Oxidation by air leads to $Ru_2(S_2CNEt_2)_5$ which exists in two isomeric forms (Figure 1.52) [138].

In contrast, photolytic oxidation of $Ru(S_2CNR_2)_3$ in $CHCl_3$ or CH_2Cl_2 affords pentagonal bipyramidal $Ru(S_2CNR_2)_3Cl$ (apical Cl and S) and iodine gives $Ru(S_2CNR_2)_3I$, again 7-coordinate. Chloroform solutions of $Ru(S_2CNR_2)_3$ react with NO to form $Ru(NO)(S_2CNR_2)_3$ (section 1.8.5), which has 6-coordinate ruthenium with one monodentate dithiocarbamate.

1.9 Complexes of ruthenium(IV)

Compounds containing ruthenium(IV) such as the dithiocarbamates $Ru(S_2CNR_2)_3Cl$ (section 1.8.6) and the porphyrin complexes (section 1.8.6) were mentioned above. Certain phosphine complexes $RuH_4(PR_3)_3$ are best regarded as ruthenium(II) compounds: $Ru(H)_2(\eta^2\text{-}H_2)(PR_3)_3$ (section 1.8.2).

Some unusual ruthenium(IV) thiolates have been made [139]

$$Ru(MeCN)_2Cl_4^- \xrightarrow[\text{MeCN}]{\text{LiSR, RSSR}} Ru(SR)_4(MeCN)$$

($R = 2,4,6\text{-}Pr^i_3C_6H_2$, $2,3,5,6\text{-}Me_4C_6H$).

They doubtless owe their stability to the bulk of the aryl thiolate ligand; they have tbp structures with equatorial nitrile that can be displaced by CO to give rare carbonyls of a metal in the +4 oxidation state.

Another, and less surprising, example of ruthenium(IV) lies in the oxo complexes with macrocycles like 14-TMC (Figure 1.53).

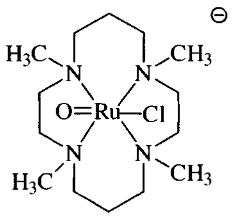

Figure 1.53 A ruthenium(IV) macrocyclic complex.

The presence of a Ru=O bond can be diagnosed from the presence of an IR band *c.* 825 cm^{-1}; the bond length, at 1.76 Å, is slightly longer than in dioxoruthenium(VI) complexes [140].

1.10 Complexes of osmium(0)

Osmium is notable for the range of binary carbonyls it forms [141]: $Os(CO)_5$, $Os_2(CO)_9$, $Os_3(CO)_{12}$, $Os_4(CO)_x$ ($x = 14, 15, 16$), $Os_5(CO)_y$ ($y = 16, 18, 19$), $Os_6(CO)_z$ ($z = 18, 21$), $Os_7(CO)_{21}$, $Os_8(CO)_{23}$ and $Os_{10}(CO)_{26}$. From the perspective of this book, the relevant compounds are $Os(PF_3)_5$, $Os[P(OMe)_3]_5$ and $Os(PMe_3)_5$, all with tbp structures [142]. The last, prepared by reduction of an osmium(II) complex:

$$\textit{trans}\text{-}OsCl_2(PMe_3)_4 \xrightarrow[\text{exc. }PMe_3]{\text{Na/THF, naphthalene}} Os(PMe_3)_5$$

It is a very reactive substance, picking up traces of H$^+$ to form $Os(PMe_3)_5H^+$ and undergoing facile metallation (Figure 1.54).

1.11 Osmium complexes in oxidation states (II–IV)

Within the osmium complexes in oxidation states (II–IV) [11, 12] the stability of the +4 oxidation state becomes more important. Ammine and tertiary phosphine complexes have been selected for detailed examination.

1.11.1 Ammine complexes

Many of the ammine complexes are osmium(III) compounds; the +2 state is less stable than with ruthenium, as expected, and osmium(II) compounds

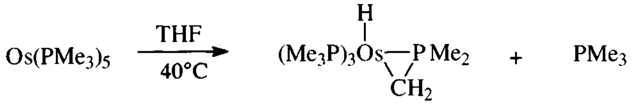

Figure 1.54 Metallation of $Os(PMe_3)_5$.

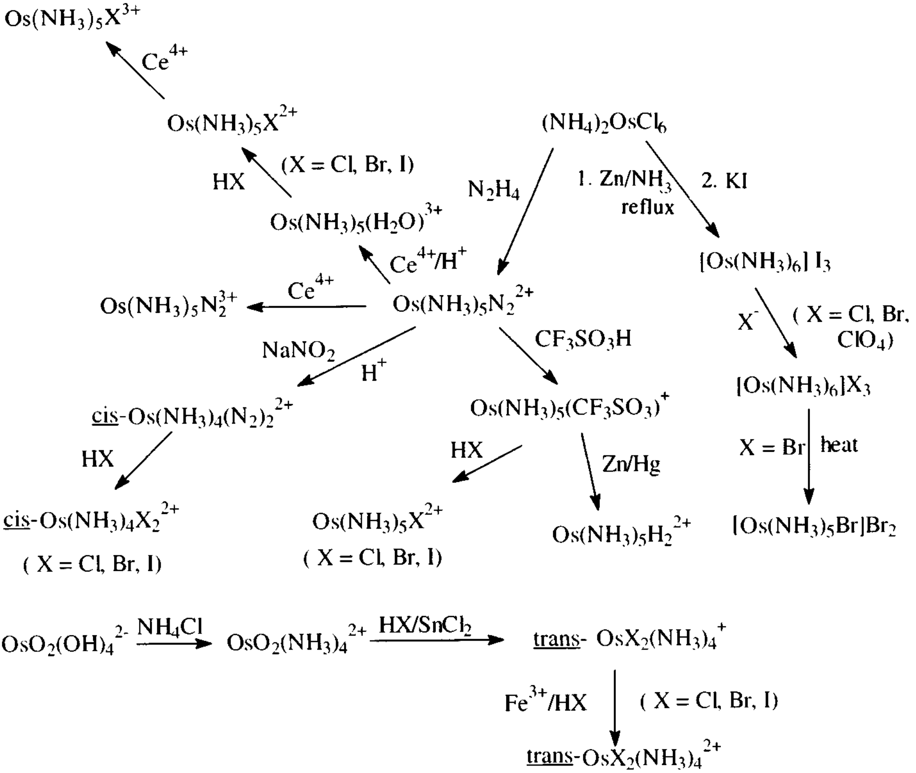

Figure 1.55 Syntheses of osmium ammine complexes.

are only really stable in the presence of good π-acceptors (N_2, CO) [143]. Osmium(IV) ammines can often be made by oxidation of the corresponding Os(III) compounds. Figure 1.55 summarizes many syntheses.

The most remarkable complex is the osmium(VI) nitrido species $OsN(NH_3)_4^{3+}$ (IR $\nu(Os{\equiv}N)$ 1090 cm^{-1}) [144].

The dinitrogen complex $[Os(NH_3)_5N_2]^{2+}$ is a useful synthetic intermediate, while the presence of the weakly nucleophilic triflate group enables it to be easily removed in the synthesis of the dihydrogen complex.

The dinitrogen complex (Figure 1.56) has a rather short $Os{-}N_2$ bond (1.842 Å) indicating some multiple bond character while the *trans*-Os–N bond is slightly longer than the others, but not significantly different. The N_2 ligand shows $\nu(N{-}N)$ at 2022 cm^{-1} in the IR spectrum [145].

Some bis(dinitrogen) complexes exist, generally as *cis*-isomers (presumably this minimizes competition for the metal t_{2g} electron density in π-bonding). Unlike ruthenium, osmium(III) dinitrogen complexes do exist, showing osmium(III) to be a better π-donor; not surprisingly, they are more labile than the osmium(II) species.

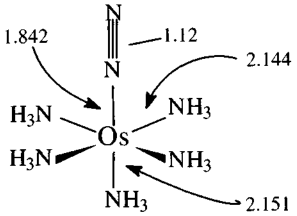

Figure 1.56 Bond lengths in $[Os(NH_3)_5(N_2)]^{2+}$.

Reaction of the osmium(III) pentammines with zinc amalgam gives an osmium species that is stable in solution for some hours (and may be $[Os^{IV}(NH_3)_5(OH)(H)]^{2+}$). It is capable of forming $Os(NH_3)_5L^{2+}$ adducts with π-acids like MeCN [146].

Osmium complexes of bi- and polydentate ammines

The simplest systems are the tris(chelates) of phen and bipy

$$K_2OsCl_6 \xrightarrow[260°C]{bipy} Os(bipy)_3^{2+} \text{ (green)} \xrightarrow{Cl_2} Os(bipy)_3^{3+}$$

$$K_2OsCl_6 \xrightarrow[260°C]{phen} Os(phen)_3^{2+} \text{ (dark brown)} \xrightarrow{Cl_2} Os(phen)_3^{3+}$$

Os–N bond lengths in $Os(bipy)_3(PF_6)_2$ (isostructural with the ruthenium analogue) and $Os(phen)_3(ClO_4)_2H_2O$ are 2.062 Å and 2.066–2.082 Å, respectively [147].

Other complexes include

$$OsX_6^{2-} \xrightarrow[\text{DMF heat}]{L-L} [Os(L-L)_2X_2]^+ \xrightarrow{Na_2S_2O_4} Os(L-L_2)X_2$$

(X = Cl, Br, I; L–L = phen, bipy)

$$OsCl_6^{2-} \xrightarrow[fuse]{Os/terpy} Os(terpy)_2^{2+} \xrightarrow{Cl_2} Os(terpy)_2^{3+}$$

With ethylenediamine, high oxidation states become a possibility (Figure 1.57), sometimes involving a deprotonated ligand (see also section 1.12.1) [148].

The structure of the deprotonated ethylenediamine complex $[Os(en\text{-}H)_2en]Br_2$ has been confirmed (Figure 1.58); the Os=NH bonds (2.11–2.19 Å) indicating clear multiple bond character. It can be used as a source of 'conventional' ethylenediamine complexes.

$Osen_2H_2^{2+}$ is in fact a dihydrogen complex (Figure 1.59).

In aqueous solution, the water molecule (L) can be replaced by other ligands including a range of biomolecules. The nature of the molecule bound affects the position and relaxation time of the dihydrogen resonance (and also J_{HD} when D_2O is present). Both the dihydrogen and the water can

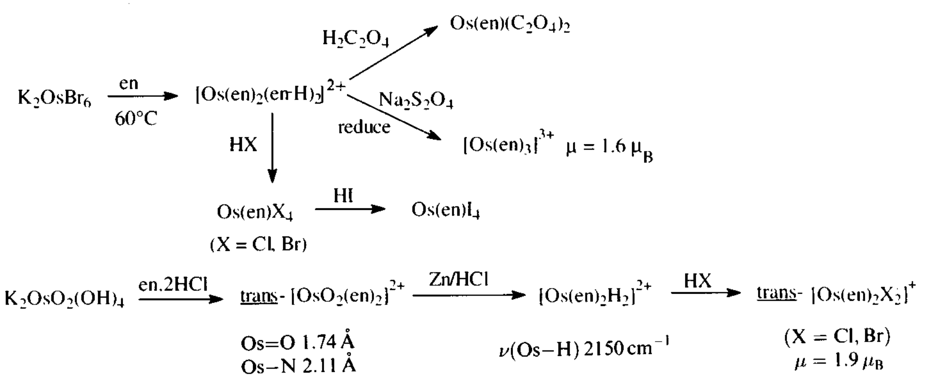

Figure 1.57 Ethylenediamine complexes of osmium.

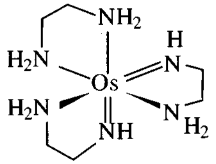

Figure 1.58 The cation in the deprotonated ethelyenediamine complex $[Os(en\text{-}H)_2en]Br_2$.

be replaced by unsaturated molecules (ethene and ethyne) [149]. On reaction with sodium acetate, $[Osen_2H_2]^{2+}$ forms $[Os(\eta^2\text{-}H_2)en_2(OAc)]^+$, which has Os–H of 1.59–1.60 Å (neutron-diffraction, H–H 1.34 Å), which is shorter than in classical hydrides like $OsH_4(PMe_2Ph)_3$ (1.66 Å) indicating the strength of the Os–H bond [150].

1.11.2 Tertiary phosphine complexes

Syntheses of some of these important tertiary phosphine complexes are summarized in Figure 1.60, which represent reactions typical of a tertiary phosphine (e.g. PMe_2Ph), showing complexes in the oxidation states +6, +4, +3 and +2 [78a].

The osmium(VI) complexes $OsO_2X_2(PR_3)_2$ are not generally obtainable with the smaller alkyl and alkyl(aryl)phosphines, which tend to be good

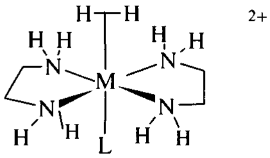

Figure 1.59 The dihydrogen complex cation $[Osen_2H_2(L)]^{2+}$(L, e.g. H_2O).

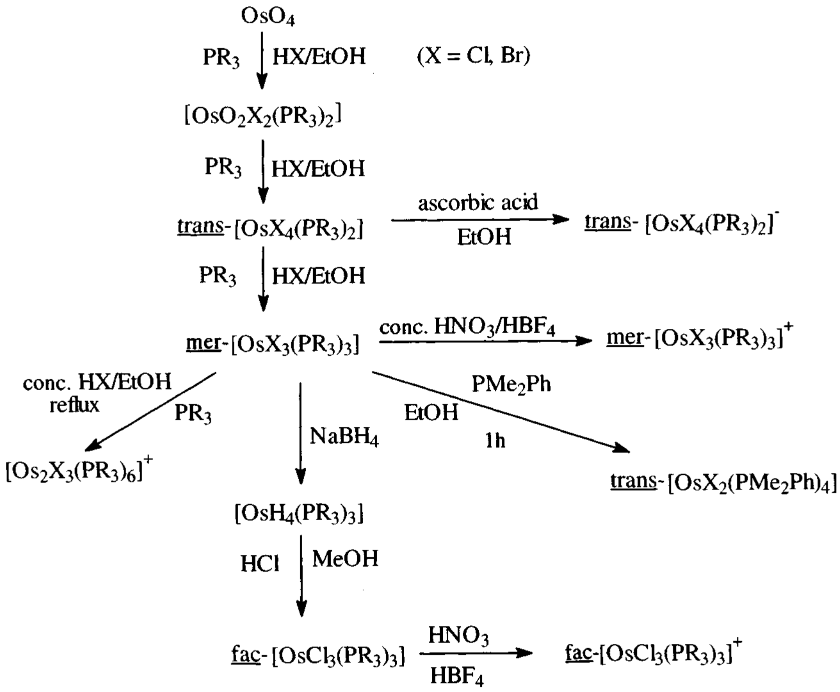

Figure 1.60 Syntheses of some osmium complexes of tertiary phosphines.

reducing agents; with the bulky PPr^i_2Ph, $OsO_2Cl_2(PPr^i_2Ph)_2$ is obtained after 3 h reflux

$$OsO_4 \xrightarrow[\text{HCl/EtOH reflux}]{Pr^i_2Ph} OsO_2Cl_2(PPr^i_2Ph)_2$$

These compounds give characteristic 'osmyl' IR bands (840 cm^{-1} in $OsO_2Cl_2(PPh_3)_2$) [151].

The osmium(IV) complexes are only obtained by this route with fairly unreactive phosphines and arsines (e.g. PBu_2Ph) but they are conveniently made by oxidation of *mer*-$OsX_3(QR_3)_3$ ($Q = P$, As) with the halogen in $CHCl_3$, or CCl_4 and refluxing.

The general product of OsO_4/acid/phospine reflux is *mer*-$OsX_3(PR_3)_3$, important starting materials for other syntheses. The *fac*-isomer cannot be made directly, instead the *mer*-isomer is treated with borohydride, making $OsH_4(PR_3)_3$, which on reaction with HX in methanol gives *fac*-$OsX_3(PR_3)_3$, though this is not a general method. (Neither can a photochemical route, as used for $IrX_3(PR_3)_3$ (section 2.13.3), be used.)

Distinguishing between the *fac*- and *mer*-isomers is theoretically possible with far-IR spectra, as the *mer*-isomer (C_{2v} symmetry in the coordination sphere) should give rise to three ν(Os–X) stretching bands, while the C_{3v}

cis-isomer should give rise to just two; in practice, both isomers tend to give just two bands (possibly owing to overlapping bands or accidental degeneracies) [78a, 152]. There are significant differences in the visible/UV spectra, but ESR spectra of these low spin d^5 complexes show clear differences: the *fac*-isomer of $OsCl_3(PBu_2Ph)_3$ has an axially symmetric g-tensor ($g_\perp = 1.83$, $g_{||} = 1.28$) while the *mer*-isomer gives rise to a 'rhombic' spectrum ($g_1 = 3.33$, $g_2 = 1.66$, $g_3 = 0.36$) [153].

The magnetic moments for these osmium(III) complexes are, as expected, in the range 1.9–2.2 μ_B. Reduction of *mer*-$OsX_3(PR_3)_3$ has been studied in various ways. The usual product of extended reflux with the phosphine/HCl mixture or from using amalgamated zinc in thf under argon is the dimeric species $[Os_2Cl_3(PR_3)_6]^+$, analogous to ruthenium complexes (section 1.8.2). However, some monomeric osmium(II) complexes can be made

$$\textit{cis-}OsH_2(PMe_2Ph)_4 \xrightarrow[MeOH/C_6H_6]{HCl} \textit{cis-}OsCl_2(PMe_2Ph)_4$$

$$OsO_4 \xrightarrow[\text{boil EtOH}]{\text{conc. HCl/PMe}_2\text{Ph}} \textit{trans-}OsCl_2(PMe_2Ph)_4$$

$$Na_2OsCl_6 \xrightarrow[\text{EtOH boil}]{PPh_3} OsCl_2(PPh_3)_3$$

$$OsCl_2(PPh_3)_3 \xrightarrow[\text{hexane}]{PMe_3} \textit{trans-}OsCl_2(PMe_3)_4$$

The last route is used analgously for ruthenium(II) complexes.

Electrochemical reduction of *mer*-$OsCl_3(PMe_2Ph)_3$ affords $[OsCl_3(PMe_2Ph)_3]^-$ [154]. At room temperature in donor solvents, a species $OsCl_2(PMe_2Ph)_3$(solvent) is formed; the initial product is the *trans,mer*-isomer which on standing reverts to the thermodynamically more stable product (Figure 1.61). *trans,mer*-$[OsCl_2(PMe_2Ph)_3(MeCN)]$ has Os–Cl = 2.432–2.447 Å, Os–N 2.06 Å and Os–P 2.350–2.362 Å (*trans* to P) and 2.298 Å (*trans* to N) [154].

A compound *trans*-$OsCl_2(PMe_2Ph)_4$ has been isolated from the solution and is believed to contain one very loosely bound phosphine, possibly attached through a metal-ring π-bond or Os–H–C agostic interaction.

By comparison, oxidation of *mer*-$Os(PR_3)_3Cl_3$ systems affords paramagnetic osmium(IV) species *mer*-$Os(PR_3)_3Cl_3^+$ (the corresponding *fac*-species can only be oxidized electrochemically) [152]. Other osmium(IV)

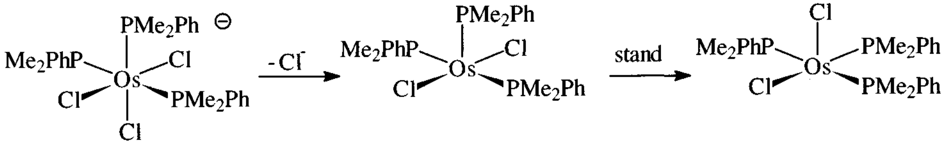

Figure 1.61 Electroreduction of $OsCl_3(PMe_2Ph)_3$.

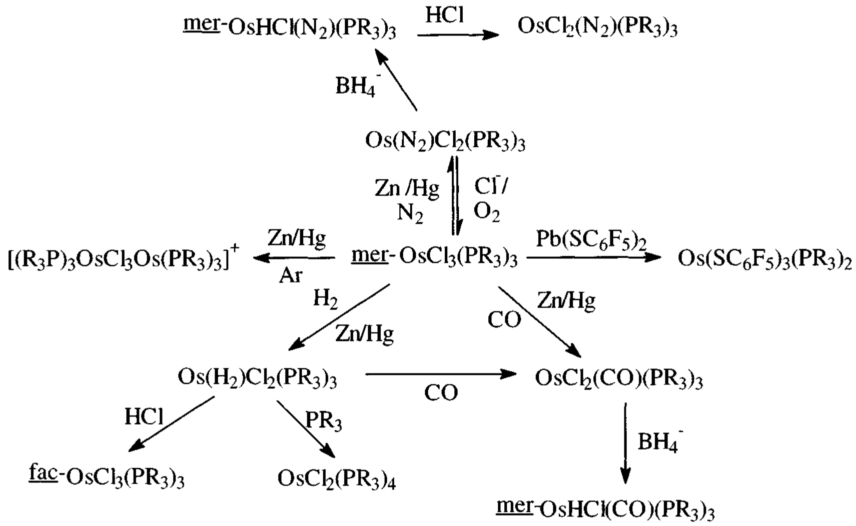

Figure 1.62 Reactions of $OsCl_3(PR_3)_3$.

complexes, *trans*-$OsX_4(PR_3)_2$, were mentioned earlier: they are paramagnetic with magnetic moments rather below the spin only value for two unpaired electrons ($\mu = 1.6\,\mu_B$ for *trans*-$OsCl_4(PEt_3)_2$). These complexes are reduced (ascorbic acid/ethanol) to *trans*-$[OsCl_4(PR_3)_2]^-$, low spin osmium(III) complexes ($\mu = 2.0\,\mu_B$ for $Ph_4P^+[OsCl_4(PEt_2Ph)_2]^-$).

The solutions of *mer*-$OsCl_3(PR_3)_3$ undergo an interesting reduction with zinc amalgam [155] to form $OsCl_2(PR_3)_2L$ (Figure 1.62), where L is a molecule abstracted from the atmosphere in the reaction flask; if a noble gas, incapable of coordination, is employed, coordinative saturation is obtained by dimerization to $[(PR_3)_3OsCl_3Os(PR_3)_3]^+$.

The dinitrogen complex is stable to borohydride reduction but the nitrogen is displaced by chloride

$$OsCl_2(N_2)(PR_3)_3 \xrightarrow{BH_4^-} OsHCl(N_2)(PR_3)$$

$$OsCl_2(N_2)(PR_3)_3 \xrightarrow{Cl^-} OsCl_3(PR_3)_3$$

The halides in *mer*-$OsCl_3(PR_3)_3$ can be replaced by a thiolate ligand to give paramagnetic $Os(SC_6F_5)_3(PR_3)_2$; an agostic Os–F–C interaction is believed to complete the coordination sphere of osmium [156].

Considerable structural information is available on osmium complexes of tertiary phosphines, arsines and stibines (Table 1.13) [152, 157].

Comparison with data (mainly obtained from EXAFS measurements) on osmium diarsine complexes (Table 1.14) shows that as the oxidation state increases, osmium–halogen bonds shorten whereas Os–P and Os–As bonds lengthen. Bond shortening is predicted for bonds with ionic character,

Table 1.13 Bond lengths in $OsY_a(QR_3)_b$ (Å)

	Oxidation state	Os–Q		Os–Y	
		trans-Q	*trans*-Y	*trans*-Y	*trans*-Q
trans-$OsCl_4(PMe_2Ph)_2$	4	2.448		2.319	
trans-$OsBr_4(AsPh_3)_2$	4	2.569		2.451–2.472	
mer-$OsCl_3(PMe_2Ph)_3$	3	2.408	2.350	2.347	2.439
trans-$OsCl_4(PEt_3)_2^-$	3	2.371–2.386		2.375–2.386	
fac-$OsCl_3(PEt_2Ph)_3$	3		2.375–2.380		2.442–2.449
trans-$OsCl_2(PMe_3)_4^+$	3	2.398–2.419		2.352	
mer-$OsBr_3(SbPh_3)_3$	3	2.640–2.654	2.644	2.507–2.508	2.522

as the size of the metal ion decreases with increasing oxidation state and electrostatic attraction. The opposite tendency in Os–P and Os–As bonds has been rationalized in terms of a weaker attraction for the 'soft' donor atom as the metal becomes a harder acid (with increasing oxidation state); steric repulsion effects may also play a part [158].

Complexes of diphosphines and diarsines can be prepared by various routes; the following are typical

$$OsO_4 \xrightarrow[\text{conc. HX}]{\text{L–L}} Os(L{-}L)_2X_2 \xrightarrow[\text{HBF}_4]{\text{conc. HNO}_3} [Os(L{-}L)_2X_2]^+BF_4^-$$

$$OsX_6^{2-} \xrightarrow[\text{reflux COH}]{\text{L–L}} Os(L{-}L)_2X_2 \xrightarrow[\text{HBF}_4]{\text{conc. HNO}_3} [Os(L{-}L)_2X_2]^+BF_4^-$$

$$\xrightarrow{\text{HClO}_4} [Os(L{-}L)_2X_2]^{2+}$$

(L–L, e.g. *o*-$C_6H_4(QMe_2)_2$ (Q = P, As), $Ph_2PC_2H_4PPh_2$, etc.).

As noted above, structural information is available from EXAFS data (Table 1.14).

In *trans*-$Os(dppe)_2Cl_2CH_2Cl_2$, Os–P is 2.348–2.372 Å, Os–Cl is 2.434 Å (compare Ru–P 2.369–2.389 Å, Ru–Cl 2.436 Å in $Ru(dppe)_2Cl_2$) [159]. In *trans*-$Os(dppe)_2Br_2$ Os–P is 2.365–2.378 Å and Os–Br is 2.674 Å.

Table 1.14 Bond lengths in *trans*-$[Os(o\text{-}C_6H_4(AsMe)_2)_2X_2]^{n+}$ (Å)

X	*n*	Oxidation state	Os–As	Os–X
Cl	0	2	2.404	2.41
Cl	1	3	2.460 (2.459 (X))	2.349 (2.337 (X))
Cl	2	4	2.512	2.278
Br	0	2	2.407	2.558,[a] 2.548[b]
Br	1	3	2.443	2.515,[a] 2.485[b]
Br	2	4	2.517	2.400,[a] 2.384[b]

Data obtained from EXAFS measurements except X (X-ray).
[a] From Os L-edge; [b] From Br K-edge.

Hydride complexes

Osmium forms a large number of hydridophosphine complexes, principally mononuclear. The three main families are $OsH_6(PR_3)_2$, $OsH_4(PR_3)_3$ and $OsH_2(PR_3)_4$.

Hexahydrides

$OsH_6(PMe_2Ph)_2$ is synthesized by reduction of $Ph_4As^+OsCl_4(PMe_2Ph)_2^-$

$$OsCl_4(PMe_2Ph)_2^- \xrightarrow[THF]{LiAlH_4} OsH_6(PMe_2Ph)_2$$

It is a pale yellow oil characterized by ^1H NMR (1 : 2 : 1 triplet showing two phosphines with $\delta = -8.6$ ppm) and IR spectroscopy (δ(Os–H) 2028, 1980, 1869 cm^{-1}) [160].

Crystalline $OsH_6(PPr^i_2Ph)_2$ was also made by reduction:

$$OsO_2Cl_2(PPr^i_2Ph)_2 \xrightarrow[THF]{LiA/H_4} OsH_6(PPr^i_2Ph)_2$$

Its ^1H NMR spectrum supports the formulation (triplet at $\delta = -9.21$ ppm, J(P–H) 9 Hz, J(Os–H) 40 Hz) and the structure was established by X-ray and neutron diffraction (Figure 1.63); unlike $IrH_5(PR_3)_2$ (section 2.15) the two phosphorus atoms are not colinear with the metal (P–Os–P 155°) [161]: the geometry round the osmium is an irregular dodecahedron.

The Os–H bonds are 1.637–1.668 Å; since the shortest H–H contacts are 1.65 Å, it is clearly a 'classical' hydride rather than a η^2-H_2 complex. Other hexahydrides OsH_6L_2 ($L = PPr^i_3$, PBu^t_2Me) have lately been reported. On protonation with HBF_4, $[OsH_7(PPr^i_3)_2]^+$ is formed, believed to be $[OsH_3(H_2)_2(PPr^i_3)_2]^+$; this reacts with MeCN forming hydrides such as $[OsH_3(MeCN)_2(PPr^i_3)_2]^+$ [162].

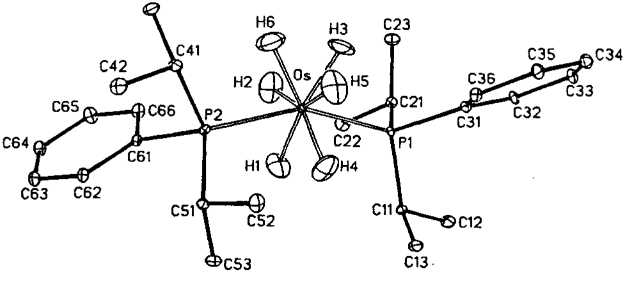

Figure 1.63 The structure of $OsH_6(PPr^i_2Ph)_2$. (Reprinted with permission from *Inorg. Chem.*, 1987., **26**, 2930. Copyright (1987) American Chemical Society.)

Tetrahydrides

Several of these complexes have been made:

$$mer\text{-}OsCl_3(PMe_2Ph)_3 \xrightarrow[EtOH]{NaBH_4} OsH_4(PMe_2Ph)_3$$

with others (L = PBu_3, PPh_3, PEt_2Ph, $AsEtPh_2$) synthesized by the same general route [160, 163].

The low-frequency NMR spectrum of $OsH_4(PMe_2Ph)_3$ shows a 1 : 3 : 3 : 1 quartet owing to coupling with three equivalent phosphines ($\delta = 8.81$ ppm, J(P–H) 6.2 Hz) and IR bands to O–H stretching at 2033, 1970, 1861 and 1806 cm^{-1} (in C_6H_6). The equivalence of the phosphines could be the result of strong P–P coupling or (more likely) of the molecule being fluxional in solution; in the solid state the structure (Figure 1.64) is a distorted pentagonal bipyramid.

The axial P–Os–P angle is 166°, so the three atoms are not quite colinear (Os–P 2.311 Å); the unique Os–P bond is slightly longer at 2.347 Å, showing a *trans*-effect of hydride. Os–H bonds average 1.663 Å [164].

In the similar $OsH_4(PEt_2Ph)_3$, the Os–P bonds are 2.296 Å (axial) and 2.339 Å (equatorial). MO calculations have been used to explain the

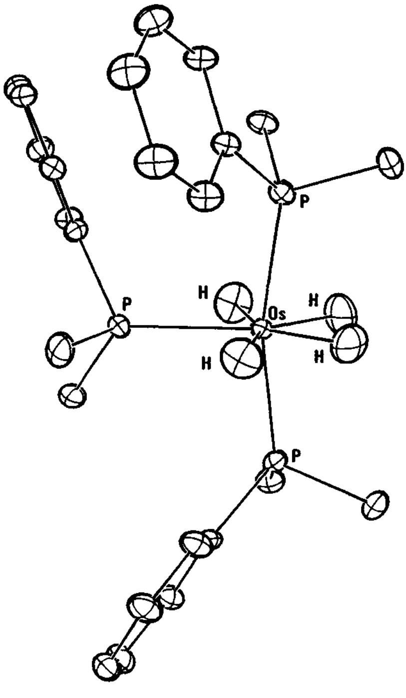

Figure 1.64 The structure of $OsH_4(PMe_2Ph)_3$. (Reprinted with permission from *J. Am. Chem. Soc.*, 1977, **99**, 7557. Copyright (1977) American Chemical Society.)

preference of neutral phosphine ligands for axial sites [165]: $OsH_4(PMe_2Ph)_3$ undergoes photodissociation

$$OsH_4(PMe_2Ph)_3 \rightarrow OsH_2(PMe_2Ph)_3 + H_2$$

Under high hydrogen pressure, $OsH_6(PMe_2Ph)_2$ is formed, with excess phosphine *cis*-$OsH_2(PMe_2Ph)_4$. However, photolysis *in vacuo* gives dimers $Os_2H_4(PMe_2Ph)_6$ and $Os_2H_4(PMe_2Ph)_5$, the former decomposing further to afford a very unusual paramagnetic osmium(III) species, $[OsH_4(PMe_2Ph)_2]^-$.

Deprotonation of $OsH_4(PMe_2Ph)_3$ with excess KH in thf at 70°C leads to lipophilic $K^+[fac\text{-}OsH_3(PMe_2Ph)_3]^-$. In the solid state, this has a dimeric structure with phenyl rings helping it present a hydrocarbon-like exterior to solvents (Os–H 1.66–1.69 Å, Os–P 2.271–2.28 Å) [166].

$$OsH_3(PMe_2Ph)_3 + KH \rightarrow H_2 + K[fac\text{-}OsH_3(PMe_2Ph)_3]$$

Dihydrides

Reaction of $OsH_4(PR_3)_3$ with tertiary phosphines gives dihydrides $OsH_2(PR_3)_4$ ($PR_3 = PMePh_2, PMe_2Ph, PEt_2Ph$, etc.) [163]:

$$OsH_4(PR_3)_3 + PR_3 \xrightarrow{\text{toluene}} OsH_2(PR_3)_4 + H_2$$

The IR spectra show two ν(Os–H) bands (1950 and 1920 cm^{-1} for $PR_3 = PMe_2Ph$); this supports a *cis*-structure (a *trans*-structure would only give one band), a conclusion supported by the NMR data. These compounds, therefore, have rigid structures.

Some diphosphines give *trans*-dihydrides

$$cis\text{-}OsX_2(L{-}L)_2 \xrightarrow{LiAlH_4} trans\text{-}OsH_2(L{-}L)_2 \qquad (L{-}L = o\text{-}C_6H_4(PEt_2)_2)$$

These have simple IR spectra with only one ν(Os–H) band.

With some bulky phosphines, $OsH_2Cl_2(PR_3)_2$ have been obtained (PR_3, e.g. PPr^i_3, $PMeBu^t_2$) [167]

$$OsCl_3.xH_2O \xrightarrow[Pr^iOH/boil]{PR_3} OsH_2Cl_2(PR_3)_2$$

These are diamagnetic 16 electron species (reaction in methanol or 2-methoxyethanol gives $OsH(CO)Cl(PR_3)_2$, presumably because the alcohol is oxidized to an aldehyde that can be a source of CO) (Figure 1.65). These

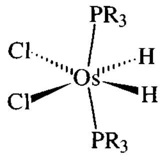

Figure 1.65 Structure of the hydride $OsH_2Cl_2(PR_3)_2$.

complexes have *cis*-arrangements of the hydride and chloride ligands with *trans*-phosphines with very distorted octahedral coordination, with R–Os–P 112° and Cl–Os–Cl 83°; they are fluxional in solution.

The $PMeBu^t_2$ and PPr^i_3 complexes react to attain an 18 electron system in various ways

$$OsH_2Cl_2(PR_3)_2 \xrightarrow{\text{exc. } PMe_3} cis\text{-}OsCl_2(PMe_3)_4$$

$$OsH_2Cl_2(PR_3)_2 \xrightarrow{BH_4^-} OsH_6(PR_3)_2$$

$$OsH_2Cl_2(PR_3)_2 \xrightarrow{CO} \text{all } trans\text{-}Os(CO)_2Cl_2(PR_3)_2$$

$$OsH_2Cl_2(PR_3)_2 \overset{H_2}{\Longleftrightarrow} OsH_4Cl_2(PR_3)_2$$

The structure of $OsH_4Cl_2(PPr^i_3)_2$ shows *cis*-chlorides and *trans*-phosphines occupying four vertices of an octahedron, but the hydrogens were not located [168].

With less bulky phosphines, 18 electron $OsH_2Cl_2(PR_3)_3$ are known

$$mer\text{-}OsCl_3(PEt_2Ph)_3 \xrightarrow[H_2/THF]{Zn/Hg} OsH_2Cl_2(PEt_2Ph)_3$$

$OsH_2Cl_2(PPr^i_2)_2$ can be converted into trihydrides $OsH_3X(PPr^i_3)_2$

$$OsH_2Cl_2L_2 \xrightarrow{Me_3SiX} OsH_2X_2L_2 \xrightarrow[-HX]{H_2} OsH_2XL_2 \xrightarrow{Ar} OsH_3XL_2$$

($L = PPr^i_3$; X = Cl, Br, I)

NMR and other evidence suggests [169] that these are 'classical' octahedral hydrides (with, as usual, *trans*-phosphines).

Cationic hydrides

Several cationic hydrides have been studied in detail [170] to assess whether they are classical hydrides or dihydrogen complexes. $OsH_3(PPh_3)_4^+$ appears to be a classical hydride but $OsH_5(PPh_3)_3^+$ is thought to be $OsH_3(\eta^2\text{-}H_2)(PPh_3)_3^+$ and $OsH_3[P(OR)_3]_4^+$ is $OsH(\eta^2\text{-}H_2)[P(OR)_3]^+$. These are typically made by protonation:

$$OsH_2[P(OR)_3]_4 \xrightarrow{HBF_4/Et_2O} OsH_3[P(OR)_3]_4^+ \qquad (R = Me, Et)$$

NMR evidence has been used to support similar structures $trans\text{-}[OsH(\eta^2\text{-}H_2)(R_2(CH_2)_2PR_2)_2]^+$ (R = Ph, Et); an X-ray diffraction study (R = Ph) has shown the planar OsP_4 arrangement but without locating the hydrogens [171]. MO calculations for $[OsH_5(PR_3)_3]^+$ predict the (observed) dodecahedral structure [172]; the crystal structure of $[OsH_5(PMe_2Ph)_3]BF_4$ shows that it is a classical hydride (Os–H 1.62–1.65 Å) but with rather short H–H distances.

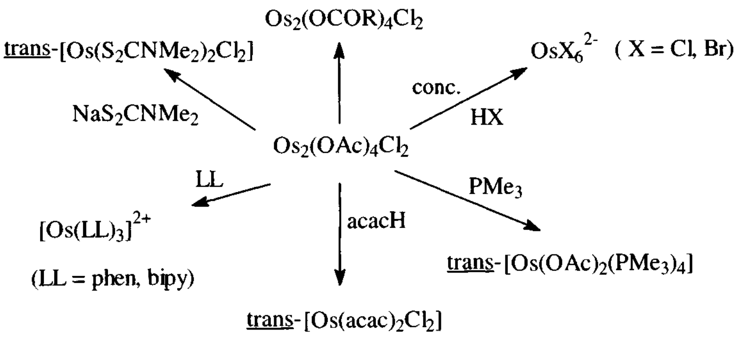

Figure 1.66 Reactions of the dimeric $Os_2(OAc)_4Cl_2$.

1.11.3 Carboxylate complexes

The carboxylates complexes of osmium have been studied less than the ruthenium analogues [173].

Reaction of $OsCl_6^{2-}$ with acetic acid/acetic anhydride mixtures containing concentrated HCl gives the diosmium compound $Os_2(OAc)_4Cl_2$ (rather than mixed-valence species, see section 1.8.3); other carboxylates can be made by carboxylate exchange:

$$OsCl_6^{2-} \xrightarrow[(MeCO)_2O/HCl]{MeCOOH} Os_2(OAc)_4Cl_2 \xrightarrow{RCO_2H} Os_2(OCOR)_4Cl_2$$

($R = C_3H_7$, CH_2Cl, $o\text{-}PhC_6H_4$, etc.).

They have binuclear tetracarboxylate-bridged 'lantern' structures: in the butyrate Os–Os is 2.301 Å and Os–Cl 2.417 Å. Most reactions involve cleavage of the Os–Os bond (Figure 1.66).

1.11.4 Nitrosyl complexes [12, 115]

The pattern of behaviour in osmium nitrosyls seems to be similar to that seen with ruthenium, though fewer data are available. The most common type of complex has octahedrally coordinated osmium(II) with linear Os–N–O linkage. Some syntheses are shown in Figure 1.67.

The $\{Os(NO)\}^6$ compound $Os(NO)Cl_3(PPh_3)_2$ doubtless has linear nitrosyls, like the ruthenium analogues (section 1.8.5) and $Os(NO)Cl_5^{2-}$.

A recent report concerns the $\{Os(NO)\}^8$ compound *trans*-$Os(NO)Cl(PPr^i_3)_2$, which has a linear Os–N–O linkage [174]

$$Os(NO)Cl(PPh_3)_3 \xrightarrow{PPr^i_3} Os(NO)Cl(PPr^i_3)_2$$

Introducing the bulky tri(isopropyl)phosphine causes a decrease in coordination number. This 16 electron compound undergoes a range of

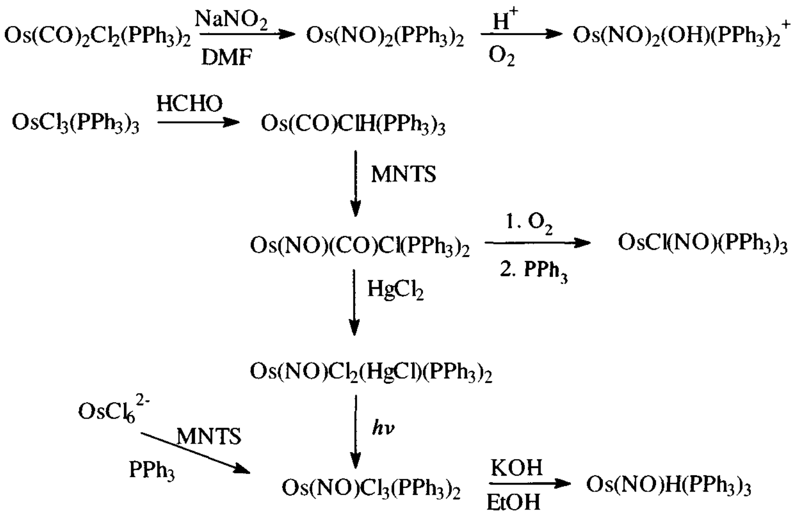

Figure 1.67 Syntheses of some osmium nitrosyl complexes.

oxidative-addition reactions to afford 18 electron species.

$$\mathrm{Os(NO)Cl(PPr^i_3)_2 + XY \rightarrow Os(NO)Cl(X)(Y)(PPr^i_3)_2}$$

$(\mathrm{XY} = \mathrm{H_2, I_2, HCl, MeI, MeOH})$

$$\begin{array}{lcl} \mathrm{Os(NO)Cl(PPr^i_3)_2 + CO} & \longrightarrow & \mathrm{Os(NO)Cl(CO)(PPr^i_3)_2} \\ \nu(\mathrm{N{-}O})\ 1700\,\mathrm{cm^{-1}} & & \nu(\mathrm{N{-}O})\ 1755\,\mathrm{cm^{-1}}, \\ & & \nu(\mathrm{C{-}O})\ 1895\,\mathrm{cm^{-1}} \end{array}$$

$\mathrm{Os(NO)_2(PPh_3)_2}$, an $\{\mathrm{Os(NO)_2}\}^{10}$ system, is tetrahedral like the ruthenium analogue (Os–N 1.771–1.776 Å, Os–N–O 174.1–178.7°; ν(N–O) 1616, 1665 $\mathrm{cm^{-1}}$) and is converted on oxidation in acid solution to the dinitrosyl $[\mathrm{Os(NO)_2(OH)(PPh_3)_2}]^+$, which has two widely separated IR bands (1842, 1632 $\mathrm{cm^{-1}}$ in the $\mathrm{BF_4}$ salt); the two modes of nitrosyl coordination are confirmed by the crystal structure (Figure 1.68) [175].

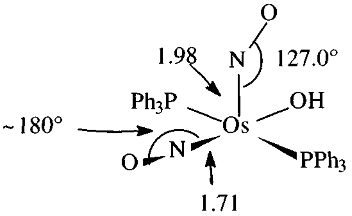

Figure 1.68 The structure of $[\mathrm{Os(NO)_2(OH)(PPh_3)_2}]^+$.

1.11.5 Other osmium complexes

Osmium forms a 6-coordinate acetylacetonate, $Os(acac)_3$, isomorphous with the ruthenium analogue; unlike ruthenium, however, the osmium(IV) complexes $Os(acac)_2X_2$ (X = Cl, Br, I) can be made (*cis*- and *trans*-isomers exist) from OsX_6^{2-} and Hacac, as can $Os(acac)X_4^-$ [176].

The pyridine complexes of osmium(III) result from reductive substitution

$$OsI_6^{2-} \xrightarrow{py} mer\text{-}Ospy_3I_3 \xrightarrow[CH_2Cl_2]{X_2} mer\text{-}Ospy_3X_3 \qquad (X = Cl, Br)$$

while under different conditions the osmium(II) complexes $Ospy_4X_2$ can be made.

The osmium(IV) complexes can be made by oxidation of the osmium(III) systems [152]:

$$mer\text{-}OsCl_3py_3 \xrightarrow{Cl_2 \text{ or } Ce^{4+}} mer\text{-}[OsCl_3py_3]^+Cl^-$$

mer-$OsCl_3py_3$ has also been made by electroreduction of $OsCl_6^{2-}$ in pyridine. The Os–Cl distances are 2.376 Å (*trans* to py) and 2.357–2.359 Å (*trans* to Cl) with corresponding Os–N distances of 2.086 (*trans* to Cl) and 2.090–2.097 Å (*trans* to N) [177].

The sulphur-containing analogue of the acetylacetonate $Os(MeCSCHCSMe)_3$ results from the reaction of OsO_4 with acetylacetone and H_2S. The most thoroughly studied complexes, as with ruthenium, are the dithiocarbamates, both $Os(S_2CNEt_2)_n$ ($n = 3, 4$) resulting from the reaction of $OsCl_6^{2-}$ with NaS_2CNEt_2. Oxidation of $Os(S_2CNEt_2)_3$ gives $Os(S_2CNEt_2)_3X$; where X is a halide, the product is probably a 7-coordinate monomer. When X = PF_6, dimeric ions $[Os_2(S_2CNEt_2)_6]^{2+}$ have been isolated in the solid state: bridging dithiocarbamate enables the osmium to have pentagonal bipyramidal 7-coordination [178]. Thiolates have also been reported in the (+4) state [179].

Dissolving $OsCl_5$ in MeCN at room temperature leads to reduction and the formation of *cis*-$OsCl_4(MeCN)_2$. Most nitrile complexes, however, feature phosphines and arsines as co-ligands. Reaction of $OsCl_3(AsPh_3)_3$ with *p*-tolylisocyanide gives the three isomers of $OsCl_3(RNC)_2(AsPh_3)$ (R = *p*-MeC_6H_4) [180].

1.12 Compounds in high oxidation states

There is a vigorously expanding chemistry of compounds of ruthenium and osmium in high oxidation states [3, 4, 11, 12], particularly of dioxo and nitrido compounds, though recently some striking developments have taken place in imide chemistry.

1.12.1 Compounds of the MO_2^{2+} *group*

The osmium MO_2^{2+} compounds are much more numerous and have greater stability.

The first component to be identified was the yellow ammine (Frémy, 1844):

$$trans\text{-}K_2OsO_2(OH)_4 \xrightarrow{NH_4Cl} trans\text{-}[OsO_2(NH_3)_4]Cl_2$$

though the most important is probably $OsO_2(OH)_4^{2-}$

$$OsO_4 \xrightarrow[EtOH]{KOH} K_2OsO_2(OH)_4$$

OsO_2^{2+}, sometimes called the 'osmyl' group, is usually linear (a few *cis*-dioxo linkages are known) with short Os–O bonds (around 1.8 Å) indicative of π-bonding. The osmium uses two orbitals (one is shown in Figure 1.69) to form two π-bonds with the two oxygen atoms, giving rise to two bonding, two non-bonding and two anti-bonding π-orbitals.

The bonding and non-bonding orbitals, together with the two Os–O σ-bonding orbitals are occupied by the 12 electrons from the two oxide ions. The two electrons from Os^{6+}occupy the low-lying d_{xy} orbital, giving rise to the observed characteristic absorptions in the IR spectrum *c.* 830–850 cm^{-1} (e.g. in $OsO_2(NH_3)_4Cl_2$ at 828 cm^{-1}, with the corresponding symmetric stretching frequency at 865 cm^{-1}) [181].

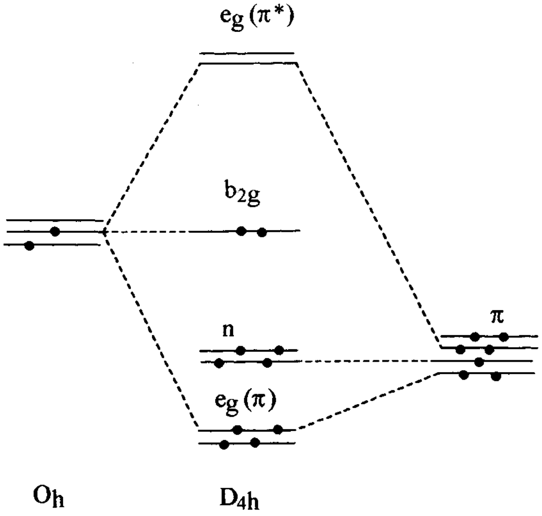

Figure 1.69 The π-bonding in the osmyl ion OsO_2^{2+}.

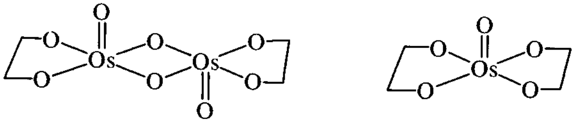

'monoester' 'diester'

Figure 1.70 Products of the reaction of OsO_4 with alkenes.

Compounds that are O- and N-donors like oxalate and ethylenediamine are able to support the +6 oxidation state

$$OsO_4 \xrightarrow[M^+]{H_2C_2O_4} M_2OsO_2(C_2O_4)_2 \qquad (M = \text{alkali metal})$$

$$OsO_2(OH)_4^{2-} \xrightarrow{\text{en.2HCl}} [OsO_2(en)_2]Cl_2$$

(the latter having Os=O 1.74 Å, Os–N 2.11 Å, O–Os–O 180°), but it is perhaps more surprising that tertiary phosphine complexes exist in this state (section 1.11.2)

$$OsO_4 \xrightarrow[\text{EtOH/HCl}]{PR_3} \textit{trans}\text{-}OsO_2Cl_2(PR_3)_2$$

(PR_3, e.g. PPh_3, PMe_2Ph, PPr^i_2Ph), though short reaction times are necessary to prevent further reduction and the trialkyl phosphines are too strongly reducing to allow the isolation of their complexes [140].

Osmate esters are important intermediates in the reactions of OsO_4 in the stereospecific *cis*-hydroxylation of alkenes and other unsaturated molecules [182].

Alkenes (R) react with OsO_4 to give two kinds of esters: the so-called monoesters $OsO_2(O_2R)$, which are actually dimers, ($Os_2O_4(O_2R)_2$) and diesters $OsO(O_2R)_2$ (Figure 1.70) [183].

The reaction of OsO_4 with alkenes is accelerated by nitrogenous bases (e.g. pyridine) forming an intermediate $OsO_2(O_2R)L_2$ that on hydrolysis gives the *cis*-diol $R(OH)_2$. Some salts are known of the type $K_2[OsO_2(O_2R)_2]$ (R, e.g. Me), which can be converted into esters

$$OsO_4 \xrightarrow[\text{MeOH}]{\text{KOH}} K_2OsO_2(OMe)_4 \xrightarrow[\text{glycol}]{\text{KOH/MeOH}} OsO(O_2R)_2$$

The product has a square pyramidal structure (IR ν(Os–O) 992 cm^{-1}) (Figure 1.71).

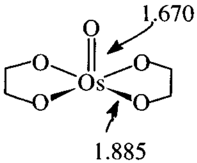

Figure 1.71 Bond lengths in the ester $OsO(OCH_2CH_2O)_2$.

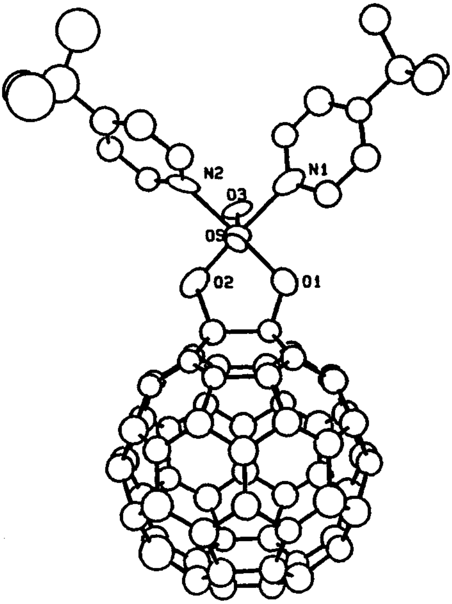

Figure 1.72 The structure of $(C_{60})OsO_4(Bu^tpy)_2$. (Reprinted with permission from *Science*, 1991, **252**, 312.) Copyright (1991) American Association for the Advancement of Science.)

A striking example of the ability of OsO_4 to add to unsaturated C–C linkages is provided by its reaction with C_{60}, buckminsterfullerene (Figure 1.72) [184]

$$C_{60} + OsO_4 \xrightarrow[\text{toluene}]{Bu^tpy} C_{60}(OsO_4)(Bu^tpy)_2$$

The olive-green osmium(VI) octaethylporphyrin complex $OsO_2(OEP)$ (IR ν(Os–O) 825 cm^{-1}) is representative of a number of 'osmyl' porphyrins [185]; they can readily be transformed into a number of osmium porphyrins in lower oxidation states (Figure 1.73).

$OsO_2(OEP)$ has Os=O 1.745 Å and Os–N 2.052 Å. $OsO_2(TMP)$ has Os=O 1.743 Å, Os–N 2.066 Å (TMP = tetramesitylporphyrin).

The osmium(VI) arylimide $Os(TTP)(NAr)_2$ (TTP = tetra(*p*-tolyl)porphyrin; Ar = *p*-$NO_2C_6H_4$) also has short Os=NAr distances (1.820–1.822 Å) [186].

One of the rare examples of a compound with a *cis*-OsO_2 group is made:

$$Os(bipy)_2CO_3 \xrightarrow[Ce^{4+}]{HClO_4} cis\text{-}[OsO_2bipy_2](ClO_4)_2$$

The green *cis*-compound isomerizes to the beige *trans*-isomer on heating in MeCN [187]. Another *cis*-compound is *cis*-$[OsO_2(OAc)_3]$, with O–Os–O 125°; two acetates are monodentate and one is bidentate.

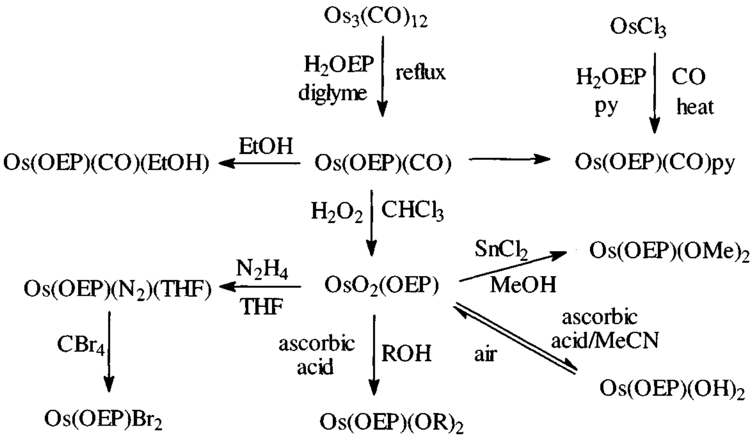

Figure 1.73 Osmium porphyrin complexes.

1.12.2 Nitride complexes

Another type of osmium(VI) compound involving multiple bonds can be viewed as a derivative of OsN^{3+}. The nitrides have attracted interest as they are often photoluminescent

$$KOsO_3N \xrightarrow{HCl\,(aq.)} K_2[OsNCl_5]$$

The Os≡N group has a strong *trans*-influence, reflected in both the labilization of the *trans*-chloride (a similar reaction occurs with $OsNBr_5^{2-}$) and in the pronounced lengthening of the *trans*-Os–Cl bond (2.605 Å versus 2.362 Å).

$$OsNCl_5^{2-} \xrightarrow{H_2O} trans\text{-}OsNCl_4(H_2O)^-$$

With large organic cluster ions (e.g. Ph_4As^+) pink 5-coordinate $OsNX_4^-$ (X = Cl, Br) is obtained. Red $OsNI_4^-$ is made:

$$OsO_3N^- \xrightarrow[Ph_4AsI]{HI\,(aq.)} (Ph_4As)^+(OsNI_4)^-$$

All the $OsNX_4^-$ complexes are distorted square pyramids (with N–Os–X angles of 103.7 to 104.5°) [188]. The stability of an osmium(VI) to iodine bond is unusual and is presumably owing to the extensive Os≡N π-bonding reducing the positive charge on the metal and stabilizing it to reduction.

IR and structural data for these species are given in Table 1.15 [189].

A definite nitrido coordination chemistry has grown up including abstraction of sulphur from thiocyanate (Figure 1.74).

$[OsN(S_2Cl_2(CN)_2)_2]^-$ is square pyramidal (Os≡N 1.639 Å, ν(Os–N) 1074 cm^{-1}).

Pyrazine (1,4-diazine) will bridge two $OsNCl_4$ fragments in $[Cl_4NOs(pyrazine)OsNCl_4]^{2-}$ where the chlorines are bent slightly away from the terminal N (IR ν(Os–N) 1105 cm^{-1}, Os–N 1.63 Å) [190].

Table 1.15 IR and structural data for $OsNX_4Y$ species

	ν(Os–N) (cm^{-1})	Os–N (Å)	Os–X (Å)	Os–Y (Å)
$OsNCl_5^{2-}$	1084	1.614	2.361	2.605
$OsNBr_5^{2-}$	1085	–	–	–
$OsNCl_4(H_2O)^-$	–	1.74	2.34	2.50
$OsNBr_4(H_2O)^-$	1109	1.67	2.486	2.42
$OsNCl_4^-$	1123	1.604	2.320	–
$OsNBr_4^-$	1119	1.583	2.457	–
$OsNI_4^-$	1107	1.616	2.662	–

Phosphine complexes like $OsN(PMe_3)_2(R_2)Cl$ ($R = CH_2SiMe_3$) with chloride *trans* to nitride, and *trans*-phosphines and *trans*-alkyls, have been made [191].

Me_3NO (but not Ph_3PO or C_5H_5NO) oxidizes a nitride group into a nitrosyl

$$OsN(terpy)Cl_2]^+ + Me_3NO \rightarrow [Os(NO)(terpy)Cl_2]^+ + Me_3N$$

The change in formal oxidation state from osmium(VI) to osmium(II) is noteworthy [192].

A similar chemistry has been found for ruthenium nitrides. They can be made, starting from ice-cold $RuO_2X_4^{2-}$ solutions:

$$RuO_2X_4^{2-} \xrightarrow[CsX]{NaN_3} Cs_2RuNX_5 \qquad (X = Cl, Br)$$

Again, with big 'organic' cations (Ph_4As, Bu_4N) 5-coordinate $RuNX_4^-$ are formed. $Ph_4AsRuNCl_4$ is isomorphous with the osmium analogue (Ru–N 1.570 Å; ν(Ru–N) 1092 cm^{-1}).

A number of dimeric nitride-bridged complexes have been synthesized [193]

$$Ru(NO)Cl_5^{2-} \xrightarrow{SnCl_2} [Ru_2NCl_8(H_2O)_8]^{3-}$$

$$OsCl_6^{2-} \xrightarrow[100°C]{NH_4OH} [Os_2N(NH_3)_8Cl_2]^{3+}$$

$$(NH_4)_2OsCl_6 \xrightarrow[2.\,HX]{1.\,X_2,\,400°C} [Os_2NX_8(H_2O)_2]^{3-} \qquad (X = Cl, Br)$$

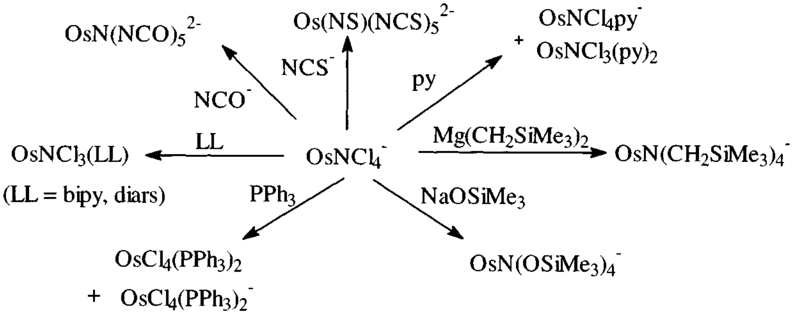

Figure 1.74 Osmium nitrido complexes.

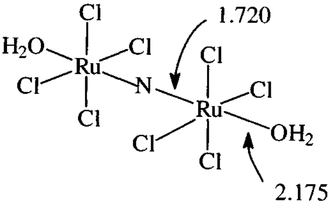

Figure 1.75 The structure of the dimeric nitrido complex $[Ru_2NCl_8(H_2O)_2]^{3-}$.

They resemble the oxygen-bridged $[M_2OCl_{10}]^{4-}$ (section 1.3.6) (Figure 1.75) with M–N stretching frequencies similar to those in the mononuclear complexes (1108 cm^{-1} in $[Os_2N(NH_3)_8Cl_2]Cl_3$).

$Os_2N(S_2CNR_2)_5$ has a dithiocarbamate bridge as well as the nitride bridge.

1.12.3 Imides

Organic imide ligands have also been used to stabilize high oxidation states. The best example of this is the osmium(VIII) compound $Os(NBu^t)_4$, which has a distorted tetrahedral OsN_4 core (N–Os–N 104.6–111.9°; Os–N 1.750 Å) [194].

$$OsO_4 \xrightarrow{NHBu^t(SiMe_3)} Os(NBu^t)_4$$

It is a volatile orange–red crystalline solid (m.p. 30°C), stable to over 100°C. On reduction with tertiary phosphines or sodium amalgam, $Os(NBu^t)_3$ is formed, which is dimeric $(Bu^tN)_2Os(\mu\text{-}NBu^t)_2Os(NBu^t)_2$. This can be oxidized to the osmium(VII) dication with concomitant shortening in the Os–Os distance from 3.1 to 2.68 Å.

The planar 3-coordinate $Os(NAr)_3$ (Figure 1.76) ($Ar = 2,6\text{-}Pr^i_2C_6H_3$) doubtless owes its monomeric character to the greater bulk of the aryl substituent.

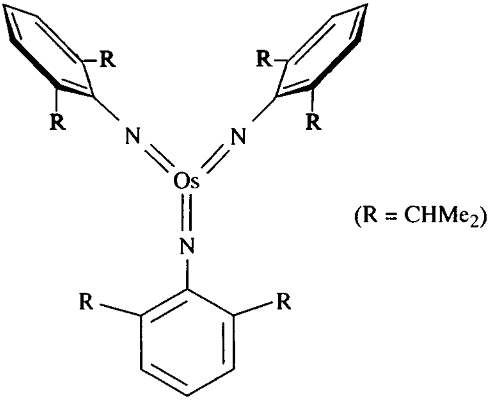

Figure 1.76 The 3-coordinate osmium(VI) imide $Os(NAr)_3$ ($Ar = 2,6Pr^i_2C_6H_3$).

In the solid state, the orientations of the rings differ markedly, but in solution only one NMR signal is seen even at −90°C. The short Os–N bonds (1.736–1.738 Å) show multiple-bond character.

When $Os(NAr)_3$ is prepared by

$$OsO_4 + ArNCO \xrightarrow[\text{reflux 20 h}]{\text{heptane}} Os(NAr)_3$$

it does not form Lewis base adducts but tends to be reduced to *trans*-$Os(NAr)_2(PR_3)_2$ (with pyHCl) and *trans*-$Os(NAr)_2(PR_3)_2$ (with phosphines). Oxidation of $Os(NAr)_2(PMe_2Ph)_2$ with Me_3NO gives $Os(NAr)_2O_2$ (IR ν(Os–O) 883, 877 cm^{-1}). OsO_4 reacts with $Mo(NAr)_2(OBu^t)_2$ to give $Os(NAr)_2O_2$ and $Os(NAr)_3O$ [195].

Imidoaryls can be made [196]:

$$OsO_2R_2 + 2Ta(NAr)(OBu^t)_3 \rightarrow Os(NAr)_2R_2 + 2TaO(OBu^t)_3$$

($R = CH_2SiMe_3$, CH_2Bu^t, CH_2CMe_2Ph; $NAr = NC_6H_3$ (2,6-$Pr^i)_2$).

1.13 Simple alkyls and aryls

Ruthenium and osmium form some remarkably stable alkyls and aryls compounds, often in unusually high oxidation states.

Like rhodium and iridium, ruthenium forms a (thermally unstable above 0°C) hexamethylate anion

$$RuCl_3(tht)_3 \xrightarrow[\text{2. tmed}]{\text{1. MeLi/Et}_2\text{O}} (Li\,tmed)_3RuMe_6$$

($tht = C_4H_8S$; $tmed = Me_2N(CH_2)_2NMe_2$).

Alkyls Ru_2R_6 ($R = CH_2CMe_3$, CH_2SiMe_3) have been made using $Ru_2(OAc)_4Cl$ as starting materials; they have staggered ethane-like structures with, formally, Ru–Ru triple bonds. Though pyrophoric and light sensitive, they are thermally stable (melting above 100°C); ruthenium inserts oxygen at low temperatures to form asymmetrically dioxygen bridged alkyls (Figure 1.77).

The short Ru–O bond has multiple-bond character (IR ν(Ru–O) 908 cm^{-1}).

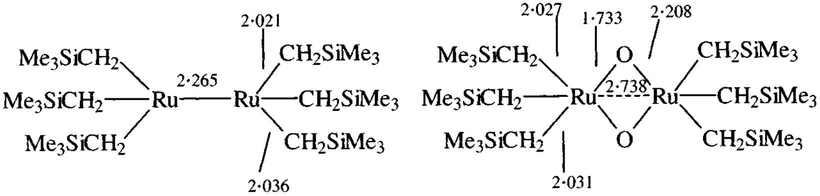

Figure 1.77 The structure of two ruthenium alkyls.

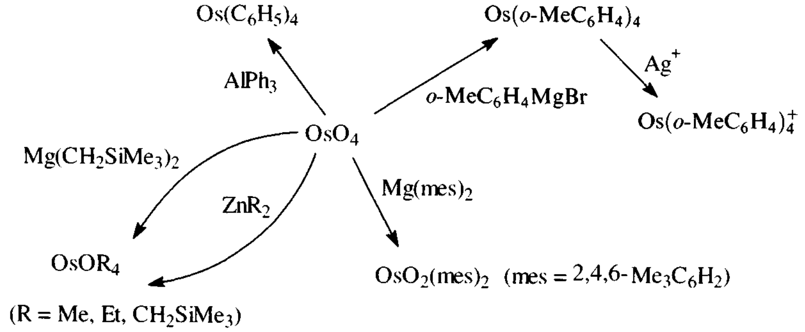

Figure 1.78 Syntheses of osmium alkyls and aryls.

Ruthenium(IV) compounds are prepared by:

$$Ru_2(OAc)_4Cl \xrightarrow{C_6H_{11}MgCl} Ru(cyclohexyl)_4$$

$$RuCl_3(tht)_3 \xrightarrow{Mg(mes)_2(Et_2O)_2} Ru(mesityl)_4$$

(tht, tetrahydrothiophen). The latter can be oxidized with $NOPF_6$ to form paramagnetic $Ru(mesityl)_4^+PF_6^-$. Both the ruthenium(IV) compounds have essentially tetrahedral geometries (Ru–C 2.01–2.02 Å; C–Ru–C 98.9–127.4° in the mesityl) [197].

Osmium forms a number of compounds in the +4, +5 and +6 states. $OsAr_4$ (Ar = Ph, *o*-tolyl, cyclohexyl) has tetrahedral coordination of osmium (e.g. Os–C 1.994 Å in $Os(C_6H_5)_4$). The tetraphenyl and tetra(cyclohexyl) compounds are air sensitive, but the *o*-tolyl is very inert (stable to O_2, CO, NO) presumably owing to the *ortho*-methyls shielding the osmium; the latter can be oxidized to paramagnetic $Os(o\text{-tolyl})_4^+$ (with little change in the Os–C bond length). Osmium(IV) tetraaryls undergo a reductive elimination in the presence of PR_3 (R, e.g. Me, OMe, OEt) by an associative mechanism [198].

$$OsAr_4 + PMe_3 \rightarrow Os(\eta^6\text{-}Ar_2)(Ar)_2(PMe_3)$$

$$Os(\eta^6\text{-}Ar_2)Ar_2(PMe_3) + 3PMe_3 \rightarrow Ar_2 + Os(Ar)_2(PMe_3)_4$$

$(Ar = 2\text{-}MeC_6H_4)$.

The volatile (50°C, 0.1 mmHg) air-stable osmium(VI) mesityl $OsO_2(mes)_2$ is also diamagnetic ($5d^2$); it has IR bands at 918–950 cm^{-1} owing to Os–O stretching. There is some distortion from tetrahedral geometry (O–Os–O 136°, C–Os–C 96°) possibly owing to the steric influence of the non-bonding electron pair. The corresponding xylyl also exists [199]. Zinc dialkyls can be used to make OsO_2R_2 systems:

$$(Ph_4P)_2[OsO_2Cl_4] \xrightarrow{ZnR_2} OsO_2R_2$$

$(R = CH_2CMe_3, CH_2SiMe_3, CH_2CMe_2Ph, \text{mesityl})$.

Alkyldene and alkylidyne compounds have also been made [200].

The diamagnetic $OsOR_4$ (again osmium(VI)) has square pyramidal structures (Os=O 1.681 Å, Os–Me 2.086 Å in $OsOMe_4$) and is volatile *in vacuo* at room temperature (IR ν(Os=O) 1013 cm^{-1}); the related $OsO(CH_2SiMe_3)_4$ melts at 15°C (IR ν(Os=O) 1040 cm^{-1}). In $OsO(CH_2CHMe_2)_4$, Os=O is 1.642 Å and Os–C 2.120 Å (ν(Os=O) 990 cm^{-1}) [201].

2 Rhodium and iridium

2.1 Introduction

Rhodium and iridium were discovered independently in the same year and also share many resemblances in their chemistry [1–10]. They form a wide range of conventional complexes as well as those of π-bonding ligands. Both metals exhibit an extensive chemistry, principally in the +3 oxidation state, with +1 also being important, and a significant chemistry of iridium +4 existing. Few compounds are known in the +2 state, in contrast to the situation for cobalt, their lighter homologue (factors responsible include the increased stability of the +3 state consequent upon the greater stabilization of the low spin d^6 configuration as 10 Dq increases).

Rhodium was discovered in 1803 by the eminent Norfolk scientist W.H. Wollaston; he dissolved platinum metal concentrates in aqua regia and found that on removing platinum and palladium he was left with a red solution. From this he obtained the salt Na_3RhCl_6, which yielded the metal on reduction with hydrogen. The rose-red colour (Greek rhodon) of many rhodium salts gave the element its name.

In the same year, Smithson Tennant was studying the black aqua regia-insoluble portion of platinum ores and found that, after fusion with soda and extraction with water, the black residue gave a blue solution in hydrochloric acid that went red when heated. The red crystals thus obtained yielded the metal on heating. Tennant gave iridium its name from the Greek iris (rainbow) ‘from the striking variety of colours which it gives’.

2.2 The elements and uses

Both rhodium (m.p. 1976°C, b.p. 3730°C) and iridium (m.p. 2410°C, b.p. 4130°C) are unreactive silvery metals, iridium being considerably more dense ($22.65\,\mathrm{g\,cm^{-3}}$) than rhodium ($12.41\,\mathrm{g\,cm^{-3}}$), the densest element known apart from osmium. Both form fcc (ccp) lattices and, like the other platinum metals, are ductile and malleable. Neither is affected by aqua regia and they only react with oxygen and the halogens at red heat.

The main use of rhodium is with platinum in catalysts for oxidation of automobile exhaust emissions. In the chemical industry, it is used in catalysts for the manufacture of ethanoic acid, in hydroformylation of alkenes and the synthesis of nitric acid from ammonia. Many applications of iridium rely on its inertness (e.g. high temperature crucibles, electrode coatings, thermocouples); it is speculated that applications include defence, nuclear and aerospace industries. The inert alloy with osmium is traditionally used in pen nibs.

2.2.1 Extraction

Rhodium and iridium are obtained from the aqua regia-insoluble residues by first smelting with PbO or $PbCO_3$ then treating the product with nitric acid to remove silver along with the lead [11]. The residue is smelted with $NaHSO_4$ which converts the rhodium into soluble $Rh_2(SO_4)_3$, while peroxide fusion of the residues leaves an insoluble residue of IrO_2. Traditionally these products were purified in several stages involving repeated precipitation and solution, ultimately affording the pure salts $(NH_4)_3MCl_6$ (M = Rh, Ir), which then yielded the metal on hydrogen reduction at 1000°C. A more up to date process uses solvent extraction to give a more efficient and rapid separation.

2.3 Halides and halide complexes [3b, 4]

2.3.1 Rhodium halides

Rhodium halides occur mainly in the +3 state. In some cases where a 'soluble' and 'insoluble' form have been reported, the former may be a hydrate.

RhF_3 [12] can be conveniently made by fluorination

$$RhCl_3 \xrightarrow[500^\circ C]{F_2} RhF_3$$

It has the VF_3 structure (Rh–F 1.961 Å) having a hcp array of fluorines with rhodium occupying 1/3 of the octahedral holes. Various hydrates have been reported

$$Rh(NO_2)_6^{3-} \xrightarrow{\text{conc. HF}} RhF_3.9H_2O$$

Insoluble red $RhCl_3$ is made by direct combination, with similar routes for the other trihalides

$$Rh \xrightarrow[800^\circ C]{Cl_2} RhCl_3$$

$$Rh \xrightarrow[\text{then } Br_2\ 400^\circ C]{45\%\ HBr/Br_2,\text{ heat}} RhBr_3\ (\text{red})$$

$$Rh \xrightarrow[400^\circ C]{I_2} RhI_3\ (\text{black})$$

All of these probably have the $AlCl_3$ structure (unconfirmed for RhI_3) with bond lengths (EXAFS) of 2.337 Å (Rh–Cl) [13] and 2.48 Å (Rh–Br) [14]. 'Soluble' chlorides and bromides are made by dissolving the oxide in the appropriate acid.

Rhodium trihalides (and complexes like K_3RhBr_6) are frequently added to photographic emulsions in trace quantities to improve the gradation of the emulsion (the 'rhodium effect') [15].

Only fluorides are known in higher oxidation states with tetra-, penta- and hexafluorides isolated.

$$RhBr_3 \xrightarrow{BrF_3} RhF_4.2BrF_3 \xrightarrow{heat} RhF_4$$

$$Rh \xrightarrow[400°C,\,6\,atm]{F_2} RhF_5$$

$$RhF_3 \xrightarrow[400°C]{F_2} RhF_5$$

$$RhF_5 \xrightarrow[250°C,\,30\,atm]{F_2} RhF_6$$

Little is known about the structure of purple paramagnetic RhF_4 ($\mu_{eff} = 1.1\,\mu_B$) but it may be similar to PdF_4 [16]. RhF_5 has a tetrameric structure [17] similar to RuF_5 and OsF_5 (section 1.3.4); the terminal Rh–F bonds are 1.808 Å and the bridges 2.01 Å. The ruby red solid (m.p. 95.5°C) has $\mu_{eff} = 2.39\,\mu_B$. Rhodium hexafluoride is a very reactive black solid (attacking glass at room temperature) vaporizing to a deep brown gas (triple point *c.* 70°C). EXAFS measurements indicate a Rh–F bond length of 1.838 Å [18].

Various ill-defined binary halides have been reported but not characterized, such as RhI_2.

2.3.2 *Iridium halides*

The pattern of iridium halides resembles rhodium, with the higher oxidation states only represented by fluorides. The instability of iridium(IV) halides, compared with stable complexes $IrCl_4L_2$ and the ions IrX_6^{2-} (X = Cl, Br, I), though unexpected, finds parallels with other metals, such as plutonium.

Preparations of the halides include [19]

$$IrF_4 \xrightarrow{400°C} IrF_3\,(black)$$

$$IrF_5 + SF_4 \xrightarrow{400°C} IrF_3 + SF_6$$

$$Ir \xrightarrow[600°C]{Cl_2} \alpha\text{-}IrCl_3\,(brown) \xrightarrow[vacuum]{750°C} \beta\text{-}IrCl_3\,(deep\ red)$$

$$Ir \xrightarrow[540°C, 8-9\,atm]{Br_2\,(sealed\,tube)} IrBr_3\ (yellow)$$

$$Ir(OH)_3 \xrightarrow[2.\,heat, 400°C]{1.\,HI\,20°C} IrI_3\ (black)$$

$$Ir + 2IrF_6 \xrightarrow{1\,to\,15\,torr} 3IrF_4\ (red-brown)\ [20]$$

$$2Ir + 5F_2 \xrightarrow{350-380°C} 2IrF_5\ (yellow-green)$$

$$Ir + 3F_2 \xrightarrow{240°C} IrF_6\ (yellow)$$

All the trihalides are known to have 6-coordinate iridium (except the unknown structure of IrI_3). IrF_3 has the PdF_3 structure; α-$IrCl_3$ and $IrBr_3$ have structures of the $AlCl_3$ type (Ir–Cl 2.30–2.39 Å in the former).

IrF_5 (until 1965 thought to be IrF_4) is paramagnetic ($\mu = 1.32\,\mu_B$) and has the same tetrameric structure as RhF_5; it has a slightly higher m.p. (104°C) than IrF_6, in keeping with the larger molecular units [21]. Like RhF_6, IrF_6 is very reactive, attacking most glass and undergoing slow photolysis to IrF_5. IrF_6 has a regular octahedral structure in the vapour (Ir–F 1.83 Å) and in the solid state (Ir–F 1.822 Å, EXAFS). It is paramagnetic with $\mu \sim 3\,\mu_B$; vibrational frequencies of the octahedral molecule have been assigned to bands at $719\,cm^{-1}$ (T_{1u}), $701.7\,cm^{-1}$ (A_{1g}) and $645\,cm^{-1}$ (E_g) [18, 22].

2.3.3 Halometallates

A wide range of MX_6^{n-} species exist, typical preparations appear below.

$$RhF_3 \xrightarrow[550°C]{KF, CsF} Cs_2KRhF_6\ (pink)$$

$$RhCl_3.3H_2O \xrightarrow[3M\,HCl]{ACl} A_3RhCl_6.H_2O \xrightarrow{heat} A_3RhCl_6\ (red)\ (A = K, Rb, Cs)$$

$$Rh(OH)_3 \xrightarrow[KBr]{HBr} K_3RhBr_6$$

$$RhF_3 \xrightarrow[NaCl]{BrF_3} Na_2RhF_6\ (yellow)$$

$$RhF_6 \xrightarrow[25°C]{NOF} (NO)_2RhF_6\ (yellow)$$

$$Cs_3RhCl_6 \xrightarrow{Cl_2\,or\,Ce^{4+}} Cs_2RhCl_6\ (dark\,green)$$

$$RhF_5 \xrightarrow[HF\,or\,IF_5, 20°C]{MF} MRhF_6\ (yellow\text{-}ochre)\ (M = K, Cs)$$

$$M_2IrF_6 \xrightarrow[MF]{N_2H_4} M_3IrF_6\ (M = K, Rb, Cs)$$

$$\mathrm{Ir} \xrightarrow[\mathrm{KCl}]{\mathrm{Cl_2}} \mathrm{K_2IrCl_6} \xrightarrow[80^{\circ}\mathrm{C}]{\mathrm{C_2O_4^{2-}}} \mathrm{K_3IrCl_6.H_2O}\ \text{(yellow)}$$

$$\mathrm{M_3IrCl_6} \xrightarrow[\mathrm{H_2O}]{\mathrm{HBr}} \mathrm{M_3IrBr_6.H_2O}\ \text{(green)}$$

$$\mathrm{Cs_3IrBr_6} \xrightarrow[160^{\circ}\mathrm{C}]{\mathrm{NaI}} \mathrm{Cs_3IrI_6}\ \text{(brown)}$$

$$\mathrm{MIrF_6} \xrightarrow{\mathrm{H_2O}} \mathrm{M_2IrF_6} + \mathrm{IrO_2} + \mathrm{O_2}\ (\mathrm{M} = \text{alkali metal})$$

$$\mathrm{IrO_2}.n\mathrm{H_2O} \xrightarrow[\mathrm{HBr}]{\mathrm{MBr}} \mathrm{M_2IrBr_6}\ \text{(purple)}$$

$$\mathrm{IrBr_3} \xrightarrow[\mathrm{BrF_3}]{\mathrm{KBr}} \mathrm{KIrF_6}\ \text{(white)}$$

$$\mathrm{IrF_6} \xrightarrow{\mathrm{NOF/F_2}} \mathrm{NO^+IrF_6^-}$$

IrI_6^{2-} does not exist: Ir^{4+} is too strongly oxidizing to coexist with the reducing I^-.

Points to note in these syntheses include the use of BrF_3 as an oxidizing agent, and the stability of IrX_6^{2-}, also used as a source of IrX_6^{3-}.

Structural data [23] (Table 2.1) confirm the presence of the hexahaloanions in these states; M_2RhF_7 (M = Sr, Pb) contain RhX_6^{3-} octahedra too, as do salts like $(MeNH_3)_4RhX_7$ (X = Cl, Br) and $(enH_2)_2RhX_7$.

Many of the compounds in higher oxidation states are reactive, and for moisture-sensitive solids that cannot be crystallized, some of the bond lengths quoted in Table 2.1 are from EXAFS measurements [24]. Raman spectroscopy is likewise well suited to studying such reactive compounds, and vibrational data for halometallates are given in Table 2.2; trends illustrated include the decrease in frequency as the oxidation state of the metal decreases, and similarly a decrease in vibrational frequency, for a given oxidation state, with increasing mass of the halogen.

Table 2.1 Bond lengths in hexahalometallate ions and related species

Rhodium	Rh–X (Å)	Iridium	Ir–X (Å)
RhF_6	1.838	IrF_6	1.822
RhF_6^-	1.855	IrF_6^-	1.910
RhF_6^{2-}	1.934	IrF_6^{2-}	1.928
RhF_6^{3-}	1.969		
$RhCl_6^{2-}$	2.313	$IrCl_6^{2-}$	2.332
$RhCl_6^{3-}$	2.330–2.354	$IrCl_6^{3-}$	2.327–2.387
		$IrBr_6^{2-}$	2.515–2.549
$RhBr_6^{3-}$	2.465–2.485	$IrBr_6^{3-}$	2.486–2.512

Table 2.2 Vibrational fundamentals in MX_6^{n-} species (cm^{-1}) (M = Rh, Ir; X = F, Cl, Br, I; $n = 0$–3)

	$\nu_1(A_{1g})$	$\nu_3(T_{1u})$		$\nu_1(A_{1g})$	$\nu_3(T_{1u})$
RhF_6			IrF_6	702	719
RhF_6^-	632	655	IrF_6^-	671	
RhF_6^{2-}	592		IrF_6^{2-}	603–610	554
RhF_6^{3-}			IrF_6^{3-}		
$RhCl_6^{2-}$	320	335	$IrCl_6^{2-}$	345–346	313–321
$RhCl_6^{3-}$	302–308	312	$IrCl_6^{3-}$	330	296
			$IrBr_6^{2-}$	215	221
$RhBr_6^{3-}$	187–190	244-260	$IrBr_6^{3-}$	198	209
			IrI_6^{3-}	149	175

The hexahalometallate(III) ions are reasonably stable, except for IrI_6^{3-}; water-sensitive Cs_3IrI_6 was made by tempering pellets of Cs_3IrBr_6 and NaI at 160°C for some days [25]. As expected for low-spin d^6 systems, these are diamagnetic, but the MX_6^{2-} species are paramagnetic with one unpaired electron [26]. Thus Cs_2RhCl_6 has $\mu_{\text{eff}} = 1.7\,\mu_B$ and various RhF_6^{2-} salts have moments of *c.* $2.0\,\mu_B$; moments in this range have been reported for IrX_6^{2-} (X = F, Cl, Br).

Salts of $IrCl_6^{2-}$ were used in the classic first ESR experiments to demonstrate delocalization of unpaired electrons onto the chloride ligand (Figure 2.1); the unpaired electron spends 30% or more of its time in ligand orbitals in this case [27].

Na_2IrCl_6 is a convenient starting material in the synthesis of iridium compounds.

$NaRhF_6$ is reported to have $\mu = 2.8\,\mu_B$.

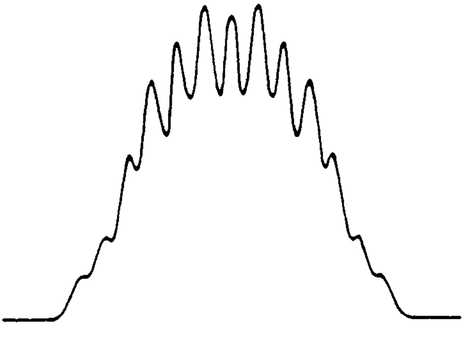

Figure 2.1 Ligand hyperfine structure in the ESR spectrum of $Na_2[(Ir, Pt)Cl_6].6H_2O$. (Reproduced with permission from *Proc. R. Soc., London, Ser. A*, 1953, **219**, 526.)

Mixed halometallates [28] can be synthesized: $RhCl_6Br_{6-x}^{3-}$ from the reaction of $RhCl_6^{3-}$ with HBr, or $RhBr_6^{3-}$ with HCl. Individual isomers have been identified in solution by ^{103}Rh NMR, which can even distinguish between stereoisomers (Figure 2.2) and shows isotopic splitting (Figure 2.3).

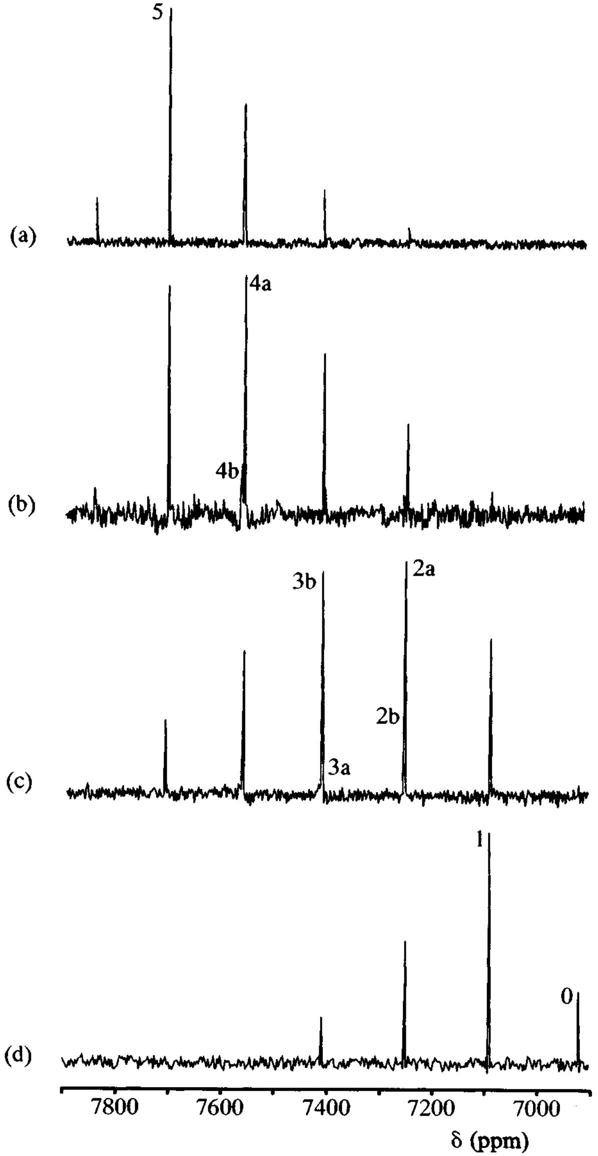

Figure 2.2 ^{103}Rh NMR spectrum of mixtures of $[RhCl_nBr_{6-n}]^{3-}$ species ($n = 0$–6; a denotes *cis,fac*-isomer, b denotes *trans,mer*-isomer). (a–d) are varying Cl : Br ratios in the starting material. (Reproduced with permission from *Z. Naturforsch., Teil B*, 1989, **44**, 1402.)

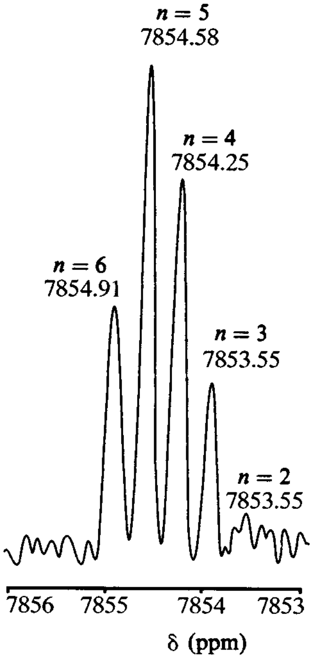

Figure 2.3 ^{103}Rh NMR spectrum of mixtures of $[Rh^{35}Cl_n^{37}Cl_{6-n}]^{3-}$ species ($n = 2$–6). (Reproduced with permission from *Z. Naturforsch., Teil B*, 1989, **44**, 1402.)

The series $[IrX_{6-x}Cl_x]^{2-}$ have likewise been made, as have the free acids $(H_3O)_2IrX_6$ (X = Cl, Br).

Various dinuclear complexes exist

$$A_3RhCl_6 \xrightarrow{H_2O} A_2RhCl_5(H_2O) \xrightarrow{\text{heat}} A_3Rh_2Cl_9$$

(A = alkali metal)

$$2RhX_6^{3-} + 6Bu_4N^+ \xrightarrow[(X=Cl,\,Br)]{CH_2Cl_2} (Bu_4N)_3Rh_2X_9 + 3Bu_4NX$$

In the latter example, the ligand abstraction is favoured by the non-polar solvent CH_2Cl_2. IR spectra distinguish between the bridging and terminal groups; thus in $Cs_3Rh_2X_9$, terminal Rh–X stretching vibrations occur in the regions 342–361 cm^{-1} (X = Cl) and 252–272 cm^{-1} (X = Br) with bridging Rh–X vibrations in the regions 267–302 cm^{-1} (X = Cl) and 171–195 cm^{-1} (X = Br) [29].

2.4 Oxides, hydrides and other binary compounds

Both rhodium and iridium form the oxides M_2O_3 and MO_2 [30]. Heating rhodium in air or oxygen (300–1000°C) yields brown Rh_2O_3, also obtained by heating rhodium nitrate at 730°C.

$$4Rh(NO_3)_3.6H_2O \rightarrow 2Rh_2O_3 + 12NO_2 + 3O_2 + 24H_2O$$

It exists in two stable forms, of which the α-form has the corundum (α-Al_2O_3) structure with octahedrally coordinated rhodium (Rh–O 2.03–2.07 Å); the β-form and a high-temperature form also have octahedral coordination. Black RhO_2 has the rutile structure (Rh–O 1.95–1.97 Å) and is best made by heating rhodium or Rh_2O_3 at 400–900°C under oxygen pressures up to 3500 atm.

Ir_2O_3 can be made by heating K_2IrCl_6 with Na_2CO_3; it is a (impure) brown solid about which little is known. Like RhO_2, IrO_2 also has the rutile structure. It is obtained by heating the metal in oxygen or by dehydrating the hydrated oxide precipitated on hydrolysis of Ir^{4+}(aq.)

The oxides decompose on heating:

$$2Ir_2O_3 \xrightarrow{500^\circ C} Ir + 3IrO_2$$

$$IrO_2 \xrightarrow{1100^\circ C} Ir + O_2$$

$$4RhO_2 \xrightarrow{680^\circ C} 2Rh_2O_3 + O_2 . 2Rh_2O_3 \xrightarrow{1050^\circ C} 4Rh + 3O_2$$

Rhodium(III) hydroxide is an ill-defined compound $Rh(OH)_3.nH_2O$ ($n \sim 3$) obtained as a yellow precipitate by careful addition of alkali to Na_3RhCl_6. Addition of imidazole solution to suitable aqua ions leads to the precipitation of 'active' rhodium(III) hydroxides formulated as $Rh(OH)_3(H_2O)_3$, $Rh_2(\mu\text{-}OH)_2(OH)_4(H_2O)_4$ and $Rh_3(\mu\text{-}OH)_4(OH)_5(H_2O)_5$ [31]. Hydrated iridium(III) hydroxide is obtained as a yellow precipitate from Ir^{3+} (aq.) at pH 8.

The metals form the usual wide range of binary compounds. Therefore, a range of sulphides and selenides are known, including MX_2 (M = Rh, Ir; X = S, Se, Te), M_3X_8 (X = S, Se), M_2S_3 and IrS_3. Of these, M_2S_3 is isostructural, containing pairs of face-sharing octahedra linked into a three-dimensional array by further sharing of sulphur. $RhSe_2$ and IrX_2 (X = S, Se) contain a special variety of the pyrite structure and are probably both represented as $M^{3+}X^{-1.5}(X_2^{3-})_{1/2}$ [32].

Other binary compounds include MAs_3 (M = Rh, Ir), which has the skutterudite ($CoAs_3$) structure [33] containing As_4 rectangular units and octahedrally coordinated M. The corresponding antimonides are similar. M_2P (M = Rh, Ir) has the anti-fluorite structure while MP_3 has the $CoAs_3$ structure. In another compound of this stoichiometry, $IrSi_3$, 9-coordination exists for iridium.

No binary hydrides have been characterized, but reactions of the metal powders with alkali metal hydrides in a hydrogen atmosphere lead to Li_3RhH_4 (planar RhH_4^{3-}) and M_3MH_6 (M = Li, Na; M = Rh, Ir) with octahedral MH_6^{3-} [34].

2.5 Aqua ions and simple salts

Aqua ions and simple salts have been thoroughly investigated recently [35]. Rhodium perchlorate, $Rh(ClO_4)_3.6H_2O$, can be made as yellow crystals by dissolving rhodium hydroxide in perchloric acid or alternatively by repeatedly heating hydrated rhodium chloride with perchloric acid. (Equilibrium is only slowly established and oligomers persist in quite acid solutions.) It contains slightly distorted $Rh(H_2O)_6^{3+}$ octahedra (Rh–O 2.128–2.136 Å); the Rh–O bonds may be lengthened slightly compared with the alum by hydrogen bonding to perchlorate ions. Solutions of iridium(III) perchlorate have been made by hydrolysis of $(NH_4)_2IrCl_6$, reacting the hydrolysis product with $HClO_4$ and then removing polymeric species by ion exchange. The alums also contain the hexaqua ion:

$$M(OH)_3 \xrightarrow{H_2SO_4} M_2(SO_4)_3(aq.) \xrightarrow{Cs_2SO_4} CsM(SO_4)_2.12H_2O$$

M–O bond lengths are 2.016 Å (Rh) and 2.041 Å (Ir), the former corresponds well to the value of 2.04 Å deduced from X-ray studies on aqueous solutions of $Rh(H_2O)_6^{3+}$ [36].

$Rh(H_2O)_6^{3+}$ is quite acidic ($pK_a = 3.4$ at 25°C). Spectroscopic study of crystals of the alums at 80 K leads to the assignment of ν_1 (A_{1g}) in $M(OH_2)_6^{3+}$ to bands at 548 cm^{-1} (Rh) and 553 cm^{-1} (Ir); in solution at room temperature they are found at 529 and 536 cm^{-1}, respectively.

Brown rhodium nitrate is reportedly formed from the reaction of RhI_3 with boiling nitric acid; it forms a hexahydrate.

The rhodium(II) aqua ion is not yet completely characterized. Cr^{2+} reduction of $Rh(H_2O)_5Cl^{2+}$ gives a diamagnetic species believed to be Rh_2^{4+} (aq.) [37], which may have the structure $(H_2O)_4Rh(\mu\text{-}OH_2)_2Rh(H_2O)_4^{4+}$.

In addition to the aqua ion, a range of mixed aquo–halo complexes are known [38], including all 10 isomers of $Rh(H_2O)_{6-x}Cl_x^{(3-x)+}$. Synthetic entry into the series is possible from either end, the determining factor being the labilizing effect of chloride:

$$Rh(H_2O)_6^{3+} \xrightarrow{Cl^-} RhCl(H_2O)_5^{2+} \xrightarrow{Cl^-} trans\text{-}RhCl_2(H_2O)_4^{+}$$

$$\xrightarrow{Cl^-} mer\text{-}RhCl_3(H_2O)_3$$

$$RhCl_6^{3-} \xrightarrow{H_2O} RhCl_5(H_2O)^{2-} \xrightarrow{H_2O} cis\text{-}RhCl_4(H_2O)^{-}$$

$$\xrightarrow{H_2O} fac\text{-}RhCl_3(H_2O)_3$$

This affects both the position of substitution and the rate; thus $RhCl(H_2O)_5^{2+}$ substitutes more than an order of magnitude faster than $Rh(H_2O)_6^{3+}$. These substitutions are all believed to follow a dissociative (S_N1) reaction. Particular compounds can sometimes be obtained under specific conditions;

thus recrystallizing a $RhCl_6^{3-}$ salt generally affords the corresponding $RhCl_5(H_2O)^{2-}$ species. Usually a mixture is formed, needing to be separated by ion-exchange: on refluxing $Rh(H_2O)_6(ClO_4)_3$ in 0.5 M HCl for 6–8 h, *mer*-$RhCl_3(H_2O)_3$ is the dominant product, while 15 min reflux of K_3RhCl_6 in dilute $HClO_4$ gives principally *fac*-$RhCl_3(H_2O)_3$. Individual species afford separate peaks in their electronic and vibrational spectra but in a mixture these will tend to overlap. However, separate signals can be seen in the ^{103}Rh NMR spectrum of such a mixture, it is even possible to discern isotopic splitting (see also Figure 2.3) [39].

Similar studies have been carried out on the corresponding bromides. Some structures have been determined; in Me_4N^+ [*trans*-$RhCl_4(H_2O)_2]^-$, Rh–O is 2.032 Å while Rh–Cl distances average 2.33 Å. $(NH_4)_2RhCl_5(H_2O)$ has Rh–O of 2.090 Å, *cis*-Rh–Cl distances average 2.347 Å while Rh–Cl *trans* to O is 2.304 Å (*trans*-influence of Cl); in the corresponding Cs salt, these distances are 2.096, 2.337 and 2.300 Å, respectively [40]. In *trans*-$[Ir(H_2O)_4Cl_2]^+$, Ir–Cl is 2.350 Å and Ir–O 2.039–2.048 Å.

2.6 Compounds of rhodium(0)

The best defined rhodium(0) compound [41] is diamagnetic $Rh_2(PF_3)_8$

$$RhCl_3 \xrightarrow[150^\circ C,\,250\,atm]{PF_3/Cu} Rh_2(PF_3)_8$$

It is believed to be metal–metal bonded $(PF_3)_4Rh{-}Rh(PF_3)_4$ and readily reacts with hydrogen

$$Rh_2(PF_3)_8 + H_2 \rightarrow 2RhH(PF_3)_4$$

Electrochemical reduction in MeCN of various $RhCl(R_3P)_3$ complexes give the diamagnetic $Rh(R_3P)_4$ ($R_3P = Ph_3P$, Me_2PhP), which are probably analogous to the PF_3 complex.

2.7 Compounds of rhodium(I)

Many important compounds are found in the +1 oxidation state [42], though unlike rhodium(III) it has no aqueous chemistry. Rhodium(I) generally forms 4-coordinate square planar and 5-coordinate species, the latter being the highest CN expected for the d^8 configuration under the 18-electron rule. (An octahedral rhodium(I) complex would involve putting two electrons in an anti-bonding orbital, as well as more steric crowding.)

2.7.1 *Tertiary phosphine complexes*

Tertiary phosphine complexes [42] are the most important rhodium(I) compounds. $RhCl(PPh_3)_3$ ('Wilkinson's compound'), a hydrogenation catalyst, is the most important, but they exist in a range of stoichiometries.

Synthesis follows several routes:

1. Substitution in rhodium(I) alkene complexes

$$RhCl_3.3H_2O \xrightarrow{C_2H_4} [RhCl(C_2H_4)_2]_2 \xrightarrow{PR_3} RhCl(PR_3)_3 \qquad (R = \text{alkyl})$$

$$RhF(C_8H_{12})_2 \xrightarrow{Pcy_3} RhF(Pcy_3)_2 \xrightarrow{NaX} RhX(Pcy_3)_2$$

$$[RhCl(C_8H_{12})_2]_2 \xrightarrow{P(OMe)_3} [RhCl\{P(OMe)_3\}_2]_2$$

2. Displacement of CO, only possible with strong π-acids

$$[RhCl(CO)_2]_2 \xrightarrow{PF_3} [RhCl(PF_3)_2]_2$$

3. Substitution of other phosphines

$$RhCl(PPh_3)_3 \xrightarrow[PMe_3]{\text{exc.}} [Rh(PMe_3)_4]^+Cl^-$$

4. Reduction using certain arylphosphines as reducing agents

$$RhCl_3.3H_2O \xrightarrow[\text{EtOH/boil}]{\text{exc. PPh}_3} RhCl(PPh_3)_3$$

2 : 1 complexes

The intensely reactive $RhX(Pcy_3)_2$ complexes are probably monomers; they bind both N_2 and SO_2 [43a], but most $RhX(PR_3)_2$ systems are dimers (R = Ph, X = Cl, OH; X-ray [43b]) (Figure 2.4)

$$[RhCl(PPr^i_3)_2]_2 + 2L \rightarrow 2RhClL(PPr^i_3)_2 \qquad (L = H_2, CO, Bu^tNC)$$

where the bridge can be cleaved

$$[RhCl(PPh_3)_2]_2 + 2PPh_3 \rightarrow 2RhCl(PPh_3)_3$$

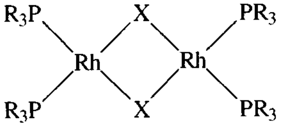

X	Rh–X	Rh–P	Rh–Rh
Cl	2.40	2.200–2.213	3.662
OH	2.06	2.185–2.207	3.278

Figure 2.4 Bond lengths in $[Rh(PPh_3)_2X]_2$ dimers.

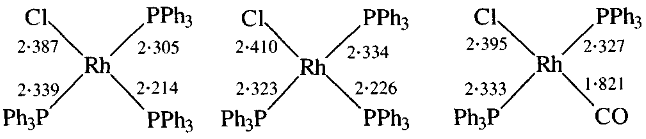

Red form Orange form

Figure 2.5 Bond lengths in $Rh(X)Cl(PPh_3)_2$ ($X = CO, PPh_3$).

3 : 1 complexes

A wide range of $RhX(QR_3)_3$ complexes exist (QR_3, e.g. PMe_3, PMe_2Ph, PPh_3, $AsPh_3$, etc.), generally made by replacing alkenes. Red $RhCl(PPh_3)_3$ [44] is made by an unusual route

$$RhCl_3 + 4PPh_3 \xrightarrow[\text{EtOH}]{\text{reflux}} RhCl(PPh_3)_3 + Ph_3PO$$

The ability of triphenylphosphine to act as a reducing agent probably involves initial formation of Ph_3PCl_2, which then undergoes solvolysis. If the synthesis is carried out using a small volume of ethanol, an orange polymorph is formed [45].

The crystal structures of both forms of $RhCl(PPh_3)_3$ show square planar coordination geometry (with a slight tetrahedral distortion). The mutually *trans* Rh–P bonds are similar to those in the less congested $RhCl(CO)(PPh_3)_2$, suggesting that steric crowding is not responsible for this distortion, which is also found in $RhCl(PMe_3)_3$ (Figure 2.5).

There are, however, short Rh–H contacts (2.77–2.84 Å) to *ortho*-hydrogens in phenyl groups. The Rh–P bond *trans* to Cl is some 0.1 Å shorter than the others, evidence of the weak *trans*-influence of chloride [46].

The ^{31}P NMR spectrum in solution [47] is in accordance with a square planar structure (Figure 2.6).

It shows a doublet of doublets owing to the pair of equivalent phosphorus nuclei, the signal being split by coupling to ^{103}Rh ($I = \frac{1}{2}$) and to the unique phosphorus; similarly the resonance owing to the third phosphorus shows coupling to two equivalent phosphorus nuclei, the resulting triplet being

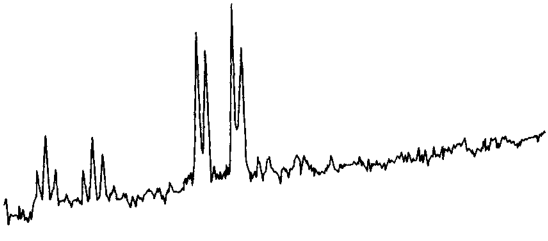

Figure 2.6 The ^{31}P NMR spectrum of $RhCl(PPh_3)_3$ at 30°C in C_6H_6 solution. (Reprinted with permission from *J. Am. Chem. Soc.*, 1972, **94**, 340. Copyright (1972) American Chemical Society.)

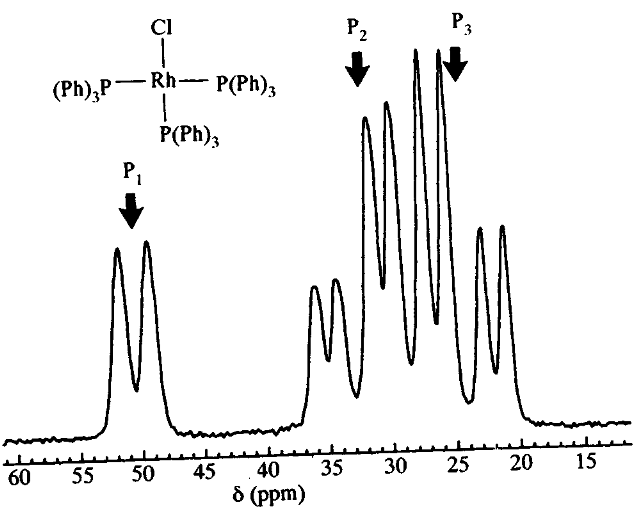

Figure 2.7 The solid-state ^{31}P NMR spectrum of $RhCl(PPh_3)_3$. (Reprinted with permission from *Organometallics*, 1992, **11**, 3240. Copyright (1992) American Chemical Society.)

split by coupling to rhodium. The solid-state ^{31}P NMR spectrum (Figure 2.7) is composed of a low-field cluster owing to the unique phosphorus split by coupling with rhodium (*cis*-P–P coupling is too small to be resolved); the multiplet has been analysed as the AB part of an ABX system, showing the two *trans*-phosphines are non-equivalent in the solid state.

$RhCl(PPh_3)_3$ is an air-stable solid (m.p. 157°C) soluble in a wide range of organic solvents with little dissociation of ligands. It does react readily with dioxygen in solution [48] forming a number of O_2 adducts (Figure 2.8); the consequent dissociation of PPh_3 is probably the reason why molecular weight measurements in incompletely deoxygenated solvents have implied

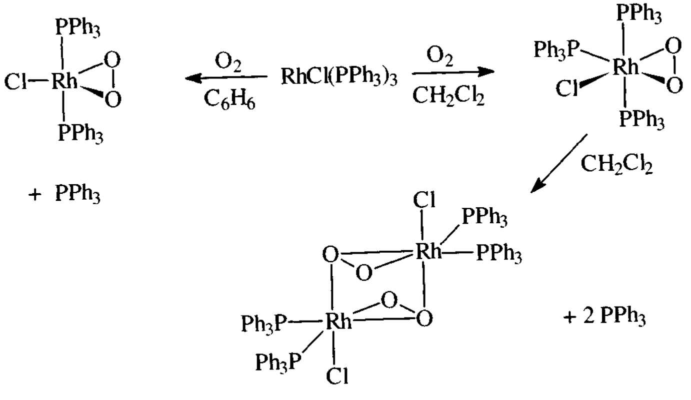

Figure 2.8 Rhodium dioxygen complexes.

dissociation for $RhCl(PPh_3)_3$. (It is notable that the isoelectronic 16-electron $Pt(PPh_3)_3$ shows no significant dissociation in solution.)

$RhCl(PPh_3)_3$ is a very active homogenous hydrogenation catalyst, because of its readiness to engage in oxidative addition reactions with molecules like H_2, forming Rh–H bonds of moderate strength that can subsequently be broken to allow hydride transfer to the alkene substrate. A further factor is the lability of the bulky triphenylphosphines that creates coordinative unsaturation necessary to bind the substrate molecules [44].

Reactions of $RhCl(PPh_3)_3$ can be divided into three classes (Figure 2.9)

1. oxidative addition (usually involving partial loss of PPh_3)
2. halide substitution
3. substitution of PPh_3 ligands (whole or partial).

In class (1), a range of small molecules adds to rhodium, usually with the loss of one PPh_3, thus maintaining the 16-electron configuration, rather than an 18-electron species unable to bind a substrate.

The reversible addition of hydrogen is the most significant of these reactions. In the presence of excess PPh_3, $RhH_2Cl(PPh_3)_3$ is formed, but generally the 5-coordinate $RhHCl_2(PPh_3)_2$ is obtained. Chlorine and HCl likewise add with fission of the X–Cl bond and loss of one PPh_3; $RhHCl_2(PPh_3)_2$ will insert ethene to form an ethyl complex.

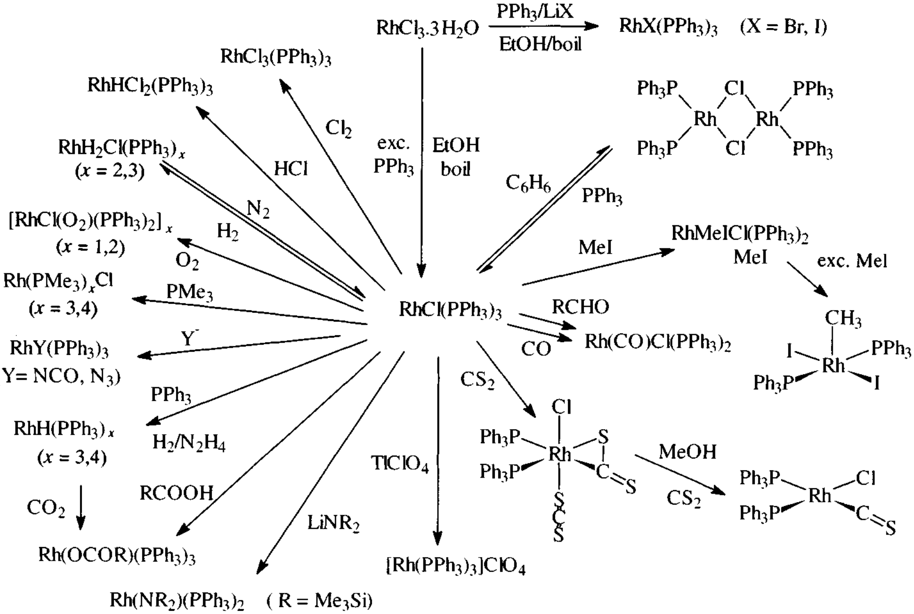

Figure 2.9 Synthesis and reactions of $RhCl(PPh_3)_3$.

The reaction with MeI proceeds in two stages. Initial reaction is oxidative addition to give a rhodium(III) species, isolated as a MeI adduct

$$RhCl(PPh_3)_3 + 2MeI \rightarrow RhClIMe(PPh_3)_2MeI + PPh_3$$

This then eliminates MeCl on recrystallization from benzene

$$RhClIMe(PPh_3)_2(MeI) \rightarrow MeCl + RhI_2(Me)(PPh_3)_2$$

Replacement reactions frequently involve a simple substitution of halide by an anionic ligand (e.g. N_3, NCO, S_2CNR_2). While chloride can be replaced by bis(trimethylsilyl)amide, $N(SiMe_3)_2$, most alkylamides are unstable to α-hydride elimination, forming the hydride $RhH(PPh_3)_3$ [49] (which is also obtained in the attempted preparation of $Rh(CH_2CH_2Me)((PPh_3)_3)$. The hydride ligand can be identified in the ^1H NMR spectrum of $RhH(PPh_3)_3$ by its high-field line (doublet, $\delta = -8.3$ ppm, J(Rh–H) = 12.4 Hz). The ^{31}P NMR spectrum at room temperature is a doublet (J(Rh–P) 164 Hz) but on cooling a fluxional process slows down and the spectrum converts into a double doublet and a double triplet (Figure 2.10) that overlap slightly.

The double triplet results from the unique phosphorus, split into a triplet by interaction with two equivalent phosphorus atoms (J(P–P) 25 Hz) then split into a doublet by rhodium (J(Rh–P) 145 Hz).

The double doublet corresponds to P_B, with splitting owing to phosphorus A (*cis*) (J(P–P) 25 Hz) and rhodium (J(Rh–P) 172 Hz). The fluxional behaviour is consistent with a rapidly rearranging (at room temperature) square planar structure rather than a tetrahedral one (Figure 2.11).

Determination of this crystal structure of the complex did not locate the hydride ligand but its position can be deduced from the distortion from

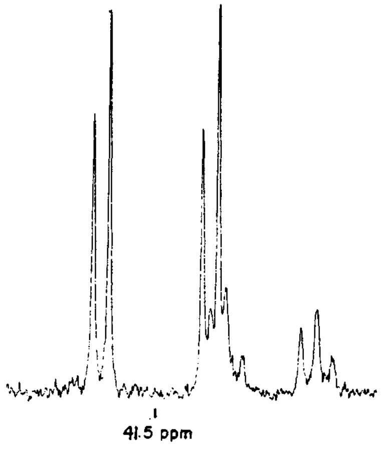

Figure 2.10 ^{31}P NMR spectrum of $RhH(PPh_3)_3$. (Reprinted with permission *Inorg. Chem.*, 1978, 17, 3066. Copyright (1978) American Chemical Society.)

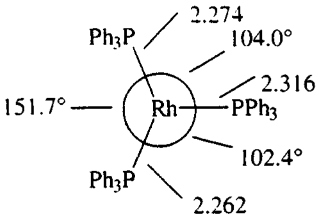

Figure 2.11 Bond lengths in $RhH(PPh_3)_3$ (hydride not shown).

regular trigonal geometry and the lengthened Rh–P bond *trans* to hydride. ($RhH(PPh_3)_4$, however, has a regular RhP_4 core so that here hydride has no stereochemical influence.)

Alkylation of $RhCl(PPh_3)_3$ yields unstable alkyls that undergo CO_2 insertion; $Rh(OCOPh)(PPh_3)_3$ has monodentate benzoate (X-ray).

Halide abstraction in donor solvents (with e.g. $TlClO_4$) affords [50] pseudo-tetrahedral $[Rh(solvent)(PPh_3)_3]^+$ ions (solvent, e.g. MeCN, Me_2CO, ROH) (Figure 2.12), which on recrystallization from CH_2Cl_2 gives $Rh(PPh_3)_3^+ClO_4^-$ (Figure 2.13) [51].

This has a distorted trigonal planar (nearly T-shaped) geometry with weak Rh–C and Rh–H interactions owing to the close approach of a phenyl group (Rh–H 2.56 Å, Rh–C 2.48 Å) supplementing the three Rh–P bonds in what is formally a 14-electron species. This ion is also formed by protonation of $RhH(PPh_3)_4$ (note the hydride ligand behaving as H^-).

$$RhH(PPh_3)_4 \xrightarrow{H_2C(SO_2CF_3)_2} [Rh(PPh_3)_3]^+HC(SO_2CF_3)_2^- + H_2 + PPh_3$$

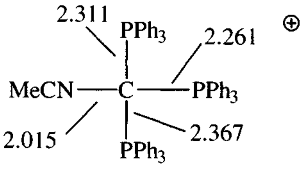

Figure 2.12 Bond lengths in $[Rh(MeCN)(PPh_3)_3]^+$.

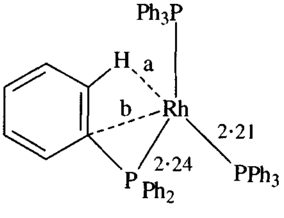

Figure 2.13 Bond lengths in $[Rh(PPh_3)_3]^+ClO_4^-$ showing short Rh–H and R–C contacts. a = 2.56 Å; b = 2.48 Å.

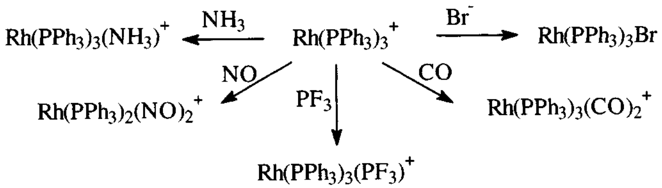

Figure 2.14 Reactions of $[Rh(PPh_3)_3]^+$.

^{31}P NMR spectra indicate the T-shape geometry is retained in solution at −30°C but that the molecule is fluxional at room temperature. $Rh(PPh_3)_3^+$ undergoes a range of addition reactions with Lewis bases (CO, PF_3, NH_3) to afford various 16- and 18-electron species (Figure 2.14).

Substitution reactions of $RhCl(PPh_3)_3$ where PPh_3 is completely displaced are relatively rare, though this is achieved with PMe_3, affording $Rh(PMe_3)_3Cl$ and $Rh(PMe_3)_4^+Cl^-$. More usually, as with CO, DMSO and C_2H_4, one phosphine is displaced; indeed the stability of *trans*-$RhCl(CO)(PPh_3)_2$ is such that aldehydes are decarbonylated by $RhCl(PPh_3)_3$. The reaction with CS_2 to give the analogous $RhCl(CS)(PPh_3)_2$ is more complicated than was first believed. If the reaction is carried out in neat CS_2, an intermediate species $RhCl(\eta^1\text{-}SCS)(\eta^2\text{-}CS_2)(PPh_3)_2$ is isolated, which readily decomposes in more polar solvents ($CHCl_3$, MeOH) forming $RhCl(CS)(PPh_3)_2$ (for its structure, see section 2.7.2).

$RhCl(PPh_3)_3$ as a homogenous hydrogenation catalyst [44, 45, 52]. The mechanism of this reaction has been the source of controversy for many years. One interpretation of the catalytic cycle is shown in Figure 2.15; this concentrates on a route where hydride coordination occurs first, rather than alkene coordination, and in which dimeric species are unimportant. (Recent NMR study indicates the presence of binuclear dihydrides in low amount in the catalyst system [47].)

The initial catalytic step involves reversible binding of H_2 to afford a rather crowded 18-electron species $RhH_2Cl(PPh_3)_3$. The ^{31}P NMR spectrum at −25°C it consists of a doublet of doublets owing to the *trans* phosphorus atoms (P_A) and a doublet of triplets owing to the unique phosphorus (P_B) (Figure 2.15) [47]. On warming to room temperature, broadening occurs as a result of phosphine ligand exchange; the loss of the couplings involving P_B shows that this is the phosphine dissociating, forming a 16-electron species $RhH_2Cl(PPh_3)_2$ that can bind an alkene (again affording an 18-electron species). This dihydride can now transfer the hydrogens to the unsaturated linkage (any alkyl intermediate is presumably shortlived as spectroscopic measurements have failed to detect them); addition is stereospecifically *cis*. Once the alkane is eliminated, the resulting coordinatively unsaturated 14-electron $RhCl(PPh_3)_2$ can rapidly undergo oxidative addition with H_2 to regenerate the dihydride intermediate.

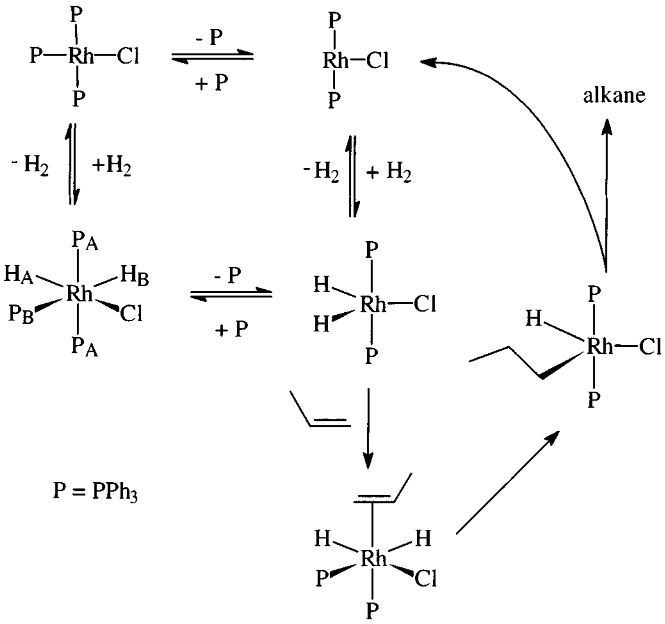

Figure 2.15 Cycle for the hydrogenation of alkenes catalysed by $RhCl(PPh_3)_3$.

Because the unsaturated hydrocarbon has to bind to rhodium in the presence of bulky PPh_3 groups, the catalyst favours unsubstituted double bonds ($RCH{=}CH_2$ rather than $RR^IC{=}CR^{II}R^{III}$). Since the alkyl intermediate is shortlived, there is little tendency to β-elimination with concomitant alkene isomerization. Although both alkene and alkyne functions are reduced, in general carbonyl or carboxylic groups and benzene rings are not, though aldehydes are frequently decarbonylated. Peroxides tend to oxidize and thus destroy the catalyst, so that substrates need to be purified carefully before use.

An example of a rhodium(I) complex with a tridentate phosphine is shown in Figure 2.16; it is formed by the usual route, reaction of the phosphine with $[RhCl(cycloocta\text{-}1.5\text{-}diene)]_2$.

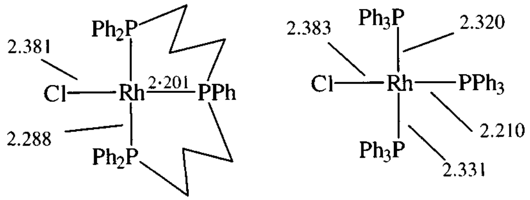

Figure 2.16 Bond lengths in a rhodium(I) complex of a tridentate phosphine compared with those in $RhCl(PPh_3)_3$.

It has an approximately square planar geometry, with bond lengths very similar to $RhCl(PPh_3)_3$ (Figure 2.5); like the latter, it undergoes a range of addition reactions, some involving no formal change in oxidation state, others a change to rhodium(III) species (Figure 2.17).

These are generally analogous to those of Wilkinson's compound, with the important difference that ligand dissociation cannot occur, so that the product of oxidative addition with H_2 cannot have a vacant site to bind an alkene and will thus not act as a hydrogenation catalyst [53].

4 : 1 complexes

The 4 : 1 complexes tend to be formed only by less bulky phosphines and even then tend to be coordinatively saturated.

$$RhCl(PPh_3)_3 \xrightarrow[X^-]{PR_3} Rh(PR_3)_4^+X^- \quad (X, \text{e.g. } PF_6, BF_4;\ PR_3 = PMe_3, PHPh_2)$$

Related compounds occur with bidentate phosphines

$$[RhCl(cod)]_2 \xrightarrow[X^-]{\text{diphos}} Rh(\text{diphos})_2^+X^-$$

(cod = cycloocta-1.5-diene; diphos = $Ph_2P(CH_2)_2PPh_2$, $Me_2P(CH_2)_2PMe_2$).

$Rh(Ph_2P(CH_2)_2PPh_2)_2^+ClO_4^-$ has essentially square planar coordination of rhodium (Rh–P 2.289–2.313 Å) [54].

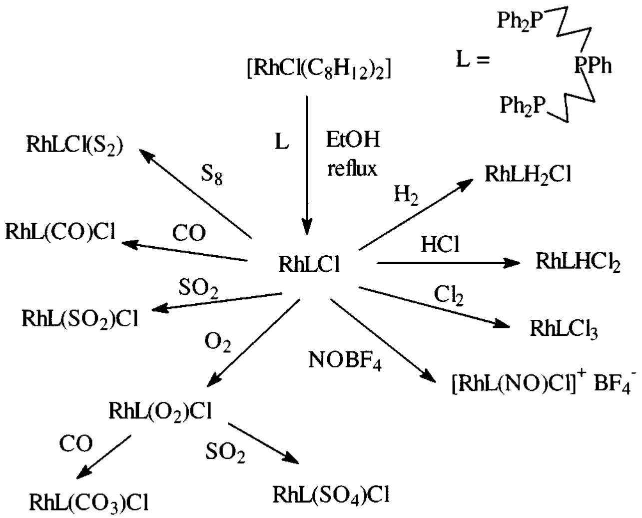

Figure 2.17 Reactions of the rhodium(I) complex of a tridentate phosphine.

5 : 1 complexes

Few of the 5:1 complexes [55] have been prepared, all with trialkylphosphites

$$[\mathrm{RhCl(cod)}]_2 \xrightarrow{\mathrm{P(OR)_3}} \{\mathrm{Rh[P(OR)_3]_5}\}^+\mathrm{X}^-$$

($X = BPh_4$, PF_6; R = Me, Et, Bu).

2.7.2 *Carbonyl complexes*

Three of the rhodium(I) carbonyl complexes are particularly important and are selected for special study.

$[RhCl(CO)_2]_2$

Reduction of hydrated $RhCl_3$ with CO at 100°C (best results are with CO saturated with methanol or ethanol) yields volatile red crystals of the dimer

$$\mathrm{RhCl_3.3H_2O} \xrightarrow[100^\circ\mathrm{C}]{\mathrm{CO}} [\mathrm{RhCl(CO)_2}]_2$$

This has been shown to have an unusual dimeric structure (Figure 2.18) in which the two planar units are at an angle of 124° [56a].

The Rh–Rh distance is 3.12 Å, long compared with Rh–Rh single bonds (2.624 Å in $Rh_2(MeCN)_{10}^{4+}$, 2.73 Å in $Rh_4(CO)_{12}$); there is a weaker (3.31 Å) intermolecular attraction. Dipole moment and IR studies indicate that the structure is retained in solution and is, therefore, a consequence of electronic rather than solid-state packing effects. Furthermore, it is found for some other (but not all) $[RhCl(alkene)_2]_2$ and $[RhCl(CO)(PR_3)]_2$ systems. SCF MO calculations indicate that bending favours a Rh–Cl bonding interaction which also includes a contribution from Rh–Rh bonding [56b].

$[RhCl(CO)_2]_2$ undergoes a range of reactions (Figure 2.19) generally involving bridge cleavage and is, therefore, a useful starting material.

$RhH(CO)(PPh_3)_3$

$RhH(CO)(PPh_3)_3$ [57] is most conveniently prepared by

$$\mathrm{RhCl(CO)(PPh_3)_2} \xrightarrow[\mathrm{EtOH}]{\mathrm{N_2H_4}} \mathrm{RhH(CO)(PPh_3)_3}$$

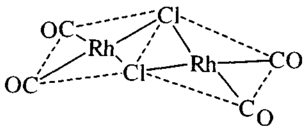

Figure 2.18 The structure of $[RhCl(CO)_2]_2$.

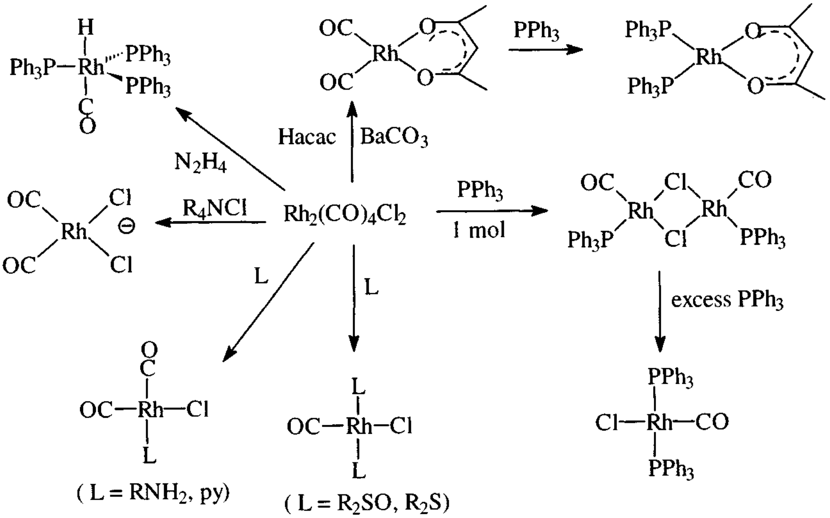

Figure 2.19 Reactions of $[RhCl(CO)_2]_2$.

It shows ν(Rh–H) and ν(C–O) at 2041 and 1918 cm^{-1}, respectively, in the IR spectrum (Nujol) and the low-frequency hydride resonance at $\delta = -9.30$ ppm in the ^{1}H NMR spectrum. It has a tbp structure (Figure 2.20) with the rhodium displaced out of the P_3 plane by 0.36 Å towards the CO.

It is an 18-electron species but in solution it tends to lose one PPh_3 to give $RhH(CO)(PPh_3)_2$, an active catalyst for hydroformylation and, to a lesser extent, hydrogenation of alkenes. (Evidence for the dissociation includes the fact that in the presence of other phosphines, mixed species $RhH(CO)(PPh_3)_2(PR_3)$ are formed by scrambling.) Initial coordination of the alkene is, in the absence of added CO, followed by hydrogenation (presumably via coordination of H_2 and an alkyl (intermediate)). Under a pressure of CO, hydroformylation occurs, with a high stereoselectivity in favour of straight-chain aldehydes, especially in the presence of added PPh_3. This supports the involvement of a crowded species (Figure 2.21) as the intermediate [58].

This process has been used commercially at the 100 kilotonne per year level running at around 100°C/20 atm.

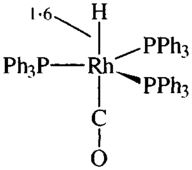

Figure 2.20 The structure of $RhH(CO)(PPh_3)_3$.

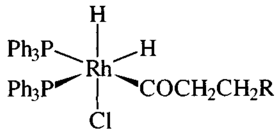

Figure 2.21 Probable structure of the intermediate in alkene hydroformylation catalysed by $RhH(CO)(PPh_3)_3$.

trans-$RhCl(CO)(PPh_3)_2$ and related compounds

trans-$RhCl(CO)(PPh_3)_2$ [59] is the rhodium analogue of 'Vaska's compound' (section 2.10.2) and undergoes analogous oxidative addition reactions. It is a yellow solid (IR ν(C–O) 1980 cm^{-1} ($CHCl_3$)) conveniently obtained by the following route using methanal as the source of the carbonyl group.

$$RhCl_3 \xrightarrow[\text{EtOH reflux}]{PPh_3/HCHO} RhCl(CO)(PPh_3)_2$$

The *trans*-geometry (confirmed by X-ray) keeps the bulky PPh_3 groups as far apart as possible (Figure 2.22).

Other $RhX(CO)(PPh_3)_2$ compounds can be made as shown in Figure 2.23; metathesis with an alkali metal halide or pseudohalide is often convenient, but the most versatile route, as with the iridium analogues, is a two-stage process in which the fluoro complex is first prepared, the fluorine then being readily displaced.

Attempted synthesis of $RhY(CO)(PPh_3)_2$ in undried solvents (Y = a weakly coordinating anion, e.g. BF_4, ClO_4, SO_3CF_3) leads to $[Rh(H_2O)(CO)(PPh_3)_2]^+Y^-$. The water molecule is bound sufficiently strongly not to be displaced by alkenes (ethene, phenylethanol) but is removed by pyridine or CO (at 1 atm) yielding $Rh(CO)_3(PPh_3)_2^+$.

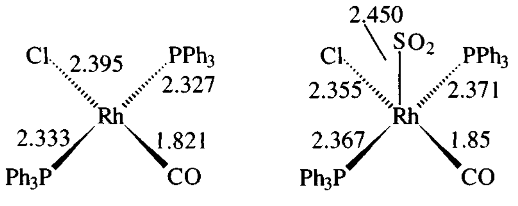

(X = Cl; Q = Ph)

X	Q	*n*	Rh–P	Rh–X	Rh–C
Cl	O	0	2.327–2.33	2.395	1.821
I	O	0	2.316–2.336	2.683	1.81
SH	O	0	2.314	2.416	1.767
Cl	S	0	2.335–2.337	2.386	1.787
OH_2	O	1	2.351	2.122	1.792

Figure 2.22 Bond lengths in $RhCl(CO)(PPh_3)_2$, $RhX(CQ)(PPh_3)_2]$ and $[Rh(OH_2)(CO)(PPh_3)_2]^+$ as well as in the SO_2 adduct.

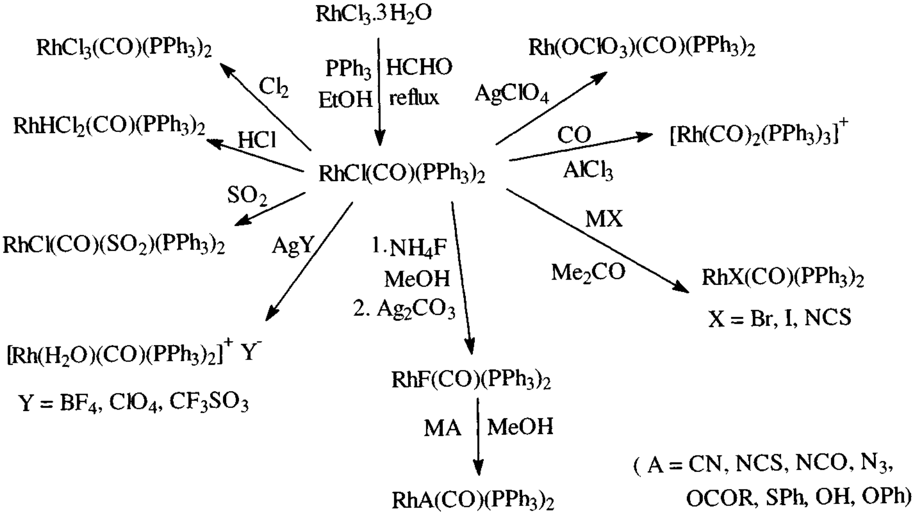

Figure 2.23 Reactions of $RhCl(CO)(PPh_3)_2$.

The mercapto complex $Rh(SH)(CO)(PPh_3)_2$ can be made by an unusual route [60] involving COS, where an intermediate with CS bound COS has been suggested.

$$RhH(PPh_3)_4 + COS \xrightarrow{\text{toluene}} Rh(\eta^2\text{-}COS)H(PPh_3)_3$$
$$\rightarrow Rh(SH)(CO)(PPh_3)_2 + 2PPh_3$$

The ^1H NMR spectrum of $Rh(SH)(CO)(PPh_3)_2$ in the mercaptide region (Figure 2.24) shows a 1 : 2 : 1 triplet owing to coupling to two equivalent (mutually *trans*) phosphines (J(P–H) 18.1 Hz), each line split into a doublet by a weaker coupling to ^{103}Rh (J(Rh–H) 1.6 Hz).

Structures have been determined for a number of these compounds, showing that the Rh–P bonds are little affected by the *cis*-ligands (Figure 2.22). The shorter Rh–C distance in the thiocarbonyl is probably a result of greater Rh=C back-bonding. Addition of SO_2 results in the formation of a 5-coordinate (sp) adduct with the expected lengthening in all bonds.

Other $RhCl(CO)(PR_3)_2$ compounds ($PR_3 = PEt_3$, PBu_3, $Palkyl_2Ph$, $PalkylPh_2$, $P(OR)_3$, PBu^t_2 alkyl) have been synthesized by the general route

$$[Rh(CO)_2Cl]_2 + 4PR_3 \xrightarrow{\text{MeOH}} 2RhCl(CO)(PR_3)_2 + 2CO$$

Structures have been determined for $PR_3 = PMe_2Ph$ and PBu^t_3 [61]. In the former, the square planar geometry is retained (with slightly shorter Rh–P bonds (2.316 Å) than for $PR_3 = PPh_3$), but in the latter, there is pronounced lengthening of the Rh–P bonds (Rh–Cl 2.395 Å, Rh–P 2.425-2.430 Å, Rh–C 1.784 Å) and a distortion towards a tetrahedral structure (P–Rh–P

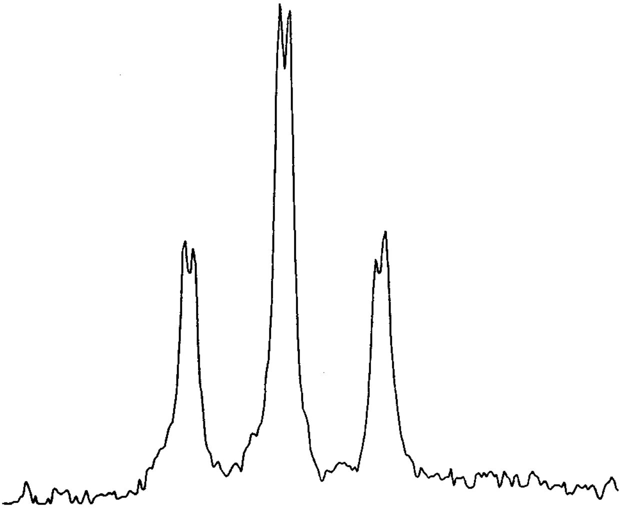

Figure 2.24 NMR spectrum of $Rh(SH)(CO)(PPh_3)_2$ in the mercaptide region. (Reprinted with permission from *Inorg. Chem.*, 1982, **21**, 2858. Copyright (1982) American Chemical Society.)

162.5°, C–Rh–Cl 150.7°) and some bending of the Rh–C–O bond (162.3°). Some short O–H and Cl–H intramolecular contacts may be responsible for the distortion though it has been suggested that in a distorted tetrahedral environment there may be an interaction between Rh d_{xz} electrons and the CO π^*-orbital causing bending.

Further evidence of steric crowding owing to bulky phosphines is found in $RhCl(CO)(PBu^t_2\text{ alkyl})_2$. Study of the ^{31}P NMR spectra at low temperature, 'freezing in' the rotational conformers shows separate signals for each (Figure 2.25) [62].

$RhCl(CO)(PR_3)_2$ (R = Et, Me, Ph) and the corresponding iridium systems undergo UV photolysis with the loss of CO, generating short-lived $RhCl(PR_3)_2$ species that act as catalysts for alkane carbonylation. Thus photolysis for 16.5 h under 1 atm CO using $RhCl(CO)(PMe_3)_2$ in pentane gives 2725% hexanal with high regioselectivity (45 : 1 hexanal to 2-methylpentanal) [63].

The complexes $[RhCl(CO)(PR_3)]_2$ can exist as *cis*- and *trans*-isomers (Figure 2.26).

The *cis*-structure (like $[Rh(CO)_2Cl]_2$ folded, with an angle of 123°) has been confirmed for PMe_2Ph (X-ray) whereas the $P(NMe_2)_3$ analogue is *trans* (IR). Comparison of solid-state and solution IR spectra indicates that both isomers are present in solution ($PR_3 = PMe_3$, PMe_2Ph, $P(NMe_2)_3$) [64].

Anionic carbonyl complexes of both rhodium(I) and (III) are synthesized by decarbonylation of formic acid, with reduction to rhodium(I) occurring

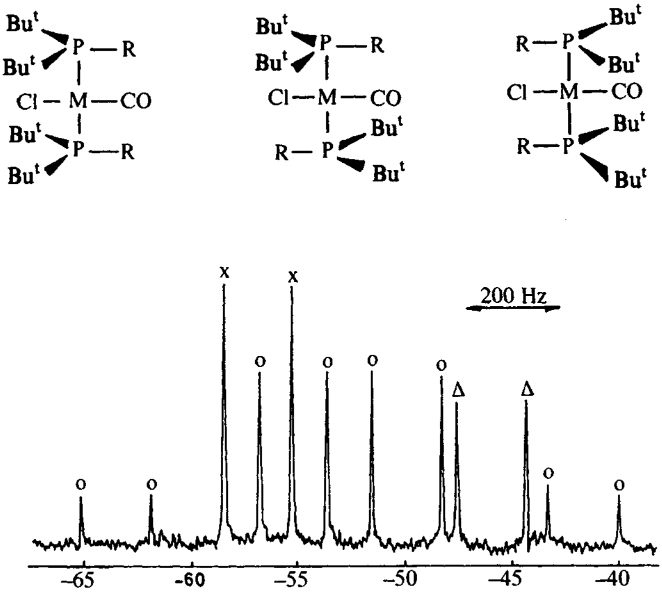

Figure 2.25 ^{31}P NMR spectrum of *trans*-$RhCl(CO)(PBu^t_2Et)_2$ at −60°C. The patterns ×, ○, △ correspond to the three conformers. (Reproduced with permission from *Chem. Comm.*, 1971, 1103.)

on extended reflux

$$RhX_3 \xrightarrow[\text{MX reflux}]{\text{HCOOH}} Rh(CO)X_5^{2-} \xrightarrow[\text{reflux}]{\text{HCOOH}} Rh(CO)_2X_2^-$$

Such a complex, *cis*-$Rh(CO)_2I_2^-$, is the active species in the Monsanto process for low-pressure carbonylation of methanol to ethanoic acid. The reaction is first order in iodomethane and in the rhodium catalyst; the rate-determining step is oxidative addition between these followed by

$$Rh(CO)_2I_2^- + MeI \Leftrightarrow Rh(CO)_2(Me)I_3^-$$

methyl migration generating $(MeCO)Rh(CO)I_3^-$. This can then add CO, eliminate MeCOI (subsequently hydrolysed to the acid) and regenerate $Rh(CO)_2I_2^-$.

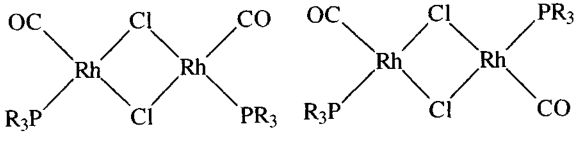

cis- trans-

Figure 2.26 Isomers of $[RhCl(CO)(PR_3)]_2$.

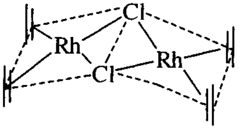

Figure 2.27 The structure of $[RhCl(C_2H_4)_2]_2$.

2.7.3 *Alkene complexes*

If ethene is bubbled through a methanolic solution of $RhCl_3.3H_2O$, red–orange crystals of $[RhCl(C_2H_4)_2]_2$ precipitate in a redox reaction.

$$2RhCl_3 + 6C_2H_4 + 2H_2O \rightarrow [RhCl(C_2H_4)_2]_2 + 2MeCHO + 4HCl$$

This has a 'folded' structure (Figure 2.27) similar to that of rhodium carbonyl chloride (Figure 2.18) with ethene acting as a two-electron donor, but ethene is more weakly held and readily displaced by CO and certain alkenes (e.g. cycloocta-1,5-diene).

Reaction under controlled conditions with tertiary phosphines leads to partial displacement of alkene retaining the dimeric structure [65].

Reaction of the dimer with Na(acac) leads to cleavage of the bridge giving yellow crystals of $Rh(alkene)_2(acac)$:

$$[RhCl(C_2H_4)_2]_2 + 2Na(acac) \rightarrow 2NaCl + 2(C_2H_5)Rh(acac)$$

C_2F_4 displaces one ethene to give $Rh(C_2H_4)(C_2F_4)(acac)$, as does hexafluorodewarbenzene, whereas other alkenes (e.g. propene, styrene, vinyl chloride) displace both ethenes. Comparison of the structures of two complexes (Figure 2.28) shows that the Rh–C bonds are shorter to tetrafluoroethene, because C_2F_4 is a better π-acceptor, with concomitant strengthening of the Rh–C bond.

NMR spectra show the ethene molecules to undergo a 'propeller' type rotation about the metal–alkene axis: the fluxionality is removed on cooling; such rotation is not observed with coordinated C_2F_4, indicating a higher barrier to rotation, in keeping with the stronger Rh–C bonds [66].

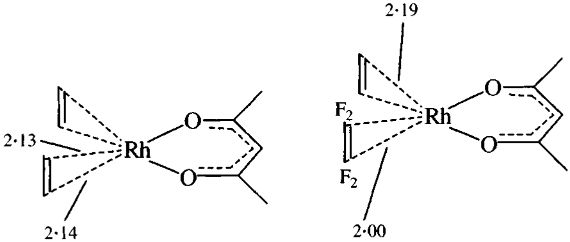

Figure 2.28 The structures of $Rh(acac)(C_2H_4)_2$ and $Rh(acac)(C_2H_4)(C_2F_4)$.

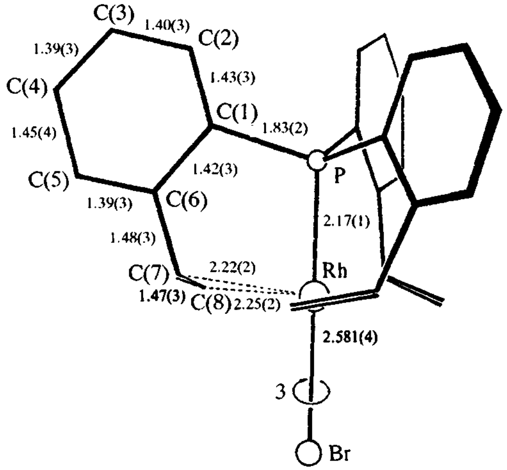

Figure 2.29 The structure of RhBr((*o*-vinylphenyl)$_3$P). (Reproduced with permission from *J. Chem. Soc., Dalton Trans.*, 1973, 2202.)

A number of tertiary phosphine ligands have been synthesized that also contain an alkene linkage capable of coordinating to a metal. A good example of this kind of coordination is formed in the complex of (tri-*o*-vinylphenyl)phosphine (Figure 2.29); with each alkene acting as a two-electron donor, a noble gas configuration is achieved [67].

2.7.4 *Isocyanide complexes*

Isocyanide complexes [68] can readily be prepared using excess isocyanide as the reducing agent:

$$[\mathrm{RhCl(CO)_2}]_2 \xrightarrow[\mathrm{RNC}]{\mathrm{exc.}} \mathrm{Rh(RNC)_4^+} \xleftarrow[\mathrm{RNC}]{\mathrm{exc.}} \mathrm{RhCl_3.3H_2O}$$

(R, e.g. alkyl, Ph)

In solution the compounds exhibit solvent-dependent colours; in dilute solution in non-polar solvents, planar monomers are present but in more concentrated solutions oligomerization occurs. In the solid state a dimeric structure has been identified (X-ray, Figure 2.30); with R = Ph there is a staggered configuration (Rh–Rh 3.193 Å) but with other isocyanides (R = 4-FC_6H_4) the configuration is eclipsed.

The weak Rh–Rh bond is taken to occur by d_{z^2}-d_{z^2} overlap.

Like other planar rhodium(I) complexes, $Rh(RNC)_4^+$ undergoes oxidative addition with halogens to form 18-electron rhodium(III) species and also add other small molecules (SO_2, NO^+) (Figure 2.31).

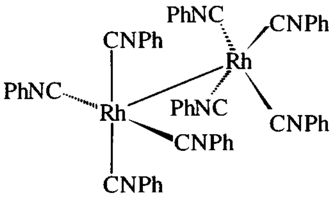

Figure 2.30 The dimeric structure of $[Rh_2(PhNC)_8]^{2+}$ in the solid state.

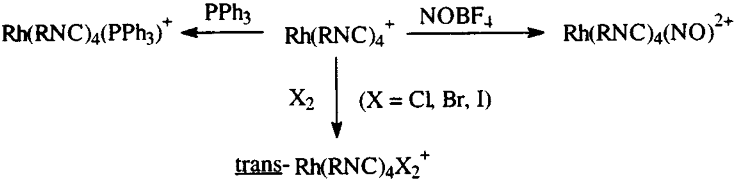

Figure 2.31 Reactions of $[Rh(RNC)_4]^+$.

2.8 Rhodium(II) complexes

Until recently, well-authenticated cases of the rhodium(II) oxidation state were rare, with the exception of the dinuclear carboxylates. They fall into two main classes, although there are other rhodium(II) complexes:

1. paramagnetic complexes ($4d^7$) with bulky phosphines, usually of the type $Rh(PR_3)_2X_2$
2. diamagnetic dinuclear carboxylates, and related dimers.

2.8.1 Phosphine complexes

Reaction of $RhCl_3.3H_2O$ with bulky tertiary phosphines at room temperature or below generally leads to reduction to rhodium(II).

$$RhCl_3.3H_2O \xrightarrow[0-25°C]{PR_3} trans\text{-}RhCl_2(PR_3)_2$$

($PR_3 = P(o\text{-tolyl})_3$, Pcy_3, PBu^t_2R' (R' = Me, Et, Pr^n etc.).

Oxidative cleavage may be used

$$[RhX(Pcy_3)_2]_2 \xrightarrow{X_2} trans\text{-}RhX_2(Pcy_3)_2 \qquad (X = Cl, Br)$$

(Other syntheses are mentioned in section 2.9.5.)

These compounds are paramagnetic ($PR_3 = P(o\text{-tolyl})_3$, $\mu_{eff} = 2.3\,\mu_B$; $PR_3 = Pcy_3$, $\mu = 2.24\,\mu_B$), deeply coloured (usually blue–green) and have IR spectra resembling those of *trans*-$PdCl_2(PR_3)_2$ systems. The structure has been determined for $PR_3 = PPr^i_3$ (Rh–P 2.366 Å, Rh–Cl 2.298 Å) [69].

A more unusual complex is formed by the very bulky tris(2,4,6-trimethoxyphenyl)phosphine (tmpp) [70].

$$[Rh_2(MeCN)_{10}](BF_4)_4 \xrightarrow{\text{tmpp}} 2[Rh(tmmp)_2]^{2+} + 4BF_4^-$$

The complex ion (Figure 2.32) contains Rh_2^+ bound *cis* to two phosphorus atoms (2.216 Å) and more distantly to four oxygens (2.201–2.398 Å), exhibiting a distortion ascribed to the Jahn–Teller effect; it is paramagnetic ($\mu = 1.80\,\mu_B$) and exhibits an ESR spectrum (Figure 2.33) showing rhodium hyperfine coupling as the doublet for $g_{||}$.

The complex reacts with CO reversibly via a series of redox reactions. $Rh(TMPP)_2^{2+}$ forms adducts with bulky isocyanides RNC (R = Bu^t, Pr^i), retaining the +2 state but changing to a *trans*-geometry (Figure 2.34) with monodentate phosphines (and uncoordinated ethers) (R = Bu^t, $\mu_{eff} = 2.04\,\mu_B$; $g_\perp = 2.45$, $g_{||} = 1.96$).

2.8.2 Dimers

The second class of rhodium(II) complexes is the dimers [71]. The dimeric

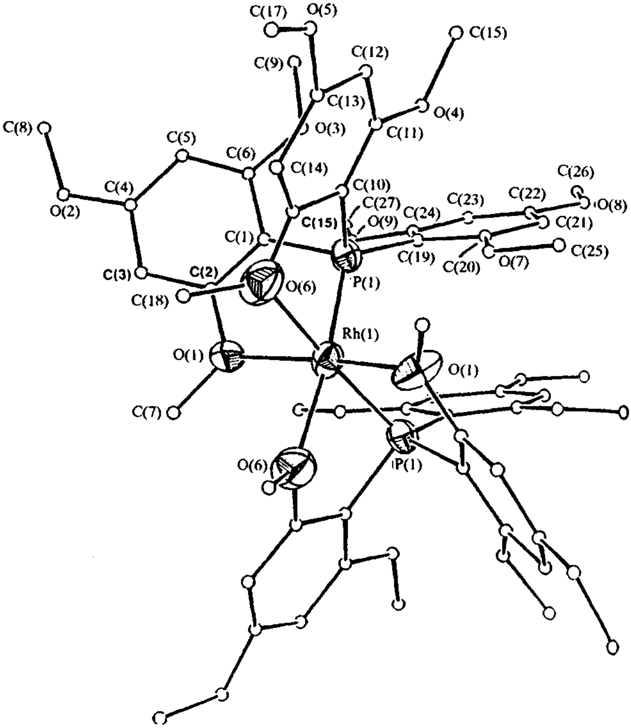

Figure 2.32 The structure of $[Rh(tmpp)_2]^{2+}$. (Reprinted with permission from *J. Am. Chem. Soc.*, 1991, **111**, 5504. Copyright (1991) American Chemical Society.)

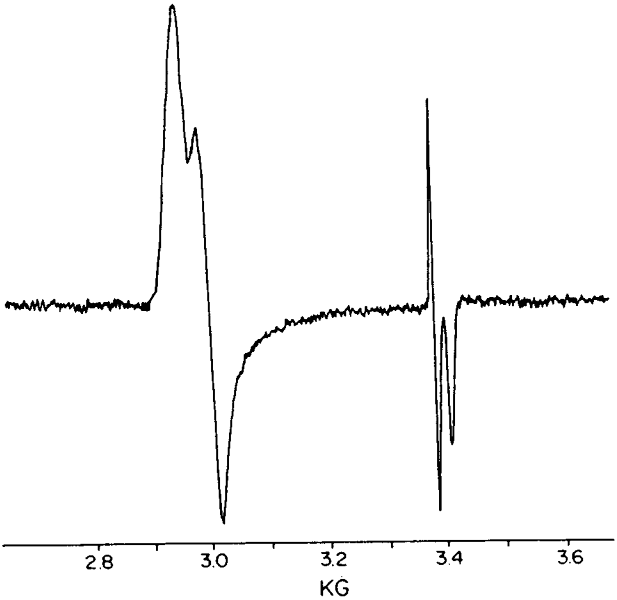

Figure 2.33 The ESR spectrum of $[Rh(tmpp)_2]^{2+}$ in CH_2Cl_2/toluene at 8 K. (Reprinted with permission from *J. Am. Chem. Soc.*, 1991, **111**, 5504. Copyright (1991) American Chemical Society.)

acetate can conveniently be prepared as a green methanol solvate:

$$RhCl_3.xH_2O \xrightarrow[\text{MeCH reflux}]{\text{MeCOOH/MeCOONa}} Rh_2(OCOMe)_4.2MeOH$$

The methanol can be removed by heating gently *in vacuo*. Similar compounds can be made with other carboxylate groups, either by using this method or by heating the acetate with excess carboxylic acid. Treatment of the anhydrous carboxylate with various neutral ligands (L) or anionic donors (X^-) forms $Rh_2(OCOR)_4L_2$ and $[Rh_2(OCOR)_4X_2]^{2-}$, respectively. The colour of the adduct depends on the donor atom in L (or X):

blue to green: oxygen
pink to red: nitrogen
orange to brown–red: phosphorus or sulphur.

These compounds all have the ‘lantern’ structure shown in Figure 2.35.

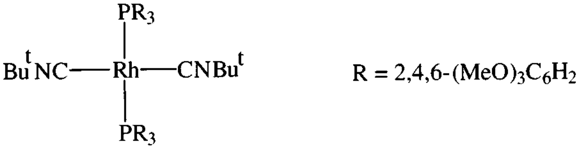

$$Bu^tNC—\overset{PR_3}{\underset{PR_3}{Rh}}—CNBu^t \qquad R = 2,4,6\text{-}(MeO)_3C_6H_2$$

Figure 2.34 Isocyanide adducts of $[Rh(tmpp)_2]^{2+}$.

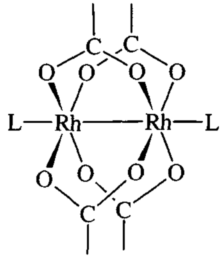

Figure 2.35 The 'lantern' structure adopted by dimeric rhodium(II) carboxylates.

Structural data for many carboxylates (Table 2.3) consistently show the presence of a metal–metal bond around 2.4 Å, shorter than that in rhodium metal (2.7 Å).

There is a slight dependence on the nature of the carboxylate group and upon the axial ligand, but they are not imposed by the steric requirements of the carboxylates. Some points are germane to this:

1. Adducts are formed with hard and soft donors, including π-acids such as CO, PF_3 and PPh_3. DMSO bonds through S for R = Me and Et, but through O when R = CF_3.

Table 2.3 Bond lengths in rhodium(II) carboxylates (Å)

(a) $Rh_2(OCOMe)_4L_2$

L	Rh–Rh	Rh–L
MeOH	2.377	2.286
MeCN	2.384	2.254
H_2O	2.3855	2.310
py	2.399	2.227
Me_2SO	2.406	2.451
$P(OMe)_3$	2.4556	2.437
$P(OPh)_3$	2.445	2.418
PPh_3	2.4505	2.477
PF_3	2.4215	2.340
CO	2.4193	2.091
Cl^-	2.3959	2.585
PhSH	2.4024	2.548
$AsPh_3$	2.427	2.576

(b) $Rh_2(OCOR)_4(H_2O)_2$

R	Rh–Rh	$Rh–OH_2$
Me	2.3855	2.310
CMe_3	2.371	2.295
CF_3	2.394	2.243

2. The long Rh–P bonds in the tertiary phosphine adducts show little dependence upon the tertiary phosphine and are interpreted in terms of a largely σ-component in the Rh–P bond; they are also affected by the strong *trans*-influence of the Rh–Rh bond.
3. ESCA data support a rhodium(II) oxidation state in these compounds. Therefore, the Rh $3d_{5/2}$ binding energy is *c.* 309.2 eV in simple carboxylates, midway between those in typical rhodium(I) complexes (*c.* 308.5 eV) and rhodium(III) complexes (*c.* 310.7 eV) [72].
4. The diamagnetism of all these rhodium(II) compounds indicates spin pairing via a metal–metal bond.
5. The lantern structure is quite stable, unlike certain other Rh_2 dimers. Protonation was formerly claimed to give 'Rh_2^{4+}' aqua ions, but they are believed now to be $[Rh_2(OCOMe)_3]^+$ (aq.) and $[Rh_2(OCOMe)_2]^{2+}$ (aq.) [73].
6. One-electron oxidation to $[Rh_2(OCOMe)_4(H_2O)_2]^+$ leads to an ion (violet to orange, depending on solvent) with a shorter Rh–Rh bond (2.317 Å) than that in the neutral molecule (2.385 Å), suggesting the electron has been removed from an orbital with anti-bonding character.

Unsolvated $[Rh_2(OCOR)_4]_2$ can be obtained by sublimation. The 'lantern' structure is retained with the axial position occupied by oxygens from neighbouring dimer units. The presence of axial ligands has little effect on the Rh–Rh bond; therefore, in $[Rh_2(OCOCF_3)_4]$ Rh–Rh is 2.382 Å compared with 2.394 Å in $[Rh_2(OCOCF_3)_4(H_2O_2)]$ and 2.418 Å in $Rh_2(OCOCF_3)_4(MeCN)_2$ [74].

The assignment of the Rh–Rh stretching frequency in the vibrational spectra of these compounds has been controversial for some 20 years, with ν(Rh–Rh) assigned variously to bands in the 150–170 and 280–350 cm^{-1} regions. Recent resonance Raman studies (Figure 2.36) exciting the metal-based $\sigma \rightarrow \sigma^*$ transition in $Rh_2(OCOMe)_4(PPh_3)_2$ showed enhancement of the symmetric stretching mode, at 289 cm^{-1}.

Isotopic (^2H, ^{18}O) labelling of the carboxylate groups has virtually no effect, as expected, on this band but produces shifts of 6–14 cm^{-1} in bands at 321 and 338 cm^{-1}, showing them to arise from Rh–O stretching [75].

Complexes of thiocarboxylic acids, $Rh_2(SCOR)_4L_2$, similarly adopt the 'lantern' structure. Rh–Rh distances are significantly greater than in the analogous carboxylates (R = Me_3C, L = py, Rh–Rh 2.514 Å; R = Ph, L = py, Rh–Rh 2.521 Å; R = Me_3C, L = PPh_3, Rh–Rh 2.584 Å). Raman studies on $Rh_2(SCOMe)_4L_2$ (L = PPh_3, $AsPh_3$, $SbPh_3$, MeCOSH) assign ν(Rh–Rh) to bands in the region of 226–251 cm^{-1}, significantly lower than in the carboxylates, consistent with the longer and weaker Rh–Rh bond [76].

Part of the upsurge in interest in rhodium(II) carboxylates since the early 1970s results from the discovery that they have potential as anti-tumour

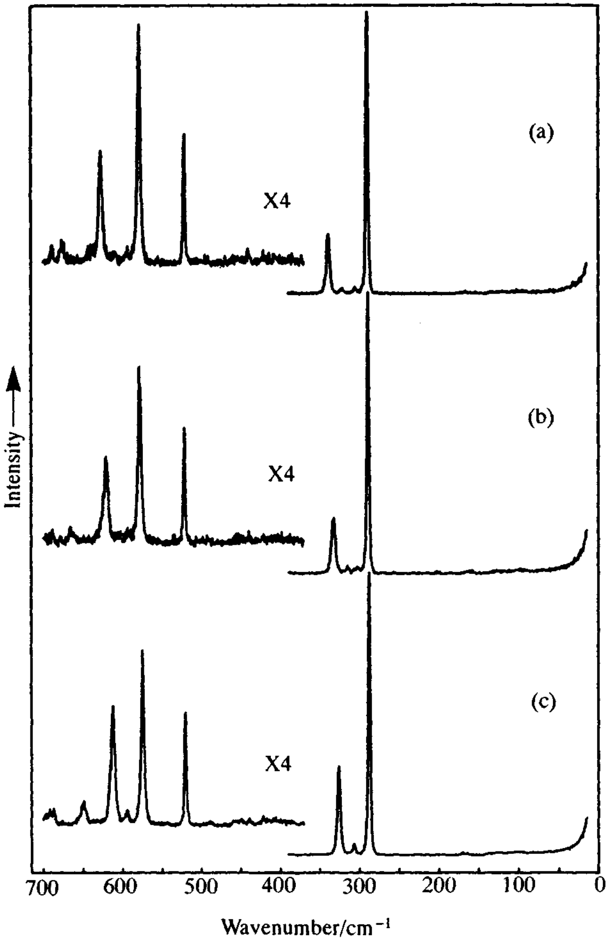

Figure 2.36 Resonance Raman spectra of (a) $Rh_2(^{16}O_2)CMe_4(PPh_3)_2$; (b) $Rh_2(^{18}O_2)CMe_4(PPh_3)_2$; (c) $Rh_2(^{16}O_2)C(CD_3)_4(PPh_3)_2$. Recorded as KCl discs at 80 K, L = 363.8 nm. (Reprinted with permission from *J. Am. Chem. Soc.*, 1986, **108**, 518. Copyright (1986) American Chemical Society.)

agents. The dimers form adducts with many biologically important N-donors but react irreversibly with some compounds containing SH groups. It seems that they may inhibit DNA synthesis by deactivating sulphydryl-containing enzymes [77].

Bonding in the dimers

Several MO schemes are suggested, most with a single bond but differing to some extent on the ordering of the energy levels [78] (Figures 2.37 and 2.38). The most recent results indicate the highest occupied MO (HOMO) is of σ-symmetry, consistent with ESR results on $[Rh_2(OCOR)_4(PR_3)_2]^+$.

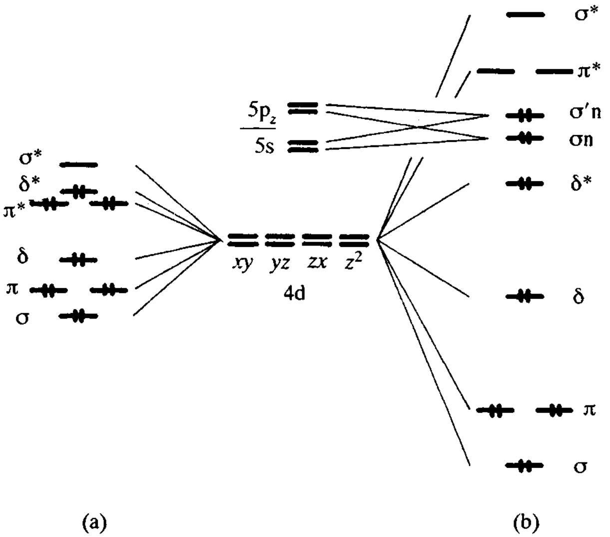

Figure 2.37 Models for the metal–metal bonding in $Rh_2(O_2CR)_4$. (a) corresponds to a single-bond; (b) corresponds to a triple-bond model in which there is a greater interaction between the rhodium 4d orbitals than between the 4d and 5s, 5p manifolds. (Reprinted with permission from *J. Am. Chem. Soc.*, 1981, **103**, 364. Copyright (1981) American Chemical Society.)

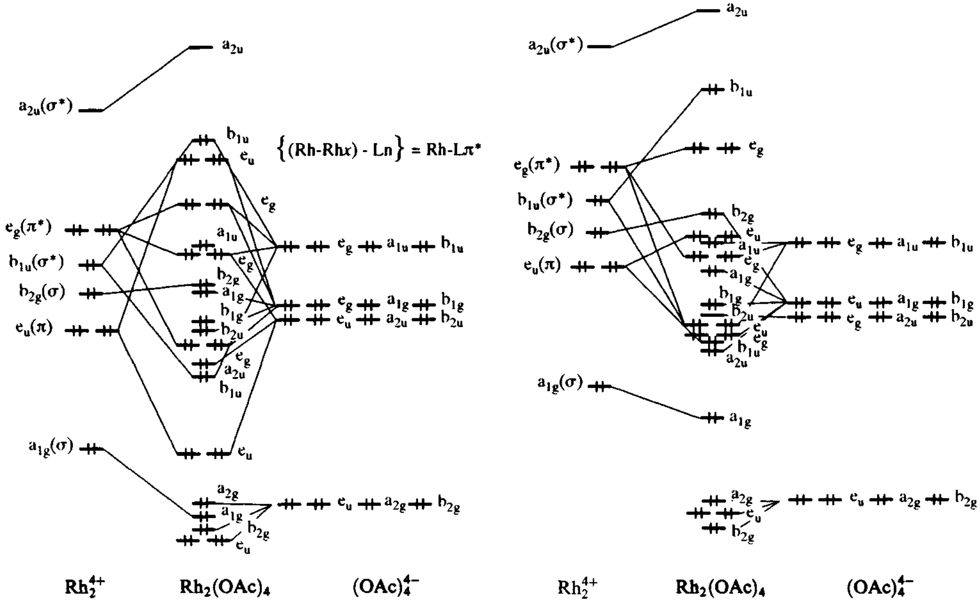

Figure 2.38 The effect of varying the relative energies of the metal and ligand orbitals upon the final molecular orbital scheme for a dimeric rhodium carboxylate. (Reprinted from *Coord. Chem. Rev.*, **50**, 109, 1983, with kind permission from Elsevier Science S.A., P.O. Box 564, 1001 Lausanne, Switzerland.)

In the MO scheme the rhodium atoms use their $d_{x^2-y^2}$ orbitals to form the Rh–O bonds, the remaining 4d orbitals are used to form four pairs of bonding and anti-bonding MOs (σ, δ and π) (Figure 2.37a).

The ligands interact with the two orbitals of σ-symmetry modifying the ordering somewhat (Figure 2.37b). As has been pointed out, altering the relative positions of the metal orbitals relative to those of the carboxylates affects the final scheme considerably (Figure 2.38).

Other compounds with the lantern structure include the acetamidates $Rh_2(MeCONH)_4L_2$ and the mixed-valence anilinopyridinate $Rh_2(ap)_4Cl$ (Figure 2.39), which has an unusual ESR spectrum in that the electron is localized on one rhodium [79].

Bridging ligands are not essential for the stability of dimers. Reduction of $[Rh(H_2O)_5Cl]^{2+}$ is believed to give a dimer $[Rh_2(H_2O)_{10}]^{2+}$.

Extended reflux of a MeCN solution of $Rh_2(OCOMe)_4$ with excess $Et_3O^+BF_4^-$ leads to successive replacement of the acetates [80]:

$$Rh_2(OCOMe)_4 \rightarrow [Rh_2(OCOMe)_2(MeCN)_6]^{2+} \rightarrow [Rh_2(MeCN)_{10}]^{4+}$$

$[Rh_2(MeCN)_{10}]^{4+}$ has a staggered structure (minimizing inter-ligand repulsions) with a Rh–Rh distance of 2.624 Å (presumably corresponding to a Rh–Rh single bond uninfluenced by bridging ligands (Figure 2.40).

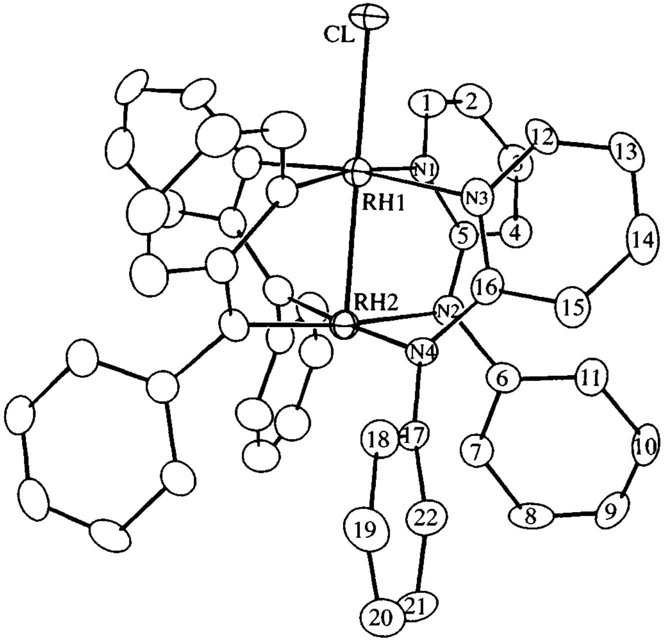

Figure 2.39 The 'lantern' structure of the dimeric rhodium antipyrine complex $Rh_2(ap)_4Cl$. (Reprinted with permission from *Inorg. Chem.*, 1988, **27**, 3783. Copyright (1988) American Chemical Society.)

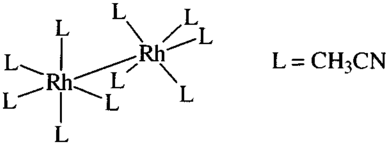

Figure 2.40 The staggered structure of the dimeric ion $[Rh_2(MeCN)_{10}]^{2+}$.

Reaction of $Rh_2(OCOR)_4$ with dimethylglyoxime leads to a non-bridged dimer [81].

$$Rh_2(OCOMe)_4 \xrightarrow{DMGH} Rh_2(DMG)_4$$

The bis(PPh_3) adduct has a long Rh–Rh bond of 2.936 Å, whereas in the 'mixed' dimer $Rh_2(OCOMe)_2(DMG)_2(PPh_3)_2$ where only two acetates bridge, Rh–Rh is 2.618 Å (Figure 2.41).

2.8.3 *Other complexes*

Photolysis of the rhodium(III) complex of octaethylporphyrin gives a rhodium(II) dimer that readily undergoes addition reactions to afford rhodium(III) species (Figure 2.42).

With more bulky porphyrins like TMP, a stable low-spin monomer Rh(TMP) can be isolated ($g_{\perp} = 2.65$, $g_{\parallel} = 1.915$), which forms a paramagnetic CO adduct.

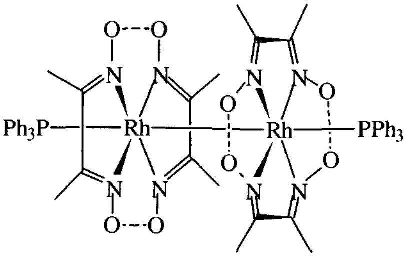

Figure 2.41 A dimeric non-bridged rhodium dimethylglyoxime complex (for clarity the hydrogen atoms in the hydrogen bonds are not shown).

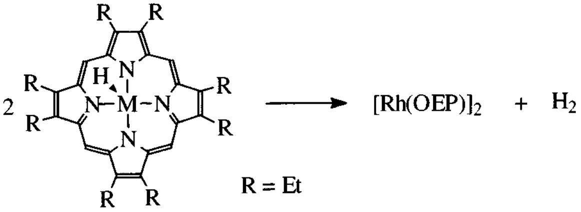

Figure 2.42 Synthesis of a dimeric rhodium(II) octaethylporphyrin complex.

A number of rhodium(III) complexes of thiacrown ligands can be reduced to give rhodium(II) species identifiable in solution. Thus controlled potential electrolysis of $Rh(9S_3)_2^{3+}$ ($9S_3$ = 1,4,7-trithiacyclononane) gives $Rh(9S_3)_2^{2+}$ ($g_1 = 2.085$, $g_2 = 2.042$, $g_3 = 2.009$) [82].

2.9 Rhodium(III) complexes

A considerable number of rhodium(III) complexes exist. Their stability and inertness are as expected for a low-spin d^6 ion; any substitution leads to a considerable loss of ligand-field stabilization.

2.9.1 *Complexes of O-donors*

The yellow acetylacetonate contains octahedrally coordinated rhodium (Rh–O 1.992 Å; O–Rh–O 95.3°) [83].

$$Rh(NO_3)_3 \xrightarrow[\text{pH 7}]{\text{acac}^-} Rh(acac)_3$$

The corresponding tri- and hexa-fluoroacetylacetonates may be similarly prepared. The stability of the acetylacetonate is such that not only can it be resolved on passage through a column of D-lactose, but the enantiomers retain their integrity on nitration or bromination.

Extended refluxing of hydrated $RhCl_3$ with excess oxalate leads to the tris complex, the potassium salt crystallizing as orange–red crystals with Rh–O 2.000–2.046 Å.

$$RhCl_3.3H_2O \xrightarrow[\text{reflux, 6 h}]{\text{aq. } K_2C_2O_4 \text{ (6 mol)}} K_3Rh(C_2O_4)_3.4\tfrac{1}{2}H_2O$$

$Rh(C_2O_4)_3^{3-}$ was resolved by Werner as the strychnine salt but other ions, such as $Coen_3^{3+}$ and $Niphen_3^{3+}$, have been used more regularly for this [84].

The dinuclear rhodium(II) acetate is described in section 2.8.2; the dinuclear structure is retained on one-electron oxidation, but when ozone is used as the oxidant, a compound with a trinuclear Rh_3O core is formed, analogous to those formed by Fe, Cr, Mn and Ru. (It can also be made directly from $RhCl_3$.)

$$RhCl_3.3H_2O \xrightarrow[\text{2. } ClO_4^-]{\text{1. MeCOOAg}} [Rh_3O(O_2CMe)_6(H_2O)_3]^+ClO_4^-$$

$$Rh_2(O_2CMe)_4 \xrightarrow[\text{2. } ClO_4^-]{\text{1. } O_3\text{/boiling MeCOOH}} [Rh_3O(O_2CMe)_6(H_2O)_3]^+ClO_4^-$$

Rhodium forms an EDTA complex isomorphous with the corresponding ones of Ru, Fe, Ga and Cr. In $Rh(EDTAH)(H_2O)$ one carboxylate is protonated and thus the acid is pentadentate, the water molecule completing the octahedron (Figure 2.43).

Next Page

A number of rhodium(III) complexes of thiacrown ligands can be reduced to give rhodium(II) species identifiable in solution. Thus controlled potential electrolysis of $Rh(9S_3)_2^{3+}$ ($9S_3$ = 1,4,7-trithiacyclononane) gives $Rh(9S_3)_2^{2+}$ ($g_1 = 2.085$, $g_2 = 2.042$, $g_3 = 2.009$) [82].

2.9 Rhodium(III) complexes

A considerable number of rhodium(III) complexes exist. Their stability and inertness are as expected for a low-spin d^6 ion; any substitution leads to a considerable loss of ligand-field stabilization.

2.9.1 Complexes of O-donors

The yellow acetylacetonate contains octahedrally coordinated rhodium (Rh–O 1.992 Å; O–Rh–O 95.3°) [83].

$$Rh(NO_3)_3 \xrightarrow[\text{pH 7}]{\text{acac}^-} Rh(acac)_3$$

The corresponding tri- and hexa-fluoroacetylacetonates may be similarly prepared. The stability of the acetylacetonate is such that not only can it be resolved on passage through a column of D-lactose, but the enantiomers retain their integrity on nitration or bromination.

Extended refluxing of hydrated $RhCl_3$ with excess oxalate leads to the tris complex, the potassium salt crystallizing as orange–red crystals with Rh–O 2.000–2.046 Å.

$$RhCl_3.3H_2O \xrightarrow[\text{reflux, 6 h}]{\text{aq. } K_2C_2O_4 \text{ (6 mol)}} K_3Rh(C_2O_4)_3.4\tfrac{1}{2}H_2O$$

$Rh(C_2O_4)_3^{3-}$ was resolved by Werner as the strychnine salt but other ions, such as $Coen_3^{3+}$ and $Niphen_3^{3+}$, have been used more regularly for this [84].

The dinuclear rhodium(II) acetate is described in section 2.8.2; the dinuclear structure is retained on one-electron oxidation, but when ozone is used as the oxidant, a compound with a trinuclear Rh_3O core is formed, analogous to those formed by Fe, Cr, Mn and Ru. (It can also be made directly from $RhCl_3$.)

$$RhCl_3.3H_2O \xrightarrow[\text{2. } ClO_4^-]{\text{1. MeCOOAg}} [Rh_3O(O_2CMe)_6(H_2O)_3]^+ClO_4^-$$

$$Rh_2(O_2CMe)_4 \xrightarrow[\text{2. } ClO_4^-]{\text{1. } O_3\text{/boiling MeCOOH}} [Rh_3O(O_2CMe)_6(H_2O)_3]^+ClO_4^-$$

Rhodium forms an EDTA complex isomorphous with the corresponding ones of Ru, Fe, Ga and Cr. In $Rh(EDTAH)(H_2O)$ one carboxylate is protonated and thus the acid is pentadentate, the water molecule completing the octahedron (Figure 2.43).

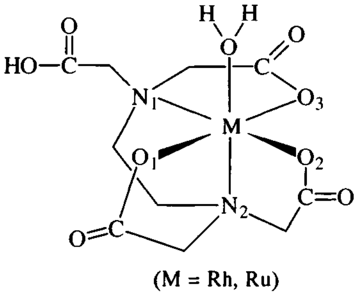

	Rh	Ru
M-OH2	2.096	2.131
M-N1	2.082	2.13
M-N2	1.988	2.038
M-O1	2.001	1.988
M-O2	2.007	2.007
M-O3	2.03	2.06

Figure 2.43 Ruthenium and rhodium EDTA complexes. Comparative bond lengths are given in Table 2.4.

Table 2.4 Bond lengths in M(EDTAH)(H_2O) (M = Ru, Rh) (Å)

	Ru	Rh
$M-OH_2$	2.131	2.096
$M-N_1$	2.130	2.082
$M-N_2$	2.038	1.988
$M-O_1$	1.988	2.001
$M-O_2$	2.007	2.007
$M-O_3$	2.060	2.030

The bond lengths make a more regular octahedron than in the d^5 ruthenium analogue, possibly partly a consequence of the symmetrical electron distribution in the d^6 Rh^{3+} ion (Table 2.4) [85].

2.9.2 *Complexes of ammines*

Amine complexes are an important class of rhodium(III) complex. Figure 2.44 shows some relationships.

Hexammines

Hexammines are more difficult to prepare than the pentammines, one route to $Rh(NH_3)_6^{3+}$ involving substitution under forcing conditions [86]:

$$[Rh(NH_3)_5Cl]Cl_2 \xrightarrow[100^\circ C\text{ sealed tube}]{NH_3\text{ (aq.)}} [Rh(NH_3)_6]Cl_3$$

It is more convenient to start with the triflate ion $[Rh(NH_3)_5(CF_3SO_3)]^{2+}$ since triflate is a much better leaving group than chloride and is immediately replaced by liquid ammonia [87]. A third route involves acid hydrolysis of the cyanate complex $[Rh(NH_3)_5(NCO)]^{2+}$, which proceeds quantitatively (probably via a carbamic acid complex). Vibrational studies on $Rh(NH_3)_6^{3+}$ assign stretching vibrations as $\nu_1(A_{1g})$ at 514 cm^{-1}, $\nu_2(E_g)$ at 483 cm^{-1} and $\nu_3(T_{1u})$ at 472 cm^{-1} [88].

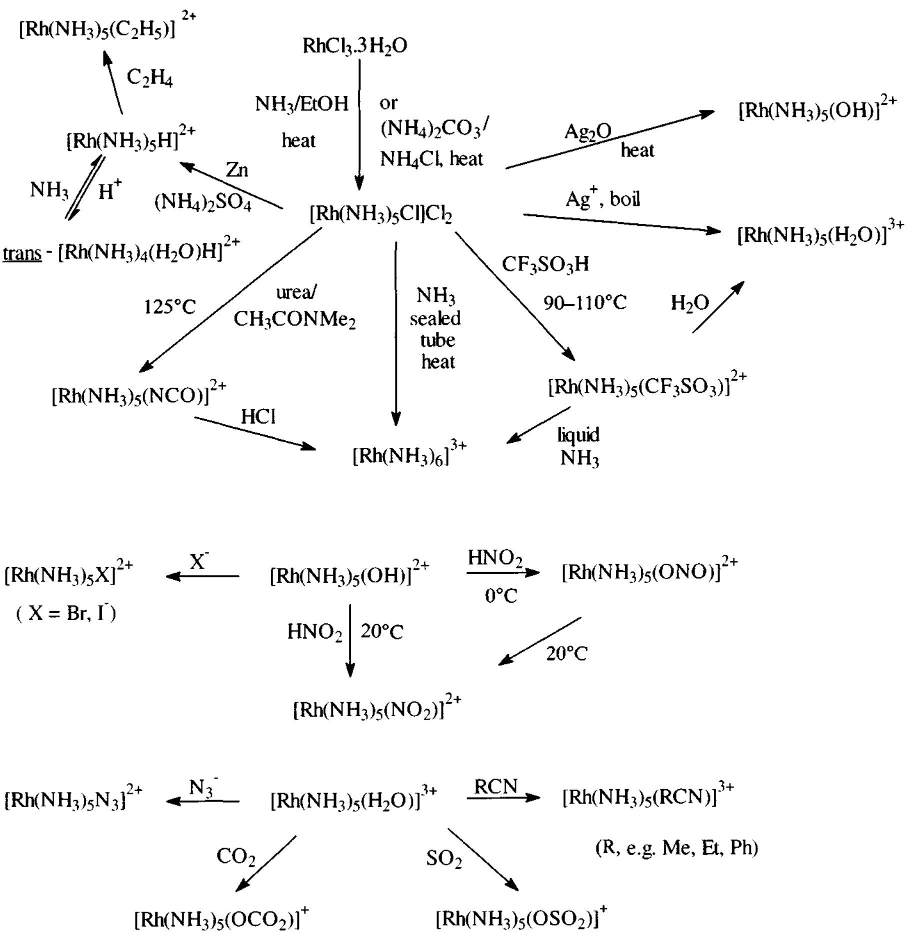

Figure 2.44 Syntheses and reactions of rhodium(III) ammine complexes.

Pentammines

The most important of the pentammines is the chloride $[Rh(NH_3)_5Cl]Cl_2$, prepared by one of two routes [89]:

$$RhCl_3.3H_2O \xrightarrow[EtOH]{NH_3\,(aq.)} [Rh(NH_3)_5Cl]Cl_2$$

The ethanol is implicated in forming a rhodium(I) complex that catalyses the reaction. The second method produces a mixture

$$RhCl_3.3H_2O \xrightarrow[H_2O,\,heat]{(NH_4)_2CO_3/NH_4Cl} [Rh(NH_3)_5Cl]Cl_2 + [Rh(NH_3)_4Cl_2]Cl$$

which is easily separable because the yellow pentammine precipitates while the more soluble tetrammine stays in solution. Other pentammines can be made by metathesis with NaX or by substitution of the aquo complex.

$$[Rh(NH_3)_5(H_2O)]^{3+} \xrightarrow{X^-} [Rh(NH_3)_5X]^{2+} \qquad (X = Cl, Br, I)$$

X-ray diffraction studies on $[Rh(NH_3)_5X]X_2$ (X = Cl, Br) yield Rh–N 2.051–2.061 Å (X = Cl) and 2.052–2.062 Å (X = Br) with Rh–Cl 2.355 Å and Rh–Br 2.491 Å, respectively [90].

The most remarkable pentammine is the hydride $[Rh(NH_3)_5H]^{2+}$ [91], produced by zinc (powder) reduction of the chloropentammine salt. It shows ν(Rh–H) at 2079 cm^{-1} in the IR spectrum (of the sulphate) and the low-frequency hydride NMR resonance at $\delta = -17.1$ ppm as a doublet showing Rh–H coupling (14.5 Hz). Its crystal structure shows the pronounced *trans*-influence of hydride, with the Rh–N bond *trans* to H some 0.17 Å longer than the *cis* Rh–N bond (Figure 2.45) [92].

Kinetic inertness, evidently caused by the electronic configuration, leads to a remarkable unreactivity of the Rh–H bond to hydrolysis. In the absence of air, it is unaffected by ammonia solution: in dilute solution, the ammonia *trans* to hydride is reversibly replaced by water, showing that the hydride has a *trans*-effect parallel to its *trans*-influence.

$$Rh(NH_3)_5H^{2+} + H_2O \Leftrightarrow Rh(NH_3)_4(H)(H_2O)^{2+} + NH_3$$

Both these hydrides insert alkenes and alkynes; the crystal structure of $[Rh(NH_3)_5(C_2H_5)]^{2+}Br_2$ shows the ethyl group has a *trans*-influence comparable to that of the hydride [93].

The hydroxypentammine is a useful starting material for the nitro and nitrito linkage isomers, the nitrito form separating under mild conditions but transforming to the nitro isomer on standing, especially when heated.

$$\begin{tikzcd}
{[Rh(NH_3)_5OH]^{2+}Cl_2} \arrow[r, "NaNO_2", "12\,M\,HCl\,0°C"'] & {[Rh(NH_3)_5(ONO)]Cl_2} \arrow[d, "\text{stand, heat}"] \\
 & {[Rh(NH_3)_5(NO_2)]Cl_2}
\end{tikzcd}$$

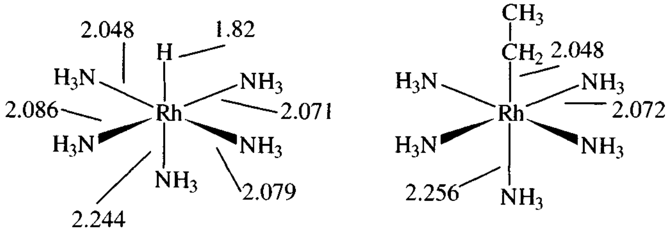

Figure 2.45 Comparative bond lengths in $[Rh(NH_3)_5H]^{2+}$ and $[Rh(NH_3)_5Et]^{2+}$.

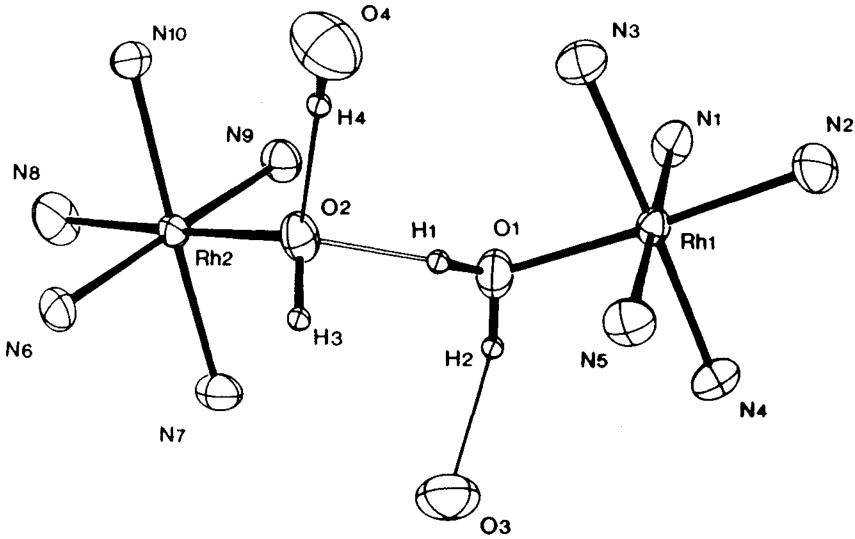

Figure 2.46 The structure of $[(NH_3)_5Rh(H_7O_4)Rh(NH_3)_5]^{5+}$. (Reproduced with permission from *Z. Naturforsch., Teil B*, 1988, **43**, 189.)

$[Rh(NH_3)_5OH]^{2+}$ reacts with $[Rh(NH_3)_5(H_2O)]^{3+}$ to form $[(NH_3)_5Rh(H_7O_4)$-$Rh(NH_3)]^{5+}$ (Figure 2.46) in which there is a μ-H_3O_2 bridge between the coordinated H_2O and OH groups [94].

Tetrammines

A useful route into the tetrammine series starts from the readily available chloropentammine, substitution with oxalate giving the (necessarily) *cis*-tetrammine, conveniently isolable as a perchlorate [95]:

$$Rh(NH_3)_5Cl^{2+} \xrightarrow[120^\circ C,\, 14\,h]{Na_2C_2O_4/H_2C_2O_4} [Rh(NH_3)_4(C_2O_4)]^+$$

The oxalate can then be replaced by chloride or bromide:

$$cis\text{-}[Rh(NH_3)_4(C_2O_4)]^+ \xrightarrow{HCl} cis\text{-}[Rh(NH_3)_4Cl_2]^+$$

The *trans*-isomer can be obtained as a second product in the pentammine synthesis, also by

$$[Rh(NH_3)_5H]^{2+} \xrightarrow[2.\, H_2O_2/HCl\, pH\, 1]{1.\, KCl\, pH\, 6} trans\text{-}[Rh(NH_3)_4Cl_2]^+Cl^-$$

In this reaction, the ammonia *trans* to hydride then the hydride itself are both replaced. In *trans*-$[Rh(NH_3)_4Cl_2]^+Cl^-$, Rh–N is 2.07 Å and Rh–Cl 2.31 Å [96].

Photochemical reactions of rhodium(III) ammines

Though thermally stable, rhodium ammines are light sensitive and irradiation of such a complex at the frequency of a ligand-field absorption band causes substitution reactions to occur (Figure 2.47) [97]. The charge-transfer transitions occur at much higher energy, so that redox reactions do not compete.

Irradiation of solutions of *cis*-$[Rh(NH_3)_4Cl_2]^+$ at 366 nm formed mainly *trans*-$[Rh(NH_3)_4Cl(H_2O)]^{2+}$ with a little *cis*-isomer. *Trans*-$[Rh(NH_3)_4Cl_2]^+$ behaves similarly. The isomeric chloro aqua complexes photochemically interconvert but eventually form a stationary state.

The *cis*/*trans* ratio is the same for both reactions, suggesting a common intermediate. In an important reinvestigation, it was found that *cis*-$[Rh(NH_3)_4Cl(H_2O)]^{2+}$, *cis*-$[Rh(NH_3)_4Cl_2]^+$ and the corresponding *trans*-isomers give the same mixture of 17% *cis*- and 83% *trans*-$[Rh(NH_3)_4Cl(H_2O)]^{2+}$,

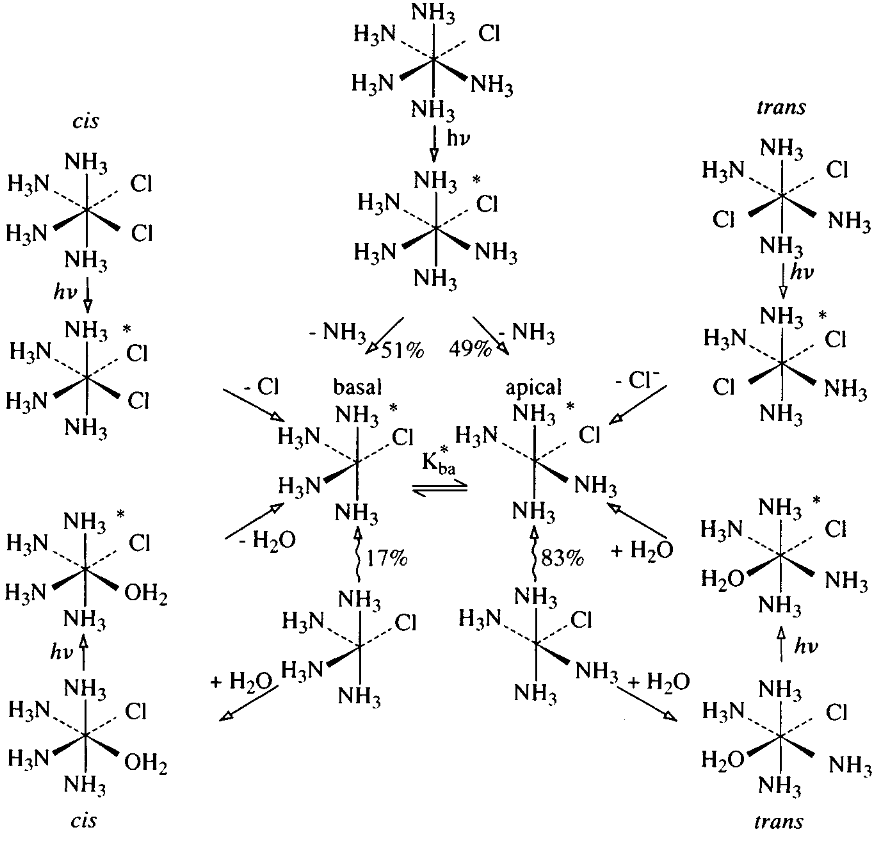

Figure 2.47 The limiting photosubstitution mechanism for rhodium(III) ammine complexes. (Reprinted from *Coord. Chem. Rev.*, **94**, 151, 1989, with kind permission from Elsevier Science S.A., P.O. Box 564, 1001 Lausanne, Switzerland.)

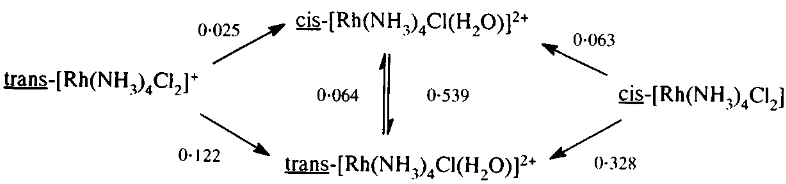

Figure 2.48 Quantum yields for the photolysis of rhodium(III) ammine complexes.

implying that photolysis takes a dissociative pathway leading to a 5-coordinate intermediate that can equilibrate with its isomer before being attacked by a water molecule to give the final $[\mathrm{Rh(NH_3)_4Cl(H_2O)}]^{2+}$ ion (Figure 2.48).

Solvent can affect the product yields. $[\mathrm{Rh(NH_3)_5Cl}]^{2+}$ tends to lose $\mathrm{Cl^-}$ in polar media, but in less polar solvents (MeOH, DMSO) that cannot solvate $\mathrm{Cl^-}$ so well, ammine loss predominates. $[\mathrm{Rh(NH_3)_5N_3}]^{2+}$ in HCl solution undergoes mainly substitution to give $[\mathrm{Rh(NH_3)_5Cl_2}]^+$ and $\mathrm{N_2}$, but other products include $[\mathrm{Rh(NH_3)_5(NH_2OH)}]^{3+}$.

2.9.3 *Complexes of other N-donors*

A range of pyridine complexes can be made [98]

$$trans\text{-}\mathrm{Rhpy_4Cl_2^+} \xleftarrow[\text{trace EtOH}]{\text{py}} \mathrm{RhCl_6^{3-}} \xrightarrow[\text{py}]{\text{neat}} fac \text{ and } mer\text{-}\mathrm{RhCl_3py_3}$$

Apart from ethanol, other primary alcohols catalyse the formation of the dichloro complex, probably via a rhodium(I) intermediate rather than a rhodium(III) hydride. $\mathrm{Rhpy_4X_2^+}$ compounds have anti-bacterial activity.

Though it is not possible to replace the remaining two chlorides in $[\mathrm{Rhpy_4Cl_2}]^+$ by pyridine, possibly owing to steric effects, it can be used as a starting material for a number of syntheses. With ammonia it gives $[\mathrm{Rh(NH_3)_5Cl}]^{2+}$, and with bidentate amines (en, phen) it gives ions like *trans*-$[\mathrm{Rhen_2Cl_2}]^+$ (excess amine leads to $\mathrm{Rhen_3^{3+}}$).

Nitrile complexes are synthesized by a variety of routes (Figure 2.49).

$\mathrm{Rh(NO_2)_6^{3-}}$ is of some importance in the traditional extraction of rhodium. Impure $\mathrm{RhCl_3}$ is neutralized and treated with $\mathrm{NaNO_2}$; $\mathrm{Na_3Rh(NO_2)_6}$ is soluble under these conditions (though base metals precipitate), but when ammonium chloride is added, $\mathrm{(NH_4)_3Rh(NO_2)_6}$ precipitates. The potassium salt is similarly relatively insoluble. All these salts are believed

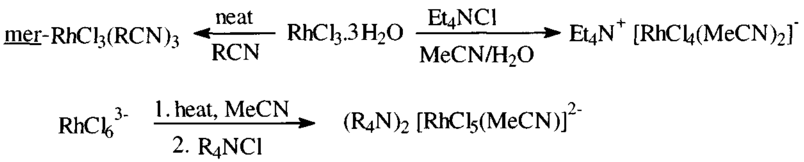

Figure 2.49 Synthesis of rhodium(III) nitrile complexes.

to involve N-bonded NO_2 groups; confirmed (X-ray) for $Na_3Rh(NO_2)_6$ (Rh–N 2.056 Å) [99].

Polydentate N-donors

The synthesis of $Rhen_3^{3+}$, mentioned above, is again accelerated by a trace of ethanol catalyst

$$RhCl_3.3H_2O \xrightarrow[\text{aq. EtOH}]{\text{en}} Rhen_3Cl_3$$

It exists as optical isomers and was first resolved by Alfred Werner. The route to the bis complexes generates the ammine *in situ* and is applicable to other ammines (tren, trien, etc.) yielding principally the *trans*-isomer

$$RhCl_3.3H_2O \xrightarrow[\text{2. 2 equiv. NaOH}]{\text{1. 2 equiv. en HCl reflux}} \textit{trans}\text{-}[Rhen_2Cl]^+Cl^-$$

Entry into the *cis*-diammine system (Figure 2.50) uses the chelating ligand oxalate, as with the ammines; use of $NaBH_4$ as catalyst speeds this up.

The oxalate can be removed by acid hydrolysis. *cis*-$Rhen_2X_2^+$ complexes have also been resolved for X = Cl, NO_2 and $\frac{1}{2}C_2O_4$ [100].

With the more rigid phen and bipy, *cis*-$Rh(L{-}L)_2X_2^+$ can be prepared using ethanol in a reaction reminiscent of the synthesis of $Rhpy_4Cl_2^+$

$$RhCl_3.3H_2O \xrightarrow{\text{L–L/EtOH}} \textit{cis}\text{-}Rh(L{-}L)_2Cl_2^+ \qquad (\text{L–L} = \text{phen, bipy})$$

$$RhX_6^{3-} \xrightarrow{\text{phen}} Rh(phen)X_4^- \xrightarrow{\text{phen}} \textit{cis}\text{-}Rh(phen)_2X_2^+ \qquad (X = Cl, Br)$$

A recent facile synthesis of $Rh(L{-}L)_3^{3+}$ is:

$$RhCl_3.3H_2O \xrightarrow{AgL_2^+X^-} Rh(L{-}L)_3^{3+}(X^-)_3$$

(X = ClO_4, NO_3; L = phen, bipy).

Like the ammines, rhodium complexes of ligands like bipy and phen have a significant photochemistry. Therefore, on irradiation, solutions of *cis*-$[Rh(L{-}L)_2X(H_2O)]^{2+}$ (X = halogen) gradually convert to *cis*-$[Rh(L{-}L)_2X(H_2O)]^{2+}$, though much more slowly than with the ammines [101].

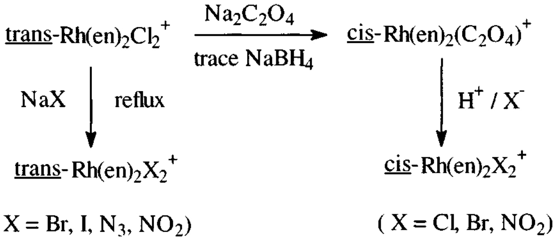

Figure 2.50 Synthesis of rhodium(III) complexes of ethylenediamine.

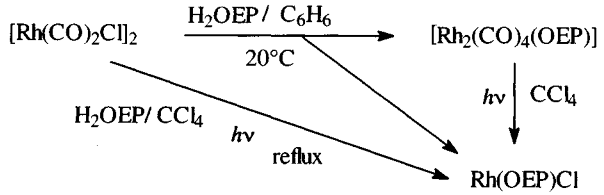

Figure 2.51 Synthesis of rhodium porphyrin complexes.

Macrocycles

Reaction of $[Rh(CO)_2Cl]_2$ with porphyrins (e.g. H_2TPP) leads to Rh(porphyrin)(CO)Cl, which readily lose CO. Some of the chemistry of the octaethylporphyrin complexes [102] is shown in Figures 2.51 and 2.52.

Two forms of the methyl complex have been characterized by X-ray diffraction; the Rh–C distances differ slightly at 1.97 and 2.01 Å, though the sp coordination geometry is the same.

The rhodium(II) compound is a diamagnetic dimer; with oxygen it forms a paramagnetic monomeric O_2 adduct, probably a superoxide complex represented as $(porph)Rh^{3+}O_2^-$.

2.9.4 Complexes of S-donors

The thiocyanate $(Ph_4P)_3[Rh(SCN)_6]$ is S-bonded, with Rh–S 2.372 Å; however, linkage isomers $[Rh(NCS)_n(SCN)_{6-n}]^{3-}$ exist, separable by chromatography [103].

A series of sulphide complexes can be made by refluxing the rhodium trihalide with the appropriate organic sulphide in methanol or ethanol:

$$RhX_3 + 3R_2S \xrightarrow[\text{reflux}]{\text{MeOH}} mer\text{-}RhX_3(R_2S)_3$$

(R = Me, Et, Pr; $R_2 = (CH_2)_4$).

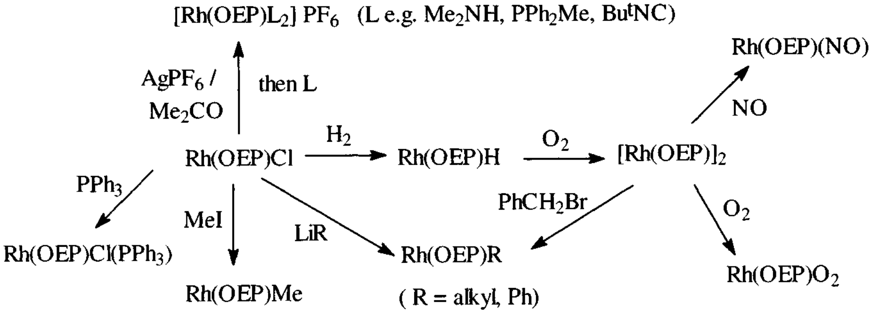

Figure 2.52 Reactions of rhodium porphyrin complexes.

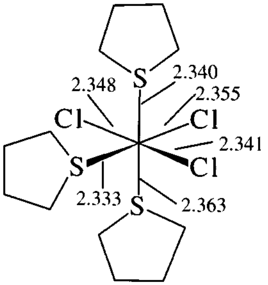

Figure 2.53 Structure of $RhCl_3$(tetrahydrothiophene)$_3$.

Similar reactions with PhSR (R = Me, Et, Pr, Bu) give *mer*-$RhX_3(PhSR)_3$ and some *fac*-isomer for R = Et, Bu. X-ray diffraction confirms (Figure 2.53) the *mer*-structure for the tetrahydrothiophene complex $RhCl_3(C_4H_8S)_3$, which has been used as a convenient starting material for making organo-rhodium compounds.

^1H NMR shows no exchange with added C_4H_8S [104].

Tris-chelates with bidentate S-donors are made conventionally (Rh–S 2.368 Å for $Rh(S_2CNEt_2)_3$)

$$RhCl_3.3H_2O \xrightarrow[H_2O/EtOH\ heat]{NaY} RhY_3 \qquad (Y = S_2CNR_2, S_2P(OEt)_2)$$

On oxidation of $Rh(S_2CNMe_2)_3$, an unusual dimer is formed (Figure 2.54) with different rhodium environments; the $Rh_2(S_2CNMe_2)_5^+$ has no metal–metal bond (Rh–Rh 2.556 Å) [105].

The dithioacetylacetonate is made by preparing the ligand *in situ*; the stable red crystals have 6-coordinate rhodium (Rh–S 2.314–2.333 Å;

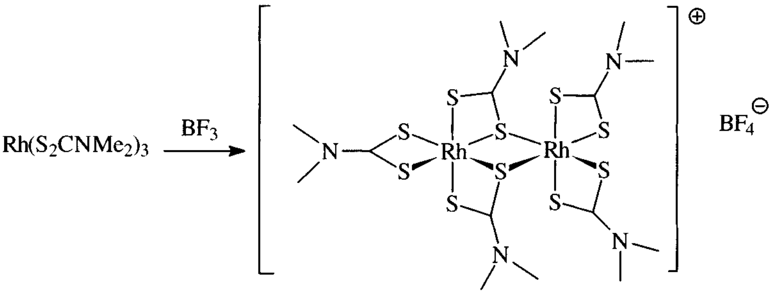

Figure 2.54 Synthesis of $[Rh_2(S_2CNMe_2)_5]^+$.

Table 2.5 Complexes formed by reaction of $RhCl_3$ with tertiary phosphines

Phosphine	Example		Complex formed
Small trialkyl	Me_3P		*fac*- and *mer*-$RhCl_3(PR_3)_3$
Large trialkyl	Bu_3P		*mer*-$RhCl_3(PR_3)_3$
Arylalkyl	Me_2PhP		*mer*-$RhCl_3(PR_3)_3$
Bulky alkyl	Bu^t_2PrP	(cold)	$RhCl_2(PR_3)_2$
	Bu^t_2PrP	(heat)	$RhHCl_2(PR_3)_2$
	Bu^t_3P	(heat)	$RhH_2Cl(PR_3)_2$
Triaryl	Ph_3P	(cold)	$RhCl_3(PR_3)_3$
	Ph_3P	(heat)	$RhCl(PR_3)_3$
	(*o*-tolyl)$_3$P	(cold)	$RhCl_2(PR_3)_2$

S–Rh–S 97°) in a geometry very similar to the acetylacetonate (section 2.9.1) [106].

$$RhCl_3.3H_2O + MeCOCH_2COMe \xrightarrow[HCl/EtOH,\,0^\circ C]{H_2S} Rh(MeCSCHCSMe)_3$$

Thiacrown ether and related systems also tend to involve octahedrally coordinated rhodium(III) [107].

2.9.5 *Tertiary phosphine complexes*

Rhodium(III) forms a wide range of complexes with tertiary phosphines and arsines [108, 109], though in some cases other oxidation states are possible. Table 2.5 summarizes the complexes produced from reaction of $RhCl_3$ with stoichiometric quantities of the phosphine.

Other halides can be introduced by metathesis. Figure 2.55 summarizes some of the complexes isolable with dimethylphenylphosphine, similar in general to the corresponding iridium complexes (section 2.13.3), including the photochemical isomerization of the *mer*-isomer.

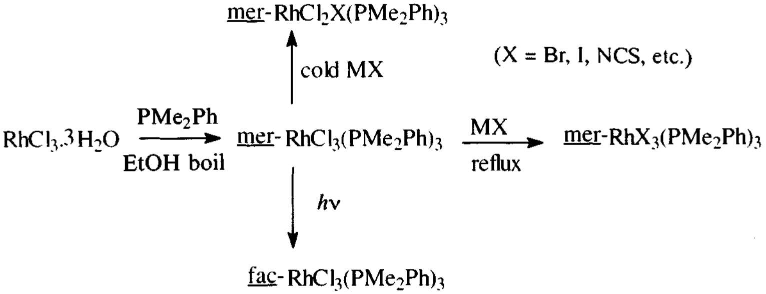

Figure 2.55 Synthesis of rhodium dimethylphenylphosphine complexes.

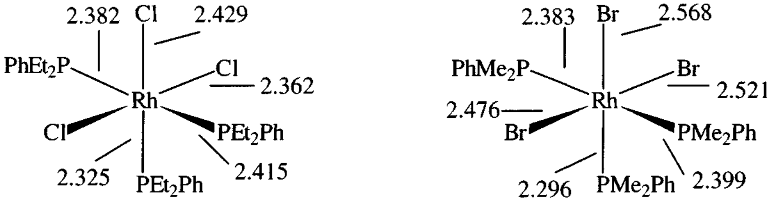

Figure 2.56 Bond lengths in octahedral rhodium(III) complexes of dialkylphenyl phosphines.

Crystal structures have been determined (Figure 2.56) for $RhCl_3(PEt_2Ph)_3$ and $RhBr_3(PMe_2Ph)_3$ (in both cases *mer*-isomer) – in each case, the Rh–X bond length shows the *trans*-influence of a tertiary phosphine [110].

Using less than 3 mol of phosphine affords binuclear complexes $Rh_2Cl_6(PR_3)_n$ ($n = 3, 4$), also obtained by reproportionation (Figure 2.57).

The structures of the two tri(*n*-butyl)phosphine complexes of this type have been determined (Figure 2.58), again showing the high *trans*-influence of PR_3 compared with Cl (Figure 2.58).

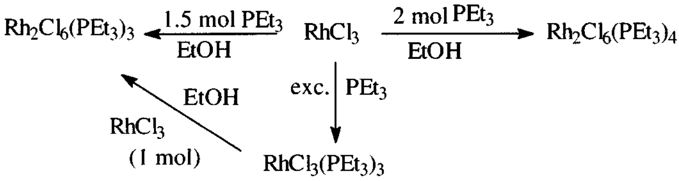

Figure 2.57 Interconversion between rhodium triethylphosphine complexes.

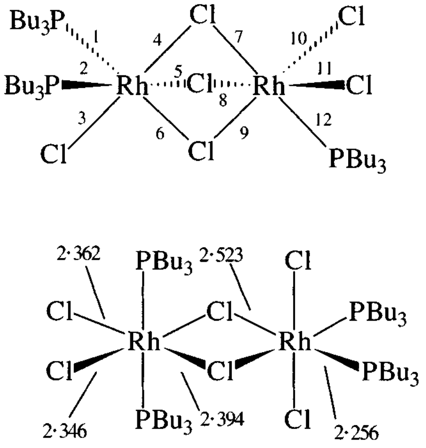

1 = 2.264; 2 = 2.249; 3 = 2.314
4 = 2.362; 5 = 2.504; 6 = 2.462
7 = 2.573; 8 = 2.365; 9 = 2.359
10 = 2.282; 11 = 2.291; 12 = 2.249

Figure 2.58 Bond lengths in rhodium complexes of tributylphosphines.

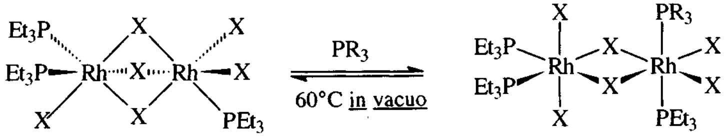

Figure 2.59 Interconversion between dimeric triethylphosphine complexes.

^{31}P NMR shows that when a tertiary phosphine is added to $Rh_2X_6(PEt_3)_3$, one isomer is exclusively produced, the process being reversible (Figure 2.59).

Similarly, adding 2.5 mol PEt_3 to 1 mol of $Rh_2Br_6(PEt_3)_4$ yields exclusively *mer*-$RhBr_3(PEt_3)_3$ [111, 112].

Hydride groups can be introduced by various methods [113], either abstraction of hydrogen from a solvent or a reducing agent, or by oxidative addition:

$$RhCl_3(PMePh_2)_3 \xrightarrow[EtOH]{H_3PO_2} RhHCl_2(PMePh_2)_3$$

$$RhCl_3 \xrightarrow[H_2O/Pr^iCH\text{ reflux}]{PBu^tPr_2} RhHCl_2(PBu^tPr_2)_2$$

$$RhCl(PBu^t_3)_2 \xrightarrow[hexane]{H_2} RhH_2Cl(PBu^t_3)_2$$

Bond lengths in $RhH_2Cl(PBut_3)_2$ are shown in Figure 2.60.

Carbonyl derivatives can be made similarly, either by abstracting CO from the solvent, by direct introduction or by oxidative addition to a Vaska-type complex:

$$RhCl_3 \xrightarrow[EtOH]{PPhEt_2/CO} RhCl_3(CO)(PPh_3)_2$$

$$RhCl(CO)(PPh_3)_2 \xrightarrow{Cl_2} RhCl_3(CO)(PPh_3)_2$$

NMR spectra of $RhX_3(PR_3)_3$ complexes

NMR spectra of tertiary phosphine complexes are often helpful in assigning stereochemistries [114] and two examples of *mer*-isomers are illustrated here.

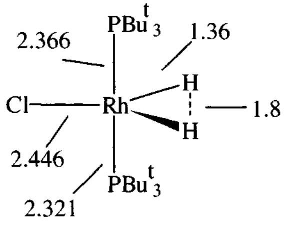

Figure 2.60 Bond lengths in $RhH_2Cl(PBu^t_3)_2$.

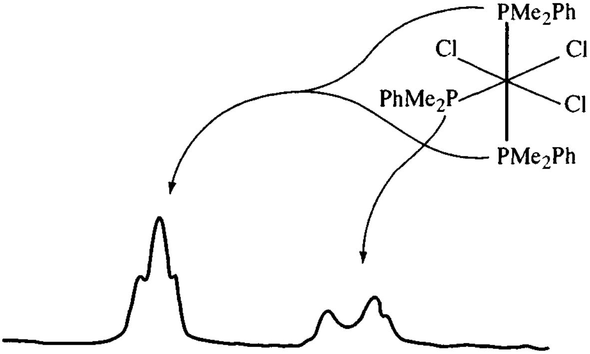

Figure 2.61 The methyl region of the ^{1}H NMR spectrum of *mer*-$RhCl_3(PMe_2Ph)_3$ demonstrating the 'virtual coupling' of the resonances as a result of the mutually *trans*-phosphines. (Reproduced with permission from S.A. Cotton and F.A. Hart, *The Heavy Transition Elements*, published by Macmillan Press Ltd, 1975.)

The methyl region of the ^{1}H NMR spectrum of *mer*-$RhCl_3(PMe_2Ph)_3$ is illustrated in Figure 2.61.

The resonance of the methyl in the unique phosphine is a doublet (splitting owing to coupling with ^{31}P, $I = \frac{1}{2}$), while the corresponding resonance for the methyls in the mutually *trans*-phosphines appears to be a 1 : 2 : 1 triplet. Such a triplet would be expected if the hydrogens were equally coupled to the two phosphorus nuclei – this cannot be the case: (^2J(P–H) could scarcely be the same as ^4J(P–H)). The phenomenon is known as 'virtual coupling' and is commonly found in complexes of PMe_2Ph and certain other methyl-substituted tertiary phosphines, with 4d and 5d metals. (If the case is treated as an $A_3XX'A'_3$ spin system, when $J(X{-}X)'$ is much larger than $J(A{-}X)$, a 1 : 2 : 1 triplet obtains with a spacing equal to $1/2J(A{-}X)$. It arises because with heavy metals $J(P{-}P)_{trans}$ is much greater than $J(P{-}P)_{cis}$.)

The ^{31}P NMR spectrum of *mer*-$RhCl_3(PMe_3)_3$ is shown in Figure 2.62; again two of the ligands are equivalent, so the spectrum is a doublet for

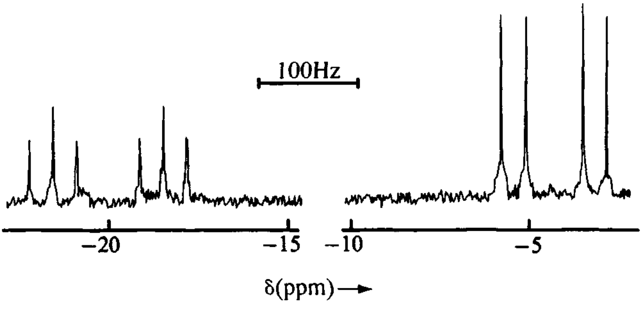

Figure 2.62 The ^{31}P NMR spectrum of *mer*-$RhCl_3(PMe_3)_3$, with random noise decoupling of the protons. (Reproduced with permission from *J. Chem. Soc., Dalton Trans.*, 1973, 704.

the two equivalent phosphines, split by the third, and a triplet for the third phosphine (split by two equivalent P), each signal in turn split by coupling to ^{103}Rh ($I = \frac{1}{2}$). (Doublet $\delta = -20.0$ Hz, J(Rh–P) = 112.1 Hz; J(P–P) = 24.2 Hz. Triplet $\delta = -4.3$ Hz, J(Rh–P) = 83.8 Hz). The ^{31}P NMR of *fac*-$RhCl_3(PEt_3)_3$ where all phosphines are equivalent is a doublet, the only splitting is owing to Rh–P coupling (114 Hz) similar to that found for P *trans* to Cl in the *mer*-isomer.

Case studies of phosphine complexes

An immense number of phosphine complexes of rhodium have been synthesized and detailed compilations of information are available [3d]. In this section, some case studies are presented to illustrate the variations that arise as a result of changes in the steric requirements of the phosphine.

Complexes of trimethylphosphine (cone angle 118°) [115]. Syntheses are shown in Figure 2.63. The rhodium(III) complexes can be made by the usual routes or by oxidation of rhodium(I) complexes. Note that in contrast with the bulkier PPh_3, refluxing $RhCl_3$ with PMe_3 does not result in reduction.

Complexes of triphenyl phosphine (cone angle 145°). Fusing anhydrous $RhCl_3$ with PPh_3 is reported to afford $RhCl_3(PPh_3)_3$, also prepared by chlorine oxidation of $RhCl(PPh_3)_3$. Normally, however, particularly on refluxing with excess PPh_3, reduction occurs and the important rhodium(I)

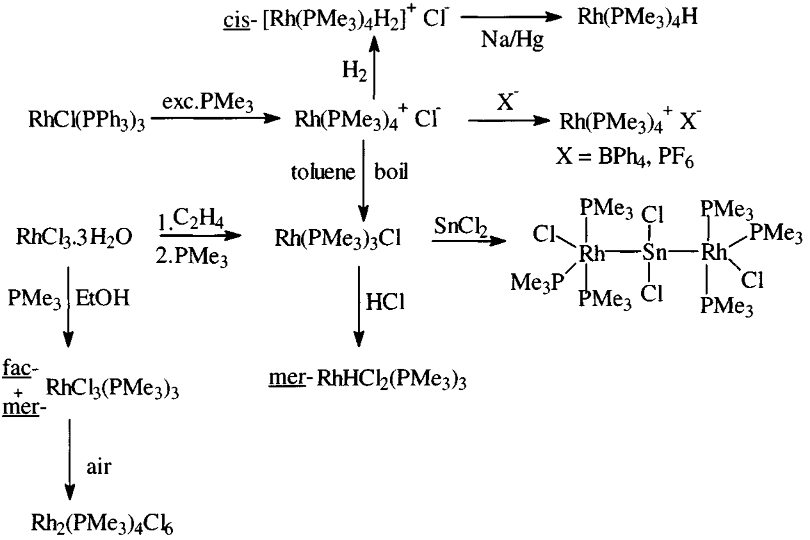

Figure 2.63 Syntheses and interrelationships between rhodium complexes of trimethylphosphine.

complex $RhCl(PPh_3)_3$ is obtained (section 2.7.1). A few other arylphosphines similarly act as reducing agents [45]. Wilkinson's catalyst contains traces of a paramagnetic impurity, long believed to be $RhCl_2(PPh_3)_2$. This has recently been reported as a serendipitous product of the cleavage of a rhodium diene complex, but the preparation has not yet been repeated [116].

Complexes of triisopropylphosphine (cone angle 160°) [69, 117]. In contrast to less bulky trialkylphosphines, a complex $RhCl_3(PPr^i_3)_3$ has only been made by reaction at 0°C: at higher temperatures, hydrides like $RhHCl_2(PPr^i_3)_2$ result (the less bulky tri(*n*-propyl)phosphine gives the 3 : 1 complex at reflux).

Recently, cleavage of the dimeric cyclooctene complex with PPr^i_3 under either hydrogen or nitrogen has been shown to afford $RhClH_2(PPr^i_3)_2$ and $RhCl(N_2)(PPr^i_3)_2$ (Figure 2.64); these compounds have trigonal bipyramidal and planar structures, respectively.

Controlled chlorination with *N*-chlorosuccinimide results in the formation of square pyramidal $RhHCl_2(PPr^i_3)_2$ and planar $RhCl_2(PPr^i_3)_2$ (Figure 2.65).

Reaction of $RhCl_3$ and sodium amalgam with triisopropylphosphine under a hydrogen atmosphere yields a distorted square planar complex $RhH(PPr^i_3)_3$ (Figure 2.66).

Its structure shows the *trans*-influence of hydride and pronounced distortion from square planar geometry (H–Rh–P 70.7°) owing to steric crowding. $(RhH(PPh_3)_3$ is rather less distorted (H–Rh–P 75.8°) [118a]. This 16-electron complex shows no tendency to add an extra molecule of phosphine, unlike the less hindered $RhH(PEt_3)_3$. It is, however, an active

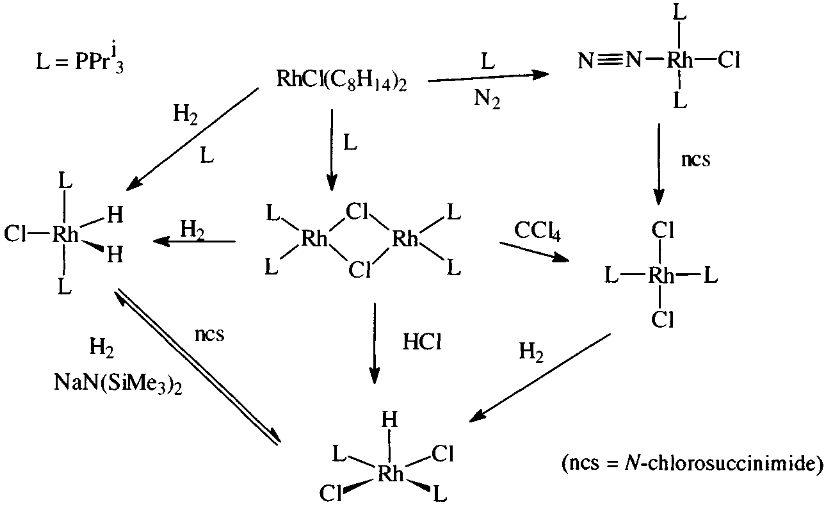

Figure 2.64 Interrelationships between rhodium complexes of triisopropylphosphine.

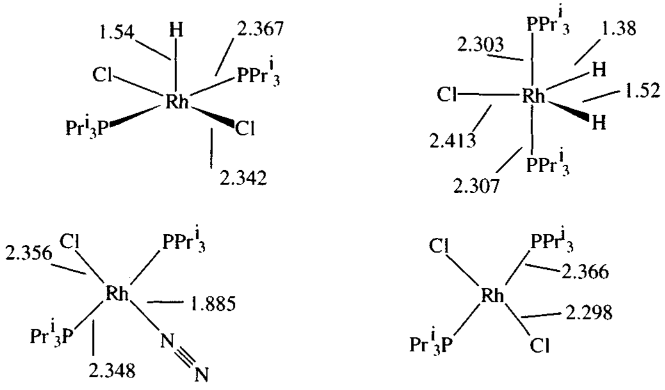

Figure 2.65 Bond lengths in rhodium complexes of triisopropylphosphine.

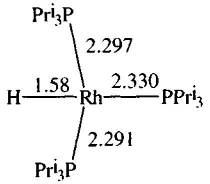

Figure 2.66 Bond lengths in $RhH(PPr^i_3)_3$.

catalyst for the hydrogenation of nitrites – this may result from dissociation to $RhH(PPr^i_3)_2$, as occurs with known $RhH(Pcy_3)_2$. A dimer, $[Rh_2H_4(PPr^i_3)_4]$ is also known [118b], it has the structure $[Pr^i_3P)_2Rh(\mu\text{-}H)_3RhH(PPr^i_3)_2]$.

Complexes of t-*butyl phosphines (PBu^t_3 cone angle 182°, PBu^t_2Me cone angle 161°)* [119]. Reaction of an excess of bulky trialkylphosphines with $RhCl_3.3H_2O$ does not yield $RhCl_3(PR_3)_3$ species; instead there is reduction to a rhodium(II) species $RhCl_2(PBu^t_2R)_2$ (R = Me, Et, Pr). However, if this synthesis is carried out at elevated temperatures, hydride abstraction occurs to give 5-coordinate $RhHCl_2(PBu^t_2R)_2$ (Figure 2.67); these compounds have NMR hydride signals at unusually high fields ($\delta \sim -30$ ppm). These undergo rapid carbonylation with alcoholic methoxide to give Vaska-type complexes

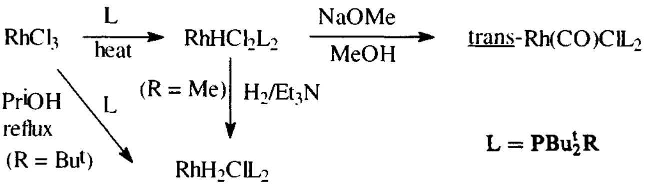

Figure 2.67 Syntheses of rhodium complexes of bulky di(*t*-butyl)alkylphosphines.

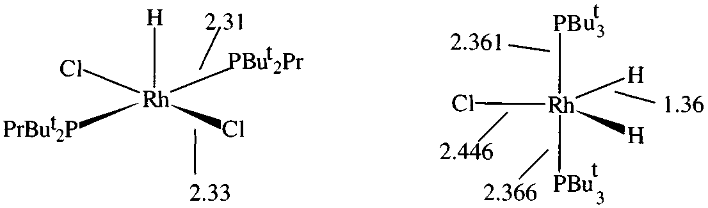

Figure 2.68 Bond lengths in two 5-coordinate rhodium hydride complexes with bulky tertiary phosphines.

(Figure 2.68); while 5-coordinate (tbp) dihydrides have also been synthesized [119b].

The ^{31}P NMR spectrum of $RhH_2Cl(PBu^t_2)_2$ is shown in Figure 2.69; the triplets show coupling with two equivalent hydrogens, split further by coupling with rhodium (*J*(Rh–P) 110.3 Hz; *J*(P–H) 14.9 Hz).

2.10 Iridium(I) complexes

Like rhodium(I), the iridium(I) complexes are stabilized by π-bonding ligands such as PR_3 and CO, with 4- and 5-coordinate geometries.

2.10.1 *Tertiary phosphine complexes*

$IrCl(PPh_3)_3$, the iridium analogue of Wilkinson's compound, illustrates the differences that can arise between two very similar metals. Unlike $RhCl(PPh_3)_3$, it cannot be made by heating $IrCl_3$ with excess phosphine, using the phosphine as a reducing agent, as hydride complexes are formed, a characteristic of iridium. Stable hydrides can also be made by oxidative addition to $IrCl(PPh_3)_3$ (Figure 2.70) [120].

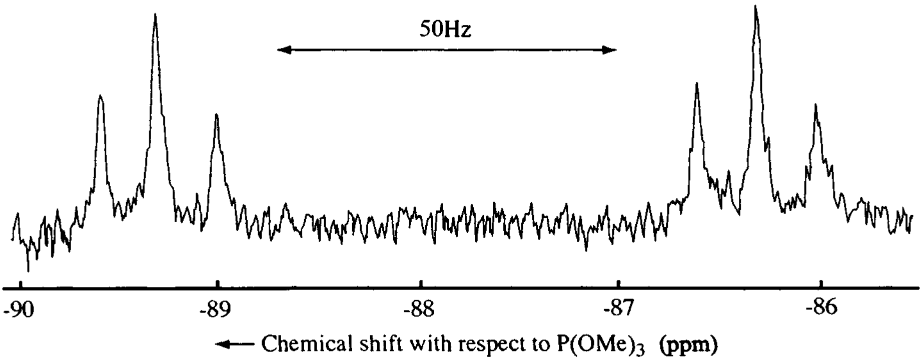

Figure 2.69 The ^{31}P NMR spectrum of $RhH_2Cl(PBu^t_3)_3$, with decoupling of the protons. (Reproduced with permission from *J. Chem. Soc., Series A*, 1971, 3684.)

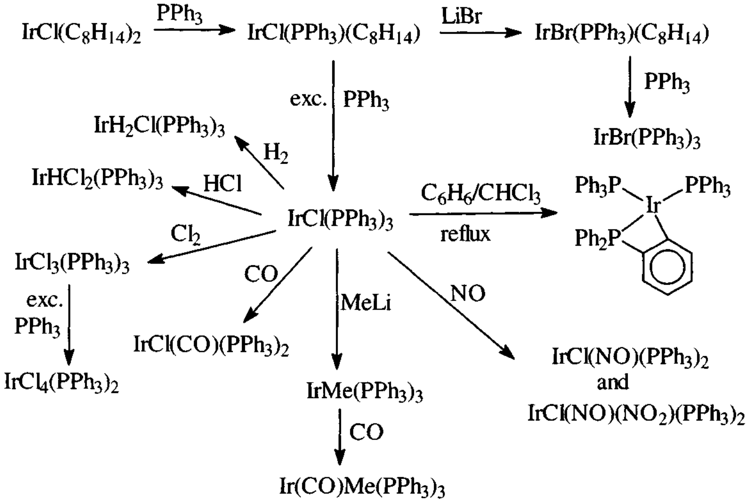

Figure 2.70 Synthesis and reaction of $IrCl(PPh_3)_3$.

$IrCl(PPh_3)_3$, which can be made by displacing alkene from IrCl(cyclooctene)$_2$, does not act as a hydrogenation catalyst for two main reasons: (a) the strong Ir–H bonds do not permit hydride transfer to coordinated alkene; (b) the hydride complexes like $IrH_2Cl(PPh_3)_3$ do not dissociate so there is no vacant coordination site capable of binding an alkene. The iridium methyl shown in Figure 2.70 is unstable to cyclometallation; recent study of the alkyls $Ir(PMe_3)_3(CH_2EMe_3)$ (E = C, Si) shows them to be thermally unstable too, metallating via a 6-coordinate iridium(III) hydride complex without dissociating a phosphine (Figure 2.71) [121].

A number of $Ir(PR_3)_4^+$ complexes exist [122]:

$$IrCl(CO)(PPh_3)_2 \xrightarrow[MeCN]{AgClO_4} Ir(CO)(MeCN)(PPh_3)_2^+$$
$$\xrightarrow[PPh_2Me]{exc.} Ir(PPh_2Me)_4^+ClO_4^-$$

The cation has significant tetrahedral distortion from square planar geometry (P–Ir–P ~150°) to minimize non-bonding interactions. It undergoes various oxidative addition reactions

$$Ir(PPh_2Me)_4^+ \xrightarrow{XY} IrXY(PPh_2Me)_4^+ \qquad (XY = H_2, HCl, Cl_2)$$

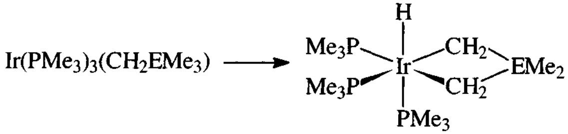

Figure 2.71 Cyclometallation of an iridium neopentyl.

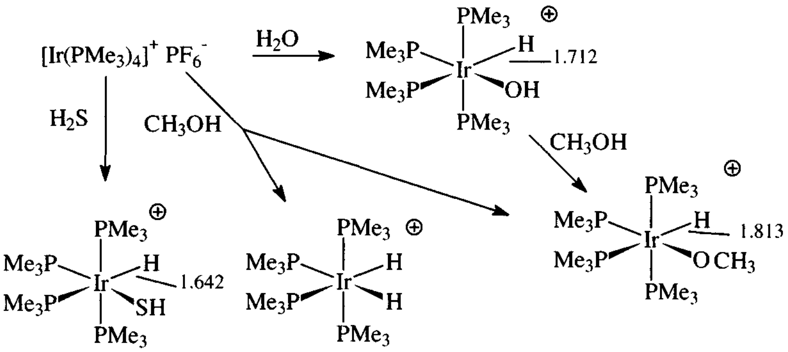

trans-Ligand	Ir—P
OH	2.259
OMe	2.274
SH	2.298
Trimethylphosphine	2.336–2.355
H	2.369–2.378

Figure 2.72 Oxidative additive reactions of $[Ir(PMe_3)_4]^+$ and bond lengths.

The similar species $Ir(PMe_3)_4^+$ likewise shows tetrahedral distortion from square planar geometry (P–Ir–P 152.6–158.9°). It undergoes some remarkable oxidative addition reactions with species like H_2O and H_2S (Figure 2.72).

The Ir–P bond lengths in the complexes allow the ligands to be placed in order of *trans*-influence.

Using the chelating phosphine bis(diphenylphosphino)ethane (dppe) a related complex $Ir(dppe)_2^+$can be made [123]

$$IrCl(CO)(PPh_3)_2 \xrightarrow[C_6H_6]{dppe} [Ir(dppe)_2CO]^+Cl^-$$

$$\xrightarrow[toluene]{100°C} Ir(dppe)_2^+Cl^- + CO$$

The orange complex, though quite air stable in the solid state, forms an 'irreversible' dioxygen adduct (IR ν(O–O) 845 cm^{-1}) in solution within a few minutes. The complex likewise adds H_2, HCl, HBr and, reversibly, CO. An adduct with MeNC is formed by a photochemical route:

$$Ir(MeNC)_4^+ \xrightarrow[h\nu]{dppe} Ir(dppe)_2(CNMe)^+$$

The square planar iridium isocyanide complexes [124]

$$IrCl_3 \xrightarrow[150°C]{CO} [IrCl(CO)_3]_x \xrightarrow{RNC} Ir(CNR)_4^+$$

(R, e.g. cyclohexyl, *p*-tolyl) readily undergo oxidative addition with molecules like Cl_2 and MeI to give iridium(III) complexes

$$Ir(CNR)_4^+ + XY \rightarrow IrXY(CNR)_4^+$$

2.10.2 Vaska's compound

The 1961 report that Vaska's compound ($IrCl(CO)(PPh_3)_2$) reversibly binds dioxygen sparked off an intense study of addition reactions of this and related compounds that has continued unabated up to the present day [125].

Vaska's compound may be prepared as yellow air-stable crystals by various reactions, such as conventional substitution

$$IrCl(CO)_3 \xrightarrow{PPh_3} IrCl(CO)(PPh_3)_2 + 2CO$$

or, more usually, by CO abstraction

$$IrCl_3.xH_2O \xrightarrow[MeOCH_2CH_2OH \text{ or } DMF]{PPh_3/\text{reflux}} IrCl(CO)(PPh_3)_2$$

The complex has a *trans*-structure [126] (Figure 2.73).

It undergoes a wide range of addition reactions with molecules XY:

$$IrCl(CO)(PPh_3)_2 + XY \rightarrow IrClXY(CO)(PPh_3)_2$$

If X–Y bond fission occurs, the product is a 6-coordinate iridium(III) complex (Table 2.6); otherwise a 5-coordinate (or pseudo-5-coordinate) adduct is obtained in which Ir formally retains the (+1) state (Table 2.7). This distinction can be somewhat artificial; $IrCl(O_2)CO(PPh_3)_2$ can be regarded as an iridium(III) peroxo complex.

Solutions of Vaska's compound react with oxygen to form $IrCl(O_2)(CO)(PPh_3)_2$; the dioxygen molecule can be removed by heating the solid *in vacuo* to 100°C or by simply flushing the solution with nitrogen. Under the same conditions, it reacts with hydrogen forming the stable octahedral complex $IrClH_2(CO)(PPh_3)_2$; CO is reversibly absorbed as $IrCl(CO)_2(PPh_3)_2$ while SO_2 forms a stable (but reversible) adduct $IrCl(SO_2)(CO)(PPh_3)_2$, where the SO_2 is bound to iridium by sulphur. An indication of the bond strength in the SO_2 adduct, about $40\,kJ\,mol^{-1}$, has been obtained by differential scanning calorimetry (a second molecule of SO_2 can be bound, probably via an $Ir{-}Cl \rightarrow SO_2$ linkage).

Adduct formation by $IrCl(CO)(PPh_3)_2$ and similar compounds results in a shift in the IR carbonyl stretching frequency (Table 2.8).

With the exception of the CO adduct, as might be expected, the adducts have higher stretching frequencies. The largest values are found for the 'irreversible' adducts with the halogens, corresponding to the higher positive charge on the metal. Therefore, as electrons are removed from the metal in

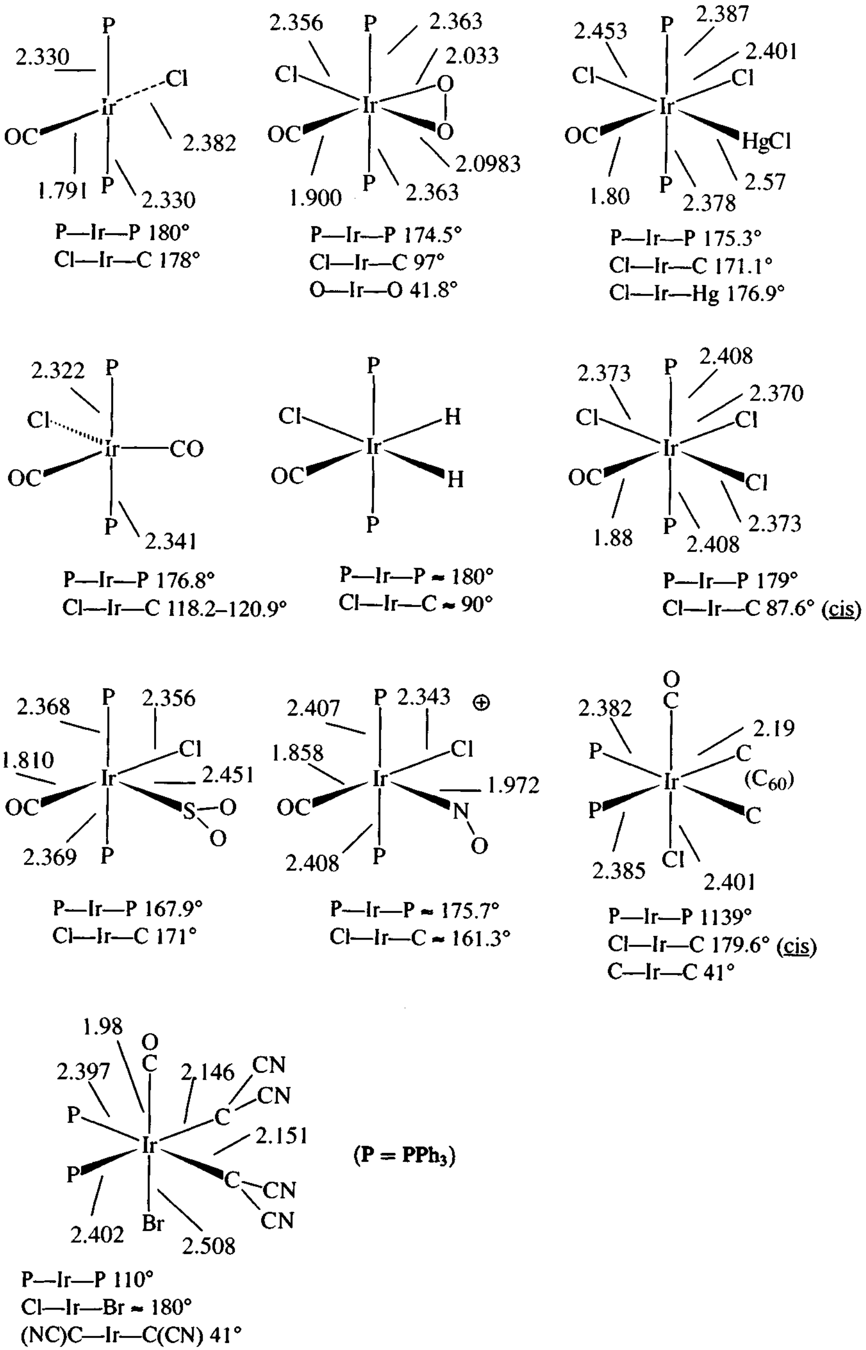

P—Ir—P 180°
Cl—Ir—C 178°

P—Ir—P 174.5°
Cl—Ir—C 97°
O—Ir—O 41.8°

P—Ir—P 175.3°
Cl—Ir—C 171.1°
Cl—Ir—Hg 176.9°

P—Ir—P 176.8°
Cl—Ir—C 118.2–120.9°

P—Ir—P ~ 180°
Cl—Ir—C ~ 90°

P—Ir—P 179°
Cl—Ir—C 87.6° (cis)

P—Ir—P 167.9°
Cl—Ir—C 171°

P—Ir—P ~ 175.7°
Cl—Ir—C ~ 161.3°

P—Ir—P 1139°
Cl—Ir—C 179.6° (cis)
C—Ir—C 41°

P—Ir—P 110°
Cl—Ir—Br ~ 180°
(NC)C—Ir—C(CN) 41°

(P = PPh_3)

Figure 2.73 Structural data for Vaska's compound and its adducts.

Table 2.6 Formation of 6-coordinate products from Vaska's compound

Reactant	Product
H_2	$IrClH_2(CO)(PPh_3)_2$
HCl	$IrCl_2H(CO)(PPh_3)_2$
Cl_2	$IrCl_3(CO)(PPh_3)_2$
$HgCl_2$	$IrCl_2(HgCl)(CO)(PPh_3)_2$
$SiHCl_3$	$IrClH(SiCl_3)(CO)(PPh_3)_2$
$SiEtHCl_2$	$IrClEt(SiHCl_2)(CO)(PPh_3)_2$
MeI	$IrClMeI(CO)(PPh_3)$
Cl_2S	$IrCl_2(SCl)(CO)(PPh_3)_2$
SiH_3Cl	$IrCl_2(SiH_3)(CO)(PPh_3)_2$
$S(CN)_2$	$IrCl(NCS)CN(CO)(PPh_3)_2$
HCN	$IrClH(CN)(CO)(PPh_3)_2$

Table 2.7 Formation of 5-coordinate (or pseudo-5-coordinate) products from Vaska's compound

Reactant	Product
O_2	$IrCl(O_2)(CO)(PPh_3)_2$
CO	$IrCl(CO)_2(PPh_3)_2$
SO_2	$IrCl(SO_2)(CO)(PPh_3)_2$
BF_3	$IrCl(BF_3)(CO)(PPh_3)_2$
$(NC)_2C{=}C(CN)_2$	$IrCl[(NC)_2C_2(CN_2)](CO)(PPh_3)_2$
$RC{\equiv}CR$	$IrCl(RCCR)(CO)(PPh_3)_2$
C_2F_4	$IrCl(F_2CCF_2)(CO)(PPh_3)_2$
N_2H_4/PPh_3	$IrH(CO)(PPh_3)_3$
$PhCON_3$	$IrCl(N_2)(PPh_3)_2$
C_n ($n = 60, 70$)	$IrCl(C_n)(CO)(PPh_3)_2$

Table 2.8 IR data for adducts of $IrCl(CO)(PPh_3)_2$

Molecule added	$\nu(CO)$ (cm^{-1})[a]
–	1967
O_2	2015
SO_2	2021
BF_3	2067 (C_6H_6)
HCl	2046
MeI	2047
C_2F_4	2052
$(NC)_2C{=}C(CN)_2$	2057
I_2	2067
Br_2	2072
Cl_2	2075
D_2	2034
CO	1934, 1988
C_{60}	2014 (mull)
C_{70}	2002 (sh 2012) (mull)

[a] Solution in $CHCl_3$ unless noted.

forming the adduct, the ability of the metal to participate in back-donation to the anti-bonding CO π^*-orbitals is reduced; as a result, the CO bond order increases.

Structures of some adducts [127] together with the parent compound are shown in Figure 2.73. If oxygen is treated as a monodentate ligand, then the structure of the oxygen adduct can be called trigonal bipyramidal similar to the CO adduct. The PPh_3 groups adopt *trans*-positions, favoured on steric grounds, which are also formed in the adducts with the halogens and $HgCl_2$. When the bulkier groups such as $(NC)_2C{=}C(CN)_2$ or C_n ($n = 60$, 70, 84) bind to iridium, the halogen and carbonyl groups occupy the 'axial' positions, as axial phosphines would involve non-bonding interactions with the bulky electron donors. Study of the structural data in Figure 2.73 shows a tendency for bond length to increase upon adduct formation though the more ionic Ir–Cl bonds seem to be less affected.

The structures of several adducts can be rationalized on the basis [128] that in a 5-coordinate low-spin d^8 tbp system, the acceptor ligands prefer to occupy an equatorial site ($IrCl(CO)_2(PPh_3)_2$) whereas a π-donor prefers an axial site. In a square pyramidal situation, it is weakly bonded acceptors that prefer the apical position, e.g. ($IrCl(SO_2)(CO)(PPh_3)_2$.

Some syntheses for other $IrX(CO)(PPh_3)_2$ complexes follow:

$$IrCl(CO)(PPh_3)_2 \xrightarrow[MeCN]{AgClO_4} Ir(MeCN)(CO)(PPh_3)_2^+ \xrightarrow{X^-} IrX(CO)(PPh_3)_2$$

$$(X = Br, I, CN, NCS, CNO, OH)$$

$$IrCl(CO)(PPh_3)_2 \xrightarrow[Ag_2CO_3]{NH_4F} IrF(CO)(PPh_3)_2$$

$$IrCl(CO)(PPh_3)_2 \xrightarrow{NaOR} Ir(OR)(CO)(PPh_3)_2 \quad (R = Me, Ph, Bu^t, C_6F_5)$$

$$IrCl(CO)(PPh_3)_2 \xrightarrow{MeLi} Ir(Me)(CO)(PPh_3)_2$$

The most versatile route involves the synthesis of the MeCN complex; the weakly bound nitrite is readily replaced by a variety of anions. These generally react in a similar way to the chloride, IR data for these and their dioxygen adducts are given in Table 2.9 [129].

Structures for a number of *trans*-$IrX(CO)(PR_3)_2$ systems have been determined (Table 2.10).

The Ir–P bonds show little dependence upon the *cis*-ligand X, as expected [130].

Complexes with other phosphines can be prepared by the general route of refluxing $IrCl_3$ or $IrCl_6^{2-}$ in an alcohol that acts as the source of CO, then adding the phosphine. In certain cases, a displacement reaction can be used

$$IrCl(CO)(PPh_3)_2 + 2PMe_3 \rightarrow IrCl(CO)(PMe_3)_2 + 2PPh_3$$

Table 2.9 IR data for $IrX(CO)(PPh_3)_2$ and its O_2 adducts (cm^{-1})

X	ν(CO)[a]		O_2 adduct		
	Mull	Solution	ν(CO) (mull)	ν(O–O) (mull)	Rev/irrev[b]
F	1944	1957	2005	850	
Cl	1960	1965	2005	855	rev
Br	1955	1966		862	rev
I	1975	1967	2005	850	irrev
OH	1930, 1950	1949			
Me	1935 (KBr)	1937 (C_6H_6)	1967	827	irrev
NCS	1970	1976	2015	855	rev
SH	1945	1965 (KBr)	1960	845	irrev
C_6F_5	1965 (KBr)	1990	no adduct		
NCO	1965	1968	2010	855	rev
C≡CPh	1955	1955 (CH_2Cl_2)	1990	835	irrev
SPh		1950			
CN		1990			
NCSe		1987			

[a] Solution in $CHCl_3$ unless noted; [b] Reversible or irreversible.

IR data [131] shows a trend to increasing ν(C–O) as the substituents on the phosphine became more electron withdrawing (Table 2.11) so that as the σ-donor power of the phosphine decreases and the π-acceptor power increases, the electron density at Ir decreases and electrons are removed from the π^*-orbital of CO [132].

There is a similar trend relating ν(C–O) to the π-acceptor strength of X (Figure 2.74).

The stereochemistry and mechanism of oxidative addition

In general when a molecule AB adds to a complex $IrX(CO)L_2$ [10, 133], second-order kinetics are exhibited

$$\text{rate} = k[\text{Ir complex}][\text{AB}]$$

Table 2.10 Bond lengths in *trans*-$IrX(CO)(PR_3)_2$ (Å)

PR_3	X	Ir–C	Ir–P	Ir–X
PPh_3	Cl	1.791	2.330	2.382
P(*o*-tolyl)$_3$	Cl[a]	1.67	2.338	2.43
P(*o*-tolyl)$_3$	Cl	1.817	2.331	2.364
Pcy_3	Cl	1.808	2.339	2.398
PPh_3	OPh	1.795	2.328, 2.344	2.049
PPh_3	Me[a]	1.835	2.300	2.17
P(*p*-tolyl)$_3$	Me	1.867	2.302, 2.305	2.206
PPh_3	OH	1.797	2.312, 2.314	2.110
PPh_3	C_6F_5	1.891	2.305, 2.326	2.090
PPh_3	OC_6F_5	1.798	2.320, 2.321	2.058
PPh_3	$C_6H_2Me_3$	1.848	2.313, 2.319	2.143

[a] Disordered structure, accuracy limited.

Table 2.11 IR data for $IrCl(CO)(PR_3)_2$ (cm^{-1})

PR_3	$\nu(CO)$		
	Toluene	$CHCl_3$	Mull
Pcy_3	1932	1927	1931
PPr^i_3	1935	1933	
PBu_3	1940	1943	
$PBuPh_2$	1955	1949	
PBz_3	1956	1956	
P(*p*-tolyl)$_3$	1963	1964	
PPh_3	1967	1971	1960
$P(OPh)_3$	2001	2003	
P(*o*-tolyl)		1960	
PMe_3			1938
$AsPh_3$			1958
PBu^t_3	1920[a]		1916

[a] Solution in pentane.

The reaction rates depend on several factors: the halide X, ligand L, even the solvent. Therefore, when MeI adds to $IrX(CO)(PPh_3)_2$ the rate increases in the order I < Br < Cl whereas for the addition of H_2 or O_2, the relative order is reversed.

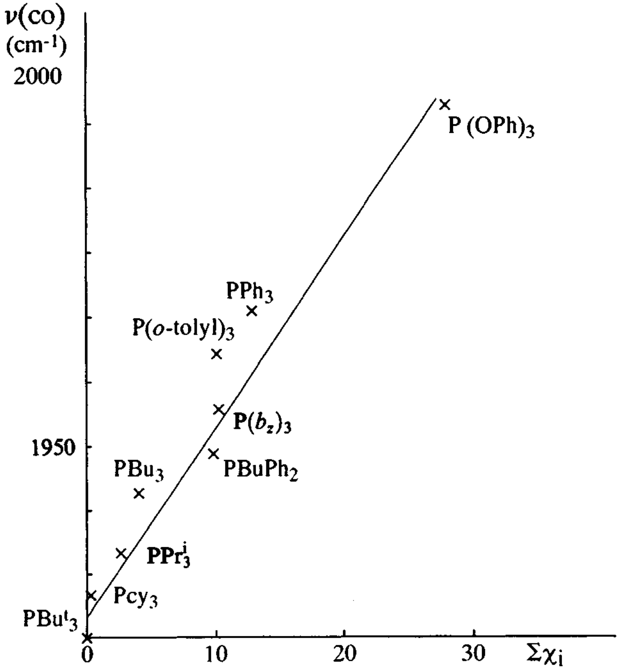

Figure 2.74 Relationship between ν(C–O) for *trans*-$IrCl(CO)(PPh_3)_2$ (in $CHCl_3$ solution) and $\sum\chi_i$ (Tolman's additivity substituent contribution for electronic effects in R_3P). (See *Chem. Rev.*, 1977, **77**, 313.)

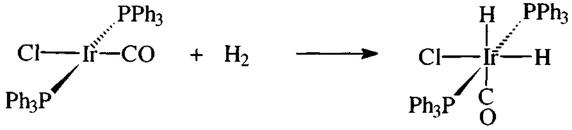

Figure 2.75 Oxidative addition of dihydrogen to Vaska's compound.

No single mechanism accounts for all the reactions. One pathway involves a concerted one-step process involving a cyclic transition state. This of necessity affords a *cis*-product. Another possibility, more favoured in polar solvents, involves a cationic 5-coordinate intermediate $[IrX(A)(CO)L_2]^+$, which undergoes subsequent nucleophilic attack by B^-. Other possibilities include a S_N2 route, where the metal polarizes AB before generating the nucleophile, and radical routes. Studies are complicated by the fact that the thermodynamically more stable isolated product may not be the same as the 'kinetic product' formed by initial addition.

When the adding species AB retains an A–B bond after addition (e.g. O_2), addition is necessarily *cis*. This is also the case when H_2 adds (Figure 2.75); the stereochemistry of this addition keeps the bulky tertiary phosphines apart.

Additionally, MO calculations indicate the lowest energy orientation occurs with the three strongest *trans*-influence ligands (two hydrides and a PPh_3) in a facial configuration. Calculations on compounds $IrX(CO)(PR_3)_2$ indicates that weak donors X and strong π-acceptors PR_3 favour addition in the XIrCO plane [134, 135].

When H_2 adds to *cis*-IrCl(CO)(dppe) (Figure 2.76), two pathways are found [136, 137].

The first product is formed in high yield at low temperatures but subsequently equilibrates with the thermodynamically more stable second product. The direction of the initial addition of H_2 in the P–Ir–CO plane is ascribed to the electron-withdrawing influence of the carbonyl group.

Using more basic (electron-donating) ligands generally speeds up the reactions while bulky ligands slow it down. The use of tris(*o*-tolyl)phosphine is an extreme example of the latter as IrCl(CO)[P(*o*-tolyl)$_3$]$_2$ fails to add O_2, H_2 or SO_2 and only adds HCl slowly; the reason is that methyls in an *ortho*-position tend to 'block' the axial positions (Figure 2.77) [126b].

Different results can be found in the solid state and solution; gaseous HX (X= halide) adds *cis* to solid $IrCl(CO)(PPh_3)_2$ and in benzene solution, but in polar solvents like methanol a mixture of *cis*- and *trans*-products is found.

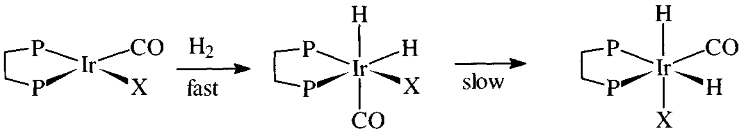

Figure 2.76 Oxidative addition to *cis*-Ir(CO)Cl(dppe).

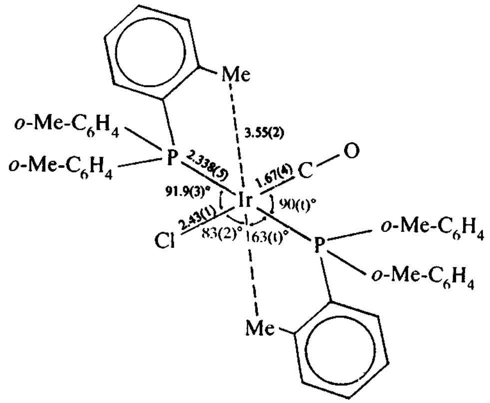

Figure 2.77 The structure of $IrCl(CO)[P(o\text{-tolyl})_3]_2$. (Reprinted with permission from *Inorg. Chem.*, 1975, **14**, 2669. Copyright (1975) American Chemical Society.)

2.11 Dioxygen complexes

Discovery of the ability of $IrCl(CO)(PPh_3)_2$ reversibly to bind dioxygen prompted considerable synthetic and structural study of dioxygen complexes [138]. Early reports of the structures of $IrX(CO)(O_2)(PPh_3)_2$ (X = Cl, Br, I) gave O–O distances of 1.30, 1.36 and 1.509 Å, respectively, compared with 1.21 Å in O_2^{2-}; since the first two were 'reversible' and the iodide an 'irreversible' adduct, it was postulated that the O–O distance correlated with this. Therefore, if electron transfer occurred from non-bonding metal d orbitals to anti-bonding orbitals of O_2, the O–O distance increased with electron donation (with the benefit of hindsight, the insensitivity of ν(O–O) in the IR spectrum contrasted strongly with the apparent variation in the O–O distance). Subsequently, increased structural data (see Table 2.12) indicated that O–O distances fell into a narrower range of 1.41–1.52 Å. It is now believed that some of the earlier studies gave anomalous results because of disorder in the crystal (and possible decomposition).

The presently accepted model for bonding in these dioxygen complexes regards them as essentially peroxo complexes. This view is supported [139] by the similarity in O–O distance to that in O_2^{2-}; likewise the similarity in ν(O–O) in the IR spectrum (Table 2.9) to that in H_2O_2 (880 cm^{-1}), Na_2O_2 (880 cm^{-1}) and $Na_2O_2.8H_2O$ (843 cm^{-1}). ^{17}O NQR studies on $IrCl(CO)O_2(PPh_3)_2$ show resonances at similar frequencies to H_2O_2 [140]. MO calculations suggest that the O_2 ligand donates about 0.1 electron from its $1\sigma_g$ -orbital and 0.2 electron from its π-orbital and accepts around 1.2 electrons from the metal dπ-orbital into its π_g-orbital. This back donation is primarily responsible for weakening the O–O bond [141].

Table 2.12 Bond lengths in dioxygen complexes (Å)

	d(O–O)
$[IrCl(CO)O_2(PPh_2Et)_2]^-$	1.469
$[IrO_2(PMe_2Ph)_4]^+BPh_4^-$	1.49
$[RhO_2(PMe_2Ph)_4]^+BPh_4^-$	1.43
$[RhO_2(AsMe_2Ph)_4]^+ClO_4^-$	1.46
$[IrO_2(Ph_2PCH_2PPh_2)_2]^+ClO_4^-$	1.486
$[IrO_2(Ph_2PCH_2PPh_2)_2]^+PF_6^-$	1.453
$[IrO_2(Ph_2PCH_2CH_2PPh_2)_2]^+PF_6^-$	1.52
$[IrO_2(Ph_2PCH_2PPh_2)_2]^+C(CN)_3^-$	1.39–1.43

The structural changes occurring upon oxygenation can be seen by comparison of the structures of $IrCl(CO)(PPh_3)_2$ and $IrCl(CO)(O_2)(PPh_2Et)_2$ (Figure 2.78); the latter is a more accurate determination than the disordered PPh_3 analogue. The former is essentially square planar, with virtually linear P–Ir–P and Cl–Ir–C geometries.

On reaction with O_2, the P–Ir–P colinearity is maintained (174.5°), keeping these bulky ligands apart, but the Cl–Ir–C angle closes (to 97.4°) to accommodate the incoming O_2 molecule. The geometry of the O_2 adduct can be described as distorted octahedral, with Ir, Cl, C and the two O atoms essentially coplanar. As expected as the coordination number increases, there is a general increase in bond length (except for Ir–Cl).

The S_2 and Se_2 groups are stabilized by bonding to iridium (and rhodium) [142]

$$Ir(dppe)_2Cl + \tfrac{1}{4}Y_8 \xrightarrow{CH_2Cl_2} [Ir(dppe)_2(Y_2)]^+Cl^- \qquad (Y = S, Se)$$

The S–S distance increases from 1.899 Å in S_8 to 2.066 Å (Figure 2.79).

The S_2 group is removed by Hg or R_3P, oxidized by periodate to coordinated S_2O or SO and methylated by Me_3SO_3F.

Iridium(I) can stabilize unusual species like CS, and SO, as well as N_2. The dinitrogen analogue of Vaska's compound is conveniently made as shown in Figure 2.80 [143].

It is essential that reagent grade $CHCl_3$ is used in the synthesis as the trace of ethanol 'stabilizer' removes the aryl isocyanate byproduct and prevents it

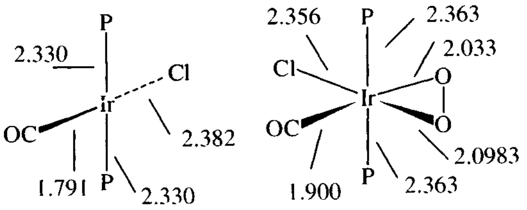

Figure 2.78 A comparison of the structures of $IrCl(CO)(PPh_3)_2$ and $IrCl(CO)O_2(PPh_2Et)_2$.

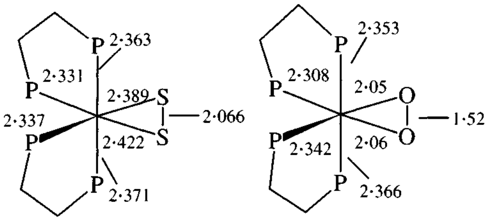

Figure 2.79 A comparison of bond lengths in *cis*-$[Ir(dppe)_2X_2]^+$.

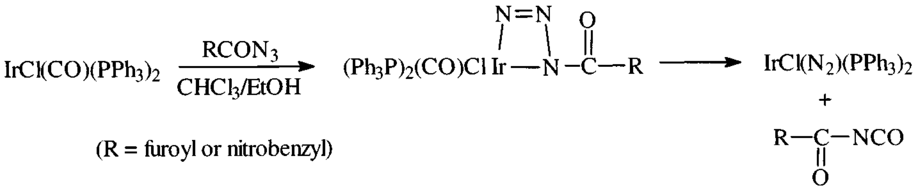

Figure 2.80 Synthesis of the dinitrogen complex $IrCl(N_2)(PPh_3)_2$.

reacting with the dinitrogen complex. The yellow N_2 complex (IR $\nu(N{\equiv}N)$ $2105\,cm^{-1}$) is thermally stable but the N_2 ligand is labile and readily replaced by other ligands (Figure 2.81).

The orange thiocarbonyl is air stable (IR $\nu(C{=}S)$ $1332\,cm^{-1}$); its synthesis proceeds via an isolable C_2S_5 complex that is desulphurized by refluxing with PPh_3 [144]:

$$\begin{aligned} IrCl(N_2)(PPh_3)_2 &\xrightarrow{CS_2} IrCl(C_2S_5)(PPh_3)_2 \\ &\xrightarrow{PPh_3} IrCl(CS)(PPh_3)_2 + Ph_3PS \end{aligned}$$

A green–black SO complex (dec. 155°C) with a bent Ir–S–O linkage has been synthesized (Figure 2.82) [145].

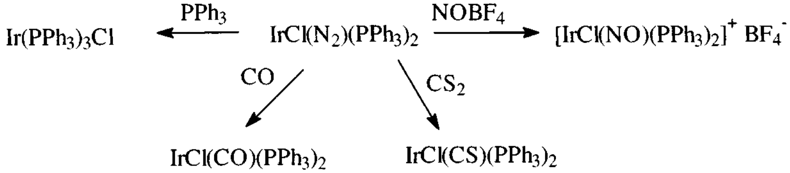

Figure 2.81 Reactions of the dinitrogen complex $IrCl(N_2)(PPh_3)_2$.

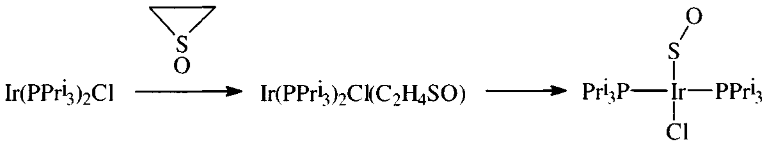

Figure 2.82 Synthesis of an SO complex.

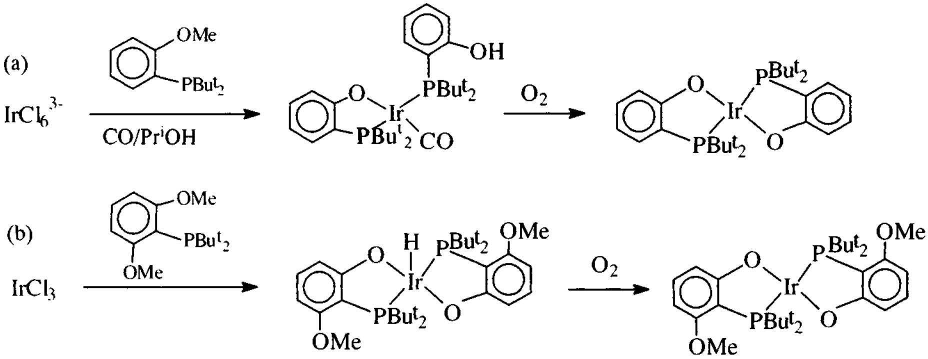

Figure 2.83 Syntheses of iridium(II) phosphine complexes.

2.12 Iridium(II) complexes

The iridium(II) complexes are rarer that those of rhodium(II). Iridium does not seem to form carboxylates $Ir_2(O_2CR)_4$ with the 'lantern' structure; complexes analogous to *trans*-$RhX_2(PR_3)_2$ are not formed with bulky tertiary phosphines, probably because the greater strength of Ir–H bonds leads to $IrHX_2(PR_3)_2$.

The best characterized complexes [146] are prepared as shown in Figure 2.83. In synthesis (a) the first step involves demethylation of both ligands; only one phosphine chelates, demonstrating the stability of square planar d^8 iridium(I); on oxidation, the CO is displaced (as CO_2) and both ligands chelate.

In synthesis (b), the initial product is a 5-coordinate (sp) iridium(III) hydride complex, which is rapidly oxidized in solution to the planar iridium(II) complex. Both of the compounds are paramagnetic with one unpaired electron, as expected for square planar d^7 complexes.

The square planar ion $[Ir(C_6Cl_5)_4]^{2-}$ also contains iridium(II) [147].

2.13 Iridium(III) complexes

A wide range of iridium complexes are formed in the +3 oxidation state, the most important for iridium, with a variety of ligands. The vast majority have octahedral coordination of iridium.

The aqua ion $Ir(H_2O)_6^{3+}$ and halide complexes IrX_6^{3-} have already been mentioned above. The kinetic inertness of the low spin d^6 complexes means that hydrolysis of $IrCl_6^{3-}$ is slow: complexes up to $IrCl_2(H_2O)_4^+$ have been produced and separated from mixtures by high-voltage electrophoresis.

Next Page

Previous Page

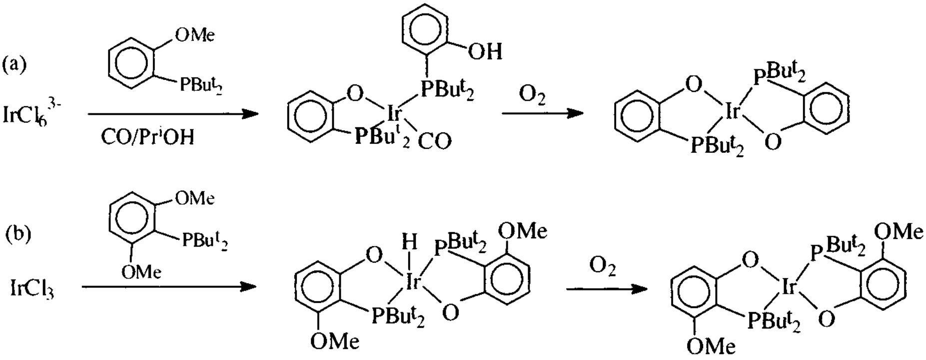

Figure 2.83 Syntheses of iridium(II) phosphine complexes.

2.12 Iridium(II) complexes

The iridium(II) complexes are rarer that those of rhodium(II). Iridium does not seem to form carboxylates $Ir_2(O_2CR)_4$ with the 'lantern' structure; complexes analogous to *trans*-$RhX_2(PR_3)_2$ are not formed with bulky tertiary phosphines, probably because the greater strength of Ir–H bonds leads to $IrHX_2(PR_3)_2$.

The best characterized complexes [146] are prepared as shown in Figure 2.83. In synthesis (a) the first step involves demethylation of both ligands; only one phosphine chelates, demonstrating the stability of square planar d^8 iridium(I); on oxidation, the CO is displaced (as CO_2) and both ligands chelate.

In synthesis (b), the initial product is a 5-coordinate (sp) iridium(III) hydride complex, which is rapidly oxidized in solution to the planar iridium(II) complex. Both of the compounds are paramagnetic with one unpaired electron, as expected for square planar d^7 complexes.

The square planar ion $[Ir(C_6Cl_5)_4]^{2-}$ also contains iridium(II) [147].

2.13 Iridium(III) complexes

A wide range of iridium complexes are formed in the +3 oxidation state, the most important for iridium, with a variety of ligands. The vast majority have octahedral coordination of iridium.

The aqua ion $Ir(H_2O)_6^{3+}$ and halide complexes IrX_6^{3-} have already been mentioned above. The kinetic inertness of the low spin d^6 complexes means that hydrolysis of $IrCl_6^{3-}$ is slow: complexes up to $IrCl_2(H_2O)_4^+$ have been produced and separated from mixtures by high-voltage electrophoresis.

2.13.1 Complexes of ammines

The iridium(III) complexes are broadly similar to the rhodium(III) ammines; a selection of synthesis is shown in Figure 2.84.

As with rhodium (and cobalt), introduction of five ammonia molecules is relatively straightforward, but the sixth substitution is difficult, requiring more forcing conditions. One versatile route involves the formation of the pentammine triflate complex ion $[Ir(NH_3)_5(O_3SCF_3)]^{2+}$, where the labile triflate group is readily replaced by water, then by a range of anionic ligands [148].

A recently reported synthesis involves refluxing a mixture of $IrCl_3$ and ethanoic acid with urea; hydrolysis of the urea proceeds steadily generating the ammonia ligands. This resulting mixture of the penta-, tetra- and triammines can be separated chromatographically [149].

No structural studies have been reported on these complexes, but detailed study of their vibrational spectra permits the assignments shown in Table 2.13. Like the rhodium analogues, iridium ammines are photoactive; therefore, on excitation of ligand-field bands, solutions of $[Ir(NH_3)_6]^{3+}$ or $[Ir(NH_3)_5Cl]^+$ afford $[Ir(NH_3)_5(H_2O)]^{3+}$.

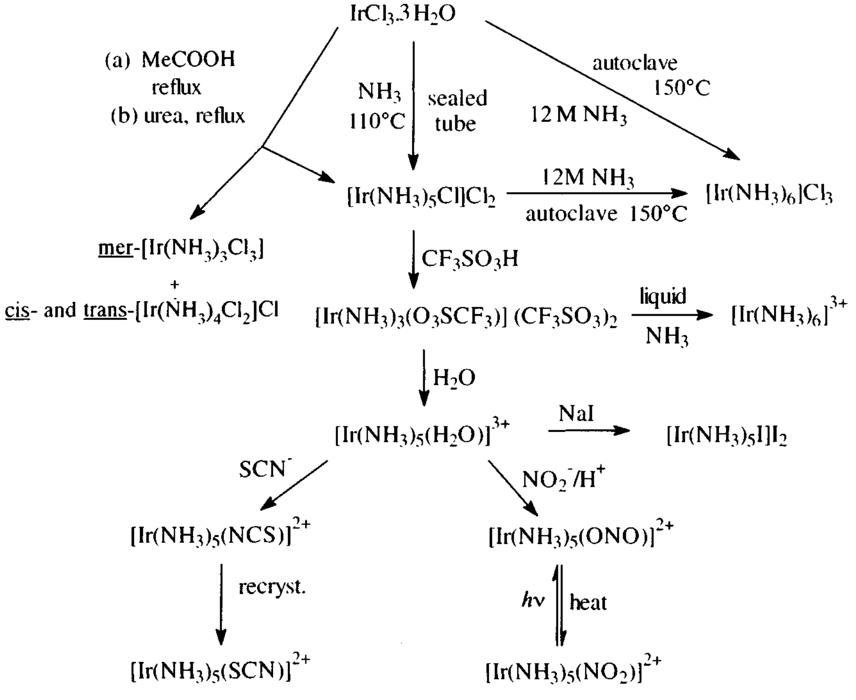

Figure 2.84 Synthesis of iridium(III) ammine complexes.

Table 2.13 Vibrational spectra of iridium(III) ammines (cm^{-1})

	ν(Ir–N)	ν(Ir–Cl)	ν(Ir–Br)
$Ir(NH_3)_6Cl_3$	527, 500, 475		
$[Ir(NH_3)_5Cl]Cl$	526, 512, 501, 479	306	
$[Ir(NH_3)_5Br]Br_2$	523, 509, 492, 478		200

Complexes with N-donor heterocyclics can be synthesized [150]:

$$IrCl_6^{3-} \xrightarrow[EtOH]{py} trans\text{-}Irpy_4Cl_2^+Cl^- \xrightarrow[UV]{py} mer\text{-}IrCl_3py_3$$

$$K_2IrCl_5(H_2O) \xrightarrow{pyrazine} K_2IrCl_5(pyrazine)$$

The latter is a case of monodentate pyrazine, also found in $IrCl_3(pyrazine)_3$ and $[IrCl_4(pyrazine)_2]^-$.

Complexes of the bidentate ligand ethylenediamine show similar patterns to simple ammines [151]

$$Na_3IrCl_6 \xrightarrow[145°C,\ sealed\ tube]{en/H_2O} Iren_3^{3+} \xrightarrow{KI} Iren_3I_3$$

Other anions can be introduced by ion exchange. One method for bis complexes is

$$K_3IrCl_6 \xrightarrow[MeCOOH]{en} cis\text{- and } trans\text{-}Iren_2Cl_2^+Cl^-$$

The resultant mixture can be separated by fractional crystallization as the *trans*-isomer is more soluble; the *cis*-isomer can be resolved into its enantiomers using optically active anions like α-bromocamphor π-sulphonate. These chlorides can be converted into the bromide or iodide complex by refluxing with a solution of the appropriate potassium halide.

2.13.2 Complexes of S-donors

Relatively few complexes of S-donors are well characterized [152]

$$(NH_4)_2IrCl_6 \xrightarrow[reflux]{Et_2S/EtOH} fac\text{-}IrCl_3(Et_2S)_3 + [IrCl_2(Et_2S)_4]^+[IrCl_4(Et_2S)_2]^-$$

The mixture of products can be separated by dissolving the yellow neutral complex in benzene; the red 'ionic' complex is crystallized from chloroform.

Among complexes of bidentate ligands, the dithiocarbamate $Ir[S_2CN(CH_2)_4]_3$ has octahedrally coordinated iridium (Ir–S 2.38 Å) [153].

This is synthesized by a standard method, while another synthetic method uses insertion reactions:

$$K_3IrCl_6 + 3NaS_2CN(CH_2)_4 \longrightarrow Ir[S_2CN(CH_2)_4]_3 + 3KCl + 3NaCl$$

$$mer\text{-}IrH_3(PPh_3)_3 \xrightarrow{CS_2} IrH_2(S_2CH)(PPh_3)_2$$

2.13.3 Tertiary phosphine and arsine complexes

A considerable number of the tertiary phosphine and arsine complexes of iridium(III) have been synthesized [4, 8]; they generally contain 6-coordinate iridium and are conventionally prepared by refluxing Na_2IrCl_6 with the phosphine in ethanol or 2-methoxyethanol [154]

$$IrCl_6^{2-} \xrightarrow[EtOH/HCl]{PR_3} IrCl_3(QR_3)_3$$

($QR_3 = PMe_2Ph, PEt_2Ph, Et_3As, Et_2PhAs, P(alkyl)_3$, etc.). This preparation affords a mixture of the *fac*- and (principally) the *mer*-isomer of $IrCl_3(QR_3)_3$, usually with some of the salt $R_3QH^+IrCl_4(QR_3)_2^-$. Bromides and iodides can be made directly or by metathesis

$$IrBr_6^{2-} \xrightarrow[\text{butanone, heat}]{PEt_2Ph} mer\text{-}IrBr_3(PEt_2Ph)_3$$

$$mer\text{-}IrCl_3(PEt_3)_3 \xrightarrow[\text{butanone, reflux}]{NaI} mer\text{-}IrI_3(PEt_3)_3$$

The *fac*-isomers are conveniently made by a general reaction involving irradiation (fluorescent tube) of a solution of the *mer*-isomer [155]

$$mer\text{-}IrX_3(PR_3)_3 \xrightarrow[C_6H_6]{h\nu} fac\text{-}IrX_3(PR_3)_3$$

as can pseudohalide complexes

$$mer\text{-}IrCl_3(PEt_3)_3 \xrightarrow[h\nu]{Y^-/Me_2CO} fac\text{-}IrY_3(PEt_3)_3 \qquad (Y = NCS, NCO, N_3)$$

The *fac*- and *mer*-isomers can be distinguished by physical methods (IR, NMR spectra, dipole moments); they also differ in reactivity:

$$fac\text{-}IrX_3(PR_3)_3 \xrightarrow[\text{boil}]{EtOH} IrHX_2(PR_3)_3$$

The *mer*-isomer does not react under these conditions. The properties of coordinated anions (e.g. Cl^-) in these complexes depend on the *trans*-ligand in various ways. Thus in *mer*-$IrCl_3(PR_3)_3$, the chloride *trans* to phosphine is more labile and thus readily removed by aqueous $AgNO_3$ (unlike the other two chlorides). Likewise ν(Ir–Cl) in the IR spectra of these complexes depends on the ligand *trans* to chloride.

Carbon monoxide can be introduced directly

$$\textit{fac}\text{-}IrCl_3(PEt_3)_3 \xrightarrow[MeO(CH_2)_2OH]{CO,\ reflux} \textit{fac}\text{-}IrCl_3(CO)(PEt_3)_2$$

or by oxidative addition to iridium(I) carbonyl species

$$\textit{trans}\text{-}IrBr(CO)(PEt_2Ph)_2 \xrightarrow{MeBr} IrBr_2(Me)(CO)(PEt_2Ph)_2$$

The stability of carbonyls of a metal in the +3 oxidation state is unusual; because $d\pi$–$p\pi$ back donation is necessary to stabilize the Ir–C bond, generally only one CO group can be bonded to the electron-deficient Ir^{3+}.

2.13.4 *Hydride complexes*

Hydride complexes are especially well characterized and important for iridium(III), with typical general formulae $IrHX_2L_3$, IrH_2XL_3, $IrH_3L_3$and $IrH_4L_3^+$. They are frequently readily interconvertible, as shown in Figure 2.85 for some diethylphenylphosphine complexes [156].

An 'early' preparation used 1 mol base in alcoholic solution as the reducing agent:

$$\textit{mer}\text{-}IrCl_3(PEt_3)_3 + KOH + C_2H_5OH$$
$$\xrightarrow{boil} IrHCl_2(PEt_3)_3 + KCl + H_2O + MeCHO$$

(The ethanal was converted to its 2,4-DNP derivative, obtained in 87% yield.) It may also be noted that for this redox reaction, iridium retains the +3 state throughout. The more labile chloride *trans* to phosphine is replaced

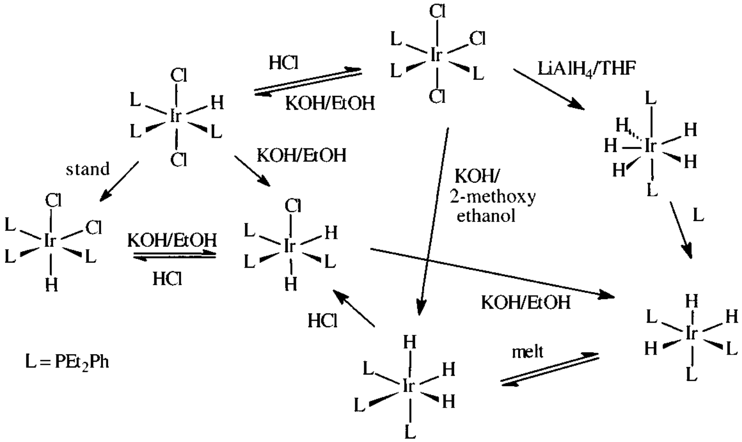

Figure 2.85 Iridium hydrido complexes.

in the reaction; reaction of HCl with the hydride regenerates the starting complex.

Extended reflux with larger quantities of base, especially in higher-boiling alcohols, can afford di- and trihydrides, while oxidative addition can be used

$$\mathrm{Ir(PMe_2Ph)_4^+ + H_2 \rightarrow IrH_2(PMe_2Ph)_4^+}$$

With bulky phosphines, 6-coordinate structures are not possible [157]

$$\mathrm{IrCl_6^{3-} \xrightarrow[\text{reflux}]{\text{exc. PBu}^t_2\text{R}} IrHCl_2(PBu^t_2R)_2}$$

$$\mathrm{IrCl_3.3H_2O \xrightarrow[\text{EtOH reflux}]{\text{HCl/PPr}^i_3} IrHCl_2(PPr^i_3)_2}$$

These compounds are generally believed to have square pyramidal structures (X-ray, $\mathrm{PPr^i_3}$) [157d] and have typical spectroscopic properties of transition-metal hydrides ($\mathrm{IrHCl_2(PBu^t_2Me)_2}$ ν(Ir–H) 1998 $\mathrm{cm^{-1}}$).

$\mathrm{Ir(H)_2X(PBu^t_2R)_2}$ (X = Cl, Br, I; R = Me, Ph) has a tbp structure (axial phosphines) (Ir–H 1.512–1.553 Å for X = Cl, R = Ph) but is fluxional in solution [157e]. Low-temperature NMR studies indicate hindered rotation about Ir–P bonds in $\mathrm{IrHCl_2(PBu^t_2Me)_2}$ [158]. $\mathrm{IrH_2Cl(PPr^i_3)_2}$ undergoes HID exchange with deuterated solvents and acts as an alkane dehydrogenation catalyst [159].

Trihydrides can be made more readily by using $\mathrm{LiAlH_4}$ or $\mathrm{NaBH_4}$ as reducing agents:

$$\mathrm{IrCl_3(QR_3)_3 \xrightarrow[\text{THF}]{\text{NaBH}_4\text{ or LiAlH}_4} IrH_3(QR_3)_3}$$

($\mathrm{PR_3}$, e.g. $\mathrm{PPh_3}$, $\mathrm{PEt_2Ph}$, $\mathrm{PMe_2Ph}$, $\mathrm{AsEt_2Ph}$). These preparations afford mixtures of the *fac*- and *mer*-isomers, separable by fractional crystallization and distinguishable spectroscopically. Figure 2.86 show the ^{1}H NMR spectrum in the hydride region of the two isomers of $\mathrm{IrH_3(PEt_2Ph)_3}$ [160].

Trihydrides lose some or all of the hydride ligands with suitable reagents

$$\mathrm{IrH_3(PPh_3)_3 \xrightarrow{\text{HBr}} IrHBr_2(PPh_3)_3}$$

The structures of *fac*-$\mathrm{IrH_3(PMe_2Ph)_3}$, $\mathrm{IrH_2Cl(PMe_2Ph)_3}$ and $\mathrm{IrHCl_2(PMe_2Ph)_3}$ (2-isomers) have been determined (see section 2.13.5) as well as those of *mer*-$\mathrm{IrH_3(PPh_3)_3}$ and *fac*-$\mathrm{IrH_3(PMePh_2)_3}$ (Figure 2.87) [161]. They all involve octahedrally coordinated iridium, with hydride ligands occupying individual positions in the coordination sphere.

Protonation of *mer*-$\mathrm{IrH_3(PMe_2Ph)_3}$ with $\mathrm{HBF_4}$ leads to $\mathrm{[IrH_4(PMe_2Ph)_3]^+}$, believed to be a non-classical hydride $\mathrm{[IrH_2(\eta^2\text{-}H_2)(PMe_2Ph)_3]^+}$ [162]. It catalyses *fac–mer* isomerism of $\mathrm{IrH_3(PMe_2Ph)_3}$. $\mathrm{IrHCl_2L_2}$ (L = $\mathrm{Pcy_3}$, $\mathrm{PPr^i_3}$)

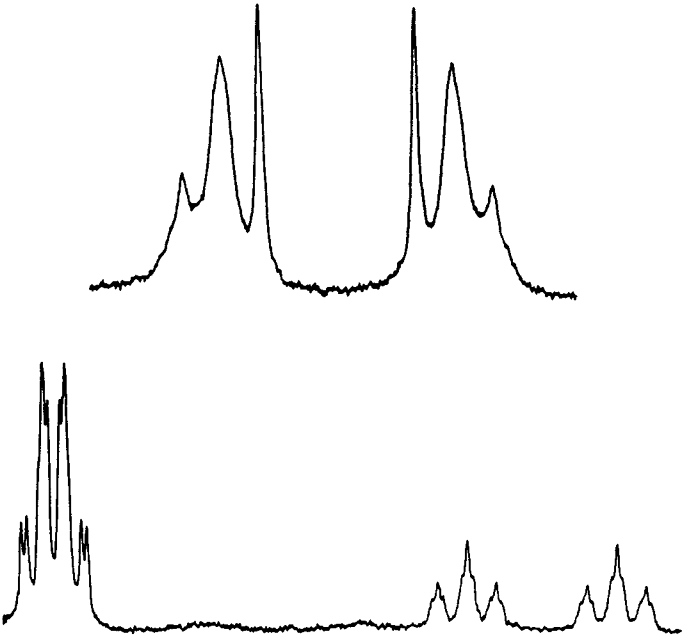

Figure 2.86 The ^{1}H NMR spectrum in the hydride region of the isomers of $[IrH_3(PEt_2Ph)_3]$: top, *fac*-isomer; bottom, *mer*-isomer. (Reproduced with permission from E.L. Muetterties (ed.), *Transition Metal Hydrides*, published by Marcel Dekker, 1971, p. 80.)

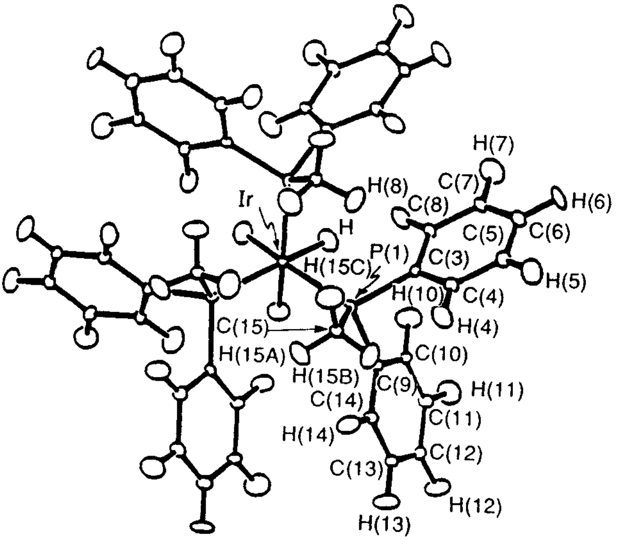

Figure 2.87 The structure of *fac*-$[IrH_3(PPh_2Me)_3]$. Ir–H 1.627 Å, Ir–P 2.314 Å; H–Ir–H 83.4°, P–Ir–P 98.6°. (Reproduced with permission from *J. Chem. Soc., Dalton Trans.*, 1993, 3359.)

reversibly binds H_2, probably as another η^2-hydrogen complex $IrH(\eta^2\text{-}H_2)Cl_2(PR_3)_2$.

Formally iridium(V) hydrides are discussed in section 2.15.

2.13.5 *Case study of dimethylphenylphosphine complexes*

The PMe_2Ph complexes have been studied in particular detail [163–165], since their ^1H NMR spectra lend themselves to assigning the stereochemistry of the complexes. Figure 2.88 shows the relationships between a large number of these complexes, which are in general typical of iridium(III) phosphine complexes.

The initial synthesis of $IrCl_3(PMe_2Ph)_3$ leads mainly to the *mer*-isomer (I) (and a certain amount of the $(HPMe_2Ph)^+[IrCl_4(PMe_2Ph)_2]^-$ (III) byproduct), which can be isomerized to the *fac*-isomer (II) by irradiation (section 2.13.3) [104]. Refluxing in alcohols, particularly in the presence of base, leads to hydride complexes (V and VI): the labilizing effect of the phosphine on the chloride *trans* to it should be noted in the synthesis of (V). Hydride ligands can be replaced by halide or pseudo-halide (VIII); a hydride (VII) isomeric with (V) can be produced by treatment of (VI) with HCl; in this case only the hydride *trans* to phosphine is replaced. In contrast, *fac*-$IrCl_3(PMe_2Ph)_3$ (II) requires gentle boiling in ethanol for a few hours to introduce a hydride ligand giving (XIII).

An indication of the *trans*-labilizing influence of phosphine is given by the reaction of *mer*-$IrCl_3(PMe_2Ph)_3$ with NaI; the chloride *trans* to phosphines is replaced within 3.5 h reflux in butanone, forming VIII ($X = I$) whereas 48 h reflux is needed to replace all three chlorides (forming XIV).

Another way of replacing chloride *trans* to phosphine involves using silver salts; reaction with $AgPF_6$ and $AgNO_3$ introduces, respectively, a water molecule (XII) and a nitrate group (IX), which may in turn be replaced by a range of Lewis bases, giving (VIII), (X) and (XXV).

The cationic species $[IrX_2(CO)(PMe_2Ph)_3]^+$ (XVI, $Q = CO$) undergoes nucleophilic attack by methoxide forming the carboxylate complex (XXI). In the presence of very strong base, a cyclometallation of a methyl group occurs forming (XXIV) [165].

One or more methyl groups can be introduced. Using excess MeMgCl results in a change in configuration from *mer*- to *fac*-(XVIII); replacing one or two of these methyl groups results in the readoption of the *mer*-configuration for the phosphines (XIX, XX). (Presumably the *mer*-configuration is more stable for $d\pi$–$p\pi$ bonding but this has to be balanced against electronic and other steric factors [166].)

Variable temperature NMR studies of $[IrCl_2(PMe_2Ph)_4]^+$ (XXV; $L = PMe_2Ph$) show a broad line in the ^{31}P spectrum at room temperature but on cooling to 80°C a mass of sharp lines are observed, owing to three to four rotational isomers (Figure 2.89); the predominant ABCD pattern is

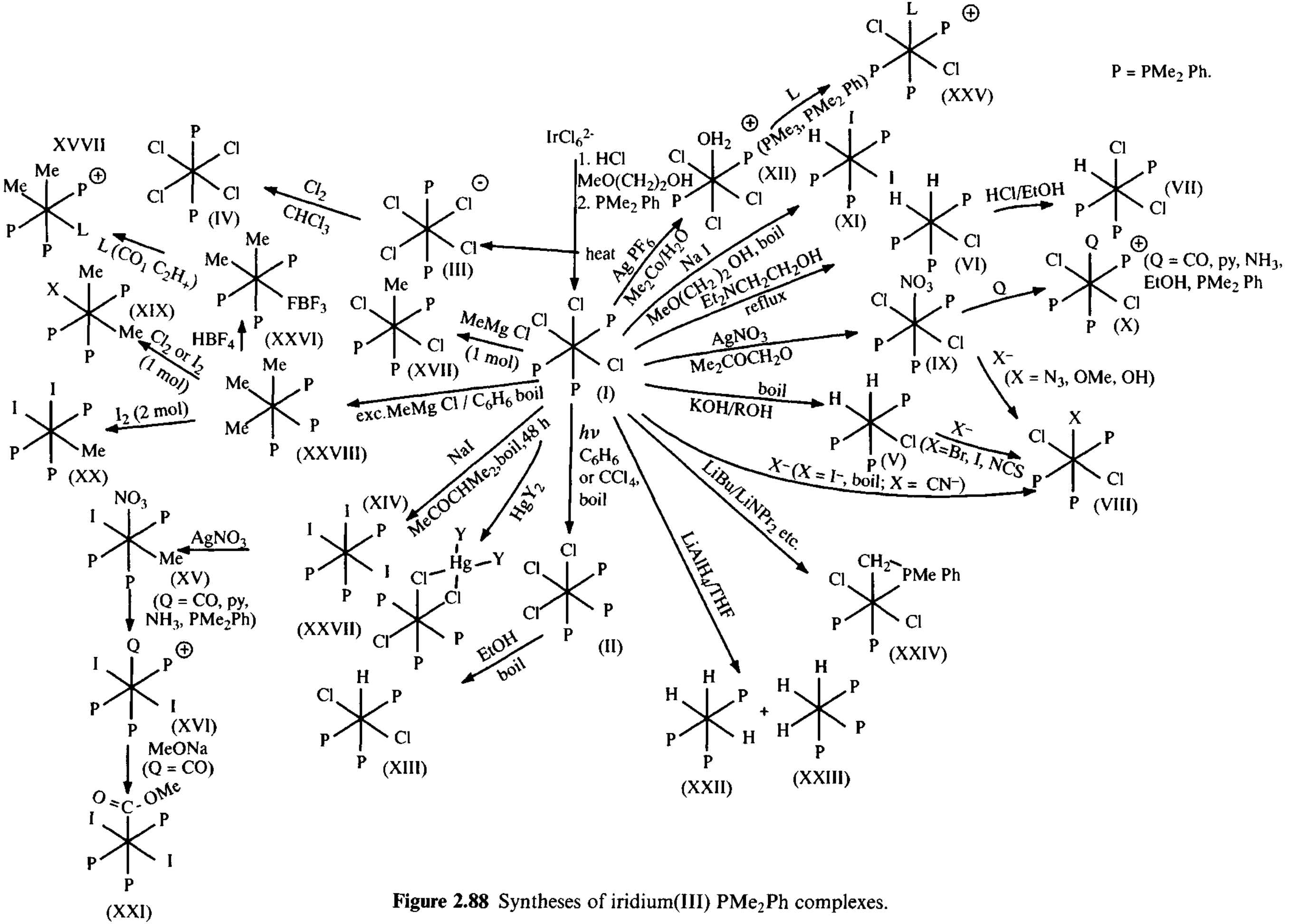

Figure 2.88 Syntheses of iridium(III) PMe₂Ph complexes.

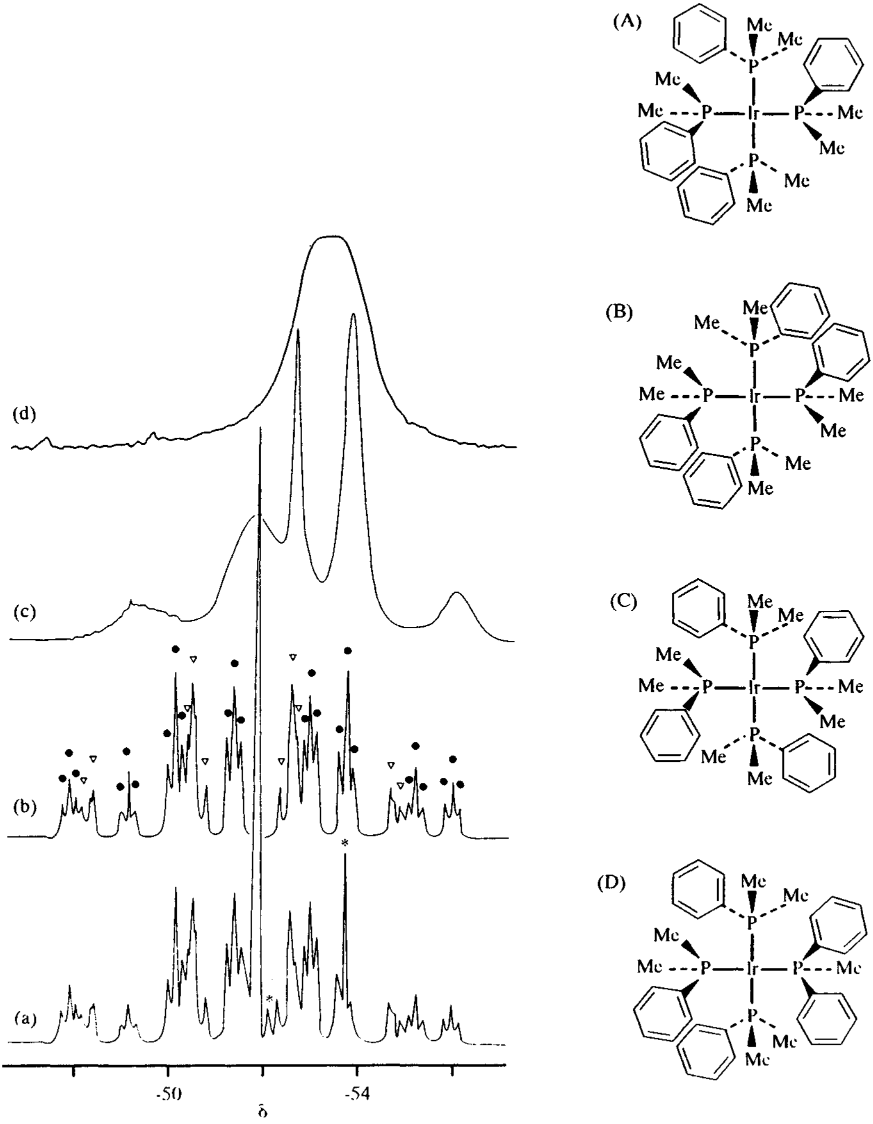

Figure 2.89 $^{31}P\{^1H\}$ NMR spectrum of $[IrCl_2(PMe_2Ph)_4]^+ClO_4$ at (a) −80°C; (c) −5°C; and (d) 25°C; together with a computer simulation (b). Signals owing to rotameric isomers are denoted •, ▽ and *. The four possible rotamers are shown as A–D. (Reproduced with permission from *J. Chem. Soc., Chem Commun.*, 1989, 1351.)

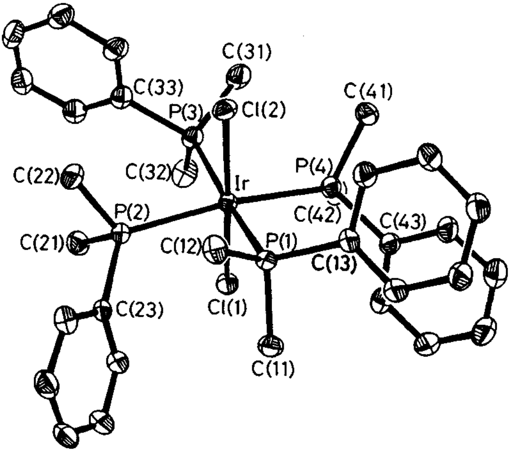

Figure 2.90 The structure of the cation in $[IrCl_2(PMe_2Ph)_4]ClO_4$. (Reproduced with permission from *J. Chem. Soc., Chem Commun.*, 1989, 1351.)

assigned to isomer A, the form adopted in the solid state (Figure 2.90). (One interesting point about this substance is the phenomenon of parallel phenyl groups (3.8 Å apart) noted in certain other substances like *cis*-$UCl_4(Ph_3PO)_2$ [167].)

As already remarked, in compounds *mer*-$IrX_3(PMe_2Ph)_3$, the most labile ligand is the group X (X = H, Me, halogen) *trans* to a phosphine. The Ag^+-assisted removal of chloride in (I) yields $[IrCl_2(H_2O)(PMe_2Ph)_3]^+$ (XII) where the H_2O is very weakly bound (Ir–O 2.189 Å, compare $Ir(H_2O)_6^{3+}$ 2.041 Å) and readily replaced.

Similarly protonation of *fac*-$IrMe_3(PMe_2Ph)_3$ with HBF_4 gives $IrMe_2(BF_4)(PMe_2Ph)_3$ (XXVI), which has weakly bound BF_4 (Ir–F 2.389 Å): in solution the BF_4 is easily displaced by neutral donors to give (XXVII) [168].

Structural data

Figure 2.91 compares bond lengths for a range of these complexes [169]. Comparison of Ir–P bond lengths (e.g. for compounds I, II and V) shows the shortest Ir–P bonds *trans* to Cl and the longest for P *trans* to H. A similar effect is seen on Ir–Cl bond lengths by comparing the same compounds.

Examining the *mer*-$IrH_{3-x}Cl_x(PMe_2Ph)_3$ systems (I, V, VI, VII) it has been noted that the Ir–P bonds *trans* to a particular ligand shorten as the number of hydride ligands increases (increments of about 0.04 Å). This is not simply caused by interligand repulsions as the Ir–Cl bonds do not show this variation; it has been concluded that both non-bonding interligand forces and metal–ligand bonding forces are involved. Comparing

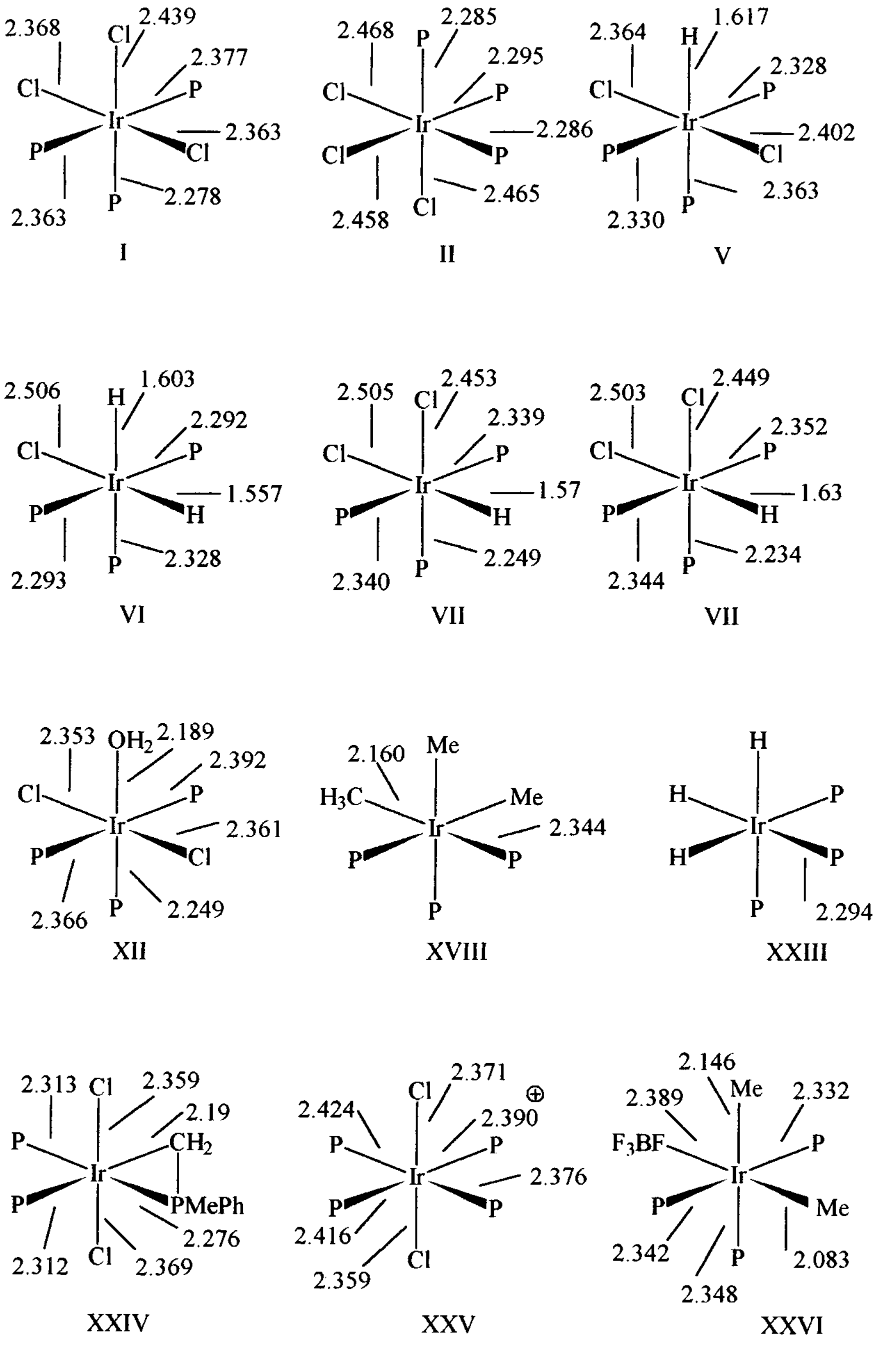

Figure 2.91 Structural data for iridium(III) complexes of dimethylphenylphosphine.

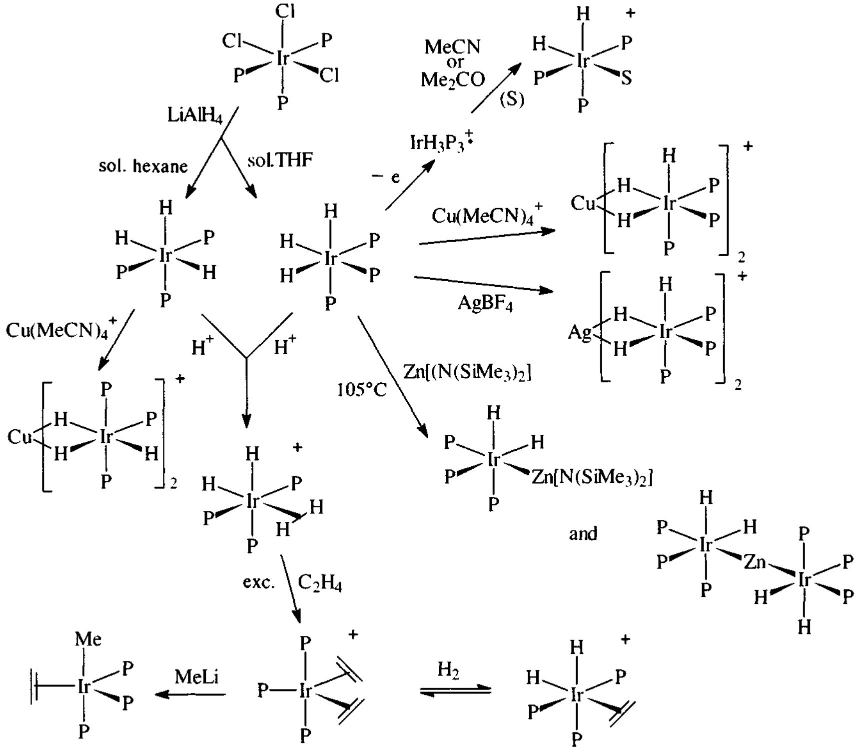

(P = PMe$_2$Ph)

Figure 2.92 Reactions of iridium(III) dimethylphenylphosphine trihydro and trimethyl complexes.

fac-IrX$_3$(PMe$_2$Ph)$_3$ compounds (X = Cl, H, Me: II, XXIII and XVIII) shows a very significant effect of methyl on the Ir–P bond.

Recent study of these complexes has focused on the reactions of trimethyls and trihydrides (Figure 2.92) as on protonation they generate reactive co-ordinatively unsaturated species

$$\mathrm{IrX_3P_3} \xrightarrow{\mathrm{H^+}} \mathrm{IrHX_3P_3^+} \rightarrow \mathrm{IrXP_3^+} + \mathrm{HX} \qquad (\mathrm{X} = \mathrm{H, Me})$$

LiAlH$_4$ reduction of *mer*-IrCl$_3$(PMe$_2$Ph)$_3$ gives a separable mixture of *fac*- and *mer*-IrH$_3$(PMe$_2$Ph)$_3$ (XXII and XXIII); these are rigid 6-coordinate complexes (readily binding electrophilic complexes like Cu(MeCN)$_4^+$ to form hydride-rich clusters) but on protonation (HBF$_4$) they form [IrH$_4$(PMe$_2$Ph)$_3$]$^+$, which appears to be the dihydrogen complex [Ir(η^2-H$_2$)H$_2$(PMe$_2$Ph)$_3$]$^+$: similar intermediates [IrMe$_2$(PMe$_2$Ph)$_3$]$^+$ can be made by protonation of IrMe$_3$(PMe$_2$Ph)$_3$ [170].

2.14 Iridium(IV) complexes

The chemistry of the iridium +4 oxidation state is limited, owing to the stability of the low-spin d^6 Ir^{3+} complexes, which makes their oxidation difficult. The best known are IrX_6^{2-} (X = F, Cl, Br) (see section 2.3).

A variety of complexes of neutral donors IrX_4L_2 have been made [171]:

$$IrX_3.nH_2O \xrightarrow[HX/EtOH]{L} HL + IrX_4L_2^- \xrightarrow[CHCl_3]{X_2} IrX_4L_2$$

($X = Cl$, $L = PMe_3$, PMe_2Ph, PEt_3, PEt_2Ph, PPr_3, $AsPr_3$, py)
($X = Br$, $L = PEt_3$, $AsEt_3$, PMe_2Ph, $AsMe_2Ph$, py)

$$IrX_3.nH_2O \xrightarrow[HX, L]{R_4NX} R_4N^+IrX_4L_2^- \xrightarrow{X_2} IrX_4L_2$$

($X = Cl$, $L = Me_2S$, Me_2Se; $X = Br$, $L = Me_2S$)

$$[Ir(C_8H_{12})Cl]_2 \xrightarrow{PPh_3} Ir(PPh_3)_3Cl \xrightarrow{Cl_2} IrCl_4(PPh_3)_2$$

The choice of starting material is important, as IrX_3L_3 (L, e.g. PR_3) usually cannot be oxidized.

The complexes are strongly coloured (purple chlorides, green bromides) light-sensitive solids that undergo facile reduction. In general, only the *trans*-isomer is formed (though *cis*-$IrCl_4py_2$ has been made by oxidizing the corresponding iridium(III) species). Magnetic and spectroscopic properties are as expected for a low-spin d^5 system, magnetic moments at room temperature being in the range 1.6–1.9 μ_B; *trans*-$IrCl_4(AsPr_3)_2$ shows the ESR spectrum expected for a *trans*-isomer ($g_\perp = 2.43$, $g_\| = 0.80$).

Comparison of the far-IR spectra of the two isomers of $IrCl_4py_2$ shows two ν(Ir–Cl) bands for the *trans*-isomer (330, 317 cm^{-1}) and three for the *cis*-isomer (346, 328, 272 cm^{-1}), as predicted by group theory. The *trans*-geometries are confirmed by X-ray diffraction for $IrCl_4(PMe_2Ph)_2$ (Ir–Cl 2.324 Å, Ir–P 2.392 Å) and $IrBr_4(AsEt_3)_2$ (Ir–Br 2.459 Å, Ir–As 2.489 Å) (Figure 2.93).

The *cis*-complexes can be made using chelating bidentate ligands, the syntheses again following the route of oxidation of the iridium(III) analogue.

$$IrX_3.nH_2O \xrightarrow[L-L]{HX} Ir(L-L)X_4^- \xrightarrow[\text{or } HNO_3]{X_2} IrX_4(L-L)$$

(L–L = phen, bipy, X = Cl, Br)

$$IrCl_3.nH_2O \xrightarrow{L-L} Ir(L-L)Cl_3 \xrightarrow{R_4NCl} Ir(L-L)Cl_4^- \xrightarrow{X_2} Ir(L-L)Cl_4$$

(L–L = $RQ(CH_2)_2QR$ (R = Me, Ph; Q = S, Se); $MeS(CH_2)_3SMe$).

The structure of *cis*-Ir(phen)Cl_4 is shown in Figure 2.94.

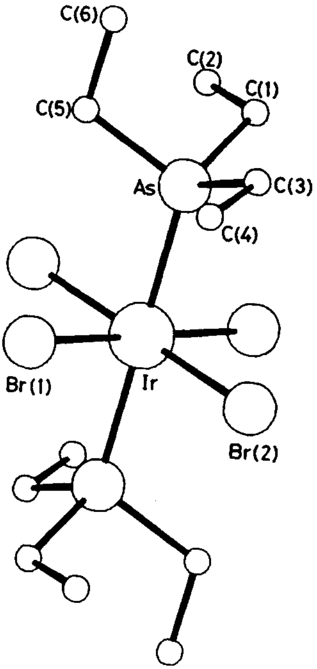

Figure 2.93 The structure of *trans*-[Ir(AsEt$_3$)$_2$Br$_4$]. (Reproduced with permission from *J. Chem. Soc., Dalton Trans.*, 1987, 1901.)

Anionic complexes Et$_4$N[IrCl$_5$L] (L = py, Me$_2$S, Me$_2$Se, PPh$_3$, AsPh$_3$, SbPh$_3$) have been synthesized:

$$trans\text{-IrCl}_4\text{py}_2 \xrightarrow[\text{CH}_2\text{Cl}_2]{\text{HCl/Et}_4\text{NCl}} \text{Et}_4\text{NIrCl}_5\text{py}$$

$$\xrightarrow[\text{3. Cl}_2\text{/CH}_2\text{Cl}_2]{\text{1. reduce;}\quad \text{2. L, EtOH}} \text{Et}_4\text{NIrCl}_5\text{L}$$

These iridium(IV) complexes have UV–visible spectra dominated by intense absorptions around 500 nm (X = Cl) and 700 nm (X = Br) assignable to $\pi x \rightarrow \text{Ir}(t_{2g})$ ligand-to-metal charge-transfer bonds.

IrCl$_4$(PMe$_2$Ph)$_2$ undergoes a redox reaction with ferrocene forming

$[\text{Fe}(\text{C}_5\text{H}_5)_2]^+[\text{IrCl}_4(\text{PMe}_2\text{Ph})_2]^-$

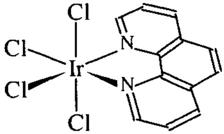

Figure 2.94 The structure of *cis*-Ir(phen)Cl$_4$.

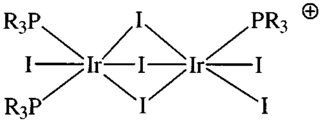

Figure 2.95 The structure of the dimeric cation $[Ir_2I_5(PR_3)_4]^+$.

No IrI_4 complexes have so far been characterized: $Ir(PR_3)_4^+$ ($PR_3 = PMe_2Ph$, $P(OMe)Ph_2$) is oxidized by iodine giving complexes analysing as $IrI_4(PR_3)_2$. They are in fact dimeric iridium(III) complexes $Ir_2I_5(PR_3)_4^+I_3^-$, containing the cation shown in Figure 2.95 [122a].

Recently two rare paramagnetic iridium(IV) hydride complexes have been reported [172].

$$(NH_4)_2IrCl_6 \xrightarrow[\text{EtOH/conc. HCl}]{PR_3} IrH_2Cl_2(PR_3)_2 \qquad (R = Pr^i, cy)$$

As expected, they are deeply coloured ($R = Pr^i$, deep red; R = cy, red–violet) and have typical magnetic moments of 1.5–1.6 μ_B and ESR g values 2.064, 2.038, 2.007 (for $R = Pr^i$); others [157d] have suggested that the structures were obtained on disordered molecules. In solution, at room temperature, they tend to decompose

$$2IrH_2Cl_2(PR_3)_2 \Leftrightarrow IrHCl_2(PR_3)_2 + IrH(\eta^2\text{-}H_2)Cl_2(PR_3)_2$$

$Ir(OH)_6^{2-}$ is formed by a substitution reaction and is isolable as red crystals. Similar complexes have been isolated for the heavier group (II) metals.

$$K_2IrCl_6 \xrightarrow{KOH} K_2Ir(OH)_6$$

On heating they afford M_2IrO_3 (M = Na, K; $\frac{1}{2}$Ca, $\frac{1}{2}$Sr, $\frac{1}{2}$Ba), which can in some cases be made by heating the appropriate metal oxide with IrO_2, though M_2IrO_4 (M = Ca, Sr) can also be made. All probably have 6-coordinate Ir^{4+} [173].

Red moisture-sensitive crystals of $K_2Ir(NO_3)_6$, isomorphous with the Pt analogue and believed to contain 12-coordinate iridium, with bidentate nitrates are made by:

$$K_2IrBr_6 \xrightarrow{N_2O_5} K_2Ir(NO_3)_6$$

The rubidium and caesium analogues can also be synthesized [174].

The mixed valence (III, IV) ions $Ir_3N(SO_4)_6(H_2O)_3^{4-}$ and $Ir_3O(SO_4)_9^{10-}$ have been made by reactions of H_2SO_4 with $(NH_4)_2IrCl_6$ and K_2IrCl_6, respectively. They have structures similar to trinuclear carboxylates $M_3O(RCO_2)_6(H_2O)_3^{n+}$ based on Ir_3X cores with bridging sulphates.

2.15 Iridium(V) complexes

Compounds $IrH_5(PR_3)_2$ (PR_3, e.g. PEt_2Ph, PMe_3, PEt_3, PPr^i_3) are prepared by $LiAlH_4$ reduction of THF solutions of $IrCl_3(PR_3)_3$ or $IrHCl_2(PPr^i_3)_2$. ($IrH_5(PEt_2Ph)_2$ was originally though to be a trihydride on the basis of analytical data.)

$$IrCl_3(PR_3)_3 \xrightarrow[\text{THF}]{\text{LiAlH}_4\text{ or NaBH}_4} IrH_5(PR_3)_2$$

Other syntheses include

$$IrHCl_2(PBu^t_2R) \xrightarrow[C_6H_6]{NaOPr^i/H_2} IrH_5(PBu^t_2R)_2 \qquad (R = Me, Ph, Bu^t)$$

Two hydrogen atoms are readily displaced by a molecule of a Lewis base

$$IrH_5(PEt_3)_2 + AsMe_2Ph \rightarrow mer\text{-}IrH_3(PEt_3)_2(AsMe_2Ph) + H_2$$

$$IrH_5(PEt_2Ph)_2 + L \rightarrow mer\text{-}IrH_3(PEt_2Ph)_2L + H_2$$

($L = PPh_3$, $AsMe_2Ph$, MeNC, Me_2S, CO).

The facile displacement of H_2 might suggest that the pentahydrides were dihydrogen complexes of iridium(III), $IrH_3(\eta^2\text{-}H_2)(PR_3)_2$. However, the structure of $IrH_5(PPr^i_3)_2$ has been determined by X-ray and neutron diffraction (Figure 2.96), showing the molecule to be pentagonal bipyramidal with *trans*-phosphines and five equivalent equatorial hydrides (Ir–P 2.309 Å; Ir–H 1.603 ± 0.025 Å) [175].

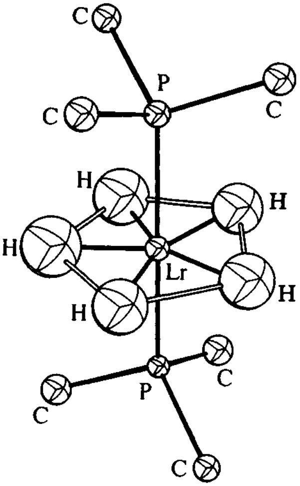

Figure 2.96 The structure of $IrH_5(PPr^i_3)_2$. (Reprinted with permission from *J. Am. Chem. Soc.*, 1985, **107**, 7212. Copyright (1985) American Chemical Society.)

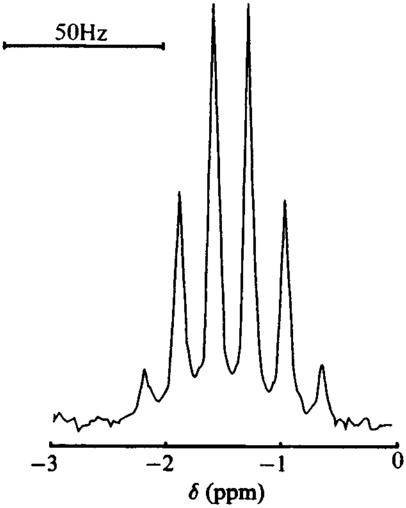

Figure 2.97 ^{31}P NMR spectrum (ethyl protons decoupled) of $IrH_5(PEt_2Ph)_2$. (Reprinted from *J. Inorg. Nucl. Chem.*, 1973, 33, 2195. Copyright (1973) with kind permission from Elsevier Science Ltd, The Boulevard, Langford Lane, Kidlington OX5 1GB, UK.)

The IR spectrum shows ν(Ir–H) at 1950 cm^{-1}and a triplet in the ^1H NMR at $\delta = -11$ ppm (J(P–H) 12 Hz) confirming the presence of two phosphines. The ^{31}P NMR of $IrH_5(PEt_2Ph)_2$ (Figure 2.97) is a sextet, showing the presence of five hydride ligands.

These pentahydrides have attracted attention as catalysts for hydrogenation of the double bond in alkenes. $IrH_5(PPr^i_3)_2$ catalyses vinylic H–D exchange between terminal alkenes and benzene, the isomerization of α,β-ynones, isomerization of unsaturated alcohols and dehydrogenation of molecules such as secondary alcohols [176].

Recently an orange compound $IrH_4Cl(PPr^i_3)_2$ has been isolated (IR ν(Ir–H) 2204 and 2152 cm^{-1}) as has the Pcy_3 analogue [177].

$$IrCl_3.3H_2O \xrightarrow[\text{Na naphthalenide}]{H_2/PPr^i_3/THF} IrH_4Cl(PPr^i_3)_2$$

It is stable in the solid state only under a hydrogen atmosphere, tending to eliminate H_2 reversibly.

$$IrH_4Cl(PPr^i_3)_2 \underset{+H_2}{\overset{-H_2}{\rightleftharpoons}} IrH_2Cl(PPr^i_3)_2 + H_2$$

X-ray diffraction has not located the hydrides, but NMR evidence favours a structure of the type (Figure 2.98) with one (η^2-H_2) ligand.

Protonation of $IrH_5(Pcy_3)_2$ affords a fluxional complex thought to be $IrH_6(Pcy_3)_2^+$ with two (η^2-H_2) ligands and two classical hydrides (Figure 2.99) from the ^1H NMR ($\delta = -8.3$ ppm at room temperature;

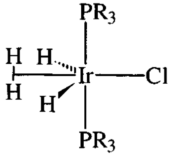

Figure 2.98 The structure of $IrH_4Cl(PR_3)_2$.

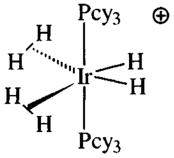

Figure 2.99 The structure of $[IrH_6(Pcy_3)_2]^+$.

$\delta = -5.05$ ppm (intensity 4) and -15.2 ppm (intensity 2) at low temperature). It can, therefore, be viewed as an iridium(III) complex [178].

2.16 Nitrosyls of iridium and rhodium

Two factors have contributed particularly to the interest in the iridium and rhodium nitrosyl compounds [179]:

1. The report in 1968 of the first crystallographically characterized bent metal–nitrosyl linkage in $[IrCl(NO)(CO)(PPh_3)_2]^+BF_4^-$ [180].
2. The discovery that $[Ir(NO)_2(PPh_3)_2]^+$ reacts with CO forming the carbonyl $Ir(CO)_3(PPh_3)_2^+$, which then regenerates the starting material in reacting with NO [181]

$$Ir(NO)_2(PPh_3)_2^+ + 4CO \rightarrow Ir(CO)_3(PPh_3)_2^+ + CO_2 + N_2O$$

$$Ir(CO)_3(PPh_3)_2^+ + NO \rightarrow Ir(NO)_2(PPh_3)_2^+$$

This has obvious potential for removing undesirable NO and CO from automobile exhaust gases.

Bent metal–NO bonding is traditionally associated with NO bonding as NO^-, whereas linear coordination is associated with NO^+. The latter is predicted to involve shorter M–N bonds as both σ- and π-donation can be involved.

$$Ir{-}N^+{\equiv}O^-: \qquad Ir{=}N^+{=}\ddot{O}:$$

On this basis, the bent nitrogens with square pyramidal structures like $Ir(NO)Cl_2(PPh_3)_2$ are assigned to the M^{III} (d^6) oxidation state in keeping with other examples of this stereochemistry, such as $RhCH_3I_2(PPh_3)_2$.

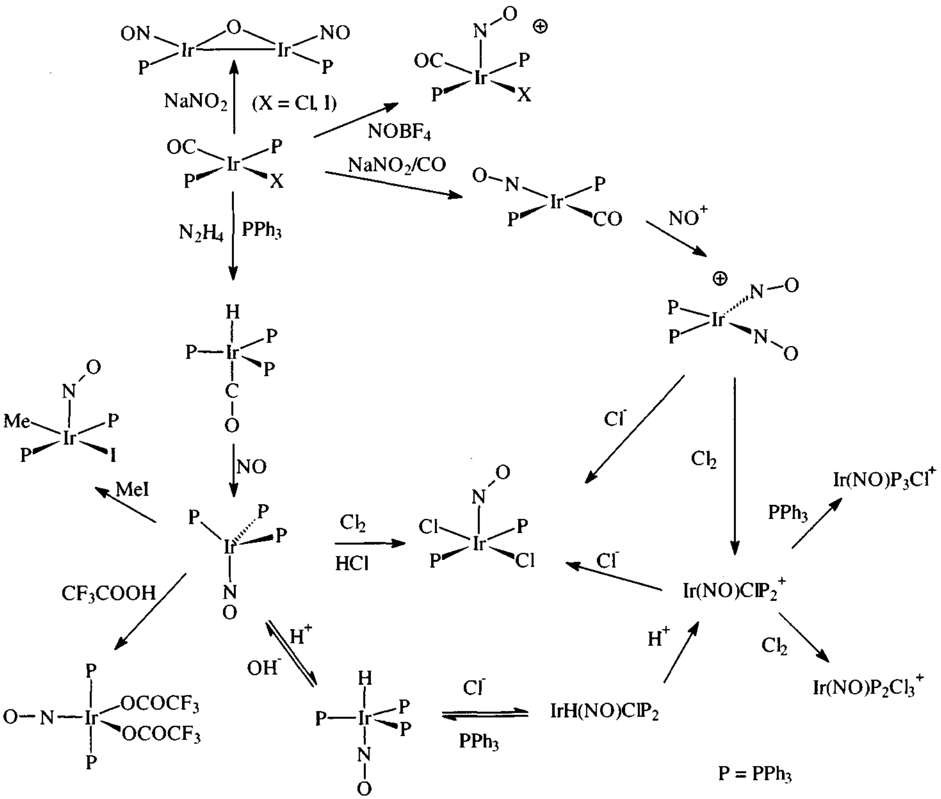

Figure 2.100 Synthesis of some iridium nitrosyl complexes.

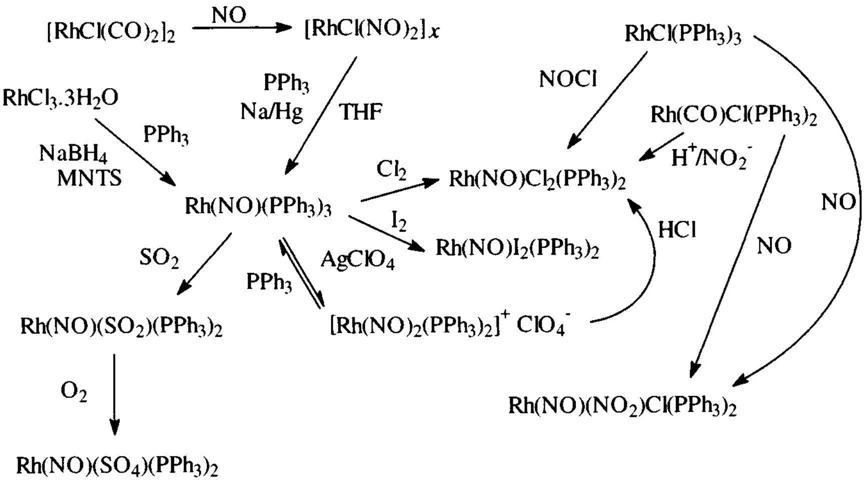

Figure 2.101 Synthesis of some rhodium nitrosyl complexes.

Table 2.14 Structural data for iridium nitrosyl complexes

	Ir–N (Å)	Ir–N–O (°)	ν(NO) (cm^{-1})
$Ir(NO)(PPh_3)_3$	1.67	180	1600
$[IrH(NO)(PPh_3)_3]^+ClO_4^-$ (black isomer)	1.68	175	1780
(brown isomer)	1.77	167	1720
$[IrCl(NO)(PPh_3)]_2O$	1.77	176	1831–1854
$[Ir(NO)_2(PPh_3)_2]^+ClO_4$	1.77	164	1715–1760
$[Ir(NO)(\eta^3\text{-}C_3H_5)(PPh_3)_2]^+BF_4^-$	1.95	129	1631
$[IrI(NO)(CO)(PPh_3)_2]^+BF_4^-$	1.89	125	1720
$[IrCl(NO)(CO)(PPh_3)_2]^+BF_4^-$	1.97	124	1680
$IrCl_2(NO)(PPh_3)_2$	1.94	123	1560
$IrI(NO)CH_3(PPh_3)_2$	1.92	120	1525
$[Ir(NO)(phen)(PPh_3)_2]^{2+}(PF_6)_2$	1.70	180	1805
$Ir(NO)(O_2CCF_3)_2(PPh_3)_2$	1.59	178	1800
$Ir(NO)(CO)(PPh_3)_2$	1.787	174	1645
$K_2Ir(NO)Cl_5.H_2O$	1.760	174	2006

It has frequently been assumed that linear M–N–O linkages are associated with higher ν(N–O) frequencies than bent M–NO linkages. Unfortunately there is a region of overlap between (roughly) 1600 and 1720 cm^{-1} where both linkages have been found to absorb. X-ray diffraction and, latterly, ^{15}N NMR spectra have been most useful in resolving the situation [182].

Syntheses of many of these compounds are shown in Figures 2.100 and 2.101, with structural data in Tables 2.14 and 2.15. Apart from NO itself, convenient reagents for introducing the group include NO$^+$ salts and MNTS (*N*-methyl-*N*-nitrosotoluene-*p*-sulphonamide, *p*-$MeC_6H_4SO_2N(NO)Me$).

$[IrCl(NO)(PPh_3)_2]^+$ is the nitrosyl analogue of Vaska's compound [183]. These are various synthetic routes to it

$$[IrH(NO)Cl(PPh_3)_2]^+ \xrightarrow{HX} [IrCl(NO)(PPh_3)_2]^+X^- + H_2$$

Table 2.15 Structural data for rhodium nitrosyl complexes

	Rh–N (Å)	Rh–N–O (°)	ν(NO) (cm^{-1})
$[Rh(NO)_2(PPh_3)_2]^+ClO_4^-$	1.818	159	1754, 1759
$Rh(NO)(PPh_3)_3$	1.759	157	1610
$Rh(NO)(\eta^2\text{-}SO_2)(PPh_3)_2$	1.802	140.4	1600
$Rh(NO)Cl_2(PPh_3)_2$	1.912	124.8	1630
$Rh(NO)(O_2CCF_3)_2(PPh_3)_2$	1.93	122	1665
$[Rh(NO)(MeCN)_3(PPh_3)_2]^{2+}[PF_6^-]_2$	2.026	118	1720

($X = ClO_4$, PF_6, BF_4) (note the hydrogen bound to iridium behaving here as H^-).

$$IrCl(CO)(PPh_3)_2 \xrightarrow{RCON_3} IrCl(N_2)(PPh_3)_2 \xrightarrow{NO^+BF_4^-} [IrCl(NO)(PPh_3)_2]^+$$

This synthesis is possible with other halide ligands

$$[Ir(NO)_2(PPh_3)_2]^+ \xrightarrow[(1\,mol)]{Cl_2} [IrCl(NO)(PPh_3)_2]^+$$

Counting NO as a three-electron donor, $[IrCl(NO)(PPh_3)_2]^+$ is, therefore, a 16-electron species isoelectronic with Vaska's compound, isolable as a red crystalline hexafluorophosphate (m.p. 211°C, ν(N–O) 1870 cm^{-1}) or similar perchlorate and tetrafluoroborate; a *trans*-structure is indicated by spectroscopic data, and it is presumed to have a linear Ir–N–O grouping.

Unlike Vaska's compound, it does not undergo oxidative addition with O_2, H_2, SO_2 or $(NC)_2C{=}(CN)_2$. (The isoelectronic ruthenium nitrosyl $RuCl(NO)(PPh_3)_2$ likewise binds SO_2 and O_2.) This has been ascribed to the increased positive charge on iridium and also to the nitrosyl group syphoning off π-electron density. The iridium compound will, however, undergo a number of addition reactions with both neutral donors and anionic ligands (Figure 2.102).

These reactions are accompanied by pronounced shifts in the positions of ν(N–O) in the IR spectrum, almost certainly associated with the transition to bent Ir–N–O linkages, known from X-ray data for two of the products.

Comparison of four pairs of compounds where the structures of both rhodium and iridium analogues are known shows dangers of drawing correlations between spectra and structure, even with isoelectronic compounds.

1. $[M(NO)_2(PPh_3)_2]^+$. The coordination number of the metal in both is four, in a distorted tetrahedral geometry. The position of ν(N–O) in the IR spectrum is essentially the same, and the rhodium and iridium compounds have similar slight bending of the M–N–O linkage.

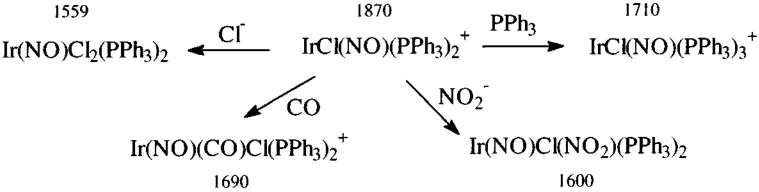

Figure 2.102 Addition reactions for iridium nitrosyl complexes (ν(N–O) (cm^{-1}) is shown for each compound).

2. $M(NO)(PPh_3)_3$. Though the M–N–O bond angles are very different (180° (Ir) and 157° (Rh)), ν(N–O) occurs at virtually the same position in the IR spectrum.
3. $M(NO)Cl_2(PPh_3)_2$. Both these compounds have a square pyramidal structure with bent apical M–N–O linkage and similar bond angles. There is, however, a difference of 70 cm^{-1} in ν(N–O).
4. $M(NO)(OCOCF_3)_2(PPh_3)_2$. Both these complexes have 5-coordinate geometries with monodentate carboxylates. The rhodium compound has a square pyramidal structure with bent Rh–N–O (122°) but the iridium compound has a tbp structure with 'straight' equatorial Ir–N–O (178°). The position of ν(N–O) reflects this difference (1800 cm^{-1} (Ir) and 1665 cm^{-1} (Rh)).

The balance between linear and bent nitrosyl coordination is delicate, illustrated by the case of the allyl complex $[Ir(NO)(C_3H_5)(PPh_3)_2]^+$. When precipitated as the PF_6^- salt, it exhibits ν(N–O) at 1763 cm^{-1}; the BF_4^- salt shows ν(N–O) at 1631 cm^{-1}. Solutions of either compound show both bands, with the intensity of the 1763 cm^{-1} band increasing on cooling. NMR shows that the allyl group is present as a π-allyl throughout. The solid-state structure of the BF_4 salt shows a bent nitrosyl (Ir–N–O 129°; X-ray) so that the higher value of ν(N–O) is associated with a straight Ir–N–O linkage; the two isomeric forms are thus in equilibrium in solution (Figure 2.103) [184].

Many of the nitrosyls studied are 5-coordinate, and analysis of crystallographic results indicates that, in general, in the trigonal bipyramid structures NO is found in the equatorial position in a linear geometry whereas in a square pyramidal structure, there is a bent M–N–O linkage in an apical position. A further point of interest is that in compounds like $Ir(NO)Cl_2(PPh_3)_2$, the nitrosyl group bends in the more hindered (P–Ir–P) plane.

Extended-Hückel calculations have been carried out [185] for systems such as $IrCl_4(NO)^{2-}$, based on a slightly distorted square pyramid of C_{4v} symmetry (crystallographically studied 5-coordinate systems do not have a planar base but exhibit this slight distortion). Figure 2.104 shows how the

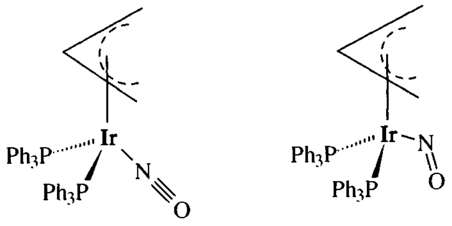

ν_{NO} 1763 cm^{-1} ν_{NO} 1631 cm^{-1}

Figure 2.103 Bent and linear allyl nitrosyls.

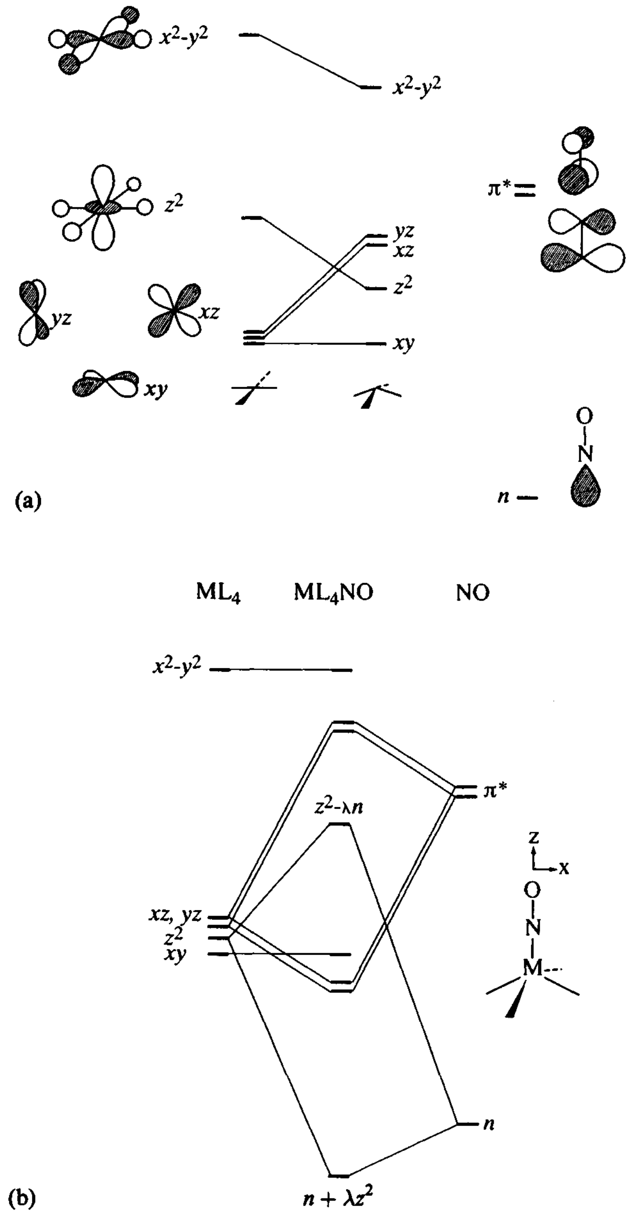

Figure 2.104 (a) Energy levels of (left) square planar and (centre) pyramidally distorted complexes, together with (right) key donor and acceptor orbitals of a nitrosyl ligand. (b) Interaction diagram for a linear nitrosyl in the apical position of a square pyramidal $ML_4(NO)$ system. (Reprinted with permission from *Inorg. Chem.*, 1974, **13**, 2667. Copyright (1974) American Chemical Society.)

metal d orbitals in a C_{4v} MX_4 situation interact with the orbitals of a linear NO; principally this involves d_{z^2} mixing with the lone pair on N (n) and the π-interaction between metal d_{xz}, d_{yz} and the π^* pair of NO orbitals, as shown in Figure 2.104.

In a complex $Ir(NO)Cl_4^{2-}$or $Ir(NO)Cl_2(PR_3)_2$ there are 10 electrons associated with these levels. A system widely used to represent this situation (developed by Enemark and Feltham) neglects the two electrons in the orbital $(n + \lambda z^2)$ largely derived from the N lone pair, thus describing $Ir(NO)Cl_4^{2-}$as $\{MNO\}^8$, meaning that there are eight electrons associated with the metal d orbitals and NO π^*-orbitals; this counts the metal and NO together and gets rid of any dichotomy surrounding assignment of the oxidation state of the metal. Thus for $Ir(NO)Cl_4^{2-}$, in Figure 2.104, the MOs are occupied up to and including $z^2 - \lambda n$.

The effect of bending the Ir–N–O linkage in the xz plane is shown in the Walsh diagram (Figure 2.105).

As the Ir–N–O angle decreases below 180°, two interactions change. Firstly, the d_{z^2} interactions with the nitrogen one pair n grows weaker; as Figure 2.105 shows, in a linear case it is destabilizing so that lessening it increases stability. Secondly d_{z^2} begins to form a bonding interaction with π^*_{xz}, while the interactions of d_{xz} with π^* decreases.

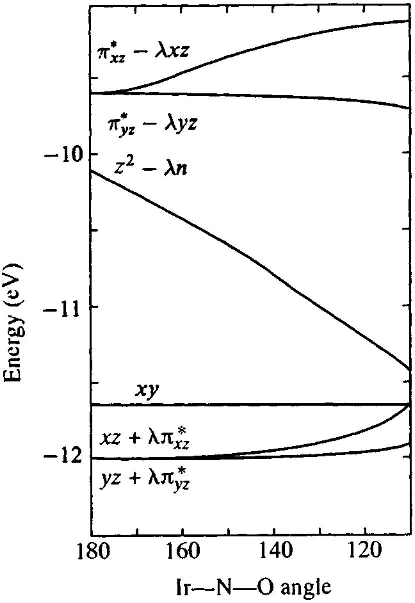

Figure 2.105 Walsh diagram for an $[IrCl_4(NO)]^{2-}$ system. (Reprinted with permission from *Inorg. Chem.*, 1974, **13**, 2667. Copyright (1974) American Chemical Society.)

Reference to the Walsh diagram (Figure 2.105) shows that for a $\{MNO\}^8$ system, bending produces a net stabilization, thus rationalizing the M–N–O bond angle of *c.* 120° found for systems like $M(NO)Cl_2(PR_3)_2$.

The energies of the d_{z^2} and d_{xz} orbitals can also be significantly altered by changing ligands, with strong π-donors increasing the levels of the metal π-orbitals and tending to favour bending.

Calculations for trigonal bipyramidal $ML_4(NO)$ systems with axial NO-like $[Ir(NO)(PPh_3)_3H^+]$ give a d orbital sequence of $xz, yz < x^2 - y^2, xy < z^2$ so that in such an $\{IrNO\}^8$ system, the z^2 orbital is unoccupied; not only does bending not produce any stabilization but in fact d_{xz}, $d_{yz} - \pi^*$ back-bonding is lost, favouring a linear Ir–N–O bond.

2.17 Simple σ-bonded alkyls and aryls of rhodium and iridium

A number of the simple σ-bonded alkyls and aryls of rhodium and iridium have been synthesized in recent years. There are three types of rhodium(III) methyl derivative

$$MCl_3(C_4H_8S)_3 \xrightarrow[Et_2O,\,tmed]{6MeLi} [Li(tmed)]_3(MMe_6)^{3-} \qquad (M = Rh, Ir)$$

$$\xrightarrow[(M=Rh)]{PMe_3} fac\text{-}RhMe_3(PMe_3)_3$$

The hexamethyl anions are analogous to the series formed by the lanthanides; they have octahedrally coordinated metals (Rh–C 2.13 Å; Ir–C 2.16 Å) but decompose above 20°C. A different compound of the formula $RhMe_3(PMe_3)_3$, possibly the *mer*-isomer, is made from $Rh_2(O_2CMe)_4$ and PMe_3, using $MgMe_2$ as the alkylating agent [186]. Other *fac*-alkyls, Rh(alkyl)(1,4,7-trialkyl-1,4,7-triazacyclononame) compounds have been made (alkyl = Me, neohexyl) [187].

Aryls have recently been synthesized [188], including a rare rhodium(II) compound (Figure 2.106).

The rhodium(III) triaryls have pseudo-octahedral structures; therefore, in the air-stable trimesityl rhodium, the three mesityl groups are arranged in *fac*-positions, with *ortho*-methyls blocking the other coordination sites (Figure 2.107).

Trimesityl rhodium is reduced by PMe_2Ph to give a square planar rhodium(I) aryl

$$Rh(2,4,6\text{-}Me_3C_6H_2)_3 \xrightarrow{PMe_2Ph} Rh(2,4,6\text{-}Me_3C_6H_2)(PMe_2Ph)_3$$

Anhydrous $IrCl_3$ reacts with excess mesityllithium to form air-stable tetramesityliridium, which has a distorted tetrahedral structure; as expected

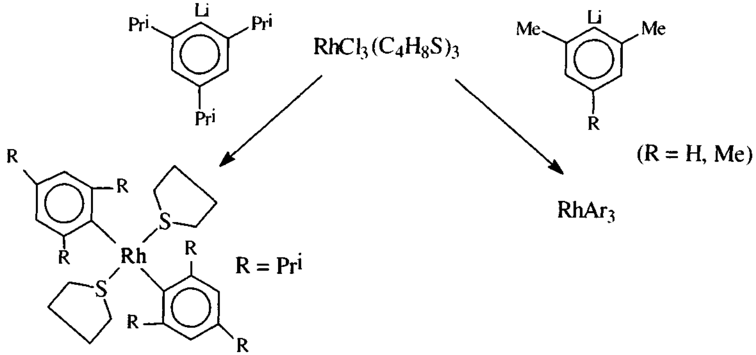

Figure 2.106 Synthesis of rhodium aryls.

for iridium(IV), low spin d^5, it gives an ESR signal ($g_\perp = 2.005$; $g_\parallel = 2.437$) [189].

The trimesityl of iridium can be made by reaction of $IrCl_3(tht)_3$ with MesMgBr, while $IrMes_4$ can be oxidized to the cationic iridium(V) species $[IrMes_4]^+$, also tetrahedral (with concomitant slight Ir–C bond changes from 1.99–2.04 Å in the neutral compound to 2.004–2.037 Å in the cation). Another iridium(V) species, $IrO(Mes)_3$ has been made [190], it has a tetrahedral structure (Ir=O 1.725 Å).

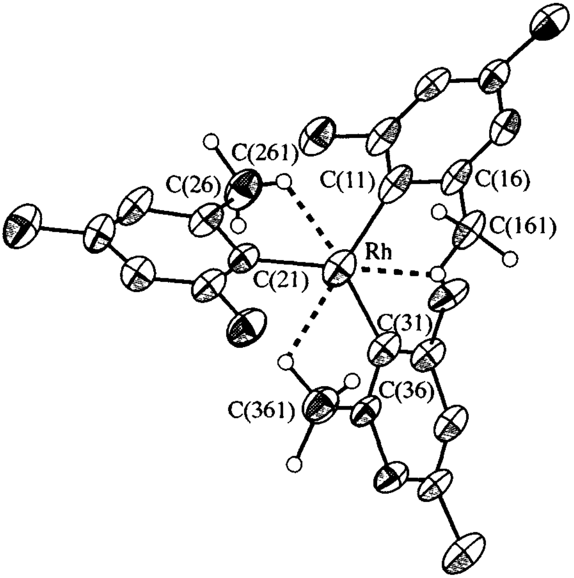

Figure 2.107 The structure of trimesitylrhodium. (Reproduced with permission from *J. Chem. Soc., Chem. Commun.*, 1990, 1242.)

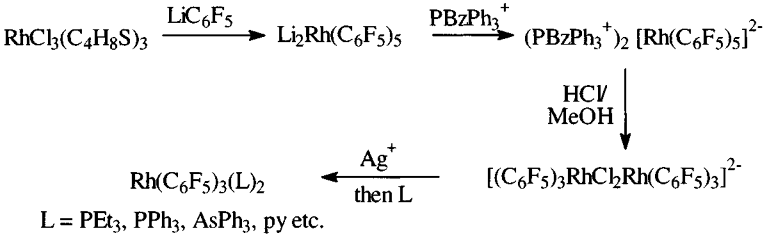

Figure 2.108 Synthesis of rhodium pentafluophenyl complexes.

Reaction of an 'aberrant batch' of $IrCl_3.xH_2O$ with mesityllithium has given a substituted hexadienyl rather than $IrMes_4$ [191].

Using the electron-withdrawing pentafluorophenyl group, two types of 5-coordinate compound have been made (Figure 2.108).

The anionic pentafluorophenyls have square pyramidal structures but are evidently non-rigid in solution (^{19}F NMR shows all ligands equivalent). The neutral adducts are also square pyramidal (apical C_6F_5, *trans*-L) [192].

3 Palladium and platinum

3.1 Introduction

Palladium and platinum are the longest known and most studied of the six platinum metals [1–11], a reflection of their abundance and consequent availability. Platinum occurs naturally as the element, generally with small amounts of the other platinum metals. It was used as a silver substitute by Colombian Indians and first observed there by Ulloa (1736), who called it platina del Pinto ('little silver of the Pinto river') but the first sample was actually brought to Europe in 1741 by Charles Wood, Assay Master of Jamaica. Palladium was isolated in 1803 by W.H. Wollaston, who was studying the aqua regia-soluble portion of platinum ores (he announced his discovery by an anonymous leaflet advertising its sale through a shop in Soho) and named it after the newly discovered asteroid Pallas [12].

These two metals resemble each other more closely than any of the other 'pairs' in this book. Their chemistry is largely that of the +2 and +4 oxidation states, though there are a few, formally, +1 and +3 compounds and there is an important group of zero valent tertiary phosphine complexes though no stable carbonyl comparable to $Ni(CO)_4$. Unlike nickel(II), where there are large numbers of tetrahedral complexes, these metals adopt almost exclusively square planar geometries in this oxidation state. As expected, they form more compounds in high oxidation states than nickel, partly a consequence of the lower ionization energies (Table 3.1).

Significant differences include:

1. The +4 oxidation state is more stable for platinum.
2. Platinum complexes are usually less labile.
3. There are many more examples of *cis*- and *trans*-isomers for platinum (a consequence of (2)).

Platinum in particular forms numbers of stable σ-bonded alkyls and aryls in both the +2 and +4 states.

3.2 The elements and uses

Both palladium and platinum are shiny, silvery metals (with ccp structures), easily drawn and worked when pure. Palladium has the lower melting and boiling points (1552 and 3141°C, respectively); the corresponding figures

Table 3.1 Ionization energies (kJ mol^{-1})

	Ni	Pd	Pt
I_1	736.7	805	870
I_2	1753	1875	1791
I_3	3393	3174	(2800)
I_4	5300	(4100)	(3900)

Values in parentheses are estimated.

for platinum are 1772 and 3825°C. Palladium is the more reactive, attacked by air at 700°C and by moist halogens at 20°C; it dissolves in hot oxidizing mineral acids whereas platinum is only dissolved by aqua regia. Both are attacked by molten caustic alkali.

Uses

The main uses of palladium [13] are in the electronics and electrical industries, in circuitry and in dental alloys. It finds many catalytic applications in industry, as well as in diffusion cells for the synthesis of hydrogen, and in automobile catalysts. Jewellery and 'three way' auto-catalysts are the principal uses of platinum, which fulfils a wide range of roles in the chemical industry.

The 'three way' catalysts are a major present day use for platinum and rhodium, and a lesser one for palladium; their role in minimizing exhaust emissions (while maximizing energy release) from petrol engines entails complete combustion of hydrocarbons, conversion of CO into CO_2 and also removal of nitrogen oxides as N_2 (reduction of NO_x). Platinum metal catalysts are thermally stable and operate at relatively low temperatures. They are prepared by dispersing a mixture of these three metals and alumina, together with certain additives like ceria, over a ceramic or metal matrix to obtain a large surface area. Platinum is the best alkane (and CO) oxidation catalyst while palladium is superior for alkenes. The role of the CeO_2 lies partly in the ability of cerium to switch oxidation states and thus act as a local oxygen store.

Fuel cells essentially reverse the electrolytic process. Two separated platinum electrodes immersed in an electrolyte generate a voltage when hydrogen is passed over one and oxygen over the other (forming H_3O^+ and OH^-, respectively). Ruthenium complexes are used as catalysts for the electrolytic breakdown of water using solar energy (section 1.8.1).

3.2.1 *Extraction*

The principal countries where platinum and palladium are extracted (along with nickel) are South Africa, Canada and the former USSR, though significant amounts come from Colombia, China and Western Australia [14]. The ores include all six platinum metals, with palladium and platinum most abundant; relative amounts vary, with the Merensky reef (South Africa) richer in platinum, roughly equal amounts in Sudbury (Ontario), and the Noril'sk deposits (Siberia) richer in palladium. They tend to occur along with nickel and copper ores, e.g. cooperite (PtS), braggite (MS) and sperrylite ($PtAs_2$).

The metals are obtained from the metallic phase of the sulphide matte or the anode slime from electrolytic refining of nickel. In the traditional process for the platinum metals, their separation was facilitated by their solubility in aqua regia and convertibility into $PdCl_4^{2-}$ or $PtCl_6^{2-}$ salts. Nowadays, substantial amounts are obtained using solvent extraction.

3.3 Halides

As expected, the heavier metal favours higher oxidation states (Table 3.2): the MX_3 compounds are not genuine M^{3+} species but are diamagnetic, with equal amounts of M^{2+} and M^{4+}. PtF_5, however, is a platinum(V) compound.

3.3.1 Palladium halides

Syntheses of palladium halides often involve direct reaction with a halogen:

$$Pd \xrightarrow[500^\circ\text{C reflux}]{F_2} PdF_3 \xrightarrow{SeF_4 \text{ or } SF_4} PdF_2$$

$$Pd \xrightarrow[>260^\circ\text{C}]{Cl_2} PdCl_2$$

$$Pd \xrightarrow{HBr/Br_2} PdBr_2$$

$$PdCl_2 \xrightarrow[\text{sealed tube } 140^\circ\text{C}]{5\%\ HI} PdI_2$$

$$PdF_3 \xrightarrow[300^\circ\text{C}]{F_2} PdF_4$$

$$Pd \xrightarrow[900-1700\ \text{Pa}]{\text{atomic F}} PdF_6$$

PdF_2 is that rare substance, a paramagnetic palladium compound, explicable in terms of (distorted) octahedral coordination of palladium with octahedra sharing corners [15]. It exists in two forms, both having $\mu_{\text{eff}} \sim 2.0\,\mu_B$, rather below the spin only value for two unpaired electrons. Bond lengths are Pd–F 2.172 Å (two) and 2.143 Å (four) in the tetragonal form (rutile structure).

The other palladium(II) halides are all diamagnetic. $PdCl_2$ exists in well defined α- and β-forms [16] (as well as a γ-form); the former has a $PdCl_{4/2}$

Table 3.2 Characteristics of palladium and platinum halides

	Palladium				Platinum			
	F	Cl	Br	I	F	Cl	Br	I
MX_2	Pale violet solid	Red solid, dec. >600°C	Brown solid	Black (α), deep red (β), black (γ), dec. >350°C		Black–brown solid	Brown solid	Black solid, dec. >500°C
MX_3	Black solid					Green–black solid	Black–green crystal	Black solid
MX_4	Brick red solid, rapid dec. >350°C				Yellow–brown solid	Red–brown crystal, dec. >350°C	Dark red solid, dec. >180°C	Black crystal, slow dec. RT
MX_5					Red solid, m.p. 80°C			
MX_6	Dark red solid, dec. ~0°C				Dark red solid, m.p. 61.3°C			

M, palladium or platinum; X, halide.

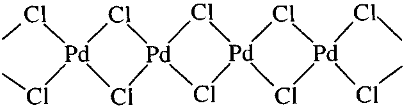

Figure 3.1 The chain structure of α-$PdCl_2$.

chain structure (Figure 3.1) while the β-form, synthesized by subliming the α form at 430–460°C) is Pd_6Cl_{12}, similar to the platinum analogue.

$PdBr_2$ also has a chain structure, but puckered, unlike α-$PdCl_2$, with planar coordination (somewhat irregular: Pd–Br 2.34, 2.57 Å). PdI_2 has three modifications, all made starting from the black γ-form precipitated from aqueous $PdCl_2$ reacting with HI at 140°C; it is traditionally used, because of its insolubility, in the gravimetric determination of palladium. The α-form of PdI_2 has a structure with tetragonal PdI_4 units forming side-by-side chains (Pd–I 2.60 Å) while in the β-form there are planar Pd_2I_6 units (Pd–I 2.61–2.62 Å) cross-linked with two distant iodines (3.29, 3.49 Å) to give distorted 6-coordination.

PdF_3 is really $Pd^{2+}PdF_6^{2-}$; both palladiums have an octahedral environment (Pd^{2+}–F 2.17 Å; Pd^{4+}–F 1.90 Å); like PdF_2, it is paramagnetic with a magnetic moment of 1.75 μ_B per palladium. It is possible that application of pressure causes the Pd–F bonds to even out, so that at high pressures the compound could become PdF_3 (genuine alkali metal salts of PdF_6^{3-} do exist) [17].

PdF_4 is the only stable palladium(IV) halide [18] (testimony to the oxidizing nature of palladium(IV)) and is a very moisture-sensitive diamagnetic red solid; the structure is based on Pd_6F_{24} hexameric units linked three-dimensionally. It has octahedrally coordinated palladium with two terminal (*cis*) fluorines and four bridging ones. Despite the absence of other tetrahalides, the complete series of PdX_6^{2-} exist (cf. Ir).

PdF_6 has been reported [19] (but not confirmed) to result from the reaction of powdered palladium with atomic fluorine under pressure (900–1700 Pa) as a dark red solid, unstable at 0°C that oxidizes both oxygen and water. An IR band at 711 cm^{-1} has been assigned as ν(Pd–F). There are unsubstantiated claims for PdF_5.

3.3.2 *Platinum halides*

Syntheses of platinum halides [20] include

$$Pt \xrightarrow[500^\circ C]{Cl_2} PtCl_2$$

$$Pt \xrightarrow{Br_2} PtBr_3 + PtBr_4 \xrightarrow{250^\circ C} PtBr_2$$

$$H_2PtBr_6.xH_2O \xrightarrow[180\text{–}280^\circ C]{\text{heat}} PtBr_2$$

$$\mathrm{Pt} \xrightarrow[525^\circ\mathrm{C},\ \textit{in vacuo}]{\mathrm{I_2}} \alpha\text{-}\mathrm{PtI_2}$$

$$\mathrm{K_2PtI_6} \xrightarrow[\text{sealed ampoule}]{240^\circ\mathrm{C}} \beta\text{-}\mathrm{PtI_2}$$

$$\mathrm{Pt} \xrightarrow[400\text{–}600^\circ\mathrm{C}]{\mathrm{Cl_2}/\text{sealed tube}} \mathrm{PtCl_3}$$

$$\mathrm{PrBr_2} \xrightarrow[125^\circ\mathrm{C}]{\mathrm{Br_2},<3\ \text{atm}} \mathrm{PtBr_3}$$

$$\mathrm{Pt} \xrightarrow[\text{sealed tube, }160^\circ\mathrm{C}]{\mathrm{KI/I_2/H_2O}} \mathrm{PtI_3}$$

$$\mathrm{Pt} \xrightarrow[140^\circ\mathrm{C}]{\text{exc. }\mathrm{KI/I_2/H_2O}} \alpha\text{-}\mathrm{PtI_4}$$

$$\mathrm{Pt} \xrightarrow[\text{sealed tube, }350^\circ\mathrm{C}]{\mathrm{SO_2Cl_2}} \mathrm{PtCl_4}$$

$$\mathrm{PtCl_2} \xrightarrow[<200^\circ\mathrm{C}]{\mathrm{F_2}} \mathrm{PtF_4}$$

$$\mathrm{Pt} \xrightarrow[150^\circ\mathrm{C}]{\mathrm{Br_2}} \mathrm{PtBr_4}$$

$$\mathrm{PtCl_2} \xrightarrow[350^\circ\mathrm{C}]{\mathrm{F_2}} \mathrm{PtF_5}$$

$$\mathrm{Pt\ (hot\ wire)} \xrightarrow[\text{2. condense}]{\text{1. }\mathrm{F_2}} \mathrm{PtF_6}$$

PtF_2 is unknown, presumably unstable with respect to the disproportionation

$$2\mathrm{PtF_2} \rightarrow \mathrm{Pt} + \mathrm{PtF_4}$$

This would occur as a consequence of the stability of the low spin d^6 platinum(IV) state and of the oxidizing power of fluorine. $PtCl_2$, like the other platinum dihalides, is insoluble in water. It has two crystalline forms: the β-form is similar to β-$PdCl_2$ (Figure 3.2; Pt–Cl 2.34–2.39 Å, Pt–Pt 3.32–3.40 Å). This transforms to the α-form at 500°C; this form has square planar coordination of platinum (Pt–Cl 2.299–2.310 Å) in a chain structure [21]. $PtBr_2$ is isomorphous with β-$PtCl_2$, and thus believed to be Pt_6Br_{12}, while β-PtI_2 is isomorphous with β-PdI_2 [20].

All the trihalides are mixed valence compounds. PtF_3 is isostructural with $PdF_3 \cdot PtX_3$ (X = Cl, Br, I) cannot be made by straightforward thermal decomposition of PtX_4 [22] under open conditions but by routes involving continuous decomposition and formation under closed, equilibrium conditions.

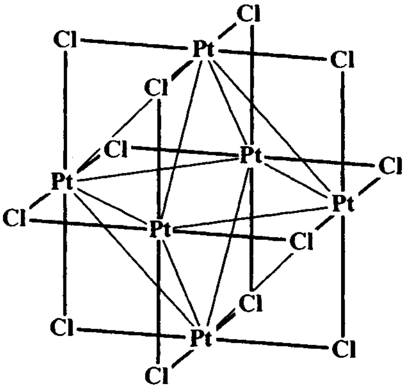

Figure 3.2 The structure of β-$PtCl_2(Pt_6Cl_{12})$. (Reproduced with permission from S.A. Cotton and F.A. Hart, *The Heavy Transition Elements*, Macmillan Press Ltd, 1975, p. 109.)

$PtCl_3$ and $PtBr_3$ (Figure 3.3) are isomorphous and contain both Pt_6X_{12} clusters and $[PtX_2X_{4/2}]_\infty$ chains, thus representing a 'half way' stage in decomposing PtX_4 [20].

PtF_4 prepared by various routes, including fluorination (BrF_3) of $PtCl_4$ or heating PtF_6, is isostructural with PdF_4 (Pt–F (terminal) 1.818 Å, Pt–F (bridge) 2.048 Å) [23]. The other tetrahalides similarly have chain structures (Figure 3.4) with two *cis*-terminal halides.

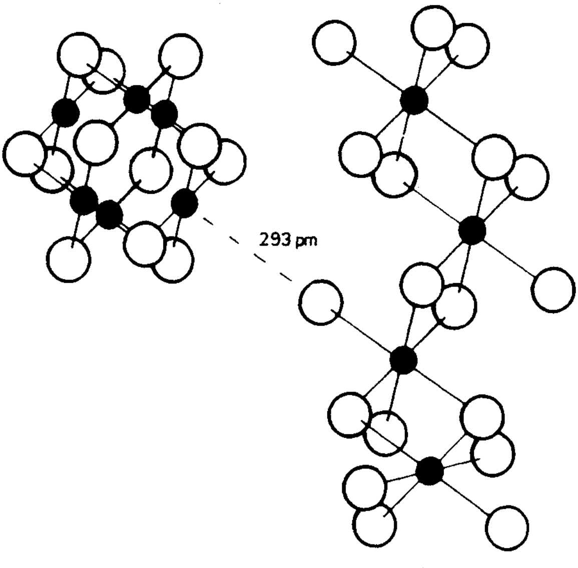

Figure 3.3 The structure of $PtBr_3$, showing the Pt_6Br_{12} and ${}^1_\infty[PtBr_2Br_{4/2}]$ structural units. (Reproduced with permission from *Transit. Met. Chem.*, 1975/6, **1**, 45.)

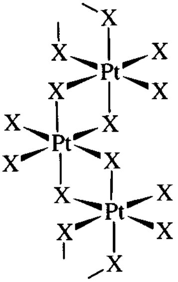

Figure 3.4 The chain structure adopted by PtX_4 in the solid state.

The iodide is polymorphic, with the α- and γ-forms known to have this structure (bond lengths are 2.65–2.72 Å (γ-PtI_4), 2.62–2.78 Å (α-PtI_4) 2.41–2.54 Å ($PtBr_4$).

On heating, $PtCl_4$ and $PtBr_4$ give PtX_2 but PtI_4 first yields PtI_3 or Pt_3I_8, depending on conditions [24].

Evaporation of solutions of platinum in aqua regia gives yellow crystals of the hydrates *trans*-$[PtCl_4(H_2O)_2].3H_2O$ and *fac*-$[PtCl_3(H_2O)_3]Cl.\frac{1}{2}H_2O$ [25].

PtF_5, made by fluorination of $PtCl_2$ at 350°C disproportionates above its m.p.

$$2PtF_5 \rightarrow PtF_4 + PtF_6$$

Its structure is not known but it may be a tetramer, like RhF_5.

The original synthesis of PtF_6 [26] involves electrical ignition of a platinum wire in a fluorine atmosphere then rapidly cooling the vapour (liquid nitrogen); it is also reported to result from the reaction of the elements under pressure at 200°C. It has a molecular structure (Pt–F 1.839 Å) and is intensely reactive, forming PtF_5 and PtF_4 on heating, vigorously decomposing water to O_2, and even attacking dry glass. It also is readily reduced:

$$O_2 + PtF_6 \rightarrow O_2^+PtF_6^-$$

3.3.3 *Halide complexes*

An extensive range of mono- and binuclear halide complexes of platinum and palladium exist. Of the tetrahalometallate(II) ions, some like PtF_4^{2-} and PdI_4^{2-} are elusive, the latter only having been characterized in solution.

$$PdCl_2 \xrightarrow[HCl]{MCl} M_2PdCl_4 \text{ (red–brown) (M, e.g. K, } NH_4\text{) (Pt similarly)}$$

$$K_2PdCl_4 \xrightarrow{Br^-} K_2PdBr_4 \text{ (dark red)}$$

$$K_2PtCl_4 \xrightarrow{NaBr/HBr} K_2PtBr_4 \text{ (brown)}$$

$$K_2PtCl_4 \xrightarrow[KI]{exc.} K_2PtI_4 \text{ (black)}$$

Table 3.3 Bond lengths in MX_4^{2-} together with M–X stretching frequencies (cm^{-1})

Ion	Cation	M–X (Å)	Ion	$\nu_1(A_{1g})$	$\nu_2(B_{1g})$	$\nu_6(E_u)$
$PdCl_4^{2-}$	NH_4^+	2.299	K	310	275	336
$PtCl_4^{2-}$	K^+	2.308	Bu_4N	330	312	317
$PdBr_4^{2-}$	K^+	2.438	(aq.)	188	172	225
$PtBr_4^{2-}$	K^+	2.445	–	208	194	243
PtI_4^{2-}	(in $(MeNH_3)_4Pt_3I_{11}$)	2.625	(aq.)	155	142	–

They have square planar structures; corresponding bond lengths and vibrational frequencies are given in Table 3.3.

PtI_4^{2-} has been identified in the unusual $(MeNH_3)_4Pt_3I_{11}$, a mixed-valence compound with PtI_4^{2-}, PtI_6^{2-} and $Pt_2I_6^{2-}$ ions all present (K_2PtI_4 has not definitely been confirmed) [27].

Genuine palladium(III) fluoroferrates have been made [28]

$$PdF_3 + 2AF + BF \xrightarrow[3\,kbar]{400°C} A_2BPdF_6$$

(A = K, Rb, Cs; B = Li, Na, K).

The beige to green solids have the elpasolite structure. Magnetic measurements confirm the $t_{2g}^6e_g^1$ configuration; they give strong ESR signals (Na_3PdF_6 $g_\perp = 2.312$, $g_\| = 2.025$) and exhibit a peak in the photoelectron spectra intermediate between those for palladium(II) and palladium(IV). K_2NaPdF_6 has been shown (X-ray) to have Jahn–Teller-distorted PdF_6^{3-} octahedra with Pd–F = 1.95 Å (four) and 2.14 Å (two).

'Chloroplatinic acid', $(H_3O)_2PtCl_6.xH_2O$ ($x \sim 2$), is obtained as brown-red crystals by dissolving platinum in aqua regia, followed by one or two evaporations with hydrochloric acid; it is a very useful starting material. Thermogravimetric data show that, after initial dehydration (up to 125°C), $PtCl_4$ is formed at 220°C and β-$PtCl_2$ at 350°C, before final decomposition to platinum around 500°C [29]. The Pt–Cl bond length is 2.323 Å in $(H_3O)_2PtCl_6$ [30].

All eight possible octahedral MX_6^{2-} (X = F, Cl, Br, I) have been made [31]:

$$A_2PdCl_6 \xrightarrow[200-300°C]{F_2} A_2PdF_6 \qquad (A = K\ to\ Cs)$$

$$M \xrightarrow[2.\,ACl]{1.\,aqua\ regia} A_2MCl_6 \qquad (M = Pd, Pt)$$

$$K_2PtCl_6 \xrightarrow{KHF_2\ melt} K_2PtF_6$$

$$A_2PdBr_4 \xrightarrow{Br_2} M_2PdBr_6$$

$$PdCl_6^{2-} \xrightarrow[CsI]{exc.} Cs_2PdI_6$$

Table 3.4 Bond lengths in MX_6^{2-} (Å)

Pd complexes	Counter-ion	M–X	Pt complexes	Counter-ion	M–X
PdF_6^{2-}	XeF_5^+	1.893	PtF_6^{2-}	NH_4^+	1.942
	K^+	1.896		K^+	1.922
$PdCl_6^{2-}$	NH_4^+	2.300	$PtCl_6^{2-}$	K^+	2.315–2.316
	K^+	2.309			
	Me_4N^+	2.312			
$PdBr_6^{2-}$	$(en)H_2^{2+}$	2.466–2.470	$PtBr_6^{2-}$	K^+	2.481
			PtI_6^{2-}	pyH^+	2.661–2.670
				Cs^+	2.673

$$PtCl_4 \xrightarrow{HCl} H_2PtCl_6 \xrightarrow{ACl} M_2PtCl_6 \qquad (A = K \text{ to } Cs)$$

$$Pt \xrightarrow[2.\,A^+]{1.\,HBr/Br_2} A_2PtBr_6$$

$$H_2PtCl_6 \xrightarrow{exc.\,AI} A_2PtI_6$$

The palladium compounds are generally, as expected, less stable. Therefore, PdF_6^{2-} is decomposed by water while PtF_6^{2-} can be synthesized in aqueous solution. The M_2PdCl_6 salts decompose on heating to 200°C. Bond lengths for a selection of the MX_6^{2-} ions are given in Table 3.4 and the structure of K_2PtCl_6 is shown in Figure 3.5 (based on the fluorite structure with K^+ in the fluoride positions and $PtCl_6^{2-}$ taking the place of the potassium) [32].

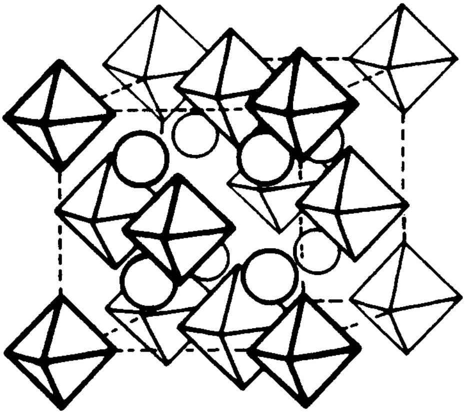

Figure 3.5 The crystal structure of K_2PtCl_6. (Reproduced from A.F. Wells, *Structural Inorganic Chemistry*, 4th edn, 1975, p. 387, by permission of Oxford University Press.)

Table 3.5 Comparing bond lengths in MF_6^{n-} (Å)

	M–F
PtF_6	1.839
$KPtF_6$	1.886
K_2PtF_6	1.926
K_2PdF_6	1.896
K_2NaPdF_6	1.95–2.14[a]

[a] Jahn–Teller distorted.

Synthesis for the octahedral MF_6^- ions include [33]

$$PdF_4 \xrightarrow[HF]{KrF_2/O_2 \text{ or } NaF} X^+PdF_6^- \qquad (X = O_2, Na)$$

$$Pd \xrightarrow[320°C,\ 60\,000\ psi]{F_2/O_2} O_2^+PdF_6^-$$

$$PtF_6 \xrightarrow{O_2} O_2^+PtF_6^- \xrightarrow[IF_5]{MF} M^+PtF_5^- \qquad (M = K \text{ to } Cs)$$

The magnetic moment for PtF_6^- (K^+ salt) is 0.87 μ_B (t_{2g}^5). The bond lengths for this ion are, as expected, intermediate between PtF_6 and PtF_6^{2-} (Table 3.5).

Both these ions are strong oxidizing agents; PtF_6^- will, unlike PtF_6^{2-}, oxidize water to O_2 and O_3. Vibrational data for a number of MX_6^{n-} species are listed in Tables 3.6 and 3.7.

As expected, there is a shift to lower frequency as the oxidation state of the metal decreases and as the mass of the halogen increases.

Mixed haloplatinate(IV) ions have been synthesized [34] by use of substitution reactions on $PtCl_6^{2-}$ and $PtBr_6^{2-}$; using the stronger *trans*-influence of Br, the *cis*-isomers can be made by treating $PtBr_6^{2-}$ with Cl^- (in the presence of Br_2):

$$PtBr_6^{2-} \xrightarrow{Cl^-} PtBr_5Cl^{2-} \rightarrow cis\text{-}PtBr_4Cl_2^{2-} \rightarrow fac\text{-}PtBr_3Cl_3^{2-}$$

$$\rightarrow cis\text{-}PtBr_2Cl_4^{2-} \rightarrow PtBrCl_5^{2-} \rightarrow PtCl_6^{2-}$$

Table 3.6 Vibrational frequencies in MX_6^{2-} (M = Pd, Pt; X = F, Cl, Br, I)

	PdF_6^{2-}	$PdCl_6^{2-}$	$PdBr_6^{2-}$	PtF_6^{2-}	$PtCl_6^{2-}$	$PtBr_6^{2-}$	PtI_6^{2-}
Counter-ion	NO^+	K^+	K^+	Cs^+	K^+	K^+	(aq.)
ν_1	573	317	198	591	351	218.5	150
ν_2	554	292	176	566	321	195.5	131
ν_3	602	357	253	571	345	244.5	186
ν_4	–	175	130	281	184		
ν_5	246	164	100	221	174	114.5	69.5

Data from: Y.M. Bosworth and R.J.H. Clark (1974) *J. Chem. Soc., Dalton Trans.*, 1749; M.P. Laurent *et al.* (1981) *Inorg. Chem.* **20**, 372; D.M. Adams *et al.* (1981) *J. Chem. Phys.* **74**, 2800; W. Preetz and G. Rimkus (1982) *Z. Naturforsch., Teil B*, **37**, 579.

Table 3.7 Comparative vibrational data for MF_6^{n-} (cm^{-1})

	PdF_6	PdF_6^-	PdF_6^{2-}	PtF_6	PtF_6^-	PtF_6^{2-}
ν_1		643	573	656	647	591
ν_2		570	554	601	590/572	566
ν_3	711		602	705	630	571
ν_4				273		281
ν_5			246	242	249/236	221
ν_6				211		

The *trans*-isomers can be made by substitution of Br^-

$$PtBrCl_5^{2-} \xrightarrow{Br^-} trans\text{-}PtBr_2Cl_4^{2-} \rightarrow mer\text{-}PtBr_3Cl_3^{2-} \quad \text{etc.}$$

Reaction mixtures can be separated by chromatography. Individual isomers can be identified by their vibrational spectra.

In the case of $PtF_nCl_{6-n}^{2-}$, it has even been possible to synthesize isotopically labelled species using isotopically labelled HCl (Figure 3.6).

Spectra of *trans*-$Pt^{35}Cl_2F_4^{2-}$ and the *cis*-isomer show the simpler spectra expected from the *trans*-isomer (three Pt–F and two Pt–Cl stretches) compared with the *cis*-isomer (four Pt–F and two Pt–Cl stretches). The complexity of the spectrum of the *cis*-isomer is also the result of the lack of a centre of symmetry in the *cis*-form; the selection rules allow all bands to be seen in both the IR and the Raman spectra (in theory, at least).

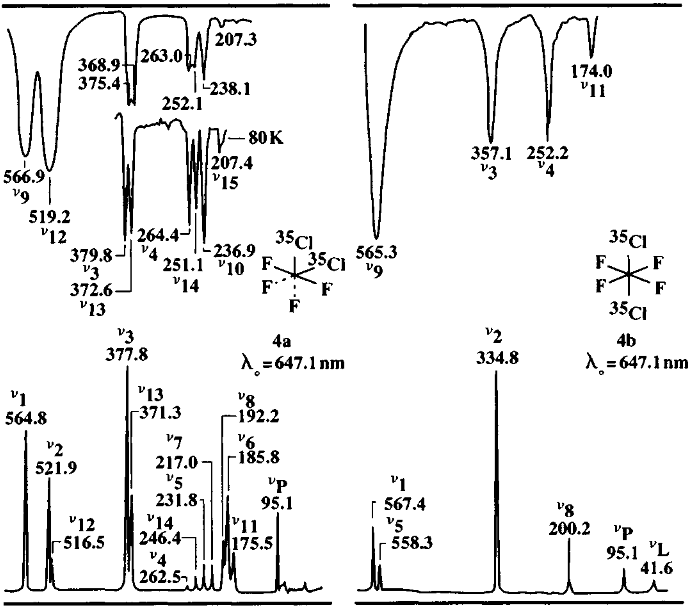

Figure 3.6 IR (upper) and Raman (lower) spectra of $Cs_2[Pt^{35}Cl_2F_4]$: *cis*-isomer on the left; *trans*-isomer on the right. (Reproduced with permission from *Z. Naturforsch., Teil B*, 1989, **44**, 619.)

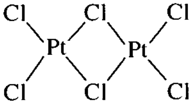

Figure 3.7 The dimeric structure of $[Pt_2Cl_6]^{2-}$.

The structures of *fac*-$(py_2CH_2)[PtF_3Cl_3]$ and *mer*-$(py_2CH_2)[PtF_3Cl_3]$ show the greater *trans*-influence of chloride. The Pt–F bonds are 1.950–1.995 Å in the *fac*-isomer and 1.936–1.937 (*trans* to F) and 1.972 Å (*trans* to Cl) in the *mer*-isomer; similarly Pt–Cl is 2.265–2.285 Å in the *fac*-isomer and 2.271 (*trans* to F) and 2.292–2.303 Å (*trans* to Cl) in the *mer*-isomer [35].

The $M_2X_6^{2-}$ salts are the simplest binuclear complexes [36]

$$MCl_4^{2-} \xrightarrow[H_2O]{Ph_3MeAsCl} (Ph_3MeAs)_2M_2Cl_6 \qquad (M = Pd, Pt)$$

$$MCl_4^{2-} \xrightarrow[H_2O]{cyclo\text{-}C_3H_7C_3^+Cl^-} (cyclo\text{-}C_3H_7C_3)_2M_2Cl_6$$

$$MBr_2 \xrightarrow[H_2O]{Et_4NBr} (Et_4N)_2M_2Br_6$$

$$MI_2 \xrightarrow[e.g.\ EtOH]{Et_4NI} (Et_4N)_2M_2I_6$$

They have di-μ-halogen bridged structures and are planar (Figure 3.7).

Typical bond lengths in $Pd_2Cl_6^{2-}$ are Pd–Cl 2.27 Å (terminal) and 2.32 Å (bridge) with Pd–Pd 3.41 Å and in $Pd_2Br_6^{2-}$ Pd–Br 2.398–2.405 Å (terminal) and 2.445–2.452 Å (bridge).

Dinuclear platinum(IV) complexes have recently been reported:

$$PtX_6^{2-} \xrightarrow[heat]{CF_3CO_2H} Pt_2X_{10}^{2-} \qquad (X = Cl, Br)$$

They have edge-sharing bioctahedral structures [37].

3.4 Other binary complexes

Palladium is notable for its ability to absorb (and desorb) hydrogen; diffusion through thin palladium films can be used to separate hydrogen from other gases. At 300 K, the Pd/H phase diagram shows an α-phase up to $PdH_{0.03}$, a two-phase region up to $PdH_{0.56}$ after which the β-phase becomes the sole species. The greatest H : Pd ratio obtainable is ~0.83 : 1 (at 195 K). The hydride reportedly has a defect NaCl structure.

The ability of palladium and platinum to catalyse hydrogenation reactions is of considerable industrial importance.

Tertiary hydrides can be made [38, 39]

$$\mathrm{AH + Pd\,sponge} \xrightarrow[20\,\mathrm{kbar},\,400^\circ\mathrm{C}]{H_2} A_2PdH_4 \qquad (A = \mathrm{Rb, Cs})$$

$$\mathrm{AH + Pd\,sponge} \xrightarrow[70\,\mathrm{kbar},\,300-350^\circ\mathrm{C}]{H_2} A_3PdH_5 \qquad (A = \mathrm{K, Rb, Cs})$$

Na_2PdH_4, A_2PtH_4 (M = Na, K) and K_2PtH_6 are similarly made, only K_2PtH_6 requiring any high hydrogen pressure.

All A_2MH_4 contain square planar MH_4^{2-} units, but at high temperatures the A_2MH_4 salts adopt the K_2PtCl_6 structure with hydrogens able to move between different square planar orientations. M_2PdH_2 (M = Li, Na) compounds have metallic lustre and display metallic conductivity [40].

Palladium and platinum combine on heating with the group V (15) and VI (16) elements [41].

The important oxides are black PdO and brown PtO_2. The former can be made by heating palladium in oxygen; other methods include heating $PdCl_2$ in an $NaNO_3$ melt at 520°C. A hydrated form precipitates from aqueous solution, e.g. when $Pd(NO_3)_2$ solution is boiled. It has 4-coordinate square planar palladium (Figure 3.8).

Black PdO_2 (rutile structure) is claimed to result from heating PdO with $KClO_3$ under pressure at 950°C, then rapidly cooling to room temperature. PtO_2, however, is well authenticated; it is made in hydrated form by hydrolysis (with Na_2CO_3) of boiling $PtCl_6^{2-}$ solution. It dehydrates on heating.

PtS (PdO structure) and PdS (similar) are prepared from M^{2+}(aq.) and H_2S or Li_2S. They have square planar coordination of M^{2+} (Figure 3.9).

On heating with sulphur, MS_2 result. PtS_2 has the 6-coordinate CdI_2 structure whereas PtS_2 is $Pd^{2+}(S_2^{2-})$ in a distorted pyrite structure (4-coordinate PdPd–S 2.30 Å) confirming the preference for the divalent state for

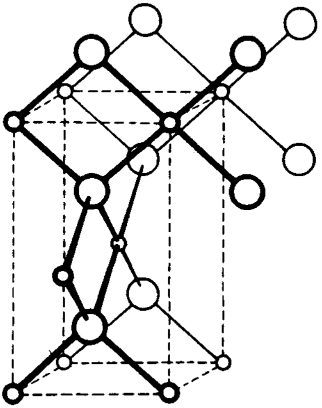

Figure 3.8 The structure of PdO and PtO. (Reproduced from A.F. Wells, *Structural Inorganic Chemistry*, 4th edn, 1975, p. 446, by permission of Oxford University Press.)

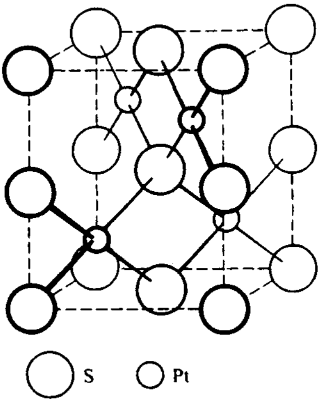

Figure 3.9 The structure of PtS. (Reproduced from A.F. Wells, *Structural Inorganic Chemistry*, 4th edn, 1975, p. 661, by permission of Oxford University Press.)

palladium. Other phases like $Pd_{2.2}S$, Pd_3S and Pd_4S (the last two both alloy like) exist. The former is a superconductor below 1.63 K.

The tellurides MTe reportedly have the NiAs structure.

The pyrites structure is exhibited by several pnictides: MAs_2 and MSb_2 (M = Pd, Pt) and PtP_2 (Figure 3.10).

PdP_2, however, contains continuous chains of phosphorus atoms (with, as expected, planar 4-coordinate Pd) while PdP_3 has the $CoAs_3$ structure (P_4 rings).

3.5 Aqua ions

Syntheses of palladium and platinum aqua ions [42] include

$$PdO \xrightarrow{HClO_4} Pd(H_2O)_4^{2+}$$

$$PtCl_4^{2-} \xrightarrow{AgClO_4} Pt(H_2O)_4^{2+}$$

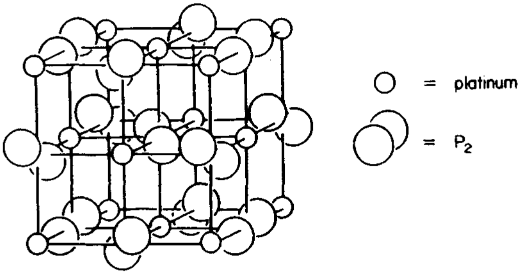

Figure 3.10 The structure of PtP_2. (Reproduced with permission from S.A. Cotton and F.A. Hart, *The Heavy Transition Elements*, Macmillan Press Ltd, 1975, p. 111.)

Hydrated palladium perchlorate has been isolated as brown needles of $Pd(H_2O)_4(ClO_4)_2$ by first dissolving palladium sponge in concentrated HNO_3, adding 72% $HClO_4$, evaporating until it fumes strongly and then crystallizing. $Pd(NO_3)_2(H_2O)_2$ is made by the reaction of palladium with nitric acid; it is also brown.

3.6 Palladium(0) and platinum(0) compounds

3.6.1 Tertiary phosphine complexes

The tertiary phosphine complexes are the most important zerovalent compounds. They are frequently prepared by reductive methods, often using the phosphine as the reducing agent [43], e.g.

$$Pd(\eta^5\text{-}C_5H_5)(\eta^3\text{-}C_3H_5) \xrightarrow{PR_3} Pd(PR_3)_2$$

($R = Bu^t$, cy; $PR_3 = PPhBu^t_2$)

$$trans\text{-}PtCl_2(Pcy_3)_2 \xrightarrow{Na/Hg} Pt(Pcy_3)_2$$

$$[\text{2-methylallyl}\,PdCl]_2 \xrightarrow{\text{exc.}\,PR_3} Pd(PR_3)_n$$

($PR_3 = PMe_3$, PMe_2Ph, PBu^n_3 ($n = 4$); $PR_3 = Pcy_3$, PPr^i_3, Pbz_3 ($n = 3$); $PR_3 = PBu^t_2Ph$ ($n = 2$))

$$cis\text{-}PtCl_2(PPh_2CF_3)_2 \xrightarrow[NaBH_4]{PPh_2CF_3} Pt(PPh_2CF_3)_3$$

Compounds with high coordination numbers sometimes eliminate a molecule of phosphine on heating:

$$M(PR_3)_4 \xrightarrow[\textit{in vacuo}]{70^\circ C} M(PR_3)_3 \qquad (M = Pd, Pt;\ R = Bu, Et)$$

$$M(PPr^i_3)_3 \xrightarrow[\textit{in vacuo}]{\text{heat}} M(PPr^i_3)_2 \qquad (M = Pd, Pt)$$

Tetrahedral structures have been established for $Pd(PPh_3)_4$ (rather long Pd–P bonds at 2.443 Å), $Pd[P(CH_2OH)_3]_4$ (Pd–P 2.321 to 2.326 Å), $Pt(PF_3)_4$ (electron diffraction: Pt–P 2.229 Å), $Pd[P(C{\equiv}CPh)_3]_4$, $Pt(PEt_3)_4$ and $Pt(PMe_2Ph)_4$ [44]. Trigonal planar structures are found for $Pt(Pcy_3)_3$, $Pd(PPh_3)_3$ (Pd–P 2.307–2.322 Å) and $Pt(PPh_3)_3$ (Pt–P 2.262–2.271 Å) [45] and essentially linear 2-coordination for $M(PBu^t_2Ph)_2$ (M = Pd, Pt; M–P 2.285 and 2.252 Å, respectively), $M(Pcy_3)_2$ (Pd–P 2.26 Å, Pt–P 2.231 Å) and $Pd(PBu^t_3)_2$ (Pd–P 2.285 Å). The last named has a P–Pd–P angle of 180° while the PBu^t_2Ph complexes are virtually linear but with some short metal *ortho*-hydrogen contacts. Curiously, the Pcy_3 complexes have

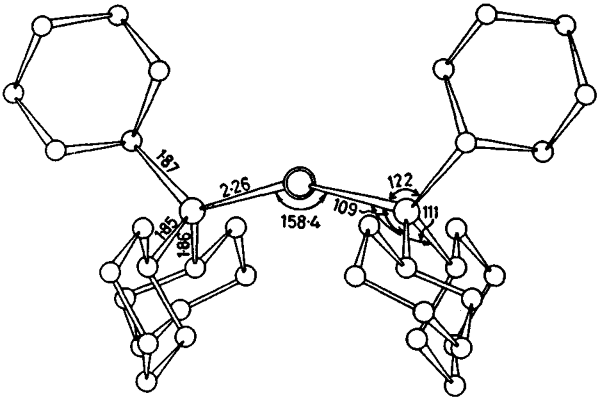

Figure 3.11 The structure of $Pd(Pcy_3)_2$. (Reproduced with permission from *J. Chem. Soc., Chem. Commun.*, 1974, 400.)

significantly 'bent' P–M–P bonds (158.4° M = Pd; 160.5° M = Pt) (Figure 3.11). $Pd(P(o\text{-tolyl})_3)_2$ has linear P–Pd–P coordination [46].

As expected, the Pt–P bond increases from 2.231 Å in the 2-coordinate $Pt(Pcy_3)_2$ to 2.303 Å in 3-coordinate $Pt(Pcy_3)_3$. (Similarly in $Pd(PPh_3)_n$ ($n = 3, 4$), from 2.31 Å ($n = 3$) to 2.443 Å ($n = 4$).)

Most of these compounds are solids (though a few such as $Pt(PEt_3)_3$, $Pt(PBu^n_3)_3$ and $Pt(PF_3)_4$ are oils at room temperature). Their stoichiometry in solution has been studied, most particularly by ^{31}P NMR at low temperatures, to determine which species are present [47]. Table 3.8 shows that the coordination number is principally determined by the bulk of the ligand

Table 3.8 $M(PR_3)_n$ complexes isolated in the solid state (S) and detected in solution (✓)

PR_3	Cone angle (°)	PtL_4	PtL_3	PtL_2	PdL_4	PdL_3	PdL_2
PF_3	104	S					
$P(OEt)_3$	109	S✓	X				
PMe_3	118	S✓	X		S✓	X	
PMe_2Ph	122	S✓			S✓	X	
PEt_3	132	S✓	S✓	X	S✓	✓	
PBu^n_3	132	S✓	S✓		S✓	✓	
$PMePh_2$	136	S✓			S✓		
PPh_3	145	S	S✓		S✓	S✓	S
$P(o\text{-tolyl})_3$	145	X	S✓				S✓
PPr^i_3	160		S✓	S✓		✓	✓
$P(O\text{-}o\text{-tolyl})_3$	141		S✓	X			
Pbz_3	165		S✓	X		✓	
PBu^t_2Ph	170		X	S✓		X	S✓
Pcy_3	170		S✓	S✓		✓	S✓
PBu^t_3	182			S✓			S✓

(conveniently measured in terms of its cone angle), i.e. the bulkier the ligand, the lower the coordination number of the complex isolated.

Steric requirements also affect the stability of compounds; therefore, for the complexes $Pt(PR_3)_4$, the PEt_3 complex (cone angle 132°) loses 1 mol phosphine *in vacuo* at 50°C, but the PMe_3 complex (cone angle 118°) is unaffected.

Steric factors are not the only ones to affect stability; $Ni(Pcy_3)_3$ does not dissociate, while $M(Pcy_3)_2$ (M = Pd, Pt) is stable, the reverse of what would be expected on steric grounds. Similarly with P(*o*-tolyl)$_3$, nickel forms NiL_4 while platinum forms PtL_3. Such discrepancies may be accounted for by taking into account the electron-donating power (basicity) of the phosphine and the electronic properties of the metal; thus electron-donating phosphines like PPr^i_3 can satisfy the electron demand of the metal better than aryl phosphines such as P(O-*o*-tolyl)$_3$ [48]. Compression of the cone angle or meshing of the ligands may also be important [45c]. Tricyclohexylphosphine has a cone angle of 170° yet meshing of the ligands leads to the isolability of $Pt(Pcy_3)_3$ from solution at −15°C (only $Pt(Pcy_3)_2$ is detected in solution above 0°C). Corresponding palladium and platinum complexes generally resemble each other closely, but there are differences; $Pd(PPh_2Me)_4$ does not dissociate while the platinum analogue does. $Pd(PBu^t_2Ph)_2$ binds oxygen reversibly, the platinum analogue binds irreversibly; PtL_2 (L = PPr^i_3, Pcy_3, PBu^t_2Ph) adds hydrogen reversibly whereas the palladium analogues do not.

In these compounds, compared with the palladium and platinum complexes, nickel generally exhibits higher coordination numbers, an effect similar to that seen with copper and silver compared with gold (section 4.1). Consideration of the d–s and s–p separations (Table 3.9) suggests that 2-coordination may be favoured for large s–p or small d–s separations (while relativistic effects may be significant for platinum, the general similarity between platinum and palladium suggests that it is not an important factor).

In addition to the tertiary phosphine complexes, a few others such as $Pt(QBu_3)_4$ (Q = As, Sb) and $Pt(QPh_3)_4$ have been made, but they have been the subjects of few studies.

Compounds $M(PPh_3)_2$ (M = Pd, Pt) have been postulated as kinetic intermediates but controversy has surrounded their isolation. It seems some '$M(PPh_3)_2$' species reported could have been $M(PPh_3)_2L$ (L, e.g. H_2,

Table 3.9 Values for d–s and s–p separations (eV)

	d^{10}–d^9s	d^9s–d^9p	d^{10}–d^9p^1
Ni	−1.8	3.52	1.72
Pd	0.81	3.42	4.23
Pt	0.76	4.04	3.28

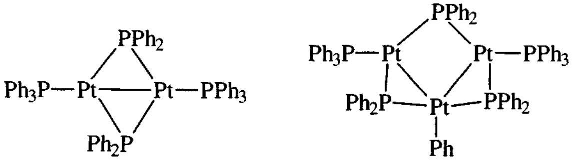

Figure 3.12 Complexes produced by refluxing solutions of $Pt(PPh_3)_4$.

N_2, C_2H_4) or internally metallated species. Reactions such as extended refluxing of $Pt(PPh_3)_4$ in benzene yields clusters [49] (Figure 3.12).

Recently, however, $Pd(PPh_3)_2$ has been reported to result from reduction of palladium(II) complexes as a very reactive yellow solid [50]:

$$Pd(C_3H_5)(PPh_3)_2^+ \xrightarrow{Ph_2MeSiLi} Pd(PPh_3)_2$$

Electrochemical reduction of *cis*-$PtCl_2(PR_3)_2$ (R = Ph, Et) generates very reactive $Pt(PR_3)_2$ species [51] (though it has been suggested that corresponding palladium compounds may be anionic, e.g. $Pd(PR_3)_2Cl_2^{2-}$)

$$Pt(PR_3)_2Cl_2 \xrightarrow{2e^-} Pt(PPR_3)_2 + 2Cl^-$$

They can be trapped by reactive molecules

$$Pt(PEt_3)_2 \xrightarrow[X=Cl,CN]{PhX} trans\text{-}Pt(Ph)X(PEt_3)_2$$

UV irradiation of $Pt(PEt_3)_2(C_2O_4)$ under a dihydrogen atmosphere yields a hydride by trapping [52]:

$$Pt(PEt_3)_2C_2O_4 \xrightarrow{h\nu} Pt(PEt_3)_2 + 2CO_2 \xrightarrow{H_2} trans\text{-}PtH_2(PEt_3)_2$$

Thermolysis of *cis*-$PtH(CH_2CMe_3)(cy_2PC_2H_2Pcy_2)$ at 45–80°C yields a bent platinum(0) complex (Figure 3.13) that is intensely reactive to a whole range of unactivated C–H bonds in saturated and unsaturated hydrocarbons.

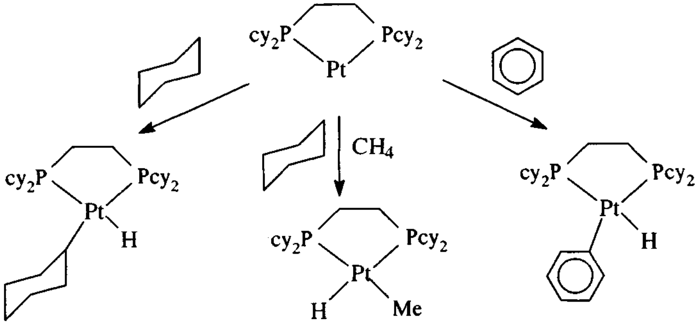

Figure 3.13 Addition reactions of $Pt(cy_2PCH_2CH_2Pcy_2)$.

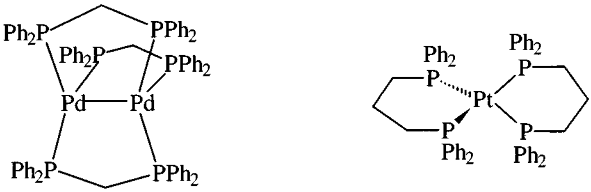

Figure 3.14 Zerovalent complexes of polydentate phosphines.

Zerovalent complexes are also obtained with polydentate phosphines [53]:

$$Pd_2Cl_2(dppm)_2 \xrightarrow[\text{exc. dppm}]{\text{NaBH}_4} Pd_2(dppm)_3$$

$$PtCl_2(cod) \xrightarrow{\text{dppp}} PtCl_2(dppp) \xrightarrow[\text{NaBH}_4]{\text{dppp}} Pd(dppp)_2$$

Their structures are shown in Figure 3.14.

3.6.2 Reactions of Pt(PPh_3)$_n$ and related species

Pt(PPh_3)$_n$ ($n = 3$, 4) species [54] have been studied with profit for many years; they undergo a wide range of addition reactions with attendant loss of phosphine, the kinetically active species probably being $Pt(PPh_3)_2$. (The palladium analogues generally behave similarly but are much less studied.)

Though many of the products shown in Figure 3.15 are clearly platinum(II) species, some are formally platinum(0).

However, it seems that these are best viewed as platinum(II) species too, so that two-electron metal-to-ligand transfer has been effected. The structures of $Pt(PPh_3)_2Z$ ($Z = \eta^2\text{-}O_2$, $\eta^2\text{-}C_3H_4$, $\eta^2\text{-}CS_2$) (Figure 3.16) all involve 'square planar' coordination as expected for platinum(II) rather than the tetrahedral 4-coordination anticipated for platinum(0).

Similarly, ESCA data show the platinum $4f_{7/2}$ binding energy in $Pt(PPh_3)_2O_2$ (73.2 eV) to be nearer to that in $Pt(PPh_3)_2Cl_2$ (73.4 eV) rather than $Pt(PPh_3)_4$ (71.7 eV) or platinum metal (71.2 eV) [55]. Like many of the rhodium and iridium dioxygen adducts (section 2.11) adduct formation with O_2 is irreversible (though that with SO_2 is reversed on heating). With unsaturated compounds (alkenes, alkynes, benzene) η^2-coordination is the rule. Reactions with alkyl and some aryl halides affords a route to mono alkyls and aryls. The reactions with halogens gives a route to *cis*-$Pt(PPh_3)_2X_2$ (X = Br, I); if an excess of halogen is used and the reaction stopped after a few minutes (to prevent oxidation to platinum(IV)) the initial *trans*-product is isolated (the halogen oxidizes liberated PPh_3 and prevents it catalysing, as occurs so often with platinum(II), the *trans–cis* isomerization). Other reactions can involve coupling (NO) and decoupling (C_2N_2).

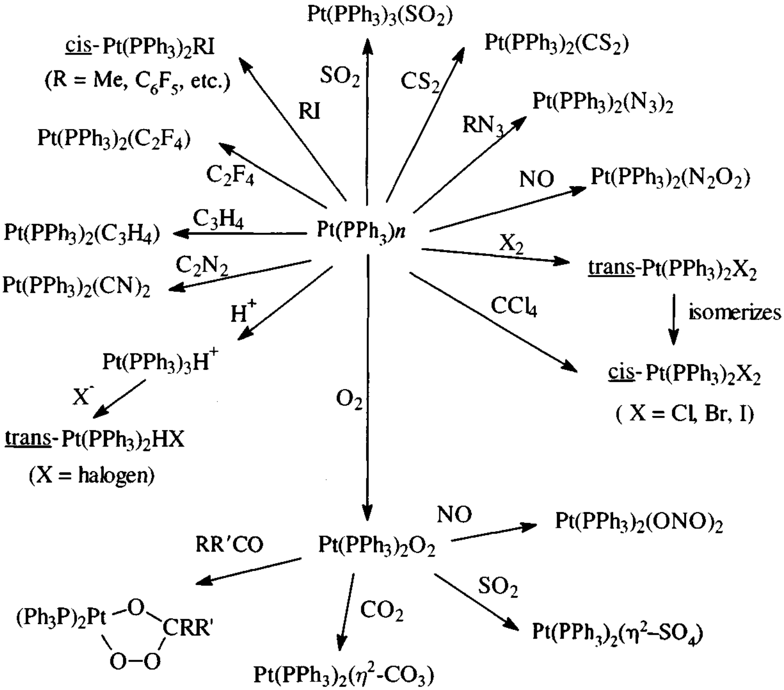

Figure 3.15 Reactions of $[Pt(PPh_3)_n]$.

The O_2 adduct has a rich chemistry of its own (Figure 3.15) reacting with small electrophiles in processes involving oxidation of the substrate. Thus NO couples to give nitrite and N_2O_4 nitrate; SO_2 is turned into sulphate and CO_2 into carbonate. In several cases, as with aldehydes and ketones, a peroxychelate ring results.

Other zerovalent phosphine complexes sometimes exhibit different reactions. $Pt(PPh_3)_3$ does not react with dihydrogen but $Pt(PEt_3)_3$ forms $Pt(PEt_3)_3H_2$. $Pt(PR_3)_3$ (R = Et, Pr^i) adds H_2O to form hydroxybases $[Pt(PEt_3)_3H^+OH]^-$ and $[Pt(PPr^i_3)_2H(solvent)]^+OH^-$. $Pd(Pcy_3)_2$ reacts with the strong acid HBF_4 to give *trans*-$[Pd(Pcy_3)_2H(H_2O)]^+BF_4^-$ and with carboxylic acids to form $[Pd(Pcy_3)_2H(OCOR)]$; with phenols it gives $[Pd(Pcy_3)_2H(OC_6X_5)]$

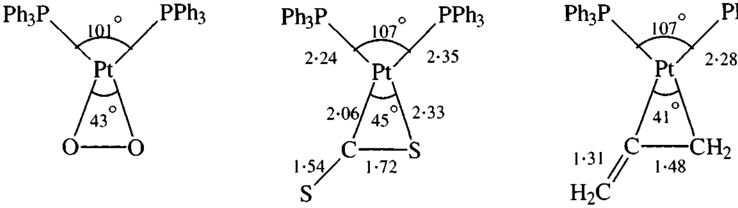

Figure 3.16 Structures of $Pt(PPh_3)_2Z$ ($Z = O_2, CS_2, C_3H_4$).

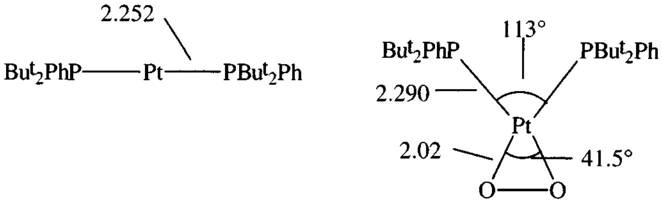

Figure 3.17 A comparison between the geometeries of $[Pt(PBu^t_2Ph)_2]$ and $[Pt(PBu^t_2Ph)_2(O_2)]$.

(X = H, F). The platinum analogue behaves similarly, and it also reacts with H_2 to form *trans*-$Pt(Pcy_3)_2H_2$.

Both $M(PPhBu^t_2)_2$ compounds (M = Pd, Pt) add O_2, the former reversibly. They are nearly isostructural, with a slightly longer O–O bond in the platinum compound (1.43 Å) than in the palladium analogue (1.37 Å). Compared with the parent platinum compound (Figure 3.17) the Pt–P bonds are some 0.04 Å longer in the dioxygen compound, but though the P–Pt–P angle has closed from 180° to 113.1°, this is a good deal larger than the value in the PPh_3 analogue (101°) and suggests steric crowding.

The adoption of a planar structure in these adducts, rather than the sterically more favourable tetrahedral one, is in keeping with a platinum(II) oxidation state. The side-on bonding of the O_2 molecule is believed to involve two components, as in Zeise's salt (Figure 3.18).

There is (a) σ-donation from a filled oxygen orbital to an empty platinum orbital and (b) π back-bonding from a filled metal d orbital into an empty oxygen π^*-anti-bonding orbital.

There has been considerable study of reactivity patterns and reaction mechanisms for oxidative additions of $Pt(PR_3)_n$ species. Reactivity is determined by (a) steric factors, thus complexes like $Pt(Pcy_3)_2$ are very reactive and (b) the basicity of the phosphine. The more basic the phosphine, the more facile is oxidative addition; therefore $Pt(PEt_3)_3$ will add PhCl and PhCN while the less nucleophilic $Pt(PPh_3)_3$ will not. It is thought that many of these reactions involve initial dissociation of a phosphine, as in the addition of benzyl halides to $Pd(PPh_3)_4$, proceeding generally by inversion through a S_N2 mechanism. Either ionic or radical mechanisms are possible. Radical pathways can be detected in three ways:

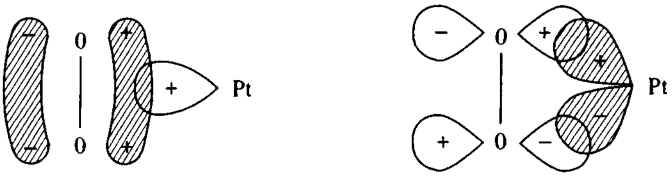

Figure 3.18 Metal–dioxygen bonding in platinum–dioxygen complexes.

1. Addition of radical inhibitors (e.g. duroquinone, galvinoxyl), which will slow up any pathway involving radicals.
2. Adding a radical trap like Bu^tNO to the reaction mixture; this reacts with radicals ($R^\bullet$) forming nitroxide radicals $Bu^t(R^\bullet)NO$ that can be detected by ESR.
3. Observation of CIDNP effects in the resonances of either reactant or product species in the NMR spectrum of the reaction mixture.

In the case of the reaction of $PhCH_2Br$ with $Pt(PEt_3)_3$, it is thought that $Pt(PEt_3)_2(PhCH_2)Br$ is formed via a S_N2 route where the platinum forms a cationic complex that undergoes immediate attack by Br^- while some $Pt(PEt_3)_2Br_2$ is formed in a very rapid reaction unaffected by radical scavengers.

$$Pt(PEt_3)_3 + PhCH_2Br \rightarrow Pt^I(PEt_3)_nBr + PhCH_2^\bullet$$

$$Pt(PEt_3)_nBr + BrCH_2Ph \rightarrow Pt(PEt_3)_2Br_2 + PhCH_2^\bullet$$

This is in contrast with the reaction of $Pt(PEt_3)_3$ with Me_3CCH_2Br, which is affected by radical scavengers like galvinoxyl, where the radicals are sufficiently long lived to undergo side reactions with the solvent – in toluene, some $Pt(PEt_3)_2(PhCH_2)Br$ is formed – giving credence to a radical chain mechanism. In the reactions of alkyl halides (EtI, MeI, $PhCH_2Br$) to $Pt(PPh_3)_3$, believed to proceed by a non-chain radical process, addition of radical traps results in the formation of ESR-active radicals. This reaction is very solvent dependent; in benzene MeI adds to give solely $Pt(PPh_3)_2MeI$ while in THF $Pt(PPh_3)_2I_2$ is the main product [56]. A detailed study of this reaction in benzene shows that the most important steps are

$$Pt(PPh_3)_3 \rightleftharpoons Pt(PPh_3)_2 + PPh_3$$

$$Pt(PPh_3)_2 + MeI \rightarrow Pt(PPh_3)_2(Me)I + PPh_3$$

Undissociated $Pt(PPh_3)_3$ is much less reactive.

Addition of RX to a $Pt(PR_3)_n$ species may occur by two main pathways:

1. S_N2 attack of the electron-rich platinum(0) on the alkyl halide to give the $Pt^{II}(R)X$ species directly, possibly via an ionic intermediate.
2. Platinum removes a halogen atom from the halide, causing homolytic fission of the C–halogen bond. The resulting Pt^I–XR radical pair can either react to form $Pt^{II}(R)X$ or separate, with subsequent reaction with RX leading to either PtX_2 or PtRX species or reaction with solvent molecules.

3.6.3 Carbonyl complexes

$Ni(CO)_4$ is a most important nickel carbonyl compound and can even be prepared directly from its constituents yet the corresponding palladium and platinum compounds do not exist (at least, at room temperature). If platinum (or palladium) is vaporized from a hot rod (around 1800°C) to produce gaseous platinum atoms, and co-condensed with CO in an argon matrix, IR spectra indicate the presence of metal carbonyl species $M(CO)_x$ ($x = 1$–4). On controlled warming, diffusion takes place with successive CO addition taking place to yield $M(CO)_4$ as the stablest product (ν(C–O) 2052, 2070, 2053 cm^{-1} for nickel, palladium and platinum tetracarbonyls, respectively). Analysis of spectra leads to metal–carbon force constants of 1.80, 0.82 and 1.28 mdyn Å^{-1} for nickel, palladium and platinum tetracarbonyls, respectively. This indicates the weakness of the Pd–C and Pt–C bonds; they decompose if the matrices are warmed above *c.* 80 K [57, 58].

The M–CO bond is stabilized by the presence of tertiary phosphines

$$Pt(PPh_3)_3 + CO \xrightarrow{Me_2CO} Pt(PPh_3)_3CO$$

$$PtCl_2 + 2PPh_3 + 2CO + Zn \rightarrow ZnCl_2 + Pt(PPh_3)_2(CO)_2$$

Both $Pt(PPh_3)_3CO$ and $Pt(PPh_2Et)_2(CO)_2$ have essentially tetrahedral coordination of platinum.

The reason for the greater stability of $M(PR_3)_n$ over $M(CO)_4$ must lie in the difference in donor characteristics of the two kinds of ligand. CO is a poor σ-donor but a strong π-acceptor, while tertiary phosphines are much better σ-donors.

In a binary carbonyl both σ- and π-components are important in the metal–carbon bond: a σ-bond owing to $M \leftarrow :C$ donation and a π-bond owing to back-bonding from filled metal d orbitals to empty CO π^*-orbitals. The relative energies of the metal d orbitals are in the order of 4d (Pd) > 5d (Pt) > 3d (Ni) so that the strength of the σ-component would be in the order of Pd < Pt < Ni (this also correlates with the electronegativities of the metals). The ability of the metal to donate electrons may correlate with the ionization energies; I_1 values are 737 (Ni), 805 (Pd) and 870 (Pt) kJ mol^{-1}, giving a π-bonding order Pt < Pd $\ll$ Ni. Therefore, on both grounds the Ni–C bond is predicted to be the strongest.

3.6.4 Carbonyl clusters

Apart from the mixed phosphine/carbonyl species $Pt(PPh_3)_{4-n}(CO)_n$ ($n = 1, 2$), there are polynuclear species $Pt_3L_n(CO)_3$ ($n = 3, 4$; $L = PR_3$), and additionally some remarkable anionic binary carbonyl clusters, formed by reductive carbonylation of $Na_2PtCl_6.6H_2O$ with general formulae $[Pt_3(CO)_6]_n^{2-}$. These contain $Pt_3(CO)_3(\mu^2\text{-}CO)_3$ clusters stacked along a three-fold axis but with a twist or sliding minimizing repulsions in adjacent layers [59].

3.6.5 Isocyanide complexes

A few isocyanides of palladium and platinum are known in the zerovalent oxidation state. The best characterized compounds involve triangular M_3 clusters with M–M bonds.

$$\mathrm{Pt(PBu^t_3)_2} \xrightarrow{\mathrm{Bu^tNC}} \mathrm{[Pt(CNBu^t)_2]_3}$$

$$\mathrm{Pt(cod)_2} \xrightarrow{\mathrm{Pr^iNC}} \mathrm{[Pt(CNPr^i)_2]_3}$$

The palladium compound $[Pd(CNcy)_2]_3$ has been made by metal vapour synthesis, from Pd atoms and a solution of cyNC at 160 K. It has an analogous structure $[Pd_3(CNcy)_3(\mu^2\text{-}CNcy)_3]$ [60].

3.7 Palladium(I) and platinum(I) compounds

A limited chemistry of the +1 oxidation state of palladium and platinum has developed since the 1970s, mainly involving metal–metal bonded dinuclear complexes [61].

3.7.1 Phosphine complexes

Phosphine complexes can be synthesized by reduction or reproportionation. Complexes of dppm are the most important and can undergo both substitution reactions and insertions (Figure 3.19).

Using a 2-diphenylphosphinopyridine as the bridging ligand (with a similar 'bite' to dppm) leads to a similar dimer (Figure 3.20).

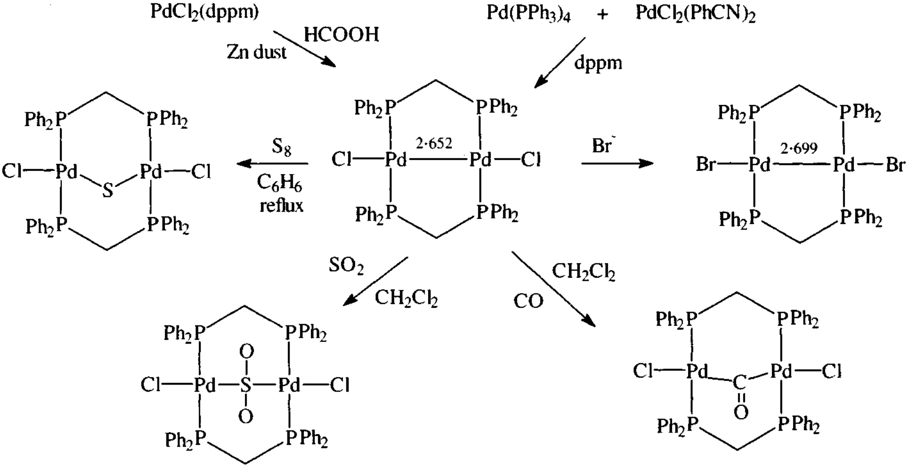

Figure 3.19 Synthesis and reactions of palladium(I) bis(diphenylphosphino)methane complexes.

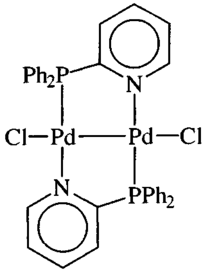

Figure 3.20 A palladium(I) 2-diphenylphosphinopyridine complex.

Hydrogen reduction of (dppp)Pd$(CF_3SO_3)_2$(dppp)$Ph_2P(CH_2)_3PPh_2$ affords $[dpppPd]_2(CF_3SO_3)_2$, which has agonistic Pd–phenyl interactions as well as normal Pd–P coordination and a Pd–Pd bond (2.701 Å) (Figure 3.21).

Several *cis*-platinum(II) dihydrides lose H_2 reversibly in solution, forming dinuclear platinum(I) hydrides $[(diphosphine)PtH]_2$ [62].

Isocyanide complexes can also be made by reproportionation.

3.7.2 *Isocyanide complexes*

Isocyanide complexes can be synthesized by:

$$PdX_2(Bu^tNC)_2 + Pd(Bu^tNC)_2 \rightarrow [PdX(Bu^tNC)_2]_2$$

$$PdCl_4^{2-} \xrightarrow{MeNC} [Pd_2(MeNC)_6]_2(PF_6)_2$$

The methylisocyanide complex has a dimeric structure with a direct metal–metal bond (2.531 Å) and only terminal isocyanides, in a staggered configuration (Figure 3.22).

The platinum analogue is similarly made.

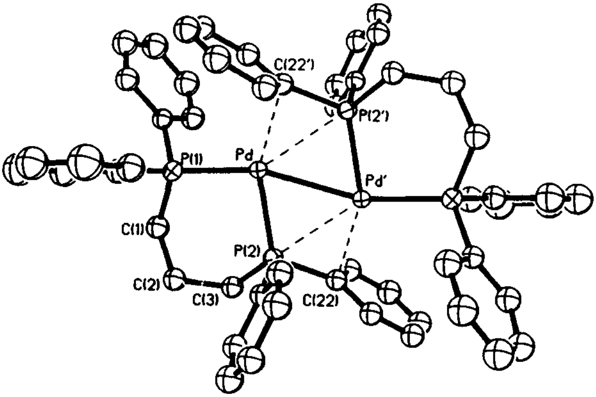

Figure 3.21 Structure of the dimeric palladium(I) complex $[(dppp)Pd]_2(CF_3SO_3)_2$. (Reprinted with permission from *Organometallics*, 1992, **11**, 23. Copyright (1992) American Chemical Society.)

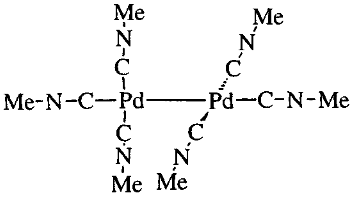

Figure 3.22 The staggered structure of $[Pd_2(MeNC)_6]^{2+}$.

3.8 Complexes of palladium(II) and platinum(II)

A wide variety of complexes are formed by both metals in the +2 oxidation state; indeed, it is the most important one for palladium. The complexes can be cationic, neutral or anionic. Both Pd^{2+} and Pt^{2+} are 'soft' acids so that many stable complexes are formed with S or P as donor atoms but few with O-donors, though there are important ammines. There are pronounced similarities between corresponding palladium and platinum complexes; the latter are more studied (and less labile).

3.8.1 Complexes of O-donors

Complexes of O-donors are relatively rare, explicable by the 'soft' nature of the divalent ions. A telling indication is that sulphoxide ligands will only bind through O if steric effects make S-bonding impractical. The most important complexes are diketonates and carboxylates (for the aqua ions see section 3.5).

Diketonates

Two kinds of platinum diketonate may be made

$$PtCl_4^{2-} + MeCOCH_2COMe \xrightarrow{KOH} KPtCl(acac)_2$$

$$\xrightarrow[\text{exc. }MeCOCH_2COMe]{KOH} Pt(acac)_2$$

$Pt(acac)_2$ has the expected square planar coordination by oxygen (Pt–O 1.979–2.008 Å) with bidentate diketonates; this has also been confirmed for $Pd(PhCOCHCOMe)_2$, which is obtainable as *cis*- and *trans*-isomers that can be crystallized and separated manually (Figure 3.23).

In $[PtCl(acac)_2]^-$, 4-coordination is possible because one of the diketonates is C-bonded (Figure 3.24).

The diketonates can form Lewis base adducts such as 5-coordinate $Pd[P(o\text{-}tolyl)_3](CF_3COCHCOCF_3)_2$ (Figure 3.25), though with acetylacetone square planar adducts of the type $M(acac)_2(PR_3)_2$ are usually obtained, where the diketone is monodentate O-bonded [63].

Next Page

Previous Page

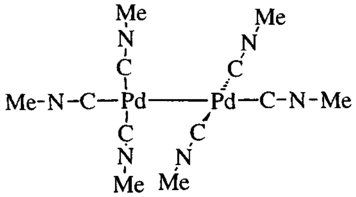

Figure 3.22 The staggered structure of $[Pd_2(MeNC)_6]^{2+}$.

3.8 Complexes of palladium(II) and platinum(II)

A wide variety of complexes are formed by both metals in the +2 oxidation state; indeed, it is the most important one for palladium. The complexes can be cationic, neutral or anionic. Both Pd^{2+} and Pt^{2+} are ‘soft’ acids so that many stable complexes are formed with S or P as donor atoms but few with O-donors, though there are important ammines. There are pronounced similarities between corresponding palladium and platinum complexes; the latter are more studied (and less labile).

3.8.1 Complexes of O-donors

Complexes of O-donors are relatively rare, explicable by the ‘soft’ nature of the divalent ions. A telling indication is that sulphoxide ligands will only bind through O if steric effects make S-bonding impractical. The most important complexes are diketonates and carboxylates (for the aqua ions see section 3.5).

Diketonates
Two kinds of platinum diketonate may be made

$$PtCl_4^{2-} + MeCOCH_2COMe \xrightarrow{KOH} KPtCl(acac)_2$$

$$\xrightarrow[\text{exc. MeCOCH}_2\text{COMe}]{\text{KOH}} Pt(acac)_2$$

$Pt(acac)_2$ has the expected square planar coordination by oxygen (Pt–O 1.979–2.008 Å) with bidentate diketonates; this has also been confirmed for $Pd(PhCOCHCOMe)_2$, which is obtainable as *cis*- and *trans*-isomers that can be crystallized and separated manually (Figure 3.23).

In $[PtCl(acac)_2]^-$, 4-coordination is possible because one of the diketonates is C-bonded (Figure 3.24).

The diketonates can form Lewis base adducts such as 5-coordinate $Pd[P(o\text{-tolyl})_3](CF_3COCHCOCF_3)_2$ (Figure 3.25), though with acetylacetone square planar adducts of the type $M(acac)_2(PR_3)_2$ are usually obtained, where the diketone is monodentate O-bonded [63].

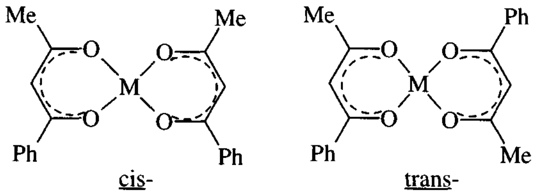

Figure 3.23 The *cis*- and *trans*-isomers of [Pd(PhCOCHCOMe)$_2$].

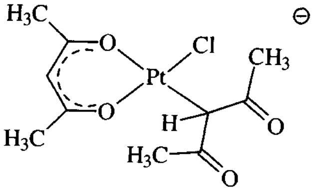

Figure 3.24 The structure of [PtCl(acac)$_2$]$^-$.

Carboxylates

The acetates are important compounds (Figure 3.26) with somewhat different structures [64], the palladium compound being a trimer (Pd–Pd 3.10–3.20 Å; Pd–O 1.99 Å) while platinum acetate is a tetramer (Pt–O 2.00–2.16 Å; Pt–Pt 2.492–2.498 Å).

There is significant metal–metal bonding in the platinum compound, whose geometry involves a square of platinum atoms; another important difference is that the coordination geometry is square planar in palladium acetate but octahedral in the platinum analogue. Different oligomers exist in solution, broken down by adduct formation. Palladium(II) acetate may be obtained as brown crystals from the following reaction [65]:

$$\mathrm{Pd} \xrightarrow[\mathrm{HNO_3}]{\mathrm{MeCOOH}} \mathrm{Pd(OCOMe)_2}$$

The importance of palladium acetate lies in its ability to catalyse a wide range of organic syntheses: functionalizing C–H bonds in alkanes and in aromatics, and in oxidizing alkenes. It has been used industrially in the

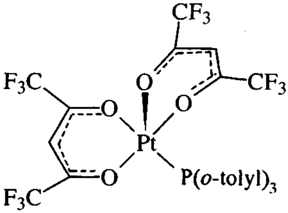

Figure 3.25 The structure of [Pt(CF$_3$COCHCOCF$_3$)$_2${P(*o*-tolyl)$_3$}].

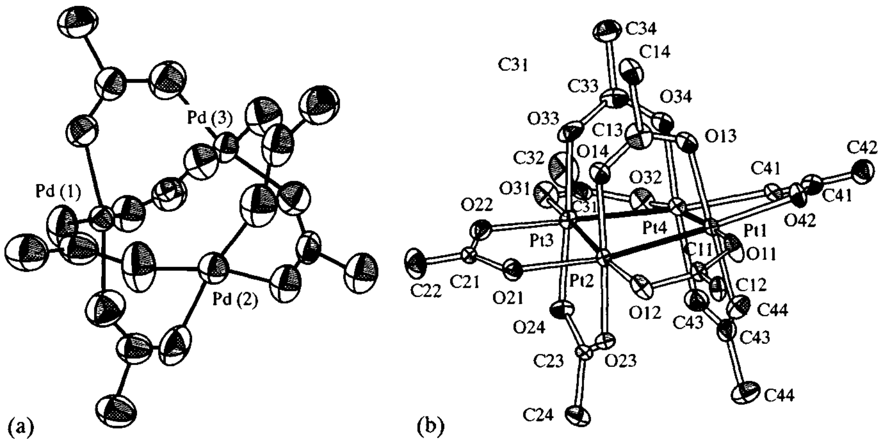

Figure 3.26 The structures of (a) palladium acetate and (b) platinum acetate. (Reproduced with permission from *J. Chem. Soc., Chem. Commun.*, 1970, 659 and *Acta Crystallogr. Sect. B*, 1978, **34**, 1857.)

synthesis of vinyl acetate from ethene; it will also catalyse the conversion of benzene into phenol or benzoic acid. It usually is used in conjunction with a reoxidation catalyst (peroxides, O_2, $K_2S_2O_8$) so that it seems the ability of palladium to switch oxidation states may be important [66],

3.8.2 *Complexes of N-donors*

Ammines

The preparation of the isomeric forms of $Pt(NH_3)_2Cl_2$ is discussed in terms of the *trans*-effect in section 3.8.9 [67].

$$PtCl_4^{2-} \xrightarrow{\text{aq. NH}_3} cis\text{-}Pt(NH_3)_2Cl_2$$

$$Pt(NH_3)_4^{2+} \xrightarrow[\text{heat}]{\text{HCl (aq.)}} trans\text{-}Pt(NH_3)_2Cl_2$$

A more convenient synthesis of the latter is

$$Pt(NH_3)_4Cl_2 \xrightarrow[\textit{in vacuo}]{190^\circ\text{C}} trans\text{-}Pt(NH_3)_2Cl_2 + 2NH_3$$

These *cis*-complexes of palladium are unstable and rapidly isomerize but can be made via the *cis*-diaqua complex [68]

$$Pd(NH_3)_4^{2+} \xrightarrow[\text{HClO}_4]{\text{H}_2\text{O}} cis\text{-}Pd(NH_3)_2(H_2O)_2^{2+}$$

$$\xrightarrow[(\text{X} = \text{Cl,Br,I})]{\text{NaX}} cis\text{-}Pd(NH_3)_2X_2$$

$$Pd(NH_3)_4Cl_2 \xrightarrow{\text{H}^+} trans\text{-}Pd(NH_3)_2Cl_2$$

Although the bisammine complexes of platinum(II) are the most important because of the medical applications of the *cis*-isomer (section 3.10), the synthesis of the others [69] is also important:

$$PtCl_6^{2-} \xrightarrow[HCl]{SO_2} H_2PtCl_4 \xrightarrow[heat]{conc. NH_3} [Pt(NH_3)_4]Cl_2$$

Pt–N distances are 2.046–2.047 Å in the methane sulphonate salt of $[Pt(NH_3)_4]^{2+}$ [63].

High yield synthesis of $Pt(NH_3)_3Cl^+$ is difficult [67]: the traditional method of Chugaev (*J. Chem. Soc.*, 1915, 1247), which relies on the hydrolysis of NCO^- to generate ammonia, is the most widely used

$$cis\text{-}Pt(NH_3)_2Cl_2 \xrightarrow[heat]{KNCO} Pt(NH_3)_3Cl^+$$

Another route ultimately relies on replacement of a labile water molecule:

$$trans\text{-}Pt(NH_3)_2Cl_2 \xrightarrow[24\,h]{KI} trans\text{-}Pt(NH_3)_2ClI \xrightarrow[boil]{AgNO_3}$$

$$trans\text{-}[Pt(NH_3)_2Cl(H_2O)]^+NO_3^- \xrightarrow[heat]{NH_3} [Pt(NH_3)_3Cl]Cl$$

For the monoammine [67, 70]

$$cis\text{-}Pt(NH_3)_2Cl_2 \xrightarrow{CH_3COOH/KCl} Pt(NH_3)Cl_3^-$$

$$\xrightarrow{Pt(NH_3)_4^{2+}} Pt(NH_3)_4[Pt(NH_3)Cl_3]_2$$

$$\xrightarrow{K_2PtCl_4} KPt(NH_3)Cl_3$$

More conveniently

$$cis\text{-}Pt(NH_3)_2Cl_2 \xrightarrow[MeCONMe_2\ 100°C,\ 6\,h]{Et_4NCl/N_2} Pt(NH_3)Cl_3^-$$

Replacement of the chlorines in *cis*-$Pt(NH_3)_2Cl_2$ is facile (Figure 3.27).

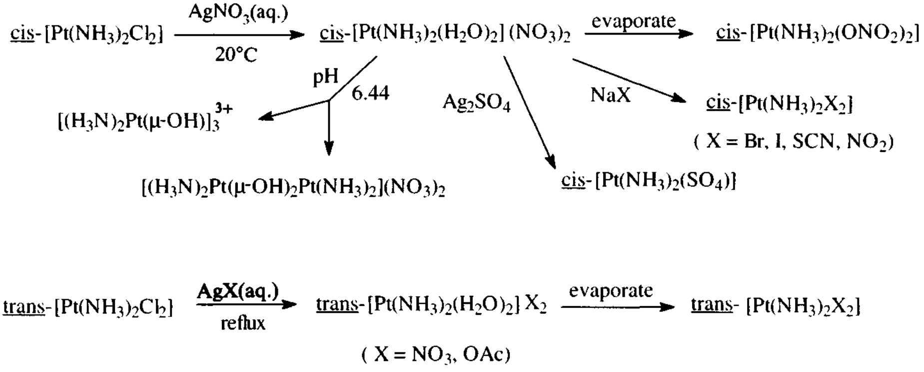

Figure 3.27 Reactions of *cis*- and *trans*-$[Pt(NH_3)_2Cl_2]$.

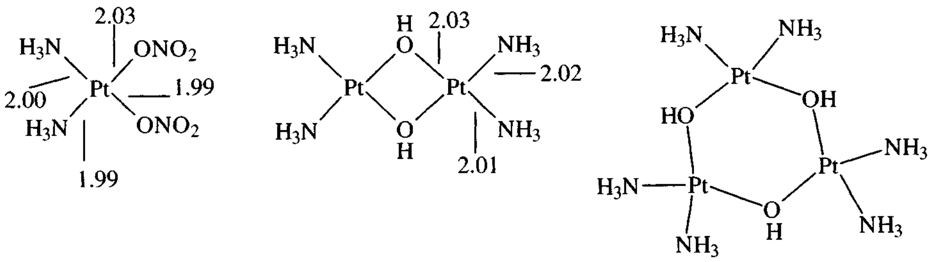

Figure 3.28 Structures of platinum ammine complexes.

It is believed that this occurs when cisplatin is used as an anti-cancer agent. In cells where chloride levels are low, after cisplatin has been transported through the cell wall, the aqua complex (from which other *cis*-complexes are easily made) is formed and is the real anti-cancer agent. At higher pH (~6.5) oligomerization occurs, giving a colourless di-μ-hydroxo bridged dimer and a yellow tri-μ-hydroxo bridged trimer (Figure 3.28) [71, 72].

Kurnakov's test (1893) is generally applicable to *cis*- and *trans*-ammine dihalides. Addition of thiourea (tu, $(H_2N)_2CS$) to the *cis*-complex leads to successive replacement of all the ligands (Figure 3.29); here the lability of the Pt–Cl bond (see section 3.8.9) causes substitution of a chloride.

Since thiourea has a high *trans*-influence, the ammonia *trans* to it is replaced, repetition of the sequence causing the formation of yellow needles of $Pt(tu)_4Cl_2$.

In the case of the *trans*-complex, only the two chloride ions are substituted, the *trans*-effect of ammonia being too low to give substitution with the result that white needle crystals of *trans*-$[Pt(NH_3)_2(tu)_2]Cl_2$ are formed [73].

Another example of reactivity difference lies in the reaction with silver nitrate. Solutions of the *cis*-isomer react with silver nitrate in a few hours at room temperature while the *trans*-isomer needs refluxing for many hours to remove all the chloride [71, 72, 74]. A quantitative method for measuring concentrations of each isomer in mixtures involves reaction

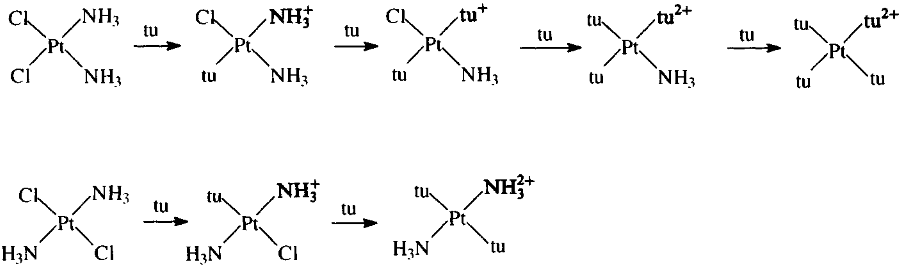

Figure 3.29 Substitution of *cis*- and *trans*-$[Pt(NH_3)_2Cl_2]$ by thiourea (tu) in Kurnakov's test.

with allyl alcohol, which quickly forms a complex $Pt(NH_3)_2Cl(allylalcohol)^+$ with the *trans*-isomer (but not the *cis*-isomer); this can be monitored spectrophotometrically at 252 nm [75].

Distinguishing between cis- and trans-$Pt(NH_3)_2Cl_2$

The relatively recent discovery that *cis*-$Pt(NH_3)_2Cl_2$ possesses significant anti-tumour activity while the *trans*-isomer is inactive has made distinguishing the isomers of greater importance.

Traditionally, the distinction could be achieved by chemical reactions, notably Kurnakov's test, above; the increased scope of physical methods means that several physical techniques can be used in addition to X-ray diffraction studies [76].

Release of coordinated chloride from *trans*-$Pt(NH_3)_2Cl_2$ is much harder and requires heating; *trans*-$PtCl(OH)(NH_3)_2$ (Pt–O 1.989 Å; Pt–N 2.024 and 2.048 Å) and *trans*-$Pt(OH)_2(NH_3)_2$ have been isolated from such mixtures [72].

Among physical methods, dipole moments will distinguish between the two; the *cis*-isomer has a dipole moment while in the *trans*-isomer the bond dipoles cancel. Mixtures of the isomers can be separated chromatographically at low pH [77]. The *cis*- and *trans*-isomers have significantly different vibrational spectra, the PtN_2Cl_2 chromophores approximating to D_{2h} (*cis*) and C_{2v} (*trans*) symmetry, respectively. The *cis*-isomer should give two peaks in the Pt–Cl stretching region of the far-IR spectrum, whereas in the *trans*-isomer only one of the two Pt–Cl stretching vibrations is IR active. Comparison of the far-IR spectra of *cis*-$Pt(NH_3)_2X_2$ (X = Cl, Br) identifies the broad band at 320 cm^{-1}, composed of two overlapping bands, as owing to Pt–Cl stretching. In comparison there is one sharp band in the spectrum of the *trans*-isomer (Figure 3.30) [78]. Raman spectra can similarly be used.

NMR can be used in more than one way [74]. Both isomers will give only one peak in the ^{15}N NMR spectrum, with satellites owing to $^{15}N–^{195}Pt$ coupling. The coupling constant will depend on the atom *trans* to N; for the *cis*-isomer (N *trans* to Cl) *J*(Pt–N) is 303 Hz while in the *trans*-isomer (N *trans* to N) it is 278 Hz. The ^{195}Pt spectrum will in each case be a 1:2:1 triplet owing to coupling of Pt with two equivalent nitrogens (though the value of *J* varies). The ^{195}Pt chemical shifts are virtually identical.

NQR spectra of the two isomers give resonances at different frequencies and also show that the Pt–Cl bond is more ionic in the *cis*-isomer, while there are significant differences in both the absorption and MCD spectra [79].

Apart from *cis*- and *trans*-$Pt(NH_3)_2Cl_2$, a third compound of this composition can be obtained; unlike the others, it is a 1:1 electrolyte:

$$\underset{\text{colourless}}{Pt(NH_3)_4^{2}(aq.)} + \underset{\text{red}}{PtCl_4^{2-}(aq.)} \rightarrow \underset{\text{green}}{[Pt(NH_3)_4]^{2+}[PtCl_4^{2-}]}$$

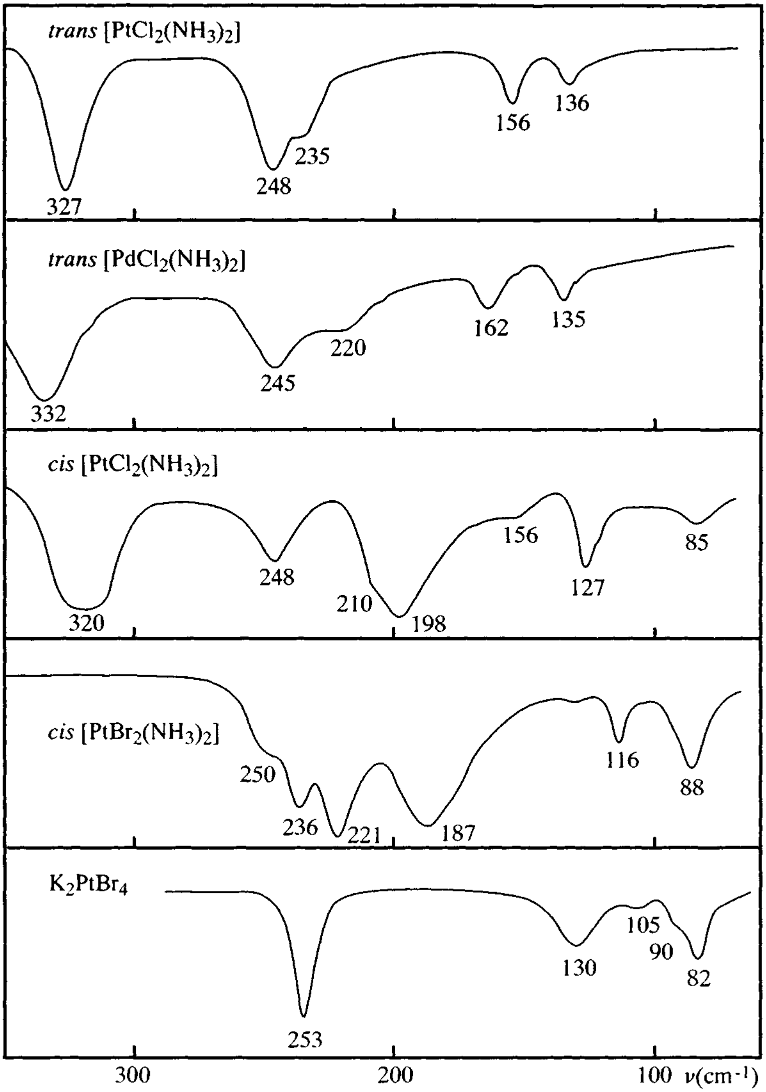

Figure 3.30 IR spectra of *trans*-$[M(NH_3)_2Cl_2]$ (M = Pd, Pt), *cis*-$[Pt(NH_3)_2X_2]$ (X = Cl, Br) and K_2PtBr_4. (Reproduced with permission from *Spectrochim. Acta, Part A*, 1968, **24**, 819.)

The crystal structure (Figure 3.31) shows the cations and anions to be stacked alternately [80] with a Pt–Pt separation of 3.25 Å.

The metal–metal interaction and conductivity increase with pressure; using bulkier ammines increases the Pt–Pt distance. Although palladium-containing ions can be substituted for the platinum species, the optical properties and metal–metal interaction causing pronounced dichroism are

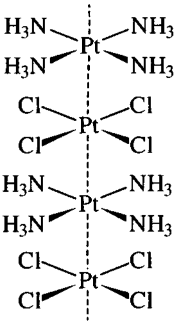

Figure 3.31 Chain structure of $[Pt(NH_3)_4][PtCl_4]$.

associated with the presence of platinum. The Pt–Pt distance is not short enough for metallic conductivity, unlike in the cyanides (section 3.8.4).

On boiling the Magnus salt with ammonia solution, it is converted into the tetraammine

$$Pt(NH_3)_4PtCl_4 + 4NH_3 \rightarrow 2Pt(NH_3)_4Cl_2$$

Magnus' green salt takes its name from its discoverer (1828), H.G. Magnus, Professor of Physics and Technology at the University of Berlin. Pink $[Pd(NH_3)_4]PdCl_4$, Vauqelin's salt, was discovered slightly earlier (1813) by L.-N. Vauquelin, Professor of Chemistry at the Collège de France.

The *cis*- and *trans*-isomers of $Ptpy_2X_2$ can be made by various routes, for example that shown in Figure 3.32.

This synthesis is of course analogous to those for the bisammine complexes. It can be applied to substituted pyridines and other halides (Br, I, NCS) [81].

A recent convenient synthesis for *cis*- and *trans*-$PtpyI_2$ proceeds as follows

$$PtCl_4^{2-} \xrightarrow[KI]{exc.} PtI_4^{2-} \xrightarrow{py} cis\text{-}Ptpy_2I_2$$

This *cis*-isomer is dissolved in DMSO; the initial substitution product is *cis*-$[Ptpy_2(DMSO)I]^+$, which undergoes rapid substitution by iodide to give *trans*-$Ptpy(DMSO)I_2$. Addition of a slight excess of pyridine now gives *trans*-$Ptpy_2I_2$ [82].

It has recently been shown that ^1H NMR spectra can distinguish between *cis*- and *trans*-isomers of this type. The $^3J(Pt{-}H)$ coupling constants between platinum and the α-hydrogen of the pyridines are slightly higher for the *cis*-isomers; therefore for *cis*-$Ptpy_2Cl_2$ $^3J(Pt{-}H)$ is 42 Hz while $^3J(Pt{-}H)$ is 34 Hz for the *trans*-isomer [83].

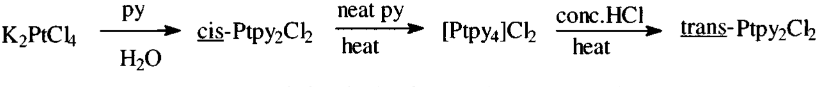

Figure 3.32 Synthesis of *cis*- and *trans*-$Ptpy_2Cl_2$.

Nitrile complexes $M(RCN)_2Cl_2$ [84] are useful starting materials for the synthesis of other complexes (e.g. phosphine complexes section 3.8.3) as the nitrites are easily displaced. Synthesis include

$$K_2PCl_4 \xrightarrow[25°C, 8d]{\text{exc. MeCN}} cis\text{- and } trans\text{-}Pt(MeCN)_2Cl_2$$

$$PtCl_2 \xrightarrow[\text{heat}]{\text{PhCN}} cis\text{- and } trans\text{-}Pt(PhCN)_2Cl_2$$

Mixtures may be separated by chromatography or by using solubility differences. Isomerization often occurs on heating; solutions of *cis*-$Pt(RCN)_2Cl_2$ give mixtures of the *cis*- and *trans*-forms, while solid *cis*-$Pt(PhCN)_2Cl_2$ gives the *trans*-isomer.

Multidentate amines form many complexes with these metals.

$$K_2MCl_4 \xrightarrow[EtOH/H_2O]{\text{phen}} M(phen)Cl_2$$

$$K_2PtCl_4 \xrightarrow[\text{reflux, 20 h}]{terpy/H_2O} [Pt(terpy)Cl]^+Cl^-$$

Examples confirmed by X-ray diffraction, all square planar, include *cis*-$Pt(en)Cl_2$ (Pt−N 2.032, Pt−Cl 2.318 Å), *cis*-$Pd(en)Cl_2$ (Pd−N 1.978 Å), $Pd(en)_2Cl_2$ (Pd−N 2.036 Å) [85] and $Pd(bipy)_2(PF_6)_2$ (Pd−N 2.032–2.039 Å). Adoption of a strictly square planar geometry in the last compound would give rise to non-bonded interactions between hydrogens on opposite rings, so that a slight distortion towards a tetrahedral geometry takes place to accommodate this (dihedral angle of 24.1°). In other cases $[Pd(L{-}L)_2](PF_6)_2$ (L−L = bipy, phen), strain is minimized by bowing of the chelating ligands and by the cation assuming a step conformation [86]. Distortion is even more marked in complexes of 2,9-dimethyl-1,10-phenanthroline (diaphen), PtX_2(dimphen) (X = Cl, Br, I), their structures showing the increase in Pt−N bond length as the *trans*-influence of the halogen increases (Table 3.10).

They form adducts with Lewis bases in which the phenanthroline is monodentate, PtX_2(dimphen)L (L = Me_2S, Me_2SO, PhNO) [87].

cis-$Pt(bipy)Cl_2$ exists in yellow and red forms, the difference in colour results from different stacking modes in the solid state, with respective Pt−Pt distances of 4.435 and 3.45 Å [88].

Table 3.10 Distortion of geometry in PtX_2 (dimphen)

X	Pt−N (Å)	Pt−X (Å)
Cl	2.045, 2.046	2.301, 2.313
Br	2.049, 2.058	2.419, 2.421
I	2.062, 2.082	2.580, 2.584

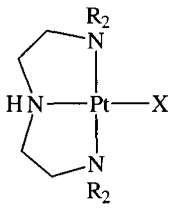

Figure 3.33 The structure of complexes of tridentate amines such as diethylenetriamine.

With tridentate amines like diethylenetriamine (dien) and its relatives, 4-coordination is again the rule, as with $[Pt(dien)Br]^{+}Br^{-}$ (Figure 3.33; $R = H$, $X = Br$) and $[Pt(Et_4dien)I]^{+}I^{-}$ ($R = Et$, $X = I$).

The steric crowding introduced in the latter by the four ethyl substituents inhibits nucleophilic attack at platinum, so that complexes of this type tend to undergo substitution by a dissociative mechanism [89]. The complex of the more rigid ligand, 2,2′,2″-terpyridyl, $Pt(terpy)Cl^{+}$, is found to be about 10^3 to 10^4 times more reactive to substitution than the dien analogue; this is ascribed to steric strain [90], which is reflected in the short Pt–N bond to the 'central' nitrogen (Pt–N some 0.03 Å shorter than the other two Pt–N bonds) and N–Pt–N bond angles of 80–82°).

Another rare example of monodentate phenanthroline is provided by $PtCl(PEt_3)_2(phen)$; the non-bonding Pt–N distance is 2.843 Å (Figure 3.34). A bidentate phenanthroline would involve considerable non-bonding interactions between the tertiary phosphines and the benzene rings [91].

With their preference for square planar coordination, palladium(II) and platinum(II) are well suited to binding to porphyrins and related N_4 donor macrocycles. Therefore, Pd(octaethylporphyrin) is readily synthesized starting from the labile PhCN complex (like the platinum analogue) [92]

$$MCl_2 + H_2OEP \xrightarrow[195^{\circ}C,\,4\,h]{PhCN} 2HCl + M(OEP)$$

It has square planar coordination (Pd–N 2.010–2.017 Å) similar to the value of 2.009 Å in the tetraphenylporphyrin analogue, prepared by a similar route. As with nickel, macrocycle complexes can be made by *in situ* template

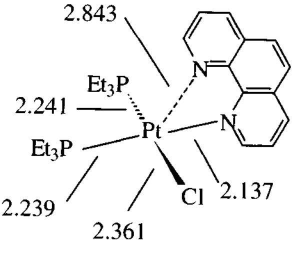

Figure 3.34 The structure of $PtCl(PEt_3)_2(phen)$ showing the monodentate phenanthroline ligand.

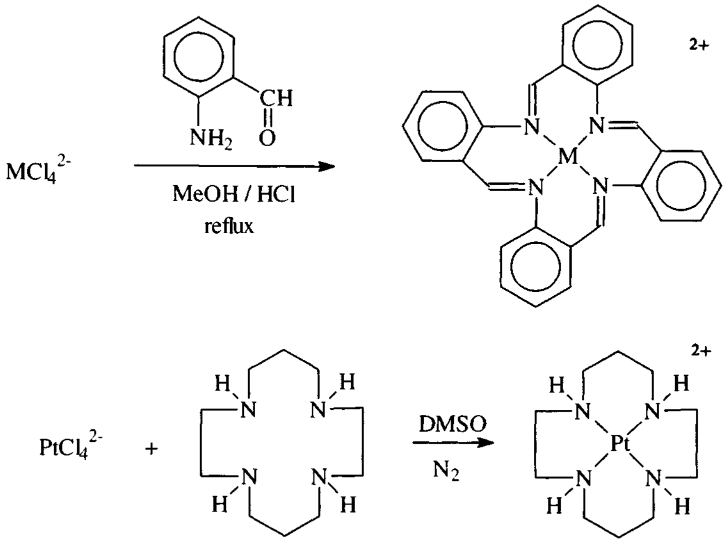

Figure 3.35 Syntheses of complexes of macrocycles.

synthesis (Figure 3.35) using *o*-aminobenzaldehyde [93], or by insertion into a preformed system in the case of the 14aneN$_4$ ligand.

'Platinum blues'

When solutions containing the aqua complexes derived from cisplatin react with pyrimidines and other bases and are exposed to air, blue solutions (and solids) result [94]. These are mixed-valence oligomers ($n = 4$). Some have anti-tumour activity but have not yet found clinical use.

The first structural information was obtained for an α-pyridone complex $[Pt_2(NH_3)_4(pyridone)_2]_2(NO_3)_5$ (Figure 3.36).

It has a chain structure, with one unpaired electron per tetramer unit ($\mu_{eff} = 1.81\,\mu_B$) and can be regarded as a $Pt_3^{II}Pt^{III}$ compound. ESR data suggest that the unpaired electron resides in a MO based on platinum $5d_{z^2}$ orbitals directed along the tetramer chain.

The original 'blue' (K.A. Hofmann, 1908) was obtained from the reaction of $Pt(MeCN)_2Cl_2$ with silver salts over some hours. Under these conditions, the nitrite is hydrolysed to acetamide. Very recently, the structure of the complex $[(H_3N)_2Pt(MeCONH)_2Pt(NH_3)_2]_4(NO_3)_{10}$ has been determined (Figure 3.37). The average oxidation state of the platinums in the octamer is 2.25.

3.8.3 *Tertiary phosphine complexes*

Tertiary phosphine complexes of platinum and palladium $M(PR_3)_2X_2$ are important [95]. The *cis*- and *trans*-isomers are readily obtained for platinum,

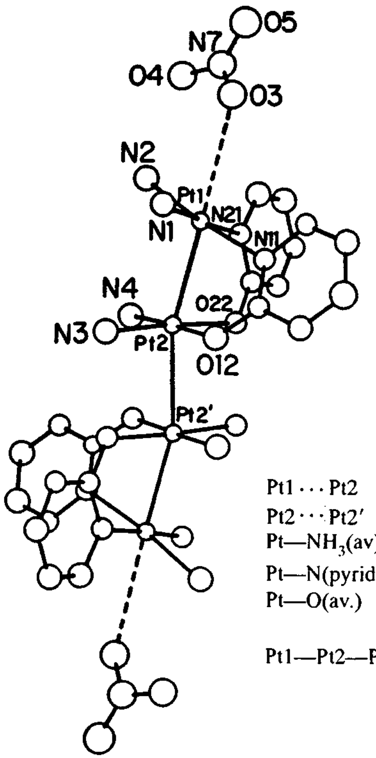

	Distance (Å)
Pt1 · · · Pt2	2.779
Pt2 · · · Pt2′	2.885
Pt—NH_3(av)	2.06
Pt—N(pyridone)	2.05
Pt—O(av.)	2.04
Pt1—Pt2—Pt2′	164.5°

Figure 3.36 Structure of the α-pyridone complex $[Pt_2(NH_3)_4(pyridone)_2]_2(NO_3)_5$. (Reprinted with permission from *J. Am. Chem. Soc.*, 1978, **100**, 3785. Copyright (1978) American Chemical Society.)

but, as found with the ammines (section 3.8.2), *cis*-$Pd(PR_3)_2X_2$ rapidly isomerizes to the *trans*-isomer.

Reaction of K_2PtCl_4 with a trialkyl phosphine initially gives the Magnus-type compound $Pt(PR_3)_4^{2+}PtCl_4^{2-}$. This isomerizes over some weeks (more rapidly on heating) to a mixture of *cis*- and *trans*-$Pt(PR_3)_2Cl_2$, from which the more soluble yellow *trans*-isomer can be extracted with light petroleum, leaving the white *cis*-form to be re-crystallized from ethanol. If the *cis*-form is heated (e.g. in an oil bath) to just above its melting point for around an hour, it will isomerize to the *trans*-isomer.

For the corresponding bromides and iodides, preparation starts with K_2PtX_4 (X = Br, I) formed *in situ* from $PtCl_4^{2-}$ with KX. For *trans*-$Pd(PR_3)_2Cl_2$, shaking alcoholic $PdCl_2$ or Na_2PdCl_4 with the phosphine yields a solution of the yellow complex.

For the triphenylphosphine complexes, where the *cis*-form is particularly stable, irradiation causes the *cis–trans* isomerization

$$K_2PtCl_4 \xrightarrow[\text{reflux}]{PPh_3/\text{xylene}} cis\text{-}Pt(PPh_3)_2Cl_2 \xrightarrow[366\,\text{nm}]{h\nu} trans\text{-}Pt(PPh_3)_2Cl_2$$

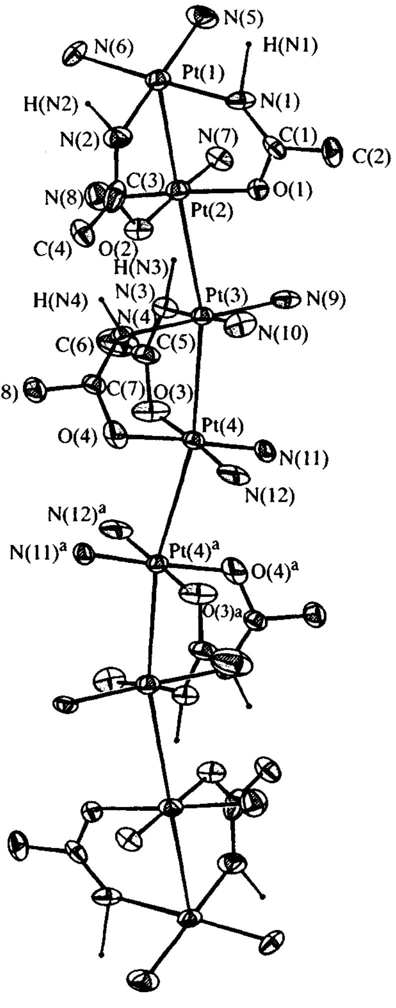

Figure 3.37 Structure of the cation in the acetamide complex $[(NH_3)_2Pt(MeCONH_2)Pt(NH_3)_2]_4$-$(NO_3)_{10}.4H_2O$. (Reprinted with permission from *J. Am. Chem. Soc.*, 1992, **114**, 8110. Copyright (1992) American Chemical Society.)

When halogens add to $Pt(PPh_3)_3$, the initial product is *trans*-$Pt(PPh_3)_2X_2$, isolable after a short reaction time (in the presence of excess X_2, which removes free PPh_3, catalyst for the isomerization to the *cis*-form).

With less bulky phosphines, 5-coordinate $M(PR_3)_3X_2$ can be obtained

$$M(PMe_2Ph)_2X_2 \xrightarrow[CH_2Cl_2]{PMe_2Ph} M(PMe_2Ph)_3X_2$$

$Pd(PMe_2Ph)_3Cl_2$ has a distorted sp structure with a distant axial chlorine (Pd–P 2.265–2.344 Å; Pd–Cl (basal) 2.434 Å; Pd–Cl (axial) 2.956 Å) [96].

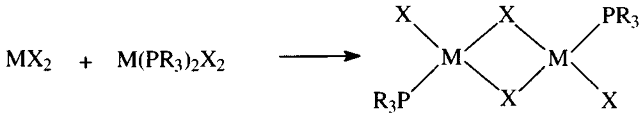

Figure 3.38 Synthesis of the halogen-bridged 1 : 1 phosphine complexes.

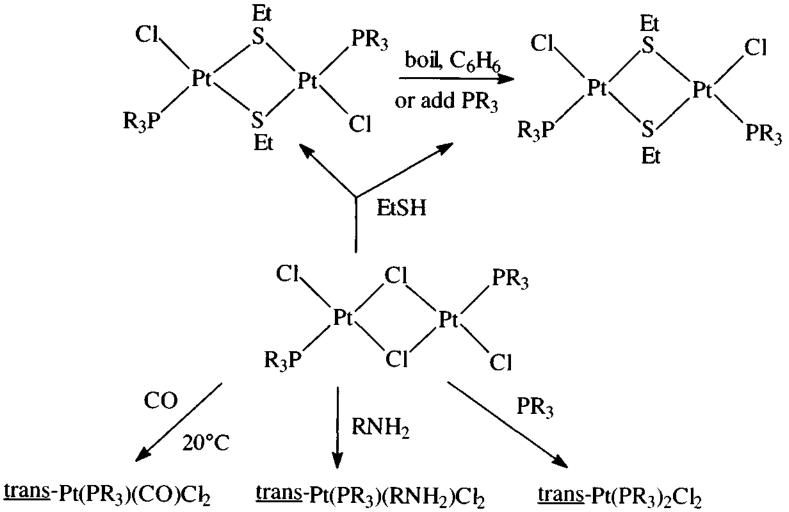

Figure 3.39 Reactions of halogen-bridged 1 : 1 phosphine complexes.

Halogen-bridged 1 : 1 complexes can be made by heating together the stoichiometric amounts of MX_2 and $M(PR_3)_2X_2$ in a high boiling solvent (for Pt, naphthalene or xylene: for Pd, ethanol or chloroform) in a reproportionation (Figure 3.38) [97].

Direct synthesis is possible

$$2PtCl_2 + 2PPr^n_3 \xrightarrow{200°C} Pt_2Cl_4(PPr^n_3)_2$$

Various ligands cleave the bridge (Figure 3.39) while thiols substitute at the bridge.

Pfeiffer (1913) pointed out that $[Pt(PR_3)X_2]_2$ complexes can potentially exist in three isomeric forms, but only the symmetric *trans*-isomer has been characterized (Figure 3.40).

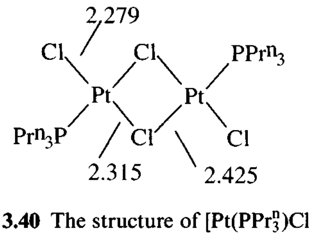

Figure 3.40 The structure of $[Pt(PPr^n_3)Cl_2]_2$.

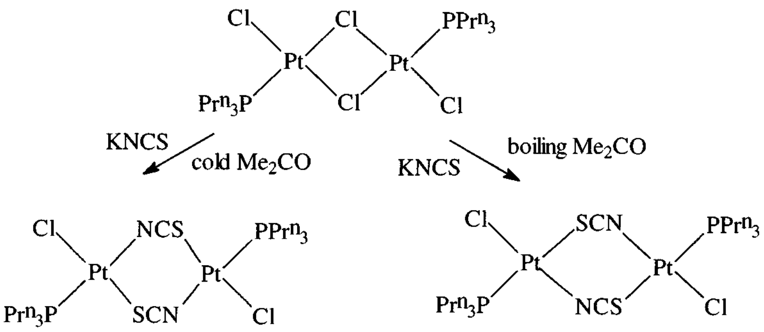

Figure 3.41 Isomerism in bridged thiocyanate complexes.

The greater *trans*-influence of the tertiary phosphine manifests itself in the Pt–Cl bond lengths.

Some interesting cases of isomerism in bridged complexes do arise. The thiocyanate bridged complex shown in Figure 3.41 is a good example of the ambidentate behaviour of the thiocyanate (confirmed by X-ray) while in the complexes $[Pt(PR_3)(SR)(SR')]_2$ the choice of isomer is determined by the order in which the thiolate groups are introduced (Figure 3.42).

Hydride complexes

One and, sometimes, two hydrogen atoms can be introduced into hydride complexes [98]. A variety of synthetic routes has been utilized, using methods

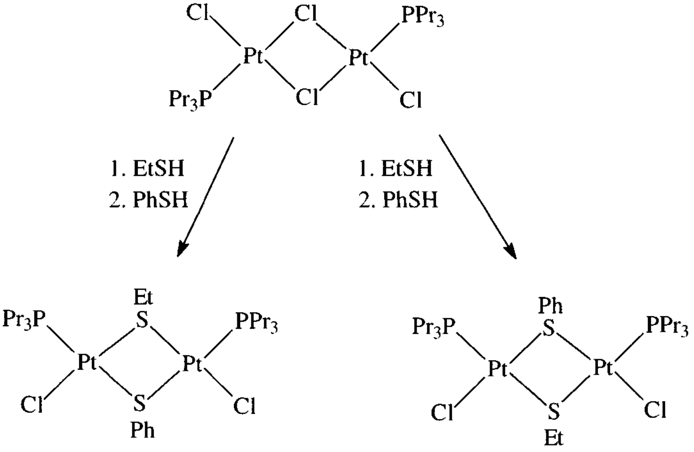

Figure 3.42 Isomerism in bridged thiolate complexes.

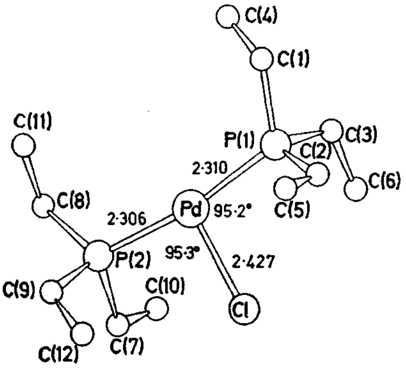

Figure 3.43 The structure of *trans*-$Pd(PEt_3)_2HCl$ (hydride not located). (Reproduced with permission from *J. Chem. Soc., Dalton Trans.*, 1973, 354.)

as diverse as hydrometallate reduction and protonation

$$Pt(PPh_3)_3 \xrightarrow{CF_3CO_2H} [Pt(PPh_3)_3H]^+[(CF_3CO_2)_2H]^-$$

$$cis\text{- or } trans\text{-}Pt(PEt_3)_2Cl_2 \xrightarrow[\text{heat}]{KOH/EtOH} trans\text{-}Pt(PEt_3)_2HCl$$

$$trans\text{-}Pd(PEt_3)_2Cl_2 \xrightarrow{Me_3GeH} trans\text{-}Pd(PEt_3)_2HCl$$

Some of these monohydrides were among the first transition metal hydride complexes to be synthesized and at the time their geometry was uncertain until X-ray diffraction studies were carried out. The structure of *trans*-$Pd(PEt_3)_2HCl$ shows the geometry to be square planar with the hydrogen exerting stereochemical influence (the hydrogen atom was not located in this study, as hydrogens are poor scatterers of X-rays) (Figure 3.43) [99].

The presence of the hydride group in these complexes can be detected by the observation of ν(M–H) in the IR spectrum (very sensitive to deuteration, by a factor of 0.717 ($\sqrt{\frac{1}{2}}$) (Figure 3.44) and the observation of a low-frequency NMR resonance.

The spectrum of $Pt(PEt_3)_2HCl$ (Figure 3.45) shows a 1 : 2 : 1 central resonance owing to coupling of the hydrogen with two equivalent phosphines; the satellites are owing to coupling with ^{195}Pt ($I = 1/2$, 33.8%) [100].

Dihydrides are more difficult to prepare but are most easily obtained with very bulky tertiary phosphines [101a]

$$trans\text{-}Pt(PR_3)_2Cl_2 \xrightarrow[\text{EtOH}]{\text{exc. } NaBH_4} trans\text{-}Pt(PR_3)_2H_2$$

($PR_3 = PBu^t_2$ alkyl, Pcy_3, etc.).

$PtH_2(Pcy_3)_2$ has the IR absorption owing to ν(Pt–H) at 1710 cm^{-1} (a lower frequency than the monohydride owing to the mutually *trans*-hydrogens) and low-frequency NMR line ($\delta = -3.15$ ppm, ^2J(P–H) 17 Hz,

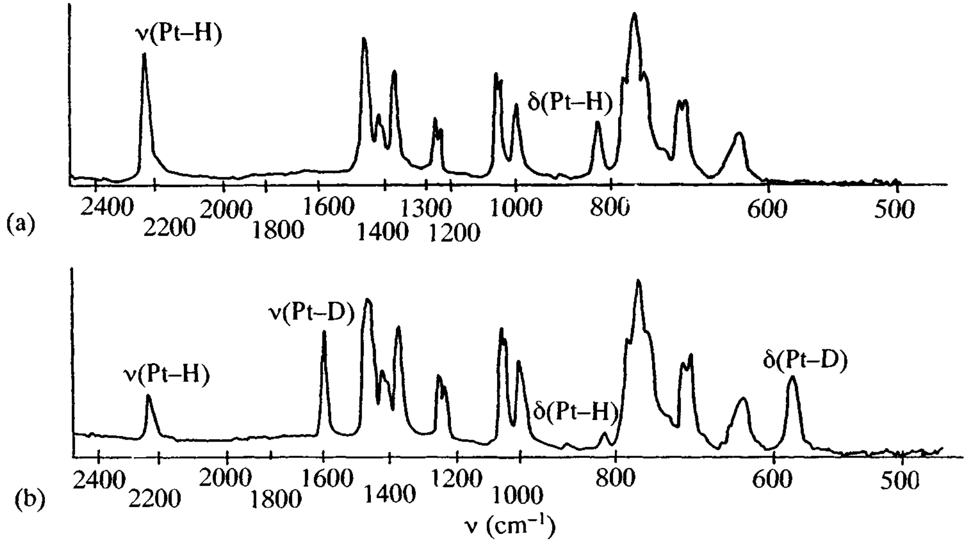

Figure 3.44 IR spectrum of (a) *trans*-Pt(PEt$_3$)$_2$HCl and (b) *trans*-Pt(PEt$_3$)$_2$DCl. (Reproduced with permission from *Proc. Chem. Soc.*, 1962, 321.)

^1J(Pt–H) 790 Hz). The PMe$_3$ analogue can be prepared by sodium naphthalenide reduction; it is only stable under a hydrogen atmosphere but has, like the Pcy$_3$ complex, had its structure determined and has the expected spectral properties (IR 1715 cm^{-1}; NMR $\delta = -2.7$ ppm, ^2J(P–H) = 20 Hz, ^1J(Pt–H) 807 Hz). It also exists as the (less stable) *cis*-isomer and is intensely reactive. *trans*-PtH$_2$(Pcy$_3$)$_2$ will insert CO$_2$ to form a formate complex:

$$trans\text{-Pt(Pcy}_3)_2\text{H}_2 \xrightarrow{\text{CO}_2} trans\text{-Pt(Pcy}_3)_2\text{H(OCOH)}$$

The ion PtH$_3$(PBu$^t_2$)$_2^+$ (formed from PtH$_2$(PBu$^t_3$)$_2$ and CF$_3$SO$_3$H) is believed to be a dihydrogen complex, [Pt(H)(H$_2$)(PBu$^t_3$)$_2$]$^+$ [101b].

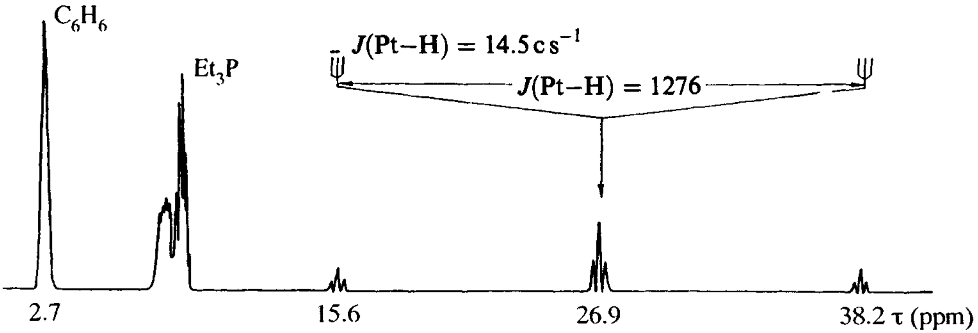

Figure 3.45 ^{1}H NMR spectrum of *trans*-Pt(PEt$_3$)$_2$HCl in benzene solution. The τ scale can be converted to the δ scale now used by the relationship $\delta = 10 - \tau$. (Reproduced with permission from *Proc. Chem. Soc.*, 1962, 321.)

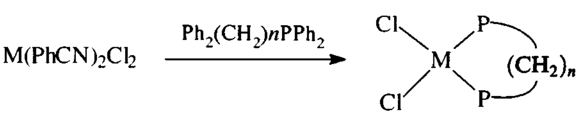

Figure 3.46 Synthesis of 1 : 1 diphosphine complexes (M = Pd, Pt).

Complexes of bidentate phosphines

Reaction of the diphosphines $Ph_2P(CH_2)_nPPh_2$ ($n = 1$–3) with $MCl_2(PhCN)_2$ affords 1 : 1 *cis*-complexes (Figure 3.46) [102]. (Note the use of the labile PhCN adducts; if the MCl_4^{2-} salts are used, 'Magnus' type compounds $M(P{-}P)_2^{2+}MCl_4^{2-}$ are formed.) Similar complexes are formed with other halides: for the thiocyanates see section 3.8.6. The structures of the palladium complexes have been determined (Table 3.10) with 'square' coordination only achieved for $n = 3$ with the formation of a six-membered metal-chelate ring.

With longer carbon chains in the diphosphine (n, e.g. 5, 6) oligomers are formed, thus $PdCl_2[Ph_2P(CH_2)_6PPh_2]$ is a dimer (Figure 3.47) with Pd–Cl 2.300–2.316 Å, Pd–P 2.342–2.344 Å. (Comparison with the *cis*-complexes in Table 3.10 shows that Pd–P bonds *trans* to P are longer, and Pd–Cl *trans* to Cl are shorter, owing to the *trans*-influence.)

Platinum generally behaves similarly to palladium, though $Pt[Ph_2P(CH_2)_3PPh_2]Cl_2$ is thought to be oligomeric; the monomer $Pt[Ph_2P(CH_2)_5PPh_2]Cl_2$ has a *cis*-structure. It is likely that both monomers and oligomers can be made, depending on choice of reaction conditions and starting materials.

With bulky diphosphines $Bu^t_2P(CH_2)_nPBu^t_2$ ($n = 8$–12), similar reactions of the diphosphines with $MCl_2(PhCN)_2$ give separable mixtures of monomer, dimer and trimer. With small phosphines ($n = 5$–7) dimers predominate (Figure 3.48).

Specific examples where structures have been determined are *trans*-$Pt[Bu^t_2P(CH_2)_{12}PBu^t_2]Cl_2$ and dimeric $[Pd(Bu^t_2P(CH_2)_nPBu^t_2)Cl_2]_2$ ($n = 5$, 7, 10).

The factors determining which complex is obtained are not completely delineated. In a study of a range of $Ph_2P(CH_2)_nPPh_2$ ($n = 2$, 6–12, 16) *cis*-complexes (usually monomer–dimer mixtures) were made from the phosphine and K_2PtCl_4 in refluxing $MeOCH_2CH_2OH$, while using the phosphine

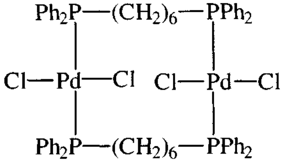

Figure 3.47 The dimeric diphosphine-bridged complex $[Pd\{Ph_2P(CH_2)_6PPh_2\}Cl_2]_2$.

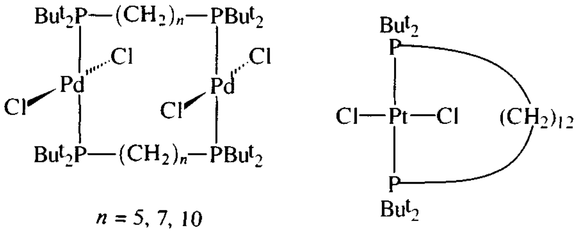

Figure 3.48 The diphosphine complexes $[Pd\{Bu^t_2P(CH_2)_nPBu^t_2\}Cl_2]_2$ and $[Pt\{PBu^t_2P(CH_2)_{12}$-$PPBu^t_2\}Cl_2]$.

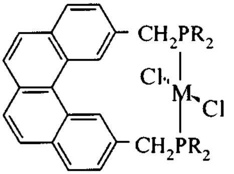

Figure 3.49 The *trans*-complexes of a phenanthrene-derived diphosphine ligand (M = Pd, Pt).

and Zeise's salt in $Me_2CO/CHCl_3$ gave a mixture of monomeric and dimeric *trans*-complexes.

Rigid diphosphines have been used to enforce *trans*-geometries; thus with the phenanthrene-derived diphosphine (Figure 3.49, R = Et) the complexes $PdLCl_2$ and $PtLCl_2$ have closely similar geometries (Pd–P 2.307 Å, Pd–Cl 2.306 Å, P–Pd–P 177.4°; Pt–P 2.293 Å, Pt–Cl 2.304 Å, P–Pt–P 177.1°) [103].

Many, but not all, bidentate phosphine and arsine ligands form 2 : 1 complexes with these metals. $M(diars)_2X_2$ (diars = o-$C_6H_4(AsMe_3)_2$) contain 6-coordinate metals; *trans*-$Pd(diars)_2I_2$ has long Pd–I bonds (3.52 Å). These complexes are 1 : 1 electrolytes in solution, suggesting the presence of 5-coordinate $M(diars)_2X^+$ ions.

Complexes of bulky phosphines and internal metallation reactions

The molecular structures of complexes of the platinum metals with tertiary phosphines often show short metal–carbon or metal–hydrogen contacts [104]. When complexes of bulky tertiary phosphines are heated, internal metal–carbon bond formation frequently occurs (Figure 3.50).

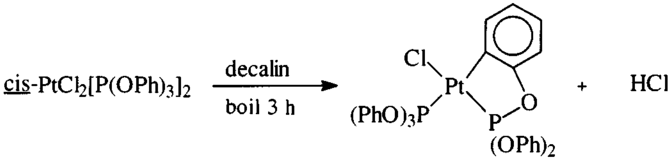

Figure 3.50 Internal metallation of *cis*-$PtCl_2[P(OPh)_3]_2$.

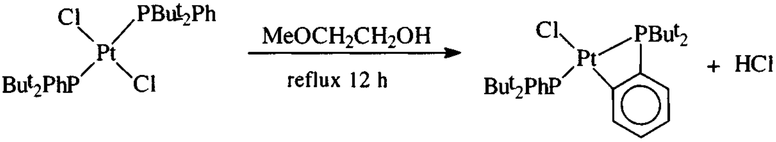

Figure 3.51 Internal metallation of *trans*-$PtCl_2(PBu^t_2Ph)_2$.

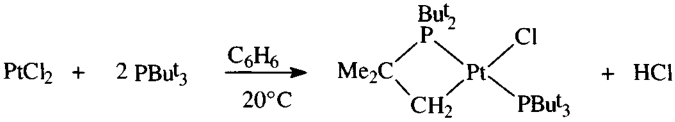

Figure 3.52 Formation of a metallated complex with PBu^t_3 under mild conditions.

This reaction goes less easily with the bromide and not at all with the iodide, nor with any palladium analogue. In another example (Figure 3.51), similar reactions do not occur with less bulky phosphines (PMe_2Ph) and occur less readily with ligands having only one bulky group (e.g. PBu^tPh_2). With the even bulkier PBu^t_3, reflux is not necessary for metallation (Figure 3.52) and there is no evidence for $PtCl_2(PBu^t_3)_2$.

In the case of palladium, *trans*-$PdCl_2(PBu^t_3)_2$ can be isolated, which in solution slowly converts into the internally metallated complex, in keeping with the unwillingness of palladium to metallate. The reason for this may lie in a mechanism involving oxidative addition forming a M(IV) intermediate (Figure 3.53) that then eliminates HCl; the decreased stability of palladium(IV) could make the activation energy for this step too high. Figure 3.54 includes other reactions involving the *t*-butylphosphines showing the effect of steric crowding on metallation.

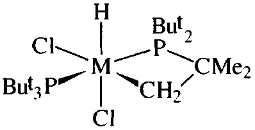

Figure 3.53 Possible M^{IV} intermediate in the formation of a metallated complex with PBu^t_3.

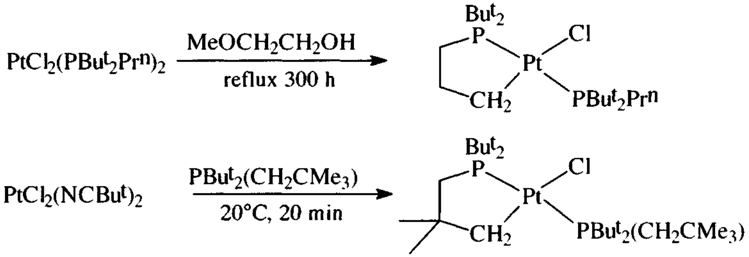

Figure 3.54 The effect of the bulk of tertiary phosphine ligands upon the ease of the formation of a metallated complex.

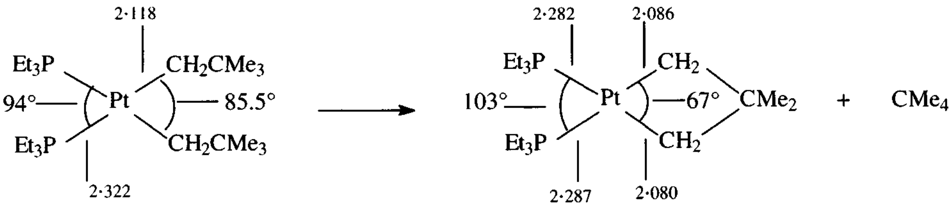

Figure 3.55 Structural evidence for the reduction in strain attending the formation of a metallated complex.

The use of bulky alkyl groups to promote elimination depends on steric crowding; comparison of bond lengths in a bis(neopentyl) and the metallated product (Figure 3.55) shows crowding in the bis(neopentyl) to manifest itself in slight lengthening of the Pt–P bonds (the Pt–C bond is 'normal', see Table 3.11) and a slight twist between the P–Pt–P and C–Pt–C planes (18.7°). The platinacyclobutane product has rather shorter Pt–P and Pt–C bonds.

3.8.4 Complexes of C-donors [105]

Alkyls

Alkyl compounds can be synthesized by substitution, oxidative addition and insertion reactions

$$trans\text{-}PtCl_2(PR_3)_2 \xrightarrow{MeMgX} trans\text{-}Pt(PR_3)_2MeCl$$

$(PR_3 = PMe_2Ph, PPh_3)$

$$Pt(PPh_3)_3 \xrightarrow{MeI} Pt(PPh_3)_2MeI$$

$$trans\text{-}Pt(PEt_3)_2HCl + C_2R_4 \rightleftharpoons trans\text{-}Pt(PEt_3)_2Cl(CR_2CR_2H) \quad (R = H, F)$$

In the last reaction, use of C_2F_4 drives the equilibrium to the right.

Table 3.11 Bond lengths (Å) in palladium and platinum alkyls and aryls: $M(PR_3)_2R^1X$

	M	PR_3	R^1	X	M–X	M–C	M–P
trans-Isomer	Pt	$PMePh_2$	Me	Cl	2.412	2.081	2.291, 2.292
	Pt	$PMePh_2$	CF_2CF_3	Cl	2.363	2.013	2.326–2.341
	Pt	PMe_2Ph	CH_2SiMe_3	Cl	2.415	2.079	2.292
	Pt	PEt_3	Me	Cl	2.346	2.018	2.293
	Pt	PPh_3	CF_3	Cl	2.400	2.080	2.328
	Pt	PPh_3	Ph	Ph	–	2.080	2.299
cis-Isomer	Pt	$PMePh_2$	Me	Me	–	2.119–2.122	2.284–2.285
	Pd	$PMePh_2$	Me	Me	–	2.089–2.092	2.321–2.326
	Pt	PEt_3	Et	Cl	2.384	2.087	2.210, 2.350

The structures of the series *trans*-$Pt(PMePh_2)_2RCl$ ($R = Me$, CF_2CF_3) show Pt–C bonds of 2.081 and 2.013 Å, respectively, with the electron-withdrawing fluoroalkyl leading to a shorter and stronger bond. (Data for some other platinum alkyls are discussed in section 3.8.10.)

Palladium alkyls are generally less stable than their platinum analogues. This is not reflected, however, in the molecular dimensions of *cis*-$MMe_2(PMePh_2)_2$: Pt–C 2.120 Å, Pd–C 2.090 Å, Pt–P 2.284, Pd–P 2.323 Å, suggesting that such instability is kinetic rather than thermodynamic in origin [106a]. Planar 4-coordination is general as usual; therefore, in $Pd(C_6F_5)_2$(terpy), the 2,2′:6′,2″-terpyridyl ligand is bidentate [106b].

Reaction of MeLi with $Pt(PPh_3)_2(Me)_2$ gives $Li_2Pt(Me)_4$; $Pt(Me)_4^{2-}$ is of marginal stability in solution. Use of electron-withdrawing groups like C_6Cl_5 confers greater stability; $(Bu_4N)_2[Pt(C_6Cl_5)_4]$ has square planar platinum (Pt–C 2.086 Å). Adduct formation with, for example, tertiary phosphines and arsines can confer considerable stability on alkyls and aryls; thus *cis*-$Pt(PEt_3)_2(Me)_2$ can be distilled at 85°C *in vacuo* (10^{-4} mmHg) without decomposition.

Isomerization and elimination reactions of alkyls and aryls

Isomerizations of mono-alkyls and aryls have been widely studied [107]; many *cis*-$Pt(PR_3)_2ArCl$ undergo rapid isomerization in the presence of free phosphine, a reaction inhibited by Cl^- with a mechanism believed to involve a 3-coordinate $Pt(PR_3)_2Ar^+$ intermediate that is then attacked by Cl^-. The *cis*- and *trans*-isomers of $Pt(PEt_3)_2(Ph)Cl$ undergo reversible isomerization when irradiated at the wavelength of charge-transfer transitions (254 and 280 nm).

Elimination reactions have been particularly studied in the case of dialkyls. They depend on the alkyl groups being *cis*; *trans*-complexes have to isomerize before they can eliminate, and a complex with a *trans*-spanning diphosphine ligand is stable to 100°C (Figure 3.56).

A dissociative mechanism is indicated by the fact that excess phosphine inhibits elimination from molecules like *cis*-$Pd(PPh_3)_2Me_2$ and $Pt(PPh_3)_2Bu_2$. On thermolysis of mixtures where one molecule contains deuterium, such as

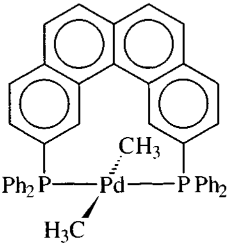

Figure 3.56 A rigid *trans*-dialkyl complex that is particularly stable to thermal elimination.

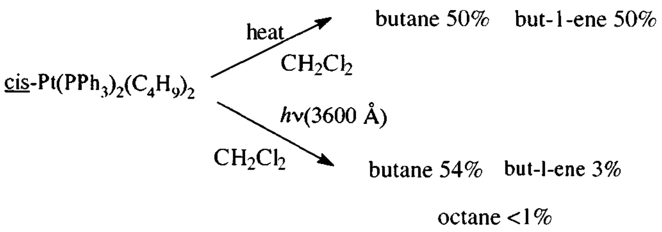

Figure 3.57 The effect of reaction conditions upon decomposition of *cis*-$Pt(PPh_3)_2(C_4H_9)_2$.

cis-$Pd(PR_3)_2Me_2$ and $Pd(PR_3)_2(CD_3)_2$, only C_2H_6 and C_2D_6 were formed, indicating an intramolecular mechanism (similar results were obtained with mixtures of *cis*-$Pt(PPh_3)_2(CH_2CD_2CH_2Me)_2$ and $Pt(PPh_3)_2(C_4H_9)_2$.)

Alkyls with groups that cannot β-eliminate (Me, CH_2SiMe_3) are more stable than those that can (e.g. ethyls). *Trans*-complexes that cannot eliminate by reductive coupling may β-eliminate:

$$trans\text{-}Pd(PMe_2Ph)_2Et_2 \xrightarrow{\text{heat}} C_2H_4 + C_2H_6$$

$$cis\text{-}Pd(PMe_2Ph)_2Et_2 \xrightarrow{\text{heat}} C_4H_{10}$$

When photolysed, the *cis*- and *trans*-isomers both give ethene, ethane and butane (in a 2:2:1 ratio), the route doubtless involves a photochemical isomerization. If extra PMe_2Ph is added, then dissociative coupling is inhibited, and β-elimination giving C_2H_4 and C_2H_6 is favoured. When *cis*-$Pt(PEt_3)_2Et_2$ is heated to 118°C in solution, β-elimination occurs (yielding C_2H_6 and $Pt(PEt_3)_2(C_2H_4)$) with a mechanism involving phosphine dissociation. Another case where both routes have been examined is shown in Figure 3.57.

The evidence is that the thermolytic route does not involve radicals but the photochemical one does. A dissociative mechanism for the thermolytic route is indicated by its inhibition by added phosphine; it is likely that once a phosphine group has dissociated, a metal–hydrogen bond is formed, with generation of a coordinated alkene (Figure 3.58).

On heating, the neopentyl $Pt(PEt_3)_2(CH_2CMe_3)_2$ undergoes an intramolecular metallation elimination [108a] (Figure 3.59), which appears to involve initial phosphine loss affording a platinum(IV) metallacycle.

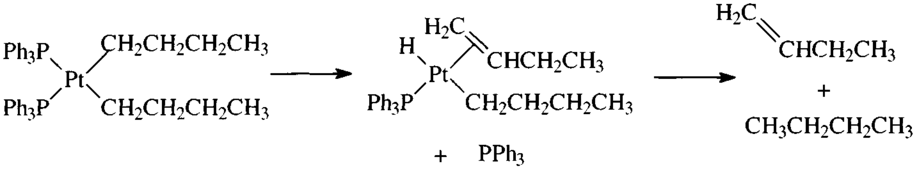

Figure 3.58 A possible mechanism for the thermolytic decomposition of *cis*-$Pt(PPh_3)_2(C_4H_9)_2$.

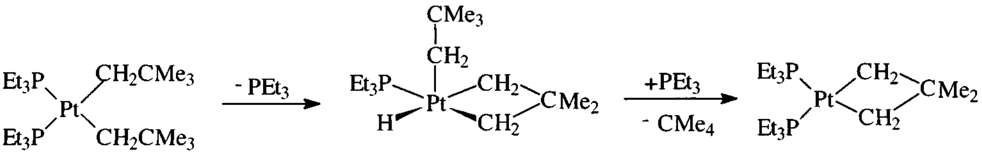

Figure 3.59 A possible mechanism for the thermolytic decomposition of *cis*-Pt$(PEt_3)_2$-$(CH_2CMe_3)_2$.

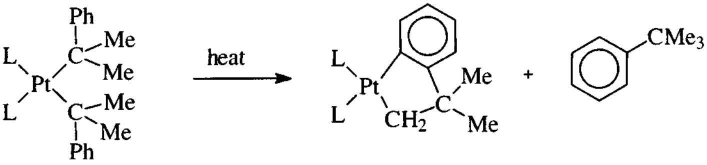

L = PEt_3, PPh_3, ½ phen, ½ bipy, ½ diphos

Figure 3.60 The thermolytic decomposition of $PtL_2(CMe_2Ph)_2$.

Detailed kinetic studies of the decomposition of platinum(II) dineophyls show (Figure 3.60) the exclusive formation of *t*-butylbenzene and an internally metallated platinum complex (3,3-dimethylplatininadan).

The suggested mechanism involves breaking of a platinum–ligand bond, again forming a platinum(IV) hydride that can then eliminate the alkane.

Compounds like *cis*-$[PdMe_2(PR_3)_2]$ (R = Me, Et) have been suggested as chemical vapour deposition (CVD) precursors for palladium [108b].

Platinum (II) carbenes should be mentioned as σ-bonded organometallics. An important general synthesis by cleavage of an electron-rich alkene affords a pair of isomers, the *trans*-form isomerizing to the thermodynamically more stable *cis*-form on heating (Figure 3.61).

The *cis*-isomer has the shorter and stronger Pt–C bond, a reflection of the lower *trans*-influence of chloride [109].

Zeise's salt

Although Zeise's salt is a complex of a π-bonding ligand, this compound must be included in an account of the chemistry of these metals, if only as

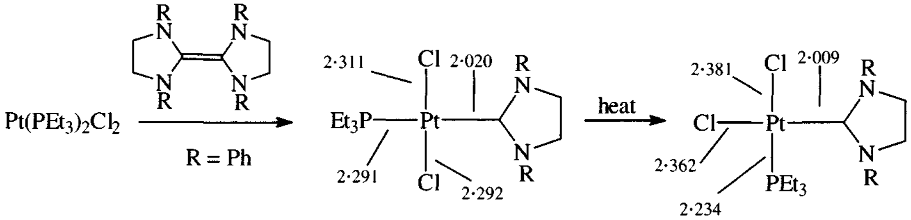

Figure 3.61 The synthesis and structure of two platinum(II) carbenes.

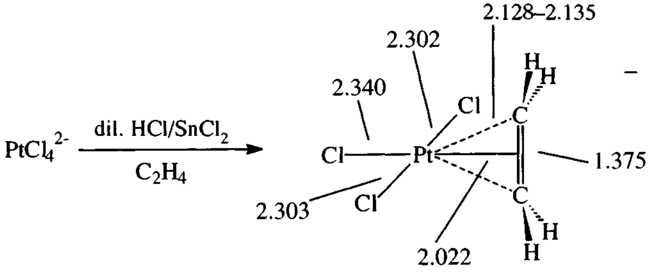

Figure 3.62 Synthesis and structure of Zeise's salt.

the first organometallic to be synthesized (1825) [110a]. It is an important model for the catalytic oxidation of alkenes to aldehydes. Zeise originally obtained it by refluxing an ethanolic mixture of $PtCl_2$ and $PtCl_4$ and extracting the resulting black solid with KCl/HCl. A more convenient method for obtaining yellow crystals of $KPtCl_3(C_2H_4)$ is shown in Figure 3.62, together with its structure.

Features to note in the structure [110b] are:

1. The *trans*-influence of ethene on the Pt–Cl bond
2. At 1.375 Å, the C–C bond in coordinated ethene is some 0.038 Å longer than in free ethene
3. Bending of the four hydrogens away from platinum (the carbons are 0.16 Å out of the plane of the four hydrogens).

Features (2) and (3) are explicable in terms of the Dewar–Chatt–Duncanson model for bonding in alkene complexes (Figure 3.63), which involves

1. Formation of a σ-bond by donation from the π-orbital of ethene into a vacant metal dsp^2 hybrid orbital
2. Back-bonding, with formation of a π-bond, from a filled metal d orbital to an anti-bonding π^*-ethene orbital.

This involves partial occupation of the π^*-orbital and hence a lengthening of the C–C bond; moreover, as the bonding at carbon changes, acquiring some sp^3 character, so the bond angle at carbon will decrease below 120°.

In the Wacker process, the coordinated ethene undergoes nucleophilic attack by OH^-. In the course of the redox reaction, palladium(II) is reduced

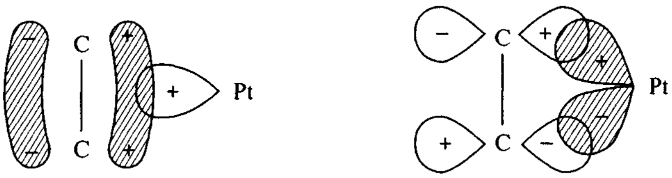

Figure 3.63 Platinum–alkene bonding in Zeise's salt. (Reproduced with permission from S.A. Cotton and F.A. Hart, *The Heavy Transition Elements*, Macmillan Press Ltd, 1975, p. 126.)

to palladium metal but is reoxidized by $CuCl_2/O_2$ *in situ*. In simple form

1. $PdCl_2 + C_2H_4 + H_2O \rightarrow Pd + 2HCl + MeCHO$
2. $Pd + 2CuCl_2 \rightarrow PdCl_2 + 2CuCl$
3. $2CuCl + 2HCl + \frac{1}{2}O_2 \rightarrow 2CuCl_2 + H_2O$

Overall:

$$C_2H_4 + \tfrac{1}{2}O_2 \rightarrow MeCHO$$

Cyanide complexes [111]

Reactions of $PtCl_4^{2-}$ with excess KCN gives yellow $K_2Pt(CN)_4.3H_2O$ (Gmelin, 1822). It contains square planar $Pt(CN)_4^{2-}$ ions stacked parallel (Pt–Pt 3.478 Å) with the groups rotated by 16° relative to the groups above and below (minimizing non-bonding interactions). The palladium analogue $K_2Pd(CN)_4.H_2O$ can be prepared similarly. The C≡N stretching vibrations give rise to strong Raman (2145, 2165 cm^{-1}) and IR (2123 and 2134 cm^{-1}) bands.

The tetracyanometallates exhibit strongly polarized luminescence that can be shifted between the near UV and the near IR (as it is very sensitive to the Pt–Pt distance) by choice of cation and by varying the pressure.

Partial oxidation gives compounds like the bronze 'Krogmann salts', anion deficient $K_2Pt(CN)_4Br_{0.3}.3H_2O$ (Pt–Pt 2.88 Å) or the cation deficient $K_{1.75}Pt(CN)_4.1.5H_2O$ (Pt–Pt 2.96 Å). These compounds are, because of the short Pt–Pt distances, one-dimensional metallic conductors. This is thought to arise through Ptd_{z^2} (or d_{z^2}–p_z) orbitals overlapping along the axes of the 'stacked' $Pt(CN)_4$ units (Figure 3.64) [112].

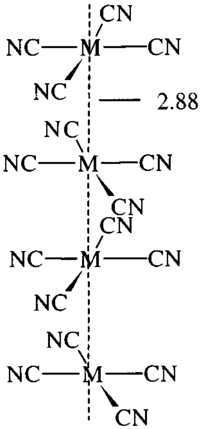

Figure 3.64 The stacking of anions in $K_2Pt(CN)_4Br_{0.3}.3H_2O$.

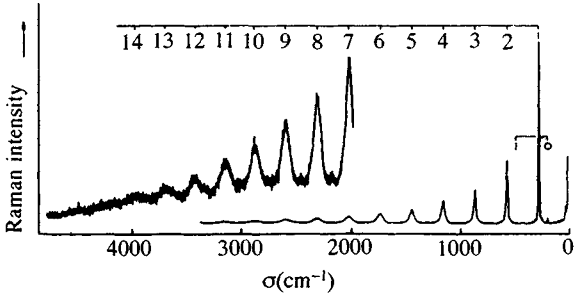

Figure 3.65 Resonance Raman spectra of $[Pt(en)_2][Pt(en)_2Cl_2]_3[CuCl_4]_4$ in a KCl disk at 80 K, $\lambda = 568.2$ nm. (Reproduced with permission from *J. Chem. Soc., Dalton Trans.*, 1980, 2492.)

Other one-dimensional chain compounds [112]

The compound $Pt(EtNH_2)_4Cl_3.H_2O$, Wolffram's red salt, is in fact a mixed-valence compound with alternating square planar $Pt^{II}(EtNH_2)_4^{2+}$ and octahedral $Pt^{IV}(EtNH_2)_4Cl_2^{2+}$ units. This is a prototype for a large number of related compounds with mono-, bi- and multidentate ligands. They have intense colours owing to intervalence charge-transfer transitions polarized along the chain (moving to shorter wavelengths as the halide changes from chloride to iodide and as the platinum–halide bridge shortens; the conductivity similarly increases). These dichroic compounds also exhibit strong resonance Raman spectra with vibrational progressions of the symmetric $X{-}Pt^{IV}{-}X$ stretching mode (Figure 3.65) [113].

^{15}N solid-state NMR studies on complexes like $[Pt(en)X_2][Pt(en)X_4]$ (X = halogen) (Figure 3.66) show that not only can separate ^{15}N environments be discerned for the Pt^{II} and Pt^{IV} sites, but the platinum environments become more similar as the halogen becomes less electronegative, the halogen becoming more centrally placed in the chain leading to higher chain conductivity [114].

3.8.5 *Complexes of S-donors*

Reactions of RSH with MCl_4^{2-} in aqueous solution lead to precipitates of the neutral thiolates $M(SR)_2$; with small alkyl and aryl substituents, the products are oligomeric: $Pd(SPr^i)_2$ is hexameric with square planar palladium (Figure 3.67) [115].

Reactions in acetonitrite lead to anionic thiolates

$$Pd(NO_3)_2 \xrightarrow[\text{MeCN}]{\text{1. NaSPh} \quad \text{2. Ph}_4\text{PBr}} (Ph_4P)_2Pd_2(SPh)_6$$

$$PtCl_4^{2-} \xrightarrow[\text{MeCN/Me}_2\text{CO}]{\text{1. NaSPh} \quad \text{2. Et}_4\text{NBr}} (Et_4N)_2Pt(SPh)_4$$

The platinum complex is square planar, while the palladium dimer also has planar 4-coordination (for other examples of mercaptide bridges see section 3.8.3) [116].

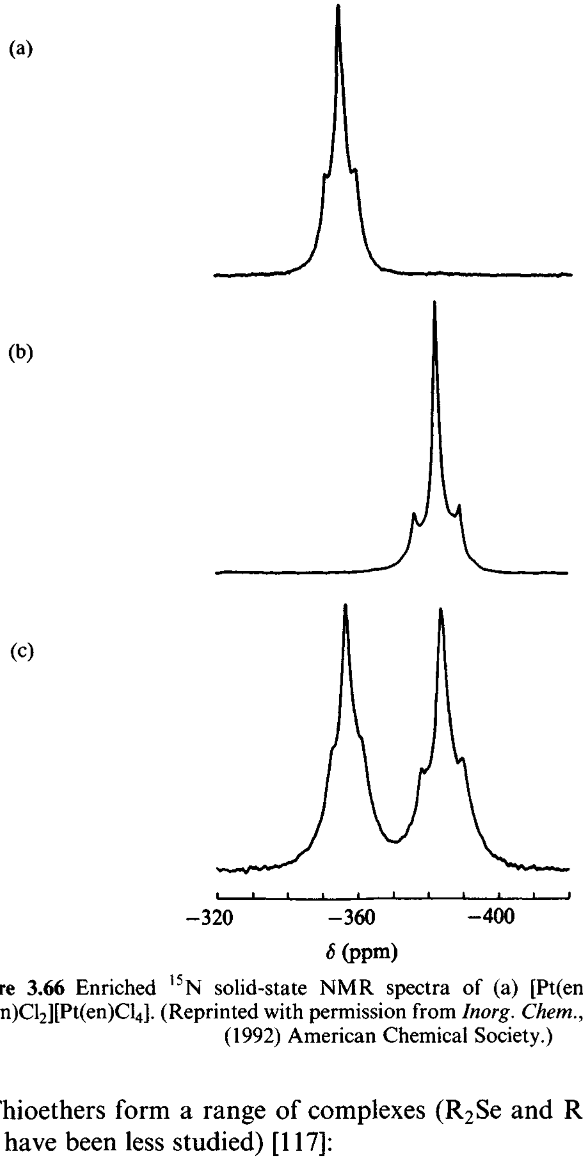

Figure 3.66 Enriched ^{15}N solid-state NMR spectra of (a) $[Pt(en)Cl_4]$; (b) $[Pt(en)Cl_2]$; (c) $[Pt(en)Cl_2][Pt(en)Cl_4]$. (Reprinted with permission from *Inorg. Chem.*, 1992, **31**, 4281. Copyright (1992) American Chemical Society.)

Thioethers form a range of complexes (R_2Se and R_2Te behave similarly but have been less studied) [117]:

$$PdX_4^{2-} \xrightarrow{R_2Q} trans\text{-}Pd(R_2S)_2X_2 \qquad (Q = S, Se, Te)$$

In $Pd(Et_2Se)_2Cl_2$, Pd−Se is 2.424 Å, Pd−Cl 2.266 Å

$$MI_2 \xrightarrow{C_4H_8S} trans\text{-}MI_2(C_4H_8S)_2 \qquad (M = Pd, Pt)\ [118]$$

$$PtCl_4^{2-} \xrightarrow[(2\,mol)]{R_2S} trans\text{-}Pt(R_2S)_2Cl_2 \xrightarrow[R_2S]{exc.} cis\text{-}Pt(R_2S)_2Cl_2$$

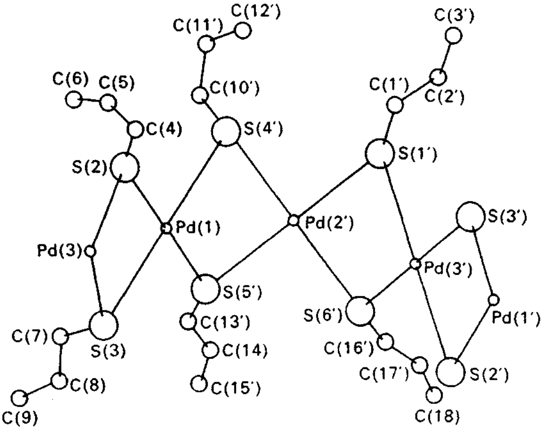

Figure 3.67 Part of the hexameric $[Pd(SPr^i)_2]_6$ molecule showing square-planar coordination of palladium. (Reproduced with permission from *Acta Crystallogr. Sect. B*, 1968, **24**, 1623.)

The structures of the *cis*- and *trans*-isomers of $Pt(1,4\text{-thioxane})_2Cl_2$ have been determined. The Pt–S distance (2.298 Å) is longer in the *trans*-isomer than in the *cis*-form (2.273 Å) showing the *trans*-influence of thioxane to be greater than that of chloride [119].

The two tetrahydrothiophen complexes above are isostructural [118]. Cationic complexes can be made

$$cis\text{-}Pt(Me_2S)_2Cl_2 \xrightarrow[\text{1 mol}]{AgNO_3/SMe_2} [Pt(Me_2S)_3Cl]NO_3$$

$$Pt(OH)_2 \xrightarrow[CF_3SO_3H]{Me_2S} [Pt(Me_2S)_4](CF_3SO_3)_2$$

The 4 : 1 complex has square planar coordination of platinum (Pt–S 2.317–2.321 Å); similar bond lengths are found in the corresponding complex with 1,4-thioxane [120]. Complexes with thiourea are important in Kurnakov's test (section 3.8.2); $Pdtu_4Cl_2$ has square planar coordination (Pd–S 2.33 Å).

Various bidentate ligands like dithiocarbamate afford monomeric square planar complexes; specific examples are $Pt(S_2CNEt_2)_2$ and $Pt(Se_2CNBu)_2$ (confirmed by X-ray). A similar structure is found for the dithiobenzoate $Pd(S_2CPh)_2$; one form of the dithioacetate is dimeric, a second form is a mixture of monomers and dimers.

Mixed mono-complexes can be made (Figure 3.68); the *trans*-influence of tertiary phosphine on the Pt–S bond is noticeable [121].

The series *cis*-$Pt(PhSC_2H_4SPh)X_2$ (X = Cl, Br, I) have been studied structurally (Table 3.12) and show little difference in the *trans*-influence of the halide ions on the Pt–S bond [122].

Crown thiaethers can form *mono*- or *bis*-complexes, depending upon the number of sulphurs in the ring (Figure 3.69).

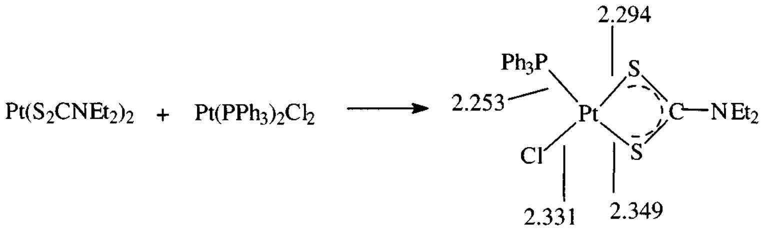

Figure 3.68 Synthesis and structure of $Pt(Ph_3P)Cl(S_2CNEt_2)$.

Table 3.12 Bond lengths (Å) in *cis*-$Pt(PhSC_2H_4SPh)X_2$

X	Pt–X	Pt–S
Cl	2.313–2.317	2.243–2.257
Br	2.430–2.434	2.248–2.249
I	2.601	2.262–2.268

To give some specific examples, in both $Pd(9S_3)_2^{2+}$ and $Pd(10S_3)_2^{2+}$ there is tetragonally distorted octahedral coordination; in the latter, Pd–S (equatorial) is 2.27 Å, Pd–S (axial) is 3.11 Å, the axial interaction being strong enough to give these complexes blue–green colours rather than the orange–yellow norm for square planar palladium(II). Brown $Pd(18S6)^{2+}$ has equatorial Pd–S distances of 2.31 Å and axial distances of 3.27 Å.

$Pt(9S_3)_2^{2+}$ is not isostructural with the palladium analogue but has square pyramidal coordination of platinum Pt–S (axial) 2.246–2.305 Å, (apical) 2.885 Å; $Pt(14S4)^{2+}$ has planar coordination (Pt–S 2.271–2.301 Å) with very distant axial contacts (3.680–3.721 Å) [123].

3.8.6 *Complexes of ambidentate ligands*

An ambidentate ligand has the choice of using two different types of donor atom. Two that have been extensively studied in their bonding to platinum and palladium are sulphoxides and thiocyanate.

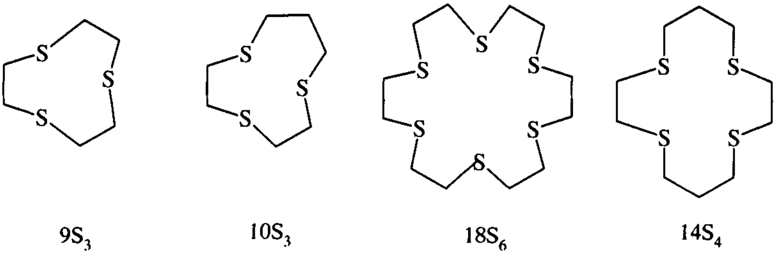

Figure 3.69 Crown thiaethers forming palladium and platinum complexes.

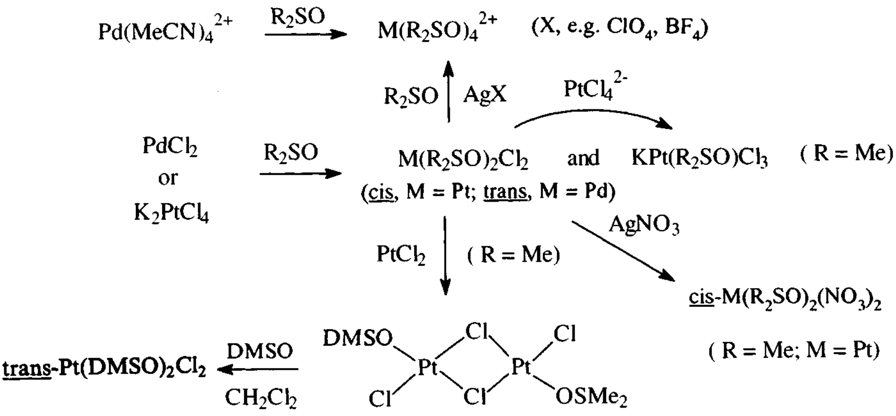

Figure 3.70 Synthesis of dialkylsulphoxide complexes.

Sulphoxide complexes [124]

Since the Pd^{2+} and Pt^{2+} ions are 'soft' acids, coordination by sulphur would be predicted. However, steric effects sometimes dictate bonding via oxygen. Some syntheses are shown in Figure 3.70.

The sterochemistry adopted between these complexes appears to be a balance between steric and electronic effects.

Thus $Pd(DMSO)_2Cl_2$ is the *trans*-isomer (S-bonded) while the platinum analogue is usually obtained as the S-bonded *cis*-isomer. The complex of Pr_2SO with $PtCl_2$ initially forms as the *trans*-isomer (presumably obtained as a result of the kinetic *trans*-effect for S-bonded sulphoxides) but isomerizes on standing to form an equilibrium mixture with the thermodynamically more stable *cis*-isomer. The isoamylsulphoxide complex $Pt[(Me_2CHCH_2CH_2)_2SO]_2Cl_2$ seems to be isolated as the (S-bonded) *trans*-isomer. The nitrate complexes $M(DMSO)_2(NO_3)_2$ have *cis*-(S-bonded) structures with monodentate nitrates (X-ray) (Figure 3.71) while the cationic complexes $[M(DMSO)_4]^{2+}X_2$ (X, e.g. BF_4, ClO_4) contain two S- and two O-bonded sulphoxides (*cis*-configuration presumably on steric grounds.

Steric crowding increases as bigger alkyl groups are introduced so that $[Pt[(Me_2CHCH_2CH_2)_2SO]_4](ClO_4)_2$ has only O-bonded sulphoxides (IR). IR spectra can be used to distinguish between S- and O-bonded sulphoxide:

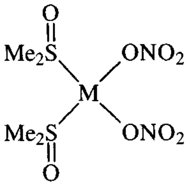

Figure 3.71 The coordination geometry of $M(DMSO)_2(NO_3)_2$ (M = Pd, Pt).

Figure 3.72 IR spectra of $[Pt(DMSO)_4](ClO_4)_2$ in the ν(S–O) region (the broad band at 1100 cm^{-1} is owing to the perchlorate group). (Reprinted with permission from *Inorg. Chem.*, 1972, **11**, 1280. Copyright (1972) American Chemical Society.)

when S-bonded, ν(S=O) increases from the free ligand value (*c.* 1050 cm^{-1}) to 1100–1160 cm^{-1}, whereas when the sulphoxide is O-bonded, ν(S–O) decreases into the region 900–960 cm^{-1} (Figure 3.72).

Crystallographic data can be used to draw up a *trans*-influence series. Comparing the Pt–Cl bond lengths in the compounds in Figure 3.73 shows that DMSO has a greater lengthening effect than the picoline, which in turn produces a slightly greater effect than chloride.

A synthetic route for the two picoline complexes relies on the fact that when the base was added to *cis*-$Pt(DMSO)_2Cl_2$, the *trans*-isomer is formed first. On standing, partial isomerization occurs to the *cis*-form, which can

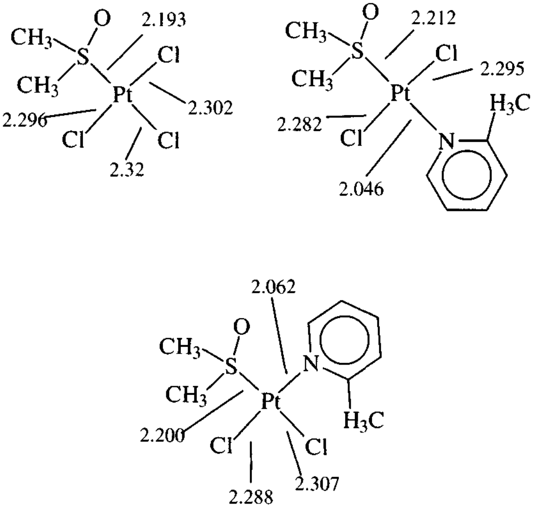

Figure 3.73 Structures of platinum complexes of DMSO.

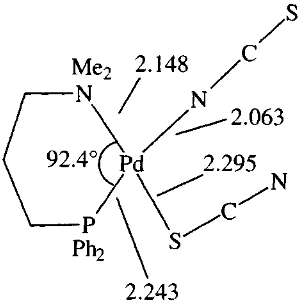

Figure 3.74 The structure of $Pd[Me_2N(CH_2)_3PPh_2](NCS)(SCN)$.

be induced to crystallize first by adding water.

$$cis\text{-}Pt(DMSO)_2Cl_2 \xrightarrow[\text{DMSO}]{\text{L}} trans\text{-}Pt(DMSO)LCl_2 + cis\text{-}Pt(DMSO)LCl_2$$

Thiocyanates [125]

Reaction of $PdCl_4^{2-}$ with KNCS leads successively to a precipitate of $Pd(SCN)_2$ and the soluble salt $K_2Pd(SCN)_4$ (square planar, Pd–S 2.31–2.39 Å). This reacts with Ph_3As to form the S,S-bonded $Pd(SCN)_2(AsPh_3)_2$ (kinetic product), which on heating gives the thermodynamically more stable N,N-bonded isomer:

$$K_2Pd(SCN)_4 \xrightarrow{AsPh_3} Pd(SCN)_2(AsPh_3)_2 \qquad (\text{IR } 2119\,\text{cm}^{-1})$$

$$\xrightarrow{\text{solid}} Pd(NCS)_2(AsPh_3)_2 \qquad (\text{IR } 2089\,\text{cm}^{-1})$$

Similar isomerizations have been noted for a number of complexes. As with metal nitrosyls, IR spectra can be used to indicate the manner of bonding, but there is an 'overlap' region around 2080–2100 cm^{-1} where ν(C–N) is found for both N- and S-bonded thiocyanates (additionally, S-bonded thiocyanates usually give a much sharper ν(C–N) band). ^{14}N NQR has been shown to be a reliable discriminator, but X-ray diffraction is ultimately the most reliable method.

In many cases, it has been found that π-bonding ligands favour S-bonding. In a complex with both N- and S-bonded thiocyanate (Figure 3.74) the N-bonded group is *trans* to P while the sulphur-bonded thiocyanate is *trans* to the 'harder' nitrogen ('anti-symbiosis').

However, the energy difference between N- and S-bonded thiocyanate is very small and is influenced by an interplay of several factors: steric effects, solvent and the counter-ion in ionic complexes. To illustrate the last point, in complexes $[Pd[Et_2N(CH_2)_2NH(CH_2)_2NH_2]NCS]^+$, the PF_6^- salt is N-bonded, as it is in the unsolvated BPh_6^- salt. However, though the acetone solvate of the tetraphenylborate is N-bonded, the methanol solvate is S-bonded [126].

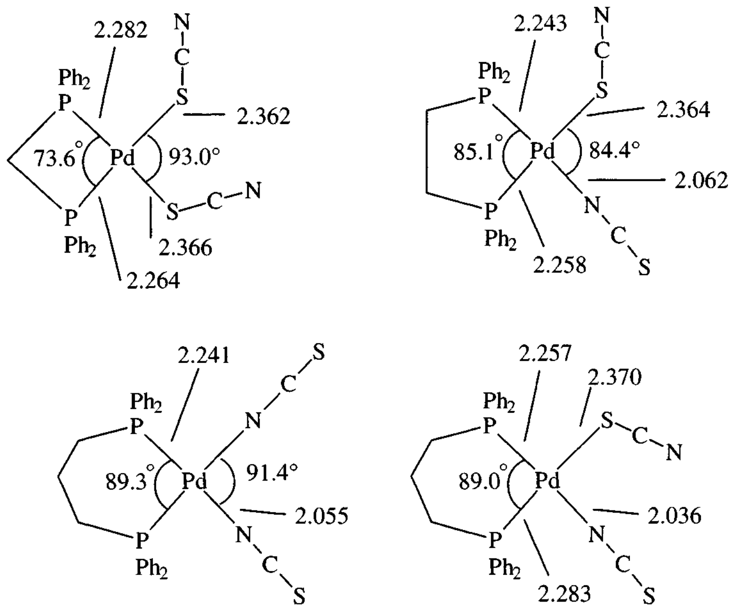

Figure 3.75 The structures of Pd[$Ph_2P(CH_2)_nPPh_2$]$(NCS)_2$ (n = 1–3).

In a classic study (1975) it was shown that in the series Pd[$Ph_2P(CH_2)_n$-PPh_2]$(NCS)_2$ (n = 1–3) the bonding of the thiocyanate changes from all-S to all-N coordinated as n increases (Figure 3.75) [127].

Subsequently it was shown that the P–Pd–P angles were essentially the same as in the corresponding chloride complexes (section 3.8.3): as a result, as the P–Pd–P angle increases, concomitant upon the increase in the length of the methylene chain, steric effects enforce N-bonded thiocyanate, which is less sterically demanding that the non-linear Pd–SCN linkage (favoured on HSAB considerations since Pd^{2+} is a 'soft' acid and sulphur is a 'soft' base).

Subsequent ^{31}P NMR study of solutions indicated that a mixture of isomers was present, with a distribution strongly dependent upon solvent; therefore, the energy difference between isomeric molecules was small. Moreover, the N,S-bonded isomer of the $Ph_2P(CH_2)_3PPh_2$ complex was also isolated in the solid state, as well as being found to be the predominant isomer in some solvents (DMF, Me_2CO, CH_2Cl_2). The isolation of the N,N-bonded isomer may have been a fortuitous success with this particular ligand, as it has not been achieved with other chelating ligands.

Two isomers have again [128] been obtained (S,S- and N,S-form) with the ligand dpbz (bis(diphenylphosphino)benzene) (Figure 3.76).

Such thiocyanate complexes are usually made by reaction of the ligand (L–L) with $Pd(SCN)_4^{2-}$ in a solvent like ethanol. A substantial amount of the Magnus-type salt [Pd(L–L)$_2$][$Pd(SCN)_4$] is often produced, convertible to the neutral Pd(L–L)$(NCS)_2$ by dissolution in hot DMF and reprecipitating with water.

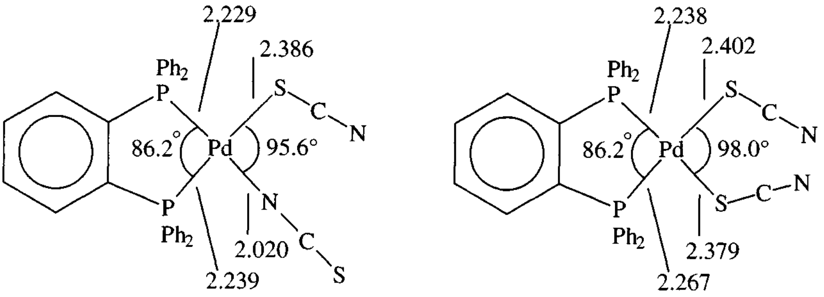

Figure 3.76 Isomers of $Pd[C_6H_4(PPh_2)_2](NCS)_2$.

It now appears that the most usual coordination mode in *cis*-di(thiocyanate) complexes is one N-bound and one S-bound thiocyanate, as an angular Pd–SCN bond minimizes interaction with the other bound thiocyanate and with the other ligands.

Most of the studies of ambidentate behaviour among thiocyanates concern palladium complexes; a recent report [129], however, investigated $Pt(bipy)(NCS)_2$

$$Pt(bipy)Cl_2 \xrightarrow[2.\,KSCN/H_2O]{1.\,AgClO_4/DMSO} Pt(bipy)(SCN)_2 \qquad \text{yellow, IR 2119, 2131 cm}^{-1}$$

$$\xrightarrow{150°C} Pt(bipy)(NCS)_2 \qquad \text{red, IR 2117 cm}^{-1}\text{ (broad)}$$

The yellow form is stable at room temperature but isomerizes on warming in the solid state or solution. EXAFS measurements indicate that the yellow form has Pt bound to N and S (i.e. the thiocyanate is S-bonded) while the red form has no Pt–S bonds (Figure 3.77); therefore, the thiocyanate is N-bonded (there are also indications of distant Pt–Pt contacts (3.2 Å), possibly by 'stacking' of the planar $Pt(bipy)(NCS)_2$ units).

3.8.7 *Stability of* cis *and* trans-*isomers* [130]

For complexes like PtL_2X_2 (X = halogen; L = NH_3, PR_3, etc.) where *cis*- and *trans*-isomers exist, the *trans*-isomer is usually thermodynamically more stable. The *cis*-isomer may be formed first in a reaction and, in the case of platinum, may be relatively inert to substitution. (Thermodynamic data are relatively scarce; *trans*-$Pt(NH_3)_2Cl_2$ is some 13 kJ mol^{-1} more stable than the *cis*-isomer.)

Isomerization frequently occurs on heating. Solid *cis*-$Pt(NH_3)_2Br_2$ turns into the *trans*-isomer at 250°C while solid *cis*-$Pt(PMe_2Ph)_2MeCl$ also isomerizes on heating. These are presumably intramolecular processes involving pseudo tetrahedral intermediates. Some *trans*- to *cis*-isomerizations occur: solid *trans*-$Pt(Et_2SO)pyCl_2$ turns into the *cis*-isomer at 134°C, while

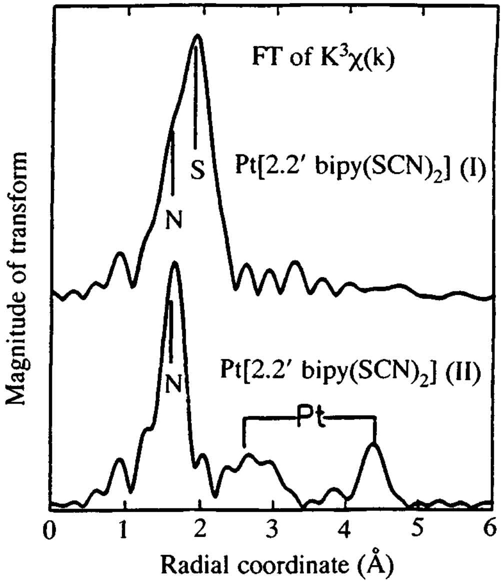

Figure 3.77 EXAFS spectra of the isomers of Pt(bipy)(NCS)$_2$. (Reprinted with permission from *Inorg. Chem.*, 1992, **31**, 1752. Copyright (1992) American Chemical Society.)

rans-Pt(PPr$_3$)$_2$Cl$_2$ partly turns into the *cis*-isomer in benzene solution. (In contrast the palladium analogue does not isomerize.) The π-bonding effects have been used to explain the unexpectedly high stability of some *cis*-isomers, as more d orbitals are involved in dπ–pπ overlap (Figure 3.78).

Thermal isomerizations can be used in the synthesis of, in particular, Pt(PR$_3$)$_2$X$_2$ isomers [131a] (section 3.8.3). *Trans*-Pt(PR$_3$)$_2$X$_2$ (X = Cl,

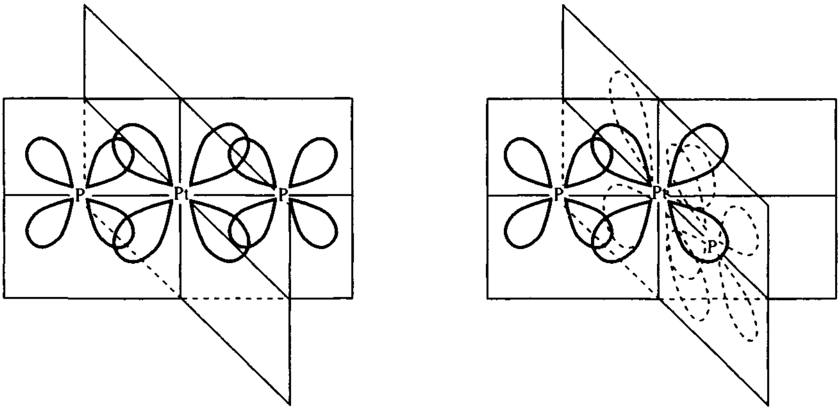

Figure 3.78 Postulated π-bonding in *cis*- and *trans*-phosphine complexes. (Reproduced with permission from S.A. Cotton and F.A. Hart, *The Heavy Transition Elements*, Macmillan Press Ltd, 1975, p. 119.)

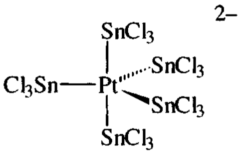

Figure 3.79 The trigonal bipyramidal $[Pt(SnCl_3)_5]^{3-}$.

R = Bu; X = Br, R = Et, Pr, Bu; X = I; R = Et, Pr) can be prepared by solid state isomerization of the *cis*-form at a temperature just below the melting point; by comparison, complexes of trimethyl- and triphenylphosphine decompose without change. Isomerization of $PtCl_2(EtCN)_2$ has likewise been studied [131b].

3.8.8 *Five-coordinate compounds*

Despite the fact that PtL_3X_2 and PtX_5^{3-} species have an 18-electron configuration, 5-coordinate palladium(II) and platinum(II) compounds are rare. One of the first examples to be established was $Pt(SnCl_3)_5^{3-}$

$$PtCl_4^{2-} \xrightarrow[2.\ Ph_3PMe+MCl]{1.\ SnCl_2/HCl} (Ph_3PMe)_3[Pt(SnCl_3)_5]$$

It has a tbp structure (Figure 3.79) with Pt–Sn 2.553 Å (axial) and 2.5722 Å (equatorial) (in the corresponding $(Me_4N)_3Pt(GeCl_3)_5$, the Pt–Ge distances are 2.400 and 2.434 Å, respectively); the shorter axial bond lengths are ascribed to differences in Pt–Sn π-bonding.

^{195}Pt and ^{119}Sn NMR data show $Pt(SnCl_3)_5^{3-}$ to be non-rigid (on the NMR timescale) down to 183 K, owing to an intramolecular process, possibly a ‘Berry twist’ mechanism [132].

Stable anionic complexes $[Pt(SnCl_3)_3L_2]^-$ are formed by tertiary phosphines and arsines with small cone angles (L = PR_3, AsR_3; R = Me, Et, OEt), confirmed by X-ray diffraction for $[Pt(SnCl_3)_3(AsMe_3)_2]^-$, which has axial arsines (Pt–As 2.427–2.445 Å; Pt–Sn 2.579–2.614 Å). With larger ligands, steric constraints mean that planar species like *trans*-$Pt(SnCl_3)_2[P(OPh)_3]_2$ are obtained [133]. In solution, $[Pt(SnBr_3)_5]^{3-}$ is unstable with respect to dissociation into $[PtBr_2(SnBr_3)_2]^{2-}$ and $[PtBr_3(SnBr_3)]^{2-}$ in the absence of added $SnBr_2$ [134]; salts $M_3[Pt(SnBr_3)_5]$ (M = Bu_4N, $PhCH_2PPh_3$) have been prepared in the solid state.

Some 5-coordinate phosphite complexes (fluxional at room temperature) exist

$$PtCl_2 \xrightarrow[2.\ NaBPh_4]{1.\ (MeO)_3P/MeOH} Pt[P(OMe)_3]_5^{2+}(BPh_4)_2$$

Again, steric effects prevent more than four bulky phosphites coordinating [135].

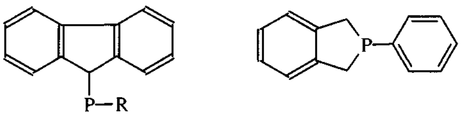

I, R = Et; II, R = Me III

Figure 3.80 Phosphine ligands forming the 5-coordinate palladium and platinum complexes.

A number of tertiary phosphine complexes with bulky ligands (Figure 3.80) have modified square pyramidal structures, examples being $M(I)_3Br_2$, $Pt(II)_3Br_2$ and $Pd(III)_3Br_2$ (all X-ray) [136].

One crystalline form of *trans*-$Pd(PMe_2Ph)_2I_2$ has a pseudo-sp structure in the solid state as an iodine atom from a neighbouring molecule occupies a distant 'axial' position [137a]. Other complexes of PMe_2Ph, $M(PMe_2Ph)_3X_2$ (M = Pd, Pt; X = halogen), are likely to be 5-coordinate, confirmed for $Pd(PMe_2Ph)_3Cl_2$ [89]. $[Pd(tmpp)_2]^{2+}$ exhibits short axial Pd–O bonds (2.632–2.671 Å) and is regarded as a distorted octahedral complex [137b].

Complexes of bulky substituted phenanthrolines $[Pt(N{-}N)LX_2]$ (L, X both monodentate; N–N, e.g. 2,9-dimethyl-1,10-phenanthroline) can be 5-coordinate tbp when a good π-acceptor (e.g. C_2H_4) is present or 4-coordinate with monodentate phenanthrolines. Hartree–Fock calculations indicate that the π-acceptors reduce the electron density at platinum so that the metal can accept charge from another donor. Species of this kind may be involved in alkene hydrogenation [138].

3.8.9 The trans-*effect*

In the 1920s, the Russian chemist Il'ya Il'ich Chernyaev systematized reactions of complexes of several metals, particularly platinum(II and IV), by noting that a ligand bound to a metal ion influenced the ease of replacement of the group *trans* to it in the complex [139].

The *trans*-effect has been defined [140] as 'the effect of a coordinated group upon the rate of substitution reactions of ligands opposite to it. Metals in which the rate influence of opposite, or *trans*-groups, is definitely greater than the influence of adjacent, or *cis* groups, will be considered to show a *trans*-effect'. The *trans*-effect is, therefore, a kinetic phenomenon, related presumably to the transition state, as well as the ground state, in the substitution reaction. It is not the same as *trans*-influence. The *trans*-influence of a ligand is a measure of the effect of a ligand on the strength of a bond opposite to it in a complex: it is a ground-state effect, which can be measured in terms of lengthening of bonds (X-ray diffraction) or vibrational spectra (sections 3.8.10 and 3.8.11).

The trans-*effect and substitution reactions*

Square planar complexes of palladium(II) and platinum(II) readily undergo ligand substitution reactions. Those of palladium have been studied less but appear to behave similarly to platinum complexes, though around five orders of magnitude faster (ascribable to the relative weakness of the bonds to palladium).

For a substitution reaction of the type

$$PtL_3X + Y \rightarrow PtL_3Y + X$$

the rate law is generally found to be of the form

$$\text{Rate} = \frac{-d[PtL_3X]}{dt} = (k_1 + k_2[Y])[PtL_3X] = k_1[PtL_3X] + k_2[Y][PtL_3X]$$

suggesting two competing pathways.

The k_1 term is independent of Y and would, therefore, appear to be dissociative, but it is in fact found to be solvent-dependent and so it is thought to be associative. (It is also found to be sensitive to steric effects in the same manner as the k_2 pathway.) A plausible pathway for the k_1 route is slow solvolysis followed by fast substitution

$$PtL_3X + S \xrightarrow{\text{slow}} PtL_3S + X \xrightarrow[Y]{\text{fast}} PtL_3Y + S$$

The k_2 term suggests a simple bimolecular process in which nucleophilic attack by Y leads to a S_N2 reaction. Associative paths will involve a 5-coordinate (sp or tbp) intermediate, and the relative rarity of isolable 5-coordinate platinum(II) species – compared with 4-coordinate – is not inconsistent with their involvement as reactive intermediates (Figure 3.81).

Retention of configuration occurs in these substitution reactions, as expected for a process involving a 5-coordinate intermediate in which the entering and leaving ligands are simultaneously bound.

Kinetic study [141] of complexes of the type *trans*-$Pt(PEt_3)_2XCl$ was of great value in establishing the strong *trans*-effect of hydride (Table 3.13); examination of the data for a wide range of reactions gives rise to a series

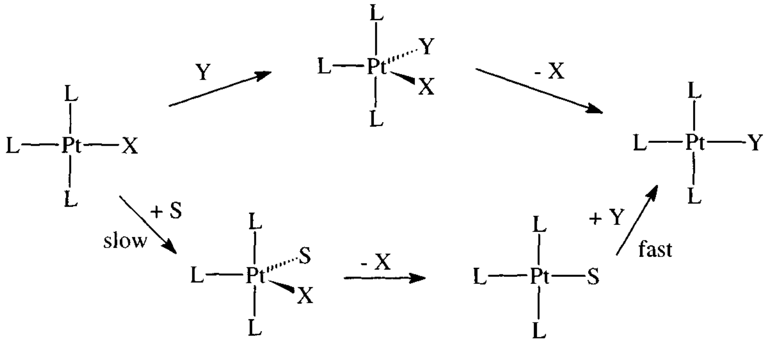

Figure 3.81 Pathways for substitution of a square planar species PtL_3X.

Table 3.13 Comparison of the effect of the *trans*-ligand on substitution of Cl by py in *trans*-$PtClX(PEt_3)_2$ at 25°C

X	k_1 (s^{-1})	k_2 ($M^{-1} s^{-1}$)
PEt_3	1.7×10^{-2}	3.8
H^{-a}	1.8×10^{-2}	4.2
Me^-	1.7×10^{-4}	6.7×10^{-2}
Ph^-	3.3×10^{-5}	7.5×10^{-4}
Mesityl	1.7×10^{-6}	3.7×10^{-4}
Cl^-	1.0×10^{-6}	4.0×10^{-4}

[a] For H^-, measured at 0° (reaction too fast to measure at 25°C).

with *trans*-effect defined as the ability of a coordinated ligand to labilize a ligand *trans* to it.

The *trans*-effect is, therefore, a kinetic labilizing effect rather than a thermodynamic one. An approximate series is:

$$CN^-, CO, C_2H_4 > PR_3, H^- > Me^- > tu \sim R_2S > NO_2^-, I^- > SCN^- > Br^- > Cl^- > pyridine > NH_3 > OH^- > H_2O$$

Two examples of steric effects deserve attention. In aryl complexes *cis*-$Pt(PR_3)_2ArCl$, introducing *ortho*-substituents into the phenyl group slows down substitution considerably, as these block the position of attack (Figure 3.82).

From the data in Table 3.14, note the greater range of values of *k* for the *cis*-isomers, showing their greater sensitivity to steric effects (the similarity of the value for the phenyl and *p*-tolyl derivatives may also be noted).

In contrast, the *trans*-isomers are much less affected by the substituents in the benzene ring, as there is interaction in the transition state [142].

Comparison of results for complexes of tridentate amines $R_2N(CH_2)_2NH(CH_2)_2NR_2$ show similar effects. With dien (R = H), rapid substitution of chloride in $Pt(dien)Cl^+$ by bases occurs at room temperature; however with Et_4dien (R = Et) the reaction is considerably slowed, since the four ethyl groups crowd the metal above and below the plane of the molecule (Figure 3.82) making nucleophilic attack harder. Such a complex can be attacked more easily by a small nucleophile rather than a 'better' nucleophile which happens to be larger [89].

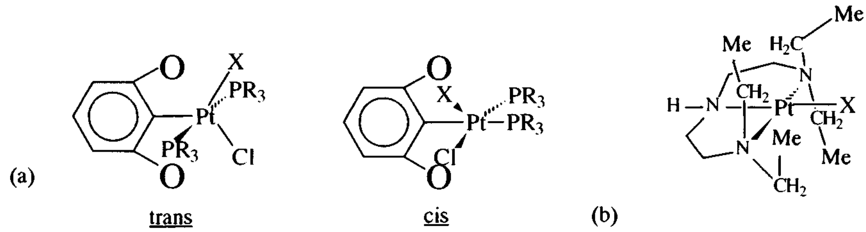

Figure 3.82 (a) The effect of *ortho*-substituents on substitution reactions of *cis*-$Pt(PR_3)_2ArCl$ complexes; (b) the effect of alkyl substituents on substitution reactions of dien complexes.

Table 3.14 Rates of attainment of equilibrium in the reaction between $Pt(PR_3)_2RCl$ and pyridine

R	k_1 (s^{-1}) *cis*-isomer (0°C)	k_1 (s^{-1}) *trans*-isomer (25°C)
Me	6.0×10^{-2}	1.7×10^{-4}
Ph	3.8×10^{-2}	3.3×10^{-5}
o-Tolyl	8.6×10^{-5}	6.7×10^{-6}
p-Tolyl	5.0×10^{-2}	–
Mesityl	4.2×10^{-7}	1.2×10^{-6}

Theoretical explanation of the *trans*-effect (and *trans*-influence) has centred on two theories, one based on σ-bonding the other on π-bonding. The σ-bonding argument considers two *trans*-ligands sharing a metal p orbital (Figure 3.83).

A strong σ-donor contributes high electron density, weakening the bond *trans* to it. This is essentially a ground-state argument, as in a 5-coordinate reaction intermediate the two groups will not be competing for electron density in just this one orbital. This would give rise to a σ-bonding order such as $H^- > PR_3 > SCN^- > I^-$, NCS, CO, $CN^- > Br^- > Cl^- > NH_3 > OH^-$.

One or two ligands such as CO and CN that have high observed *trans*-effects (and therefore are out of place in the above series) do possess empty orbitals that can act as π-acceptors to remove electron density from the metal ion, making the region *trans* to the ligand electron deficient and able to be attacked by the nucleophile in the transition state (Figure 3.84).

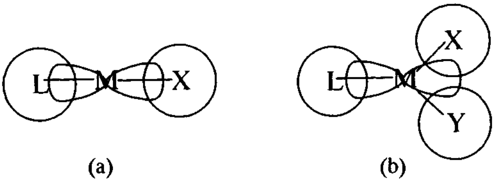

(a) (b)

Figure 3.83 (a) Ground state weakening; (b) Weakening reduced with lessening competition in the transition state.

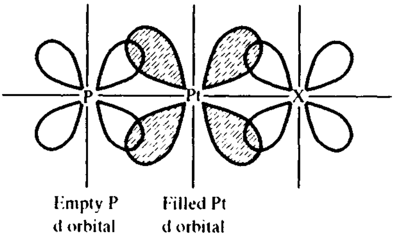

Figure 3.84 Effect of a π-bonding ligand in acting as a π-acceptor. (Reproduced with permission from S.A. Cotton and F.A. Hart, *The Heavy Transition Elements*, published by Macmillan Press Ltd, 1975, p. 118.)

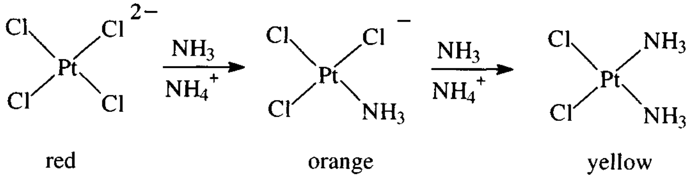

Figure 3.85 Synthesis of *cis*-$Pt(NH_3)_2Cl_2$.

This would give rise to an order of the kind $R_2C{=}CR_2$, CO > CN^- > NO_2^- > SCN^- > I^- > Br^- > NH_3 > OH^-. Therefore, a combination of σ- and π-effects can be considered to give rise to the observed *trans*-effect series.

Explanations of the *trans*-effect and *trans*-influence have considered σ- and π-bonding, often to the point of mutual exclusion.

Theories based on σ-effects consider that the more electronegative a ligand the more polarization of the metal occurs, weakening the bond *trans* to it. This can alternatively be viewed in terms of electronic transmission via a σ-type (p) orbital shared by the two ligands.

A π-bonding explanation notes that several ligands high in the *trans*-effect series are good π-acceptors and thus siphon off π-density, making the region *trans* to it electron deficient and thus attractive to ligands that are electron rich.

Synthetic applications of the trans-*effect* [139b, 143]

The classic application of the *trans*-effect lies in the synthesis of the *cis*- and *trans*-isomers of $Pt(NH_3)_2Cl_2$, known as Peyrone's salt and Reiset's salt after their respective discoverers in 1844.

The *cis*-isomer is made by reacting $PtCl_4^{2-}$ with ammonia solution (Figure 3.85).

Because Cl^- has a stronger *trans*-effect than NH_3, a group opposite to Cl^- is replaced in the second substitution. Similarly, in the synthesis of the *trans*-isomer by heating $Pt(NH_3)_4^{2+}$ with Cl^-(Figure 3.86), it is the ligand *trans* to chloride that is again replaced in the second step.

The *cis*- and *trans*-isomers of $[Pt(NH_3)(NO_2)Cl_2]^-$ have been synthesized from $PtCl_4^{2-}$ merely by choice of the order of ligand substitution (Figure 3.87). (In the second step, chloride *trans* to chloride is more labile.) The second substitution is dictated by NO_2 having a higher position in the *trans*-effect series than chloride [144].

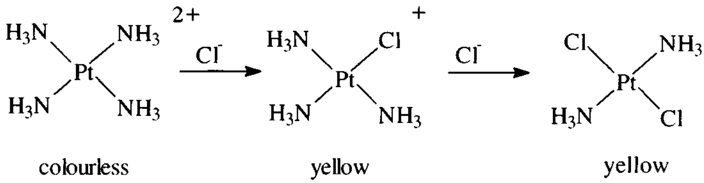

Figure 3.86 Synthesis of *trans*-$Pt(NH_3)_2Cl_2$.

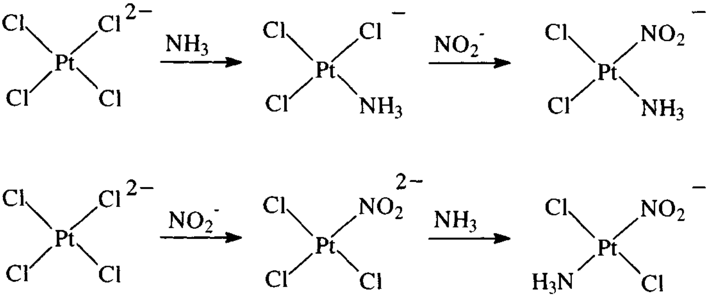

Figure 3.87 Synthesis of the isomers of $[Pt(NH_3)(NO_2)Cl_2]^-$.

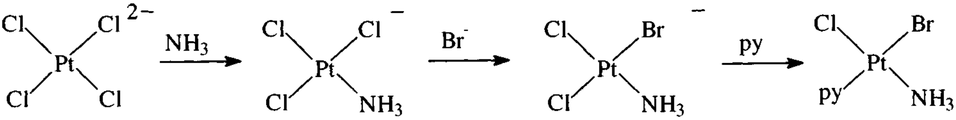

Figure 3.88 Synthesis of the first isomer of $PtClBr(NH_3)py$.

Square planar complexes of the type MABCD have three geometric isomers and in several cases all have been synthesized. Therefore, the isomers of $[PtClBr(NH_3)py]$ can be synthesized as shown in Figures 3.88–3.90.

The second substitution relies on the (observed) fact that anionic ligands (e.g. Cl^-) are more readily replaced than neutral ones (e.g. NH_3), so that chloride *trans* to chloride is substituted rather than NH_3 *trans* to chloride. In the third step, the chloride *trans* to bromide is replaced, in keeping with the *trans*-effect order Br > Cl. In Figure 3.89, the second step again relies on the observed kinetic weakness of the Pt–Cl bond, while the third substitution again involves replacement of the chloride *trans* to the group highest in the *trans*-effect series. The third isomer is produced by a sequence in which the second step is again an example of the kinetic weakness of the Pt–Cl

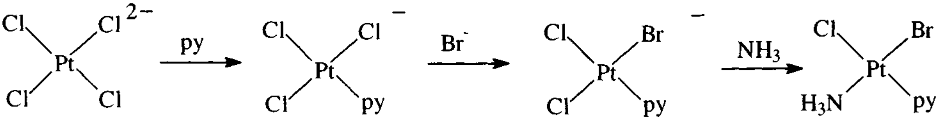

Figure 3.89 Synthesis of the second isomer of $PtClBr(NH_3)py$.

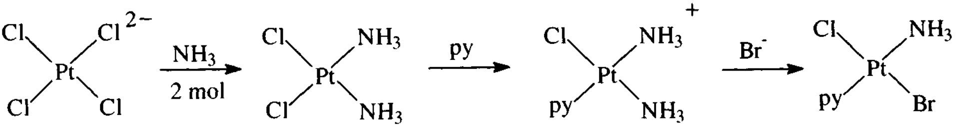

Figure 3.90 Synthesis of the third isomer of $PtClBr(NH_3)py$.

Table 3.15 Pt–Cl bond lengths in ions $PtLCl_3^-$

L	Pt–Cl *trans* to L	Pt–Cl *cis* to L	Pt–L
PEt_3	2.382	2.299–2.302	2.215 (P)
C_2H_4	2.340	2.303	2.022[a]
NH_3	2.321	2.30–2.32	2.06 (N)
2,6-Me_2py	2.309	2.302	2.024 (N)
CO	2.289	2.290–2.294	1.82 (C)
MeCN	2.266	2.293–2.301	1.960 (N)
Me_2SO	2.309	2.271–2.275	2.185 (S)
py	2.305	2.293–2.299	2.018 (N)

[a] To midpoint of C–C bond.

bond compared with the Pt–NH_3 bond. The *trans*-effect series again predicts the replacement of the group *trans* to Cl in the third step [145].

Similarly, all three isomers have been isolated for $PtBr(NO_2)NH_3(py)$ and $PtCl(NO_2)(NH_3)(MeNH_2)$ while Chernyaev used the synthesis of all three isomers of $[Pt(NH_3)py(NH_2OH)(NO_2)]^+Cl^-$ as evidence for a square planar geometry [146].

3.8.10 Structural evidence for trans-*influence*

A considerable amount of X-ray data has now been accumulated to support the concept of *trans*-influence. In a series of ions, $PtLCl_3^-$ (L = neutral ligand), the Pt–Cl bond *trans* to the neutral ligand displays much more sensitivity to L than do the *cis*-chlorines (Table 3.15) [147].

Variation of *cis*-bond lengths has been noted in some cases and is believed to reflect steric interaction. Therefore, in the series $PtX(PEt_3)_3^+$ (X = H, Cl, F) the *trans*-bond to X shows a dependence upon the electronegativity of X, while the *cis*-Pt–P bond shows no such dependence (Figure 3.91) [148], instead increasing as X becomes larger.

Similar dependence is noted in the complexes $PtH_xCl_{2-x}(PPr^i_3)_2$ ($x = 0, 1, 2$) where the Pt–P bond increases by 0.04 Å for each successive replacement of hydrogen by the bulkier chlorine (Figure 3.92) [149].

A number of mainly *trans*-$M(PR_3)_2XY$ compounds (X, Y = Cl, Me, H, Br, Ph, I) have been studied (Figure 3.93) [150].

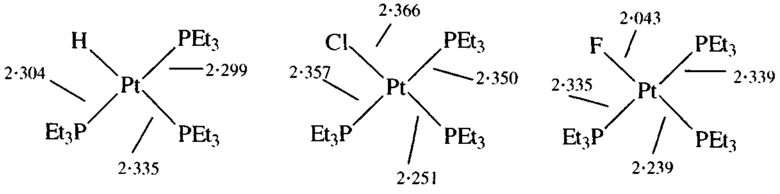

Figure 3.91 Bond lengths in the ions $[PtX(PEt_3)_3]^+$ (X = H, Cl, F).

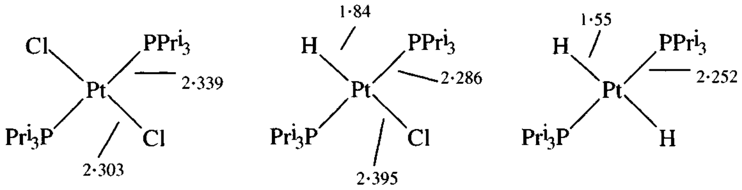

Figure 3.92 Bond lengths in the compounds PtH$_x$Cl$_{2-x}$(PPr$^i_3$)$_2$.

They display the considerable *trans*-influence of hydride and aryl groups (the Pt–Cl bond lengths should be compared with the value of *c.* 2.31 Å in PtCl$_4^{2-}$). The Pt–P bond lengths are more insensitive to the phosphine, but by synthesis of *cis*-Pt(PR$_3$)(PR$'_3$)Cl$_2$ [150] complexes, it has been possible to study the effect of electron-withdrawing substituents on the Pt–P bond, as well as on the *trans*-influence of the phosphine (Figure 3.94).

Very bulky ligands, of course, cause steric effects. The similarity of the Pt–P bond lengths in *trans*-Pt(PR$_3$)$_2$H$_2$ (R = Me, cy) suggest that the bonding is similar in these two compounds (Table 3.16 and Figure 3.95)

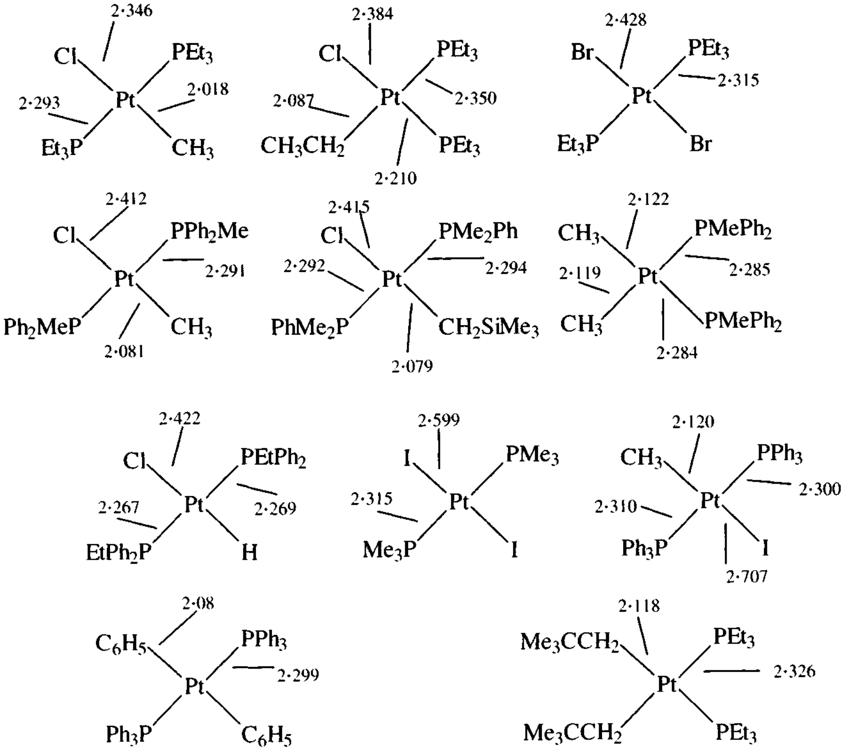

Figure 3.93 Bond lengths in compounds *trans*-Pt(PR$_3$)$_2$XY.

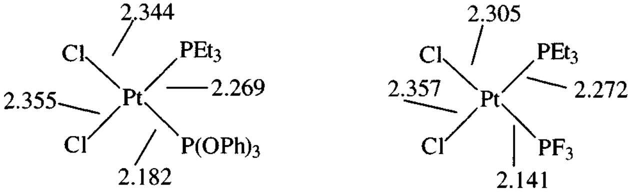

Figure 3.94 Bond lengths in compounds *cis*-$Pt(PR_3)(PR'_3)Cl_2$.

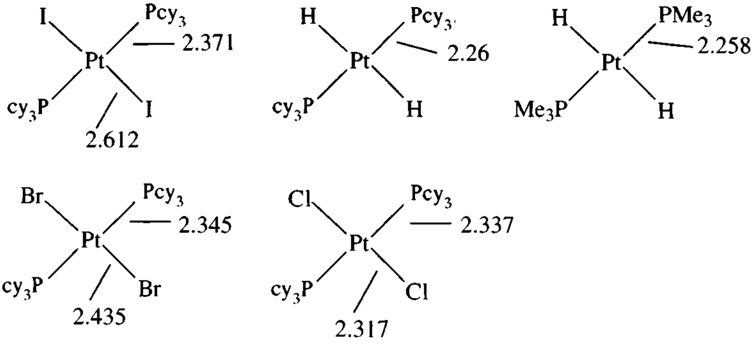

Figure 3.95 Bond lengths in compounds *trans*-$Pt(Pcy_3)_2X_2$ (X = H, halogen).

but on passing to the iodide *trans*-$Pt(Pcy_3)_2I_2$, the long Pt–P (and Pt–I) bond lengths indicate crowding; chemical evidence of this is that, on heating, the iodide eliminates a molecule of phosphine affording the halogen-bridged dimer $[Pt(Pcy_3)I_2]_2$.

Careful comparison of Pt–P bond lengths for the series *trans*-$Pt(Pcy_3)_2X_2$ (X = H, Cl, Br, I) with those for *trans*-$Pt(PR_3)_2X_2$ (PR_3 = PMe_3 or PEt_3) shows a more definite increase in Pt–P with anion size for the cyclohexylphosphine complexes (Table 3.16) believed to be owing to intermolecular X···H and X···C non-bonded interactions arising from overcrowding [151].

A series of phosphine complexes with '*cis*-PtP_2Cl_2' geometries have been compared (Table 3.17).

The Pt–P (and Pt–Cl) bond lengths correlate with the electron-donating ability of the phosphine (Tolman's χ_i factor) rather than steric factors (the cone angle of the tertiary phosphine) [150b].

Table 3.16 Pt–P bond lengths for *trans*-$Pt(PR_3)_2X_2$ complexes (Å)

X	$Pt(Pcy_3)_2X_2$	$Pt(PR_3)_2X_2$
H	2.26	2.259 (R = Me)
Cl	2.337	2.30 (R = Et)
Br	2.345	2.315 (R = Et)
I	2.371	2.315 (R = Me)

Table 3.17 Phosphine *cis*-PtP_2Cl_2 complexes

	Pt–P (Å)	Pt–Cl (Å)	Cone angle (°)	$\sum X_i$
cis-$Pt(PEt_3)_2Cl_2$	2.258	2.361	130	5.4
cis-$Pt(PMe_3)_2Cl_2$	2.248	2.376	118	7.8
cis-$Pt(PMe(C_6F_5)_2)_2Cl_2$	2.236	2.344	130	16.4
cis-$Pt(PEt_3)(P(OPh)_3)Cl_2$	2.182	2.344	128	29.1
cis-$Pt(PEt_3)(PF_3)Cl_2$	2.141	2.305	104	54.6

Table 3.18 IR and NMR data for *trans*-$Pt(PEt_3)_2HX$

X	Cl	Br	I	NCS	$SnCl_3$	CN
ν (Pt–H) (cm^{-1})	2183	2178	2156	2112	2105	2041
δ (ppm) (hydride)	−16.9	−15.6	−12.7	−13.2	−9.2	−7.8

3.8.11 Spectroscopic evidence for trans-*influence*

Infrared

Study of a series of complexes *trans*-$Pt(PEt_3)_2HX$ shows a pronounced dependence of ν(Pt–H) upon the *trans*-ligand (Table 3.18).

Similarly, in complexes PtL_2Cl_2, the Pt–Cl stretching frequency is relatively insensitive to L in the *trans*-isomer but shows considerable dependence in the *cis*-isomer (Table 3.19) [100].

NMR evidence

Table 3.18 shows how the position of the low-frequency hydride resonance is affected by the *trans*-ligand, while study of a series of complexes *trans*-$[Pt(PMe_2Ph)_2(Me)L]^+$ and neutral *trans*-$Pt(PMe_2Ph)_2(Me)X$ shows the *trans*-influence of the ligand on $^2J(^{195}Pt-^1H)$ with better donors tending to reduce the value of J (Table 3.20) [152].

Platinum ammine complexes have been a fertile area for studying *trans*-influence. Table 3.21 lists data for a range of ammines showing how $^1J(^{195}Pt-^{15}N)$ depends upon the *trans*-atom [153]. (A further selection of data can be found in: R.V. Parish, *NMR, NQR, EPR and Mössbauer Spectroscopy in Inorganic Chemistry*, Ellis-Horwood, Chichester, 1991, pp. 76, 87.) Possibly the most detailed study (of complexes of tribenzylphosphine) examined over a hundred neutral and cationic complexes [154] (Table 3.22).

Table 3.19 ν (Pt–Cl) in complexes PtL_2Cl_2 (cm^{-1})

L	NH_3	PEt_3	Et_2S	py	$AsEt_3$
trans-Isomer	331.5	340	342	342.6	339
cis-Isomer	326	303, 281	330, 318	343, 328	314, 287.5
Average	326	292	324	335.5	301

Table 3.20 The *trans*-influence of ligands on $^{2}J(^{195}Pt-^{1}H)$ in *trans*-A^+ and *trans*-AX^a

L	X	J (Hz)
$SbPh_3$		55
PMe_2Ph		57
$P(OPh)_3$		58
PPh_3		60
CO		63
Py		74
PhCN		79
	Cl	85
	Br	83
	I	80

^{a} A is $Pt(PMe_2Ph)_2$ MeL

Putting the ligands in order of their effect on the value of δ, the position of the hydride resonance, gives H $\gg$ CO, PR_3 > CN > tu > NO_2 > SMe_2 > SCN, I > Br > Cl > NH_3, py. A not dissimilar order is found for their effect on ν(Pt–H) in the IR spectrum (H $\gg$ CN > PR_3 > I > SCN ~ NO_2 ~ tu ~ CO ~ Cl > SMe_2 > Br > NH_3 > py). Data correlate well with those for other tertiary phosphines, e.g. Pcy_3.

A seminal paper [155] examined platinum–phosphorus NMR coupling constants in a series of *cis*- and *trans*-platinum(II and IV) complexes. The *trans*-influence had hitherto been explained in terms of dπ–pπ bonding, in other words, such a mechanism dominated with *trans*-effect

Table 3.21 $J(^{195}Pt-^{15}N)$ values (Hz) for platinum(II) amine complexes

	NH_3 *trans* to			
	O	N	Cl	S
cis-$Pt(NH_3)_2Cl_2$			326	
trans-$Pt(NH_3)_2Cl_2$		278		
cis-$Pt(NH_3)_2(H_2O)_2^{2+}$	391			
trans-$Pt(NH_3)_2(H_2O)_2^{2+}$		312		
$Pt(NH_3)_4^{2+}$		287		
$Pt(NH_3)_3Cl^+$		281	331	
$Pt(NH_3)_3(H_2O)^{2+}$	376	299		
cis-$Pt(NH_3)_2tu_2^{2+}$				237
cis-$Pt(NH_3)_2tu_2^{2+}$				263
cis-$Pt(NH_3)_2(SCN)_2$				250
$Pt(NH_3)_3tu^{2+}$		277		243
$Pt(NH_3)_3SCN^+$		282		264
$Pt(NH_3)_3(Me_2SO)^{2+}$		303		243

Table 3.22 NMR and IR data [154] for complexes *trans*-$Pt(Pbz_3)_2HX$ and *trans*-$[Pt(Pbz_3)_2HL]^+$

X/L	ν(Pt–H) (cm^{-1})	δ (ppm)	*J*(Pt–H) (Hz)	*J*(Pt–P) (Hz)
H	1734	−2.4	800	–
Cl	2210	−17.36	1290	2969
Br	2221	−16.47	1345	2925
I	2192	−13.62	1359	2882
SCN	2203	−13.58	1186	
CN	2059	−8.69	776	
NH_3	2256	−18.16	1042	2928
Py	2290	−18.89	1022	2919
PPh_3	2140, 2123	−6.87	783	2717
Pbz_3	2145	−7.28	714	2682
$P(OPh)_3$	2165	−5.85	758	2620
SMe_2	2219	−13.30	1094	2820
CO	2207	−6.12	840	
tu	2205	−10.09	1134	
NO_2	2200	−12.09	1008	

and *trans*-influence. The results in Table 3.23 show that the ratio $J_{cis} : J_{trans}$ is similar in the platinum(II) and platinum(IV) complexes.

Since π bonding is believed to be more important in low oxidation states, as d orbitals contract with increasing oxidation state leading to poorer dπ–pπ overlap, this would not be expected on the basis of a π-bonding mechanism. Similarly, one can compare *J*(Pt–P) for pairs of isomers in the +2 and +4 states; in a planar platinum(II) complex, the platinum 6s orbital is shared by four ligands whereas in an octahedral platinum(IV) complex it is shared by six ligands. Therefore, the 6s character is expected to be only 2/3 as much in the platinum(IV) complexes, correlating well with the *J*(Pt–P) values, which can be taken to be a measure of the σ-character in the bond.

Table 3.23 NMR coupling constants for platinum phosphine complexes [155]

	$J(^{195}Pt-^{31}P)$ (Hz)
cis-$PtCl_2(PBu_3)_2$	3508
cis-$PtBr_2(PBu_3)_2$	3479
cis-$PtI_2(PBu_3)_2$	3372
trans-$PtCl_2(PBu_3)_2$	2380
trans-$PtBr_2(PBu_3)_2$	2334
trans-$PtI_2(PBu_3)_2$	2200
cis-$PtCl_4(PBu_3)_2$	2070
trans-$PtCl_4(PBu_3)_2$	1462
cis-$PtCl_2[P(OEt)_3]_2$	5698
cis-$PtBr_2[P(OEt)_3]_2$	5662
cis-$PtI_2[P(OEt)_3]_2$	5472

Table 3.24 NMR coupling constants for platinum amine complexes [156]

	$J(^{195}Pt-^{15}N)$ (Hz)
cis-PtL_2Cl_2	351
cis-PtL_2Cl_4	249
trans-PtL_2Cl_2	290
cis-PtL_2Br_2	334
cis-PtL_2Br_4	223
trans-PtL_2Br_2	279

$L = C_{12}H_{25}NH_2$

Support for this view is found in the $^{195}Pt-^{15}N$ coupling constants for dodecylamine complexes of platinum(II) and platinum(IV), where π-bonding cannot of course occur, which exhibit similar trends (Table 3.24) [156].

As already mentioned, a purely π-bonding mechanism cannot account for the position of hydride in *trans*-effect and *trans*-influence series. Overall, therefore, a major role (though not necessarily the only one) for σ-bonding is implied.

3.9 Palladium(III) and platinum(III) compounds

Mononuclear complexes of palladium and platinum in the +3 oxidation state have only recently been unequivocally characterized [157]. The major advance has come in complexes with macrocyclic ligands such as 1,4,7-trithiacyclononane (ttcn) and 1,4,7-triazacyclononane (tacn) (Figure 3.96).

Complexes of the divalent metals $[M(ttcn)_2]^{2+}$ undergo electrochemical oxidation to paramagnetic $[M(ttcn)_2]^{3+}$. Red $[Pd(ttcn)_2]^{3+}$ has a tetragonally distorted octahedral structure (d^7, Jahn–Teller distortion) with Pd–S 2.356–2.369 Å (equatorial) and 2.545 Å (axial) in keeping with the ESR spectrum ($g_\perp = 2.049$, $g_\parallel = 2.009$) which also displays ^{105}Pd hfs. Similarly, electrochemical oxidation of the palladium(II) tacn complex (at a rather lower

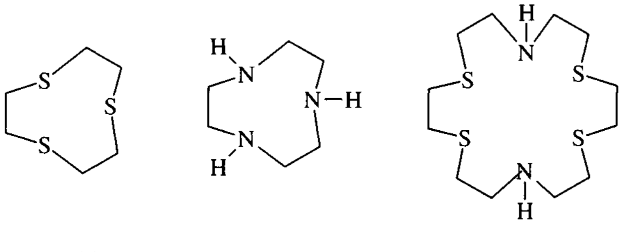

ttcn ($9S_3$) tacn 18[ane]N_2S_4

Figure 3.96 Macrocyclic ligands used to stabilize palladium(III) and platinum(III).

Next Page

Previous Page

Table 3.24 NMR coupling constants for platinum amine complexes [156]

	$J(^{195}Pt-^{15}N)$ (Hz)
cis-PtL_2Cl_2	351
cis-PtL_2Cl_4	249
trans-PtL_2Cl_2	290
cis-PtL_2Br_2	334
cis-PtL_2Br_4	223
trans-PtL_2Br_2	279

$L = C_{12}H_{25}NH_2$

Support for this view is found in the $^{195}Pt-^{15}N$ coupling constants for dodecylamine complexes of platinum(II) and platinum(IV), where π-bonding cannot of course occur, which exhibit similar trends (Table 3.24) [156].

As already mentioned, a purely π-bonding mechanism cannot account for the position of hydride in *trans*-effect and *trans*-influence series. Overall, therefore, a major role (though not necessarily the only one) for σ-bonding is implied.

3.9 Palladium(III) and platinum(III) compounds

Mononuclear complexes of palladium and platinum in the +3 oxidation state have only recently been unequivocally characterized [157]. The major advance has come in complexes with macrocyclic ligands such as 1,4,7-trithiacyclononane (ttcn) and 1,4,7-triazacyclononane (tacn) (Figure 3.96).

Complexes of the divalent metals $[M(ttcn)_2]^{2+}$ undergo electrochemical oxidation to paramagnetic $[M(ttcn)_2]^{3+}$. Red $[Pd(ttcn)_2]^{3+}$ has a tetragonally distorted octahedral structure (d^7, Jahn–Teller distortion) with Pd–S 2.356–2.369 Å (equatorial) and 2.545 Å (axial) in keeping with the ESR spectrum ($g_{\perp} = 2.049$, $g_{\parallel} = 2.009$) which also displays ^{105}Pd hfs. Similarly, electrochemical oxidation of the palladium(II) tacn complex (at a rather lower

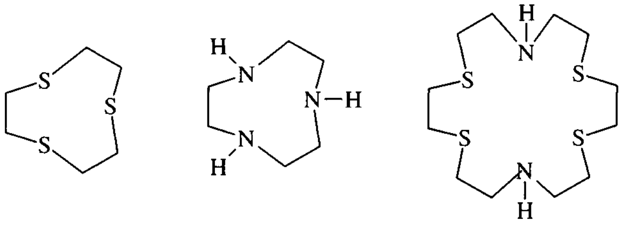

ttcn ($9S_3$) tacn 18[ane]N_2S_4

Figure 3.96 Macrocyclic ligands used to stabilize palladium(III) and platinum(III).

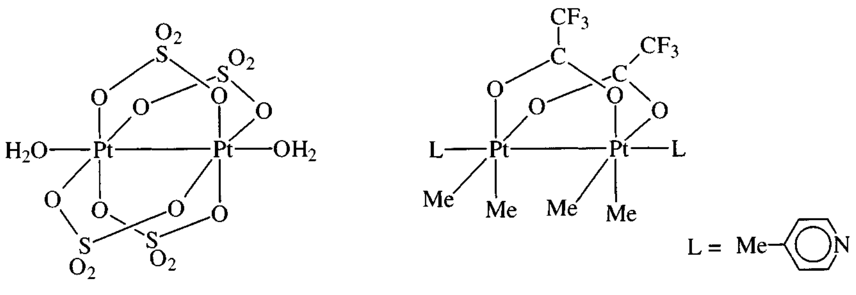

(a) (b)

Figure 3.97 Dinuclear platinum(III) compounds.

potential than the ttcn complex) gives $[Pd(tacn)_2](PF_6)_3$, again with a tetragonally distorted octahedral structure (Pd–N (equatorial) 2.111–2.118 Å; Pd–N (axial) 2.180 Å). The palladium(III) complex of the N_2S_4 macrocycle ([18]ane N_2S_4) (Figure 3.96) has been synthesized by electrochemical oxidation and detected in solution by ESR.

Oxidation of $[Pt(C_6Cl_5)_4]^{2-}$ yields the unusual paramagnetic organometallic $[Pt(C_6Cl_5)]_4^-$ with square planar coordination of platinum

$$[Pt(C_6Cl_5)_4]^{2-} \xrightarrow{Cl_2} [Pt(C_6Cl_5)]_4^-$$

Rather more dinuclear platinum(III) compounds are known [158]; formally the Pt_2^{6+} unit is isoelectronic with Rh_2^{4+}. The first species to be characterized was $Pt_2(SO_4)_4(H_2O)_2^{2-}$ (Figure 3.97a):

$$Pt(NO_2)_4^{2-} \text{ or } Pt(NH_3)_2(NO_2)_2 \xrightarrow[\text{heat}]{\text{conc. } H_2SO_4} [Pt_2(SO_4)_4(H_2O)_2]^{2-} + NO_x$$

Analogous compounds have been made with HPO_4^{2-} bridges; Pt–Pt distances in these compounds are 2.46–2.50 Å. Other dimers include $[Pt_2(\mu\text{-}O_2CMe)_4(H_2O)_2]^{2+}$ [158].

Binuclear platinum(III) methyls have been made, these complexes utilizing carboxylate bridges (Figure 3.97b)

$$\begin{tikzcd}
PtCl_2(R_2S)_2 \arrow[r, "Me_2Mg"] & {[PtMe_2(R_2S)]_2} \\
\arrow[r, "AgO_2CR^1"] & Pt_2Me_4(O_2CR^1)_2(R_2S)_2 \arrow[d, "py"] \\
& Pt_2Me_4(O_2CR^1)_2py_2
\end{tikzcd}$$

while related structures have been made using 2-oxopyridine as the bridging ligand. The compounds with two instead of four such bridges tend to have longer Pt–Pt distances (2.54–2.58 Å) [159].

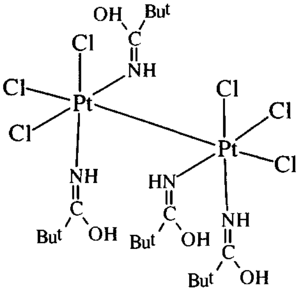

Figure 3.98 A dimeric platinum(III) complex with no bridging ligands.

The presence of bridging ligands is, however, not essential [160].

$$cis\text{-PtCl}_2\{2\text{NCBu}^t\} \xrightarrow[\text{CH}_2\text{Cl}_2]{\text{1. KOH} \quad \text{2. HCl}} cis\text{-PtCl}_2\{\text{NH=C(OH)Bu}^t\}_2 \xrightarrow{\text{Cl}_2} \text{Pt}_2\text{Cl}_6\{\text{NH=C(OH)Bu}^t\}_4$$

The long Pt–Pt bond (2.694 Å) follows the trend observed in rhodium dimers as the number of bridging ligands decreases (Figure 3.98).

As with the 'trihalides', some formally platinum(III) compounds are in fact mixed-valence species [161]. Thus:

$$cis\text{-Pt(NH}_3)_2\text{(SCN)}_2 \xrightarrow{\text{I}_2} \text{Pt(NH}_3)_2\text{(SCN)}_2\text{I}$$

the compound in fact being $[\text{Pt}^{\text{II}}(\text{NH}_3)_2(\text{SCN})_2][\text{Pt}^{\text{IV}}(\text{NH}_3)_2(\text{SCN})_2\text{I}_2]$ [152].

3.10 Complexes of platinum(IV)

Platinum(IV) forms complexes with a range of ligands [1, 2, 10, 11].

3.10.1 *Complexes of N-donors*

The full range of platinum(IV) ammines can readily be prepared [162].

Hexammines

$$(\text{NH}_4)_2\text{PtX}_6 \xrightarrow[-40^\circ\text{C}]{\text{liq. NH}_3} [\text{Pt(NH}_3)_6]\text{X}_4 \qquad (\text{X} = \text{Cl, Br, I})$$

The reaction is best carried out at −40°C, otherwise amide bridged species $[(\text{NH}_3)_4\text{Pt(NH}_2)_2\text{Pt(NH}_3)_4]\text{Cl}_6$ are obtained.

Pentammines

Introducing more than five molecules of ammonia is difficult (hence the use of liquid ammonia in the synthesis of the hexammine), but Chugaev's synthesis of the pentammine is facile:

$$K_2PtCl_6 \xrightarrow[\text{reflux, 10 min}]{NH_3/Na_2HPO_4} [Pt(NH_3)_5Cl]PO_4 \xrightarrow[HCl]{\text{conc.}} [Pt(NH_3)_5Cl]Cl_3$$

Tetrammines

The chloride and bromide can be made by oxidative addition.

$$[Pt(NH_3)_4]Cl_2 \xrightarrow[HCl\,(aq.)]{Cl_2} \textit{trans}\text{-}[Pt(NH_3)_4Cl_2]Cl_2$$

In the triflate salt, Pt–Cl is 2.302–2.309 Å, while Pt–N distances are in the range 2.049–2.059 Å [163].

$$[Pt(NH_3)_4](MeSO_3)_2 \xrightarrow{Br_2} \textit{trans}\text{-}[Pt(NH_3)_4Br_2](MeSO_3)_2$$

The Pt–Br distance is 2.447 Å while Pt–N distances are 2.065–2.068 Å [163].

The *cis*-dichloro complex can be made in a synthesis that makes use of the lability of a Pt–Cl bond *trans* to chloride.

$$\textit{mer}\text{-}[Pt(NH_3)_3Cl_3]^+Cl^- \xrightarrow{NH_3} \textit{cis}\text{-}[Pt(NH_3)_4Cl_2]Cl_2$$

Triammines

$$\textit{cis}\text{-}Pt(NH_3)_2Cl_2 \xrightarrow[2.\ HCl]{1.\ (NH_4)_2HPO_4/\text{reflux}} \textit{mer}\text{-}[Pt(NH_3)_3Cl_3]^+Cl^-$$

This reaction may involve ammoniolysis, followed by oxidative addition [164].

Diammines

$$\textit{cis}\text{-}Pt(NH_3)_2Cl_2 \xrightarrow[80^\circ C]{Cl_2} \textit{cis}\text{-}Pt(NH_3)_2Cl_4$$

$$\textit{trans}\text{-}Pt(NH_3)_2Cl_2 \xrightarrow[100^\circ C]{Cl_2} \textit{trans}\text{-}Pt(NH_3)_2Cl_4$$

These syntheses again involve the retention of configuration on oxidation. In the *cis*-isomer Pt–N is 2.059 Å and Pt–Cl is 2.318 Å (*trans* to N) and 2.322 Å (*trans* to Cl) [165].

Monoammine

$$K[Pt(NH_3)Cl_3] \xrightarrow{Cl_2} K[Pt(NH_3)Cl_5]$$

In this anion, Pt–N is 2.065 Å and Pt–Cl 2.314–2.331 Å (*cis*) and 2.313 Å (*trans*).

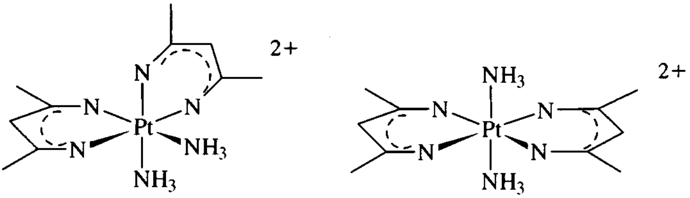

Figure 3.99 Platinum(IV) diimine complexes.

Vibrational spectra of these ammines indicate Pt–N stretching frequencies around 550 cm^{-1} (Raman) and 530 cm^{-1} (IR) [166].

Platinum(IV) ammines react with diketones to give diimmines, a reaction proceeding via deprotonation of one ammonia [167].

A second diimine group can be introduced, obtainable as *cis*- and *trans*-isomers (Figure 3.99).

The platinum(IV) ammines studied in most detail recently [168] have been hydroxy species (Figure 3.100).

The diisopropylamine complex (a) has undergone clinical trials as the drug 'iproplatin' (CHIP); the simple ammonia analogue (b) 'oxoplatin' has shown promising anti-tumour activity (see also section 3.10).

Their synthesis uses H_2O_2 to carry out oxidative addition to platinum(II) ammines

$$\textit{cis}\text{-Pt}(\text{RNH}_2)_2\text{Cl}_2 \xrightarrow{\text{H}_2\text{O}_2} \textit{cis,cis,trans}\text{-Pt}(\text{RNH}_2)_2\text{Cl}_2(\text{OH})_2$$

(R = H, Me_2CH). They are obtained as H_2O_2 adducts (perhydrates) containing lattice H_2O_2. The perhydrate adducts cleave DNA but the unsolvated compounds do not.

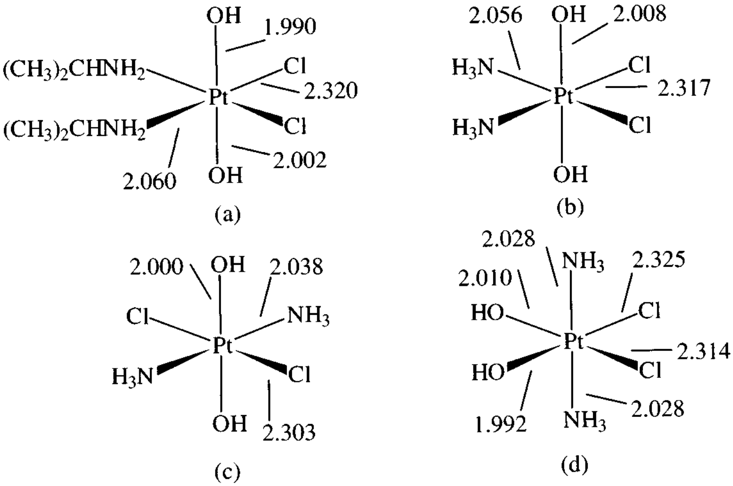

(a) (b)

(c) (d)

Figure 3.100 Bond lengths in platinum(IV) ammine hydroxy complexes.

Table 3.25 The structure of platinum(IV) en complexes

	Pt–N (Å)	Pt–X (Å)
cis-$Pt(en)_2Cl_2^{2+}$	2.045–2.068	2.30–2.31
trans-$Pt(en)_2Cl_2^{2+}$	2.074–2.087	2.313
trans-$Pt(en)_2Br_2^{2+}$	2.04–2.07	2.459
trans-$Pt(en)_2I_2^{2+}$	2.059–2.060	2.681

Oxidation of *trans*-$Pt(NH_3)_2Cl_2$ with H_2O_2 affords the all-*trans* isomer (Figure 3.100c); this isomerizes on recrystallization to give (d). Presumably (c) is the kinetic product while (d) is thermodynamically more stable.

trans-$[Pt(NH_3)_4(OH)_2]Cl_2$ has the expected octahedral coordination with Pt–N and Pt–O distances of 2.042 and 2.004 Å, respectively, distances very similar to those in the all-*trans*-isomer of $Pt(NH_3)_2(OH)_2Cl_2$ [169].

Several complexes with 1,2-diaminoethane have been studied in detail [170].

$$cis\text{-PtenX}_2 \xrightarrow{X_2} cis\text{-PtenX}_4 \qquad (X = Cl, Br)$$

$$(\text{Pten}_2)X_2 \xrightarrow{X_2} [trans\text{-Pten}_2X_2]X_2 \qquad (X = Cl, Br, I)$$

$$(\text{Pten}_2)Cl_2 + 2HCl \xrightarrow[\text{HCl}]{\text{conc.}} trans\text{-}[Pt(enHCl)_2Cl_2]$$

$$\xrightarrow[\text{heat}]{H_2O_2} cis\text{-Pten}_2Cl_2^{2+}Cl_2$$

$$H_2PtCl_6.6H_2O \xrightarrow[80°C]{\text{en/EtOH}} (\text{Pten}_3)Cl_4$$

The Pten_3^{3+} and *cis*-$\text{Pten}_2Cl_2^{2+}$ ions have been resolved, the former by Werner.

Structures of several of these complexes have been determined: data are summarized in Table 3.25.

Another platinum(IV) ammine complex studied as a possible anti-tumour compound is shown in Figure 3.101 [171]; *cis*-(1,2-diaminocyclohexane)tetrachloroplatinum has undergone clinical trials but was found to be too neurotoxic.

Complexes of the more rigid 2,2′-bipyridyl and 1,10-phenanthroline are made:

$$cis\text{-Pt(L–L)Cl}_2 \xrightarrow{Cl_2} cis\text{-Pt(L–L)Cl}_4 \qquad (\text{L–L} = \text{phen, bipy})$$

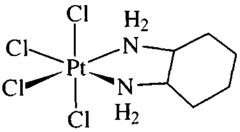

Figure 3.101 *cis*-(1,2-Diaminocyclohexane)tetrachloroplatinum.

Reaction of iodine with $Pt(phen)Cl_2$ gives compounds with the unusual stoichiometrics $Pt(phen)I_x$ ($x = 5, 6$); these contain $Pt(phen)I_4$ molecules and free iodine molecules in the lattice. $Pt(bipy)I_4$ has also been made [172].

Macrocyclic complexes of platinum(IV) are readily made by oxidation:

$$\mathrm{Pt(TPP)} \xrightarrow[\text{2. HCl}]{\text{1. } H_2O_2/CH_3COOH} \mathrm{Pt(TPP)Cl_2}$$

$$\mathrm{Pt[[14]aneN_4]Cl_2} \xrightarrow[O_2]{\text{HCl(aq.)}} \mathrm{[Pt[[14]aneN_4]Cl_2]Cl_2}$$

Six-coordination is confirmed for the latter by X-ray diffraction (Pt–N 2.04 Å, Pt–Cl 2.307 Å) [173].

3.10.2 Tertiary phosphine complexes

The most important of the tertiary phosphine complexes of platinum(IV) are $Pt(QR_3)_2X_4$, generally prepared by halogen oxidation [174] of *cis*- or *trans*-$Pt(QR_3)_2X_2$ ($Q = P$, As, $R =$ alkyl; $Q = Sb$, $R = Me$), since direct reaction of the platinum(IV) halides with the ligands leads to reduction. Once made, the platinum(IV) compounds are stable to reduction:

$$Pt(QR_3)_2X_2 + X_2 \rightarrow Pt(QR_3)_2X_4$$

Generally the configuration is retained on oxidation, though a certain amount of isomerization can take place. (Br_2 added *trans* to *trans*-$Pt(PEt_3)_2Cl_2$ in the dark, but scrambling was found in the light [175].) Anionic and cationic complexes can be made:

$$Pr_4N^+PtX_3L^- + X_2 \rightarrow Pr_4N^+PtX_5L^- \qquad (\text{L, e.g. } PMe_3;\ X = Cl, Br, I)$$

$$Pt(PMe_3)_3Cl^+BF_4^- + Cl_2 \rightarrow mer\text{-}Pt(PMe_3)_3Cl_3^+BF_4^-$$

The structures of the *cis*- and *trans*-isomers of $Pt(PEt_3)_2Cl_4$ have been determined [176]. Table 3.26 shows the bond lengths depend slightly on the *trans*-ligand.

The *cis*-isomer shows slight deviation from regular octahedral symmetry (P–Pt–P 98.1°). The *cis*- and *trans*-isomers can be distinguished in various ways; the far-IR spectra [177] of the *cis*-isomers (*cis*-PtL_2X_4 has 'local' C_{2v} symmetry) has more bands owing to Pt–X stretching between *c.* 280 and 350 cm^{-1} than the *trans*-isomer (D_{4h} symmetry) (Figure 3.102).

Table 3.26 Bond lengths in $Pt(PEt_3)_2Cl_4$ (Å)

	trans-$Pt(PEt_3)_2Cl_4$	*cis*-$Pt(PEt_3)_2Cl_4$
Pt–P (*trans* to P)	2.393	
Pt–P (*trans* to Cl)		2.335
Pt–Cl (*trans* to Cl)	2.332	2.321
Pt–Cl (*trans* to P)		2.394

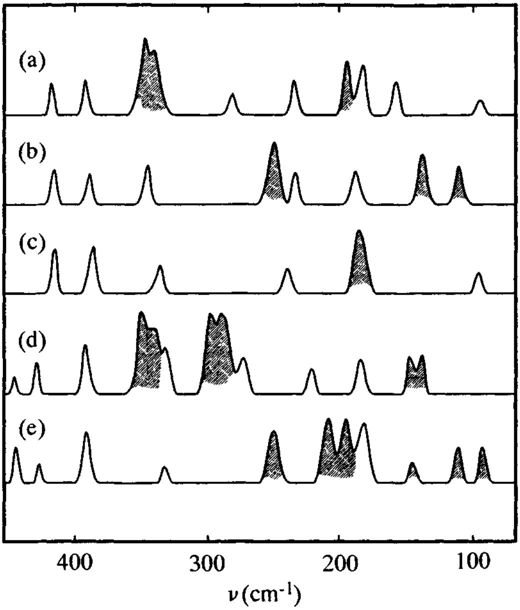

Figure 3.102 Far-IR spectra of (a) *trans*-$Pt(PEt_3)_2Cl_4$; (b) *trans*-$Pt(PEt_3)_2Br_4$; (c) *trans*-$Pt(PEt_3)_2I_4$; (d) *cis*-$Pt(PEt_3)_2Cl_4$; (e) *cis*-$Pt(PEt_3)_2Br_4$. Platinum–halogen vibrations are shaded. (Reproduced with permission from *J. Chem Soc. (A)*, 1967, 1009.)

In the ^{31}P NMR spectra, there is a significant difference in, for example, the $^{195}Pt{-}^{31}P$ coupling constant [155]. Therefore, for *cis*-$Pt(PBu_3)_2Cl_4$, $J = 2070$ Hz; *trans*-isomer, $J = 1462$ Hz).

Some platinum(IV) hydride complexes have been synthesized *in situ* (Figure 3.103).

Solid $PtH_2X_2(PEt_3)_2$ (X = Cl, Br) is isolated by removal of solvent at −20°C; the order of stability is Cl > Br > I and solutions decompose at room temperature, eliminating H_2. Monohydrides $PtHX_3(PR_3)_2$ are less stable [178].

Complexes are similarly formed by polydentate phosphine and arsine ligands; synthetic routes involve oxidation of the platinum(II) complex, either with the halogen or with nitric acid:

$$cis\text{-}Pt(L{-}L)X_2 \xrightarrow[CCl_4]{X_2} cis\text{-}Pt(L{-}L)X_4$$

(L–L, e.g. $Ph_2PCH_2CH_2PPh_2$, $Me_2As(CH_2)_3AsMe_2$, X = Cl, Br)

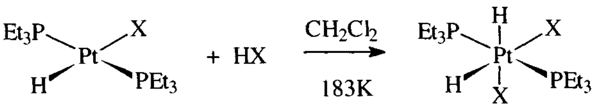

Figure 3.103 Synthesis of a platinum(IV) hydride complex.

$$trans\text{-Pt}[o\text{-}C_6H_4(QMe_2)_2]X_2 \xrightarrow{HNO_3} trans\text{-Pt}[C_6H_4(QMe_2)_2]_2X_2^{2+}$$

(Q = P, As; X = Cl, Br, I).

The structure of the iodo complex (Q = As) shows Pt–As 2.446–2.454 Å, Pt–I 2.669–2.672 Å [179].

3.10.3 *Complexes of S-donors*

The most interesting complexes with Pt–S bonds involve polysulphide rings [180]. The classically simple $[Pt(S_5)_3]^{2-}$ was first reported in 1903; more recently it has been resolved into its enantiomers using (+)-$[Ru(phen)_3]^{2+}$.

$$H_2PtCl_6 \xrightarrow{(NH_4)_2S_5} (NH_4)_2Pt(S_5)_3$$

This was only the third purely 'inorganic' ion (with no carbons) to be resolved [180b], the previous two being 'Werner's hexol' $Co[(\mu\text{-}OH)_2Co(NH_3)_4]_3^{6+}$ (*Chem. Ber.*, 1914, **47**, 3087) and F.G. Mann's *cis*-$[Rh(OH_2)_2[SO_2(NH_2)_2]_2]^-$ (*J. Chem. Soc.*, 1933, 412). The ammonium salt has quite regular octahedral (S–Pt–S 90.9–92.8°) coordination of platinum (Pt–S 2.365–2.428 Å); in the potassium salt, Pt–S distances are 2.332–2.479 Å.

Reaction of $Pt(S_5)_3^{2-}$ with concentrated HCl affords PtS_{17}^{2-}; on treatment with Ph_4P^+ and slow crystallization, disproportionation occurs:

$$3PtS_{17}^{2-} \rightarrow 2Pt(S_6)_3^{2-} + Pt(S_5)_3^{2-}$$

$(Ph_4P)_2Pt(S_6)_3$ again has octahedral coordination by sulphur (Pt–S 2.350–2.366 Å; S–Pt–S 98.4–100.7°) (Figure 3.104) [181].

The thiocyanate $K_2[Pt(SCN)_6].2H_2O$ contains octahedrally coordinated platinum, confirming the readiness of platinum(IV) to bind to a 'soft' donor atom like sulphur [182].

3.10.4 *Application of the* trans-*effect to synthesis of platinum(IV) complexes*

In addition to the methods already outlined for platinum(II) complexes, simultaneous crystallization can be used to prepare mixed complex halides (Figure 3.105).

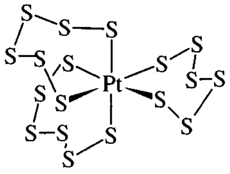

Figure 3.104 Structure of $[Pt(S_6)_3]^{2-}$.

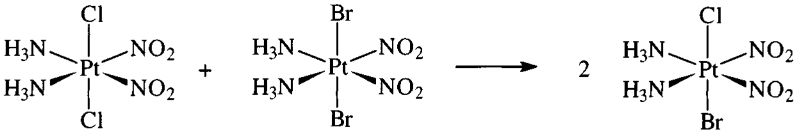

Figure 3.105 Synthesis of $PtBrCl(NH_3)_2(NO_2)_2$ by cocrystallization.

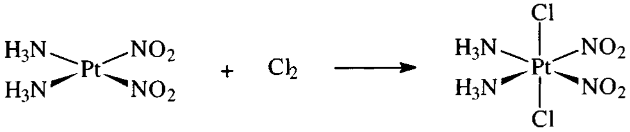

Figure 3.106 Synthesis of a platinum(IV) complex by *trans*-oxidative addition of a platinum(II) complex.

Halogen oxidation of platinum(II) complexes generally occurs *trans*, as does reaction with H_2O_2 to afford dihydroxy complexes (Figure 3.106).

The isomers of $[PtCl_2(NH_3)_4]Cl_2$ may be prepared as shown in Figure 3.107.

The last step is the synthesis of the *cis*-complex involving the *trans*-effect and the lability of Pt—Cl bonds.

The five isomeric forms of $PtBr_2Cl_2(NH_3)_2$ have been isolated by a variety of methods [183]. Isomer 1 is produced by the method shown in Figure 3.108.

The 'obvious' route by *trans*-addition of Br_2 was found to give the desired product contaminated by tri- and tetrabromo species because of substitution reactions (Figure 3.109).

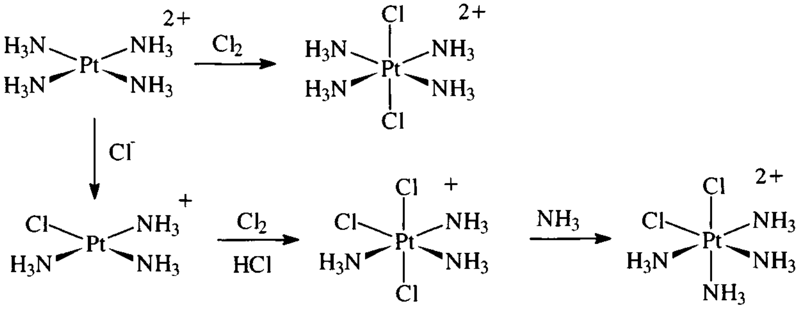

Figure 3.107 Synthesis of the isomers of $[PtCl_2(NH_3)_4]^{2+}$.

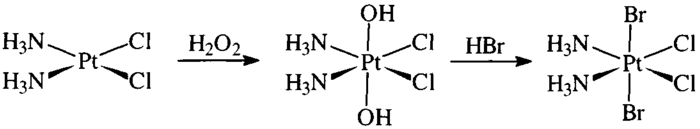

Figure 3.108 Synthesis of the *trans,cis,cis*-isomer (isomer 1) of $PtBr_2Cl_2(NH_3)_2$.

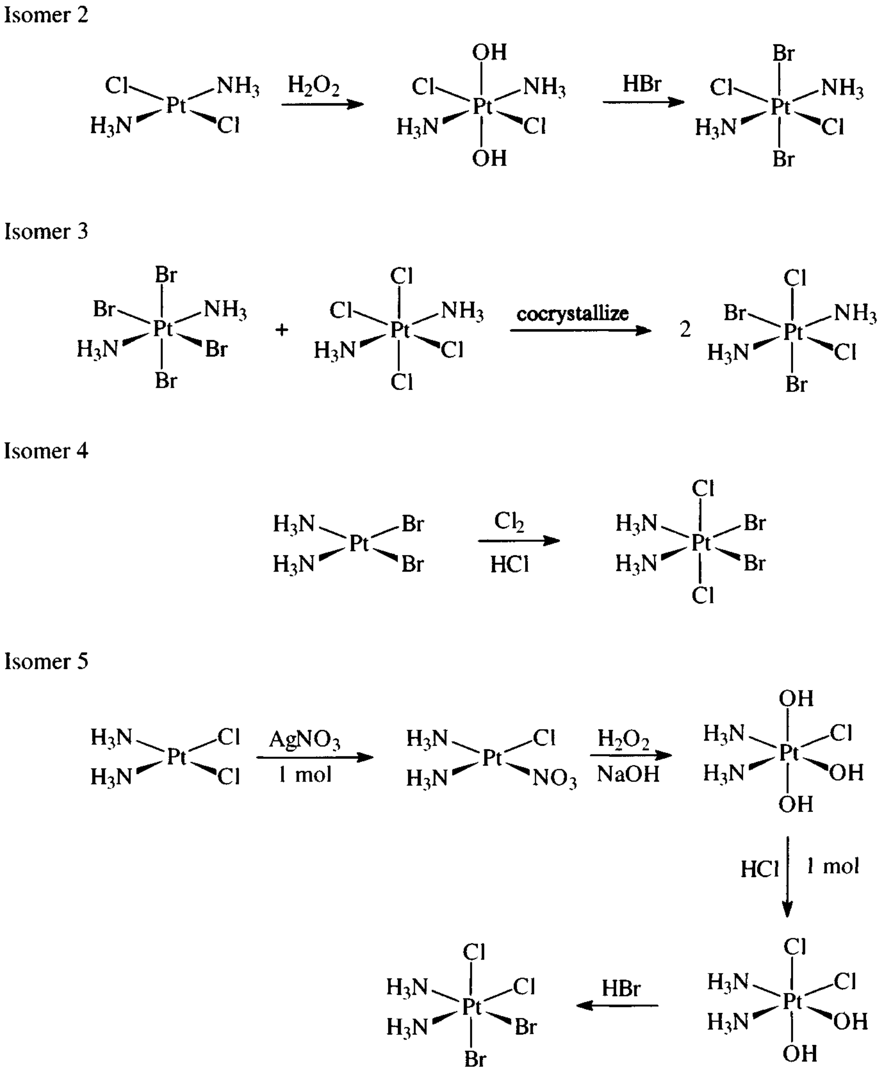

Figure 3.109 Synthesis of the other isomers of $PtBr_2Cl_2(NH_3)_2$.

Complexes of the form 'PtABCDEF' potentially have 15 isomeric forms, and a number of the isomers of $Pt(NH_3)py(NO_2)IBrCl$ have been made [184]. One such synthesis is shown in Figure 3.110.

3.10.5 The trans-*influence in some platinum(IV) complexes*

Table 3.27 shows bond lengths for a number of platinum(IV) and related platinum(II) complexes.

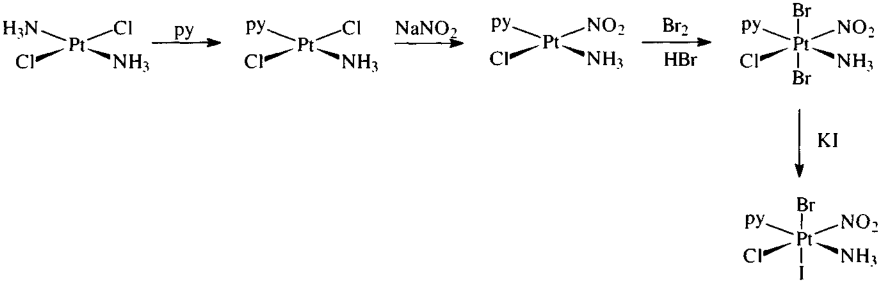

Figure 3.110 Synthesis of one PtABDEF isomer.

The Pt–Cl bond lengths in $PtCl_4^{2-}$ and $PtCl_6^{2-}$ are virtually identical [185], implying that the shortening in bond length consequent upon the increase in oxidation state from +2 to +4 is almost exactly cancelled out by the increase in bond length accompanying an increase in coordination number from 4 to 6. A comparison of *cis*-$Pt(PEt_3)_2Cl_2$ with *cis*-$Pt(PEt_3)_2Cl_4$ [186] indicates that the more 'ionic' Pt–Cl bond is less sensitive to the increase in oxidation state than is the Pt–P bond. Similar effects can be seen in the $PtLCl_x^-$ (L = PEt_3, py; $x = 3, 5$) ions [187].

As far as *trans*-influence is concerned, comparing *cis*- and *trans*-$Pt(PEt_3)_2Cl_4$ [186] shows a considerable *trans*-influence of the tertiary phosphine on the Pt–Cl bond lengths, also found in $Pt(PEt_3)Cl_5^-$. (The pronounced lengthening of the *trans*-Pt–C bond compared with the *cis* bond in $Pt(PEt_3)Cl_5^-$ is greater than that in $Pt(PEt_3)Cl_3^-$, implying the *trans*-influence of the phosphine is greater in the platinum(IV) compound.)

Table 3.27 Bond lengths in platinum(II) and platinum(IV) complexes (Å)

	Pt–Cl (*trans*-Cl)	Pt–Cl (*trans*-L)	Pt–L (*trans*-Cl)	Pt–L (*trans*-L)
$PtCl_4^{2-}$	2.310			
$PtCl_6^{2-}$	2.314			
$Pt(PEt_3)Cl_3^-$	2.300	2.382	2.215	
$Pt(PEt_3)Cl_5^-$	2.316	2.424	2.308	
$PtpyCl_3^-$	2.296[a]	2.305	2.018	
$PtpyCl_5^-$	2.319[a]	2.313	2.062	
cis-$Pt(PEt_3)_2Cl_2$	2.301		2.258	
cis-$Pt(PEt_3)_2Cl_4$	2.321	2.394	2.335	
trans-$Pt(PEt_3)_2Cl_4$	2.332			2.393

[a] Average value.

3.11 Complexes of palladium(IV)

Compared with the plethora of platinum(IV) compounds, the palladium(IV) complexes are as yet relatively few in number [10, 11]. When isolable, they tend to resemble the corresponding platinum compounds.

The PdX_6^{2-} (X = halogen) complexes are described in section 3.3.1. A limited range of complexes have been made by oxidation of palladium(II) species [188]:

$$trans\text{-}PdL_2Cl_2 \xrightarrow{Cl_2} trans\text{-}PdL_2Cl_4$$

(L = NH_3, py, PPr_3, $AsMe_2Ph$)

$$trans\text{-}Pd(Me_3N)_2Br_2 \xrightarrow{Br_2} trans\text{-}Pd(Me_3N)_2Br_2$$

$$R_4N^+PdX_3L^- \xrightarrow{X_2} R_4N^+PdX_5L^-$$

(X = Cl, L = $AsEt_3$, NMe_3, py, Me_2S, Me_2Se; X = Br, L = $AsEt_3$, PEt_2Ph, py, Me_2S, Me_2Se)

$$Pd(L{-}L)Cl_2 \xrightarrow[CCl_4]{Cl_2} Pd(L{-}L)Cl_4$$

(L–L = phen, bipy, $Me_2NC_2H_4NMe_2$).

The limited stability of these compounds is shown by the fact that other tertiary phosphines and arsines do not yield isolable products.

With chelating phosphine and arsine ligands, two types of complex have been isolated:

$$Pd(L{-}L)X_2 \xrightarrow{X_2} Pd(L{-}L)X_4$$

(L–L, e.g. $Me_2P(CH_2)_2PMe_2$, $o\text{-}C_6H_4(AsMe_2)_2$; X = Cl, Br)

$$Pd(L{-}L)_2Cl_2 \xrightarrow{Cl_2} Pd(L{-}L)Cl_4$$

(L–L = $o\text{-}C_6H_4(AsMe_2)_2$, $Ph_2QC_2H_4QPh_2$; Q = P, As)

$$Pd(L{-}L)_2X_2 \xrightarrow[HX,\,0^\circ C]{conc.\ HNO_3} Pd(L{-}L)_2X_2^{2+}$$

(L–L = $Me_2P(C_2H_4)PMe_2$, $o\text{-}C_6H_4(QMe_3)_2$; Q = P, As).

Crystallography confirms structures for $Pd(bipy)Cl_4$ (Pd–N 2.037–2.044 Å; Pd–Cl *trans* to N 2.289–2.290 Å, Pd–Cl *trans* to Cl 2.302–2.310 Å) and $Pd[C_6H_4(AsMe_2)_2]_2Cl_2(ClO_4)_2$ (Pd–Cl 2.302 Å; Pd–As 2.452–2.455 Å) (Figure 3.111). Other compounds isolated include a complex of the tetradentate (N_4) macrocycle cyclam $[Pd(cyclam)Cl_2](NO_3)_2$, a tellerate $Na_8K_2H_4[Pd_2Te_4O_{24}H_2].20H_2O$, and some methyl palladium complexes such as *fac*-$PdMe_3(bipy)I$.

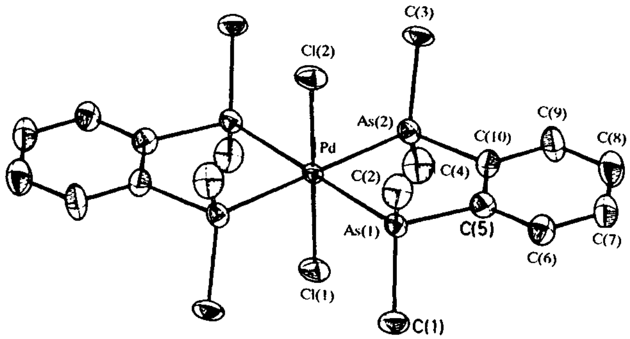

Figure 3.111 The structure of the cation in $[Pd\{o\text{-}C_6H_4(AsMe_2)_2\}Cl_2]ClO_4$. (Reproduced with permission from *J. Chem. Soc., Dalton Trans.*, 1983, 133.)

Just as many palladium(IV) complexes are produced by halogen oxidation of the corresponding palladium(II) complex, so the palladium(IV) compounds tend to decompose by the reverse process, usually on heating:

$$cis\text{-}Pd(bipy)Cl_4 \rightarrow Cl_2 + cis\text{-}Pd(bipy)Cl_2$$

3.12 The σ-bonded organometallics of palladium(IV) and platinum(IV)

Palladium and platinum form a wide range of very stable alkyls and aryls in the (+2) state (section 3.8.4) generally with 'supporting' ligands like tertiary phosphines [85, 189].

There is also a considerable chemistry, especially of platinum, in the +4 state, some of these being among the most stable σ-bonded organometallics known. The prototype compound $PtMe_3I$ was reported as long ago as 1907 (Pope and Peachey) and certain of its features have become clear particularly as a result of studies since the 1960s.

1. No homoleptic tetramethyl has been made, though $PtMe_6^{2-}$ and Lewis base adducts $PtMe_4L_2$ ($L = PMe_2Ph$, 1/2 bipy etc.) can be made.
2. Platinum(IV) exhibits an exceptionless preference for octahedral coordination in these complexes, using bridging ligands when necessary to achieve this.

Many of these compounds are trimethyls [190]. A selection of syntheses and structures are shown in Figures 3.112 and 3.113.

While $(Bu_4N)_2PtMe_6$ is only stable at room temperature under nitrogen, the trimethyls in particular are rather stable: bond energies of 160–210 kJ mol^{-1} have been estimated for Pt–Me bond energies in various platinum(IV) methyls [191].

The β-diketonates demonstrate that, like platinum(II), platinum(IV) can bond to both carbon and oxygen atoms in the diketonate ligand.

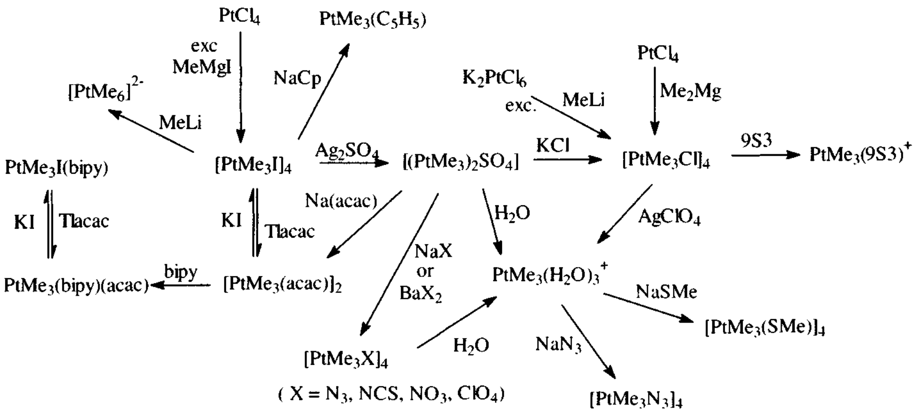

Figure 3.112 Syntheses and reactions of methylplatinum(IV) compounds.

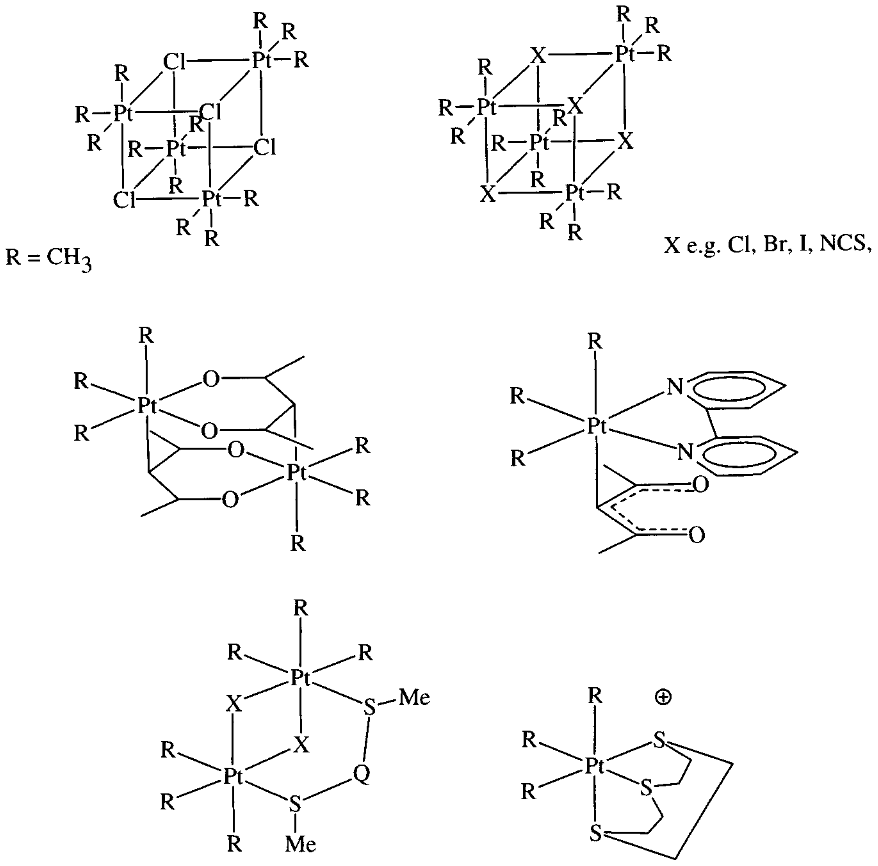

Figure 3.113 Structures of some methylplatinum(IV) compounds

Six-coordination is obtained in $[PtMe_3(acac)]_2$ by bidentate (O,O′) behaviour and by a bond to the γ-carbon, a situation maintained in solution at room temperature (on warming, the bond to the γ-carbon breaks). In the bipyridyl adduct, it is the bond to the γ-carbon that completes the octahedral coordination [192].

Complexes like $(PtMe_3X)_2MeQCH_2QMe$ (X = halogen; Q = S, Se) are rigid at low temperatures, but on warming, inversion occurs in the $Pt{-}Q{-}CH_2{-}Q{-}Pt$ rings, then above 0°C the bridging dithioether (or selenoether) switches synchronously from one platinum to another. The thioether 1,4,7,10-tetrathiocyclododecane is only tridentate in *fac*-$PtMe_3(C_8H_{16}S_4)^+$ and in solution there is exchange between bound and unbound sulphur; this is in contrast to the complex of the tridentate 1,4,7-trithiacyclononane where all three sulphurs are simultaneously bound [193].

All the trimethylplatinum(IV) species have a *fac*-arrangement of the methyls; this is enforced in the $[PtMe_3X]_4$ oligomers, but nevertheless appears to reflect a genuine stereochemical preference (e.g. the isoelectronic *fac*-$Ir(PMe_2Ph)_3Me_3$, section 2.13.5).

The *trans*-influence can be monitored in $PtMe_3$ complexes by both NMR and IR spectra. The coupling constants between the platinum and the methyl hydrogens ($^2J(^{195}Pt{-}^1H)$) is sensitive to the other atoms bound to platinum, ranging from 81.7 Hz ($(PtMe_3Cl)_4$) to 60.8 Hz ($PtMe_3(CN)_3^-$), the order being $CN < py < NH_3 < SCN < I < H_2O < Br < Cl$ [194].

A strong line is seen in the Raman spectra of these complexes that is assigned to ν(Pt–C); typical values are 600 cm^{-1} ($PtMe_3(H_2O)_3^+$), 581 cm^{-1} ($(PtMe_3Cl)_4$) and 553 cm^{-1} ($PtMe_3(CN)_3^-$); here the frequency order is $CN < I < SCN < Br < py < Cl < NH_3 < H_2O$, correlating better with other *trans*-influence series based on vibrational spectra.

Although they are η^5-organometallics, it is pertinent to mention compounds like $PtMe_3(\eta^5\text{-}C_5H_5)$; the cyclopentadienyl group can be thought of as occupying three coordination sites, so that the complexes may, again, be considered to involve octahedrally coordinated platinum(IV). With a volatility comparable to a metal carbonyl (b.p. 20°C at 0.01 mmHg) it decomposes to platinum metal and methane on heating (*c.* 165°C) or on irradiation; laser photolysis of complexes of this type is being actively studied as a way of depositing thin platinum films. Other trimethylplatinum(IV) species undergo photoemission with reductive elimination to platinum(II) species [195].

The only homoleptic organoplatinum(IV) compound synthesized so far is $Pt(C_6Cl_5)_4$, produced by electrochemical oxidation of the platinum(III) analogue or by chemical oxidation with Cl_2 in the presence of $AlCl_3$

$$[Pt(C_6Cl_5)_4]^- \xrightarrow{Cl_2} [Pt(C_6Cl_5)_4]$$

The diamagnetic orange compound is air and moisture-stable but eliminates $C_6Cl_5{-}C_6Cl_5$ on standing. The crystal structure shows that the octahedral

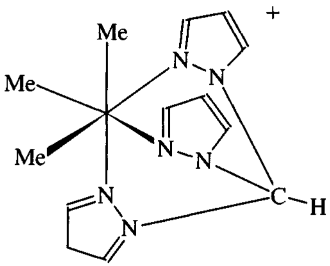

Figure 3.114 Structure of *fac*-$[PdMe_3(pz_3CH)]^+$.

coordination characteristic of Pt(IV) is attained by four Pt—C σ-bonds and two Pt—*o*-Cl interactions [196].

Very recently a significant organopalladium(IV) chemistry has begun to emerge [197], with isolable species like *fac*-$PdMe_3$(bipy)I (stable at 20°C but decomposing in solution in 30–40 min at room temperature) and *fac*-$[PdMe_3(pz_3CH)]^+I^-$ (Figure 3.114) (isomorphous with the platinum analogue).

Methylplatinum phosphine complexes have been synthesized in both the +2 and +4 oxidation states (see also section 3.8.4). Syntheses for a number of these with the tertiary phosphine PMe_2Ph, which appear to be typical, are shown in Figure 3.115.

(The use of this phosphine facilitates assignment of configuration as 'virtual coupling' is observed when the phosphines are *trans* (section 2.9.5).) Syntheses follow established routes using methyllithium as an alkylating agent; the platinum(IV) complexes can be made by direct alkylation of platinum(IV) compounds or by oxidative addition to platinum(II) species.

Assignment of stereochemistry for these compounds follows from NMR spectra (also from electric dipole moments). Therefore, when *trans*-$PtMeX(PMe_2Ph)_2$ (dipole moments 3.8–3.95 Debye) adds X_2, the resulting $PtMeX_3(PMe_2Ph)_2$ is assigned configuration (I) in Figure 3.115b, as NMR shows the phosphines still to be *trans* while the dipole moment is virtually unchanged (4.3 Debye, X = Cl). When *trans*-$PtMeX(PMe_2Ph)_2$ adds MeX forming *cis,cis,trans*-$PtMe_2X_2(PMe_2Ph)_2$ (Figure 3.115b, II), the NMR spectrum shows the phosphines to remain *trans*; the complex can also be made by treating $PtMe_3Cl(PMe_2Ph)_2$ with Cl_2, causing loss of MeCl. NMR shows that $PtMe_4(PMe_2Ph)_2$ is *cis* (Figure 3.115b, IV) as the methyl resonances are a doublet rather than the 'virtual' 1:2:1 triplet for a *trans*-arrangement.

Addition of MeCOX to *cis*-$PtMe_2(PMe_2Ph)_2$ yields $PtMe_2X(COMe)(PMe_2Ph)_2$ (Figure 3.15b,V); here the acetyl group *cis* to the methyls doubtless assists the elimination of Me_2CO on pyrolysis, as will be seen in the next section [198].

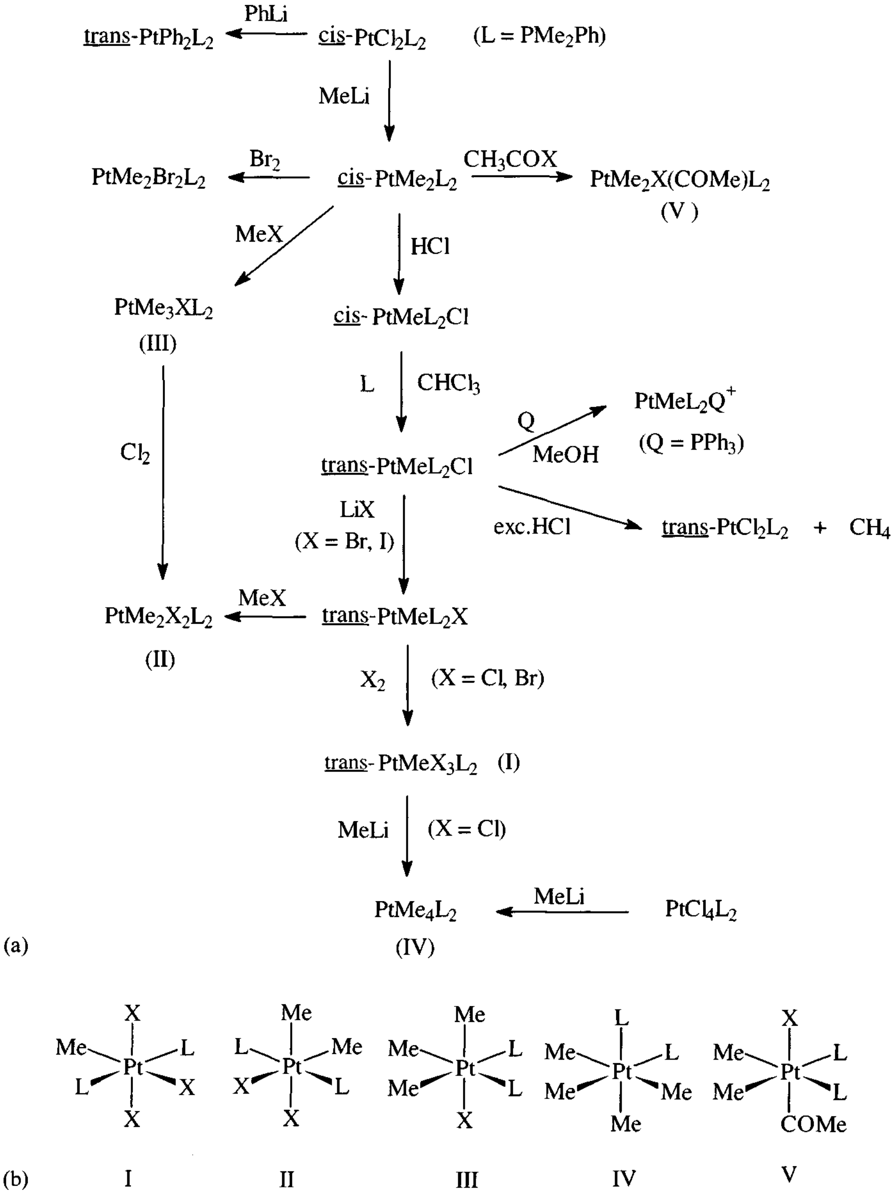

Figure 3.115 (a) Syntheses of organoplatinum phosphine complexes; (b) structures of methylplatinum phosphine complexes.

3.12.1 Reductive elimination reactions

Many platinum(IV) alkyls undergo this process on heating to 150–180°C, with the elimination of a small organic molecule and formation of a platinum(II) product [198, 199].

Reactions often proceed solely by one route:

$$\mathrm{PtMe_2(COMe)X(PMe_2Ph)_2} \xrightarrow{130^\circ\mathrm{C}} \mathrm{Me_2CO} + trans\text{-}\mathrm{PtMeX(PMe_2Ph)_2}$$

$$cis\text{-}\mathrm{PtMe_4(PMe_2Ph)_2} \xrightarrow{160^\circ\mathrm{C}} \mathrm{C_2H_6} + cis\text{-}\mathrm{PtMe_2(PMe_2Ph)_2}$$

$$fac\text{-}\mathrm{PtMe_3I(PMe_2Ph)_2} \xrightarrow{165^\circ\mathrm{C}} \mathrm{C_2H_6} + trans\text{-}\mathrm{PtMeI(PMe_2Ph)_2}$$

Mixtures are, however, often obtained:

$$mer\text{-}\mathrm{PtMeX_3(PMe_2Ph)_2} \rightarrow \mathrm{MeX} + cis\text{- and } trans\text{-}\mathrm{PtX_2(PMe_2Ph)_2}$$

$(X = \mathrm{Cl, Br})$

$$fac\text{-}\mathrm{PtMe_3Cl(PMe_2Ph)_2} \rightarrow \mathrm{C_2H_6}\,(90\%) + trans\text{-}\mathrm{PtMeCl(PMe_2Ph)_2} + \mathrm{MeCl}\,(10\%)$$

Compounds with N-donor ligands tend to be more stable and not to undergo reductive elimination:

$$\mathrm{PtMe_3Xpy_2} \xrightarrow{-\mathrm{py}} [\mathrm{PtMe_3Xpy}]_2 \xrightarrow{-\mathrm{py}} [\mathrm{PtMe_3X}]_4$$

The Pt–CF_3 bond is stronger than the Pt–Me bond so that the latter is preferentially broken

$$\mathrm{PtMe_2(CF_3)I(PMe_2Ph)_2} \xrightarrow{180^\circ\mathrm{C}} trans\text{-}\mathrm{Pt(CF_3)I(PMe_2Ph)_2} + \mathrm{C_2H_6}$$

$$\mathrm{PtMe(CF_3)I_2(PMe_2Ph)_2} \xrightarrow{225^\circ\mathrm{C}} trans\text{-}\mathrm{Pt(CF_3)I(PMe_2Ph)_2} + \mathrm{MeI}$$

A kinetic study of the reaction, retarded by excess phosphine [189],

$$fac\text{-}\mathrm{PtMe_3X(PMe_2Ph)_2} \rightarrow \mathrm{C_2H_6} + trans\text{-}\mathrm{PtMeX(PMe_2Ph)_2}$$

indicates prior dissociation of a tertiary phosphine followed by an intramolecular elimination of C_2H_6. When the chelating diphosphine ($Ph_4PC_2H_4PPh_2$) analogue is decomposed, the elimination occurs without prior dissociation of the phosphine (the decomposition of *fac*-$PdMe_3I$(bipy) is first order and retarded by iodide, suggesting that here iodide loss is followed by decomposition of a 5-coordinate intermediate).

Study of the reductive elimination reactions of *fac*-$PtMe_3$(dppe)I leads to estimated Pt–Me and Pt–I bond energies of 132 and 196 kJ mol^{-1}, respectively [200].

$$fac\text{-}\mathrm{PtMe_3(dppe)I} \rightarrow cis\text{-}\mathrm{PtMe_2(dppe)} + \mathrm{MeI}$$

and

$$cis\text{-}\mathrm{PtMeI(dppe)} + \mathrm{C_2H_6}$$

A Pt–Si bond energy of 233 kJ mol^{-1} has been estimated from study of the process

$$PtMe_2I(SiMe_3)(bipy) \rightarrow Me_4Si + PtMeI(bipy)$$

Some reactions of $PtMe_4L_2$ systems do not involve reductive elimination; thus reaction of $PtMe_4(NN)$ (NN = phen, bipy) with organic acids yielding $PtMe_3A(NN)$ (A = formate, acetate, benzoate, salicylate) is first order in both reactants [201].

3.13 Anti-tumour activity of platinum complexes

The initial discovery of a potential anti-tumour activity of platinum complexes [202] was made in the 1960s by Barnett Rosenberg's research group, who were studying the effect of an electric current on the bacterium *Escherichia coli*: cell division was prevented although cell growth continued if platinum electrodes were used. The platinum had reacted with ammonium chloride buffer to form ammine complexes. Tests showed that *cis*-$Pt(NH_3)_2Cl_4$ and *cis*-$Pt(NH_3)_2Cl_2$ were active compounds.

Anti-tumour screening showed that *cis*-$Pt(NH_2)_2Cl_2$ (but not the *trans*-isomer) was a very active agent and clinical tests were started in 1971. A number of side-effects were experienced – kidney toxicity, neurotoxicity, nausea, vomiting, inner ear damage and loss of sensation in head and feet – combated by pre- and post-hydration treatment and forced diuresis with mannitol solutions. Used in conjunction with other drugs, intravenous *cis*-$Pt(NH_3)_2Cl_2$ (cisplatin) received Food & Drug Administration (FDA) approval in 1979 and has been found to give 90% long-term remission of testicular cancer, with good results for ovarian, bladder, head and neck tumours. Obviously there is a need for drugs to counter the more common cancers, those of the lung and breast for example. There has, therefore, been an intensive screening programme investigating many compounds (not just involving platinum) of which a number have been investigated clinically, but at the time of writing only two platinum complexes have received FDA approval.

It has been found that certain features are desirable, if not essential, in 'active' platinum complexes:

1. Two ammine groups (with at least one H per N) in a *cis*-configuration (or a bidentate ammine)
2. The presence of good leaving groups like chloride or carboxylate in a *cis*-configuration
3. An uncharged complex.

Palladium(II) complexes with these features are inactive, owing to their greater lability. Platinum(IV) complexes are often less toxic than their platinum(II) analogues, because of their stability to substitution, though it is believed that they undergo *in vivo* reduction to platinum(II).

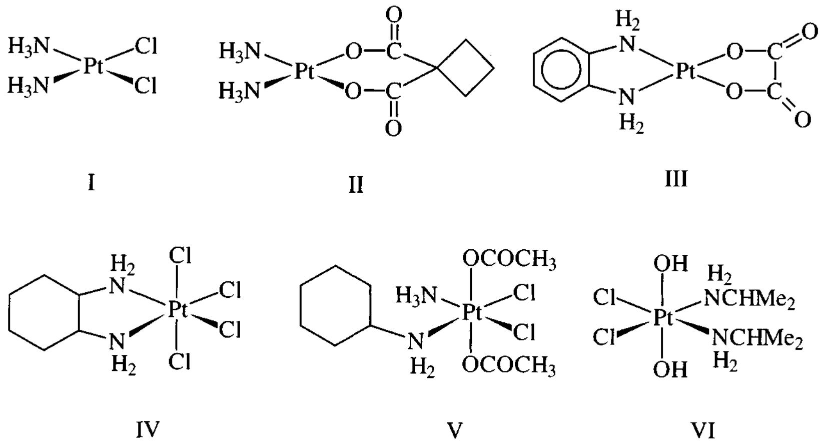

Figure 3.116 Platinum compounds studied for possible anti-tumour activity. I, *cis*-Dichlorodiammineplatinum(II); cisplatin, platinol; NSC 119875; neoplatin; platinex. II, *cis*-Diammine(1,1-cyclobutanedicarboxylato)platinum(II); JM-8; paraplatin; NSC 241240. III, Oxiplatin. IV, Tetraplatin. V, Amminediacetatodichloro(cyclohexylamine)platinum(IV). VI, *cis*-Dichloro-*trans*-dihydroxy-*cis*-bis(isopropylamine)platinum(IV); iproplatin; JM-19; CHIP; NSC 256927.

The platinum(IV) compound that has shown most promise is carboplatin (paraplatin), which received FDA approval in 1990. Features to note in its structure are the use of hydroxy and carboxylate groups to improve water solubility. As noted above, the ammine ligand has been found to need at least one hydrogen, possibly for hydrogen-bonding to phosphate groups in the DNA (Figure 3.116).

Carboplatin is less nephrotoxic than cisplatin and it also causes less nausea, though it does cause lowered platelet levels. It is being used to treat ovarian tumours. Interest in alternative methods of ingestion is leading to the study of compounds capable of being administered orally (Figure 3.117a) and that are reduced *in situ* to reactive platinum(II) species (Figure 3.117b). Compounds of this type are under review for activity [203], with JM-216 (bis(acetato-*O*)amminedichloro(cyclohexylamine)platinum(IV)) undergoing worldwide clinical trials.

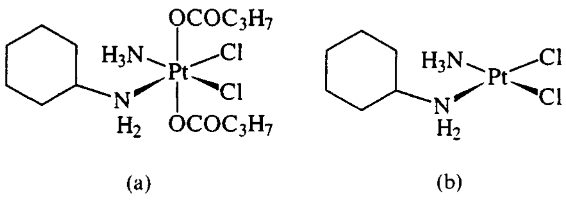

Figure 3.117 (a) JM-216, a platinum(IV) compound under clinical tests as an orally administered anti-tumour agent; (b) the platinum(II) product of *in vivo* reduction, likely to be the active species.

Dimeric complexes like $[Cl(NH_3)Pt\{H_2N(CH_2)_4NH_2\}Pt(NH_3)Cl]Cl_2$ are also being investigated as they bind to DNA in a different way to that involved in cisplatin binding and are active in cisplatin-resistant human tumour cells. They are more potent than cisplatin in lung cancer models *in vivo* and are likely to go on clinical trials in the near future [204].

How cisplatin works [202, 205]

Cisplatin cannot be taken orally owing to hydrolysis in gastric juice. In blood, some is bound to plasma protein and excreted venally, the rest is transported in the blood as uncharged $Pt(NH_3)_2Cl_2$ molecules, which pass unaltered through cell walls. Once through the cell walls, however, the cisplatin undergoes hydrolysis to *cis*-$[Pt(NH_3)_2Cl(H_2O)]^+$ and, more slowly, to *cis*-$[Pt(NH_3)_2(H_2O)_2]^{2+}$, owing to the lower intracellular Cl^- concentration (4 mM, compared with 100 mM outside)

$$\textit{cis}\text{-}[Pt(NH_3)_2Cl_2] + H_2O \rightarrow Cl^- + \textit{cis}\text{-}[Pt(NH_3)_2Cl(H_2O)]^+$$

$$\textit{cis}\text{-}[Pt(NH_3)_2Cl(H_2O)]^+ + H_2O \rightarrow Cl^- + \textit{cis}\text{-}[Pt(NH_3)_2(H_2O)_2]^{2+}$$

Loss of Cl^- makes the platinum complex more reactive, since water is better leaving group than Cl^-.

The ability of cisplatin to be toxic to tumour cells is believed to relate to its binding to DNA, but since *trans*-$[Pt(NH_3)_2Cl_2]$ also binds to DNA, the reason for the inactivity of the *trans*-form is more complex.

Cisplatin has been shown to form adducts with DNA mainly by forming intrastrand cross-links (Figure 3.118); it does so by binding to adjacent guanines (mainly) or adjacent guanine and adenine groups: these occupy the *cis*-positions originally filled by Cl^-, as seen in the model compound *cis*-$[Pt(NH_3)_2\{d(pGpG)\}]$ (Figure 3.119). This structure also shows an

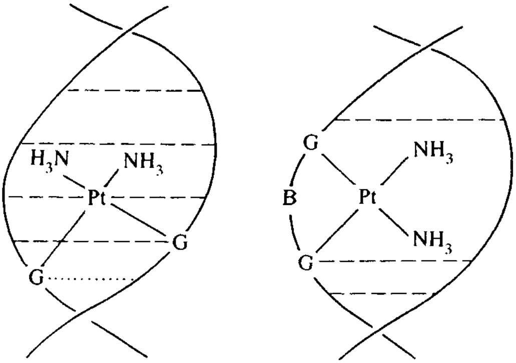

Figure 3.118 Possible modes of cisplatin binding to DNA strands. (Reproduced from J.J.R. Frausto da Silva and R.J.P. Williams, *The Biological Chemistry of the Elements*, 1994, p. 539, by permission of Oxford University Press.)

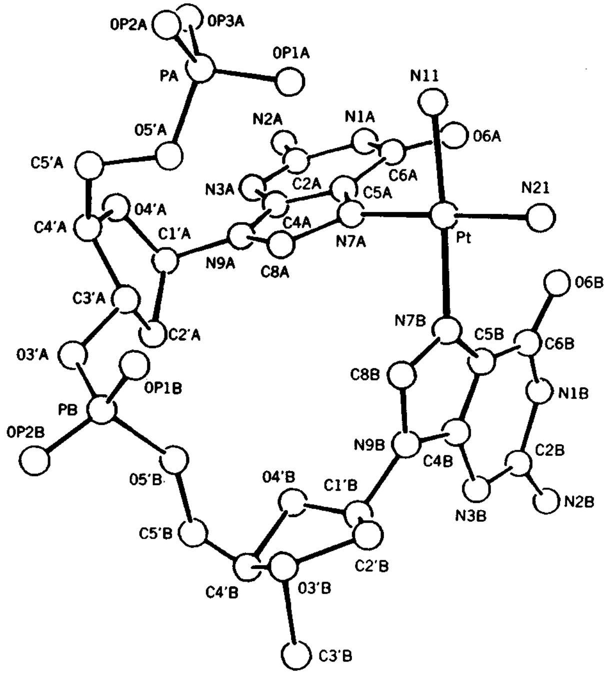

Figure 3.119 *cis*-$Pt(NH_3)_2[d(pGpG)]$, model compound for the binding of cisplatin to DNA. (Reprinted with permission from *Science*, 1985, **230**, 430. Copyright (1985) American Association for the Advancement of Science.)

intramolecular hydrogen bond to a phosphate group, which probably explains the need for amine ligands with at least one hydrogen. The need to replace two Cl^- explains why species like $[Pt(dien)Cl]^+$, with only one labile Cl^-, are inactive. Because of the different geometry of *trans*-$Pt(NH_3)_2Cl_2$ molecules, they are unable to emulate cisplatin by forming intrastrand 1,2-d(GpG) or 1,2-d(ApG) cross-links with neighbouring guanines and adenines; instead they form *interstrand* cross-links or intrastrand 1,3-d(GpNpG) links (where N represents another, intervening, nucleotide base).

Binding of cisplatin to the neighbouring bases in the DNA disrupts the orderly stacking of the purine bases; when it forms a 1,2-intrastrand cross-link, it bends the DNA helix by some 34° towards the major groove and unwinds the helix by 13°. These cross-links are believed to block DNA replication.

Cisplatin-modified DNA specifically binds certain proteins, several of which are known to contain the high-mobility group (HMG) domain of 80 amino acids. It is thought that HMG-domain proteins recognize cis-platinated DNA adducts in the cancer cell and are diverted from their usual binding sites on the genome, thus shielding the point of cisplatin binding from the DNA repair enzymes. This maintains the ability of the bound cisplatin to stop replication from happening and results in death of the tumour cell [205].

The body excretes platinum in various ways, mainly through urine; the complex Pt(L-methionine-SN)$_2$ is one of the few characterized products [206].

Table 3.28 Bond lengths for palladium and platinum congeners (Å)

	Bond	M		Ref.
		Pd	Pt	
$M(PBu^t_3)_2$	M–P	2.285	2.249	207(a)
$M(PBu^t_2Ph)_2$	M–P	2.285	2.252	207(b)
$M(Pcy_3)_2$	M–P	2.26	2.231	207(c)
$M(PPh_3)_3$	M–P	2.307–2.322	2.262–2.277	207(d)
trans-$MI_2(C_4H_8S)_2$	M–S	2.316–2.329	2.309–2.310	207(e)
	M–I	2.603–2.625	2.606–2.610	
cis-MCl_2 (bipy)	M–N	2.03	2.001	207(f)
	M–Cl	2.297	2.306	
cis-$M(Me_2)(PPh_2Me)_2$	M–P	2.323	2.284	207(g)
	M–C	2.090	2.120	
cis-$MCl_2(PMe_3)_2$	M–P	2.257	2.238	207(h)
	M–Cl	2.368	2.372	
MCl_4^{2-}	M–Cl	2.299	2.308	207(i)
MBr_4^{2-}	M–Br	2.438	2.445	207(j)
MF_6^{2-}	M–F	1.896	1.922	207(k)
MCl_6^{2-}	M–Cl	2.309	2.315	207(l)
MBr_6^{2-}	M–Br	2.466–2.470	2.481	207(m)
MCl_4(bipy)	M–N	2.307–2.044	2.038–2.044	207(n)
	M–Cl (*trans*-Cl)	2.302–2.310	2.316–2.320	
	M–Cl (*trans*-N)	2.289–2.290	2.306–2.307	
trans-$MCl_2(Pcy_3)_2$	M–P	2.363	2.337	207(o)
	M–Cl	2.301	2.317	
$M(PPh_3)_2C_{60}$	M–P	2.315–2.330	2.253–2.303	207(p)
	M–C	2.086–2.123	2.115–2.145	
$MMe_3[(pz)_3CH]^+$	M–C	2.039–2.060 (av. 2.048)	2.031–2.056 (av. 2.048)	207(q)
	M–N	2.191–2.225 (av. 2.208)	2.156–2.189 (av. 2.169)	
$M(DMSO)_4^{2+}$	M–S	2.240–2.249 (av. 2.245)	2.205–2.208 (av. 2.207)	207(r)
	M–O	2.061–2.065 (av. 2.063)	2.040–2.051 (av. 2.045)	
$M(PBu^t_2Ph)_2O_2$	M–P	2.357–2.360	2.290	207(s)
	M–O	2.05–2.06	2.02	
trans-$M(P–P)Cl_2$[a]	M–P	2.307	2.293	207(t)
	M–Cl	2.306	2.304	
MCl_2(dppe)	M–P	2.226–2.223 (av. 2.230)	2.208	207(u)
	M–Cl	2.357–2.361 (av. 2.359)	2.341–2.355 (av. 2.348)	
$[M(CNMe)_4](PF_6)_2$	M–C	1.981	1.990	207(v)

[a] P–P = 2,11-bis(diethylphosphinomethyl)benzo[c]phenanthrene.

3.14. Bond lengths in palladium and platinum analogues

Table 3.28 compares bond lengths for a series of congeners of platinum and palladium [207]. One fact that emerges is that bonds from a given atom to palladium and platinum have very similar lengths. There is, however, a pattern; *in general* for the more ‘ionic’ (e.g. metal–halogen) bonds; the bond to platinum is often slightly longer, whereas for the more ‘covalent’ bonds (e.g. metal–nitrogen or phosphorus) it is the bond to palladium that is slightly longer.

4 Silver and gold

4.1 Introduction

For many years, the chemistry of silver and gold was believed to be more similar than is now known to be the case [1–10]. In the Cu–Ag–Au triad, the stability of oxidation states does not follow the usual trend of increasingly stable high oxidation state on descending the group; for copper, the +2 state is the most important, for silver it is the +1 state and, though oxidation states between −1 and +7 are claimed, for gold it is the +1 and +3 states that dominate its chemistry. The types of compound are summarized in Table 4.1.

A plausible reason (or one of the reasons) for the relative stabilities of the oxidation states lies in the ionization energies (Table 4.2) [11]. The value of I_1 is lower for silver than for copper, as would be expected, but I_2 is higher for silver (this electron is removed from a 4d orbital, where the electrons are farther apart and repelled less, than in 3d orbitals); I_3 is again lower for silver, correlating with the increased stability of silver(III) and the tendency of silver(II) to disproportionate. The high I_1 value for gold results from the relativistic contraction of the 6s shell (from which this electron is removed) while the low I_3 value is in keeping with the stability of the +3 state, reinforced by the large ligand field splitting for the $5d^8$ ion. The preference of gold for the +3 state has been attributed to relativistic effects, according to Hartree–Fock calculations [12].

All three M^+ ions are known to form compounds with the unusual digonal linear coordination (see also section 4.9.7), though this is most common for gold. As a result, complexes R_3PMX of copper and silver are normally di- and tetranuclear species with 3- or 4-coordinate metals, while the gold analogues are 2-coordinate monomers. This is the reverse of what would be expected on steric grounds [13, 14].

Mixing of gold $5d_{z^2}$ and 6s orbitals, facilitated by the small d^{10}–d^9s separation (and also the large d^9s–d^9p separation, Table 4.3) gives rise to two orbitals Ψ_1 and Ψ_2 (Figure 4.1). The electron pair initially in $5d_{z^2}$ occupies Ψ_1, away from the two ligands (considered to lie along the z axis). The orbital Ψ_2 can mix further with $6p_z$, to afford two orbitals Ψ_3 and Ψ_4, which have (empty) lobes pointing along the z axis that can accept electron pairs from the two ligands (Figure 4.1). Recent Hartree–Fock calculations do indicate significant 5d involvement.

Table 4.1 Compounds of copper, silver and gold

Oxidation state	Copper	Silver	Gold
−1			With very electropositive metal (e.g. Cs^+Au^-)
+1	Stable if insoluble or complexed; usually 4-coordinate	Found with variety of ligands, e.g. NH_3, PR_3, Cl; usually 4-coordinate	Occurs with wide range of ligands; most often 2-coordinate
+2	Stable in aq. solution; found with wide variety of ligands, 4–6-coordinate	Usually found with N-, O-, F-donors; 4–6-coordinate	Rare, stabilized by 'suspect' ligands
+3	Rare, usually stabilized by F	Most often found bound to N, O, F; 4- and 6-coordinate	Common with wide range of ligands; usually square planar
+4			One example with a 'suspect' ligand
+5			Fluorine as ligand 6-coordinate
+7			Not confirmed, F as ligand

4.2 The elements and uses

Both silver (m.p. 962°C, b.p. 2212°C) and gold (m.p. 1065°C, b.p. 2807°C) have characteristic brilliant white and yellow colours in bulk but when finely divided are black or, in the case of gold, can be purple, ruby red or blue. Thus reduction of gold compounds by $SnCl_2$ gives the colloid known as 'Purple of Cassius', which is used as a ceramic colorant.

Table 4.2 Ionization energies (kJ mol^{-1})

	Cu	Ag	Au
I_1	745	731	890
I_2	1958	2073	1978
I_3	3554	3361	(2900)
I_4	5326	(5000)	(4200)

Estimated values in parentheses.

Table 4.3 Energy separations (eV)

	Cu^+	Ag^+	Au^+
d^{10}–d^9s	2.72	4.86	1.86
d^9s–d^9p	5.72	5.07	5.96
d^{10}–d^9p	8.44	9.93	7.82

Neither metal is attacked by oxygen, but silver reacts with H_2S in town air forming a black tarnish of Ag_2S. Both dissolve in cyanide under oxidizing conditions. Non-oxidizing acids have no effect, but silver dissolves in concentrated HNO_3 and gold in aqua regia. Both silver and gold react with the halogens, and gold can, therefore, be dissolved in mixtures of halogens and ionic halides in a polar solvent (e.g. $Cl_2/Et_4NCl/MeCN$ or $I_2/KI/MeOH$) [15].

Like copper, both gold and silver have fcc (ccp) lattices (Au–Au 2.88 Å, Ag–Ag 2.889 Å) in which the metals are 12-coordinate.

4.2.1 Extraction [16]

Although silver does not often occur native, principal ores are AgCl ('horn silver') and Ag_2S (argentite), sometimes associated with copper ores; main ore-containing countries are Mexico, Canada, Peru, Australia, the USA, the former USSR and Poland. Gold is largely formed as the metal (USA, former USSR, South Africa, Canada) deposited in quartz, though erosion can lead to veins in rocks or deposits in rivers; it is sometimes found in sulphide minerals like pyrites and chalcopyrite ($CuFeS_2$) or arsenopyrite (FeAsS). Bacteria have been implicated in the accumulation of gold while various complexes like $AuCl_2^-$ and $Au(SH)_2^-$ are thought to also be responsible for gold transport and accumulation.

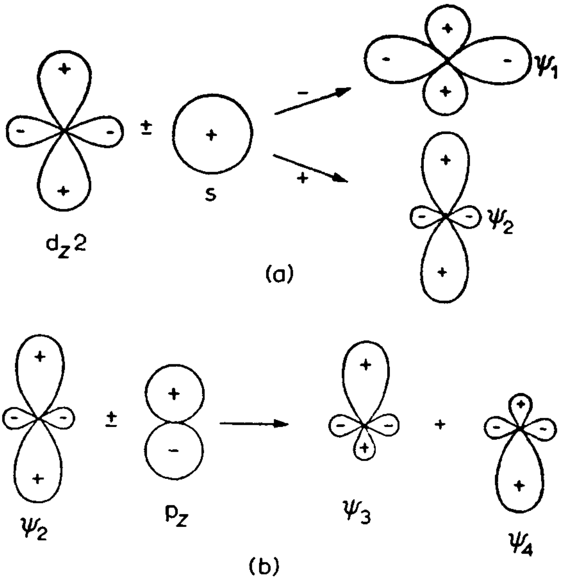

Figure 4.1 Mixing of atomic orbitals to give hybrid orbitals capable of generating digonal 2-coordination. (From J.E. Huheey, *Inorganic Chemistry*, Harper and Row, London, 1975. Reprinted by permission of Addison-Wesley Educational Publishers Inc.)

Silver was formerly extracted by cyanide solution of Ag_2S, the resulting $Ag(CN)_2^-$ being treated with zinc to afford the metal; roasted ores could also be extracted with mercury to give silver amalgam. Presently much silver is extracted by workup of the anode slime from the preparation of non-ferrous metals (Pb, Cu); pure silver is obtained by electrolysis of $AgNO_3$.

Gold ores can be concentrated by froth flotation, the resulting concentrate being roasted at 600–800°C to oxidize off sulphur and arsenic as their oxides. The product is extracted with cyanide under oxidizing conditions (using either peroxide or air itself) before displacement with powdered zinc. More reactive metals (silver etc.) can be removed by chlorination of molten gold.

An alternative route increasingly investigated is bio-oxidation using bacteria to oxidize pyrite or arsenopyrites at 45°C.

Final purification can be done by electrolysis using $HAuCl_4$ electrolyte.

4.2.2 Gold plating and other methods of gold deposition

Electrolysis of solutions containing $Au(CN)_2^-$ is widely used to recover gold from solution (electrowinning) [17]. The process is also used to deposit gold coverings for electrons (e.g. printed circuit boards, electrical connectors) and most recently for hip and shoulder joint replacement surgery.

Where insulated surfaces are to be joined, two other processes are employed: the 'immersion' and 'electroless' methods. Immersion gold plating is based on displacement reactions, where a copper or nickel object is coated with a thin film of gold from a solution of gold complex, usually in slightly acid solution (about 90°C); the process is self-terminating when a film of *c.* 0.2 μm is attained. Electroless processes use a reducing agent ($NaBH_4$, dimethylaminoborane, sodium hypophosphite) usually in hot alkaline solution (70–90°C) to reduce a gold complex such as $Au(CN)_2^-$.

4.3 Halides

The halides of silver and gold are listed in Table 4.4; as expected gold has more in higher oxidation states [18c].

4.3.1 Silver halides

The subfluoride Ag_2F can be prepared by reaction of silver with aqueous AgF or by electrolysis of AgF in HF:

$$Ag + AgF \rightarrow Ag_2F$$

It has the anti-CdI_2 structure, with alternating double layers of silver and intercalated fluorides. It is a metallic conductor.

Table 4.4 Characteristics of silver and gold halides

	Silver				Gold			
	F	Cl	Br	I	F	Cl	Br	I
M_2X	Bronze							
MX	Colourless, m.p. 435°C	Colourless, m.p. 455°C	Cream, m.p. 432°C	Yellow, m.p. 558°C		Yellow-white, dec. 170°C	Light yellow, dec. 115°C	Lemon, dec. 120°C
MX_2	Black					Black[a]		
MX_3	Bright red[b]				Gold-yellow, dec. 500°C[b]	Red, dec. 254°C	Dark brown, dec. 97°C	
MX_5					Yellow-brown			
MX_7					Pale yellow			

M, silver or gold; X, halide.

[a] $AuCl_2$ is, in fact, Au_4Cl_8, containing Au(I) and (III); [b] Ag_3F_8 and Au_2F_5 are also obtained.

Anhydrous AgF is best made by fluorination of finely divided silver at room temperature; alternatively it can be made by dissolving silver(II) oxide in hydrofluoric acid and crystallizing:

$$\mathrm{Ag} \xrightarrow{\mathrm{F_2/N_2\,(1:10)}} \mathrm{AgF}$$

As expected from the similarity of ionic radii between Ag^+ (1.15 Å) and Na^+ (1.01 Å), one form has the NaCl structure (it is trimorphic) with other forms having the CsCl and inverse NiAs structures. Unlike the other silver(I) halides, it is very soluble in water (up to 14 M) and forms di- and tetrahydrates; it is decomposed by UV rather than visible light and melts unchanged at 435°C.

The other silver(I) halides are traditionally prepared by ionic precipitation, on account of their insolubility:

$$\mathrm{Ag^+(aq.) + X^-(aq.) \rightarrow AgX(s)} \qquad (\mathrm{X = Cl, Br, I})$$

which increases in the order Cl < Br < I, just as their covalent character increases and their colour deepens (as the energy of the charge transfer process $Ag^+X^- \rightarrow AgX$ decreases) [19]. AgCl and AgBr also have the 6-coordinate NaCl structure but the repulsion between I^- in a NaCl-type lattice is such that the stable (γ) form at room temperature of AgI has the 4-coordinate ZnS structure. Comparison between experimental lattice energies (derived from Born–Haber cycle calculations) and values calculated using the Kaputinskii equation show increasing discrepancy in the order F < Cl < Br < I, demonstrating increasing divergence from an ionic model as the larger halide ion becomes more polarizable by Ag^+ (this contributes to the lattice energy being greater than predicted on an ionic model, which in turn leads to a more positive enthalpy of solution, sufficient to ensure their insolubility rather than the solubility predicted from the similarity in size between Ag^+ and Na^+). Silver iodide also exists with the hexagonal ZnO structure (136–146°); above 146°C, it passes into the α-form which has a rigid bcc structure in which there is a fixed array of I^-, but the Ag^+ can move almost at will through the structure. This causes α-AgI to have the highest conductivity of any ionic solid: interest has centred on creating ionic conductors with high conductivities at room temperature [20].

The silver(I) halides are, of course, important in the photographic process, AgBr being most commonly used; in this process a photon causes an electron to be lost from a halide ion and gained by a silver ion, thus forming silver atoms. Subsequent development with hydroquinone intensifies the image by reducing those AgBr grains containing silver atoms, followed by 'fixing' the image, a process in which thiosulphate removes unreacted AgBr as the complex ion $Ag(S_2O_3)_2^{3-}$. Since the light-sensitive AgBr has been removed, the image is now stable.

Silver(II) fluoride AgF_2 is a genuine silver(II) compound exhibiting Jahn–Teller tetragonal distortion (4F at 2.07 Å; 2F at 2.59 Å); it exhibits a low magnetic moment ($1.07\,\mu_B$) owing to anti-ferromagnetic coupling. In the absence of excess fluorine, it decomposes at 150–200°C but under a fluorine atmosphere melts at ~620°C. It is prepared from the elements at 200°C and is quite a strong fluorinating agent.

AgF_3 has recently been characterized [21] as a red diamagnetic solid, isostructural with AuF_3; it is best made by adding a fluoroacid (BF_3, PF_5) to solutions of AgF_4^- salts in anhydrous HF

$$AgF_4^- + BF_3 \rightarrow AgF_3 + BF_4^-$$

The elongated octahedral coordination of silver has Ag–F 1.863 Å (×2) 1.990 Å (×2) and 2.540 Å (×2). When dry, it is stable for some weeks at room temperature, though it loses fluorine on standing in HF to form Ag_3F_8 and is a strong fluorinating agent. Ag_3F_8 is $Ag^{II}Ag_2^{III}F_8$ ($\mu_{eff} = 1.92\,\mu_B$); Ag_2F_5 ($Ag^{II}Ag^{III}F_5$) has also been made.

4.3.2 *Gold halides*

Only AuF of the gold(I) halides is unknown in the solid state; its stability can be examined by means of a Born–Haber cycle, assuming that it would have an ionic lattice like AgF. (AuF has been generated in the gas phase from Au^+ and CH_3COF [22].)

			ΔH (kJ mol^{-1})
Au(s)	→	Au(g)	343.1
Au(g)	→	$Au^+(g) + e^-$	890.1
$\frac{1}{2}F_2(g)$	→	F(g)	79.0
$F(g) + e^-$	→	$F^-(g)$	−322
$Au^+(g) + F^-(g)$	→	AuF(s)	−778
$Au(s) + \frac{1}{2}F_2(g)$	→	AuF(s)	+212.2

Its instability relative to its constituent elements is the result of the high value of I_1 of gold and to its large enthalpy of atomization, which are not compensated for by the small lattice energy.

AuCl, AuBr and AuI are all prepared by cautious heating of Au_2X_6 (X = Cl, Br) or, in the case of AuI, direct synthesis

$$Au_2Cl_6 \xrightarrow{150^\circ C} 2Cl_2 + 2AuCl \xrightarrow{200^\circ C} 2Au + Cl_2$$

$$Au_2Br_6 \xrightarrow{250^\circ C} 2Br_2 + 2AuBr \xrightarrow{250^\circ C} 2Au + Br_2$$

$$2Au + I_2 \longrightarrow 2AuI$$

$$AuCl_4^-(aq.) \xrightarrow{I_2} AuI$$

Table 4.5 Energy values[a] for gold halides

		F	Cl	Br	I	Ref.[b]
AuX	ΔH	(+75)	−35	−19	1.7	1
	ΔG		−16	−15	−3.3	1
	ΔH	+212[c]	−34.7	−13.8	0	2
AuX_3	ΔH	−360	−121	−67.3		1
	ΔG		−54	−36		1
	ΔH	−363.6	−117.6	(−49.3) (+62.8)		2

[a] All values in $kJ\,mol^{-1}$; estimated values in parentheses.
[b] Data taken from:
1. R.J. Puddephatt (1978) *The Chemistry of Gold*, Elsevier, Oxford.
2. M.W.M. Hisham and S.W. Benson (1987) *J. Phys. Chem.*, **91**, 3631.

[c] This book.

Other methods are available, especially for AuCl, such as the decomposition of Au(CO)Cl. AuCl tends to disproportionate slowly at room temperature as predicted from the data in Table 4.5.

$$6AuCl \rightarrow 2AuCl_3 + 4Au \qquad \Delta G = -12\,kJ\,mol^{-1}$$

Decomposition is rapid in solution, so that AuCl needs to be stored in an anhydrous state. All three gold(I) halides have a zig-zag chain structure (Figure 4.2) with linear coordination of gold; AuCl has a 'wide' Au–X–Au angle (93°) and AuI a narrower angle (72°), while AuBr exists in both crystalline forms.

Bond lengths are Au–Cl 2.36 Å, Au–Br 2.40–2.44 Å, Au–I 2.62 Å [23].

A compound $AuCl_2$ is, as might be expected from its black colour, the mixed valence $Au^{I}_2Au^{III}_2Cl_8$; it is prepared from the reaction of CO with excess $AuCl_3$ in $SOCl_2$:

$$2AuCl_3 + CO \rightarrow 2AuCl_2 + COCl_2$$

The gold(I) atoms have linear coordination (Figure 4.3) and the gold(III) atoms square planar coordination [24].

There are various routes for the synthesis of the trihalides:

$$Au + BrF_3 \rightarrow AuF_3.BrF_3 \xrightarrow[in\ vacuo]{300°C} AuF_3 \xrightarrow{500°C} Au + F_2$$

$$Au \xrightarrow[1000°C,\ 15\,bar]{F_2} AuF_3 \quad [26]$$

$$2Au + 3Cl_2 \xrightarrow{240°C} Au_2Cl_6$$

$$2Au + 3Br_2 \rightarrow Au_2Br_6$$

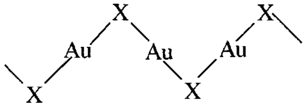

Figure 4.2 The structure of gold(I) halides in the solid state.

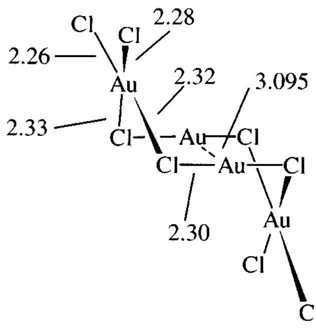

Figure 4.3 The structure of $AuCl_2$.

Two structures are exhibited, both involving 4-coordinate gold, giving rise to the diamagnetism expected for square planar d^8 systems. Like AgF_3, AuF_3 has [26] a fluorine-bridged helical structure (Figure 4.4) and is a strong fluorinating agent too.

The chloride [12] and bromide [27] are dimeric Au_2X_6 (Figure 4.5) with Au–Cl 2.243–2.249 Å (terminal) and 2.334 Å (bridge); some ligands break the bridges to form adducts $AuX_3.L$ while others reduce them to gold(I) species.

Gold(III) iodide has not been definitely characterized in the solid state; substances with this formula in the solid state are probably gold(I) polyiodides $Au^+I_3^-$; AuI_3 has also been detected in the gas phase (mass spectra).

The higher fluorides of gold, AuF_5 and AuF_7, have been reported; the former is well characterized [28]:

$$\mathrm{Au} \xrightarrow[350-380^\circ\mathrm{C}]{\mathrm{O_2/F_2\,(1:4)}} \mathrm{O_2^+AuF_6^-} \xrightarrow[160-200^\circ\mathrm{C}]{\text{sublime}} \mathrm{AuF_5} + \mathrm{O_2} + \tfrac{1}{2}\mathrm{F_2}$$

$$\mathrm{Au} \xrightarrow[0-20^\circ\mathrm{C}]{\mathrm{KrF_2/HF}} \mathrm{KrF^+AuF_6^-} \xrightarrow[\textit{in vacuo}]{40-60^\circ\mathrm{C}} \mathrm{AuF_5}$$

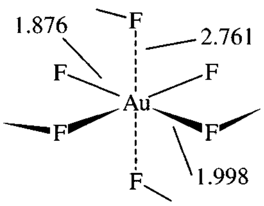

Figure 4.4 The structure of AuF_3.

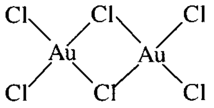

Figure 4.5 The structure of Au_2Cl_6.

It is an intensely reactive and hygoscopic yellow–brown substance (m.p. 75–78°C); its volatility suggests a low molecular mass; Mössbauer spectra indicate 6-coordinate gold while the Raman spectrum is interpreted in terms of *cis*-bridged octahedral units. In the gas phase at 170°C, it comprises dimers and trimers [29] (electron diffraction).

AuF_7 is reported to result from the reaction of fluorine atoms (produced in a high-voltage plasma) with AuF_5 at 120–130°C, being condensed out at −196°C as a very reactive and volatile pale yellow solid (vapour pressure >30 mmHg at room temperature) with an intense IR band at 734 cm^{-1} (vapour). It decomposes to AuF_5 above 100°C and affords Au_2O_3 and Au on hydrolysis [18].

4.4 Oxides and other binary compounds

The main silver oxides are Ag_2O and AgO. The former is obtained as a dark brown precipitate when OH^- are added to solutions of Ag^+ salts; it tends to retain traces of water and alkali, even on drying. It is basic, giving slightly alkaline solutions in water (it is a convenient mild alkali in organic chemistry) and reacting with atmospheric CO_2. On heating to 160°C, it forms silver. Isostructural with Cu_2O, it has tetrahedral coordination of silver. When fused with alkali metal oxides, mixed oxides like KAgO are formed that have $Ag_4O_4^{4-}$ units with 2-coordinate silver. Analogous gold compounds are known (but not Au_2O) [30].

Black AgO is prepared by oxidation of silver salts with O_3, $S_2O_8^{2-}$ and, most recently, SO_2/air mixtures, as well as by anodic oxidation [31]. Neutron diffraction shows it to be $Ag^IAg^{III}O_2$ with 2-coordinate Ag^I and square planar Ag^{III} sites. It is stable to around 100°C and gives solutions of Ag^{2+} when dissolved in dilute acid. Treatment with alkaline periodate retains the disproportionation

$$4AgO + 6OH^- + 4IO_4^- \rightarrow 2Ag(IO_6)_2^{7-} + Ag_2O + H_2O + 4H^+$$

It finds important applications in batteries.

Less important oxides are Ag_2O_3, obtained impure by extended anodic oxidation of silver, and Ag_3O, obtained hydrothermally from Ag/AgO at 80°C, 4000 bar, which is a metallic conductor with the anti-BiI_3 structure containing an hcp array of silvers with oxide ions occupying 2/3 of the octahedral holes [32].

The only important gold oxide is brown Au_2O_3, obtained hydrated by alkaline precipitation of Au^{3+}(aq.); single (ruby) crystals have been produced by hydrothermal crystallization at 235–275°C (from $HClO_4/KClO_4$). It has a polymeric structure [33] with square planar Au^{3+} (Au–O 1.93–2.07 Å) though with four more distant oxygens (at 2.81–3.19 Å). It decomposes to the elements on gentle heating and dissolves in strong alkali as

$Au(OH)_4^-$. There have been claims for an AuO_2, which may have been impure Au_2O_3.

The ternary oxides M_3AuO (M = Rb, Cs) contain Au^-, however [34].

Other binary compounds include the very insoluble black Ag_2S ($k_{sp} \sim 10^{-51}$) and Au_2S. The latter has the cuprite structure while Ag_2S has three polymorphs; 2- and 3-coordination is found in the low-temperature form while at high temperatures Ag_2S is a conductor owing to movement of silver atoms between the framework of sulphurs. AuS and AuSe are, as would be expected, $Au^IAu^{III}X_2$ with digonal gold(I) and square planar gold(III) [35]; little is known about Au_2X_3 (X = S, Se, Te). $AuTe_2$ 'calverite' has 4 + 2-coordination of gold by tellurium [36]. Various polyanions such as $Au_2S_8^{2-}$, AuS_9^- and $Au_{12}S_8^{4-}$ have been made; the first two have rings with linear coordination of gold (as in $Au_2Se_5^{2-}$ and $Au_2Se_6^{2-}$) while the latter has a cube of sulphurs with golds at the middle of each edge [37]. Selenide complexes of silver [38] and gold [39] have been studied lately. Silver selenide complexes show dependence in structure on counter-ion as in $[Ph_4PAg(Se_4)]_n$, $[Me_4NAg(Se_5)]_n$, $[Et_4NAg(Se_4)]_4$ and $(Pr_4N)_2[Ag_4(Se_4)_3]$.

Gold forms no simple phosphide; Au_2P_3 is $Au_4^I(P_6^{4-})$ with P–Au–P angles of 171 and 180°.

4.5 Aqua ions

Only Ag^+ and Au^{3+} are stable in aqueous solution, the latter always being complexed. The relevant potentials (in acid solution) are:

$$Ag^+(aq.) + e^- \rightarrow Ag(s) \qquad E^0 = +0.799\,V$$

$$Ag^{2+}(aq.) + e^- \rightarrow Ag^+(aq.) \qquad E^0 = +1.980\,V$$

$$Au^+(aq.) + e^- \rightarrow Au(s) \qquad E^0 = +1.83\,V$$

$$Au^{3+}(aq.) + 2e^- \rightarrow Au^+(aq.) \qquad E^0 = -1.36\,V$$

From the Ag^+/Ag^{2+} potential, it is seen that the silver(II) ion is a strong oxidizing agent and is only fairly stable in strong acid; it may be prepared by ozone oxidation of Ag^+ or by reproportionation of AgO (section 4.4).

Ag^+ is stable to disproportionation in aqueous solution

$$2Ag^+(aq.) \rightarrow Ag^{2+}(aq.) + Ag(s) \qquad E^0 = -1.18\,V$$

though the potential is affected by complexation and certain silver(I) macrocyclic complexes disproportionate in solution (section 4.7).

Table 4.6 Selected electrode potentials for gold(I) and gold(III) complexes $[Au(L^{n-})_2]^{(1-2n)+}$ and $[Au(L^{n-})_4]^{(3-4n)+}$

L	Gold(I) E^0 (V)	Gold(III) E^0 (V)
H_2O	−1.83	−1.52
Cl^-	−1.15	−1.00
Br^-	−0.96	−0.85
I^-	−0.66	–
SCN^-	−0.58	−0.64
NH_3	−0.56	−0.33
CN^-	+0.61	+0.20

In the case of gold, study of the above potentials predicts correctly the disproportionation of Au^+ in aqueous solution

$$3Au^+(aq.) \rightarrow Au^{3+}(aq.) + 2Au(s) \qquad E^0 = 0.47\,V$$

For example, AuCl immediately decomposes into gold and gold(III) chloride, though some gold(I) halide complexes such as AuI_2^- are quite stable, while $Au(CN)_2^-$ is formed by oxidation of gold in the presence of CN^-:

$$Au + 2CN^- \rightarrow Au(CN)_2^- + e^- \qquad E^0 = +0.61\,V$$

Table 4.6 shows the potentials to be ligand dependent.

X-ray scattering data on solutions of Ag^+ indicate the presence of $Ag(H_2O)_4^+$ with Ag–O about 2.4 Å [40]. Soluble silver(I) salts include $AgNO_3$, $AgClO_4$ (the periodate is insoluble), $AgBF_4$, $AgClO_3$ and AgF (all other halides are insoluble). There is no evidence for perchlorate coordination in aqueous solution. Silver nitrate is prepared from the reaction of silver with concentrated nitric acid as colourless crystals m.p. 212°C. It decomposes above 350°C to silver, oxygen, nitrogen and oxides of nitrogen. Insoluble salts of silver include the bright yellow Ag_3PO_4 and (in contrast to the chlorate) the bromate and iodate. Little is known concerning gold(III) salts such as $Au(NO_3)_3$.

The oxidizing power of Ag^{2+} (aqueous) is being utilized in electrochemical cells for disposal of organic wastes; solutions of Ag^{2+} in HNO_3 were originally found to be efficient oxidants for organic nuclear waste (tributyl phosphate kerosene from solvent extraction processes) but the scope has been expanded to include rubber, certain polymers, hydraulic and lubricating oils, aromatic and aliphatic hydrocarbons, organo-phosphorus, sulphur and chloro compounds (including PCBs, notoriously difficult to oxidize) [41].

4.6 Silver(I) complexes

4.6.1 Complexes of O-donors

The aqua ion as a ligand is discussed in section 4.5. Silver forms a range of light-sensitive, insoluble carboxylates that find application in the synthesis of, for example, alkyl halides and esters. The benzoate, trifluoroacetate and perfluorobutyrate have dimeric structures; others are polymers (Figure 4.6).

Commercially, the most important complexes of O-donors are the thiosulphates, implicated in photographic 'fixing'; of several known, in $NaAgS_2O_3.H_2O$ each silver is tetrahedrally bound to three sulphurs and one oxygen while $(NH_4)_7Ag(S_2O_3)_4$ also has silver tetrahedrally bound by sulphur. Unlike other 'soft' metal ions, Ag^+ binds to Me_2SO via oxygen in $Ag(DMSO)_2ClO_4$ rather than by sulphur.

4.6.2 Complexes of N-donors

Dissolution of Ag_2O in aqueous ammonia lends to the formation of $Ag(NH_3)_2^+$ (Ag–N 2.110 Å in $Ag(NH_3)_2SO_4$); its reduction by aldehydes and reducing sugars is the basis of its use as Tollens' reagent, the 'silver mirror' test. In liquid ammonia, the tetrahedral $Ag(NH_3)_4^+$ is formed (Ag–N 2.31 Å), isolable as a perchlorate (which loses NH_3 on keeping); silver nitrate forms $[Ag(NH_3)_3]^+NO_3^-$ with a trigonally coordinated silver (Ag–N 2.281 Å) [42]. Linear coordination is formed in $Ag(pyridine)_2^+NO_3^-.H_2O$ (Ag–N 2.26 Å, bond angle 173°; four distant contacts to oxygens Ag–O *c.* 2.9 Å); an unstable $Ag(py)_4^+$ has similarly been characterized. $Ag(im)_2^+$ is linear in the nitrate, but in the perchlorate, $Ag(im)_2^+$ is associated in pairs (further grouped into triangular units). $Ag(pyrazine)NO_3$ has silver similarly bound to two nitrogens but nitrate coordination is stronger than in the pyridine complex as the chains are kinked (N–Ag–N 159°) (Figure 4.7).

An exception to the above types of structure is the cubane cluster in $(AgIpiperidine)_4$ [43].

Less study has been made of complexes with polydentate ligands. Ag–N linkages have been studied in relation to polynucleotide bases and the Ag–DNA interaction could be important in the use of the silver–sulphadiazine complex in burn treatment. Ethylenediamine is a bridging ligand in $AgenClO_4$ (2-coordinate silver) but essentially planar 5-coordination

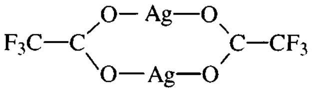

Figure 4.6 The dimeric structure adopted by some silver carboxylates such as silver trifluoroacetate.

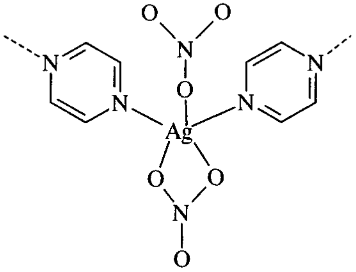

Figure 4.7 The environment of silver in Ag(pyrazine)NO_3.

occurs in Ag(quinquepyridine)PF_6; $[Ag(PPh_3)_2(terpy)]ClO_4$ has trigonal bipyramidal coordination [44].

Ag(4,4′-bipy)NO_3 has a three-dimensional structure with silver ions diagonally coordinated by two bipy ligands (N–Ag–N 173.7°) in extended infinite chains, the chains being cross-linked by Ag–Ag bonds (2.970 Å) [45].

4.6.3 Tertiary phosphine and arsine complexes

The 1 : 1 phosphine complexes resemble those of copper rather than gold (Figure 4.8) [46].

More bulky phosphines favour the chair structure; $[(R_3P)AgX]_4$ (R = Et, Ph; X = Cl, Br, I) all adopt the cubane form but a second form of $[(Ph_3P)AgI]_4$ has the chair structure in which some silver atoms are 3-coordinate. Some of these clusters may dissociate into dimers in solution. In contrast to the linear gold analogue, $[(Ag(O_2CMe)(PPh_3)]_4$ has a tetrameric structure featuring 3- (1P, 2O) and 4- (1P, 3O) coordinate silver while a second form is dimeric $[(Ph_3P)Ag(\mu\text{-}O_2CMe)Ag(PPh_3)]$ with 3-coordinate silver [47]; Ag(SCN)(PPr^n_3) has a chain structure where 4-coordination is attained with cross-linking of Ag–S–Ag–S-units. $(Ph_3P)_2AgX$ (X = Cl, Br, I, SCN) are X-bridged dimers [48] and $(Ph_3P)_3AgCl$ also features tetrahedral coordination; four tertiary phosphites, though not phosphines, can bind to one silver. Four-coordination is found in monomeric and dimeric

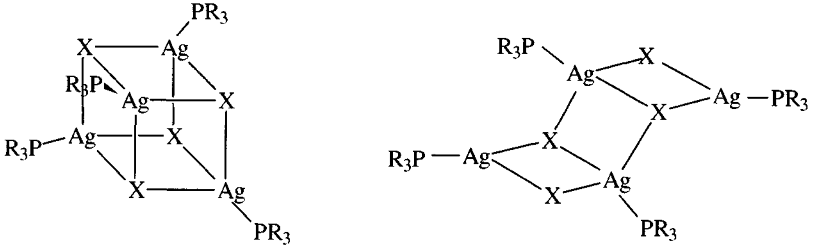

Figure 4.8 Cubane and chair structures adopted by complexes $(R_3P)AgX$.

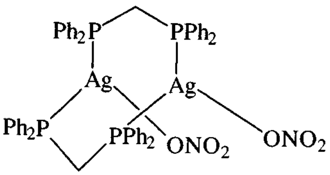

Figure 4.9 The dimeric structure adopted by $(Ph_2PCH_2PPh_2)AgNO_3$.

$(Ph_3P)_2AgNO_3$. $[(Ph_3P)_2Ag(O_2CH)]$ has 4-coordinate silver with a symmetrically bidentate formate ligand [49]. Two-coordination has been established for bulky phosphines, for $[(mesityl)_3P]_2Ag^+PF_6^-$ and probably for $(Bu^t_3P)_2Ag^+X^-$ ($X = PF_6, BF_4, ClO_4$). Among complexes of bidentate ligands, $(Ph_2PCH_2PPh_2)AgNO_3$ is a dimer with 3-coordinate silver (Figure 4.9).

The series M(PP)Cl (PP = 2,11-bis(diphenylphosphinomethyl)benzo[c]-phenanthrene; M = Cu, Ag, Au) is interesting in showing group trends (Table 4.7) where the silver and copper complexes have trigonal coordination and the gold member is linear [50].

Linear coordination is also found in Ag(tmpp)X (X = Cl, Br). Bond lengths are Ag–P 2.379 and Ag–Cl 2.342 Å in the chloride; Ag–P 2.374 and Ag–Br 2.448 Å in the bromide [51a]. The 3-coordinate monomers $Ag(PR_3)(CF_3COCHCOCF_3)$ (the diketonate chelates through the two oxygens; R = Me, Et) are volatile and thermally stable to over 100°C; they have been suggested as CVD precursors [51b]. Four-coordination occurs in $[Ag(S_2CAr)(PPh_3)_2]$ [52].

4.6.4 Complexes of halogen-donors

Silver halides dissolve in excess halide (e.g. AgCl is a hundred times more soluble in 1 M HCl than in water) forming complex ions AgX_2^- and AgX_3^{2-} [53]. These isolated anions are not often found in the solid state; thus M_2AgI_3 ($M = K, Rb, NH_4$) have corner linked tetrahedra (Figure 4.10), though $Au(S_2CNBu^n_2)_2^+AgBr_2^-$ does have digonally coordinated silver (Ag–Br 2.45 Å).

MAg_4I_5 (M = Rb, K) compounds are iodide-based solid electrolytes with high conductivities; the structures are based on packing of I^-, the ion Ag^+

Table 4.7 Structure of M(PP)Cl

M	M–P average (Å)	M–Cl (Å)	P–M–P (°)
Cu	2.237	2.222	131.9
Ag	2.434	2.514	140.7
Au	2.308	2.818	175.5

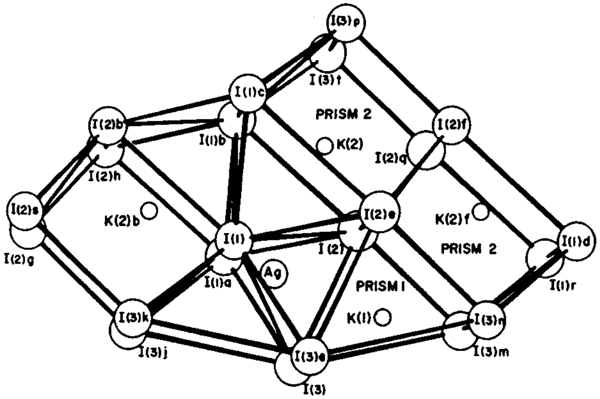

Figure 4.10 The structure of K_2AgI_3. (Reproduced with permission from *Acta Crystallogr. Sect. B*, 1975, **31**, 2339.)

(but not M^+) being mobile at room temperature, moving from one position to another with a relatively small energy barrier [54].

Trigonal coordination is also found in M(dibenzo-18-crown-6)AgX_3 (M = K, Rb; X = Cl, Br) with Ag–X bond lengths of 2.447 Å (X = Cl) and 2.550 Å (X = Br) in the rubidium salts. With the larger K(crypt-2,2,2)$^+$ counter-ion, it is possible to isolate individual ions as $AgCl_2^-$. In $(PPh_3Me)^+AgI_3^-$, Ag–I is 2.742–2.755 Å; $(Pr_4N)_4[Ag_4I_8]$, however, has cubane-type clusters [55].

4.6.5 *Complexes of C-donors*

The most important complexes with C-donors, other than organometallics, are cyanides. AgCN has a structure with Ag–C–N–Ag bonding in linear polymeric chains; it dissolves in excess KCN forming $K^+Ag(CN)_2^-$ (digonal with Ag–C 2.13 Å, $\nu(C{\equiv}N)$ 2135–2139 cm^{-1}), $Ag(CN)_3^{2-}$ and $Ag(CN)_4^{3-}$ [56].

4.6.6 *Complexes of S-donors*

Like gold, silver readily forms insoluble (yellow) thiolates $[Ag(SR)]_n$; primary alkylthiolates are thought to have non-molecular structures but with bulky tertiary alkyls ($n = \sim 8$), probably having a cyclic structure. Addition of excess thiolate leads to the formation of clusters like $Ag_6(SPh)_8^{2-}$, $Ag_5(SPh)_7^{2-}$ and $Ag_5(SBu^t)_6^-$ (phosphine adducts are known, too).

Octahedral silver clusters are also found in dithioacid complexes $[Ag(S_2CNR_2)]_6$ (R = Pr, Et) and $[Ag(S_2C{=}C(CN)_2)]_6^{6-}$, while $[Ag_8(S_2C{=}C(CN)_2)_6]^{4-}$ has a cube of silvers (Figure 4.11) [57].

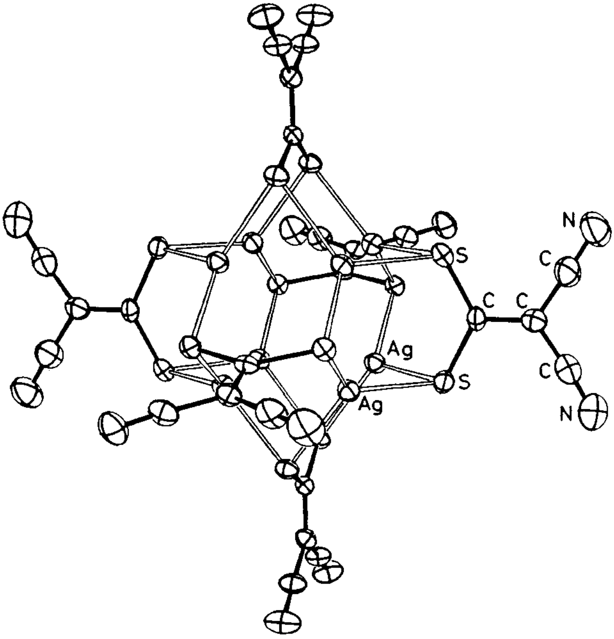

Figure 4.11 The structure of $[Ag_8\{S_2C{=}C(CN)_2\}_6]^{4-}$. (Reproduced with permission from *J. Chem. Soc., Chem. Commun.*, 1981, 323.)

A number of thiourea complexes of silver have shown the tendency to bind up to four ligands, in contrast to gold. Thus $Agtu_2X$ (X = Cl, NCS) have essentially 3-coordinate silver (one distant fourth atom); $Agtu_3ClO_4$ is a 4-coordinate dimer (Figure 4.12) [58].

Various thioether complexes have been synthesized: for example, 6-coordination is found in $[Ag(18S_6)]^+$ and $[Ag(9S_3)_2]^+$ but in $[Ag(16S_6)]^+$, tetrahedral coordination occurs, with two unused donor atoms in the ligand [59].

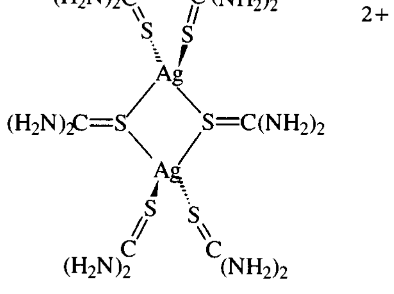

Figure 4.12 The structure of dimeric $[Ag_2(tu)_6]^{2+}$ in $Ag(tu)_3ClO_4$.

4.7 Silver(II) complexes

Stable compounds of silver(II) are found with N, O and F as donor atoms; macrocycles are, as elsewhere, able to support the higher oxidation state. As a d^9 system, Ag^{2+} imitates Cu^{2+} in displaying Jahn–Teller distortion.

Violet fluoro complexes like $BaAgF_4$ and Cs_2AgF_4 can be made by fluorination

$$BaCO_3 + Ag_2SO_4 \xrightarrow[800°C]{F_2} BaAgF_4 \qquad (\mu = 1.9\,\mu_B)$$

and have square planar silver (Ag–F 2.05 Å). $MAgF_3$ (M = K, Rb, Cs) and $CsAgMF_6$ (M = Tl, In, Sc, Fe) have also been made; $KAgF_3$ has distorted 6-coordination (perovskite structure) and $CsAgFeF_6$ has a compressed octahedral geometry [60].

Complexes of N-donor ligands have been made by chemical (ozone or persulphate) or electrochemical oxidation, such as $Agpy_4S_2O_8$, $Ag(bipy)_2(S_2O_8)$ and $Ag(bipy)_2(NO_3)_2.H_2O$. Solid $Ag(bipy)_2(S_2O_8)$ has $\mu_{eff} = 1.82\,\mu_B$; $g_\perp = 2.032$, $g_\parallel = 2.134$ (in frozen solution, hyperfine structure from both silver and nitrogen are seen). $Ag(bipy)_2(NO_3)_2.H_2O$ has distorted octahedral coordination (bidentate bipy, bridging nitrate). The value of E^0 for $Agbipy_2^+$/ $Agbipy_2^{2+}$ is 1.453 V, compared with 2.0 V for the aqua ion, demonstrating the ability of these ligands to stabilize higher oxidation states [61].

Picolinate and pyridine-2,6-carboxylate give stable complexes, with 4- and 6-coordination. Macrocycles like porphyrins afford silver(II) derivatives; most remarkable is the reaction of the macrocycle *meso*-Me_6[14]ane (Figure 4.13).

It forms a stable silver(I) complex in acetonitrile, in keeping with the ability of MeCN to solvate Ag^+; in the presence of water, disproportionation occurs [62].

$$AgClO_4 + L \xrightarrow{MeCN} [AgL]^+ClO_4^- \xrightarrow{H_2O} [AgL]^{2+}(ClO_4)_2 + Ag + L$$

Silver has square planar coordination in Ag[*meso*-Me_6[14]ane]$(NO_3)_2$ (Ag–N 2.16 Å) with distant axial oxygens (Ag–O 2.81 Å); the complex has

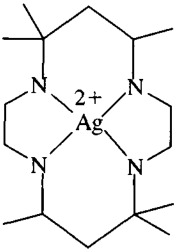

Figure 4.13 The structure of the silver(II) complex of the macrocycle *meso*-Me_6[14]ane.

$\mu_{eff} = 2.2\,\mu_B$; $g_{\|} = 2.11$, $g_{\perp} = 2.058$. Similar complexes can be obtained with other ligands [63]; some can be oxidized, chemically or electrochemically, to silver(III) complexes.

4.8 Silver(III) complexes

As mentioned in the previous section, oxidation (with $NOClO_4$) of a silver(II) complex yields the yellow diamagnetic Ag[*meso*-Me_6[14]ane]$(ClO_4)_3$; other complexes such as $AgOEPClO_4$ can be made; the Ag^{3+}/Ag^{2+} potential is 0.44 V [64].

Fluoride complexes of silver(III) are exemplified by the purple–red Cs_2KAgF_6 (elpasolite structure, octahedral Ag^{3+}; paramagnetic with $\mu = 2.6\,\mu_B$). Yellow $MAgF_4$ (M = Na, Rb, K) and $XeF_5^+AgF_4^-$ are diamagnetic and probably square planar [65].

Yellow $Ag(OH)_4^-$, synthesized by anodic oxidation of silver in strong alkali, is said to be stable for 2 h at 25°C in 1.2 M NaOH but decomposes to AgO and O_2 at pH 11 in 1–2 min [66].

The longest established silver(III) complexes are the red to brown biguanides, like the ethylene bis(biguanide) shown in Figure 4.14; persulphate oxidation of Ag^+ in the presence of this ligand gives a silver(III) complex with essentially square planar coordination.

4.9 Gold(−I) complexes

Gold has a high electron affinity (223 kJ mol^{-1}, compare with that for I of 295 kJ mol^{-1}) to fill the 6s subshell, because of relativistic contraction (see section 4.18). It, therefore, forms 1 : 1 compounds MAu with group I metals; of these Cs^+Au^- and Rb^+Au^- are ionic semi-conductors [67] with the CsCl structure ('normal' alloys of gold like those with the lighter alkali metals are metallic conductors). Au^- is also formed when gold dissolves in liquid ammonia in the presence of Cs and other alkali metals. Au^- is also found in $K_{18}Tl_{20}Au_3$, which contains $[Tl_9Au_2]^{9-}$, $[Tl_{11}]^{7-}$ and Au^-.

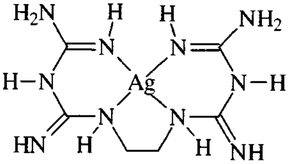

Figure 4.14 The coordination geometry of silver in the silver(III) ethylenebis(biguanide) complex.

4.10 Gold(I) complexes

4.10.1 Complexes of O-donors

Few studies have been made of these ligands; most complexes reported involve other supporting ligands as in $Au(OSiMe_3)(PPh_3)$ and $Au(OCOR)(PPh_3)$, though an important Au–O bond is formed in $[(Ph_3P)Au]_3O^+$ (section 4.17) [68]. Some air- and heat-stable alkoxides $Au(OR')(PR_3)$ (R = Ph or cy; R' = CH_2CF_3 or $CH(CF_3)_2$) have been reported [69].

4.10.2 Complexes of N-donors

The 'soft' Au^+ forms relatively few complexes compared with those of phosphines. Complexes with ammines, nitriles and diazoles like $Au(NH_3)_2^+$ and $Au(RCN)_2^+$ are known but little studied. In linear $Au(NH_3)_2^+$, Au–N is 2.01–2.03 Å [70a]. $[Au(NCPh)_2]^+$ has been used as a labile source of other gold complexes [70b]. AuCl(piperidine) is a monomer with weak tetrameric association; in contrast AuX(py) (X = Cl, Br, I) are $[Aupy_2]^+[AuX_2]^-$ with a chain structure in the solid state (and Au–Au interactions), suggesting a close balance between factors for 'molecular' and ionic structures [70c] (note also the tetrahydrothiophene complexes in section 4.10.6).

4.10.3 Tertiary phosphine and arsine complexes

The phosphine and arsine complexes of gold(I) have been intensively studied since the early 1970s. The possibilities of coordination numbers between 2 and 4 have been explored, though the use of bulky ligands is less essential than with the isoelectronic $M(PR_3)_2$ (M = Pd, Pt) compounds and the coordination numbers depend on both steric and electronic factors [71].

The usual starting material is $AuCl_4^-$, which can be reduced with the tertiary phosphine

$$AuCl_4^- + 2R_3P \rightarrow R_3P.Au.Cl + R_3PCl_2 + Cl^-$$

or more cheaply, *in situ* with 2,2'-thiodiethanol, (bis-2-hydroxyethylsulphide)

$$\begin{aligned} &AuCl_4^- + 2(HOCH_2CH_2)_2S \\ &\quad \rightarrow AuCl[S(CH_2CH_2OH)_2] + (HOCH_2CH_2)_2SO + Cl^- + 2HCl \end{aligned}$$

or via an isolable complex with a weakly bound ligand like tht, the intermediate being reacted with the tertiary phosphine (or arsine)

$$AuCl_4^- + 2R_2S + H_2O \rightarrow AuCl(R_2S) + R_2SO + 2HCl + Cl^-$$

1 : 1 complexes

X-ray diffraction shows linear coordination in $(Ph_3P)AuX$ (X = Cl, Br, I, NO_3, SCN [72], Ph [73], SR [74], CN, Me, CF_3 [75] OCOMe [76],

Table 4.8 Au–P bond lengths in the 2-coordinate complexes $(Ph_3P)AuX$

Donor atom	X	Au–P (Å)
O	NO_3	2.199
	OCOMe	2.207
	$OCOCF_3$	2.208
	$OCOCHCl_2$	2.210
	$OCOPr^i$	2.213
	SO_4	2.216
	OCOCH(OH)Me	2.219
N	NCO	2.222
	NMe_3	2.231 (ClO_4 salt)
Cl	Cl	2.235
Br	Br	2.252
I	I	2.249
S	SCN	2.252
	SPh	2.259
	S_2COEt	2.260
	S_2COMe	2.261
	S_2CPh	2.263–2.269
C	CNO	2.274
	C_6F_5	2.27
	$C{\equiv}CC_6F_5$	2.274
	Me	2.279
	CN	2.278
	$(2,6\text{-}MeO)_2Ph$	2.284
	CF_3	2.285
	Ph	2.296
P	PPh_3	2.295 ($C(CN)_3$ salt)
	PPh_3	2.311 (NO_3 salt)
	PPh_3	2.312 (PF_6 salt)
	PPh_3	2.325 (solution)

$OCOCF_3$, S_2CNEt_2, S_2COMe [77], OCOPh, NMe_3 [78], etc.), R_3PAuCl [79] (R_3 = cy_3, $Phcy_2$, Me_3P, Et_3P, Cl_3P, $(PhO)_3P$ and $(tolyl)_3P$), $Pr_3PAuC_5H_5$ and Ph_3AsAuX (X = Cl, Br). In all of these the ligand X is monodentate (note the monodentate nitrate and dithio ligands, as well as the monohapto-cyclopentadienyl). Table 4.8 shows the *trans*-influence of the ligand X on the Au–P bond length in some of these compounds; it depends on the donor atom in X rather than X itself, the bond lengths following a trend in agreement with *trans*-effect orders.

Complexes other than the chloride are prepared by a variety of reactions, including metathesis and re-distribution:

$$Ph_3PAuCl \xrightarrow{NaXCN} Ph_3PAuXCN \qquad (X = S, Se)$$

$$Ph_3PAuCl \xrightarrow{AgOAc} Ph_3PAuOAc$$

$$(Ph_3P)_2Au^+ + Au(CNO)_2^- \rightarrow (Ph_3P)Au(CNO)$$

Table 4.9 Structure and spectroscopic data for AuX(tmpp)

X	Au–P (Å)	Au–X (Å)	ν(Au–X) (cm^{-1})
Cl	2.253	2.303	313
Br	2.255	2.413	218
I	2.239	2.586	183

PF_3AuCl, prepared from Au_2Cl_6 and PF_3 in $SOCl_2$ has a vapour pressure of 10^{-4} mbar at room temperature and has been suggested as a laser CVD precursor [80].

The series AuX (tmpp) shows clear patterns [81] in structure and spectroscopic parameters (Table 4.9) (X = Cl, Br, I).

Complexes with more than one phosphine

The 2 : 1, 3 : 1 and 4 : 1 complexes have been prepared by altering the stoichiometry of the reaction mixture; the complex formed in solution depends on the cone angle of the phosphine (as with $M(PR_3)_n$ (M = Pd, Pt)) [71]. Thus PBu^t_3 and Pcy_3 form only 2 : 1 complexes (three Pcy_3 can bind to the larger Pt) whereas PBu^n_3 forms 3 : 1 complexes and with PEt_3, up to 4 : 1 complexes can be obtained. The stoichemetry of the complex isolated in the solid state depends on factors such as the coordinating power of the anion present and upon the balance between cation and anion size. Thus $(PPh_3)_2AuSCN$ is 3-coordinate, but because of the bulk of tricyclohexylphosphine, $(cy_3P)_2Au^+SCN^-$ is 2-coordinate [82].

Many structures have been determined including $(PPh_3)_2Au^{2+}X^-$ (X^-, e.g. NO_3, PF_6, $C(CN)_3$) [83], $(Pcy_3)_2Au^+X^-$ (X = NCS, PF_6, Cl) [79], $(PPh_2Me)_2Au^+PF_6^-$, $(Bu_3P)_2Au^+BPh_4$ [84] (all are linear, 2-coordinate); $(PPh_3)_2AuX$ (X = Cl, Br, I, NCS) and $(PPh_3)_3Au^+X^-$ (X = BPh_4) are 3-coordinate and $(PPh_3)_3AuX$ (X = Cl, SCN), $(PPh_2Me)_4Au^+PF_6^-$, $(PPh_3)_4Au^+BPh_4^-$ and $(SbPh_3)_4Au^+ClO_4^-$ [85] are 4-coordinate. The 3-coordinate complexes are essentially trigonal when all the ligands are the same, or slightly distorted in $(PPh_3)_2AuX$, where steric effects force the P–Au–P angle to exceed 120° [86]. The 4 : 1 complexes are distorted tetrahedra [85]. 'Mixed' 3-coordinate complexes like $[(PPh_3)Au(bipy)]^+$ have been made [87], with very asymmetric bidentate coordination (Figure 4.15).

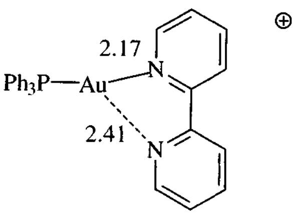

Figure 4.15 The asymmetric coordination geometry in $[(Ph_3P)Au(bipy)]^+$.

Table 4.10 Bond lengths (Å) in the complexes $(PPh_3)_nAuX$ and $(PPh_3)_2AuX$

$(PPh_3)_nAuCl$			$(PPh_3)_nAuSCN$			$(PPh_3)_2AuX$		
n	Au–P	Au–Cl	*n*	Au–P	Au–S	X	Au–P	Au–X
1	2.235	2.279	1	2.252	2.304	Cl	2.27	2.533
2	2.27	2.533	2	2.348	2.469	Br	2.323	2.625
3	2.41	2.71	3	2.396	2.86	I	2.333	2.754

Trends in Au–X and Au–P bond lengths in complexes $(PPh_3)_nAuX$ should be noted (Table 4.10); the Au–Cl bond length varies more with changes in coordination number than does the Au–P bond and is, therefore, more sensitive to the decrease in s character as the hybrid orbitals used by gold change from sp to sp^3.

Luminescence has been noted [88] in numerous gold phosphine complexes.

Rather fewer complexes with polydentate ligands have been studied [89]. Interest in possible use of $Au(dppe)_2^+$ in cancer therapy has led to the determination of the structures of $(AuCl)_2dppe$ and $Au(dppe)_2^+X^-$ (X = Cl, SbF_6). The former has the diphosphine acting as a bridging ligand while the latter has a tetrahedral cation as in $[Au(1,2\text{-}(Me_2As)_2C_6H_4)_2]^+$. The compound [Au(PP)]Cl has already been referred to in section 4.4 as an example of the preference of gold for 2-coordination [50].

The tridentate $MeC(CH_2PPh_2)_3$ gives $MeC(CH_2PPh_2AuCl)_3$.

4.10.4 Complexes of halogen-donors

The ions AuX_2^- (X = Cl, Br, I) are well known; the chloride and bromide are particularly unstable in water unless excess halide ion is present. Although AuF does not exist as a solid (section 4.3.2), it has been suggested that the unknown AuF_2^- could be stabilized by ions such as Ph_4As^+ to prevent the disproportionation:

$$3AuF_2^- \rightarrow AuF_4^- + 2Au + 2F^-$$

The series Bu_4NAuX_2 have been prepared by reactions like

$$2R_4NAuCl_4 + PhNHNH_2HCl \rightarrow R_4NAuCl_2 + R_4NPhAuCl_3 + N_2 + 4HCl$$

$$AuBr_4^- + MeCOMe \rightarrow AuBr_2^- + CH_2BrCOMe + HBr$$

$$AuBr_2^- \xrightarrow[I^-]{\text{exc.}} AuI_2^-$$

Au–X bond lengths in the series are 2.257 Å (Cl), 2.376 Å (Br) and 2.529 Å (I); they are affected by counter ions, Au–Cl being 2.281 Å in $Cs_2AuCl_2AuCl_4$. AuX_2^- exhibits Au–X stretching vibrations in the IR at 350, 254 and 210 cm^{-1} (X = Cl, Br, I, respectively, in the Bu_4N salts) and in Raman spectra at 329, 209 and 158 cm^{-1}, respectively [90].

Ions of the type AuX_2^- are found as counter ions in other complexes like $Aupy_2^+AuCl_2^-$, $Au(Bu_2NCS_2)_2^+AuBr_2^-$ and $Au(tht)_2^+AuI_2^-$.

4.10.5 Complexes of C-donors

AuCN has a similar structure to AgCN and likewise dissolves in excess cyanide to form $Au(CN)_2^-$; this is important in the extraction of gold. It has been characterized as various salts (Tl, K, Bu_4N, Cs) with Au–C 1.964 Å (Bu_4N salt [91]). The thallium salt has short Au–Au (3.10 Å) and Au–Tl (3.50 Å) interactions; extended-Hückel calculations indicate the importance of relativistic effects in these covalent interactions. Isocyanides form stable complexes:

$$AuCl(SMe_2) + MeNC \rightarrow AuCl(MeNC) + Me_2S$$

$$AuCl_4^- \xrightarrow[EtOH]{exc.\ Bu^tNC} AuCl(Bu^tNC)$$

The latter is linear with a short Au–C bond (1.92 Å); excess isocyanide lends to $Au(RNC)_2^+$ and possibly $Au(RNC)_4^+$. An unusual synthesis is

$$Ph_4AsAu(CN)_2^- \xrightarrow{MeI} MeNCAuCN$$

The linear Au(CO)Cl (ν(C–O) 2153 cm^{-1}), useful as a synthetic intermediate, is prepared by [92]

$$HAuCl_4 \xrightarrow[SOCl_2]{exc.\ CO} Au(CO)Cl + COCl_2$$

Au(CO)Br has been obtained in solution (only)

$$2Au_2Br_6 + 4CO \rightarrow 4Au(CO)Br + 4Br_2$$

while $Au(CO)_2^+$ has been isolated in various salts (section 4.16.1).

4.10.6 Complexes of S-donors

The most important complexes of S-donors are thiolates, simply regarded as $[Au(SR)]_n$, long used for treatment of rheumatoid arthritis (section 4.20). Little is known about their structures: it has been remarked that their clinical use would be unlikely to be sanctioned were they currently undergoing trial. EXAFS and Mössbauer measurements indicate that they have digonal coordination of gold (Au–S ~ 2.30 Å) and are, therefore, thiolate-bridged polymers [93a]. Hexameric structures have been suggested for some complexes with long alkyl groups that are soluble in organic solvents and have been established crystallographically for $R = 2,4,6\text{-}Pr^i_3C_6H_2$, which has a 12-membered Au_6S_6 ring in a chair configuration [93b]. Linear $Au(SH)_2^-$ is obtained from $Au(acac)_2^-$ and H_2S (Au–S 2.277–2.297 Å) [94]. Reaction with phosphines affords monomeric R_3PAuSR (e.g. auranofin);

the anion in $Ph_4As^+Au(SPh)_2^-$ [95] contains digonally coordinated gold (Au–S 2.262–2.271 Å) while in $Au(SR)_2^-$ ($R = 2,4,6\text{-}Pr^i_3C_6H_2$) Au–S is 2.288 Å [93].

Linear S–Au–S (but non-linear Au–S–C) is found in $PhAs^+Au(SCN)_2^-$ [96]; related phosphine complexes $(R_3P)_nAuSCN$ have been made (section 4.10.3). Sulphate and thiosulphate bind through sulphur; $Na_3Au(S_2O_3)_2.2H_2O$ has linear 2-coordinate gold in contrast to tetrahedral coordination of silver by sulphur and oxygen.

Among neutral ligands, thioethers form important complexes $AuCl(SR_2)$ (SR_2, e.g. Me_2S, Et_2S, $S(CH_2CH_2OH)_2$) that are synthetically useful since the sulphide is readily replaced by strong donors (e.g. tertiary phosphines) (sections 4.10.3 and 4.10.5). AuX(tht) (X = Cl, I) have been made. The iodide is $Au(tht)_2^+AuI_2^-$, but the chloride and bromide are neutral AuX(tht). The iodide remarkably can be synthesized at room temperature [97]:

$$2Au + I_2 \xrightarrow{\text{tht}} 2AuI(tht)$$

Essentially linear coordination is found in thiourea complexes $AuBr(S{=}C(NR_2)_2)$ (R = H, Me) and

$$[Au(S{=}C{-}\underline{NH{-}CH_2{-}CH_2{-}NH})_2]^+Cl^-$$

Bidentate dithiolate ligands afford complexes like $Au(S_2CNR_2)$ (R = Et, Pr, Bu) and $Au(S_2PR_2)$ (R = Pr), which have dimeric structures based on 8-membered rings with linear S–Au–S coordination and short Au–Au distances. These in turn are associated into chains (Figure 4.16) (Au–Au *c.* 3.0–3.4 Å) [99].

The dithioacetate is a tetramer, still with digonally coordinated gold [100]. Though long known, the gold complexes of terpenethiolates ('liquid gold')

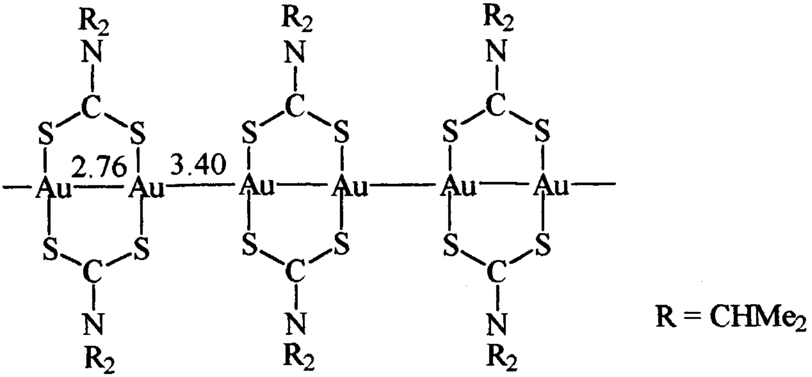

Figure 4.16 The structure of $Au(S_2CNPr^i_2)$ showing the association of dimeric units into chains.

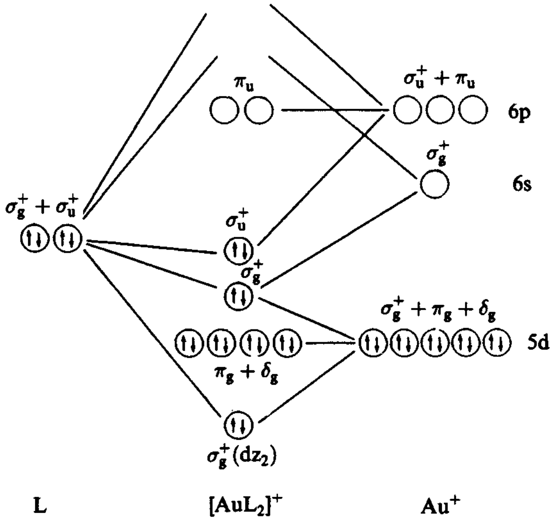

Figure 4.17 A qualitative molecular orbital scheme for a σ-bonded complex ion $[AuL_2]^+$. (Reprinted with permission from *Inorg. Chem.*, 1982, **21**, 2946. Copyright (1982) American Chemical Society.)

have, as yet, unknown structures; when painted on to pottery, then fired, they decompose to give a gold film.

4.10.7 MO schemes for 2-coordinate gold(I) complexes

A typical scheme [101] for a complex AuL_2^+ is shown in Figure 4.17.

A simple crystal field treatment predicts

$$5d_{z^2}(\sigma) > 5d_{xz,yz}(\pi) > 5d_{xy}, d_{x^2-y^2}(\delta),$$

the latter expected to be essentially non-bonding, but the relative energies will be ligand dependent, with electronegative ligands increasing d orbital participation and more electropositive ligands increasing s/p participation. There will also be gold 6s and 6p mixing into the highest ligand-field orbitals. Analysis of the spectra of $Au(CN)_2^-$ gave the ordering $d_{z^2}(\sigma) > d_{xy}$, $d_{x^2-y^2}(\delta) > d_{xz}$, $d_{yz}(\pi)$ whereas the PE spectrum of $(Me_3P)AuMe$ was interpreted in terms of $d_\pi \sim d_\delta > d_\sigma$. MO calculations for AuX_2^- (X = F to I) have recently indicated $d_\delta > d_\pi > d_\sigma$ [96].

4.11 Gold(II) complexes

Unstable dithiocarbamates $Au(S_2CNR_2)_2$ have been detected in solution by ESR but the square planar $Au(S_2C_2(CN)_2)_2^{2-}$ has been isolated as a green Bu_4N^+ salt; the gold(II) state appears to be stabilized by delocalization of

Next Page

Previous Page

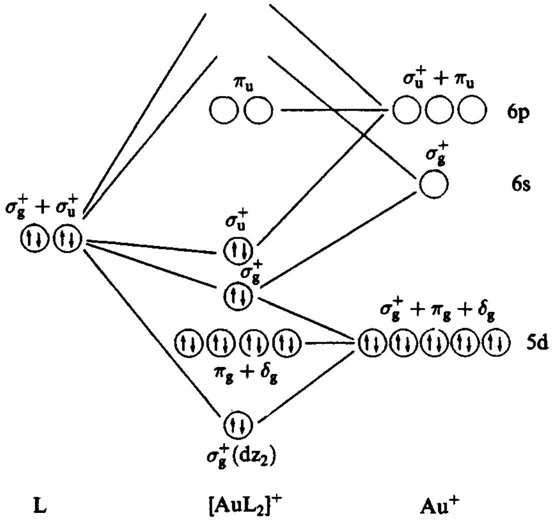

Figure 4.17 A qualitative molecular orbital scheme for a σ-bonded complex ion $[AuL_2]^+$. (Reprinted with permission from *Inorg. Chem.*, 1982, **21**, 2946. Copyright (1982) American Chemical Society.)

have, as yet, unknown structures; when painted on to pottery, then fired, they decompose to give a gold film.

4.10.7 MO schemes for 2-coordinate gold(I) complexes

A typical scheme [101] for a complex AuL_2^+ is shown in Figure 4.17.

A simple crystal field treatment predicts

$$5d_{z^2}(\sigma) > 5d_{xz,yz}(\pi) > 5d_{xy}, d_{x^2-y^2}(\delta),$$

the latter expected to be essentially non-bonding, but the relative energies will be ligand dependent, with electronegative ligands increasing d orbital participation and more electropositive ligands increasing s/p participation. There will also be gold 6s and 6p mixing into the highest ligand-field orbitals. Analysis of the spectra of $Au(CN)_2^-$ gave the ordering $d_{z^2}(\sigma) > d_{xy}$, $d_{x^2-y^2}(\delta) > d_{xz}$, $d_{yz}(\pi)$ whereas the PE spectrum of $(Me_3P)AuMe$ was interpreted in terms of $d_\pi \sim d_\delta > d_\sigma$. MO calculations for AuX_2^- (X = F to I) have recently indicated $d_\delta > d_\pi > d_\sigma$ [96].

4.11 Gold(II) complexes

Unstable dithiocarbamates $Au(S_2CNR_2)_2$ have been detected in solution by ESR but the square planar $Au(S_2C_2(CN)_2)_2^{2-}$ has been isolated as a green Bu_4N^+ salt; the gold(II) state appears to be stabilized by delocalization of

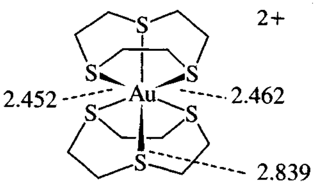

Figure 4.18 The structure of $[(1,4,7\text{-trithiacyclononane})_2Au]^{2+}$.

the unpaired electron as is likely in gold(II) phthalocyanine and in the green carbollide $(Et_4N)_2Au(C_2B_9H_{11})_2$ ($\mu = 1.79\,\mu_B$) [102]. A gold(II) complex of the macrocycle 1,4,7-trithiacyclononane (L) has octahedrally coordinated gold(II) (Figure 4.18); the gold(III) to gold(II) reduction in the course of the reaction should be noted.

$$AuCl_4^- + L \xrightarrow[\text{boil}]{HBF_4\,(aq.)} [AuL_2]^{2+}(BF_4^-)_2$$

The gold(II) complex readily undergoes one electron reduction and oxidation to the corresponding gold(I) and gold(III) complexes; the tetragonally distorted geometries for the d^8 and d^9 systems are expected, but the tetrahedral coordination in the gold(I) complex, with one monodentate and one terdentate ligand seems to be a compromise between the tendency of the ligand to utilize all its donor atoms and the usual preference of gold(I) for digonal coordination (Table 4.11) [103].

Many gold(II) complexes are diamagnetic ylids that have square planar coordination including a gold–gold bond (Figure 4.19) synthesized by oxidative addition reactions of gold(I) compounds (use of excess halogen yields a gold(III) compound, the use of a binuclear complex in this synthesis allows oxidative addition to occur in one electron steps at each gold, whereas in a mononuclear complex a two electron gold(I) to gold(III) conversion occurs) [104].

Solvated Au^{2+}, detectable by ESR, has been generated by gold reduction of $Au(SO_3F)_3$ in HSO_3F at 65°C, as well as by partial pyrolysis of $Au(SO_3F)_3$ below 140°C [105].

Table 4.11 Characteristics of $[Au([9]aneS_3)_2]^{n+}$

	n		
	1	2	3
Environment	Distorted tetrahedral	Tetragonally distorted octahedron	Strongly tetragonally distorted octahedron
Au–S (Å)	2.302, 2.345, 2.767, 2.816 (average lengths)	2.452 (×2), 2.462 (×2), 2.839 (×2)	2.348 (×2), 2.354 (×2), 2.926 (×2)

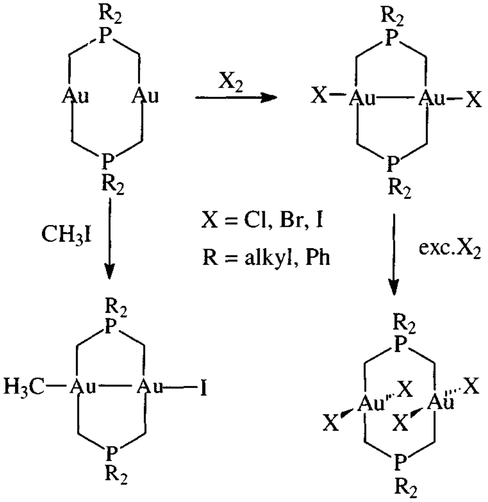

Figure 4.19 Synthesis of gold ylid complexes, including gold(II) compounds with metal–metal bonds.

Mixed-valence systems

A number of apparent gold(II) complexes are in fact mixed gold(I)–gold(III) compounds; $AuCl_2$ is $Au^{I}_{2}Au^{III}_{2}Cl_8$, AuQ (Q = S, Se, Te) is $Au^{I}Au^{III}Q_2$, $MAuX_3$ (M = alkali metal, X = halogen) is $M_2(Au^{I}X_2Au^{III}X_4)$ and $AuX_2(Sbz_2)$ is $Au(Sbz_2).AuX_3(Sbz_2)$ [106]. Study of $Cs_2Au^{I}Au^{III}Cl_6$ (Figure 4.20) in a high pressure cell mounted on a diffractometer shows that as the pressure increases, the chlorine atoms move between the gold atoms until at 5200 MPa, the gold environments are indistinguishable, formally gold(II). This is accompanied by an increase in conductivity [107].

Obviously analytical data do not distinguish between a true gold(II) complex and a mixed valence gold(I)–gold(III) species. Apart from X-ray structural determinations, techniques applicable include ESCA and ^{197}Au Mössbauer spectra [108] (which will give two sets of peaks for a mixed valence compound against one for a true gold(II) compound), magnetic susceptibility and ESR (for paramagnetic compounds) [109].

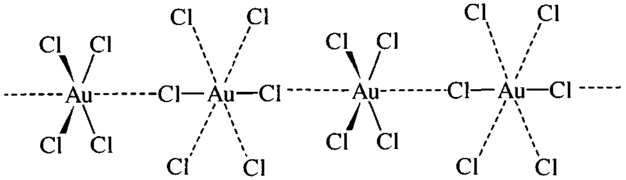

Figure 4.20 The environment of the gold atoms in $Cs_2Au^{I}Au^{III}Cl_6$. Weak Au–Cl interactions are shown as dotted lines.

4.12 Gold(III) complexes

4.12.1 Complexes of halogens

Like palladium(II) and platinum(II), gold(III) has the d^8 electronic configuration and is, therefore, expected to form square planar complexes. The d-orbital sequence for complexes like $AuCl_4^-$ is $d_{x^2-y^2} \gg d_{xy} > d_{yz}$, $d_{xz} > d_{z^2}$; in practice in a complex, most of these will have some ligand character.

The stability of gold(III) compared with silver(III) has been ascribed to relativistic effects causing destabilization of the 5d shell, where the electrons are less tightly held. Hartree–Fock calculations on AuX_4^- (X = F, Cl, Br) indicate that relativistic effects make a difference of 100–200 kJ mol^{-1} in favour of the stability of AuX_4^- (Table 4.12) [110].

The tetrahalometallates are useful starting materials.

$$Au \xrightarrow[\text{oxidizing agent}]{HX} HAuX_4 \qquad (X = Cl, Br)$$

The oxidizing agent is usually concentrated HNO_3 but can be the halogen itself; yellow fluoroaurates can be made directly or by substitution

$$Au \xrightarrow[KCl]{BrF_3} KAuF_4$$

$$AuCl_4^- \xrightarrow[\text{or } BrF_3]{F_2} AuF_4^-$$

The black iodide is unstable [3(d),112], tending to reduce to AuI_2^- in aqueous solution, but has been made *in situ*

$$Et_3N^+AuCl_4^- \xrightarrow{\text{exc. HI (liq.)}} Et_4N^+AuI_4^-$$

Typical bond lengths are 1.915 Å (X = F) [113], 2.27–2.29 Å (Cl) [114], 2.404 Å (Br) and 2.633–2.648 (I) [3(d), 115]. Other groups (CN, SCN) can also be introduced by substitution, while $Au(NO_3)_4^-$ is a classic example of monodentate nitrate (Figure 4.21) (Au–O 1.99–2.02 Å) and is prepared [116]:

$$Au_2O_3 \xrightarrow{\text{conc. } HNO_3} H_3O + Au(NO_3)_4^-$$

$$Au \xrightarrow{\text{exc. } N_2O_5} NO_2^+Au(NO_3)_4^- \xrightarrow{KNO_3} K^+Au(NO_3)_4^-$$

Table 4.12 Fundamentals from Au–X stretching in AuX_4^- (cm^{-1}) [111]

X	$\nu_1(A_{1g})$	$\nu_5(b_{1g})$	$\nu_6(Eu)$
Cl	349	324	365
Br	213	196	252
I	148	110	186

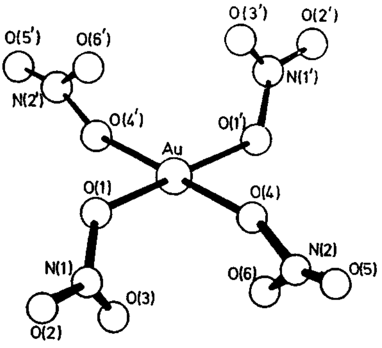

Figure 4.21 The structure of $Au(NO_3)_4$. (Reproduced with permission from *J. Chem Soc. (A)*, 1970, 3093.)

Apart from $Au(NO_3)_4^-$, relatively few complexes of gold(III), and only those with O-donors, have been examined. Two that demonstrate the preference of gold(III) for square planar coordination are $SrAu_2(MeCOO)_8$ and $SrAu_2(OH)_8$; in the latter $Au(OH)_4^-$ has Au–O 1.98 Å [117].

4.12.2 *Complexes of N-donors*

A variety of N-donors have been used to form complexes with gold(III). Some preparations of complexes with N-donors are shown in Figure 4.22; both $AuCl_3py$ and $Aupy_2Cl_2^+Cl^-$ contain square planar gold [118], as does $Au(NH_3)_4^{3+}$ (Au–N 2.02 Å), while similar bond lengths are found in $Au(NH_3)Cl_3$ (2.01 Å) and $Au(NH_3)_2Br_2^+Br^-$ (Au–N 2.04 Å, Au–Br 2.428 Å) [119]. The last can be isolated by making use of the *trans*-effect (section 4.12.6). Azide forms the square planar complex $Ph_4As^+[Au(N_3)_4]^-$

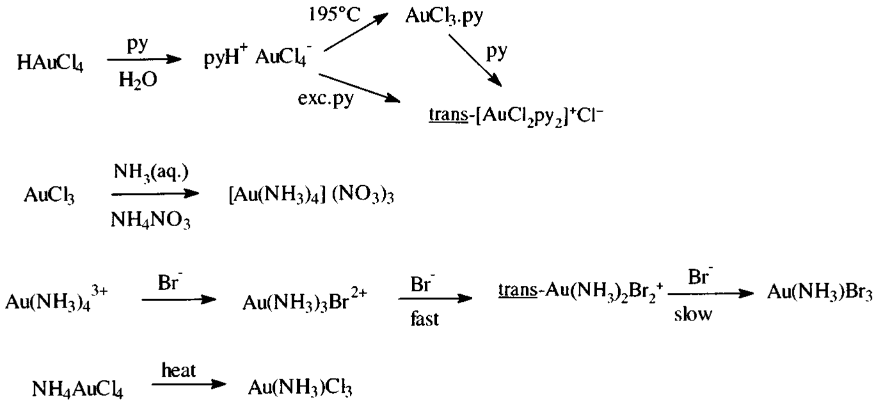

Figure 4.22 Syntheses of gold ammine complexes.

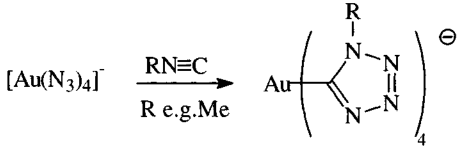

Figure 4.23 A cyclization reaction of $Au(N_3)_4$ in which 4-coordination is retained.

(Au–N 2.028 Å), which is reduced to $Au(NCO)_2^-$ by CO but in reaction with RNC undergoing an unusual cyclization (Figure 4.23) [120].

Rather less is known about complexes with bi- and tridentate ligands such as $AuCl_3$(bipy) and $AuBr_3$(phen), which are probably ionic $AuX_2L^+X^-$; with bulky ligands like 2,2-biquinolyl, 5-coordinate complexes are obtained (section 4.12.5). Ethylene-1,2-diamine affords $Au(en)_2Cl_3$, which in the solid state contains distorted $Au(en)_2Cl_2^+$ [121a]. In $Au(phen)(CN)_2Br$, the phenanthroline is monodentate [121b]. $[Au(bipy)Cl_2]^+BF_4$ also has square planar coordination of gold with Au–N 2.037 Å and Au–Cl 2.252 Å [122]. $Au(en)_2^{3+}$ reacts with β-diketones in template reactions [123] to afford complexes of tetradentate macrocycles (Figure 4.24).

With a tridentate ligand $Au(terpy)Cl_3.H_2O$ has, in fact, $AuCl(terpy)^{2+}$ with weakly coordinated chloride and water while $Au(terpy)Br(CN)_2$ has square pyramidal gold(III): the terpyridyl ligand is bidentate, occupying the axial and one basal position [124]. Macrocyclic complexes include the porphyrin complex Au(TPP)Cl (section 4.12.5); cyclam-type macrocyclic ligands have a very high affinity for gold(III) [125].

4.12.3 Tertiary phosphine and arsine complexes

While tertiary phosphines and arsines tend to reduce gold(III) to gold(I), the reverse reactions can be used synthetically [126]:

$$Ph_3PAuCl \xrightarrow{Cl_2} Ph_3PAuCl_3$$

$$Et_3PAuBr \xrightarrow{Br_2} Et_3PAuBr_3$$

The structures of both these complexes demonstrate the *trans*-influence of phosphines in lengthening the bond to the *trans*-halogen (Table 4.13).

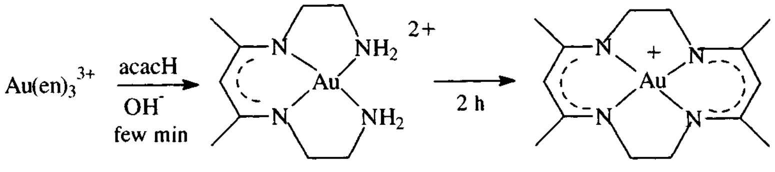

Figure 4.24 Template synthesis of a gold(III) macrocycle complex.

Table 4.13 The *trans*-influence in complexes AuX_3L

X	L	Au–X (Å)	
		X *trans* to L	X *cis* to L
Cl	PPh_3	2.347	2.273, 2.282
Cl	NH_3	2.277	2.282, 2.287
Cl	PhN	2.260	2.284, 2.289
Cl	Thianthrene	2.305	2.274
Me	PPh_3	1.923	2.100, 2.168
Ph	Cl	2.028	2.071, 2.064
Br	PEt_3	2.468	2.407, 2.416
Br	PPh_3	2.461	2.405, 2.424
Cl	Bz_2S	2.287	2.272
Br	Bz_2S	2.419	2.418, 2.425

In some cases, oxidation gives unexpected results (Figure 4.25) with concomitant formation of an Au–C bond.

Gold (I) complexes of bidentate phosphines and arsines like

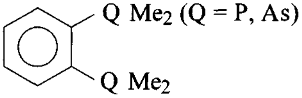

$Au(diphos)_2^+$ and $Au(diars)_2^+$ can be oxidized to gold(III) species [127]. These tend to add halide ions so that $Au(diars)_2I_2^+$ has a distorted octahedral structure with very weakly bound iodides (section 4.12.5).

4.12.4 *Other complexes*

Thiols and other sulphur ligands can be used to reduce Au^{3+} to Au^+ but gold(III) complexes can be made, for example, with tetramethylthiourea (tmu),

$$AuBr_3 \xrightarrow{tmu} trans\text{-}Au(tmu)_2Br_2^+AuBr_2^-$$

but on recrystallization, complete reduction to Au(tmu)Br occurs. Other square planar complexes characterized include $AuCl_3(SPh_2)$ [128],

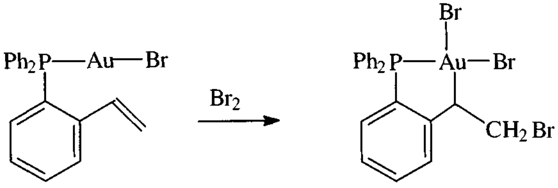

Figure 4.25 Synthesis of an organogold(III) compound by an unusual oxidative addition reaction.

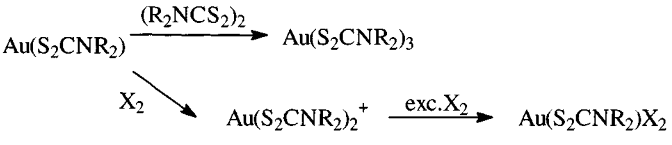

Figure 4.26 Synthesis of gold dithiocarbamate complexes.

$AuCl_3$(tht) [129], $AuX_3[S(benzyl)_2)_2]$ (X = Cl, Br) [130] and $AuCl_3$ (thianthrene). Various dithiocarbamates and dithiolene complexes have been made, some by oxidation of gold(I) complexes (Figure 4.26).

Square planar coordination is general in these; in the tris-complexes $Au(S_2CNR_2)_3$, it is obtained by two dithiocarbamates being monodentate (the third is, of course, bidentate) [131]. Such planar coordination in $[Au(S_2CNEt_2)_2]^+SbF_6^-$ involves Au–S distances of 2.316–2.330 Å [132].

An unusual example involves two complexes of formula $Au(S_2CNBu_2)$-$(S_2C_2(CN)_2)$; one has a molecular structure, the other is 'ionic' $[Au(S_2CNBu_2)_2]^+[Au[S_2C_2(CN)_2]_2]^-$ [133].

The most important complex with an 'inorganic' C-donor is $Au(CN)_4^-$, with Au–C 1.98 Å in the potassium salt [134].

$$Na^+AuCl_4^- \xrightarrow{\text{conc. KCN (aq.)}} K^+Au(CN)_4^-$$

Additionally, *trans*-$Au(CN)_2X_2^-$ can be made by oxidative addition of X_2 (X = Cl, Br, I) to $Au(CN)_2^-$.

4.12.5 Coordination numbers and gold(III)

The preference of gold(III) for planar 4-coordination is such that ligands sometimes adopt unusual denticities. Therefore, $Au(NO_3)_4^-$ has four monodentate nitrates; $Au(terpy)Cl_3.H_2O$ contains $Au(terpy)Cl^{2+}$; $Aupy_2Cl_3$ is $Aupy_2Cl_2^+Cl^-$; $Au(S_2CNBu_2)_2Br$ is $Au(S_2CNBu_2)_2^+Br^-$; $Au(S_2CNBu_2)_3$ has one bidentate and two monodentate dithiocarbamates and $Au(NH_3)_4(NO_3)_3$ has only ionic nitrates, to quote compounds already mentioned.

The tetraphenylporphyrin complex AuCl(TPP) has been claimed [135] as square pyramidal; since the gold atom lies in the plane of the porphyrin ring, and the Au–Cl distance is 3.01 Å, it should be regarded as $Au(TPP)^+Cl^-$. $Au(dien)Cl_3$ [136] has a pseudo-octahedral structure but with long Au–Cl bonds (3.12–3.18 Å) again. Five-coordination is attained in the square pyramidal 2,9-dimethylphenanthroline complexes [137] $Au(dimphen)X_3$ (X = Cl, Br) with the gold atoms some 0.1 Å above the basal plane (Figure 4.27); in contrast Au(2,2′-biquinolyl)Cl_3 is trigonal bipyramidal [138a].

Molecules of the deep blue–black compound $AuI_3(PMe_3)_2$ have a trigonal bipyramidal structure in which Au–P is 2.333–2.347 Å and Au–I is 2.709–2.761 Å. It is prepared by the reaction of gold metal with Me_3PI_2 [138b]

$$2Me_3PI_2 + Au \rightarrow [AuI_3(PMe_3)_2] + \tfrac{1}{2}I_2$$

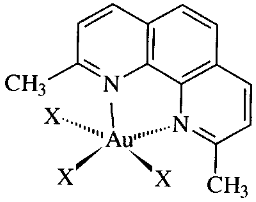

Figure 4.27 Five-coordination in the square pyramidal Au(dimphen)X_3 (X = Cl, Br).

Au(diars)$_2I_2^+I^-$ has 6-coordinate gold with rather long Au–I distances (3.35 Å) [139]. AuBr(CN)$_2$(terpy) (Figure 4.28), made as follows,

$$KAu(CN)_2Br_2 \xrightarrow[H_2O/EtOH]{1\,mol\,terpy} AuBr(CN)_2(terpy)$$

has square pyramidal coordination, with a bidentate terpyridyl occupying the apical portion and an equatorial position *trans* to bromide [140].

4.12.6 *The* trans-*effect and* trans-*influence*

Like the isoelectronic Pd^{2+} and Pt^{2+}, Au^{3+} exhibits both *trans*-effects and *trans*-influence. Table 4.13 (above) lists structural data for a number of complexes AuL_3L, showing how the disparity in Au–X distances between *cis*- and *trans*-X depends on the position of L in the *trans*-effect series; for the compounds listed, the effect is least noticeable in $AuCl_3NH_3$ as these two ligands are proximate in the series.

The *trans*-effect can be used synthetically. In the reaction of Br^- with $Au(NH_3)_4^{3+}$, the introduction of the first bromine weakens the Au–N bond *trans* to it so that the introduction of a second bromine is both sterospecifically *trans* and rapid. (A similar effect occurs in the corresponding chloride.) The third and fourth ammonia molecules are replaced with difficulty, permitting the isolation of $AuBr_2(NH_3)_2^+$ (second-order rate constants at 25°C are $k_1 = 3.40$, $k_2 = 6.5$, $k_3 = 9.3 \times 10^{-5}$ and $k_4 = 2.68 \times 10^{-2}\,l\,mol^{-1}\,s^{-1}$ at 25°C) [141].

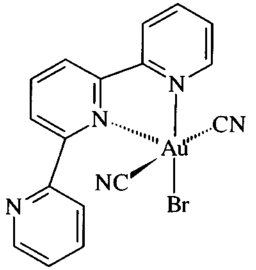

Figure 4.28 Square pyramidal 5-coordination in AuBr(CN)$_2$(terpy) made possible by terpyridyl acting as a bidentate ligand.

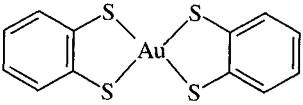

Figure 4.29 A formally gold(IV) dithiolene complex.

Factors responsible for this order include the *trans*-effect, charge neutralization, and statistical effects.

4.13 Gold(IV) complexes

A mononuclear compound containing gold in a formal oxidation state of +4 is shown in Figure 4.29; it was produced by electrochemical oxidation of the related gold(III) species [142].

The Au–S bond length at 2.30 Å is very similar to that in the gold(III) analogue (2.299–2.312 Å) and other gold(III) complexes like Au(toluene-3,4-dithiolate)$^-$ (2.31 Å) suggesting substantial covalent character in the bond.

4.14 Gold(V) complexes

A number of complexes containing the low spin d^6 ion, AuF_6^- (Au–F ~ 1.86 Å) have been made [143].

Syntheses include:

$$Au \xrightarrow[HF(liq.)]{KrF_2} KrF^+AuF_6^-$$

$$MAuF_4 \xrightarrow{F_2} MAuF_6 \qquad (M = K, Cs, NO)$$

$$AuF_3 \xrightarrow{F_2/XeF_2} (Xe_2F_{11})^+AuF_6^- \qquad (\text{Au–F } 1.86\,\text{Å})$$

AuF_5 is formed on heating $M^+AuF_6^-$ (M = NO, O_2); there has been interest in synthesizing AuF_6 by oxidation of AuF_6^- but it is likely that the t_{2g}^6 configuration is too stable to be oxidized.

4.15 Organometallic compounds of silver

Organometallic compounds of silver [2(f), 6] are restricted to the silver(I) state and are usually light, air and moisture sensitive. Simple alkyls are unstable at room temperature though some fluoroalkyls are isolable. Therefore, perfluoroisopropylsilver is stable to 60°C as a MeCN adduct. Alkenyls are more stable: styrenylsilver, prepared as follows, is stable for some days at room temperature.

$$AgNO_3 \xrightarrow{Et_3PbCH=CHPh} Ag(CH=CHPh)$$

Perfluoroisopropanylsilver sublimes *in vacuo* at 160°*C*.

Silver aryls are also stable, prepared using either diarylzinc or trialkylaryllead (or tin) compounds

$$AgNO_3 + ZnPh_2 \xrightarrow{Et_2O} AgPh + PhZnNO_3$$

AgPh is a colourless solid [144] that is rather insoluble in non-donor solvents and appears to be polymeric $(AgPh)_n$ ($n > 10$); in addition mixed compounds $(AgPh)_n.AgNO_3$ ($n = 2, 5$) can also be obtained that involve silver clusters. Mesitylsilver is a thermally stable (but light-sensitive) white crystalline solid; in the solid state it is tetrameric (in contrast to the pentameric copper and gold analogues);

$$AgCl + MesMgBr \xrightarrow{THF} [Agmes]_4$$

it tends to dissociate to a dimer in solution [145] (Figure 4.30).

With the even more sterically hindered 2,4,6-$Ph_3C_6H_2$ ligand, 1-coordinate (2,4,6-$Ph_3C_6H_2$)Ag has been claimed, though this is controversial [146].

Aryl compounds containing another donor atom in the *ortho*-position like $Ag(C_6H_4CH_2NMe_2)$ have also been isolated (they are probably clusters).

The acidic hydrogen in terminal alkynes can readily be replaced by silver, in a diagnostic test. $[(Me_3P)Ag(C{\equiv}CPh)]$ has a polymeric structure while $[(Ph_3P)Ag(C{\equiv}CPh)]_4$ is made of $[Ag(PPh_3)_2]^+$ and $[Ag(C{\equiv}CPh)_2]^-$ fragments linked so that the silver atoms form a square [147].

Apart from matrix-isolated binary carbonyls stable only at low temperatures, $Ag(CO)B(OTeF_5)_4$ (ν(C–O) 2204 cm^{-1}) has been isolated as a crystalline solid, as has $[Ag(CO)_2]^+[B(OTeF_5)_4]^-$ (linear C–Ag–C, Ag–C 2.14 Å). The IR C–O stretching vibration in the latter occurs between 2198 and 2207 cm^{-1} (depending on the counter-ion) [148a]. Under high CO pressure there is evidence for $[Ag(CO)_3]^+$ (ν(C–O) 2192 cm^{-1}) [148b]. (The area has been reviewed [149].)

A pyrazolylborate $Ag(CO)[HB(3,5(CF_3)_2pz)_3]$ loses CO under reduced pressure: it has a linear Ag–CO grouping (Ag–C–O 175.6°, Ag–C 2.037 Å; ν(C–O) 2178 cm^{-1}) [150].

4.15.1 Complexes of unsaturated hydrocarbons

Many alkenes and arenes react directly with dissolved silver salts to afford crystals of the silver complex. Examples studied by X-ray diffraction [151] include $(C_6H_6)AgX$ ($X = ClO_4, AlCl_4$) and $(C_8H_8)AgNO_3$.

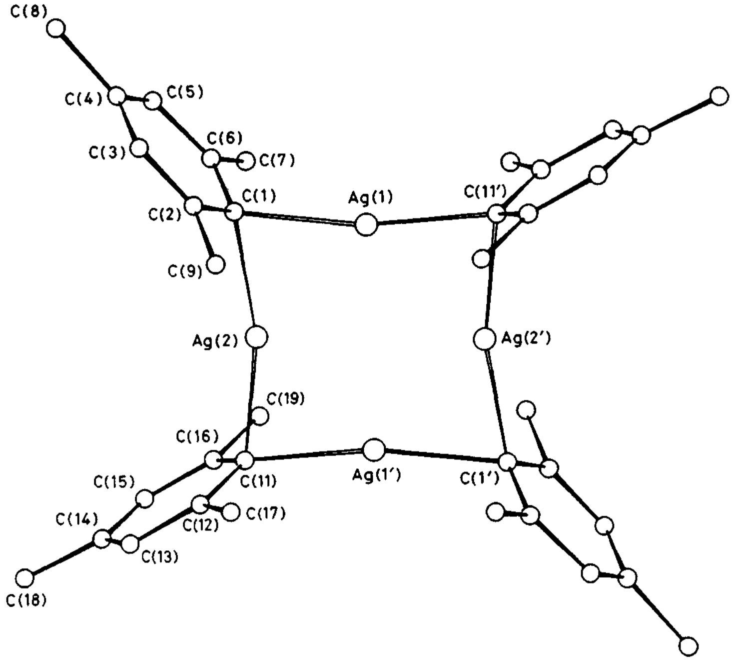

Figure 4.30 The structure of silver mesityl. (Reproduced with permission from *J. Chem. Soc., Chem. Commun.*, 1983, 1087.)

The benzene complexes have silver bound η^2 to two benzene rings in the perchlorate but only to one in the tetrachloro aluminate (Figure 4.31), while in the COT complex, each silver is bound to two double bonds in one molecule.

The Ag–C bonds tend to be asymmetric; study of silver cycloalkene complexes shows their stability to decrease in the order $C_5 > C_6 > C_7 > C_8$, corresponding to relief of strain in the cyclic molecules consequent upon the lengthening of the double bond on coordination.

Silver(I)–alkene complexation is implicated in the silver-catalysed isomerization of alkenes [152]; an example is shown in Figure 4.32.

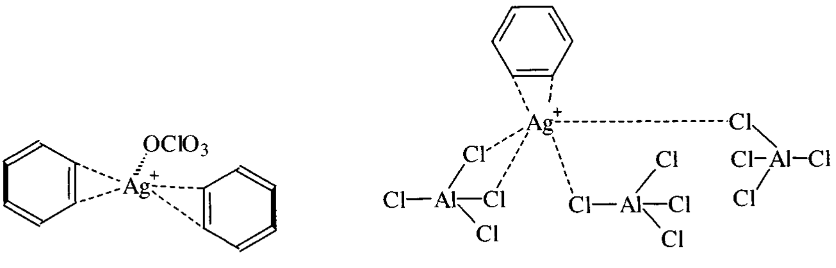

Figure 4.31 Silver(I) benzene complexes.

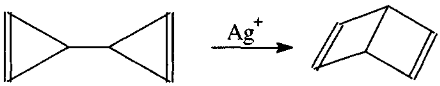

Figure 4.32 Silver-catalysed isomerization of an alkene.

Besides using chemical separations relying on different solubilities of silver–alkene complexes, mixtures of different hydrocarbons (e.g. isomeric xylenes and other polymethylated benzenes (terpenes)) can be analysed using binuclear shift reagents like $Ag^+Pr(fod)_4^-$ (fod = $Me_3CCOCHCOCF_2CF_2CF_3$). The 'soft' Lewis base (alkene or arene) binds to the silver, which in turn is bound to the paramagnetic lanthanide complex and causes shifts in the NMR spectrum of the substrate. Different xylenes, for example, afford different shifts owing to varying steric effects of the methyl groups. Using chiral shift reagents permits the observation of separate NMR signals from optically isomeric alkenes [153] (e.g. α,β-pinene).

4.16 Organometallic compounds of gold

There are considerable numbers of the organogold compounds [3(b), 9, 154], principally in the +1 and +3 oxidation states. Gold is unusual in transition metals in that, even in the +1 state, it has a marked preference for forming σ- rather than π-bonds, presumably related to the tendency of gold(I) to linear 2-coordination.

Current study in this area is prompted by laser-induced CVD of such volatile gold compounds, permitting direct laser writing in gold [155].

4.16.1 Gold(I) complexes

Simple alkyls and aryls AuR are generally unstable but coordinative saturation ensures the stability of adducts $Au(PR_3)R'$

$$Au(PR_3)Cl + LiR' \rightarrow Au(PR_3)R' + LiCl$$

(R, e.g. Me, Et, Ph; R′, e.g. Me, Ph).

These are typically colourless crystalline solids, often air and moisture stable, thermally stable to over 100°C and soluble in covalent solvents. Therefore, $Au(PMe_3)Me$ sublimes at 53°C (0.1 torr) and melts at 70–71°C; gas electron diffraction on this compound [156] confirms its linear geometry (Au–C 2.034 Å; Au–P 2.28 Å). It is a potential CVD precursor [155a]. X-ray diffraction shows $Au(PPh_3)R$ (R = Me, C_6F_5, Ph, 2,6-$(MeO)_2C_6H_3$) also to have digonal coordination. In $Au(PBu^t_3)Ph$, Au–C is 2.055 Å and Au–P is 2.305 Å; these slightly longer bond lengths reflecting the bulk of the *t*-butyl groups [157].

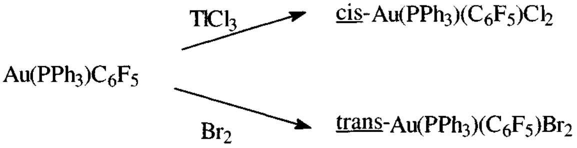

Figure 4.33 Syntheses of organogold compounds by oxidative addition to a gold(I) compound.

Another route to coordinative saturation is [158]

$$\mathrm{Au(PPh_3)Me + MeLi \xrightarrow{PMDT} Li(PMDT)^+Au(Me)_2^-}$$

(m.p. 120–123°C) (PMPT = $\mathrm{Me_2N(CH_2)_2N(Me)(CH_2)_2NMe_2}$).

The Au–C bonds in these compounds undergo cleavage with various reactants.

$$\mathrm{Au(PPh_3)Me + HgCl_2 \rightarrow Au(PPh_3)Cl + MeHgCl}$$

though sometimes if the Au–C bond is strong, oxidative addition to an organogold(III) compound occurs (Figure 4.33).

Addition with iodomethane can occur

$$\mathrm{Au(PR_3)Me \xrightarrow{MeI}} \textit{cis}\text{-}\mathrm{Au(PR_3)Me_2I} \qquad \mathrm{(PR_3 = PMe_3, PMe_2Ph)}$$

as can elimination

$$\mathrm{Au(PPh_3)Me \xrightarrow{MeI} Au(PPh_3)I + C_2H_6}$$

Fluorinated alkyls and aryls, generally more stable than the unsubstituted compounds, have been widely studied.

Several synthetic routes often exist (Figure 4.34).

$\mathrm{Au(C_6F_5)_2^-}$, also with linear coordination of gold (Au–C 2.043–2.044 Å) [159], can be made:

$$\mathrm{AuCl(SC_4H_8) \xrightarrow[Bu_4NBr]{2LiC_6F_5} (Bu_4N^+)Au(C_6F_5)_2^-}$$

One exceptional compound is the mesityl: photosensitive but thermally stable (Figure 4.35).

$$\mathrm{Au(CO)Cl \xrightarrow{(mes)MgBr} Au(mes)}$$

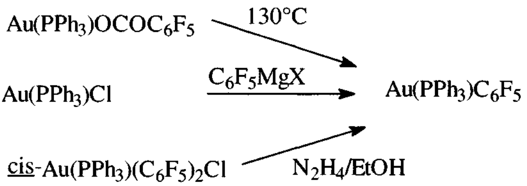

Figure 4.34 Some syntheses of a pentafluorophenylgold complex.

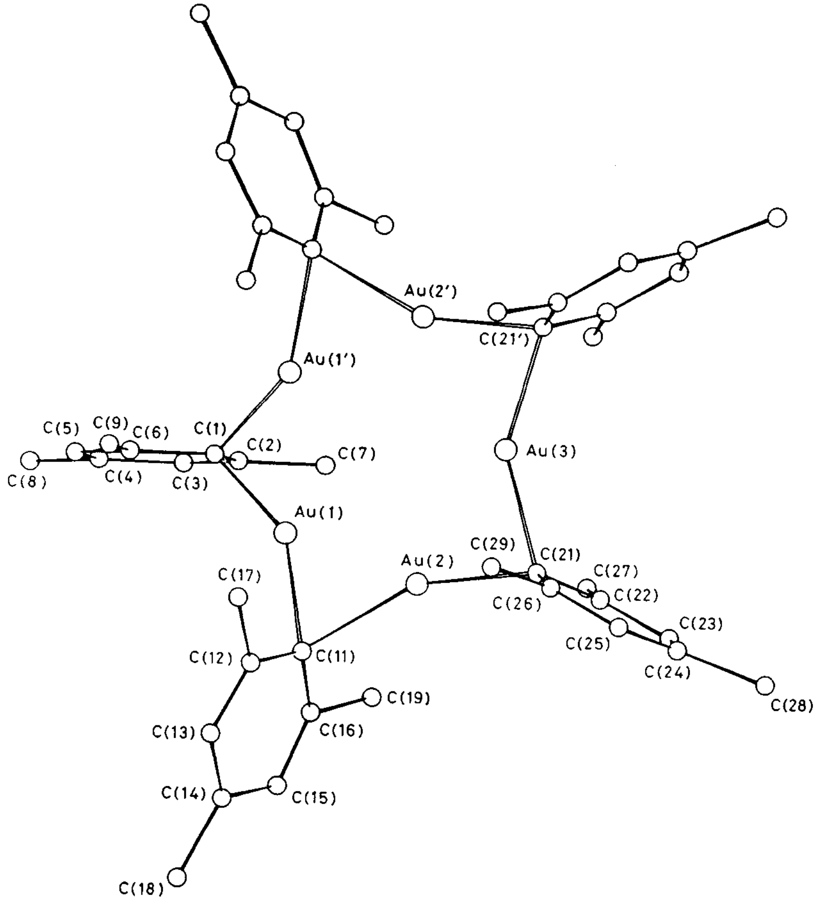

Figure 4.35 The structure of gold mesityl. (Reproduced with permission from *J. Chem. Soc., Chem. Commun.*, 1983, 1305.)

It is a pentamer with bent digonal coordination of gold (148–154°) and short Au–Au distances (2.70 Å); in solution it is a dimer. It reacts with PPh_3 to form $Au(PPh_3)(mes)$, with bidentate phosphines to afford $(mes)AuPR_2(CH_2)_nPR_2Au(mes)$ ($n = 1, 2$); and with Et_4NCl forming $Et_4N^+Au(mes)Cl^-$, all with essentially linear coordination of gold [160].

Some 2,4,6-trinitrophenyls have been made [161]

$$AuCl_2^- \xrightarrow{HgR} AuRCl^- \xrightarrow{SbPh_3} Au(SbPh_3)_4^+AuR_2^-$$

($R = 2,4,6\text{-}(NO_2)_3C_6H_2$).

o-Nitrophenyls like $Au(o\text{-}C_6H_4NO_2)(AsPh_3)$, also 2-coordinate, have likewise been made.

A range of alkynyls exist, for example:

$$\mathrm{AuX(SMe_2)} \xrightarrow[\mathrm{MeNC}]{\mathrm{MeLi}} \mathrm{Au(CNMe)Me} \qquad (\mathrm{X = Cl, Br})$$

$$\mathrm{AuX(SMe_2)} \xrightarrow{\mathrm{Me_3CC{\equiv}CLi}} \mathrm{Au(PMe_3)C{\equiv}CCMe_3}$$

X-ray diffraction confirms linear coordination in $\mathrm{Au(PPh_3)(C{\equiv}CC_6F_5)}$ and $\mathrm{Au(H_2NCHMe_2)(C{\equiv}CPh)}$ with the short Au–C bonds (1.935–1.99 Å) expected for bonds to sp hybridized carbon. Decomposition of these compounds in the vapour above 150°C is a potential route to very pure gold films [162].

(Cyclopentadienyl)gold is a very unstable, even explosive, yellow solid stabilized by adduct formation with tertiary phosphines.

$$\mathrm{Au(PPh_3)Cl} \xrightarrow{\mathrm{C_5H_5Na}} \mathrm{Au(PPh_3)(C_5H_5)}$$

IR and NMR evidence indicates it to be σ-bonded, like $\mathrm{Au(PPr_3)(C_5H_5)}$ (X-ray) [163], but at room temperature the C_5 ring hydrogens are equivalent owing to rapid site exchange ('ring whizzing').

Though matrix-isolated gold(0) species Au(CO) and $\mathrm{Au(CO)_2}$ are very unstable, the gold(I) compound Au(CO)Cl has long been known (section 4.10.5). Au(CO)Br is unstable but salts of $[\mathrm{Au(CO)_2}]^+$ of varying stability have been made; $[\mathrm{Au(CO)_2}](\mathrm{Sb_2F_{11}})$ is stable to 130°C [164].

4.16.2 Gold(III) complexes

Species $\mathrm{AuRX_2}$, $\mathrm{AuR_2X}$, $\mathrm{AuR_3}$ and $\mathrm{AuR_4^-}$ have all been made, with gold invariably achieving a square planar geometry, sometimes by adduct formation, dimerization or other polymerization. The first gold(III) alkyls were reported in 1907 and are, therefore, among the earliest known organometallics.

Alkyls

The alkyls have been studied in detail, particularly the methyls. Figure 4.36 depicts some of the interrelationships in them.

The monoalkyls are relatively unstable. Red crystals of $[\mathrm{MeAuBr_2}]_2$ are obtained by reaction of bromine with the corresponding dialkyl:

$$[\mathrm{Me_2AuBr}]_2 + 2\mathrm{Br_2} \rightarrow [\mathrm{MeAuBr_2}]_2 + 2\mathrm{MeBr}$$

An unsymmetrical structure is indicated by reactions like those in Figure 4.37 (as well as X-ray diffraction [165a]).

The dialkyls are the best characterized in this class. All the complexes $\mathrm{AuR_2X}$ (X = halogen) are planar halogen-bridged dimers, stable to 70°C or more. They are best prepared from an anhydrous halide $\mathrm{Au_2X_6}$ or adduct $\mathrm{AuX_3L}$, though if an alkyl magnesium iodide Grignard is used, the

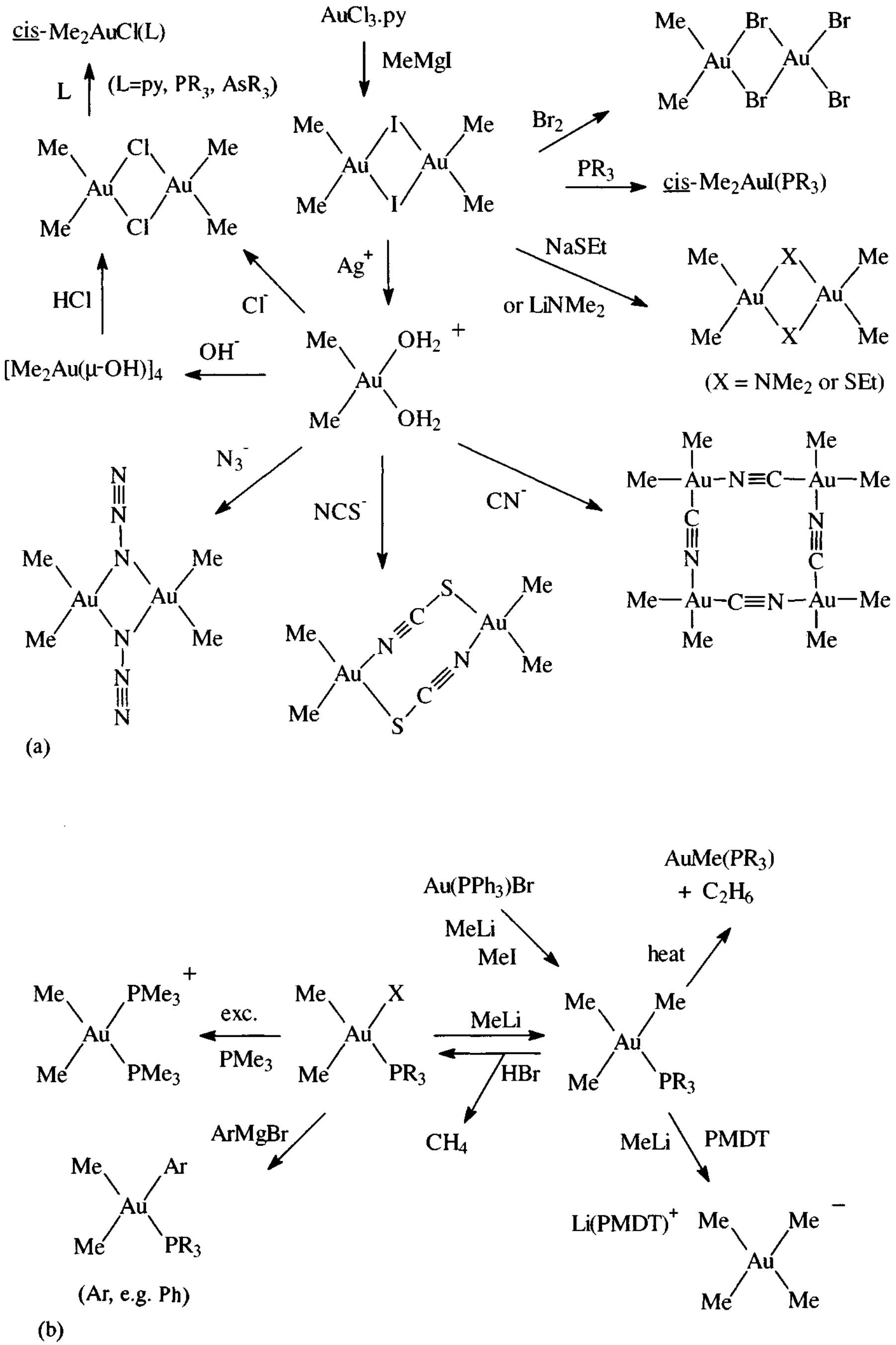

Figure 4.36 Syntheses of gold(III) methyls.

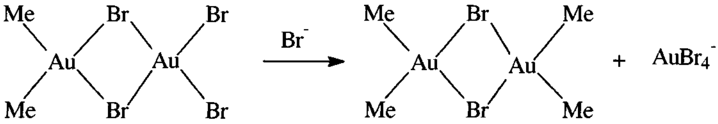

Figure 4.37 Evidence for the asymmetrical dimeric structure of methylgold dibromide.

product is the iodide $(AuR_2I)_2$. Grignards are preferred to organolithium compounds to obviate the possibilities of further substitution.

$$Au_2Br_6 \xrightarrow{MeMgI} (AuMe_2I)_2$$

$$AuBr_3py \xrightarrow{EtMgBr} (AuEt_2Br)_2$$

A recent synthesis of $(AuMeCl_2)_2$ uses $AuCl_3$ and $SnMe_4$ in methanol at −50°C [165b].

Treatment of $(AuMe_2I)_2$ with silver nitrate gives an interesting alkyl aqua ion [166] *cis*-$AuMe_2(OH_2)_2^+$, stable in aqueous solution, which reacts with pseudohalide ions to form $[AuMe_2X]_2$ ($X = N_3$, NCS or NCO); the corresponding cyanide is a tetramer since the cyanide group can only form linear bridges. In solution, the dimethyl gold aqua ion is in equilibrium with the hydroxy complex $[AuMe_2(OH)]_2$, also a tetramer in the solid state (Figure 4.36). Amides and thiolates can also act as bridging ligands in dimers, as shown by X-ray diffraction [167], but the structures shown for some of the diethyl gold complexes (Figure 4.38), notably with chelating ligands, are still tentative.

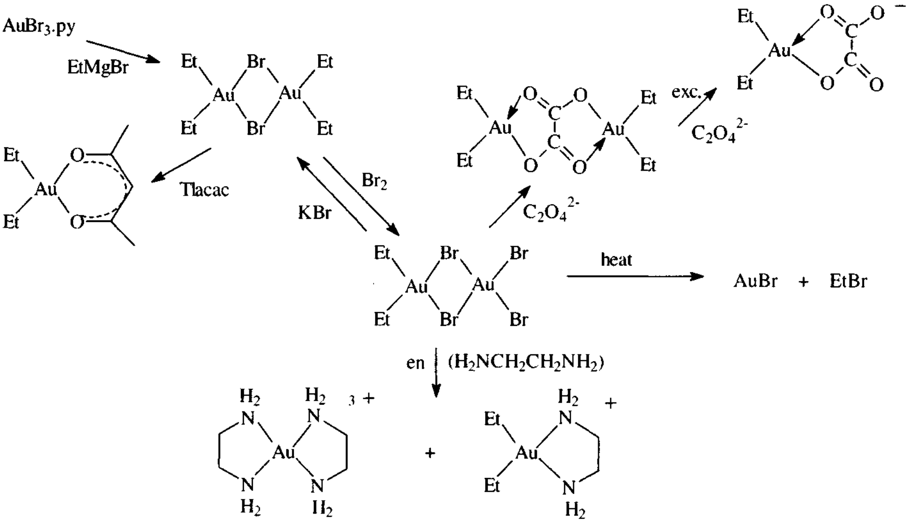

Figure 4.38 Diethyl gold(III) compounds.

Not all the gold dialkyls have dimeric structures; the halogen bridges can be cleaved with excess phosphine:

$$[\mathrm{AuMe_2Cl}]_2 \xrightarrow{\mathrm{PMe_3}} cis\text{-}\mathrm{AuMe_2Cl(PMe_3)} \xrightarrow{\text{exc. }\mathrm{PMe_3}} cis\text{-}\mathrm{AuMe_2(PMe_3)_2^+}$$

$\mathrm{AuMe_2(acac)}$ is being studied as a vehicle for laser CVD of gold films; it has the expected square planar structure in the gas phase (Au–C 2.054 Å; Au–O 2.085 Å) [168].

Trialkyls are only known as Lewis base adducts. Reaction of $\mathrm{Au_2Br_6}$ with methyllithium at 70°C affords an unstable '$\mathrm{AuMe_3}$' (which is probably $\mathrm{AuMe_3Br^-}$), but stable phosphine adducts $\mathrm{AuMe_3PR_3}$ (R, e.g. Me, Ph) can be made [169].

$$\mathrm{Au_2Br_6} \xrightarrow{\mathrm{MeLi}} \text{'}\mathrm{AuMe_3}\text{'} \xrightarrow{\mathrm{PR_3}} \mathrm{AuMe_3(PR_3)}$$

Mixed alkyls can be made

$$\mathrm{AuMe(PPh_3)} \xrightarrow{\mathrm{MeI/Bu^tLi}} trans\text{-}\mathrm{AuMe_2Bu^t(PPh_3)}$$

The latter isomerizes to the isobutyl analogue; it is inhibited by added $\mathrm{PPh_3}$ and it seems likely that the reaction proceeds via a 3-coordinate $\mathrm{AuR_3}$ species, also likely to be implicated in *cis–trans* isomerization reactions. *cis*-$\mathrm{AuMeEt_2(PPh_3)}$ has Au–P 2.371 Å, Au–C 2.10–2.14 Å; complexes of this type react with RLi, displacing $\mathrm{PPh_3}$ and forming tetraalkylaurates [170].

The tetramethyl species can be isolated as a thermally stable (but air-sensitive) salt (m.p. 86–88°C)

$$\mathrm{AuMe_3(PPh_3)} \xrightarrow{\mathrm{MeLi}} \mathrm{Li(PMDT)^+AuMe_4^-}$$

(PDMT = $\mathrm{Me_2N(CH_2)_2NMe(CH_2)_2NMe_2}$) while salts with other large cations like $\mathrm{Bu_4NAuR_4}$ (R = Me, Et) are benzene soluble [171].

Aryls

Monoaryls of gold(III) are traditionally made by an unusual reaction [172]. $\mathrm{AuCl_3}$ reacts with arenes to afford aryl halides (e.g. with benzene to give 1,2,4,5-tetrachlorobenzene) and HCl; if, however, the reaction is quenched by adding ethanol or ether, a yellow precipitate of $\mathrm{AuRCl_2}$ (R, e.g. Ph) is obtained. These are believed to be dimers in solution. Stable adducts *cis*-$\mathrm{AuRCl_2(L)}$ (L = py, $\mathrm{PMe_2Ph}$, $\mathrm{PPh_3}$, $\mathrm{SPr^i_2}$) have been obtained; the dipropyl sulphide adduct (Figure 4.39) has the Au–Cl distance *trans* to phenyl 0.11 Å longer than that *trans* to sulphur, showing the considerable *trans*-influence of an aryl group [173].

Another route to aryls, applicable to anionic derivatives [174] is:

$$\begin{aligned}&\mathrm{2R_4NAuCl_4 + PhNHNH_2HCl}\\ &\quad \rightarrow \mathrm{[R_4N][AuCl_2] + [R_4N][AuCl_3Ph] + N_2 + 4HCl}\end{aligned}$$

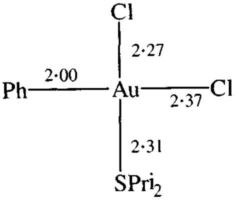

Figure 4.39 Bond lengths in *cis*-AuPhCl$_2$(SPr$^i_2$).

AuCl$_3$Ph$^-$ undergoes reversible solvolysis of the chloride *trans* to phenyl [175].

The relative stability of the gold(III) iodo species should be noted:

$$\mathrm{Bu_4NAuCl_3Ph} \xrightarrow{\mathrm{Bu_4NI}} \mathrm{Bu_4NAuI_3Ph}$$

though it cannot be recrystallized [174].

Perhalogenoaryls are more stable than the unsubstituted phenyls [176] and can be synthesized conveniently by oxidation of gold(I) complexes (demonstrating the stability of the Au–C bond). The initial product of oxidation addition seems to be the *trans*-isomer, which generally rearranges to the *cis*-form:

$$\mathrm{Au(C_6Br_5)(PPh_3)} \xrightarrow{\mathrm{Cl_2}} trans\text{-}\mathrm{AuCl_2(C_6Br_5)(PPh_3)}$$

$$\mathrm{Au(PPh_3)Cl} \xrightarrow{\mathrm{(C_6F_5)_2TlBr}} cis\text{-}\mathrm{AuCl(C_6F_5)_2(PPh_3)}$$

$$\mathrm{Au(C_6F_5)_2^-} \xrightarrow{\mathrm{X_2}} cis\text{-}\mathrm{AuX_2(C_6F_5)_2^-} \qquad (\mathrm{X = Cl, Br, I})$$

$$\mathrm{AuBr(C_6F_5)^-} \xrightarrow{\mathrm{(C_6F_5)_2TlBr}} \mathrm{AuBr(C_6F_5)_3^-}$$

A conventional synthesis may be used for the triaryl obtained as a Lewis base adduct

$$\mathrm{AuCl_3} \xrightarrow{\mathrm{C_6F_5MgBr/Et_2O}} \mathrm{Au(C_6F_5)_3(PPh_3)}$$

Structures of AuCl(C$_6$F$_5$)$_2$(PPh$_3$), AuCl(C$_6$F$_5$)$_3^-$ [177] and Au(C$_6$F$_5$)$_3$ (diars) all show the preference of gold(III) for 4-coordinate planar geometry (Figure 4.40); in the last, the diarsine is monodentate [178]. (Bu$_4$N)[AuCl$_2$(C$_6$F$_5$)$_2$] is *trans* [179].

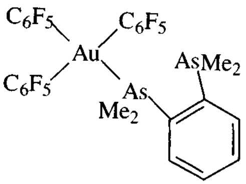

Figure 4.40 4-Coordination in AuMe$_3$(diars) made possible by a monodentate diarsine ligand.

The tetraphenylaurate ion is square planar in its Bu_4N^+ salt, while the analogous perfluorophenyl can be made:

$$AuCl_3(SC_4H_8) \xrightarrow[Bu_4NBr]{C_6F_5Li} Bu_4N[Au(C_6F_5)_4]^-$$

Average Au–C bond lengths are 2.03 and 2.08 Å, respectively [180].

Elimination reactions of aryls and mixed aryl alkyls have been widely studied [181]; aryldimethyls eliminate Ar–Me on heating.

Ylids

An extensive chemistry is developing of dinuclear gold(III) complexes with phosphorus ylid ligands (Figure 4.41). As mentioned in section 4.19, gold(I) compounds can undergo one- or two-electron oxidative additions,

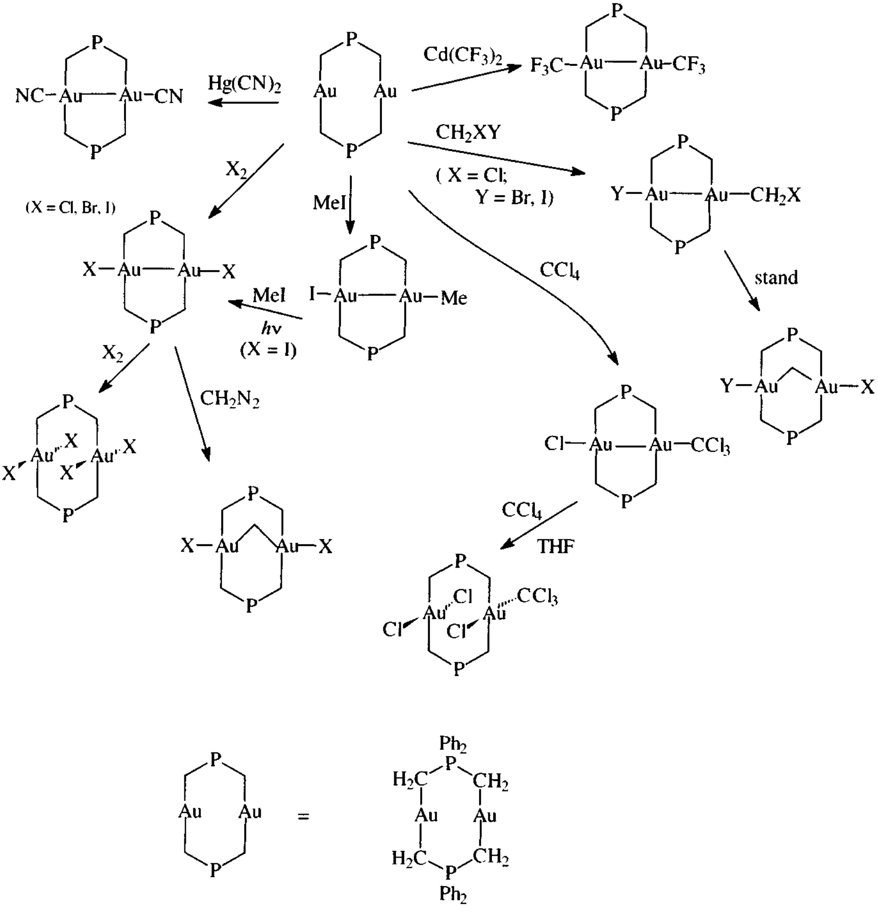

Figure 4.41 Reactions of gold ylids.

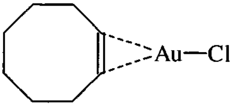

Figure 4.42 The structure of AuCl(cyclooctene).

affording gold(II) species (with a metal–metal bond) or gold(III) compounds. A selection of these reactions are shown in Figure 4.41; they also show examples where a methylene group bridges between two gold atoms, the oxidative addition of CCl_4 and a disproportionation reaction leading to a product with separate gold(I) and gold(III) centres [182].

Alkene complexes

A number of complexes AuClL have been made; those with cycloalkenes are most stable decomposing at 50–100°C. At present, few structural data are available, an exception being for AuCl(cyclooctene) (Figure 4.42) which has a structure with η^2 bonding of the alkene (Figure 4.43) [183].

4.17 Gold cluster complexes

Gold, unlike silver, forms a wide range of cluster complexes [184] where the average oxidation state of the metal is below +1; they may be synthesized by reduction of gold(I) phosphine complexes:

$$AuI(PPh_3) \xrightarrow{NaBH_4} Au_{11}I_3(PPh_3)_7$$

$$Au(NO_3)(PR_3) \xrightarrow{NaBH_4} Au_9(PR_3)_8(NO_3)_3 \qquad (R = Ph, p\text{-tolyl})$$

$$AuCl(PPh_2cy) \xrightarrow{NaBH_4} Au_6(PPh_2cy)_6^{2+}$$

Other reducing agents like Ti(η^6-toluene)$_2$ have also been used. Addition or removal of gold atoms from clusters can frequently be accomplished (Figure 4.44).

Crystallographic examination shows the clusters with eight or more gold atoms have structures based on an array of gold atoms surrounding a central gold atom. (Smaller polyhedra cannot accommodate a central gold because

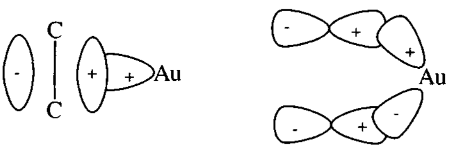

Figure 4.43 Bonding in gold alkene complexes.

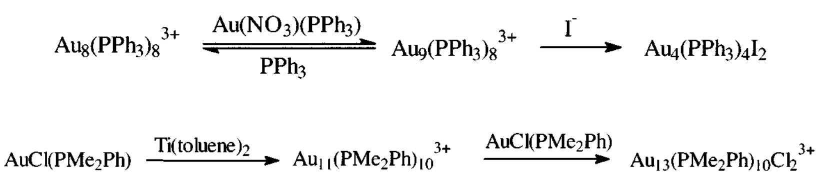

$$Au_8(PPh_3)_8{}^{3+} \underset{PPh_3}{\overset{Au(NO_3)(PPh_3)}{\rightleftharpoons}} Au_9(PPh_3)_8{}^{3+} \xrightarrow{I^-} Au_4(PPh_3)_4I_2$$

$$AuCl(PMe_2Ph) \xrightarrow{Ti(toluene)_2} Au_{11}(PMe_2Ph)_{10}{}^{3+} \xrightarrow{AuCl(PMe_2Ph)} Au_{13}(PMe_2Ph)_{10}Cl_2{}^{3+}$$

Figure 4.44 Syntheses of gold clusters.

the ‘hole’ is too small, though six golds can surround a carbon atom.) The smallest cluster, of four golds, in $Au_4I_2(PPh_3)_4$ or $[Au_4(PBu^t_3)_4]^{2+}$ has a compact tetrahedral structure [185] while $[Au_6(PPh_3)_6]^{2+}$ has an edge-sharing bitetrahedral arrangement (Figure 4.45) and $[Au_7(PPh_3)_7]^+$ is a pentagonal bipyramid.

High nuclearity clusters $[Au(AuPR_3)_n]^{x+}$ with central gold atoms adopt two types of structure; those with $12n + 18$ electrons have essentially spherical structures, whereas those with $12n + 16$ electrons have the peripheral atoms on the surface of a toroid.

$Au_{13}(PMe_2Ph)_{10}Cl_2^{3+}(PF_6)_3$ has an icosahedron of golds surrounding the central gold.

The bonding in the centred clusters is believed to involve principally gold 6s orbitals, the 5d being filled and essentially core-like, and the 6p too high in energy to be utilized. ‘Surface’ gold atoms use s/p_z hybrid orbitals, the ‘outwardly’ directed part of the hybrid is involved in forming the Au–PR_3 bond and the ‘inwardly’ directed part bonds to the central atom, overlapping with its 6s and 6p orbitals. There is also peripheral metal–metal bonding on the ‘surface’ of the cluster, but this is less important, as the Au–Au distances between surface gold atoms are 0.2–0.3 Å longer than the radial Au–Au distances.

There is evidently a flat potential energy surface for these clusters as different skeletal isomers can actually be isolated in the solid state for $Au_9[P(C_6H_4OMe)_3]_8(NO_3)_3$: a brown form has a D_{4d} crown structure and a green form has a D_{2h} structure. In solution, however, they share a common structure with identical ^{31}P NMR spectra; either the solution cluster has a regular arrangement of phosphines, or it is fluxional [186].

$[Au_{39}(PPh_3)_{14}Cl_6]Cl_2$ has a 1 : 9 : 9 : 1 : 9 : 9 : 1 layered structure in which the central gold is surrounded by other golds [187].

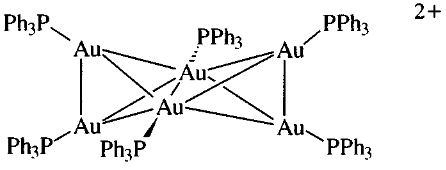

Figure 4.45 The edge-sharing bitetrahedral structure of $[Au_6(PPh_3)_6]^{2+}$. (Reproduced with permission from *J. Chem. Soc., Dalton Trans.*, 1991, 3211.)

A very large cluster $Au_{55}(PPh_3)_{12}Cl_6$ of as yet unknown structure has been reported. Physical measurements indicate the bonding to be substantially metallic in character [188].

$$Au(PPh_3)Cl \xrightarrow{B_2H_6} Au_{55}(PPh_3)_{12}Cl_6$$

Apart from gold-centred clusters, several hetero-atom clusters have been made [189]. The oxo-centred cluster has been used as a starting material in synthesis [190].

$$Au(PPh_3)Cl \xrightarrow[NaBF_4]{Ag_2O} (Ph_3PAu)_3O^+BF_4^-$$

$$[(Ph_3PAu)_3O]^+ + (MeSi)_3P \rightarrow (Ph_3PAu)_5P^{2+} + (Me_3Si)_2O$$

$$Ph_3PAuCl + C[B(OMe)_2]_4 \rightarrow (Ph_3PAu)_6C^{2+}$$

Figure 4.46 shows a MO scheme for the Au_6C framework; the six golds use 5p hybrids to overlap with the carbon s and p orbitals (as they do in

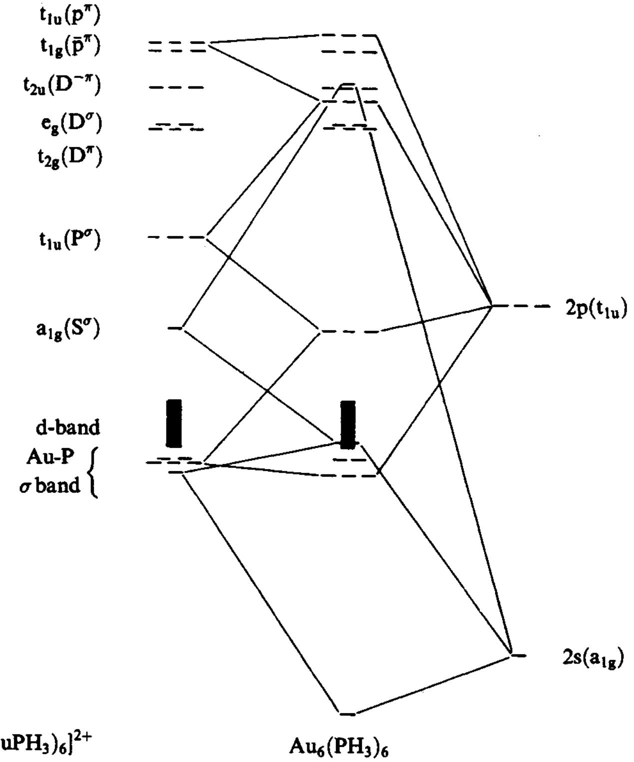

Figure 4.46 Orbital interaction diagram for the Au_6C framework in $(H_3PAu)_6C^{2+}$ showing the important bonding interactions of the carbon 2s and 2p orbitals with the MOs of the gold cluster. (Reprinted from *J. Organomet. Chem.*, **384**, 405, 1990, with kind permission from Elsevier Science S.A., P.O. Box 564, 1001 Lausanne, Switzerland.)

gold-centred clusters), resulting in four bonding orbitals (in addition to the 30 gold d orbitals).

An electron count shows (6 × 11) electrons contributed by gold, four from carbon; deducting two for the positive charge, leaves 68 electrons, which just occupy the four bonding MOs plus the gold 5d orbitals [191].

4.18 Relativistic effects in gold chemistry

For atoms of high atomic number, the properties of the valence electrons are modified [192]. The s electrons that approach the nucleus most closely are attracted strongly by the high nuclear charge and acquire velocities near enough to the speed of light to have a substantial, relativistic increase in velocity and mass. This causes contraction of the s shells. It is seen from Figure 4.47 that the effect is most pronounced at gold. (The effect occurs in addition to the 'lanthanide contraction', which itself roughly cancels out the expected increase in size of the atom owing to the outermost orbital being 6s rather than 5s in silver: without relativistic effects, the radii of silver and gold would be the same.) Outer electrons, therefore, also contract owing to orthogonality. The effect is not confined to the s orbitals; in the case of gold, as far as bonding orbitals are concerned, the effect of relativity is to stabilize 6s considerably, stabilize 6p rather less, and destabilize 5d slightly. This leads to the small 5d–6s (and large 6s–6p) separations noted for gold.

Chemical and physical effects are manyfold [193]. The contraction leads to gold forming shorter and stronger covalent bonds and is likely to be

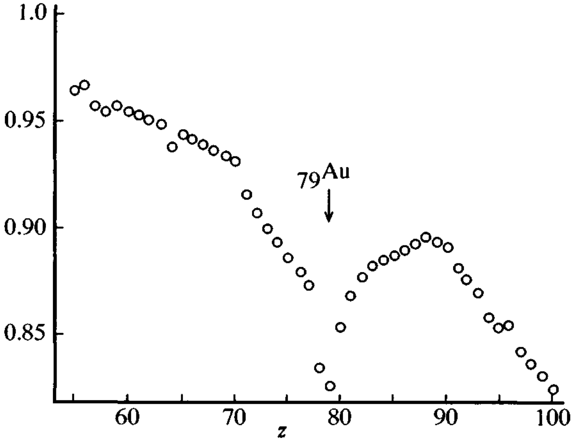

Figure 4.47 Relativistic contraction of the 6s shell in the elements Cs ($Z = 55$) to Fm ($Z = 100$) showing how relativistic effects on electrons become most pronounced at gold. (Reprinted with permission from *Acc. Chem. Res.*, 1979, **12**, 226. Copyright (1979) American Chemical Society.)

responsible for the 'aurophilic' interactions between neighbouring molecules as well as for gold clusters and gas-phase Au_2 molecules. It is responsible for the high ionization energies of gold (and hence its 'noble' character) and high electron affinity (leading to the isolability of Cs^+Au^-).

On a 'metallic' level, physical properties like the heats of atomization and boiling point are higher than extrapolation would predict. The density of gold is some 18% higher than 'non-relativistic' calculation predicts so that the Au–Au distance in gold is shorter than the Ag–Ag distance in silver. The colour of gold results from the 5d to Fermi level transitions occurring *c.* 2.3 eV, causing gold to absorb in the blue–violet region, reflecting red and yellow; the corresponding transition in silver is in the UV >3.5 eV.

The non-relativistic band structures of silver and gold are very similar so that, were it not for relativistic effects, 'gold would look silver'.

4.19 Aurophilicity

Many gold complexes have unusually short Au–Au contacts in the solid state. Therefore, linear X–Au–Y gold complexes often have packing to give Au–Au distances in the range 2.7–3.3 Å (Figure 4.48) whereas in corresponding copper or silver compounds metal–halogen contacts determine solid state packing (X, Y = halogen or neutral donor).

These short Au–Au contacts may be compared with distances of 2.88 Å in metallic gold and 2.60 Å in gaseous Au_2. The term 'aurophilicity' has been coined by H. Schmidbaur to describe the phenomenon [189, 194]. The interactions can occur as pairs, squares, linear chains or two-dimensional arrays of gold centres. Examples include the association between dimer units in the dithiocarbamates $Au(dtc)_2$ (Figure 4.16) and the ionic tetrahydrothiophen complexes $Au(tht)_2^+AuX_2^-$ (X = halogen), where cations and anions stack with Au–Au 2.97–2.98 Å (X = I). The interaction is such that $Au(S_2O_3)_2^{3-}$ pair up, despite their charge, with Au–Au 3.24 Å in the sodium salt. Likewise in $Aupy_2^+AuCl_2^-$, cations pair up at 3.42 Å apart [10, 195].

It certainly does not seem that these interactions continue in solution, so that their magnitude is weaker than solvation forces. Theoretical explanation has suggested that the unused, filled, $6s–5d_{z^2}$ hybrid (section 4.1) interacts with vacant $6p_x,p_y$ orbitals at right angles to the digonal bonds (Figure 4.49).

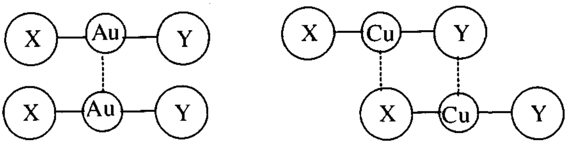

Figure 4.48 The contrast in intermolecular forces between X–Au–Y and X–Cu–Y systems (X, Y: halogen or neutral donor).

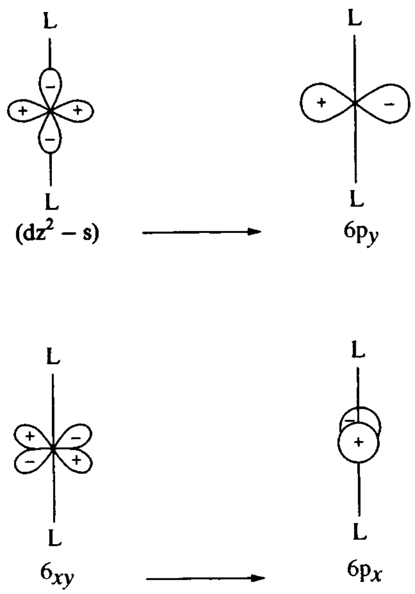

Figure 4.49 Interaction of a filled hybrid orbital with vacant $6p_x, p_y$ orbitals leading to aurophilic forces. (From K.P. Hall and D.M.P. Mingos, *Progr. Inorg. Chem.*, 1984, **32**, 264. Copyright © 1990 John Wiley. Reprinted by permission of John Wiley & Sons, Inc.)

A recent *ab initio* calculation on $(ClAuPH_3)_2$ suggests, however, that, at a distance of around 3.4 Å, the effect is largely caused by ligand dipole–dipole attractions reinforced by relativistic effects [196]. Estimates of the Au–Au forces are in the range 25–35 kJ mol^{-1}, slightly weaker than hydrogen bonds, i.e. by no means negligible [196, 197].

Intramolecular Au–Au interactions are found in some binuclear complexes $(AuX)_2$, where X is a chelating ligand like dithiocarbamate, phosphine ylid $(R_2P(CH_2)_2^-)$ or bidentate phosphines. Therefore, in $[Au(S_2CNBu_2)]_2$ the Au–Au distance is 2.78 Å (Figure 4.50).

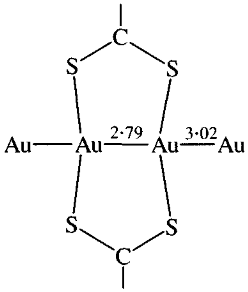

Figure 4.50 Short intramolecular Au–Au contacts in $[Au(S_2CNBu_2)]_2$.

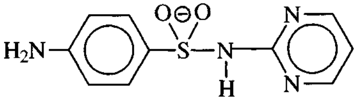

Figure 4.51 The ligand in silver(I) sulfadiazine.

4.20 Silver and gold compounds in medicine

Silver compounds have been known for a long time to possess anti-bacterial properties. Silver(I) sulfadiazine (Figure 4.51 shows the ligand) is a slow release agent for Ag^+. It is used as a cream to prevent infections in severe burns. It has a chain structure with each silver bound to three nitrogens from different pyrimidine rings and an oxygen from a sulphonyl group. (There is also a weak Ag–Ag interaction (2.92 Å)). Anti-bacterial interaction is believed to involve Ag–DNA interactions [198].

Gold compounds were first used in 1929 by French doctors to treat rheumatoid arthritis. Two of the most commonly used are aurothiomalate (myocrisin) and aurothioglucose (solganol) (Figure 4.52), given by injection of their solutions in doses of up to 25 mg a week for some years.

These drugs are gold(I) thiolates of the type $(AuSR)_n$ of ill-defined structure (they are usually obtained as powder), probably oligomers with 2-coordinate gold. Use of the S-donor ligands affords lability of the complexes in the body and also stabilizes the gold(I) state against disproportionation in aqueous solution. A disadvantage of this approach is that the compounds are restricted to vascular fluids (e.g. blood, lymph) until biological ligands break up the oligomers and they are vulnerable to ingestion by white cells [199].

The recently introduced gold(I) phosphinethioglucose derivative (auranofin, Ridura) (Figure 4.53) can be taken orally and is absorbed more slowly than myocrisin.

The monomeric non-polar molecular structure enables it to pass through cell walls relatively easily (myocrisin passes easily into the red blood cells of smokers, possibly owing to ingested cyanide in the smoke reacting to form monomeric $Au(SR)CN^-$).

$(Na^+)_2[AuSCH(CO_2^-)CH_2CO_2^-]$

(a)

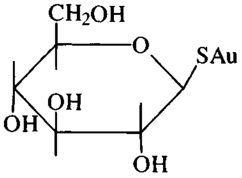

(b)

Figure 4.52 (a) Myocrysin; (b) solganol.

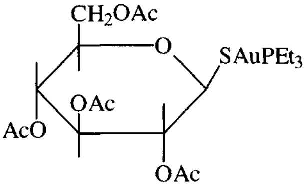

Figure 4.53 Auranofin.

Gold compounds are also being studied as possible anti-cancer agents, after the success of platinum compounds. *cis*-Complexes analogous to $Pt(NH_3)Cl_2$ have not been made; the oxidizing nature of gold(III) would make them toxic; and gold(III) complexes are kinetically more labile. The gold(I) complex $Au(dppe)_2^+Cl^-$ (section 4.10.3) has shown some activity but has been found to be a cardiovascular toxin; corresponding copper and silver complexes also appear to have some activity so that the role of the metal may be to deliver toxic diphosphine to the cells.

The compound $Au(dmamp)(O_2CMe)_2$ (dmamp = $2\text{-}Me_2NC_6H_4$) displays some anti-tumour activity and is undergoing tests on its anti-bacterial activity [200].

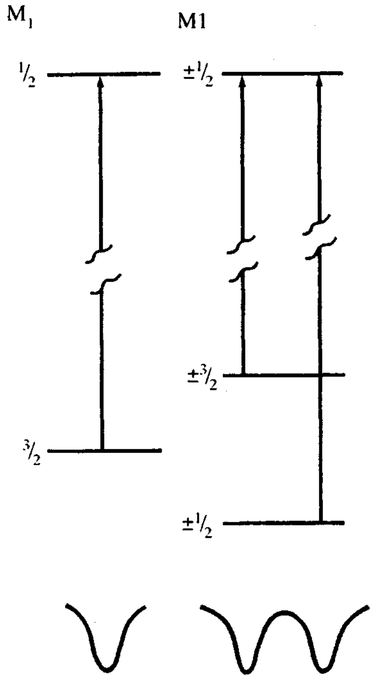

Figure 4.54 The effect of an electric field gradient (EFG) creating asymmetry in the electron distribution round a gold nucleus, leading to a quadrupole splitting in the Mössbauer spectrum. (Reproduced with permission from *Gold Bull.*, 1982, **15**, 53, published by World Gold Council.)

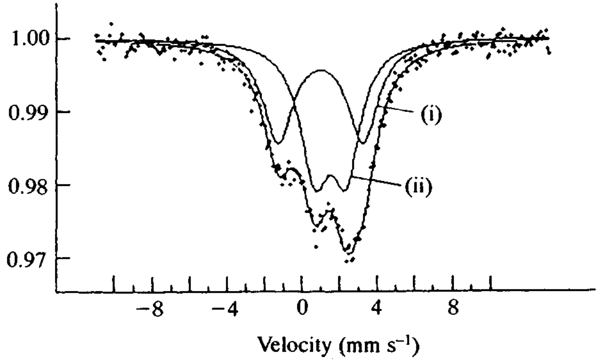

Figure 4.55 The Mössbauer spectrum of $Cs_2(AuI_2)(AuI_4)$ showing separate resonance from (i) the gold(I) and (ii) the gold(III) sites. (Reproduced with permission from *J. Chem. Soc., Dalton Trans.*, 1991, 3211.)

4.21 Mössbauer spectroscopy of gold complexes

In Mössbauer spectroscopy of gold complexes [201], γ-rays from an excited ^{197}Au nucleus (derived from ^{197}Pt (18h) by β-decay) are used to irradiate a sample of the gold compound. The gold atoms in the sample generally will have a different environment to the source, so that it is necessary to 'vibrate' the sample through a velocity range, measuring the γ-radiation, being excited from the $M_I = 3/2$ ground state to the $M_I = 1/2$ excited state. A typical spectrum shows twin peaks, a doublet. The centre of the doublet defines the **isomer shift**, a measure of the electron density at the gold nucleus, changes in which reflect changes in the 6s population principally. The splitting between the lines, the **quadrupole splitting**, reflects asymmetry in the electron distribution around the gold nucleus, which causes an electric field gradient that interacts with the quadrupole moment of the $I = 3/2$ ground state, causing it to split and give two transitions (Figure 4.54).

Mössbauer spectra with ^{197}Au can:

1. Distinguish between different oxidation states
2. Distinguish between different coordination numbers for a given donor atom
3. Show whether a compound contains gold(II) or a mixture of gold(I) and gold(III) (Figure 4.55).

References

Chapter 1

1. W.P. Griffith, *The Chemistry of the Rarer Platinum Metals*, Wiley-Interscience, New York, 1967.
2. S.E. Livingstone, in *Comprehensive Inorganic Chemistry*, eds J.C. Bailar, H.J. Emeleus, R.S. Nyholm and A.F. Trotman-Dickenson, Pergamon, Oxford, 1973, Vol. 3, p. 1163.
3. D.J. Gulliver and W. Levason, *Coord. Chem. Rev.*, 1982, **44**, 1 (high oxidation states).
4. W. Levason, in *The Chemistry of the Platinum Group Metals*, ed. F.R. Hartley, Elsevier, Amsterdam, 1991, p. 470; C.M. Che and V.W.-W. Lam, *Adv. Inorg. Chem.*, 1992, **39**, 233 (high oxidation states).
5. E.A. Seddon and K.R. Seddon, *The Chemistry of Ruthenium*, Elsevier, Amsterdam, 1984.
6. *Gmelin Handbook of Inorganic Chemistry*, System No. 63, Ruthenium. (a) Main volume, 1938 (reprint 1968); (b) Elements and compounds, Suppl. 1970.
7. J.A. Rard, *Chem. Rev.*, **85**, 1, 1985 (ruthenium).
8. M. Schroder and T.A. Stevenson, in *Comprehensive Coordination Chemistry*, eds G. Wilkinson, R.D. Gillard and J.A. McCleverty, Pergamon, Oxford, 1987, Vol. 4, p. 277 (ruthenium).
9. M.I. Bruce *et al.*, in *Comprehensive Organometallic Chemistry I*, eds G. Wilkinson, F.G.A. Stone and E.W. Abel, Pergamon, Oxford, 1982, Vol. 4, p. 651; M.I. Bruce *et al.*, in *Comprehensive Organometallic Chemistry II*, eds G. Wilkinson, F.G.A. Stone and E.W. Abel, Pergamon, Oxford, 1995, Vol. 7, p. 291 (ruthenium).
10. *Gmelin Handbook of Inorganic Chemistry*, System No. 66, Osmium. (a) Main volume, 1939; (b) Element and Compounds, Suppl, Section 1, The Metal. Alloys. Compounds, 1980.
11. P.A. Lay and W.D. Harman, *Adv. Inorg. Chem.*, 1992, **37**, 219 (osmium).
12. W.P. Griffith, in *Comprehensive Coordination Chemistry*, eds G. Wilkinson, R.D. Gillard and J.A. McCleverty, Pergamon, Oxford, 1987, Vol. 4, p. 519 (osmium).
13. R.D. Adams and J.P. Selegue, in *Comprehensive Organometallic Chemistry*, eds G. Wilkinson, F.G.A. Stone and E.W. Abel, Pergamon, Oxford, 1982, Vol. 4, p. 967; M.I. Bruce *et al.*, in *Comprehensive Organometallic Chemistry II*, eds G. Wilkinson, F.G.A. Stone and E.W. Abel, Pergamon, Oxford, 1995, Vol. 7, p. 291 (osmium).
14. For extraction, see F.R. Hartley (ed.), *Chemistry of the Platinum Group Metals*, Elsevier, Amsterdam, 1991, p. 9.
15. W.J. Casteel, A.P. Wilkinson, H. Borrmann, R.E. Serfass and N. Bartlett, *Inorg. Chem.*, 1992, **31**, 3124.
16. Y. Kobayashi, T. Okada, K. Asai, M. Katada, H. Sano and F. Ambe, *Inorg. Chem.*, 1992, **31**, 4570.
17. K. Broderson, H.-K. Breitbach and G. Thiele, *Z. Anorg. Allgem. Chem.*, 1968, **357**, 162; K. Broderson, *Angew. Chem. Int. Ed. Engl.*, 1968, **7**, 147.
18. (a) J.H. Holloway, R.D. Peacock and R.W.H. Small, *J. Chem. Soc.*, 1964, 644; (b) J.H. Holloway, E.G. Hope, G. Stanger and D.A. Boyd, *J. Fluorine Chem.*, 1992, **56**, 77; (c) E.M. Page, D.A. Rice, M.J. Almond *et al.*, *Inorg. Chem.*, 1993, **32**, 4311.
19. A.K. Brisdon, P.J. Jones, W. Levason *et al.*, *J. Chem. Soc., Dalton Trans.*, 1990, 715; A.K. Brisdon, J.H. Holloway, E.G. Hope, W. Levason and J.S. Ogden, *J. Chem. Soc., Dalton Trans.*, 1992, 447.
20. F.A. Cotton and C.E. Rice, *Inorg. Chem.*, 1977, **16**, 1865.
21. G. Thiele, H. Wockner and H. Wagner, *Z. Anorg. Allgem. Chem.*, 1985, **530**, 178.
22. E.W. Kaiser, J.S. Muenter, W. Klemperer, W.E. Falconer and W.A. Sunder, *J. Chem. Phys.*, 1970, **53**, 1411; A.K. Brisdon, J.H. Holloway, E.G. Hope, W. Levason, J.S. Ogden and A.K. Saad, *J. Chem. Soc., Dalton Trans.*, 1992, 139; S.A. Brewer, A.K. Brisdon, J.H. Holloway and E.G. Hope, *Polyhedron*, 1994, **13**, 749 (EXAFS in solution).

23. (a) O. Glemser, H.W. Roesky, K.-H. Halberg and H.-U. Werter, *Chem. Ber.*, 1966, **99**, 2652; (b) A. Veldkamp and G. Frenking, *Chem. Ber.*, 1993, **126**, 1325.
24. T. Sakurai and A. Takahashi, *J. Inorg. Nucl. Chem.*, 1979, **41**, 681.
25. K.O. Christe, D.A. Dixon, H.G. Mack *et al.*, *J. Am. Chem. Soc.*, 1993, **115**, 11279.
26. (a) S.A. Brewer, A.K. Brisdon, J.H. Holloway *et al.*, *J. Fluorine Chem.*, 1993, **60**, 13; (b) R. Bougon, W.V. Cicha and J. Isabey, *J. Fluorine Chem.*, 1994, **67**, 271.
27. J.H. Holloway, E.G. Hope, J.B. Raynor and P.T. Townson, *J. Chem. Soc., Dalton Trans.* 1992, 1131.
28. E.G. Hope, W. Levason and J.S. Ogden, *J. Chem. Soc., Dalton Trans.*, 1988, 997.
29. W.A. Sunder and F.A. Stevie, *J. Fluorine Chem.*, 1975, **6**, 449; W.E. Falconer, F.J. DiSalvo, J.E. Griffiths, F.A. Stevie, W.A. Sunder and M.J. Vasile, *J. Fluorine Chem.*, 1975, **6**, 499.
30. K. Hagen, R.J. Hobson, C.J. Holwill and D.A. Rice, *Inorg. Chem.*, 1986, **25**, 3659; W. Levason, J.S. Ogden, A.J. Rest, *J. Chem. Soc., Dalton Trans.*, 1982, 1877; H. Schäfer, R. Gerken and L. Zylka, *Z. Anorg. Allgem. Chem.*, 1986, **534**, 210.
31. K.H. Huenke and H. Schäfer, *Z. Anorg. Allgem. Chem.*, 1986, **534**, 216.
32. H. Schäfer, *Z. Anorg. Allgem. Chem.*, 1986, **535**, 219.
33. N. Bartlett, M. Gennis, D.D. Gibler, B.K. Morell and A. Zalkin, *Inorg. Chem.*, 1973, **12**, 1717.
34. E.E. Kim, K. Eriks and R. Magnusson, *Inorg. Chem.*, 1984, **23**, 393.
35. A.K. Brisdon, J.H. Holloway, E.G. Hope, W. Levason, J.S. Ogden and A.K. Saad, *J. Chem. Soc., Dalton Trans.*, 1992, 139; 1992, 447.
36. J.M. Arrieta, G. Germain, M. Vlassi, D.G. Craciunescu, E. Parrondo Iglesias and T. Debaerdemaeker, *Acta Crystallogr. Sect. C*, 1992, **48**, 1305.
37. W. Preetz, D. Ruf and D. Tensfeldt, *Z. Naturforsch., Teil B*, 1984, **39**, 1100; W. Preetz and H.J. Walter, *J. Inorg. Nucl. Chem.*, 1971, **33**, 3179; H. Muller, *J. Inorg. Nucl. Chem.*, 1966, **28**, 2081 (nuclear); G. Barka and W. Preetz, *Z. Anorg. Allgem. Chem.*, 1977, **433**, 147; *Z. Anorg. Allgem. Chem.*, 1973, **402**, 168; W. Preetz, H.J. Walter and E.W. Fries, *Z. Anorg. Allgem. Chem.*, 1973, **402**, 180.
38. (a) H.-J. Keller and H. Homberg, *Z. Anorg. Allgem. Chem.*, 1976, **422**, 261; W. Preetz and Y. Petros, *Z. Anorg. Allgem. Chem.*, 1975, **415**, 15; (b) C. Bruhn and W. Preetz, *Acta Crystallogr. Sect. C*, 1994, **50**, 1555; (c) C. Bruhn and W. Preetz, *Acta Crystallogr. Sect. C*, 1994, **50**, 1687; *Acta Crystallogr. Sect. C*, 1995, **51**, 1112; *Acta Crystallogr. Sect. C*, 1996, **52**, 321.
39. T.E. Hopkins, A. Zalkin, D.H. Templeton and M.G. Adamson, *Inorg. Chem.*, 1969, **8**, 2421; M.G.B. Drew, D.A. Rice and C.W. Timewell, *Inorg. Nucl. Chem. Lett.*, 1971, **5**, 59.
40. W. Preetz, P. Hollmann, G. Thiele and H. Hillebrecht, *Z. Naturforsch., Teil B*, 1990, **45**, 1416; P.E. Fanwick, M.K. King, S.M. Tetrick and R.A. Walton, *J. Am. Chem. Soc.*, 1985, **107**, 5009; P.A. Agaskar, F.A. Cotton, K.R. Dunbar, L.R. Favello, S.M. Tetrick and R.A. Walton, *J. Am. Chem. Soc.*, 1986, **108**, 4850; F.A. Cotton and K. Vidyasagar, *Inorg. Chim. Acta*, 1989, **166**, 109.
41. S.F. Gheller, G.A. Heath and R.G. Raptis, *J. Am. Chem. Soc.*, 1992, **114**, 7925; G.A. Heath and D.G. Humphrey, *J. Chem. Soc., Chem. Commun.*, 1990, 613; T.W. Johnson, S.M. Tetrick, P.E. Fanwick and R.A. Walton, *Inorg. Chem.*, 1991, **30**, 4146.
42. S.F. Gheller, G.A. Heath, D.C.R. Hockless, D.G. Humphrey and J.E. McGrady, *Inorg. Chem.*, 1994, **33**, 3986; B.J. Kennedy, G.A. Heath and T.J. Khoo, *Inorg. Chim. Acta*, 1991, **190**, 265; J.E. Fergusson and A.M. Greenaway, *Aust. J. Chem.*, 1978, **31**, 497; D. Appleby, R.I. Crisp, P.B. Hitchcock *et al.*, *J. Chem. Soc., Chem. Commun.*, 1986, 483.
43. J.D. Gilbert, D. Rose and G. Wilkinson, *J. Chem. Soc. (A)*, 1970, 2765; F. Bottomley and M. Mukaida, *J. Chem. Soc., Dalton Trans.*, 1982, 1933; H. Nagao, H. Nishimura, Y. Kitanaka, F.S. Howell, M. Muakida and H. Kakihana, *Inorg. Chem.*, 1990, **29**, 1693; T. Togano, N. Nagao, M. Tsuchida *et al.*, *Inorg. Chim. Acta*, 1992, **195**, 221.
44. A. Bino and F.A. Cotton, *J. Am. Chem. Soc.*, 1980, **102**, 608.
45. R. Weber, K. Dehnicke, U. Muller and D. Fenske, *Z. Anorg. Allgem. Chem.*, 1984, **516**, 214.
46. S. Perrier and J.K. Kochi, *Inorg. Chem.*, 1988, **27**, 4165; W.P. Griffith, *J. Chem. Soc. (A)*, 1969, 211; and Ref. 45.

47. R.J.H. Clark, M.L. Franks and P.C. Turtle, *J. Am. Chem. Soc.*, 1977, **99**, 2473; S.K. Harthorn, H.C. Jewiss, W. Levason and M. Webster, *Acta Crystallogr. Sect. C*, 1987, **43**, 37.
48. (a) L. Schafer and H.M. Seip, *Acta Chem. Scand.*, 1967, **21**, 737; (b) W.P. Griffith, *Chem. Soc. Rev.*, 1992, **21**, 179; (c) A.C. Dengel, A.M. El-Hendawy, W.P. Griffith, C.A. O'Mahoney and D.J. Williams, *J. Chem. Soc., Dalton Trans.*, 1994, 737.
49. G.L. Zimmermann, S.J. Riviello, T.A. Glauser and J.G. Kay, *J. Phys. Chem.*, 1990, **94**, 2399; J.G. Kay, D.W. Green, K. Duca and G.L. Zimmerman, *J. Mol. Spectrosc.*, 1989, **138**, 49.
50. W.P. Griffith, *Platinum Metals Rev.*, 1974, **18**, 94.
51. B. Krebs and K.D. Hassel, *Acta Crystallogr. Sect. B*, 1976, **32**, 1334.
52. J.C. Green, M.F. Guest, I.H . Hillier, *et al.*, *Inorg. Chem.*, 1992, **31**, 1588; B.E. Bursten, J.C. Green and N. Kaltsayannis, *Inorg. Chem.*, 1994, **33**, 2315.
53. W.P. Griffith, *Transition Met. Chem.*, 1990, **15**, 251; *Platinum Metals Rev.*, 1989, **33**, 181.
54. S.V. Ley, J. Norman, W.P. Griffith and S.P. Marsden, *Synthesis*, 1994, 639; A.C. Dengel, J.F. Gibson and W.P. Griffith, *J. Chem. Soc., Dalton Trans.*, 1991, 2799.
55. M.O. Elout, W.G. Haije and W.J.A. Maaskant, *Inorg. Chem.*, 1988, **27**, 610.
56. Y. Laurent, R. Pastuszak, P. L'Haridon and R. Marchand, *Acta Crystallogr. Sect. B*, 1982, **38**, 914; R. Pastuszak, P. L'Haridon, R. Marchand and Y. Laurent, *Acta Crystallogr. Sect. B*, 1982, **38**, 1427; P. L'Haridon, R. Pastuszak and Y. Laurent, *J. Solid State Chem.*, 1982, **43**, 29.
57. M. Kritikis, D. Novens, A.F. Andresen and P. Fischer, *J. Solid State Chem.*, 1991, **92**, 514; B. Huang, F. Bonhomme, P. Selvam, K. Yvon and P. Fischer, *J. Less Common Metals*, 1991, **171**, 301; B. Huang, K. Yvon and P. Fischer, *J. Alloys Compd.*, 1994, **210**, 243.
58. (a) P. Bernhard, H.-B. Burgi, J. Hauser, H. Lehmann and A. Ludi, *Inorg. Chem.*, 1982, **21**, 3936; P. Bernhard and A. Ludi, *Inorg. Chem.*, 1984, **23**, 870; F. Joensen and C.E. Schaffer, *Acta Chem. Scand. A*, 1984, **38**, 819; S.P. Best, J.B. Forsyth and P.L. Tregenna-Pigott, *J. Chem. Soc., Dalton Trans.*, 1993, 2711; (b) J. Chatt, G.J. Leigh, D.M.P. Mingos and R.J. Paske, *J. Chem. Soc. (A)*, 1968, 2636; J. Chatt, G.J. Leigh and D.M.P. Mingos, *J. Chem. Soc (A)*, 1969, 1674.
59. G. Laurenczy, L. Helm, A.E. Merbach and A. Ludi, *Inorg. Chim. Acta*, 1991, **189**, 131.
60. A. Patel and D.T. Richens, *Inorg. Chem.*, 1991, **30**, 3789.
61. (a) J.P. Jesson, M.A. Cushing and S.D. Ittel, *Inorg. Synth.*, 1980, **20**, 80; V.T. Kruck and A. Prasch, *Z. Anorg. Allgem. Chem.*, 1969, **371**, 1; (b) R.J. Mawby, R.N. Perutz and M.K. Whittlesey, *Organometallics*, 1995, **14**, 3268.
62. R.N. Perutz, *Chem. Soc. Rev.*, 1993, **22**, 361.
63. L. Cronin, M.C. Nicasio, R.N. Perutz, R.G. Peters, D.M. Roddick and M.K. Whittlesey, *J. Am. Chem. Soc.*, 1995, **117**, 10047.
64. S. Pell, R.H. Mann, H. Taube and J.N. Armor, *Inorg. Chem.*, 1974, **13**, 479.
65. A.D. Allen and C.V. Senoff, *J. Chem. Soc., Chem. Commun.*, 1965, 621; F. Bottomley and S.C. Nyberg, *J. Chem. Soc., Chem. Commun.*, 1966, 897; *Acta Crystallogr. Sect. B*, 1968, **24**, 1289 (structure).
66. N.E. Dixon, G.A. Lawrance, P.A. Lay and A.M. Sargeson, *Inorg. Chem.*, 1983, **22**, 846; J.F. Wishart, H. Taube, K. Breslauer and S.S. Islied, *Inorg. Chem.*, 1984, **23**, 2997; B.T. Anders, S.T. Collins and D.K. Lavalee, *Inorg. Chem.*, 1985, **24**, 2201.
67. P.A. Reynolds, C.D. Delfs, B.N. Figgis, L.M. Engelhardt, B. Moubaraki and K.S. Murray, *J. Chem. Soc., Dalton Trans.*, 1992, 2029; A.B. Blake, C.D. Delfs, L.M. Engelhardt *et al.*, *J. Chem. Soc., Dalton Trans.*, 1993, 1417; B.N. Figgis, P.A. Reynolds and A.N. Sobolev, *J. Chem. Soc., Dalton Trans.*, 1994, 1429; H.C. Stynes and J.A. Ibers, *Inorg. Chem.*, 1971, **10**, 2304.
68. C.A. Creutz and H. Taube, *J. Am. Chem. Soc.*, 1969, **91**, 3988; U. Furholz, S. Joss, H.B. Burgi and A. Ludi, *Inorg. Chem.*, 1985, **24**, 943.
69. S. Donovan-Mtunzi, R.L. Richards and J. Mason, *J. Chem. Soc., Dalton Trans.*, 1984, 2429; I.M. Treitel, M.T. Flood, R.E. Marsh and H.B. Gray, *J. Am. Chem. Soc.*, 1969, **91**, 6512.
70. M.A.A.C.F. de C.T. Carrondo, W.P. Griffith, J.P. Hall and A.C. Skapski, *Biochim. Biophys. Acta*, 1980, **627**, 332; P.M. Smith, T. Fealey, J.E. Earley and J.V. Silverton, *Inorg. Chem.*, 1971, **10**, 1943.

71. E. Krausz and J. Ferguson, *Progr. Inorg. Chem.*, 1989, **37**, 293; A. Juris, V. Balzani, F. Barigelletti, S. Campagna, P. Belser and A. von Zelewsky, *Coord. Chem. Rev.*, 1988, **84**, 85; A. Mills in *The Chemistry of the Platinum Group Metals*, ed. F.R. Hartley, Elsevier, Amsterdam, 1991, Ch. 11, p. 311; D.M. Roundhill, *Photochemistry and Photophysics of Metal Complexes*, Plenum Press, New York, 1994.
72. (a) M.M. Richter, B. Scott, K.J. Brewer and R.D. Willett, *Acta Crystallogr. Sect. C*, 1991, **47**, 2443; (b) M. Biner, H.-B. Burgi, A. Ludi and C. Rohr, *J. Am. Chem. Soc.*, 1992, **114**, 5197; (c) D.P. Rillema, D.S. Jones, C. Woods and H.A. Levy, *Inorg. Chem.*, 1992, **31**, 2935.
73. B.H. Ye, X.M. Chen, T.X. Zeng and L.N. Ji, *Inorg. Chim. Acta*, 1995, **240**, 5.
74. P.J. Smolenaers, J.K. Beattie and N.D. Hutchinson, *Inorg. Chem.*, 1981, **20**, 2202; H.J. Peresie and J.A. Stanko, *J. Chem. Soc., Chem. Commun.*, 1970, 1674; *Inorg. Synth*, 1979, **19**, 118; 1992, **29**, 164.
75. B.R. Davis and J.A. Ibers, *Inorg. Chem.*, 1970, **9**, 2768.
76. J.-P. Sauvage, J.-P. Collin, J.-C. Chambron *et al., Chem. Rev.*, 1994, **94**, 993.
77. P.M. Van Vliet, S.M.S. Toekimin, J.G. Haasnoot *et al., Inorg. Chim. Acta*, 1995, **231**, 57.
78. P.W. Armit, A.S.F. Boyd and T.A. Stephenson, *J. Chem. Soc., Dalton Trans.* 1975, 1663.
79. F.H. Jardine, *Progr. Inorg. Chem.*, 1984, **31**, 265.
80. S.J. LaPlaca and J.A. Ibers, *Inorg. Chem.*, 1965, **4**, 778.
81. N.R. Champness, W. Levason and M. Webster, *Inorg. Chim. Acta*, 1993, **208**, 189.
82. P.A. Chaloner, *Handbook of Coordination Catalysis in Organic Chemistry*, Butterworths, London, 1986, p. 39.
83. A.C. Skapski and P.G.H. Troughton, *J. Chem. Soc., Chem. Commun.*, 1968, 1230.
84. J.K. Nicholson, *Angew. Chem. Int. Ed. Engl.*, 1967, **6**, 264; G. Chioccola and J.J. Daly, *J. Chem. Soc. (A)*, 1968, 1981; F.A. Cotton, M. Matusz and R.C. Torralba, *Inorg. Chem.*, 1989, **28**, 1516; F.A. Cotton and R.C. Torralba, *Inorg. Chem.*, 1991, **30**, 2196, 3293, 4387, 4392.
85. J. Chatt and R.G. Hayter, *J. Chem. Soc.*, 1961, 896; J. Chatt and J.M. Davidson, *J. Chem. Soc.*, 1965, 843; T.S. Lobana, R. Singh and E.R.K. Tiekink, *J. Coord. Chem.*, 1990, **21**, 225.
86. C.A. Tolman, S.D. Ittel, A.D. English and J.P. Jesson, *J. Am. Chem. Soc.*, 1978, **100**, 4080.
87. F.A. Cotton, D.L. Hunter and B.A. Frenz, *Inorg. Chim. Acta*, 1975, **15**, 155.
88. C. Hall, W.D. Jones, R.J. Mawby, R. Osman, R.N. Perutz and M.K. Whittlesey, *J. Am. Chem. Soc.*, 1992, **114**, 7425; J.F. Hartwig, R.A. Andersen and R.G. Bergman, *Organometallics*, 1991, **10**, 1710.
89. G. Jia, I. Lee, D.W. Meek and J.C. Gallucci, *Inorg. Chim. Acta*, 1990, **177**, 81.
90. L. Dahlenberg and K.-M. Frosin, *Polyhedron*, 1993, **12**, 427.
91. L.D. Field, T.W. Hambley and B.C.K. Yau, *Inorg. Chem.*, 1994, **33**, 2009.
92. J. Li, R.M. Dickson and T. Ziegler, *J. Am. Chem. Soc.*, 1995, **117**, 11482.
93. R.H. Crabtree and D.G. Hamilton, *J. Am. Chem. Soc.*, 1986, **108**, 3124.
94. M. Bautista, K.A. Earl, R.H. Morris and A. Sella, *J. Am. Chem. Soc.*, 1987, **109**, 3780; M. Bautista, K.A. Earl, P.A. Maltby, R.H. Morris, C.T. Schweitzer and A. Sella, *J. Am. Chem. Soc.*, 1987, **110**, 7031.
95. A.S.C. Chan and H.-S. Shieh, *J. Chem. Soc., Chem. Commun.*, 1985, 1379 .
96. F.A. Cotton, Y. Kim and T. Ren, *Polyhedron*, 1993, **12**, 607 and references therein; T. Kimura, T. Sakurai, M. Shima, T. Togano, M. Mukaida and T. Nomura, *Bull. Chem. Soc. Japan*, 1982, **55**, 3927. For the carboxylates of Ru and Os in general, see F.A. Cotton and R.A. Walton, *Multiple Bonds between Metal Atoms*, 2nd edn, Clarendon Press, Oxford, 1993, 399 ff., 630 ff.
97. M.C. Barral, R. Jiminez-Aparicio, E.C. Royer, C. Ruiz-Valero, M.J. Saucedo and F.A. Urbanos, *Inorg. Chem.*, 1994, **33**, 2692.
98. M.C. Barral, R. Jiminez-Aparicio, J.L. Priego *et al., J. Chem. Soc., Dalton Trans.*, 1995, 2183.
99. F.A. Cotton and E. Pedersen, *Inorg. Chem.*, 1975, **14**, 388; D.S. Martin, R.A. Newman and L.M. Vlasek, *Inorg. Chem.*, 1980, **19**, 3404.
100. A.J. Lindsay, G. Wilkinson, M. Motevalli and M.B. Hursthouse, *J. Chem. Soc., Dalton Trans.*, 1985, 2321.
101. J.G. Norman, G.E. Renzoni and D.A. Case, *J. Am. Chem. Soc.*, 1979, **101**, 5256.

102. F.A. Cotton, L. Labella and M. Shang, *Inorg. Chem.*, 1992, **31**, 2385; F.A. Cotton, L.R. Favello, T. Ren and K. Vidyasagar, *Inorg. Chim. Acta*, 1992, **194**, 163.
103. M. Abe, Y. Sasaki, T. Yamaguchi and T. Ito, *Bull. Chem. Soc. Japan*, 1992, **65**, 1585; G. Powell, D.J. Richens and A.K. Powell, *Inorg. Chim. Acta*, 1993, **213**, 147.
104. (a) F.A. Cotton and J.G. Norman, *Inorg. Chim. Acta*, 1972, **6**, 411; (b) A. Spencer and G. Wilkinson, *J. Chem. Soc., Dalton Trans.*, 1972, 1570; (c) R.W. Mitchell, A. Spencer and G. Wilkinson, *J. Chem. Soc., Dalton Trans.*, 1973, 847.
105. Y. Sasaki, M. Suzuki, A. Nagasawa *et al.*, *Inorg. Chem.*, 1991, **30**, 4903; A. Symala and A.R. Chakravarty, *Polyhedron*, 1993, **12**, 1545.
106. A.C. Skapski and F.A. Stephens, *J. Chem. Soc., Dalton Trans.*, 1974, 390; R.J. Young and G. Wilkinson, *J. Chem. Soc., Dalton Trans.*, 1976, 719.
107. E. Lindner, R. Fawzi, W. Hiller, A. Carvill and M. McCann, *Chem. Ber.*, 1991, **124**, 2691.
108. E. Alessio, G. Mestroni, W.M. Attia, M. Calligaris, G. Sava and S. Zorzet, *Inorg. Chem.*, 1988, **27**, 4099; J.D. Oliver and D.P. Riley, *Inorg. Chem.*, 1984, **23**, 156; A. Mercer and J. Trotter, *J. Chem. Soc., Dalton Trans.*, 1975, 2480.
109. M. Henn, E. Alessio, G. Mestroni, M. Calligaris and W.M. Attia, *Inorg. Chim. Acta*, 1991, **187**, 39.
110. M. Calligaris, P. Faleschini and E. Alessio, *Acta Crystallogr. Sect. C*, 1993, **49**, 663.
111. E. Alessio, G. Balducci, M. Calligaris, G. Costa, W.M. Attia and G. Mestroni, *Inorg. Chem.*, 1991, **30**, 609; E. Alessio, G. Balducci, A. Lutman, G. Mestroni, M. Calligaris and W.M. Attia, *Inorg. Chim. Acta*, 1993, **203**, 205.
112. M. Calligaris, P. Faleschini, F. Todone, E. Alessio and S. Geremia, *J. Chem. Soc., Dalton Trans.*, 1995, 1653.
113. E. Alessio, M. Bolle, B. Milani *et al.*, *Inorg. Chem.*, 1995, **34**, 4716; E. Alessio, B. Milani, M. Bolle *et al.*, *Inorg. Chem.*, 1995, **34**, 4722.
114. (a) R.S. Srivastava, B. Milani, E. Alessio and G. Mestroni, *Inorg. Chim. Acta*, 1992, **191**, 15; (b) J. Chatt, G.J. Leigh and A.P. Storace, *J. Chem. Soc. (A)*, 1971, 1380; J.S. Jaswal, S.J. Rettig and B.R. James, *Can. J. Chem.*, 1990, **68**, 1808.
115. F. Bottomley, *Coord. Chem. Rev.*, 1978, **26**, 7; J.A. McCleverty, *Chem. Rev.*, 1979, **79**, 53; D.M.P. Mingos and D.J. Sherman, *Adv. Inorg. Chem.*, 1989, **34**, 293 (for nitrogen-15 NMR); A.A. Svetlov, Yu.E. Gorbunova, Yu.N. Mikhailov, A.S. Kanischeva and Yu.A. Buslaev, *Russ. J. Inorg. Chem.*, 1995, **40**, 1417.
116. A. Joly, *C. R. Hebd. Seances Acad. Sci.*, 1889, 708, 854; M.I. Khan, R. Saheb and U. Agarwala, *Ind. J. Chem., Sect. A*, 1983, **22**, 417; J.E. Fergusson and P.F. Heveldt, *J. Inorg. Nucl. Chem.*, 1977, **39**, 825.
117. A. Domenicano, A. Vaciago, L. Zambonelli, P.L. Loader and L.M. Venanzi, *J. Chem. Soc., Chem. Commun.*, 1966, 476.
118. J.B. Goodwin and T.J. Meyer, *Inorg. Chem.*, 1971, **10**, 215.
119. T. Togano, H. Kuroda, N. Nagao *et al.*, *Inorg. Chim. Acta*, 1992, **196**, 57; H. Tomiazwa, K. Harada, E. Miki *et al.*, *Bull. Chem. Soc. Japan*, 1993, **66**, 1658; R. Asanuma, H. Tomiazwa, A. Urushiyama, E. Miki, K. Mizumachi and T. Ishimori, *Bull. Chem. Soc. Japan*, 1994, **67**, 1274; H. Tomiazwa, E. Miki, K. Mizumachi and T. Ishimori, *Bull. Chem. Soc. Japan*, 1994, **67**, 1816.
120. H. Ikezawa, Y. Ikezawa, E. Miki, K. Mizumachi and T. Ishimori, *Inorg. Chim. Acta*, 1995, **238**, 89.
121. Much of the structural data for [Ru(NO)X_5] systems is found in R. Zarhloul, R. Faure and J.-P. Deloume, *J. Crystallogr. Spect. Res.*, 1992, **22**, 601; M. Rudlinger, J. Schefer, P. Fischer, N. Furer and H.U. Gudel, *J. Solid State Chem.*, 1993, **103**, 170.
122. IR data for [Ru(NO)X_5] systems is largely taken from N.L. Rogalevich, E.Y. Bobkova, G.G. Novitskii, I.K. Skutov, A.A. Svetlov and N.M. Sinitsyn, *Russ. J. Inorg. Chem.*, 1986, **31**, 694. See also D.H.F. Souza, G. Oliva, A. Teixeira and A.A. Batista, *Polyhedron*, 1995, **14**, 1031.
123. J.E. Fergusson and R.K. Coll, *Inorg. Chim. Acta*, 1993, **207**, 191; R.E. Townsend and K.J. Coskran, *Inorg. Chem.*, 1971, **10**, 1661.
124. M.H.B. Stiddard and R.E. Townsend, *J. Chem. Soc., Chem. Commun.*, 1969, 1372; J. Reed, C.G. Pierpont and R. Eisenberg, *Inorg. Synth.*, 1976, **16**, 21; M.W. Schoonover, C.P. Kubiak and R. Eisenberg, *Inorg. Chem.*, 1978, **17**, 3050.
125. C.G. Pierpont and R. Eisenberg, *Inorg. Chem.*, 1972, **11**, 1088.

126. J.J. Levison and S.D. Robinson, *J. Chem. Soc. (A)*, 1970, 2947; K.R. Grundy, K.R. Laing and W.R. Roper, *J. Chem. Soc., Chem. Commun.*, 1970, 1500; A.P. Gaughan, B.J. Corden, R. Eisenberg and J.A. Ibers, *Inorg. Chem.*, 1974, **13**, 786.
127. C.G. Pierpont and R. Eisenberg, *Inorg. Chem.*, 1972, **11**, 1094; S.T. Wilson and J.A. Osborn, *J. Am. Chem. Soc.*, 1971, **93**, 3068.
128. J.W. Bats, K.K. Pandey and H.W. Roesky, *J. Chem. Soc., Dalton Trans.*, 1984, 2081; K.K. Pandey, *J. Coord. Chem.*, 1991, **22**, 307.
129. (a) B.R. James, A. Pacheco, S.J. Rettig and J.A. Ibers, *Inorg. Chem.*, 1988, **27**, 2414; M. Ke, S.J. Rettig, B.R. James and D. Dolphin, *J. Chem. Soc., Chem. Commun.*, 1987, 1110; J.P. Collman, C.E. Nes, P.N. Swepston and J.A. Ibers, *J. Am. Chem. Soc.*, 1984, **106**, 3501; J.-S. Huang, C.-M. Che, Z.-Y. Li and C.K. Poon, *Inorg. Chem.*, 1992, **31**, 1313; M. Ke, C. Sishta, B.R. James, D. Dolphin, J.W. Sparapany and J.A. Ibers, *Inorg. Chem.*, 1991, **30**, 4766; J.-S. Huang, C.-M. Che and C.K. Poon, *J. Chem. Soc., Chem. Commun.*, 1992, 161; (b) M.J. Abrams, *Platinum Metals Rev.*, 1995, **39**, 14; (c) J.W. Buchler, C. Dreher and F.M. Kunzel, *Struct. Bonding*, 1995, **84**, 1.
130. For a review, see M.M. Taqui Khan, *Platinum Metals Rev.*, 1991, **35**, 70.
131. M.M. Taqui Khan, K. Venkatasubramanian, H.C. Bajaj and Z. Shirin, *Ind. J. Chem., Sect. A*, 1992, 306.
132. M.M. Taqui Khan, D. Chatterjee, M.R.H. Siddiqui, *et al., Polyhedron*, 1993, **12**, 1443; M.M. Taqui Khan, K. Venkatasubramanian, Z. Shirin and M.M. Bhadbhade, *J. Chem. Soc., Dalton Trans.*, 1992, 1031; M.M. Taqui Khan, D. Chatterjee, R.R. Merchant *et al., Inorg. Chem.*, 1992, **31**, 2711; M.M. Taqui Khan, M.M. Bhadbhade, K. Venkatasubramanian and M.R.H. Siddiqui, *Acta Crystallogr. Sect. C*, 1992, **48**, 1202.
133. (a) R.J. Judd, R. Cao, M. Biner *et al., Inorg. Chem.*, 1995, **34**, 5080; (b) T.S. Knowles, M.E. Howells, B.J. Howlin, G.W. Smith and C.A. Amodio, *Polyhedron*, 1994, **13**, 2197.
134. J.L. Templeton, *J. Am. Chem. Soc.*, 1979, **101**, 4906; F. Bottomley and M. Mukaida, *J. Chem. Soc., Dalton Trans.*, 1982, 1933; D.W. Reichert and H. Taube, *Inorg. Chem.*, 1972, **11**, 999; W.T. Wong and T.C. Lu, *Acta Crystallogr. Sect. C.*, 1994, **50**, 1406; M.R.J. Elsegood and D.A. Tocher, *Acta Crystallogr. Sect. C*, 1995, **51**, 40; B.J. Coe, T.J. Meyer and P.S. White, *Inorg. Chem.*, 1995, **34**, 593.
135. C. Anderson and A.L. Beauchamp, *Can. J. Chem.*,1995, **73**, 471; *Inorg. Chem.*, 1995, **34**, 6065; J. Chatlas, R. van Eldik and B.K. Keppler, *Inorg. Chim. Acta*, 1995, **233**, 59.
136. C.M. Duff and G.A. Heath, *Inorg. Chem.*, 1991, **30**, 2528; C.M. Duff, G.A. Heath and A.C. Willis, *Acta Crystallogr. Sect. C*, 1990, **46**, 2320.
137. L.H. Pignolet, *Inorg. Chem.*, 1974, **13**, 2051.
138. C.L. Raston and A.H. White, *J. Chem. Soc., Dalton Trans.*, 1975, 2410.
139. S.A. Koch and M. Millar, *J. Am. Chem. Soc.*, 1983, **105**, 3363; M. Millar, T. O'Sullivan, N. de Vries and S.A. Koch, *J. Am. Chem. Soc.*, 1985, **107**, 3714; S.P. Satsangee, J.H. Hain, P.T. Cooper and S.A. Koch. *Inorg. Chem.*, 1992, **31**, 5160.
140. C.M. Che, K.Y. Wong and T.C.W. Mak, *J. Chem. Soc., Chem. Commun.*, 1985, 988; C.M. Che, T.-F. Lai and K.Y. Wong, *Inorg. Chem.*, 1987, **26**, 2289.
141. R.K. Pomeroy, *J. Organomet. Chem.*, 1990, **383**, 387 (review); P. Rushman, G.N. van Buren and R.K. Pomeroy, *Organometallics*, 1983, **2**, 693; F.W.B. Einstein, V.J. Johnston and R.K. Pomeroy, *Organometallics*, 1990, **9**, 2754; W. Wang, F.W.B Einstein and R.K. Pomeroy, *J. Chem. Soc., Chem. Commun.*, 1992, 1737; D. Coughlin, J. Lewis, J.R. Moss, A.J. Edwards and M. McPartlin, *J. Organomet. Chem.*, 1993, **444**, C55.
142. V.T. Kruck and A. Prasch, *Z. Anorg. Allgem. Chem.*, 1969, **371**, 1; A.D. English, S.D. Ittel, C.A. Tolman, P. Meakin and J.P. Jesson, *J. Am. Chem. Soc.*, 1977, **99**, 117; S.P. Ermer, R.S. Shinomoto, M.A. Deming and T.C. Flood, *Organometallics*, 1989, **8**, 1377.
143. J.D. Buhr, J.R. Winkler and H. Taube, *Inorg. Chem.*, 1980, **19**, 2416; Z.-W. Wei, W.D. Harman, P.A. Lay and H. Taube, *Inorg. Chem.*, 1994, **33**, 3635.
144. H.-W. Lam, C.-M. Che and K.Y. Wong, *J. Chem. Soc., Dalton Trans.*, 1992, 1411.
145. J.L. Love and W.T. Robinson, *Inorg. Chem.*, 1972, **11**, 1662; P.A. Lay, R.H. Magnuson, J. Sen and H. Taube, *J. Am. Chem. Soc.*, 1982, **104**, 7658.
146. J.T. Call, K.A. Hughes, W.D. Harman and M.G. Finn, *Inorg. Chem.*, 1993, **32**, 2123.
147. H.A. Goodwin, D.L. Kepert, J.M. Patrick, B.W. Skelton and A.H. White, *Aust. J. Chem.*, 1984, **37**, 1817; M.M. Richter, B. Scott, K.J. Brewer and R.D. Willett, *Acta Crystallogr. Sect. C*, 1991, **47**, 2443.

148. F.P. Dwyer and J.W. Hogarth, *J. Am. Chem. Soc.*, 1955, **77**, 6152; M.A. Bolourtschi, H.-J. Deiseroth and W. Preetz, *Z. Anorg. Allgem. Chem.*, 1975, **415**, 25; P.A. Lay, A.M. Sargeson, B.W. Skelton and A.H. White, *J. Am. Chem. Soc.*, 1982, **104**, 6161.
149. Z. Wei and H. Taube, *J. Am. Chem. Soc.*, 1991, **113**, 8946; Z. Li and H. Taube, *Science*, 1992, **256**, 210; L. Pu, T. Hasegawa, S. Parkin and H. Taube, *J. Am. Chem. Soc.*, 1993, **115**, 2545; U. Frey, Z.-W. Li and A. Matras, *Inorg. Chem.*, 1996, **35**, 980.
150. T. Hasegawa, Z.W. Li, S. Parkin *et al.*, *J. Am. Chem. Soc.*, 1994, **116**, 4352; Z.W. Li and H. Taube, *J. Am. Chem. Soc.*, 1994, **116**, 9506.
151. D.J. Salmon and R.A. Walton, *Inorg. Chem.*, 1978, **17**, 2379; J.E. Armstrong and R.A. Walton, *Inorg. Chem.*, 1983, **22**, 1545; S.K. Harbron and W. Levason, *J. Chem. Soc., Dalton Trans.*, 1987, 633.
152. R.A. Cipriano,W. Levason, R.A.S. Mould, D. Pletcher and M. Webster, *J. Chem. Soc., Dalton Trans.*, 1990, 2609.
153. A. Hudson and M.J. Kennedy, *J. Chem. Soc. (A)*, 1968, 1116; N.J. Hill, *J. Chem. Soc., Faraday Trans. 2*, 1972, 427.
154. V.T. Coombe, G.A. Heath, T.A. Stephenson, J.D. Whitelock and L.J. Yellowlees, *J. Chem. Soc., Dalton Trans.*, 1985, 947; B.D. Yeomans, G.A. Heath and D.C.R. Hockless, *Acta Crystallogr. Sect. C*, 1995, **51**, 1807.
155. J. Chatt, G.J. Leigh and R.L. Richards, *J. Chem. Soc., Chem. Commun.*, 1969, 515; *J. Chem. Soc. (A)*, 1970, 2243; J. Chatt, D.P. Melville and R.L. Richards, *J. Chem. Soc. (A)*, 1971, 1169.
156. A. Hills, D.L. Hughes, R.L. Richards, M. Arroyo, D. Cruz-Garritz and H. Torrens, *J. Chem. Soc., Dalton Trans.*, 1991, 1281.
157. L. Aslanov, R. Mason, A.G. Wheeler and P.O. Whimp, *J. Chem. Soc., Chem. Commun.*, 1970, 30; C.C. Hinkley, M.T. Matusz and P.D. Robinson, *Acta Crystallogr. Sect. C*, 1988, **44**, 371; C.C. Hinkley, M.T. Matusz and P.D. Robinson, *Acta Crystallogr. Sect C*, 1988, **44**, 1829; R.A. Cipriano, W. Levason, R.A.S. Mould, D. Pletcher and M. Webster, *J. Chem. Soc., Dalton Trans.*, 1990, 339; N.R. Champness, W. Levason, R.A.S. Mould, D. Pletcher and M. Webster, *J. Chem. Soc., Dalton Trans.*, 1991, 2777.
158. N.R. Champness, W. Levason, D. Pletcher, M.D. Spicer and M. Webster, *J. Chem. Soc., Dalton Trans.*, 1992, 2201.
159. W. Levason, N.R. Champness and M. Webster, *Acta Crystallogr. Sect. C*, 1993, **49**, 1884; A.J. Lough, R.H. Morris and M. Schlaf, *Z. Kristallogr.*, 1995, **210**, 973.
160. P.G. Douglas and B.L. Shaw, *J. Chem. Soc. (A)*, 1970, 334.
161. P.W. Frost, J.A.K. Howard and J.L. Spencer, *Acta Crystallogr. Sect. C*, 1984, **40**, 960; N.G. Connelly, J.A.K. Howard, J.L. Spencer and P.K. Woodley, *J. Chem. Soc., Dalton Trans.*, 1984, 2005; J.A.K. Howard, O. Johnson, T.F. Koetzle and J.L. Spencer, *Inorg. Chem.*, 1987, **26**, 2930; 1991, **30**, 289.
162. K.T. Smith, M. Tilset, R. Kuhlman and K.G. Caulton, 1995, **117**, 9473.
163. B. Bell, J. Chatt and G.J. Leigh, *J. Chem. Soc., Dalton Trans.*, 1973, 997.
164. D.W. Hart, R. Bau and T.F. Koetzle, *J. Am. Chem. Soc.*, 1977, **99**, 7559; J.W. Bruno, J.C. Huffman, M.A. Green, J.D. Zubkowski, W.E. Hatfield and K.G. Caulton, *Organometallics*, 1990, **9**, 2556; P.J. Desrosiers, L. Cai, Z. Lin, R. Richards and J. Halpern, *J. Am. Chem. Soc.*, 1991, **113**, 4173.
165. F. Maseras, X.-K. Li, N. Koga and K. Morokuma, *J. Am. Chem. Soc.*, 1993, **115**, 10974.
166. J.C. Huffman, M.A. Green, S.L. Kaiser and K.G. Caulton, *J. Am. Chem. Soc.*, 1985, **107**, 5111.
167. J. Chatt, D.P. Melville and R.L. Richards, *J. Chem. Soc. (A)*, 1971, 895; M. Aracama, M.A. Esteruelas, F.J. Lahoz, J.A. Lopez, U. Meyer, L.A. Oro and H. Werner, *Inorg. Chem.*, 1991, **30**, 288; J. Espuelas, M.A. Esteruelas, F.J. Lahoz, L.A. Oro and N. Ruiz, *J. Am. Chem. Soc.*, 1993, **115**, 4683; D.G. Gusev, R. Kuhlman, J.R. Rambo, H. Berke, O. Eisenstein and K.G. Caulton, *J. Am. Chem. Soc.*, 1995, **117**, 281.
168. D.G. Gusev, V.F. Kuznetsov, I.L. Eremenko and H. Berke, *J. Am. Chem. Soc.*, 1993, **115**, 5831.
169. D.G. Gusev, R. Kuhlman, G. Sini, O. Eisenstein and K.G. Caulton, *J. Am. Chem. Soc.*, 1994, **116**, 2685.
170. M.T. Bautista, K.A. Earl and R.H. Morris, *Inorg. Chem*, 1988, **27**, 1124; M.T. Bautista, K.A. Earl, P.A. Maltby, R.H. Morris, C.T. Schweitzer and A. Sella, *J. Am. Chem. Soc.*, 1988, **110**, 4126; P. Amendola, S. Antoniutti, G. Alberti, C. Albertin and E. Borgignon, *Inorg. Chem.*, 1990, **29**, 318.

171. D.H. Farrar, P.A. Maltby and R.H. Morris, *Acta Crystallogr. Sect. C*, 1992, **48**, 28.
172. F. Maseras, N. Koga and K. Morokuma, *J. Am. Chem. Soc.*, 1993, **115**, 8313; T.J. Johnson, A. Albinati, T.F. Koetzle, J. Ricci, O. Eisenstein, J.C. Huffman and K.G. Caulton, *Inorg. Chem.*, 1994, **33**, 4966.
173. T. Behling, G. Wilkinson, T.A. Stephenson, D.A. Tocher and M.D. Walkinshaw, *J. Chem. Soc., Dalton Trans.*, 1983, 2109; A.R. Chakravarty, F.A. Cotton and D.A. Tocher, *Inorg. Chem.*, 1984, **23**, 4697.
174. H. Werner, A. Michenfelder and M. Schulz, *Angew. Chem. Int. Ed. Engl.*, 1991, **30**, 596.
175. J.E. Fergusson, W.T. Robinson and R.K. Coll, *Inorg. Chim. Acta*, 1991, **181**, 37; J.M. Waters and K.R. Whittle, *J. Chem. Soc., Chem. Commun.*, 1971, 518; K.R. Grundy, K.R. Laing and W.R. Roper, *J. Chem. Soc., Chem. Commun.*, 1970, 1500; B.L. Haymore and J.A. Ibers, *Inorg. Chem.*, 1975, **14**, 2610.
176. F.P. Dwyer and A.M. Sargeson, *J. Am. Chem. Soc.*, 1955, **77**, 1285; W. Preetz and H. Petersen, *Z. Naturforsch., Teil B*, 1979, **34**, 595.
177. A.J. Blake, G.A. Heath, G. Smith, L.J. Yellowlees and D.W.A. Sharp, *Acta Crystallogr. Sect. C*, 1988, **44**, 1836.
178. K.W. Given, S.H. Wheeler, B.S. Lick, L.J. Meheu and L.H. Pignolet, *Inorg. Chem.*, 1979, **18**, 1261; S.H. Wheeler and L.H. Pignolet, *Inorg. Chem.*, 1980, **19**, 972; L.J. Meheu and L.H. Pignolet, *J. Am. Chem. Soc.*, 1980, **102**, 6346. See also G.A. Heath and R.L. Martin, *Aust. J. Chem.*, 1970, **23**, 1721.
179. M. Arroyo, J.A. Chamizo, D.L. Hughes *et al.*, *J. Chem. Soc., Dalton Trans.*, 1994, 1819.
180. A. Araneo, G. Mercati, F. Morazzoni and T. Napoletano, *Inorg. Chem.*, 1977, **16**, 1197.
181. L.O. Atovmyan, V.G. Adrianov and M.A. Porai-Koshits, *J. Struct. Chem. USSR*, 1962, **3**, 660; J.M. Malin, E.O. Schlemper and R.K. Murmann, *Inorg. Chem.*, 1977, **16**, 165; J.M. Malin and H. Taube, *Inorg. Chem.*, 1971, **10**, 2403.
182. For OsO_4 as oxidant, see W.P. Griffith, *Transition Met. Chem.*, 1990, **15**, 251; *Platinum Metals Rev.*, 1989, **33**, 181; *Chem. Soc. Rev.*, 1992, 179.
183. A good discussion of this is: W.P. Griffith, in Ref. 10b, p. 81.
184. J.M. Hawkins, A. Meyer, T.A. Lewis, S. Loren and F.J. Hollander, *Science*, 1991, **252**, 312; J.M. Hawkins, *Acc. Chem. Res.*, 1992, **25**, 150.
185. C.-M. Che, W.-C. Chung and T.-F. Lai, *Inorg. Chem.*, 1988, **27**, 2801; C.-M. Che, C.K. Poon, W.-C. Chung and H.B. Gray, *Inorg. Chem.*, 1985, **24**, 1277.
186. J.M. Smieja, K.M. Omberg and G.L. Breneman, *Inorg. Chem.*, 1994, **33**, 614; for a recent osmium(IV) report, see J.A. Smieja, K.M. Omberg, L.N. Busuego and G.L. Breneman, *Polyhedron*, 1994, **13**, 339.
187. J.C. Dobson, K.J. Takeuchi, D.W. Pipes, D.A. Geselowitz and T.J. Meyer, *Inorg. Chem.*, 1986, **25**, 2357; T. Behling, M.V. Caparelli, A.C. Skapski and G. Wilkinson, *Polyhedron*, 1982, **1**, 840.
188. P.D. Lyne and D.M.P. Mingos, *J. Chem. Soc., Dalton Trans.*, 1995, 1635.
189. D. Bright and J.A. Ibers, *Inorg. Chem.*, 1969, **8**, 709; F.L. Phillips and A.C. Skapski, *J. Cryst. Mol. Struct.*, 1975, **5**, 83; D. Collison, C.D. Garner, F.E. Mabbs, J.A. Salthouse and T.J. King, *J. Chem. Soc., Dalton Trans.*, 1981, 1812; F.L. Phillips, A.C. Skapski and M.J. Withers, *Transition Met. Chem.*, 1975, **1**, 28; D. Pawson and W.P. Griffith, *J. Chem. Soc., Dalton Trans.*, 1975, 417; P.A. Belmonte and Z.-Y. Own, *J. Am. Chem. Soc.*, 1984, **106**, 7493.
190. W.H. Leung, M.C. Wu, C.M. Che, W.T. Wong and K.F. Chin, *J. Chem. Soc., Dalton Trans.*, 1994, 2519; D.C. Ware and H.Taube, *Inorg. Chem.*, 1991, **30**, 4598.
191. P.A. Shapley, R.M. Marshman, J.M. Shusta, Z. Gebeyehu and S.R. Wilson, *Inorg. Chem.*, 1994, **33**, 498.
192. D.S. Williams, T.J. Meyer and P.S. White, *J. Am. Chem. Soc.*, 1995, **117**, 823.
193. K.W. Given and L.H. Pignolet, *Inorg. Chem.*, 1977, **16**, 2982; M.J. Cleare and W.P. Griffith, *J. Chem. Soc. (A)*, 1970, 1117.
194. A.A. Danopoulos, G. Wilkinson, B. Hussain-Bates and M.B. Hursthouse, *J. Chem. Soc., Dalton Trans.*, 1991, 269; A.A. Danopoulos, G. Wilkinson, B. Hussain-Bates and M.B. Hursthouse, *J. Chem. Soc., Dalton Trans.*, 1991, 1855; D.W.H. Rankin, H.E. Robertson, A.A. Danopoulos, P.D. Lyne, D.M.P. Mingos and G. Wilkinson, *J. Chem. Soc., Dalton Trans.*, 1994, 1563; M.H. Schofield, T.P. Kee, J.T. Anhaus, R.R. Schrock, K.H. Johnson and W.M. Davis, *Inorg. Chem.*, 1991, **30**, 3595; A.A. Danopoulos, G. Wilkinson, B. Hussain-Bates and M.B. Hursthouse, *Polyhedron*, 1992, **11**, 2961.

195. J.R. Wolf, G.C. Bazan and R.R. Schrock, *Inorg. Chem.*, 1993, **32**, 4155.
196. A.M. La Pointe, R.R. Schrock and W.M. Davis, *Organometallics*, 1995, **14**, 2699.
197. R.S. Hay-Motherwell, G. Wilkinson, B. Hussain-Bates and M.B. Hursthouse, *Polyhedron*, 1990, **9**, 2071; R.P. Tooze, G. Wilkinson, M. Motevalli and M.B. Hursthouse, *J. Chem. Soc., Dalton Trans.*, 1986, 2711; R.S. Hay-Motherwell, G. Wilkinson, B. Hussain-Bates and M.B. Hursthouse *J. Chem. Soc., Dalton Trans.*, 1992, 3411.
198. D.T. Hardy, G. Wilkinson and G.B. Young, *Polyhedron*, 1996, **15**, 1363.
199. P. Stravropoulos, P.D. Savage, R.P. Tooze, G. Wilkinson, B. Hussain, M. Motevalli and M.B. Hursthouse, *J. Chem. Soc., Dalton Trans.*, 1987, 557; J. Arnold, G. Wilkinson, B. Hussain and M.B. Hursthouse, *J. Chem. Soc., Chem. Commun.*, 1988, 1548; *Organometallics*, 1988, **8**, 1362; P. Stravropoulos, P.G. Edwards, T. Behling, G. Wilkinson, M. Motevalli and M.B. Hursthouse, *J. Chem. Soc., Dalton Trans.*, 1987, 169; C.J. Longley, P.D. Savage, G. Wilkinson, B. Hussain and M.B. Hursthouse, *Polyhedron*, 1988, **7**, 1079.
200. A.M. La Pointe, R.R. Schrock and W.M. Davis, *J. Am. Chem. Soc.*, 1995, **117**, 4802.
201. K. Rypdal, W.A. Herrmann, S.J. Eder, R.W. Albach, P. Watzlowik, H. Bock and B. Solouki, *Organometallics*, 1991, **10**, 1331; W.A. Herrmann, S.J. Eder, P. Kiprof and P. Watzlowik, *J. Organomet. Chem.*, 1992, **428**, 183; W.A. Herrmann and P. Watzlowik, *J. Organomet. Chem.*, 1992, **437**, 363; W.A. Herrmann, S.J. Eder and W. Scherer, *J. Organomet. Chem.*, 1993, **454**, 257.

Chapter 2

1. F.R. Hartley (ed.), *The Chemistry of the Platinum Group Metals*, Elsevier, Amsterdam, 1991, p. 407.
2. W.P. Griffith, *The Chemistry of the Rarer Platinum Metals*, Wiley-Interscience, New York, 1967.
3. *Gmelin Handbook of Inorganic Chemistry*, System No. 64, Rhodium. (a) Main volume 1938 (Element and Compounds); Supplement Volumes: (b) Section 1 Compounds (Compounds with Ligands whose Donor Atoms include O, N, Halide, B, C) 1982; (c) Section 2, Coordination Compounds (Complexes with ligands containing O and N) 1984; (d) Section 3, Coordination Compounds (Complexes with ligands containing S, Se, Te, P, As, and Sb) 1984.
4. *Gmelin Handbook of Inorganic Chemistry*, System No. 67, Iridium. Main volume 1939 (Element and Compounds); Supplement Volumes: Section 1; The Metal Alloys. 1978; Section 2: Compounds. 1978.
5. S.E. Livingstone, in *Comprehensive Inorganic Chemistry*, eds J.C. Bailar, H.J. Emeleus, R.S. Nyholm and A.F. Trotman-Dickenson, Pergamon, Oxford, 1973, Vol. 3, p. 1233 (rhodium and iridium).
6. F.H. Jardine and P.S. Sheridan, in *Comprehensive Coordination Chemistry*, eds G. Wilkinson, R.D. Gillard and J.A. McCleverty, Pergamon, Oxford, 1987, Vol. 5, p. 901 (rhodium).
7. R.P. Hughes, in *Comprehensive Organometallic Chemistry I*, eds G. Wilkinson, F.G.A. Stone and E.W. Abel, Pergamon, Oxford, 1982, Vol. 5, p. 277; P.R. Sharp, in *Comprehensive Organometallic Chemistry II*, eds G. Wilkinson, F.G.A. Stone and E.W. Abel, Pergamon, Oxford, 1995, Vol. 8, p. 115 (rhodium).
8. N. Serpone and M.A. Jamieson, in *Comprehensive Coordination Chemistry*, eds G. Wilkinson, R.D. Gillard and J.A. McCleverty, Pergamon, Oxford, 1987, Vol. 5, p. 1097 (iridium).
9. G.J. Leigh and R.L. Richards, in *Comprehensive Organometallic Chemistry*, eds G. Wilkinson, F.G.A. Stone and E.W. Abel, Pergamon, Oxford, 1982, Vol. 5, p. 241; J.D. Atwood, in *Comprehensive Organometallic Chemistry II*, eds G. Wilkinson, F.G.A. Stone and E.W. Abel, Pergamon, Oxford, 1995, Vol. 8, p. 303 (iridium).
10. R.S. Dickson, *Organometallic Chemistry of Rhodium and Iridium*, Academic Press, 1983.
11. F.R. Hartley in Ref. 1, p. 9.
12. L. Grosse and R. Hoppe, *Z. Anorg. Allgem. Chem.*, 1987, **552**, 123.
13. P.A. Lee and G. Beni, *Phys. Rev. B*, 1977, **15**, 2862.

14. J. Reed and P. Eisenberger, *Acta Crystallogr. Sect. B*, 1978, **34**, 344.
15. Ref. 6, p. 1218.
16. B. Cox, D.W.A. Sharp and A.G. Sharpe, *J. Chem. Soc.*, 1956, 1242; P.R. Rao, A. Tressaud and N. Bartlett, *J. Inorg. Nucl. Chem. Suppl.*, 1976, 23.
17. B.K. Morrell, A. Zalkin, A. Tressaud and N. Bartlett, *Inorg. Chem.*, 1973, **12**, 2640.
18. A.K. Brisdon, P.J. Jones, W. Levason, J.S. Ogden, J.H. Holloway, E.G. Hope and G. Stanger, *J. Chem. Soc., Dalton Trans.*, 1990, 715; A.K. Brisdon, J.H. Holloway, E.G. Hope, W. Levason and J.S. Ogden, *J. Chem. Soc., Dalton Trans.*, 1992, 447.
19. K. Broderson, G. Thiele, H. Ohnsorge, I. Recke and F. Moers, *J. Less Common Metals*, 1968, **15**, 347.
20. W.A. Sunder and W.E. Falconer, *Inorg. Nucl. Chem. Lett.*, 1972, **8**, 537.
21. R.T. Payne and L.B. Asprey, *Inorg. Chem.*, 1975, **14**, 1111.
22. S.A. Brewer, A.K. Brisdon, J.H. Holloway and E.G. Hope, *Polyhedron*, 1994, **13**, 748.
23. L. Grosse and R. Hoppe, *Z. Anorg. Allgem. Chem.*, 1987, **552**, 123; P.J. Cresswell, J.E. Fergusson, B.R. Penfold and D.E. Scaife, *J. Chem. Soc., Dalton Trans.*, 1972, 255; J.E. Fergusson and R.R. Sherlock, *Aust. J. Chem.*, 1977, **30**, 1445; J.E. Fergusson and D.A. Rankin, *Aust. J. Chem.*, 1983, **36**, 863; R.D. Gillard, D.E. Hibbs, C. Holland, M.B. Hursthouse, K.M.A. Malik and G. Sykara, *Polyhedron*, 1996, **15**, 225; for vibrational spectra, see in particular Y.M. Bosworth and R.J.H. Clark, *J. Chem. Soc., Dalton Trans.*, 1974, 1749; K. Irmer and W. Preetz, *Z. Naturforsch., Teil B*, 1991, **46**, 1200.
24. A.K. Brisdon, J.H. Holloway, E.G. Hope and W. Levason, *Polyhedron*, 1992, **11**, 7; A.K. Brisdon, J.H. Holloway, E.G. Hope, W. Levason, J.S. Ogden and A.K. Saad, *J. Chem. Soc., Dalton Trans.*, 1992, 139.
25. W. Preetz and H.-J. Steinebach, *Z. Naturforsch., Teil B*, 1986, **41**, 260.
26. I.J. Ellison and R.D. Gillard, *Polyhedron*, 1996, **15**, 339.
27. J.H.E. Griffiths, J. Owen and J. Ward, *Proc. R. Soc. London, Series A*, 1953, **219**, 526. J. Owen and K.W.H. Stevens, *Nature*, 1953, **171**, 836; J.H.M. Thornley, *Proc. Phys. Soc., Solid State*, 1968, **1**, 1027.
28. W. Preetz and H.J. Steinebach, *Z. Naturforsch., Teil B*, 1985, **40**, 745; W. Preetz and W. Kuhr, *Z. Naturforsch., Teil B*, 1989, **44**, 1221; W. Kuhr, G. Peters and W. Preetz, *Z. Naturforsch., Teil B*, 1989, **44**, 1402.
29. W. Kuhr and W. Preetz, *Z. Anorg. Allgem. Chem.*, 1990, **584**, 165.
30. J.H.M. Biesterbos and J. Hornstra, *J. Less Common Metals*, 1973, **30**, 121; G. Bayer and H.G. Wiedermann, *Thermochim. Acta*, 1976, **15**, 213.
31. S.J. Crimp and L. Spiccia, *Aust. J. Chem.*, 1995, **48**, 447.
32. S. Jobic, P. Deniard, R. Brec, J. Rouxel, M.G.B. Drew and W.I.F. David, *J. Solid State Chem.*, 1990, **89**, 315.
33. A. F. Wells, *Structural Inorganic Chemistry*, 4th edn, Clarendon Press, Oxford, 1975, p. 215.
34. W. Bronger, M. Gehlen and G. Auffermann, *J. Alloys Compd.*, 1991, **176**, 255; W. Bronger, P. Müller, J. Kowalczyk and G. Auffermann, *J. Alloys Compd*, 1991, **176**, 262; W. Bronger, M. Gehlen and G. Auffermann, *Z. Anorg. Allgem. Chem.*, 1994, **620**, 1983.
35. P. Beutler and H. Gamsjager, *J. Chem. Soc., Chem. Commun.*, 1976, 554; R.S. Armstrong, J.K. Beattie, S.P. Best, B.W. Skelton and A.H. White, *J. Chem. Soc., Dalton Trans.*, 1983, 1973; G.D. Fallon and L. Spiccia, *Aust. J. Chem.*, 1989, **42**, 2051; S.P. Best, J.K. Beattie, R.S. Armstrong and G.P. Braithwaite, *J. Chem. Soc., Dalton Trans.*, 1989, 1771; S.P. Best, R.S. Armstrong and J.K. Beattie, *J. Chem. Soc., Dalton Trans.*, 1992, 299; J.K. Beattie, S.P. Best, F.H. Moore, B.W. Skelton and A.H. White, *Aust. J. Chem.*, 1993, **46**, 1337; M. Gajhede, K. Simonsen and L.K. Skov, *Acta Chem. Scand.*, 1993, **47**, 271.
36. M.C. Read and H. Sandstrom, *Acta Chem. Scand.*, 1992, **46**, 1177.
37. C.R. Wilson and H. Taube, *Inorg. Chem.*, 1973, **12**, 2276.
38. M.J. Pavelich and G.M. Harris, *Inorg. Chem.*, 1972, **12**, 423; D.A. Palmer and G.M. Harris, *Inorg. Chem.*, 1974, **14**, 1316; C. Carr, J.A. Glaser and M. Sandstrom, *Inorg. Chim. Acta*, 1987, **131**, 153.
39. M.C. Read, J. Glaser and M. Sandstrom, *J. Chem. Soc., Dalton Trans.*, 1992, 233.
40. (a) C.K. Thomas and J.A. Stanko, *J. Coord. Chem.*, 1972, **2**, 211; G. Bugli and C. Potvin, *Acta Crystallogr. Sect. B*, 1981, **37**, 1394; (b) C. Flensberg, K. Simonsen and L.K. Skov, *Acta Chem. Scand.*, 1993, **47**, 862.
41. See Ref. 6, p. 905.

42. Refs 3(d) and 6, p. 906.
43. (a) H.L.M. van Gaal and F.L.A. van den Bekorom, *J. Organomet. Chem.*, 1977, **134**, 237; M.D. Curtis, W.M. Butler and J. Greene, *Inorg. Chem.*, 1978, **17**, 2928; (b) P. Binger, J. Haas, G. Glaser, R. Goddard and C. Krüger, *Chem. Ber.*, 1994, **127**, 1927; (c) K.P. Wang, G. P. Rosini, S.P. Nolan and A.S. Goldman, *J. Am. Chem. Soc.*, 1995, **117**, 5082.
44. F.H. Jardine, *Progr. Inorg. Chem.*, 1981, **28**, 63 (review).
45. J.A. Osborn, F.H. Jardine, J.F. Young and G. Wilkinson, *J. Chem. Soc. (A)*, 1966, 1711; J.M. Brown and A.R. Lucy, *J. Chem. Soc., Chem. Commun.*, 1984, 914; S.B. Duckett, C.L. Newell and R. Eisenberg, *J. Am. Chem. Soc*, 1994, **116**, 10 548 and references therein.
46. M.J. Bennett and P.B. Donaldson, *Inorg. Chim. Acta.*, 1977, **16**, 655; P. Binger, J. Haas, R. Goddard and K. Kringer, *Chem. Ber.*, 1994, **127**, 1927. See also Ref. 52.
47. P. Meakin, J.P. Jesson and C.A. Tolman, *J. Am. Chem. Soc.*, 1972, **92**, 3241; for solid-state phosphorus-31 NMR, see J.W. Diesveld, E.M. Menger, H.T. Edzes and W.V. Veeman, *J. Am. Chem. Soc.*, 1982, **102**, 7935; G. Wu and R.E. Wasylishen, *Organometallics*, 1992, **11**, 3243.
48. M.J. Bennett and P.B. Donaldson, *Inorg. Chem.*, 1977, **16**, 1581, 1585.
49. S.H. Strauss, S.E. Diamond, F. Mares and D.F. Shriver, *Inorg. Chem.*, 1978, **17**, 3066.
50. Y.W. Yared, S.L. Miles, R. Bau and C.A. Reed, *J. Am. Chem. Soc.*, 1979, **99**, 7016; G. Pimblett, C.D. Garner and W. Clegg, *J. Chem. Soc., Dalton Trans.*, 1985, 1977.
51. A.R. Siedle, R.A. Newmark and R.D. Howells, *Inorg. Chem.*, 1988, **27**, 2473.
52. (a) C. Masters, *Homogeneous Transition-metal Catalysis – A Gentle Art*, Chapman & Hall, London, 1981 esp. pp. 40 ff; (b) P.A. Chaloner, *Handbook of Coordination Catalysis in Organic Chemistry*, Butterworths, London, 1986; (c) L.H. Pignolet (ed.), *Homogeneous Catalysis with Metal Phosphine Complexes*, Plenum, New York, 1983.
53. T.E. Nappier, D.W. Meek, R.M. Kirchner and J.A. Ibers, *J. Am. Chem. Soc.*, 1973, **95**, 4194.
54. R.A. Jones, F.M. Real, G. Wilkinson, A.M.R. Galas, M.B. Hursthouse and K.M.A. Malik, *J. Chem. Soc., Dalton Trans.*, 1980, 511; M.C. Hall, B.T. Kilbourn and K.A. Taylor, *J. Chem. Soc. (A)*, 1970, 2539.
55. See Ref. 6, p. 929; L.M. Haines, *Inorg. Chem.*, 1971, **10**, 1685.
56. (a) L.F. Dahl, E. Martell and D.L. Wampler, *J. Am. Chem. Soc.*, 1961, **83**, 1761; (b) J.G. Norman and D.J. Gmur, *J. Am. Chem. Soc.*, 1979, **99**, 1446.
57. *Inorg. Synth.*, 1990, **28**, 81; for a review see F.H. Jardine, *Polyhedron*, 1982, **1**, 569.
58. C. Masters, *Homogeneous Transition-metal Catalysis – A Gentle Art*, Chapman & Hall, London, 1981, pp. 55, 72, 89, 121.
59. Y.-J. Chen, J.-C. Wang and Y. Wong, *Acta Crystallogr. Sect. C*, 1991, **47**, 2441; *Inorg. Synth.*, 1968, **11**, 99; 1990, **28**, 79. For other derivatives see *Inorg. Synth.*, 1974, **15**, 65; and L. Vaska and J. Peone, *J. Chem. Soc., Chem. Commun.*, 1971, 418.
60. T. R. Gaffney and J.A. Ibers, *Inorg. Chem.*, 1982, **21**, 2857.
61. H. Schumann, S. Jurgis, M. Eisen and J. Blum, *Inorg. Chim. Acta*, 1990, **172**, 137; R.L. Harlow, S.A. Westcott, D.L. Thorn and R.T. Baker, *Inorg. Chem.*, 1992, **31**, 323.
62. B.E. Mann, C. Masters, B.L. Shaw and R.E. Stainbank, *J. Chem. Soc., Chem. Commun.*, 1971, 1103.
63. J.A. Davies and C.T. Eagle in Ref. 1, p. 230. For other reactions see S.E. Boyd, L.D. Field and M.G. Partridge, *J. Am. Chem. Soc.*, 1994, **116**, 9492; G.P. Rosini, W.T. Boese and A.S. Goldman, *J. Am. Chem. Soc.*, 1994, **116**, 9498.
64. J.J. Bonnet, Y. Jeannin, P. Kalck, A. Maissonat and R. Poilblanc, *Inorg. Chem.*, 1975, **14**, 743.
65. R.E. Cramer, *Inorg. Chem.*, 1962, **1**, 722; *Inorg. Synth.*, 1974, **15**, 14.
66. J.A. Evans and D.R. Russell, *J. Chem. Soc., Chem. Commun.*, 1971, 197; S.A. Vierkötter, C.E. Barnes, G.L. Garner and L.G. Butler, *J. Am. Chem. Soc.*, 1994, **116**, 7445; for propeller rotation, see Ref. 7, p. 418.
67. C. Nave and M.R. Truter, *J. Chem. Soc., Dalton Trans.*, 1973, 2202.
68. Ref. 7, p. 342; K.R. Mann, N.S. Lewis, R.M. Williams, H.B. Gray and J.G. Gordon, *Inorg. Chem.*, 1978, **17**, 828; H. Endres, N. Gottstein, H.J. Keller, R. Martin, W.R. Odemer and W. Steiger, *Z. Naturforsch., Teil B*, 1979, **34**, 827.
69. R.L. Harlow, D.L. Thorn, R.T. Baker and N.L. Jones, *Inorg. Chem.*, 1992, **31**, 993; T. Rappert, J. Wolf, M. Schulz and H. Werner, *Chem. Ber.*, 1992, **125**, 839.

70. K.R. Dunbar, S.C. Haefner and L.E. Pence, *J. Am. Chem. Soc.*, 1991, **111**, 5505; 1993, **113**, 9548.
71. F.A. Cotton and R.A. Walton, *Multiple Bonds between Metal Atoms*, 2nd edn, Clarendon Press, Oxford, 1993, pp. 431 ff, 630 ff; E.B. Boyar and S.D. Robinson, *Coord. Chem. Rev.*, 1983, **50**, 109; T.R. Felthouse, *Progr. Inorg. Chem.*, 1982, **29**, 73 and references therein; Ref. 6, p. 934; F.A. Cotton and J.L. Thompson, *Acta Crystallogr. Sect. B*, 1981, **37**, 2235; F.A. Cotton, B.G. DeBoer, M.D. LaPrade, J.R. Pipal and D.A. Ucko, *J. Am. Chem. Soc.*, 1970, **92**, 2926; C.G. Christoph, J. Halpern, G.P. Khare, Y.B. Koh and C. Romanowski, *Inorg. Chem.*, 1981, **20**, 3029.
72. V.I. Nefedov, Ya.V. Salyn', I.B. Barnovskii and A.G. Maiorova, *Russ. J. Inorg. Chem.*, 1980, **25**, 116; V.I. Nefedov, A.V. Shtemenko and A.S. Kotelinova, *Inorg. Chim. Acta*, 1980, **45**, L49.
73. C.R. Wilson and H. Taube, *Inorg. Chem.*, 1975, **14**, 2276.
74. F.A. Cotton, E.V. Dikarev and X. Feng, *Inorg. Chim. Acta*, 1995, **237**, 19; F.A. Cotton and Y. Kim, *Eur. J. Solid State Inorg. Chem.*, 1994, **31**, 525.
75. (a) R.J.H. Clark, *Chem. Soc. Rev.*, 1990, **19**, 107, and references therein; (b) R.J.H. Clark, A.J. Hempleman and C.D. Flint, *J. Am. Chem. Soc.*, 1986, **108**, 519.
76. E.C. Morrison and D.A. Tocher, *Inorg. Chim. Acta*, 1989, **156**, 29; N. Mehmet and D.A. Tocher, *Inorg. Chim. Acta*, 1991, **188**, 71; R.J.H. Clark, D.J. West and R. Withnall, *Inorg. Chem.*, 1992, **31**, 456.
77. Ref 75(a), p. 174; E.B. Boyar and S.D. Robinson, *Platinum Metals Rev.*, 1982, **26**, 65.
78. J.G. Norman and H.J. Kolari, *J. Am. Chem. Soc.*, 1978, **100**, 791; T. Kawamura, K. Fukamachi, T. Sowa, S. Hayashida and T. Yonezawa, *J. Am. Chem. Soc.*, 1981, **103**, 364; G.O. Christoph and Y.B. Koh, *J. Am. Chem. Soc.*, 1979, **101**, 1422.
79. J.L. Bear, L.M. Liu and K.M. Kadish, *Inorg. Chem.*, 1987, **26**, 292; J.L. Bear, C.L. Yao, F.J. Capdeville and K.M. Kadish, *Inorg. Chem.*, 1988, **27**, 3782.
80. H.J. Keller and K. Seebold, *Z. Naturforsch., Teil B*, 1970, **25**, 551.
81. K.G. Caulton and F.A. Cotton, *J. Am. Chem. Soc.*, 1969, **91**, 6517; 1971, **93**, 1914; K.R. Dunbar, *J. Am. Chem. Soc.*, 1988, **110**, 8247.
82. S. Lee, M. Mediati and B.B. Wayland, *J. Chem. Soc., Chem. Commun.*, 1994, 2299; A.J. Blake, R.O. Gould, A.J. Holder, T.I. Hyde and M. Schröder, *J. Chem. Soc., Dalton Trans.*, 1988, 1861; S.R. Cooper, S.C. Rawle, R. Yagbasan and D.J. Watkin, *J. Am. Chem. Soc*, 1991, **113**, 1601.
83. J.C. Morrow and E.B. Parker, *Acta Crystallogr. Sect. B.*, 1973, **29**, 1145.
84. B.C. Dalzell and K. Eriks, *J. Am. Chem. Soc.*, 1971, **93**, 4298; R. Kuroda, *Inorg. Chem.*, 1991, **30**, 4955; S. Uemura, A. Spencer and G. Wilkinson, *J. Chem. Soc., Dalton Trans.*, 1973, 2565; T. Glowiak, M. Kubiak and T. Symanska-Buzar, *Acta Crystallogr. Sect. B.*, 1977, **33**, 1732.
85. G.H.Y. Lin, J.D. Leggett and R.M. Wing, *Acta Crystallogr. Sect. C.*, 1973, **29**, 1023; compare Ru analogue K. Okamoto, J. Hidaka, I. Iida, K. Higashino and K. Kanamori, *Acta Crystallogr. Sect. C*, 1990, **46**, 2327.
86. T.R. Thomas and G.A. Crosby, *J. Mol. Spectrosc.*, 1971, **38**, 118; R. Bramley, B.N. Figgis and R.S. Nyholm, *J. Chem. Soc. (A)*, 1967, 861; *Inorg. Synth*, 1986, **24**, 255.
87. P.C. Ford, *Inorg. Chem.*, 1971, **10**, 2153.
88. M.W. Bee, S.F.A. Kettle and D.B. Powell, *Spectrochim. Acta*, 1974, **30A**, 139.
89. *Inorg. Synth.*, 1972, **13**, 213; 1986, **24**, 222, 254; M. Weishaupt, H. Bezler and J. Strähle, *Z. Anorg. Allgem. Chem.*, 1978, **440**, 52.
90. R.S. Evans, E.A. Hopcus, J. Bordner and A.F. Schreiner, *J. Cryst. Mol. Struct.*, 1973, **3**, 235.
91. K. Thomas, J.A. Osborn, A.R. Powell and G. Wilkinson, *J. Chem. Soc. (A)*, 1968, 1801; K. Thomas and G. Wilkinson, *J. Chem. Soc. (A)*, 1970, 356.
92. B.A. Coyle and J.A. Ibers, *Inorg. Chem.*, 1972, **11**, 1105.
93. A.C. Skapski and P.G.H. Troughton, *J. Chem. Soc., Chem. Commun.*, 1969, 666.
94. W. Frank, T. Stetzer and L. Heck, *Z. Naturforsch., Teil B.*, 1988, **43**, 189.
95. A.J. Poe and M.V. Twigg, *Can. J. Chem.*, 1972, **50**, 1089; *Inorg. Synth.*, 1986, **24**, 223; M.P. Hancock, *Acta Chem. Scand. A*, 1975, **29**, 468.
96. I.A. Baidina, N.V. Podberezskaya and L.P. Solov'eva, *J. Struct. Chem. USSR*, 1974, **15**, 34.
97. L.H. Skibsted, *Coord. Chem. Rev.*, 1985, **64**, 343; 1989, **94**, 151; L.G. Vanquickenborne and A. Ceulemans, *Inorg. Chem.*, 1978, **17**, 2730; *Coord. Chem. Rev.*, 1983, **48**, 157.

98. Ref. 6, p. 975; *Inorg. Synth.*, 1967, **10**, 64.
99. S.A. Gronilov, V.I. Alekseev, I.A. Baudina and S.P. Kharanenko, *Russ. J. Inorg. Chem.*, 1992, **37**, 306.
100. S.A. Johnson and F. Basolo, *Inorg. Chem.*, 1962, **1**, 925.
101. M. Kakoti, A.K. Deb and S. Goswami, *Inorg. Chem.*, 1992, **31**, 1302.
102. D. Whang and K. Kim, *Acta Crystallogr. Sect. C*, 1991, **47**, 2547.
103. J.-U. Vogt, O. Haeckeland and W. Preetz, *Z. Anorg. Allgem. Chem.*, 1995, **621**, 725.
104. E.A. Allen and W. Wilkinson, *J. Chem. Soc., Dalton Trans.*, 1972, 613; P.D. Clark, J.H. Machin, J.F. Richardson, N.I. Dowling and J.B. Hine, *Inorg. Chem.*, 1988, **27**, 3526.
105. C.L. Raston and A.H. White, *J. Chem. Soc., Dalton Trans.*, 1975, 2425; R.J. Butcher and E. Sinn, *J. Chem. Soc., Dalton Trans.*, 1975, 2417; A.R. Hendrickson, R.L. Martin and D. Taylor, *Aust. J. Chem.*, 1976, **29**, 269.
106. R. Beckett and B.F. Hoskins, *Inorg. Nucl. Chem. Lett.*, 1972, **8**, 263.
107. A.J. Blake, R.O. Gould, A.J. Holder, T.I. Hyde and M. Schröder, *J. Chem. Soc., Dalton Trans.*, 1988, 1861; G. Reid and M. Schröder, *Chem. Soc. Rev.*, 1990, **19**, 239; S.R. Cooper, S.C. Rawle, R. Yagbasan and D.J. Watkin, *J. Am. Chem. Soc*, 1991, **113**, 1601; A.J. Blake and M. Schröder, *Adv. Inorg. Chem.*, 1991, **35**, 1.
108. See Ref. 3(d) for a review of much of the literature.
109. For syntheses also see (a) e.g. J. Chatt, N.P. Johnson and B.L. Shaw, *J. Chem. Soc.*, 1964, 2508; (b) B.E. Mann, C. Masters and B.L. Shaw, *J. Chem. Soc. (A)*, 1972, 704; (c) S.O. Grim and L.C. Satek, *J. Coord. Chem.*, 1974, **3**, 307.
110. A.C. Skapski and F.A. Stephens, *J. Chem. Soc., Dalton Trans.*, 1973, 1789; R.B. English, *Cryst. Struct. Commun.*, 1979, **8**, 167.
111. F.H. Allen and K.M. Gabuji, *Inorg. Nucl. Chem. Lett.*, 1971, **7**, 833; J.A. Muir, M.M. Muir and A.J. Rivera, *Acta Crystallogr. Sect. B*, 1974, **30**, 2062; S.E. Boyd, L.D. Field and T.W. Hambley, *Acta Crystallogr. Sect. C*, 1994, **50**, 1019.
112. For a detailed study showing how NMR can be used to unravel the transformations and structures, see F.A. Cotton, J.L. Eglin and S.-Y. Kang, *J. Am. Chem. Soc.*, 1992, **114**, 4015; *Inorg. Chem.*, 1993, **32**, 2332; F.A. Cotton and S.-Y. Kang, *Inorg. Chem.*, 1993, **32**, 2336; F.A. Cotton, S.-Y. Kang and S.K. Mandal, *Inorg. Chim. Acta*, 1993, **206**, 29.
113. T. Yoshida, S. Otsuka, M. Matsumoto and K. Nakatsu, *Inorg. Nucl. Chem. Lett.*, 1978, **29**, L257 and references therein.
114. R.V. Parish, *NMR, NQR, EPR and Mössbauer Spectroscopy in Inorganic Chemistry*, Ellis Horwood, Chichester, 1990; G.M. Intille, *Inorg. Chem.*, 1972, **11**, 695; B.E. Mann, C. Masters and B.L. Shaw, *J. Chem. Soc., Dalton Trans.*, 1972, 707; Ref. 106(c); J.P. Jesson, in *Transition Metal Hydrides*, ed. E.L. Muetterties, Marcel Dekker, New York, 1971, p. 85; J.M. Jenkins and B.L. Shaw, *Proc. Chem. Soc.*, 1963, 279; *J. Chem. Soc. (A)*, 1966, 1407.
115. Ref. 3(d); R.A. Jones, F.M. Real, G. Wilkinson, A.M.R. Galas, M.B. Hursthouse and K.M.A. Malik, *J. Chem. Soc. Dalton Trans.*, 1980, 511; O. Blum, J.C. Calabrese, F. Frolow and D. Milstein, *Inorg. Chim. Acta*, 1990, **174**, 149; K. Osakada and T. Yamamoto, *Bull. Chem. Soc. Japan*, 1994, **67**, 3271. See also Ref. 118(b).
116. K.R. Dunbar and S.C. Haefner, *Inorg. Chem.*, 1992, **31**, 3676.
117. See Ref. 69 and T. Yoshida, D.L. Thorn, T. Okano, S. Otsuka and J.A. Ibers, *J. Am. Chem. Soc.*, 1980, **102**, 6451; T. Yoshida, T. Okano, K. Saito and S. Otsuka, *Inorg. Chim. Acta*, 1980, **44**, L135; T. Yoshida, T. Okano and S. Otsuka, *J. Chem. Soc., Chem. Commun.*, 1979, 870.
118. (a) S.H. Strauss, S.E. Diamond, F. Mares and D.F. Shriver, *Inorg. Chem.*, 1978, **17**, 3064; (b) J. Wolf, O. Nürnberg, M. Schäfer and H. Werner, *Z. Anorg. Allgem. Chem.*, 1994, **620**, 1157.
119. (a) C. Masters and B.L. Shaw, *J. Chem. Soc. (A)*, 1971, 3679; (b) T. Yoshida, S. Otsuka, M. Matsumoto and K. Nakatsu, *Inorg. Chim. Acta*, 1978, **29**, L257.
120. M.A. Bennett and D.L. Milner, *J. Am. Chem. Soc.*, 1969, **91**, 6983.
121. (a) A. Rotman and Y. Mazur, *J. Am. Chem. Soc.*, 1972, **94**, 6226; (b) T.G.P. Harper, P.J. Desrosiers and T.C. Flood, *Organometallics*, 1990, **9**, 2523.
122. (a) M.J. Nolte, E. Singleton and E. Van der Stok, *Acta Crystallogr. Sect B*, 1978, **34**, 1674; (b) G.R. Clark, C.A. Reed, W.R. Roper, B.W. Skelton and T.N. Waters, *Chem. Commun.*, 1971, 758; (c) D.L. Thorn, *Organometallics*, 1982, **1**, 197. (d) D. Milstein, J.C. Calabrese and I.D. Williams, *J. Am. Chem. Soc.*, 1986, **108**, 6387.

123. L. Vaska and D.L. Catone, *J. Am. Chem. Soc.*, 1966, **88**, 5324.
124. W.M. Bedford and G. Rouchias, *J. Chem. Soc., Chem. Commun.*, 1972, 1224; *J. Chem. Soc., Dalton Trans.*, 1974, 2531; J.W. Dart, M.K. Lloyd, R. Mason and J.A. McCleverty, *Chem. Commun.*, 1971, 1197.
125. See L. Vaska, *Acc. Chem. Res.*, 1968, **1**, 335. For syntheses, see *Inorg. Synth.*, 1991, **28**, 92; M. Rahim and K.J. Ahmed, *Inorg. Chem.*, 1994, **33**, 3003.
126. (a) M.R. Churchill, J.C. Fettinger, L.A. Buttery, M.D. Barkan and J.S. Thompson, *J. Organomet. Chem.*, 1988, **340**, 257; A.J. Blake, E.A.V. Ebsworth, H.M. Murdoch and L.J. Yellowlees, *Acta Crystallogr. Sect. C*, 1991, **47**, 657; (b) R. Brady, W.H. De Camp, B.R. Flynn, M.L. Schneider, J.D. Scott, L. Vaska and M.F. Werneke, *Inorg. Chem.*, 1975, **14**, 2669; (c) M.R. Churchill, J.C. Fettinger, B.J. Rappoli and J.D. Atwood, *Acta Crystallogr. Sect. C*, 1987, **43**, 1697; (d) M.R. Churchill, C.H. Lake, C.A. Miller and J.D. Atwood, *J. Chem. Crystallogr.*, 1994, **24**, 557.
127. (SO_2): A.J. Blake, E.A.V. Ebsworth, S.G.D. Henderson, H.M. Murdoch and L.J. Yellowlees, *Z. Krist.*, 1992, **199**, 290; (Cl_2) F. DeMartin and N. Mascioccini, *Acta Crystallogr. Sect. C*, 1983, **39**, 1225; (C_{60}): A.L. Balch, V.J. Catalano and J.W. Lee, *Inorg. Chem.*, 1991, **30**, 3980; (C_{70}): A.L. Balch, V.J. Catalano, J.W. Lee, M.M. Olmstead and S.R. Parkin, *J. Am. Chem. Soc.*, 1991, **113**, 8953; (C_{84}): A.L. Balch, A.S. Ginwalla, J.W. Lee, B.C. Noll and M.M. Olmstead, *J. Am. Chem. Soc.*, 1994, **116**, 2227; ($C_{60}O$): A.L. Balch, D.A. Costa, J.W. Lee, B.C. Noll and M.M. Olmstead, *Inorg. Chem.*, 1994, **33**, 2071; (CO): N.C. Payne and J.A. Ibers, *Inorg. Chem.*, 1969, **8**, 2714, but see also F. Abu-Hasanayn, T.J. Emge, J.A. McGuire, K. Krogh-Jespersen and A.S. Goldman, *Organometallics*, 1994, **13**, 5177; ($HgCl_2$) P.D. Brotherton, C.L. Raston, A.H. White and S.B. Wild, *J. Chem. Soc., Dalton Trans.*, 1976, 1799. For a dioxygen adduct: M.S. Weininger, E.A.H. Griffith, C.T. Sears and E.L. Amma, *Inorg. Chim. Acta*, 1982, **60**, 67; a comparable tetracyanoethylene adduct: L. Manojlvic-Muir, K.W. Muir and J.A. Ibers, *Discuss. Faraday Soc.*, 1969, **47**, 84.
128. R.R. Holmes, *Progr. Inorg. Chem.*, 1984, **32**, 134.
129. Largely based on C.A. Reed and W.R. Roper, *J. Chem. Soc., Dalton Trans.*, 1973, 1371.
130. (C_6F_5): A. Clearfield, R. Gopal, I. Bernal, G.A. Moser and M.D. Rausch, *Inorg. Chem.*, 1975, **14**, 2727; (2,4,6-$Me_3C_6H_2$): L. Dahlenberg, K. von Deuten and J. Kopf, *J. Organomet. Chem.*, 1981, **216**, 113; (OH): L. Dahlenberg and F. Mirzeei, *Cryst. Struct. Commun.*, 1982, **11**, 1577; (C_6H_5O): W.M. Rees, J.C. Fettinger, M.R. Churchill and J.D. Atwood, *Organometallics*, 1985, **4**, 2179; (Me): W.M. Rees, M.R. Churchill, Y.J. Li and J.D. Atwood, *Organometallics*, 1985, **4**, 1162; (C_6F_5O): M.R. Churchill, J.C. Fettinger, W.M. Rees and J.D. Atwood, *J. Organomet. Chem.*, 1986, **308**, 361.
131. Based mainly on W. Strohmeier and T. Onada, *Z. Naturforsch., Teil. B*, 1968, **23**, 1377.
132. L. Vaska and J. Peone, *Chem. Commun.*, 1971, 418.
133. See, e.g. J.D. Atwood, in *Inorganic and Organometallic Reaction Mechanisms*, Brooks/Cole, 1985; J.P. Collman and W.R. Roper, *Adv. Organomet. Chem.*, 1968, **7**, 54; J. Halpern, *Accounts Chem. Res.*, 1970, **3**, 386; and Ref. 10.
134. (a) C.E. Johnson, B.J. Fisher and R. Eisenberg, *J. Am. Chem. Soc.*, 1983, **105**, 7772, (b) C.E. Johnson and R. Eisenberg, *J. Am. Chem. Soc.*, 1985, **107**, 3148, 6531.
135. A.L. Sargent and M.B. Hall, *Inorg. Chem.*, 1992, **31**, 320.
136. C.E. Johnson and R. Eisenberg, *J. Am. Chem. Soc.*, 1985, **107**, 3148.
137. A.L. Sargent, M.B. Hall and M.F. Guest, *J. Am. Chem. Soc.*, 1992, **114**, 517.
138. For structures see: M. Laing, M.J. Nolte and E. Singleton, *J. Chem. Soc., Chem. Commun.*, 1975, 661; M.J. Nolte, E. Singleton and M. Laing, *J. Am. Chem. Soc.*, 1975, **97**, 6396; L. Vaska, *Accts. Chem. Res.*, 1976, **9**, 175; J.-C. Wang, L.-Y. Chou, W.-Y. Hsien and L.-K. Liu, *Acta Crystallogr. Sect. C*, 1994, **50**, 879.
139. Data largely from C.A. Reed and W.R. Roper, *J. Chem. Soc., Dalton Trans.*, 1973, 1371 .
140. S. Sasaki, K. Hori and A. Ohyoshi, *Inorg. Chem.*, 1978, **17**, 3183.
141. H.A.O. Hill and D.G. Tew, in *Comprehensive Coordination Chemistry*, eds G. Wilkinson, R.D. Gillard and J.A. McCleverty, Pergamon, Oxford, 1987, Vol. 2, p. 315.
142. A.P. Ginsberg and W.E. Lindsell, *Chem. Commun.*, 1971, 232; for structure W.D. Bonds and J.A. Ibers, *J. Am. Chem. Soc.*, 1972, **94**, 3415;.
143. J.P. Collman, M. Kubota, F.D. Vastine, J.Y. Sun and J.W. Kang, *J. Am. Chem. Soc.*, 1968, **90**, 5430.

144. M.P. Yagupsky and G. Wilkinson, *J. Chem. Soc. (A)*, 1968, 2813; J.S. Field and P.J. Wheatley, *J. Chem. Soc., Dalton Trans.*, 1972, 2269.
145. W.A. Schenk, J. Leissner and C. Burschka, *Ang. Chem. Int. Ed. Engl.*, 1984, **23**, 806.
146. H.D. Empsall, E.M. Hyde and B.L. Shaw, *J. Chem. Soc., Dalton Trans.*, 1975, 1690.
147. M.P. Garcia, M.V. Jiminez, L.A. Oro, F.J. Lahoz, M.C. Tiripicchio and A. Tiripicchio, *Organometallics*, 1993, **12**, 4660.
148. B.C. Lane, J.W. McDonald, F. Basolo and R.G. Pearson, *J. Am. Chem. Soc.*, 1972, **94**, 3786; W.P. Griffith, *J. Chem. Soc. (A)*, 1966, 899; *Inorg. Synth.*, 1963, **7**, 227; 1970, **12**, 243; 1986, **24**, 264.
149. F. Galsbøl, S.K. Hansen and K. Simonsen, *Acta Chem. Scand. A*, 1990, **24**, 796.
150. (a) M. Delepine, *Ann. Chim.*, 1923, **19**, 172.; (b) J.J. Bonnet and Y. Jeannin, *J. Inorg. Nucl. Chem.*, 1973, **35**, 4103.
151. S.A. Johnson and F. Basolo, *Inorg. Chem.*, 1962, **1**, 925; R.A. Bauer and F. Basolo, *Inorg. Chem.*, 1969, **8**, 2231; S. Kida, *Bull. Chem. Soc. Japan*, 1966, **39**, 2415.
152. G.B. Kauffmann, J.H. Tsai, R.C. Fay and C.K. Jorgensen, *Inorg. Chem*, 1963, **2**, 1133; J. Chatt, G.J. Leigh, A.P. Storace, D.A. Squire and B.J. Starkey, *J. Chem. Soc. (A)*, 1971, 899.
153. E. Sinn, *Inorg. Chem.*, 1976, **15**, 369.
154. J. Chatt, A.E. Field and B.L. Shaw, *J. Chem. Soc.*, 1963, 3371.
155. (a) P.R. Brookes, C. Masters and B.L. Shaw, *J. Chem. Soc. (A)*, 1971, 3752; (b) B.L. Shaw and R.M. Slade, *J. Chem. Soc. (A)*, 1971, 1185; (c) J.M. Jenkins and B.L. Shaw, *J. Chem. Soc.*, 1965, 6789.
156. R.S. Coffey, J. Chatt and B.L. Shaw, *J. Chem. Soc.*, 1965, 7391.
157. (a) C. Masters, B.L. Shaw and R.E. Stainbank, *J. Chem. Soc., Dalton Trans.*, 1972, 664. (b) B.E. Mann, C. Masters and B.L. Shaw, *J. Inorg. Nucl. Chem.*, 1973, **33**, 2195; (c) H.D. Empsall, E.M. Hyde, E. Mentzer, B.L. Shaw and M.F. Uttley, *J. Chem. Soc., Dalton Trans.*, 1976, 2069; (d) A. Albinati *et al.*, *J. Am. Chem. Soc.*, 1993, **115**, 7300; V.V. Grushin, A.B. Vymenits and M.E. Vol'pin, *J. Organomet. Chem.*, 1990, **382**, 185; (e) B.E. Hauger, D. Gusev and K.G. Caulton, *J. Am. Chem. Soc.*, 1994, **116**, 208.
158. J.U. Notheis, R.H. Heyn and K.G. Caulton, *Inorg. Chim. Acta*, 1995, **229**, 187.
159. J. Belli and C.M. Jensen, *Organometallics*, 1996, **15**, 1532.
160. J.P. Jesson, in *Transition Metal Hydrides*, ed. E.L. Muetterties, Marcel Dekker, New York, 1971, p. 80.
161. G.R. Clark, B.W. Skelton and T.N. Waters, *Inorg. Chim. Acta*, 1975, **12**, 235; R. Bau, W.E. Carroll, D.W. Hart, R.G. Telfer and T.F. Koetzle, *Advan. Chem. Ser.*, 1978, **167**, 73; R. Bau, C.J. Schwerdtfeger, L. Garlaschelli and T.F. Koetzle, *J. Chem. Soc., Dalton Trans.*, 1993, 3359.
162. D.G. Gusev, V.I. Bakhmutov, V.V. Grushin and M.E. Vol'pin, *Inorg. Chim. Acta*, 1990, **177**, 115; E.G. Lundquist, K. Folting, W.E. Streib, J.C. Huffman, O. Eisenstein and K.G. Caulton, *J. Am. Chem. Soc.*, 1990, **112**, 855; L.F. Rhodes and K.G. Caulton, *J. Am. Chem. Soc.*, 1985, **107**, 259.
163. For many syntheses see J.M. Jenkins and B.L. Shaw, *J. Chem. Soc.*, 1965, 6789; *J. Chem. Soc., Dalton Trans.*, 1966, 1407.
164. P.R. Brookes, C. Masters and B.L. Shaw, *J. Chem. Soc., Dalton Trans.*, 1971, 3756.
165. S. Al-Jibori, C. Crocker, W.S. McDonald and B.L. Shaw, *J. Chem. Soc., Dalton Trans.*, 1981, 1572.
166. B.L. Shaw and A.C. Smithies, *J. Chem. Soc., Dalton Trans.*, 1967, 1047; E.G. Lundquist, K. Folting, J.C. Huffman and K.G. Caulton, *Polyhedron*, 1988, **7**, 2171.
167. A.J. Deeming, G.P. Proud, H.M. Dawes and M.B. Hursthouse, *J. Chem. Soc., Dalton Trans.*, 1986, 2545; A.J. Deeming, G.P. Proud, H.M. Dawes and M.B. Hursthouse, *J. Chem. Soc., Dalton Trans.*, 1988, 2475; A.J. Deeming and G.P. Proud, *Inorg. Chim. Acta*, 1988, **144**, 253; A.J. Deeming, S. Doherty, J.E. Marshall and N.I. Powell, *J. Chem. Soc., Chem. Commun.*, 1989, 1351.
168. E.G. Lundquist, K. Folting, J.C. Huffman and K.G. Caulton, *Organometallics*, 1990, **9**, 2254; D.E. Westreib, L.F. Rhodes, J. Edwin, W.E. Geiger and K.G. Caulton, *Inorg. Chem.*, 1991, **30**, 1107.
169. G.B. Robertson and P.A. Tucker, *Acta Crystallogr. Sect. B.*, 1981, **37**, 814; *J. Am. Chem. Soc.*, 1982, **104**, 318; *Aust. J. Chem.*, 1988, **41**, 641 and refs therein.

170. L.F. Rhodes, J.C. Huffman and K.G. Caulton, *J. Am. Chem. Soc.*, 1984, **106**, 6874; R.L. Geerts, J.C. Huffman, D.E. Westenberg, K. Folting and K.G. Caulton, *New J. Chem.*, 1988, **12**, 455.
171. J. Chatt, G.J. Leigh and D.M.P. Mingos, *J. Chem. Soc. (A)*, 1968, 1674; C.E. Briant, K.A. Rowland, C.T. Webber and D.M.P. Mingos, *J. Chem. Soc., Dalton Trans.*, 1981, 1515; R.A. Cipriano, W. Levason, D. Pletcher, N.A. Powell and M. Webster, *J. Chem. Soc., Dalton Trans.*, 1987, 1901; R.A. Cipriano, L.R. Hanton, W. Levason, D. Pletcher, N.A. Powell and M. Webster, *J. Chem. Soc., Dalton Trans.*, 1988, 2483; R.A. Cipriano, W. Levason, R.A.S. Mould, D. Pletcher and N.A. Powell, *J. Chem. Soc., Dalton Trans.*, 1988, 2677.
172. P. Mura, A. Segre and S. Sostero, *Inorg. Chem.*, 1989, **28**, 2853; D. Attanasio, P. Mura, A. Maldotti, S. Sostero and O. Traverso, *New J. Chem.*, 1992, **16**, 347.
173. M.B. Bardin and P.M. Ketrush, *Russ. J. Inorg. Chem.*, 1973, **18**, 693.
174. B. Harrison, N. Logan and A.D. Harris, *J. Chem. Soc., Dalton Trans.*, 1980, 2382.
175. L. Garlaschelli, S.I. Khan, R. Bau, G. Longoni and T.F. Koetzle, *J. Am. Chem. Soc.*, 1985, **107**, 7212.
176. E. Farnetti, J. Kaspar, R. Spogliarich and M. Graziani, *J. Chem. Soc., Dalton Trans.*, 1988, 947; J.W. Faller and C.J. Smart, *Organometallics*, 1989, **8**, 602.
177. T. Le-Husebo and C.M. Jensen, *Inorg. Chem.*, 1993, **32**, 3797; L.L. Wisniewski, M. Mediati, C.M. Jensen and K.W. Zilm, *J. Am. Chem. Soc.*, 1993, **115**, 7533; J. Eckert, C.M. Jensen, G. Jones, E. Clot and O. Eisenstein, *J. Am. Chem. Soc.*, 1993, **115**, 11057 and Ref. 157(d).
178. M. Mediati, G.N. Tachibana and C.M. Jensen, *Inorg. Chem.*, 1990, **29**, 3; 1992, **31**, 1827; R.H. Crabtree and M. Lavin, *J. Chem. Soc., Chem. Commun.*, 1985, 1661; D. Ma, Y. Yu and X. Lu, *J. Org. Chem.*, 1989, **54**, 1105; X. Lu, Y. Lin and D. Ma, *Pure Appl. Chem.*, 1988, **60**, 1299.
179. R. Eisenberg and C.D. Meyer, *Accts. Chem. Res.*, 1975, **8**, 26; J.H. Enemark and R.D. Feltham, *Coord. Chem. Rev.*, 1974, **13**, 339; B.F.G. Johnson, B.L. Haymore and J.R. Dilworth, in *Comprehensive Coordination Chemistry*, eds G. Wilkinson, R.D. Gillard and J.A. McCleverty, Pergamon, Oxford, 1987, Vol. 2, 99; D.M.P. Mingos and D.J. Sherman, *Adv. Inorg. Chem.*, 1989, **34**, 293.
180. D.J. Hodgson and J.A. Ibers, *Inorg. Chem.*, 1968, **7**, 2345.
181. S. Bhaduri and B.F.G. Johnson, *J. Chem. Soc., Chem. Commun.*, 1973, 650; S. Bhaduri, K. Grundy and B.F.G. Johnson, *J. Chem. Soc., Dalton Trans.*, 1977, 20.
182. L.K. Bell, J. Mason, D.M.P. Mingos and D.G. Tew, *Inorg. Chem.*, 1983, **22**, 3497.
183. C.A. Reed and W.R. Roper, *Chem. Commun.*, 1969, 1459; *J. Chem. Soc., Dalton Trans.*, 1973, 1014.
184. M.W. Schoonover, E.C. Baker and R. Eisenberg, *J. Am. Chem. Soc.*, 1979, **101**, 1880.
185. R. Hoffmann, M.M.L. Chen, M. Elian, A.R. Rossi and D.M.P. Mingos, *Inorg. Chem.*, 1974, **13**, 2666.
186. R.A. Andersen, R.A. Jones and G. Wilkinson, *J. Chem. Soc., Dalton Trans.*, 1978, 447; R.S. Hay-Motherwell, G. Wilkinson, B. Hussain and M.B. Hursthouse, *J. Chem. Soc., Chem. Commun.*, 1989, 1436.
187. L. Wang, C. Wang, R. Bau and T.C. Flood, *Organometallics*, 1996, **15**, 491.
188. R.S. Hay-Motherwell, S.U. Koschmieder, G. Wilkinson, B. Hussain-Bates and M.B. Hursthouse, *J. Chem. Soc., Dalton Trans.*, 1991, 2821; R.S. Hay-Motherwell, G. Wilkinson, B. Hussain-Bates and M.B. Hursthouse, *J. Chem. Soc., Chem. Commun.*, 1990, 1242.
189. R.S. Hay-Motherwell, G. Wilkinson, B. Hussain-Bates and M.B. Hursthouse, *Polyhedron*, 1991, **10**, 1457.
190. A.A. Danopoulos, G. Wilkinson, B. Hussain-Bates and M.B. Hursthouse, *J. Chem. Soc., Dalton Trans.*, 1992, 3165; R.S. Hay-Motherwell, G. Wilkinson, B. Hussain-Bates and M.B. Hursthouse, *J. Chem. Soc., Dalton Trans.*, 1992, 3477; R.S. Hay-Motherwell, G. Wilkinson, B. Hussain-Bates and M.B. Hursthouse, *Polyhedron*, 1993, **12**, 2009.
191. R.S. Hay-Motherwell, B. Hussain-Bates, M.B. Hursthouse, B.E. Mann and G. Wilkinson, *J. Chem. Soc., Dalton Trans.*, 1993, 3219.
192. M.P. Garcia, L.A. Oro and F.J. Lahoz, *Angew. Chem. Int. Ed. Engl.*, 1988, **27**, 1700; M.P. Garcia, M.V. Jiminez, F.J. Lahoz, L.A. Oro, A. Tiripicchio and J.A. Lopez, *J. Chem. Soc., Dalton Trans.*, 1990, 1503.

Chapter 3

1. F.R. Hartley, *The Chemistry of Platinum and Palladium*, Elsevier, Amsterdam, 1973.
2. F.R. Hartley (ed.), *Chemistry of the Platinum Group Metals*, Elsevier, Amsterdam, 1991.
3. *Gmelin Handbook of Inorganic Chemistry*, System No. 65, Palladium. Main Volume: (a) Section 1. The Element, 1939; (b) Section 2, Compounds, 1942; (c) Supplement Volume: Part B. Compounds: Section 2, Palladium Compounds, 1986.
4. *Gmelin Handbook of Inorganic Chemistry*, System No. 68, Platinum. Main Volume. (a) Part A in Sections 1–6, 1938–1951 (Platinum Metals, Occurrence, History, Preparation, Alloys); (b) Part B: The Element in Sections 1–4, 1939–1942, Physical and Electrochemical properties of Platinum (Chemical reactions of Pt in Section 4); (c) Part C: The Compounds of Platinum. Section 1. Compounds with Noble Gases, H, O, N, Halogens, S, Se, Te, B, C,Si, P, As, Sb, Bi, 1939; (d) Section 2. Compounds with the alkali metals and ammonium, mainly the alkali metal platinum double salts, 1940;. (e) Section 3: Other Compounds, 1940; (f) Part D: Complexes with Neutral ligands, 1957. Supplement Volume; (g) Part A. Section 1. Technology of Platinum Metals. 1986; (h) Section 2. Isotopes, Atoms, Molecules and Clusters. 1989.
5. S.E. Livingstone, in *Comprehensive Inorganic Chemistry*, eds J.C. Bailar, H.J. Emeleus, R.S. Nyholm and A.F. Trotman-Dickenson, Pergamon, Oxford, 1973, Vol. 3, p. 1274 (palladium and platinum).
6. C.F.J. Barnard and M.J.H. Russell, in *Comprehensive Coordination Chemistry*, eds G. Wilkinson, R.D. Gillard and J.A. McCleverty, Pergamon, Oxford, 1987, Vol. 6, p. 1099 (palladium).
7. P.M. Maitlis, P. Espinet and M.J.H. Russell, in *Comprehensive Organometallic Chemistry I*, eds G. Wilkinson, F.G.A. Stone and E.W. Abel, Pergamon, Oxford, 1982, Vol. 6, p. 243; K.R. Dixon and A.C. Dixon, in *Comprehensive Organometallic Chemistry II*, eds G. Wilkinson, F.G.A. Stone and E.W. Abel, Pergamon, Oxford, 1995, Vol. 9, p. 193; A.J. Canty, in *Comprehensive Organometallic Chemistry II*, eds G. Wilkinson, F.G.A. Stone and E.W. Abel, Pergamon, Oxford, 1995, Vol. 9, p. 225 (palladium).
8. D.M. Roundhill, in *Comprehensive Coordination Chemistry*, eds G. Wilkinson, R.D. Gillard and J.A. McCleverty, Pergamon, Oxford, 1987, Vol. 6, p. 351 (platinum).
9. F.R. Hartley, in *Comprehensive Organometallic Chemistry*, eds G. Wilkinson, F.G.A. Stone and E.W. Abel, Pergamon, Oxford, 1982, Vol. 6, p. 471; R.J. Cross, in *Comprehensive Organometallic Chemistry II*, eds G. Wilkinson, F.G.A. Stone and E.W. Abel, Pergamon, Oxford, 1995, Vol. 9, p. 391; G.K. Anderson, in *Comprehensive Organometallic Chemistry II*, eds G. Wilkinson, F.G.A. Stone and E.W. Abel, Pergamon, Oxford, 1995, Vol. 9, p. 431 (platinum).
10. D.J. Gulliver and W. Levason, *Coord. Chem. Rev.*, 1982, **44**, 1 (high oxidation states).
11. W. Levason, in Ref. 2, p. 470 (high oxidation states).
12. I.E. Cottington, *Platinum Metals Rev.*, 1991, **35**, 141.
13. T.J. Lawton, *Platinum Metals Rev.*, 1989, **33**, 178; T.J. Truex, R.A. Searles and D.C. Sun, *Platinum Metals Rev.*, 1992, **36**, 2; D.L. Trimm, in Ref. 2, Ch. 3, p. 60; R.J. Farranto, R.M. Heck and B.K. Speronello, *Chem. Eng. News*, Sept 7 1992, 34.
14. F.R. Hartley, *Chemistry of the Platinum Group Metals*, Elsevier, Amsterdam, 1991, 9.
15. N. Bartlett and R. Maitland, *Acta Crystallogr.*, 1958, **11**, 747; A. Tressaud, J. Soubeyroux, H. Touhara, G. Demazeau and F. Langlais, *Material Res. Bull.*, 1981, **16**, 207; B. Bachmann and B.G. Müller, *Z. Anorg. Allgem. Chem.*, 1993, **619**, 387.
16. A.F. Wells, in *Structural Inorganic Chemistry*, 5th edn, Clarendon Press, Oxford, 1984, p. 414; H. Nyman, *J. Solid State Chem.*, 1976, **17**, 75; K. Broderson, G. Thiele and H. Gaedecke, *Z. Anorg. Allgem. Chem.*, 1966, **348**, 162; G. Thiele, K. Broderson and E. Kruse, *Naturwissenschaften*, 1967, **23**, 615.
17. A. Tressaud, M. Winterberger, N. Bartlett and P. Hagenmuller, *C. R. Acad. Sci. Sect. C*, 1976, **282**, 1069.
18. A.F. Wright, B.E.F. Fender, N. Bartlett and K. Leary, *Inorg. Chem.*, 1978, **17**, 748.
19. A.A. Timakov, V.N. Prusakov and Yu.V. Drobyshevskii, *Russ. J. Inorg. Chem.*, 1982, **27**, 1704.

20. M. Degner, B. Holle, J. Kamm, M.F. Pilbrow, G. Thiele, D. Wagner, W. Weigl and P. Woditsch, *Transition Met. Chem.*, 1974/5, **1**, 41.
21. B. Krebs, C. Brender and H. Schäfer, *Z. Anorg. Allgem. Chem.*, 1988, **561**, 119; K. Broderson, G. Thiele and H.G. Schnering, *Z. Anorg. Allgem. Chem.*, 1965, **337**, 120; G. Thiele, W. Wegl and H. Wochner, *Z. Anorg. Allgem. Chem.*, 1986, **539**, 141.
22. W. Wiese, H. Schäfer, H.G. von Schnering, C. Brendel and K. Rinke, *Angew. Chem. Int. Ed. Engl.*, 1970, **9**, 158.
23. B.G. Muller and M. Serafin, *Eur. J. Solid State Inorg. Chem.*, 1992, **29**, 625.
24. K. Broderson, G. Thiele and B. Holle, *Z. Anorg. Allgem. Chem.*, 1969, **369**, 154; M.F. Pilbrow, *J. Chem. Soc., Chem. Commun.*, 1972, 270; B.G. Müller and M. Serafin, *Eur. J. Solid State Inorg. Chem.*, 1992, **29**, 625.
25. F. Rau, U. Klement and K.-J. Range, *Z. Kristallogr.*, 1995, **210**, 605 and 606.
26. B.G. Müller and M. Serafin, *Eur. J. Solid State Inorg. Chem.*, 1992, **29**, 625; A.K. Brisdon, J.H. Holloway, E.G. Hope, W. Levason, J.S. Ogden and A.K. Saad, *J. Chem. Soc., Dalton Trans.*, 1992, 139.
27. Ref. 1, pp. 230ff; for structures see: H. Takazawa, S. Ohba and Y. Saito, *Acta Crystallogr. Sect. C*, 1988, **44**, 580; H. Takazawa, S. Ohba, Y. Saito and M. Sano, *Acta Crystallogr. Sect. C*, 1990, **46**, 166; D.A. Martin, J.L. Bonte, R.M. Rush and R.A. Jacobsen, *Acta Crystallogr. Sect. B*, 1975, **31**, 2538; R.F. Kroenig, R.M. Rush, D.S. Martin and J.C. Clardy, *Inorg. Chem.*, 1974, **13**, 1366; G. Thiele, H.W. Rotter and W. Bachle, *Z. Anorg. Allgem. Chem.*, 1989, **572**, 55; 1994, **620**, 1271. For spectra: D.M. Adams and D.J. Hills, *J. Chem. Soc., Dalton Trans.*, 1977, 947.
28. A. Tressuad, S. Khairoun, J.M. Dance and P. Hagenmuller, *Z. Anorg. Allgem. Chem.*, 1984, **517**, 43; A. Tressuad, S. Khairoun, H. Touhara and N. Watanabe, *Z. Anorg. Allgem. Chem.*, 1986, **540**, 291.
29. A.E. Schweitzer and G.T. Kerr, *Inorg. Chem.*, 1978, **17**, 2326.
30. F. Rau, U. Klement and K.-J. Range, *Z. Kristallogr.*, 1995, **210**, 684.
31. For vibrational and structural data see H. Hamaguchi, *J. Chem. Phys.*, 1978, **69**, 569; K. Leary, D.H. Templeton, A. Zalkin and N. Bartlett, *Inorg. Chem.*, 1973, **12**, 1726; J. Fawcett, J.H. Holloway, D.C. Puddick and D.R. Russell, *Acta Crystallogr. Sect. B*, 1980, **36**, 1921; H. Takazawa, S. Ohba and Y. Saito, *Acta Crystallogr. Sect. C*, 1988, **44**, 580; H. Takazawa, S. Ohba, Y. Saito and M. Sano, *Acta Crystallogr. Sect. C*, 1990, **46**, 166; R.J.H. Clark, V.B. Croud, H.M. Dawes and M.B. Hursthouse, *Polyhedron*, 1988, **7**, 2611; H.R. Grundy and I.D. Brown, *Can. J. Chem.*, 1970, **48**, 1151.
32. A.F. Wells, in *Structural Inorganic Chemistry*, 5th edn, Clarendon Press, Oxford, 1984, p. 458.
33. A.K. Brisdon, J.H. Holloway, E.G. Hope and W. Levason, *Polyhedron*, 1992, **11**, 7.
34. W. Preetz and G. Rimkus, *Z. Naturforsch. Teil B.*, 1982, **37**, 579; P. Erlhofer and W. Preetz, *Z. Naturforsch. Teil B.*, 1989, **44**, 619.
35. C. Bruhn, H.H. Drews, B. Meynhardt and W. Preetz, *Z. Anorg. Allgem. Chem.*, 1995, **621**, 373.
36. P.L. Goggin, *J. Chem. Soc., Dalton Trans.*, 1974, 1483; D.C. Harris and H.B. Gray, *Inorg. Chem.*, 1974, **13**, 2250.
37. P. Hollmann and W. Preetz, *Z. Anorg. Allgem. Chem.*, 1991, **601**, 47.
38. W. Bronger, *Angew. Chem. Int. Ed. Engl.*, 1991, **30**, 759 (review).
39. W. Bronger, G. Auffermann and P. Müller, *J. Alloys Compd.*, 1988, **142**, 243; *Z. Anorg. Allgem. Chem.*, 1988, **566**, 31; K. Kadir and D. Noreus, *Z. Phys. Chem.*, Munich, 1993, **179**, 237; W. Bronger and G. Auffermann, *J. Alloys Compd.*, 1992, **187**, 81, 87; *Angew. Chem. Int. Ed. Engl.*, 1994, **33**, 1112; *J. Alloys Compd.*, 1995, **228**, 119.
40. R.V. Kasowski, D. Norus, L. Wang and M-H. Whangbo, *Inorg. Chem.*, 1992, **31**, 4737.
41. See Refs 3(c), 5 and A.F. Wells, in *Structural Inorganic Chemistry*, 5th edn, Clarendon Press, Oxford, 1984, p. 539 (PdO); N.E. Brese, P.J. Squattrito and J.A. Ibers, *Acta Crystallogr. Sect. C*, 1985, **41**, 1829 (MS).
42. L. Helm, L.I. Elding and A.E. Merbach, *Helv. Chim. Acta*, 1984, **67**, 1453 (Pd); L.I. Elding, *Inorg. Chim. Acta*, 1976, **20**, 65 (Pt).
43. Syntheses see *Inorg. Synth.*, 1990, **28**, 113; S. Otsuka, T. Yoshida, M. Matsumoto and K. Nakatsu, *J. Am. Chem. Soc.*, 1976, **98**, 5850.

44. V.G. Andrianov, I.S. Akhrem, N.M. Chistovalova and Yu.T. Struchkov, *Zh. Strukt. Chem.*, 1976, **17**, 135; *J. Struct. Chem. USSR*, 1976, **17**, 111; C.L. Ritz and L.S. Bartell, *J. Organomet. Chem.*, 1976, **31**, 73; A. Immirzi and A. Musco, *Inorg. Chim. Acta*, 1977, **25**, L41; J.W. Ellis, K.N. Harrison, P.A.T. Hoye, A.G. Orpen, P.G. Pringle and M.B. Smith, *Inorg. Chem.*, 1992, **31**, 3026.
45. (a) T.A. Stromnova, V.S. Sergienko, A.V. Kisin, M.A. Porai-Koshits and I.I. Moiseev, *Izv. Akad. Nauk. SSSR Ser. Khim.*, 1987 (4) 894; *Bull. Acad. Sci. USSR Div. Chem. Sci.*, 1987, **36**, 821; (b) P.A. Chaloner, P.B. Hitchcock and G.T.L. Broadwood-Strong, *Acta Crystallogr. Sect. C*, 1989, **45**, 1309; (c) A. Immirzi, A. Musco and B.E. Mann, *Inorg. Chim. Acta*, 1977, **21**, L37.
46. S. Otsuka, T. Yoshida, M. Matsumoto and K. Nakatsu, *J. Am. Chem. Soc.*, 1976, **98**, 5850; M. Tanaka, *Acta Crystallogr. Sect. C*, 1992, **48**, 739; K.J. Moynihan and C. Chieh, *Acta Crystallogr. Sect. B*, 1979, **35**, 3060; A. Immirzi and A. Musco, *J. Chem. Soc. Chem. Commun.*, 1974, 400; A. Immirzi, A. Musco, P. Lambelli and G. Carturan, *Inorg. Chim. Acta*, 1975, **13**, L13; F. Paul, J. Pratt and J.F. Hartwig, *Organometallics*, 1995, **14**, 3030.
47. B.E. Mann and A. Musco, *J. Chem. Soc., Dalton Trans.*, 1975, 1673; 1980, 776.
48. G. Paccioni and P.S. Bagus, *Inorg. Chem.*, 1992, **31**, 4391; P. Fantucci, S. Polezzo, M. Sironi and A. Bencini, *J. Chem. Soc., Dalton Trans.*, 1995, 4121 (*ab initio* calculations).
49. N.J. Taylor, P.C. Chieh and A.J. Carty, *J. Chem. Soc., Chem. Commun.*, 1975, 448; R. Bender, P. Braunstein, A. Dedieu, P.D. Ellis, B. Huggins, P.D. Harvey, E. Sappa and A. Tiripiccio, *Inorg. Chem.*, 1996, **35**, 1223.
50. H. Urata, H. Suzuki, Y. Moro-oka and T. Ikawa, *J. Organomet. Chem.*, 1989, **364**, 235.
51. J.A. Davies, C.T. Eagle, D.E. Otis and U. Venkataraman, *Organometallics*, 1989, **8**, 1080; M. Hackett and G.M. Whitesides, *J. Am. Chem. Soc.*, 1988, **110**, 1449.
52. R.S. Paonella, A.L. Prignano and W.C. Trogler, *Organometallics*, 1985, **4**, 647.
53. R.U. Kirss and R. Eisenberg, *Inorg. Chem.*, 1989, **28**, 3373: K.A. Asker, P.B. Hitchcock, R.P. Moulding and K.R. Seddon, *Inorg. Chem.*, 1990, **29**, 4146.
54. S. Otsuka and T. Yoshida, *J. Am. Chem. Soc.*, 1977, **99**, 2134; J. Fornies, M. Green, J.L. Spencer and F.G.A. Stone, *J. Chem. Soc., Dalton Trans.*, 1977, 1006; T. Yoshida, T. Matsuda, T. Okano, T. Kitani and S. Otsuka, *J. Am. Chem. Soc.*, 1979, **101**, 2027; P. Leoni, M. Sommovigo, M. Pasquali, S. Midollini, D. Braga and P. Sabatino, *Organometallics*, 1991, **10**, 1038.
55. W.M. Riggs, *Anal. Chem.*, 1972, **44**, 830; C.D. Cook, K.Y. Wan, V. Gelius, K. Hamrin, G. Johansson, E. Olsson, H. Siegbahn, C. Nordling and K. Siegbahn, *J. Am. Chem. Soc.*, 1971, **93**, 1904; D.T. Clark, D.B. Adama and D. Brigge, *Chem. Commun.*, 1971, 602.
56. For a review, see J.D. Atwood, in *Inorganic and Organometallic Reaction Mechanisms*, Brooks/Cole, 1985, p. 128; for other references, see Refs 7 and 9.
57. D. Bell'Amico, F. Calderazzo, C.A. Veracini and N. Zandona, *Inorg. Chem.*, 1984, **23**, 3030; F. Calderazzo, *J. Organomet. Chem.*, 1990, **400**, 303; and Ref. 8, p. 475.
58. J.H. Darling and J.S. Ogden, *J. Chem. Soc., Dalton Trans.*, 1973, 1079; E. Kundig, D. McIntosh, M. Moskovits and G.A. Ozin, *J. Am. Chem. Soc.*, 1973, **95**, 7234.
59. B.K. Teo, F.J. DiSalvo, J.V. Waszczak, G. Longoni and A. Ceriotti, *Inorg. Chem.*, 1986, **25**, 2262.
60. C.G. Francis, S.I. Khan and P.R. Morton, *Inorg. Chem.*, 1984, **23**, 3680; C. Aristides, *J. Organometallic. Chem.*, 1983, **259**, 355; Y. Yamamoto, K. Takahashi, K. Matsuda and H. Yamazaki, *J. Chem. Soc., Dalton Trans.*, 1987, 1833.
61. M.P. Brown, R.J. Puddephatt, M. Rashidi, L. Manojlovic-Muir, K.W. Muir, T. Solomun and K.R. Seddon, *Inorg. Chim. Acta*, 1977, **23**, L33; P.H.M. Budzelaar, P.W.N.M. van Leeuwen, C.F. Roobeek and A.G. Orpen, *Organometallics*, 1992, **11**, 23; J.R. Boehm and A.L. Balch, *Inorg. Chem.*, 1977, **16**, 778; J.R. Boehm, D.J. Doonan and A.L. Balch, *J. Am. Chem. Soc.*, 1976, **98**, 4845.
62. D.J. Schwarz and R.A. Andersen, *J. Am. Chem. Soc.*, 1995, **117**, 4014.
63. S. Okeya, Y. Nakamura and S. Kawaguchi, *Bull. Chem. Soc. Japan*, 1982, **55**, 1460 and refs therein.
64. A.C. Skapski and M.L. Smart, *Chem. Commun.*, 1970, 658; M.A.A.F. de C. Carrondo and A.C. Skapski, *J. Chem. Soc. Chem. Commun.*, 1976, 410: *Acta Crystallogr. Sect. B*. 1978, **34**, 1857.

65. T.A. Stephenson, S.M. Morehouse, A.R. Powell, J.P. Heffer and G. Wilkinson, *J. Chem. Soc.*, 1965, 3632.
66. Y. Fujiwara, T. Jintoku and K. Takaki, *Chem Tech.*, 1990, 636.
67. (a) D.W. James and M.L. Nolan, *J. Raman Spectr.*, 1973, **1**, 259; (b) *Inorg. Synth*, 1983, **22**, 124; 1963, **7**, 240.
68. J.S. Coe and J.R. Lyons, *Inorg. Chem.*, 1970, **9**, 1775.
69. P. Khodadad and N. Rodier, *Acta Crystallogr. Sect. C*, 1989, **45**, 208.
70. Y.P. Jeannin and D.R. Russell, *Inorg. Chem.*, 1970, **9**, 778.
71. B. Lippert, C.J.L. Lock, B. Rosenberg and M. Zvagulis, *Inorg. Chem.*, 1977, **16**, 1525; R. Faggiani, B. Lippert, C.J.L. Lock and B. Rosenberg, *J. Am. Chem. Soc.*, 1977, **99**, 777.
72. J. Arpalahti, R. Sillanpää and M. Mikola, *J. Chem. Soc., Dalton Trans.*, 1994, 1499; J. Arpalahti, R. Sillanpää, K.J. Barnham and P.J. Sadler, *Acta Chem. Scand.*, 1996, **50**, 181.
73. N.S. Kurnakov, *J. Prakt. Chem.*, 1894, **50**, 481.
74. T.G. Appleton, A.J. Bailey, K.J. Barnham and J.R. Hall, *Inorg. Chem.*, 1992, **31**, 3077.
75. C.P. Hicks and M. Spiro, *J. Chem. Soc., Chem. Commun.*, 1981, 131.
76. G.H.W. Milburn and M.R. Truter, *J. Chem. Soc. (A)*, 1966, 1609.
77. F. Basolo, M. Lederer, L. Ossicini and K.H. Stephan, *J. Chromatogr.*, 1963, **10**, 262.
78. J. Hiraishi, I. Nakagawa and T. Shimanouchi, *Spectrochim. Acta*, 1968, **24A**, 821; M.J. Almond, C.A. Yates, R.H. Orrin and D.A. Rice, *Spectrochim. Acta*, 1990, **46A**, 177; A. Degen and A.J. Rowlands, *Spectrochim. Acta*, 1991, **47A**, 1263. Spectra for the palladium analogues are given in R. Layton, D.W. Sink and J.R. Durig, *J. Inorg. Nucl. Chem.*, 1966, **28**, 1965.
79. H.R. Patterson, J.C. Tewksbury, M. Martin, M-B. Krogh-Jespersen, J.A. LoMenzo, H.O. Hooper and A.K. Viswanath, *Inorg. Chem.*, 1981, **20**, 2297.
80. M.E. Cradwick, D. Hall and R.K. Phillips, *Acta Crystallogr. Sect B*, 1971, **27**, 480; A.F. Wells, in *Structural Inorganic Chemistry*, 5th edn, Clarendon Press, Oxford, 1984, p. 1238; M. Atoji, J.W. Richardson and R.E. Rundle, *J. Am. Chem. Soc.*, 1957, **79**, 3017; J.R. Miller, *Proc. Chem. Soc.*, 1960, 318.
81. P. Colamarino and P.L. Orioli, *J. Chem. Soc., Dalton Trans.*, 1975, 1656; *Inorg. Synth.*, 1963, **7**, 249; B. Viossat, N.H. Dung and F. Robert, *Acta Crystallogr. Sect C*, 1993, **49**, 84 (structures).
82. T.B.T. Ha, P. Castan, J.-P. Souchard and F.L. Wimmer, *J. Chem. Res. (S)*, 1992, 112.
83. T.B.T. Ha, J.-P. Souchard, F.L. Wimmer and N.P. Johnson, *Polyhedron*, 1990, **9**, 2647.
84. V.Yu. Kukushin and V.M. Tkachuk, *Z. Anorg. Allgem. Chem.*, 1992, **613**, 213.
85. J.R. Wiesner and E.C. Lingafelter, *Inorg. Chem.*, 1966, **5**, 1770; J. Iball, M. Macdougall and S. Scrimgeour, *Acta Crystallogr. Sect. B*, 1975, **31**, 1672; W.A. Freeman, *Inorg. Chem.*, 1976, **15**, 2235; M. Geoffroy, G. Bernardinelli, P. Castan, H. Chermette, D. Deguenon, S. Nour, J. Weber and M. Wermeille, *Inorg. Chem.*, 1992, **31**, 5056; P. Castan, D. Deguenon, P.L. Fabre and G. Bernardinelli, *Polyhedron*, 1992, **8**, 901; L.T. Ellis and T.W. Hambley, *Acta Crystallogr. Sect. C*, 1994, **50**, 1888.
86. For phen and bipy complexes see P.C. Chieh, *J. Chem. Soc., Dalton Trans.*, 1972, 1643; A. Hazell and M. Mukhopadhyay, *Acta Crystallogr. Sect. B*, 1980, **36**, 1647; A. Hazell, O. Simonon and O. Wernberg, *Acta Crystallogr. Sect. C*, 1986, **42**, 1707; S. Geremia, L. Randaccio, G. Mestroni and B. Milani, *J. Chem. Soc., Dalton Trans.*, 1992, 2117 and references therein.
87. R.J.H. Clark, F.P. Fanizzi, G. Natile, C. Paciifico, C.G. van Rooyen and D.A. Tocher, *Inorg. Chim. Acta*, 1995, **235**, 205.
88. R.S. Osborn and D. Rogers, *J. Chem. Soc., Dalton Trans.*, 1974, 1002; M. Weiser-Wallfahrer and G. Gliemann, *Z. Naturforsch. Teil B*, 1990, **45**, 652; A.J. Canty, B.W. Skelton, P.R. Traill and A.H. White, *Aust. J. Chem.*, 1992, **45**, 417; R.H. Herber, M. Croft, M.J. Coyer, B. Bilash and A. Sahiner, *Inorg. Chem.*, 1994, **33**, 2422; see also W.B. Connick and H.B. Gray, *Acta Crystallogr. Sect. C*, 1994, **50**, 1040 (iodide); C.-H. Che, L.-Y. He, C.-K. Poon and T.C.W. Mak, *Inorg. Chem.*, 1989, **28**, 3081 (cyanide); M.J. Coyer, R.H. Herber and S. Cohen, *Inorg. Chim. Acta*, 1990, **175**, 47 (cyanate).
89. W.H. Baddley and F. Basolo, *J. Am. Chem. Soc.*, 1964, **86**, 2075; 1966, **88**, 2944; J.B. Goddard and F. Basolo, *Inorg. Chem.*, 1968, **7**, 936.

90. R.J. Mureinik and M. Bidani, *Inorg. Chim. Acta*, 1978, **29**, 37; J.A. Bailey, M.G. Hill, R.E. Marsh, V.M. Miskowski, W.P. Schaefer and H.B. Gray, *Inorg. Chem.*, 1995, **34**, 4591.
91. G.W. Bushnell, K.R. Dixon and M.A. Khan, *Can. J. Chem.*, 1974, **52**, 1367; see also F.P. Fanizzi, M. Lanfranchi, G. Natile and A. Tiripicchio, *Inorg. Chem.*, 1994, **33**, 3331.
92. A.M. Stolzenberg and L.J. Schussel, *Inorg. Chem.*, 1991, **30**, 3205; A.M. Stolzenberg, L.J. Schussel, J.S. Summers, B.M. Foxman and J.L. Petersen, *Inorg. Chem.*, 1992, **31**, 1681.
93. S. Brawner and K.B. Mentner, *J. Inorg. Nucl. Chem.*, 1979, **41**, 764; D. Waknine, M.J. Heeg, J.F. Endicott and L.A. Ochrymowycz, *Inorg. Chem.*, 1991, **30**, 3691.
94. J.K. Barton, H.N. Rabinowitz, D.J. Szalda and S.J. Lippard, *J. Am. Chem. Soc.*, 1977, **99**, 2827; J.K. Barton, S.A. Best, S.J. Lippard and R.A. Walton, *J. Am. Chem. Soc.*, 1978, **100**, 3785; J.K. Barton, D.J. Szalda, H.N. Rabinowitz, T.W. Waszczak and S.J. Lippard, *J. Am. Chem. Soc.*, 1979, **101**, 1435; J.K. Barton, C. Caravana and S.J. Lippard, *J. Am. Chem. Soc.*, 1979, **101**, 7269; P. Arrizabalaga, P. Castan, M. Geoffroy and J.-P. Laurent, *Inorg. Chem.*, 1985, **24**, 3657; K. Matsumoto, K. Sakai, K. Nishio, Y. Tokisue, R. Ito, T. Nishida and Y. Shichi, *J. Am. Chem. Soc.*, 1992, **114**, 8110; K. Matsunami, H. Urata and K. Matsumoto, *Inorg. Chem.*, 1995, **34**, 202.
95. Ref. 1, pp. 456–461; T.W. Lee and R.C. Stoufer, *J. Am. Chem. Soc.*, 1975, **97**, 195; *Inorg. Synth.*, 1963, **7**, 245; 1970, **12**, 27; 1979, **19**, 114.
96. W.J. Louw, D.J.A. DeWaal and G.J. Kruger, *J. Chem. Soc., Dalton Trans.*, 1976, 2365.
97. J. Chatt and F.A. Hart, *J. Chem. Soc.*, 1960, 2807; D.L. Sales, J. Stokes and P. Woodward, *J. Chem. Soc. (A)*, 1968, 1852; J. Chatt and L.M. Venanzi, *J. Chem. Soc.*, 1955, 2787; 1957, 2351; L.M. Venanzi and R.J. Goodfellow, *J. Chem. Soc.*, 1965, 7533.
98. See Ref. 2, p. 378 for a review.
99. M.L. Schneider and H.M.M. Shearer, *J. Chem. Soc., Dalton Trans.*, 1973, 354.
100. J. Chatt, L.A. Duncanson and L.M. Venanzi, *Proc. Chem. Soc.*, 1957, 343; J. Chatt and B.L. Shaw, *J. Chem. Soc.*, 1962, 5075; J. Chatt, *Proc. Chem. Soc.*, 1962, 321.
101. (a) D.L. Packett, C.M. Jensen, R.L. Cowan, C.E. Strouse and W.C. Trogler, *Inorg. Chem.*, 1978, **24**, 3578; B.L. Shaw and M.F. Uttley, *J. Chem. Soc., Chem. Commun.*, 1974, 918; A. Immirzi, A. Musco, G. Carturan and U. Belluco, *Inorg. Chim. Acta*, 1975, **12**, L23: P.G. Leviston and M.G.H. Wallbridge, *J. Organomet. Chem.*, 1976, **110**, 271; A. Immirzi and A. Musco, *Inorg. Chim. Acta*, 1976, **22**, L35; (b) D.G. Gusev, J.U. Notheis, J.R. Rambo, B.E. Hauger, O. Eisenstein and K.G. Caulton, *J. Am. Chem. Soc.*, 1994, **116**, 7408.
102. W.L. Steffen and G.J. Palenik, *Inorg. Chem.*, 1977, **15**, 2432; C.E. Housecroft, B.A.M. Shaykh, A.L. Rheingold and B.S. Haggarty, *Inorg. Chem.*, 1991, **30**, 125; W.E. Hill, D.M.A. Minahan, J.G. Taylor and C.A. McAuliffe, *J. Am. Chem. Soc.*, 1982, **104**, 6001.
103. F. Bachechi and L. Zambonelli, *Acta Crystallogr. Sect. C*, 1992, **48**, 788.
104. A.J. Cheney, B.E. Mann, B.L. Shaw and R.M. Slade, *Chem. Commun.*, 1970, 1176; *J. Chem. Soc. (A)*, 1971, 1833; E.W. Ainscough and S.D. Robinson, *Chem. Commun.*, 1971, 130; J.R. Briggs, A.G. Constable, W.S. McDonald and B.L. Shaw, *J. Chem. Soc., Dalton Trans.*, 1982 1225; J.A. Ibers, R. DiCosimo and G.M. Whitesides, *Organometallics*, 1982, **1**, 13; R.G. Goel and W.O. Ogini, *Organometallics*, 1982, **1**, 654; A.R.H. Bottomley, C. Crocker and B.L. Shaw, *J. Organomet. Chem.*, 1983, **250**, 617; P. Foley, R. Di Cosimo and G.M. Whitesides, *J. Am. Chem. Soc.*, 1980, **102**, 6713.
105. J. Chatt and B.L. Shaw, *J. Chem. Soc.*, 1959, 705; F. Glockling, T. McBride and R.J.I. Pollock, *Inorg. Chim. Acta*, 1971, **8**, 71; M.A. Bennett, H.-K. Chee and G.B. Robertson, *Inorg. Chem.*, 1979, **18**, 1061; B. Jovanovic, L. Manojlvic-Muir and K.W. Muir, *J. Chem. Soc., Dalton Trans.*, 1974, 195; G.W. Rice and R.S. Tobias, *J. Am. Chem. Soc.*, 1977, **99**, 2141; R. Usón, J. Forniés, M. Tomás, B. Menjon, K. Sünkel and R. Bau, *J. Chem. Soc., Chem. Commun.*, 1984, 751.
106. (a) J.M. Wisner, T.J. Bartizak and J.A. Ibers, *Organometallics*, 1986, **5**, 2044. For a selection of structures see: A.N. Caldwell, L. Manojlvic-Muir and K.W. Muir, *J. Chem. Soc., Dalton Trans.*, 1977, 2265; A. Del Pra and G. Zanotti, *Cryst. Struct. Commun.*, 1979, **8**, 737; R. Bardi, A.M. Piazzessi, R. Ros and P. Cavoli, *Cryst. Struct. Commun.*, 1981, **10**, 855; R. Bardi, A.M. Pianessi and G. Bruno, *Cryst. Struct. Commun.*, 1981, **10**, 807; M.A. Bennett, H.-K. Chee and G.B. Robertson, *Inorg. Chem.*, 1979, **18**, 1061; B. Jovanovic, L. Manojlovic-Muir and K.W. Muir, *J. Chem. Soc., Dalton Trans.*, 1974, 195; J. Ertl, T. Debaerdemaeker and H.A. Brune, *Chem. Ber.*, 1982, **115**, 3860;

J.M. Wisner, T.J. Bartizak and J. A. Ibers, *Organometallics*, 1986, **5**, 2044; J.A. Ibers, R. DiCosimo and G.M. Whitesides, *Organometallics*, 1982, **1**, 13; (b) E.W. Abel, K.G. Orrell, A.G. Osborne, H.M. Pain, V. Sik, M.B. Hursthouse and K.M.A. Malik, *J. Chem. Soc., Dalton Trans.*, 1994, 3441.

107. Ref. 9; Ref. 2, pp. 303, 366; Ref. 56, p. 182; A. Gillie and J.K. Stille, *J. Am. Chem. Soc.*, 1980, **102**, 4933; R.H. Crabtree, in *The Organometallic Chemistry of the Transition Metals*, 2nd edn, John Wiley, New York, 1994, p. 151.
108. (a) P.A. Foley and G.M. Whitesides, *J. Am. Chem. Soc.*, 1979, **101**, 2732; B.C. Ankianec, D.T. Hardy, S.K. Thompson, W.N. Watkins and G.B. Young, *Organometallics*, 1992, **11**, 2591; (b) Z. Yuan, D. Jiang, S.J. Naftel, T.K. Sham and R.J. Puddephatt, *Chem. Mat.*, 1994, **6**, 2151.
109. Ref. 9, p. 505; D.J. Cardin, B. Cetinkaya, E. Cetinkaya, M.F. Lappert, L. Manojlovic-Muir and K.W. Muir, *J. Organomet. Chem.*, 1972, **44**, C 59.
110. (a) W.C. Zeise, *Mag. Pharm.*, 1830, **35**, 105; (b) R.A. Love, T.F. Koetzle, G.J.B. Williams, L.C. Andrews and R. Bau, *Inorg. Chem.*, 1975, **14**, 2653; Ref. 9, pp. 614, 633.
111. J.S. Miller and A.J. Epstein, *Progr. Inorg. Chem.*, 1976, **20**, 43; A.E. Underhill in Ref. 6., p. 133; G. Gliemann and H. Yersin, *Structure and Bonding*, 1985, **62**, 87; G.J. Kubas and L.H. Jones, *Inorg. Chem.*, 1974, **13**, 2816.
112. R.J.H. Clark, *Chem. Soc. Rev.*, 1990, **19**, 107; P. Day and M.B. Robin, *Adv. Inorg. Chem.*, 1967, **10**, 247; J.S. Miller and A.J. Epstein, *Progr. Inorg. Chem.*, 1976, **20**, 90.
113. R.J.H. Clark, M. Kurmoo, H.J. Keller, B. Kepler and E. Traeger, *J. Chem. Soc., Dalton Trans.*, 1980, 2498.
114. E.J.W. Austin, P.J. Barrie and R.J.H. Clark, *Inorg. Chem.*, 1992, **31**, 4281; 1995, **34**, 3859.
115. N.R. Kunchur, *Acta Crystallogr. Sect. B*, 1968, **24**, 1623; 1971, **27**, 2292.
116. I. Nakanishi, K. Matsumoto and S. Ooi, *Acta Crystallogr. Sect. C*, 1991, **47**, 2073.
117. P.E. Skakke and S.E. Rasmussen, *Acta Chem. Scand.*, 1970, **24**, 2634; E.A. Allen, N.P. Johnson, D.T. Rosevear and W. Wilkinson, *Chem. Commun.*, 1971, 171.
118. A. Oskarsson, B. Noren, C. Svensson and L.I. Elding, *Acta Crystallogr. Sect. C*, 1990, **46**, 748.
119. Z. Bugarcic, K. Lövquist and A. Oskarsson, *Acta Chem. Scand.*, 1993, **47**, 554.
120. Z. Bugarcic, B. Norén, A. Oskarsson, C. Stålhandske and L.I. Elding, *Acta Chem. Scand.*, 1991, **45**, 361.
121. P.T. Beurskens, J.A. Cras, T.W. Hummelink and J.H. Noordik, *J. Cryst. Mol. Str.*, 1971, **1**, 253; A.Z. Amanov, G.A. Kukina and M.A. Porai-Koshits, *Dokl. Akad. Nauk. Az. SSR*, 1977, **33**, 24 (*Chem. Abs.*, 1977, **87**, 209741); L.T. Chan, H.-W. Chen, J.P. Fackler, A.F. Masters and W.-H. Pan, *Inorg. Chem.*, 1982, **21**, 4291; for a selenium analogue, see W.-H. Pan, J.P. Fackler and H.-W. Chen, *Inorg. Chem.*, 1981, **20**, 856.
122. G. Marangoni, B.P. Heri, V. Bertolas and P. Gilli, *Inorg. Chim. Acta*, 1995, **234**, 173.
123. G.J. Grant, K.A. Saunders, W.N. Setzer and D.G. VanDerveer, *Inorg. Chem.*, 1991, **30**, 4054; A.J. Blake and M. Schroder, *Adv. Inorg. Chem.*, 1990, **35**, 1; G. Reid and M. Schroder, *Chem. Soc. Rev.*, 1990, **19**, 239.
124. J.H. Price, J.P. Birk and B.B. Wayland, *Inorg. Chem.*, 1978, **17**, 2245; B.F.G. Johnson, J. Puga and P.R. Raithby, *Acta Crystallogr. Sect. B*, 1981, **37**, 953; L.I. Elding and A. Oskarsson, *Inorg. Chim. Acta*, 1987, **130**, 209; V.K. Belsky, V.E. Konovalov, V.Yu. Kukushkin and A.I. Moiseev, *Inorg. Chim. Acta*, 1990, **169**, 101; S.G. Almeida, J.L. Hubbard and N. Farrell, *Inorg. Chim. Acta*, 1992, **193**, 149; R. Melson and F.D. Rochon, *Acta Crystallogr. Sect. B*, 1977, **33**, 3571; 1978, **34**, 1125 and references therein.
125. W. Levason and C.A. McAuliffe, *Inorg. Chim. Acta*, 1976, **16**, 167; J.L. Burmeister and F. Basolo, *Inorg. Chem.*, 1964, **3**, 1587.
126. C.P. Brock, J.L. Huckaby and T.G. Attig, *Acta Crystallogr. Sect. B*, 1984, **40**, 595.
127. G.J. Palenik, M. Mathew, W.L. Steffen and G. Beran, *J. Am. Chem. Soc.*, 1975, **97**, 1058.
128. A.J. Paviglianiti, D.J. Minn, W.C. Fultz and J.L. Burmeister, *Inorg. Chim. Acta*, 1989, **159**, 65.
129. M.J. Coyer, M. Croft, J. Chen and R.H. Herber, *Inorg. Chem.*, 1992, **31**, 1752.
130. Yu.N. Kukushkin, *Platinum Metals Rev.*, 1991, **35**, 28.
131. (a) M. Fushimi, M. Suzuki and A. Uehara, *Bull. Chem. Soc. Jap.*, 1988, **61**, 1809; (b) P. Svensson, K. Lövquist, V.Yu. Kukushkin and A. Oskarsson, *Acta Chem. Scand.*, 1995, **49**, 72. See also E.A. Allen, N.P. Johnson, D.T. Rosevear and W. Wilkinson, *Chem. Commun.*, 1971, 171.

132. J.H. Nelson and N.W. Alcock, *Inorg. Chem.*, 1982, **21**, 1196; for structure see A. Albinati, P.S. Pregosin and H. Rüegger, *Inorg. Chem.*, 1984, **23**, 3223.
133. K.H.J.O. Staezewski, P.S. Pregosin and H. Rüegger, *Helv. Chim. Acta*, 1982, **65**, 785; A. Albinati, R. Nageli, P.S. Pregosin and H. Rüegger, *Angew. Chem. Int. Ed. Engl.*, 1982, **21**, 285.
134. J.H. Nelson, W.L. Wilson, L.W. Cary, N.W. Alcock, H.J. Clase, G.S. Jas, L. Ramsay-Tassin, and J.W. Kenney, *Inorg. Chem.*, 1996, **35**, 883.
135. Ref. 8, p. 445; P. Meakin and J.P. Jesson, *J. Am. Chem. Soc.*, 1974, **96**, 5751; *Inorg. Synth.*, 1980, **20**, 78.
136. K.M. Chui and H.M. Powell, *J. Chem. Soc., Dalton Trans.*, 1974, 1879, 2117.
137. (a) N.A. Bailey, J.M. Jenkins, R. Mason and B.L. Shaw, *Chem. Commun.*, 1965, 237; (b) K.R. Dunbar and J.S. Sun, *J. Chem. Soc., Chem. Commun.*, 1994, 2387.
138. F.P. Fanizzi, L. Marescia, G. Natile, M. Lanfranchi, A. Tiripicchio and G. Pacchioni, *J. Chem. Soc., Chem. Commun.*, 1992, 333; V.G. Albano, C. Castellari, V. DeFelice, A. Panunzi and F. Ruffo, *J. Organomet. Chem.*, 1992, **425**, 173; L. Maresca and G. Natile, *Comments Inorg. Chem.*, 1993, **14**, 349.
139. (a) M.L. Tobe, in *Inorganic Reaction Mechanisms*, Nelson, New York, 1972; (b) G.B. Kauffman, *J. Chem. Educ.*, 1977, **54**, 86; (c) Ref. 53, p. 52; (d) L. Cattalini, in *Reaction Mechanisms in Inorganic Chemistry*, MTP International Review of Science: *Inorganic Chemistry Series One*, Vol. 9, ed. M.L. Tobe, Butterworths, London, 1972, p. 269; (e) R.G. Wilkins, in *Kinetics and Mechanism of Reactions of Transition Metal Complexes*, Verlag Chemie, Stuttgart, 2nd edn, 1991, p. 237. The original reference is I.I. Chernyaev, *Ann. Inst. Platine USSR*, 1926, **4**, 261.
140. F. Basolo and R.G. Pearson, in *Mechanisms of Inorganic Reactions*, 2nd edn, John Wiley, New York, 1967, p. 356.
141. F. Basolo, J. Chatt, H.B. Gray, R.G. Pearson and B.L. Shaw, *J. Chem. Soc.*, 1961, 2207.
142. See Ref. 139(a) p. 65; and Ref. 139(c) p. 57.
143. (a) F.R. Hartley, *Chem. Soc. Rev.*, 1973, **2**, 163; (b) F. Basolo and R.C. Johnson, in *Coordination Chemistry*, 2nd edn, *Science Reviews*, 1986, p. 74.
144. Ref. 143(a), p. 16, 167; Ref. 140, p. 354.
145. A.D. Gel'man, E.F. Karandashova and L.N. Essen, *Dokl. Akad. Nauk. SSSR*, 1948, **63**, 37; Ref. 1, p. 299.
146. F. Basolo and R.G. Pearson, in *Mechanisms of Inorganic Reactions*, 2nd edn, John Wiley, New York, 1968, p. 354; Ref. 144.
147. V.Yu. Kukushkin, I.A. Krol, Z.A. Starikova and V.M. Tkachuk, *Koord. Khim.*, 1990, **16**, 1406; *Soviet J. Coord. Chem.*, 1990, **16**, 746.
148. D.R. Russell, M.A. Mazid and P.A. Tucker, *J. Chem. Soc., Dalton Trans.*, 1980, 1737.
149. G.B. Robertson, P.A. Tucker and W.A. Wickramsinghe, *Aust. J. Chem.*, 1986, **39**, 1495.
150. (a) *trans*-PtMeCl(PEt$_3$)$_2$ R. Bardi, A.M. Pianessi and G. Bruno, *Cryst. Struct. Commun.*, 1981, **10**, 807; *trans*-PtMeCl(PMePh$_2$)$_2$ M.A. Bennett, H.-K. Chee and G.B. Robertson, *Inorg. Chem.*, 1979, **18**, 1061; *trans*-PtClH(PEtPh$_2$)$_2$ R. Eisenberg and J.A. Ibers, *Inorg. Chem.*, 1965, **4**, 773; *cis*-PtEtCl(PEt$_3$)$_2$ R. Bardi, A. Del Pra, A.M. Pianessi, D. Minniti and R. Romeo, *Cryst. Struct. Commun.*, 1981, **10**, 333; *trans*-Pt(CH$_2$SiMe$_3$)Cl(PMe$_2$Ph)$_2$ B. Jovanovic, L. Manojlovic-Muir and K.W. Muir, *J. Chem. Soc., Dalton Trans.*, 1974, 195; *trans*-PtI$_2$(PMe$_3$)$_2$. P.B. Hitchcock, B. Jacobson and A. Pidcock, *J. Chem. Soc., Dalton Trans.*, 1977, 2038; *trans*-PtPh$_2$(PPh$_3$)$_2$ J. Ertl, T. Debaerdemaeker and H.A. Brune, *Chem. Ber.*, 1982, **115**, 3860; *trans*-PtBr$_2$(PEt$_3$)$_2$ G.G. Messmer and E.L. Amma, *Inorg. Chem.*, 1966, **5**, 1775; *cis*-PtMe$_2$(PMePh$_2$)$_2$ J.M. Wisner, T.J. Bartizak and J.A. Ibers, *Organometallics*, 1986, **5**, 2044; *cis*-Pt(neopentyl)$_2$(PEt$_3$)$_2$ J.A. Ibers, R. DiCosimo and G.M. Whitesides, *Organometallics*, 1982, **1**, 13; for four *o*-tolyl complexes, see A.L. Rieger, G.B. Carpenter and P.H. Rieger, *Organometallics*, 1993, **12**, 842 and references therein; (b) *cis*-Pt(PR$_3$)(PR$'_3$)Cl$_2$ P.B. Hitchcock, B. Jacobson and A. Pidcock, *J. Chem. Soc., Dalton Trans.*, 1977, 2043; A.N. Caldwell, L. Manojlovic-Muir and K.W. Muir, *J. Chem. Soc., Dalton Trans.*, 1977, 2265.
151. T.S. Cameron, H.C. Clark, A. Linden and A.M. Nicholas, *Polyhedron*, 1990, **9**, 1083 and references therein.
152. H.C. Clark and J.D. Ruddick, *Inorg. Chem.*, 1970, **9**, 1226.
153. T.G. Appleton, J.R. Hall and S.F. Ralph, *Inorg. Chem.*, 1985, **24**, 4685; 1992, **31**, 3077.

154. T. Miyamoto, *J. Organomet. Chem.*, 1979, **134**, 375.
155. A. Pidcock, R.E. Richards and L.M. Venenzi, *J. Chem. Soc. (A)*, 1966, 1707.
156. P.S. Pregosin, H. Omura and L.M. Venanzi, *J. Am. Chem. Soc.*, 1973, **95**, 2047.
157. A.J. Blake, A.J. Holder, T.I. Hyde, Y.V. Roberts, A.V. Lavery and M. Schroder, *J. Organomet. Chem.*, 1987, **323**, 461; A.J. Blake, T.I. Hyde and M. Schroder, *J. Chem. Soc., Chem. Commun.*, 1987, 987; A.J. Blake, L.M. Gordon, A.J. Holder, T.I. Hyde, G. Reid and M. Schroder, *J. Chem. Soc., Chem. Commun.*, 1988, 1453; A.J. Blake, G. Reid and M. Schroder, *J. Chem. Soc., Dalton Trans.*, 1990, 3363; P.J. Alonso, R. Alcala, R. Usón and J. Fornies, *J. Phys. Chem. Solids*, 1991, **52**, 975.
158. F.A. Cotton and R.A. Walton, *Struct. Bonding*, 1985, **62**, 33 and references therein; T.G. Appleton, K.J. Barnham, K.A. Byriel, J.R. Hall, C.H.L. Kennard, M.T. Maathieson and K.G. Penman, *Inorg. Chem.*, 1995, **34**, 6040.
159. B.R. Steele and K.R. Vrieze, *Transition Met. Chem.*, 1977, **2**, 169 and references therein; see also R. Usón, J. Forniés. L.R. Favello, M. Tomás, J.M. Casas, A. Martín and F.A. Cotton, *J. Am. Chem. Soc.*, 1994, **116**, 7160.
160. R. Cini, F.P. Fanizzi, F. Pintini and G. Natile, *J. Am. Chem. Soc.*, 1991, **113**, 7805.
161. V.I. Korsunsky, G.P. Muraveiskaya and A.A. Sidorov, *Inorg. Chim. Acta*, 1991, **187**, 23.
162. All syntheses are in Ref. 67(a); see also *Inorg. Synth.*, 1974, **15**, 93; 1986, **24**, 277.
163. L. Baldé, P. Khodadad and N. Rodier, *Acta Crystallogr. Sect. C*, 1989, **45**, 859; P. Khodadad and N. Rodier, *Acta Crystallogr. Sect. C*, 1992, **48**, 743.
164. L. Baldé, P. Khodadad, N. Rodier and R. Julien, *Acta Crystallogr. Sect. C*, 1993, **49**, 2064.
165. W.P. Shao, L.J. Jiang, C.D. Li, Z.Y. Min and W.X. Tang, *Chinese J. Chem.*, 1993, **9**, 187.
166. (a) V.Yu. Kukushkin, I.G. Zenkevich, V.K. Belsky, V.E. Konovalov, A.I. Moiseev and E.O. Sidorov, *Inorg. Chim. Acta*, 1989, **166**, 79; (b) see Refs 67(b) and 165.
167. I.P. Evans, G.W. Everett and A.M. Sargeson, *J. Am. Chem. Soc.*, 1976, **98**, 8041; S.A. Brawner, I.J.B. Lin, J.-H. Kim and G.W. Everett, *Inorg. Chem.*, 1978, **17**, 1304.
168. R. Faggiani, H.E. Howard-Lock, C.J.L. Lock, B. Lippert and B. Rosenberg, *Can. J. Chem.*, 1982, **60**, 529; C.F.J. Barnard, P.C. Hydes, W.P. Griffith and O.S. Mills, *J. Chem. Res. (S)*, 1983, 302; J.F. Vollano, E.E. Blatter and J.C. Dabrowiak, *J. Am. Chem. Soc.*, 1984, **106**, 2732; R. Kuroda, S. Neidle, T.M. Ismail and P.J. Sadler, *Inorg. Chem.*, 1983, **22**, 3620.
169. P. Khodadad and N. Rodier, *Acta Crystallogr. Sect. B*, 1988, **44**, 2021.
170. C.F. Lin and J.A. Ibers, *Inorg. Chem.*, 1970, **9**, 773; R.G. Hazell, H. Toftlund, P.R. Andersen, P. Bisgard, K. Edlund, M. Eliasen, C. Herskind, T. Laursen and P.M. Pedersen, *Acta Chem. Scand. A.*, 1975, **29**, 499; H.J. Kellerand, U. Traeger, *Acta Crystallogr. Sect. B.*, 1979, **35**, 1887; B. Freckmann and K-F. Tebbe, *Acta Crystallogr. Sect. B*, 1981, **37**, 1520.
171. (a) J.L. van der Veer, W. Hinrichs and J. Reedijk, *Acta Crystallogr. Sect. C*, 1986, **42**, 534; (b) A.R. Khokhar, S. Shamsuddin and Q. Xu, *Inorg. Chim. Acta*, 1994, **219**, 193; (c) R.J. Schilder, F.P. La Creta and R.P. Perez, *Cancer Res.*, 1994, **54**, 709.
172. K.H. Buse, H.J. Keller and H. Pritzkow, *Inorg. Chem.*, 1977, **16**, 1072.
173. J.W. Buchler, K.-L. Lay and H. Stoppa, *Z. Naturforsch. Teil B*, 1980, **35**, 433; D. Waknine, M.J. Heeg, J.F. Endicott and L.A. Ochrymowycz, *Inorg. Chem.*, 1991, **30**, 3691.
174. J. Chatt, *J. Chem. Soc.*, 1950, 2301; Ref. 1, p. 260.
175. S. Al-Jibori, C. Crocker, W.S. McDonald and B.L. Shaw, *J. Chem. Soc., Dalton Trans.*, 1981, 2589.
176. P.B. Hitchcock, B. Jacobsen and A. Pidcock, *J. Organomet. Chem.*, 1977, **136**, 397; L. Aslanov, R. Mason, A.G. Wheeler and P.O. Whimp, *Chem. Commun.*, 1970, 30.
177. D.M. Adams and P.J. Chandler, *J. Chem. Soc. A.*, 1967, 1010.
178. D.W.W. Anderson, E.A.V. Ebsworth and D.W.H. Rankin, *J. Chem. Soc., Dalton Trans.*, 1973, 854, 2371.
179. L.R. Gray, D.J. Gulliver, W. Levason and M. Webster, *J. Chem. Soc., Dalton Trans.*, 1983, 133; L.R. Hanton, W. Levason and N.A. Powell, *Inorg. Chim. Acta*, 1989, **160**, 205.
180. (a) A.E. Wickenden and R.A. Krause, *Inorg. Chem.*, 1969, **8**, 719; (b) R.D. Gillard and F.L. Wimmer, *J. Chem. Soc., Chem. Commun.*, 1978, 936; (c) M. Spangenberg and W. Bronger, *Z. Naturforsch. B*, 1978, **33**, 482; P.E.Jones and L. Katz, *Acta Crystallogr. Sect. B*, 1972, **28**, 3438.

181. R.D. Gillard, F.L. Wimmer and J.P.G. Richards, *J. Chem. Soc., Dalton Trans.*, 1985, 253; R. Sillanpää, P.S. Cartwright, R.D. Gillard and J. Valkonen, *Polyhedron*, 1988, **7**, 1801.
182. J. Arpalahti, J. Hölsä and R. Sillanpää, *Acta Chem. Scand.*, 1993, **47**, 1079.
183. I.I. Chernyaev and N.N. Krasovskaya, *Russ. J. Inorg. Chem.*, 1959, **4**, 485; 1958, **3**, 2044, 2281; 1957, **2**, 2349.
184. L.N. Essen, F.A. Zakharova and A.D. Gel'man, *Zh. Neorg. Khim.*, 1958, **3**, 2654; *Zh. Neorg. Khim.*, 1956, **1**, 2475.
185. H. Takazawa, S. Ohba, Y. Saito and M. Sano, *Acta Crystallogr. Sect. C*, 1990, **46**, 166.
186. P.B. Hitchcock, B. Jacobson and A. Pidcock, *J. Organomet. Chem.*, 1977, **133**, 273; 1977, **136**, 397; L. Aslanov, R. Mason, A.G. Wheeler and P.O. Whimp, *Chem. Commun.*, 1970, 30.
187. G.W. Bushnell, A. Pidcock and M.A.R. Smith, *J. Chem. Soc., Dalton Trans.*, 1975, 572; A. Albinati, W. Kauffmann and L.M. Venanzi, *Inorg. Chim. Acta*, 1991, **188**, 145; V.Yu. Kukushkin, V.K. Bel'skii, E.A. Aleksandrova, E.Yu. Pan'kova, V.E. Konovalev, V.M. Yakovlev and A.I. Moiseev, *J. Gen. Chem. USSR*, 1991, **61**, 284.
188. L.R. Gray, D.J. Gulliver, W. Levason and M. Webster, *J. Chem. Soc., Dalton Trans.*, 1983, 133; W. Levason, M.D. Spicer and M. Webster, *Inorg. Chem.*, 1991, **30**, 967; P.K. Byers, A.J. Canty, B.W. Skelton and A.H. White, *J. Chem. Soc., Chem. Commun.*, 1986, 1723; P.K. Byers, A.J. Canty, B.W. Skelton and A.H. White, *J. Chem. Soc., Chem. Commun.*, 1987, 1023.
189. For recent reviews: (a) Pt: V.K. Jain, G.S. Rao and L. Jain, *Adv. Organomet. Chem.*, 1987, **27**, 113; (b) Pd: A.J. Canty, *Acct. Chem. Res.*,1992, **25**, 83; *Platinum Metals Rev.*, 1993, **37**, 2.
190. G. Smith, C.H.L. Kennard and T.C.W. Mak, *J. Organomet. Chem.*, 1985, **290**, C7; B. Vance, *J. Organomet. Chem.*, 1987, **336**, 441.
191. C.S. Creaser and J.A. Creighton, *J. Organomet. Chem.*, 1978, **157**, 243; G.W. Rice and R.S. Tobias, *J. Am. Chem. Soc.*, 1977, **99**, 2141; M.P. Brown, R.J. Puddephatt and C.E.E. Upton, *J. Chem. Soc., Dalton Trans.*, 1974, 2457.
192. A.G. Swallow and M.R. Truter, *Proc. R. Soc., London, Series A*, 1962, **A266**, 257.
193. E.W. Abel, A.R. Khan, K. Kite, K.G. Orrell and V. Sik, *J. Chem. Soc., Chem. Commun.*, 1979, 126; E.W. Abel, P.D. Beer, I. Moss, K.G. Orrell, V. Sik, P.A. Bates and M.B. Hursthouse, *J. Organomet. Chem.*, 1988, **341**, 559.
194. Ref. 8, p. 588; K. Kite, J.A.S. Smith and L.J. Wilkins, *J. Chem. Soc. (A)*, 1966, 1744; D.E. Clegg and J.R. Hall, *Aust. J. Chem.*, 1967, **20**, 2025; G.C. Morgan, R.D. Rennick and C.C. Soong, *Inorg. Chem.*, 1966, **5**, 372.
195. H. Kunkeley and A. Vogler, *Coord. Chem. Rev.*, 1991, **111**, 15.
196. J. Forniäs, B. Menjän, R.M. Sanz-Carillo, M. Tomßs, N.G. Connelly, J.G. Crossley and A.G. Orpen, *J. Am. Chem. Soc.*, 1995, **117**, 4295.
197. P.K. Byers, A.J. Canty, B.W. Skelton and A.H. White, *J. Chem. Soc., Chem. Commun.*, 1986, 722; 1987, 1093.
198. J.D. Ruddick and B.L. Shaw, *J. Chem. Soc. (A)*, 1969, 2801, 2965, 2969.
199. M.P. Brown, R.J. Puddephatt and C.E.E. Upton, *J. Chem. Soc., Dalton Trans.*, 1974, 2457; F. Ozawa, T. Hikida and T. Hayashi, *J. Am. Chem. Soc.*, 1994, **116**, 2844; R.H. Crabtree, in *The Organometallic Chemistry of the Transition Metals*, Wiley-Interscience, New York, 2nd edn, 1994, p. 151.
200. K.I. Goldberg, J-Y. Lau and E.M. Breitung, *J. Am. Chem. Soc.*, 1995, **117**, 6889; C.J. Levy and R.J. Puddephatt, *Organometallics*, 1996, **14**, 5019.
201. J.E. Hux and R.J. Puddephatt, *Inorg. Chim. Acta*, 1985, **100**, 1; Y. Kondo, M. Ishikawa and K. Ishihara, *Inorg. Chim. Acta*, 1996, **241**, 85.
202. For recent work, see: G. Amiraal, M. Alink, C.A. Hona, F.J. Dijt, C.J. van Garderen, R.A.G. de Graaf and J. Reedijk, *J. Am. Chem. Soc.*, 1992, **114**, 930; S.E. Sherman and S.J. Lippard, *Chem. Rev.*, 1987, **87**, 1153; B.K. Keppler, *New J. Chem.*, 1990, **14**, 389; S.L. Bruhn, J.H. Toney and S.J. Lippard, *Progr. Inorg. Chem.*, 1990, **38**, 471; W.I. Sundquist and S.J. Lippard, *Coord. Chem. Rev.*, 1990, **100**, 293; T.W. Hambley, *Chem. in Australia*, 1991, 154; C.A. McAuliffe, H.L. Sharma and N.D. Tinker in *Chemistry of the Platinum Group Metals*, ed. F.R. Hartley, Elsevier, Amsterdam, 1991, p. 546; *Chem. Eng. News*, April 20 1992, 19; B.K. Keppler, in *Metal Complexes*

in Cancer Chemotherapy, VCH, New York, 1993; W. Kaim and B. Schwederski, in *Bioinorganic Chemistry; Inorganic Elements in the Chemistry of Life*, John Wiley, 1994, p. 363 and references therein; S.J. Lippard, in *Bioinorganic Chemistry*, eds I. Bertini, H.B. Gray, S.J. Lippard and J.S. Valentine, University Science Books, California, 1994; M. Hartmann and B.K. Keppler, *Comments Inorg. Chem.*, 1995, **16**, 339.

203. L.T. Ellis, H.M. Er and T.W. Hambley, *Aust. J. Chem.*, 1995, **48**, 793; S. Neidle, C.F. Snook, B.A. Murrer and C.F.J. Barnard, *Acta Crystallogr. Sect. C.*, 1995, **51**, 822.
204. N. Farrell, T.G. Appleton, Y. Qu, J.D. Roberts, A.P. Soares Fontes, K.A. Skov, P. Wu and Y. Zou, *Biochemistry*, 1995, **34**, 15480.
205. See J.F. Hartwig and S.J. Lippard, *J. Am. Chem. Soc.*, 1992, **114**, 5646; S.E. Sherman, D. Gibson, A.H.J. Wang and S.J. Lippard, *Science*, 1985, **230**, 412; A. Laoui, J. Kozelka and J.C. Chottard, *Inorg. Chem.*, 1988, **27**, 2751; P.M. Pil and S.J. Lippard, *Science*, 1992, **256**, 234; P.M. Takahara, A.C. Rosenweig, C.A. Frederik and S.J. Lippard, *Nature*, 1995, **377**, 649 and references therein.
206. P. del S. Murdoch, J.D. Ranford, P.J. Sadler and S.J. Berners-Price, *Inorg. Chem.*, 1993, **32**, 2249; K.J. Barnham, U. Frey, P. del S. Murdoch, J.D. Ranford and P.J. Sadler, *J. Am. Chem. Soc.*, 1994, **116**, 11175.
207. (a) M. Tanaka, *Acta Crystallogr. Sect. C*, 1992, **48**, 739; K.J. Moynihan and C. Chieh, *Acta Crystallogr. Sect. B*, 1979, **35**, 3060; (b) S. Otsuka, T. Yoshida, M. Matsumoto and K. Nakatsu, *J. Am. Chem. Soc.*, 1976, **98**, 5850; (c) A. Immirzi and A. Musco, *J. Chem. Soc., Chem. Commun.*, 1974, 400; A. Immirzi, A. Musco, P. Lambelli and G. Carturan, *Inorg. Chim. Acta*, 1975, **13**, L13; (d) T.A. Stromnova, V.S. Sergienko, A.V. Kisin, M.A.Porai-Koshits and I.I. Moiseev, *Izv. Akad. Nauk. SSSR Ser. Khim.*, 1987 (4) 894; *Bull. Acad. Sci. USSR Div. Chem. Sci.*, 1987, **36**, 821; P.A. Chaloner, P.B. Hitchcock and G.T.L. Broadwood-Strong, *Acta Crystallogr. Sect. C*, 1989, **45**, 1309; (e) A. Oskarsson, B. Noren, C. Svensson and L. Elding, *Acta Crystallogr. Sect. C*, 1990, **46**, 748; (f) A.J. Canty, B.W. Skelton, P.R. Traill and A.H. White, *Aust. J. Chem.*, 1992, **45**, 417; R.S. Osborn and D. Rogers, *J. Chem. Soc., Dalton Trans.*, 1974, 1002; (g) J.M. Wisner, T.J. Bartizak, J.A. Ibers, J.J. Low and W.A. Goddard, *J. Am. Chem. Soc.*, 1986, **108**, 347; J.M. Wisner, T.J. Bartizak and J.A. Ibers, *Organometallics*, 1986, **5**, 2044; (h) G. Schulz, N.Y. Subbotini, C.M. Jensen, J.A. Golen and I. Hargittai, *Inorg. Chim. Acta*, 1992, **191**, 85; A. Del Pra and G. Zanotti, *Cryst. Struct. Commun.*, 1979, **8**, 737; (i) H. Takazawa, S. Ohba and Y. Saito, *Acta Crystallogr. Sect. C*, 1988, **44**, 580; H. Takazawa, S. Ohba, Y. Saito and M. Sano, *Acta Crystallogr. Sect. C*, 1990, **46**, 166; (j) D.A. Martin, J.L. Bonte, R.M. Rush and R.A. Jacobsen, *Acta Crystallogr. Sect. B*, 1975, **31**, 2538; R.F. Kroenig, R.M. Rush, D.S. Martin and J.C. Clardy, *Inorg. Chem.*, 1974, **13**, 1366; (k) K. Leary, D.H. Templeton, A. Zalkin and N. Bartlett, *Inorg. Chem.*, 1973, **12**, 1726; J. Fawcett, J.H. Holloway, D.C. Puddick and D.R. Russell, *Acta Crystallogr. Sect. B*, 1980, **36**, 1921; (l) H. Takazawa, S. Ohba and Y. Saito, *Acta Crystallogr. Sect. C*, 1988, 44, 580; H. Takazawa, S. Ohba, Y. Saito and M. Sano, *Acta Crystallogr. Sect. C*, 1990, **46**, 166; (m) R.J.H. Clark, V.B. Croud, H.M. Dawes and M.B. Hursthouse, *Polyhedron*, 1988, **7**, 2611; H.R. Grundy and I.D. Brown, *Can. J. Chem.*, 1970, **48**, 1151; (n) L.R. Gray, D.J. Gulliver, W. Levason and M. Webster, *J. Chem. Soc., Dalton Trans.*, 1983, 133; T.W. Hambley, *Acta Crystallogr. Sect. C.*, 1986, **42**, 49; (o) V.G. Grushin, C. Bensimon and H. Alper, *Inorg. Chem.*, 1994, **33**, 4804; A. Del Pra and G. Zanotti, *Inorg. Chim. Acta*, 1980, **39**, 137; (p) V.V. Bashilov, P.V. Petrovskii, V.I. Sokolov, S.V. Lindemann, I.A. Guzey and Yu.T. Struchkov, *Organometallics*, 1993, **12**, 991; P.J. Fagan, J.C. Calabrese and B. Malone, *Science*, 1991, **252**, 1160; (q) P.K. Byers, A.J. Canty, B.W. Skelton and A.H. White, *J. Chem. Soc., Chem. Commun.*, 1987, 1093; (r) B.F.G. Johnson, J. Puga and P.R. Raithby, *Acta Crystallogr. Sect. B*, 1981, **37**, 953; L.I. Elding and A. Oskarsson, *Inorg. Chim. Acta*, 1987, **130**, 209; (s) T. Yoshida et al., *Nouv. J. Chim.*, 1979, **3**, 761; *J. Am. Chem. Soc.*, 1977, **99**, 2134; (t) F. Bachechi and L. Zambonelli, *Acta Crystallogr. Sect. C*, 1992, **48**, 788; (u) W.L. Steffen and G.J. Palenik, *Inorg. Chem.*, 1977, **15**, 2432; D.H. Farrar, *J. Cryst. Spec. Res.*, 1982, **12**, 465; (v) J.G. Crossley and A.G. Orpen, *Acta Crystallogr. Sect. C*, 1995, **51**, 1102.

Chapter 4

1. R.J. Puddephatt, in *The Chemistry of Gold*, Elsevier, Amsterdam, 1978.
2. *Gmelin Handbook of Inorganic Chemistry*, System No. 61, Silver. Main volume (a) Part A, Sections 1–4, 1970–3 (Element); (b) Part B Section 1, 1971 (Compounds with Noble gases, H, O, N, F and Cl); (c) Section 2, 1972 (Compounds with Br, I and At); (d) Section 3, 1973 (Compounds with S, Se, Te, Po, B, C and Si); (e) Section 4, 1974 (Compounds with P, As, Sb, Bi and the Metals); (f) Section 5, 1975 (Organosilver Compounds and Organosilver Salts); (g) Section 6, 1975 (Silver(I) complexes with O and N donors); (h) Section 7, 1976 (Silver(I) Complexes with other Donor Atoms; Silver(II) and (III) complexes); (i) Part C, 1972 (Alloys).
3. *Gmelin Handbook of Inorganic Chemistry*, System No. 62. Gold. Main volume. (a) Sections 1–3, 1950–4 (The element, Ores, Alloys); (b) Organogold Compounds 1980; (c) Part B. Section 1 (Compounds with H, F, Cl, N, O) 1992. (d) Part B. Section 2 (Compounds with Br, I, S, Se, Te, Po, B and C) 1994.
4. N.R. Thompson, in *Comprehensive Inorganic Chemistry*, eds J.C. Bailar, H.J. Emeleus, R.S. Nyholm and A.F. Trotman-Dickenson, Pergamon, Oxford, 1973, Vol. 3, p. 79 (silver).
5. R.J. Lancashire, in *Comprehensive Coordination Chemistry*, eds G. Wilkinson, R.D. Gillard and J.A. McCleverty, Pergamon, Oxford, 1987, Vol. 5, p. 775 (silver).
6. (a) J.G. Noltes and G. Van Koten, in *Comprehensive Organometallic Chemistry I*, eds G. Wilkinson, F.G.A. Stone and E.W. Abel, Pergamon, Oxford, 1982, Vol. 2, p. 709; (b) G. Van Koten, S.L. James and J.T.B.H. Jastrzebskii, in *Comprehensive Organometallic Chemistry II*, eds G. Wilkinson, F.G.A. Stone and E.W. Abel, Pergamon, Oxford, 1995, Vol. 3, p. 57 (silver).
7. B.F.G. Johnson and R. Davis, in *Comprehensive Inorganic Chemistry*, eds J.C. Bailar, H.J. Emeleus, R.S. Nyholm and A.F. Trotman-Dickenson, Pergamon, Oxford, 1973, Vol. 3, p. 129 (gold).
8. R.J. Puddephatt, in *Comprehensive Coordination Chemistry*, eds G. Wilkinson, R.D. Gillard and J.A. McCleverty, Pergamon, Oxford, 1987, Vol. 5, p. 861 (gold).
9. R.J. Puddephatt, in *Comprehensive Organometallic Chemistry*, eds G. Wilkinson, F.G.A. Stone and E.W. Abel, Pergamon, Oxford, 1982, Vol. 2, p. 765; A. Grohmann and H. Schmidbaur, in *Comprehensive Organometallic Chemistry II*, eds G. Wilkinson, F.G.A. Stone and E.W. Abel, Pergamon, Oxford, 1995, Vol. 3, p. 1 (gold).
10. For reviews of gold structural chemistry see P.G. Jones, *Gold Bull.*, 1981, **14**, 102, 159; 1983, **16**, 114; 1986, **19**, 46.
11. D.W. Smith, *Inorganic Substances*, Cambridge University Press, Cambridge, 1990, p. 155.
12. P. Schwerdtfeger, P.D.W. Boyd, S. Brienne and A.K. Burrell, *Inorg. Chem.*, 1992, **31**, 3411.
13. P. Schwerdtfeger, P.D.W. Boyd, A.K. Burrell, W.T. Robinson and M.J. Taylor, *Inorg. Chem.*, 1990, **29**, 3593.
14. J.K. Burdett and O. Eisenstein, *Inorg. Chem.*, 1992, **31**, 1758.
15. Y. Nakao, *J. Chem. Soc., Chem. Commun.*, 1992, 426.
16. I. Marsden and I. House, in *The Chemistry of Gold Extraction*, Ellis Horwood, Chichester, 1992; S. Mann, *Nature*, 1992, **357**, 358; H. Colley, *Chem. Brit.*, 1992, 720; J. Barrett, M.N. Hughes, G.I. Karavaiko and P.A. Spencer, in *Metal Extraction by Bacterial Oxidation of Minerals*, Ellis Horwood, Chichester, 1992.
17. F. Simon, *Gold Bull.*, 1993, **26**, 14; C. Bocking and I.R. Christie, *Interdisciplinary Sci. Rev.*, 1992, **17**, 239.
18. A.A. Timakov, V.N. Prusakov and Yu.N. Drobyshevskii, *Dokl. Akad. Nauk SSSR*, 1986, **291**, 125; *Dokl. Chem.*, 1986, **291**, 442.
19. D.A. Johnson, in *Some Thermodynamic Aspects of Inorganic Chemistry*, 2nd edn, Cambridge University Press, Cambridge, 1982, p. 36; D.W. Smith, in *Inorganic Substances*, Cambridge University Press, Cambridge, 1990, pp. 102, 141.
20. N.W. Allcock, in *Bonding and Structure*, Ellis Horwood, Chichester, 1990, p. 268.
21. B. Zemva, K. Lutar, A. Jesih, W.J. Casteel, A.P. Wilkinson, D.E. Cox, R.B. Van Dereele, H. Borrmann and N. Bartlett, *J. Am. Chem. Soc.*, 1991, **113**, 4192.
22. D. Schröder, J. Hrnsák, I.C. Tornieporth-Oetting, T.M. Klapötke and H. Schwarz, *Angew. Chem. Int. Ed. Engl.*, 1994, **33**, 212; P. Schwerdtfeger, J.S. McFeaters, R.L. Stephens, M.J. Liddell, M. Dolg and B.A. Hess, *Chem. Phys. Lett.*, 1994, **218**, 362.

23. E.M.W. Janssen, J.C.W. Folmer and G.A. Wiegers, *J. Less Common Metals*, 1974, **38**, 71 (AuCl); E.M.W. Janssen and G.A. Wiegers, *J. Less Common Metals*, 1978, **57**, 47 (AuBr); H. Jagodzinski, *Z. Krist.*, 1959, **112**, 80 (AuI).
24. D.B. Dell'Amico, F. Calderazzo, F. Marchetti, S. Merlino and G. Perego, *J. Chem. Soc., Chem. Commun.*, 1979, 31.
25. I.C. Tornieporth-Oetting and T.M. Klapötke, *Chem. Ber.*, 1995, **128**, 957.
26. F.W.B. Einstein, P.R. Rao, J. Trotter and N. Bartlett, *J. Chem. Soc. (A)*, 1967, 478.
27. K-P. Lörcher and J. Strähle, *Z. Naturforsch. Teil. B*, 1975, **30**, 662.
28. M.J. Vasile, T.J. Richardson, F.A. Stevie and W.E. Falconer, *J. Chem. Soc., Dalton Trans.*, 1976, 351; Yu.M. Kiselev, A.I. Popov, A.V. Goryunov, N.A. Chumaevskii, L.N. Savinova, V.B. Sokolov and S.N. Spirin, *Zh. Neorg. Khim.*, 1990, **35**, 611; *Russ. J. Inorg. Chem.*, 1990, **35**, 345.
29. J. Brunvoll, A.A. Ischenko, A.A. Ivanov, G.V. Romanov, V.B. Sokolov, V.P. Spiridinov and T.G. Strand, *Acta Chem. Scand. A*, 1982, **36**, 705.
30. H.-D. Wasel-Nielen and R. Hoppe, *Z. Anorg. Allgem. Chem.*, 1968, **359**, 36; V.B. Lazarev, A.A. Zakharov and I.S. Shaplygin, *Zh. Neorg. Chem.*, 1979, **24**, 1151.
31. S. Kielhorn, D.H. Buss, O. Glemser, R. Gerner and G. Jeske, *Angew. Chem. Int. Ed. Engl.*, 1991, **30**, 1017.
32. W. Beesk, P.G. Jones, H. Rumpel, E. Schwarzmann and G.M. Sheldrick, *J. Chem. Soc., Chem. Commun.*, 1981, 664.
33. P.G. Jones, H. Rumpel, E. Schwarzmann, G.M. Sheldrick and H. Paulus, *Acta Crystallogr. Sect B*, 1979, **35**, 1435.
34. A. Pantelouris, G. Küper, J. Hornies, C. Feldmann and M. Jansen, *J. Am. Chem. Soc.*, 1995, **117**, 11753.
35. A. Rabeneau and H. Schulz, *J. Less Common Metals*, 1976, **48**, 89.
36. F. Pertlik, *Tschermaks Min. Petr. Mitt.*, 1984, **33**, 203.
37. G. Marbach and J. Strähle, *Angew. Chem.*, 1984, **96**, 229, 695; A. Müller, M. Römer, H. Bögge, E. Krickmeyer and K. Schmitz, *Inorg. Chim. Acta*, 1984, **85**, L39; for silver thiolates see I.G. Dance, *Inorg. Chem.*, 1981, **20**, 1487 and I.G. Dance, L.J. Fitzpatrick, A.D. Rae and M.L. Scudder, *Inorg. Chem.*, 1983, **22**, 3785.
38. M. Draganjac and T.B. Rauchfuss, *Angew. Chem. Int. Ed. Eng.*, 1985, **24**, 742; S. Huang and M.G. Kanatzidis, *Inorg. Chem.*, 1991, **30**, 1455.
39. S. Huang and M.G. Kanatzidis, *Inorg. Chem.*, 1991, **30**, 3572.
40. T. Yamaguchi, O. Lindqvist, J.B. Boyce and T. Claeson, *Acta Chem. Scand. A*, 1984, **38**, 423 (hydration no.). T. Yamaguchi, G. Johansson, B. Holmberg, M. Maeda and H. Ohtaki, *Acta Chem. Scand. A*, 1984, **38**, 437.
41. D.F. Steele, *Chem. Brit.*, 1991, 915.
42. U. Zachwieja and H. Jacobs, *Z. Krist.*, 1992, **201**, 207; U. Zachwieja and H. Jacobs, *Z. Anorg. Allgem. Chem.*, 1989, **571**, 37; S. Yamaguchi, H. Wakita and M. Nomura, *J. Chem. Soc., Chem. Commun.*, 1988, 433.
43. K. Nilsson and A. Oskarsson, *Acta Chem. Scand. A*, 1982, **36**, 605; C.J. Antti and B.K.S. Lundberg, *Acta Chem. Scand.*, 1971, **25**, 1758; G.W. Eastland, M.A. Mazid, D.R. Russell and M.C.R. Symons, *J. Chem. Soc., Dalton Trans.*, 1980, 1682.
44. E.C. Constable, M.G.B. Drew, G. Forsyth and M.D. Ward, *J. Chem. Soc., Chem. Commun.*, 1988, 1456; E.W. Ainscough, A.M. Brodie, S.L. Ingham and J.M. Waters, *J. Chem. Soc., Dalton Trans.*, 1994, 215.
45. F. Robinson and M.J. Zamorotko, *J. Chem. Soc., Chem. Commun.*, 1995, 2413; O.M. Yaghi and H. Li, *J. Am. Chem. Soc.*, 1996, **118**, 295.
46. B-K. Teo and J.C. Calabrese, *Inorg. Chem.*, 1976, **15**, 2474; M. Henary and J.I. Zink, *Inorg. Chem.*, 1991, **30**, 3111 and references therein (includes luminescence); R.J. Bowen, D. Camp, Effendy, P.C. Healy and B.W. Skelton, *Aust. J. Chem.*, 1994, **47**, 693.
47. N.S. Weng and A.H. Othman, *Z. Kristallogr.*, 1995, **210**, 674.
48. A. Cassel, *Acta Crystallogr. Sect B*, 1979, **35**, 174; P.G. Jones, *Acta Crystallogr. Sect. C*, 1993, **49**, 1148.
49. G.A. Bowmaker, Effendy, J.V. Hanna, P.C. Healy, G.J. Miller, B.W. Skelton and A.H. White, *J. Phys. Chem.*, 1995, **99**, 3909.
50. M. Barrow, H.B. Burgi, D.K. Johnson and L.M. Venanzi, *J. Am. Chem. Soc.*, 1976, **98**, 2356.

51. (a) L.-J. Baker, G.A. Bowmaker, D. Camp, Effendy, P.C. Healy, H. Schmidbaur, O. Steigelmann and A.H. White, *Inorg. Chem.*, 1992, **31**, 3656; (b) N.H. Dryden, J.J. Vittal and R.J. Puddephatt, *Chem. Mat.*, 1994, **5**, 765.
52. A.M.M. Lanfredi, F. Ugozzoli, F. Asaro, G. Pelizzer, N. Marisch and A. Camus, *Inorg. Chim. Acta*, 1991, **190**, 71.
53. S. Jagner and G. Helgesson, *Adv. Inorg. Chem. Radiochem.*, 1991, **37**, 1.
54. S. Geller, *Acct. Chem. Res.*, 1978, **11**, 87.
55. G. Helgesson and S. Jagner, *J. Chem. Soc., Dalton Trans.*, 1993, 1069; G.A. Bowmaker, A. Camus, B.W. Skelton and A.H. White, *J. Chem. Soc., Dalton Trans.*, 1990, 727 and references therein; S. Olson, G. Helgesson and S. Jagner, *Inorg. Chim. Acta*, 1994, **217**, 15.
56. E. Staritzky, *Anal. Chem.*, 1956, **28**, 423; P. Gans, J.B. Gill, M. Griffin and P. Cahill, *J. Chem. Soc., Dalton Trans.*, 1981, 968; see also B.F. Hoskins, R. Robson and N.V.Y. Scarlett, *J. Chem. Soc., Chem. Commun.*, 1994, 2025.
57. H. Anaker-Eickhoff, R. Hesse, P. Jennische and A. Wahlberg, *Acta Chem. Scand. A*, 1982, **36**, 251; R. Hesse and L. Nilsson, *Acta Chem. Scand.*, 1969, **23**, 825.
58. M.R. Udapa and B. Krebs, *Inorg. Chim. Acta*, 1971, **7**, 271; M.R. Udapa, G. Henkel and B. Krebs, *Inorg. Chim. Acta*, 1976, **18**, 17.
59. A.J. Blake, R.O. Gould, A.J. Holder, T.I. Hyde and M. Schröder, *Polyhedron*, 1989, **8**, 513; J.A. Clarkson, R. Yagbasan, P.J. Blower, S.C. Rawle and S.R. Cooper, *J. Chem. Soc., Chem. Commun.*, 1987, 950.
60. B. Muller and R. Hoppe, *Z. Anorg. Allgem. Chem.*, 1972, **392**, 37; G.C. Allen, R.F. McMeeking, R. Hoppe and B. Muller, *J. Chem. Soc., Chem. Commun.*, 1972, 291.
61. G.W. Bushnell and M.A. Khan, *Can. J. Chem.*, 1992, **50**, 315; J.L. Atwood, M.L. Simms and D.A. Zatko, *Cryst. Struct. Commun.*, 1973, **2**, 279.
62. M.O. Kestner and A.L. Allred, *J. Am. Chem. Soc.*, 1972, **94**, 7189.
63. K.B. Mertes, *Inorg. Chem.*, 1978, **17**, 49; H.N. Po, E. Brinkman and R.J. Doedens, *Acta Crystallogr. Sect. C*, 1991, **47**, 2310.
64. E.K. Barefield and M.T. Mocella, *Inorg. Chem.*, 1973, **12**, 2829; H.N. Po, *Coord. Chem. Rev.*, 1976, **20**, 171; L. Coghi and G. Pelizzi, *Acta Crystallogr. Sect. B*, 1975, **31**, 131.
65. R. Hoppe and R. Homann, *Naturwissenschaften*, 1966, **53**, 501; *Z. Anorg. Allgem. Chem.*, 1970, **379**, 293.
66. L.J. Kirschenbaum, J.H. Ambrus and G. Atkinson, *Inorg. Chem.*, 1973, **12**, 2832.
67. N.E. Christensen and J. Kollar, *Solid State Commun.*, 1983, **46**, 727; Z.C. Dong and J.D. Corbett, *Inorg. Chem.*, 1995, **34**, 5042.
68. Y. Yang, V. Ramamoorthy and P.R. Sharp, *Inorg. Chem.*, 1993, **32**, 1946; H. Schmidbaur, G. Weidenhiller and O. Steigelmann, *Angew. Chem. Int. Ed. Engl.*, 1991, **30**, 433; E.I. Smyslova, E.G. Perevalova, V.P. Dyadchenko, K.I. Grandberg, H.L. Slovokhotov and Yu.Y. Struchkov, *J. Organomet. Chem.*, 1981, **215**, 269.
69. S. Komiya, M. Iwata, T. Sone and A. Fukuoka, *J. Chem. Soc., Chem. Commun.*, 1992, 1109.
70. (a) D.M.P. Mingos, J. Yau, S. Menzer and D.J. Williams, *J. Chem. Soc., Dalton Trans.*, 1995, 319; (b) D.M.P. Mingos and J. Yau, *J. Organomet. Chem.*, 1994, **479**, C16; (c) V.H.N. Adams, W. Hiller and J. Strähle, *Z. Anorg. Allgem. Chem.*, 1982, **485**, 81; W. Conzelman, W. Hiller, J. Strähle and G.M. Sheldrick, *Z. Anorg. Allgem. Chem.*, 1984, **512**, 169.
71. C.C. Colburn, W.E. Hill, C.A. McAuliffe and R.V. Parish, *J. Chem. Soc., Chem. Commun.*, 1979, 218; R.V. Parish, O. Parry and C.A. McAuliffe, *J. Chem. Soc., Dalton Trans.*, 1981, 2098; A.K.H. Al-Sa'ady, C.A. McAuliffe, K. Moss, R.V. Parish and R. Fields, *J. Chem. Soc., Dalton Trans.*, 1984, 491; R.V. Parish, in *NMR, NQR, EPR and Mössbauer Spectroscopy in Inorganic Chemistry*, Ellis Horwood, Chichester, 1990, p. 152.
72. P.F. Barron, L.M. Engelhardt, P.C. Healy, J. Oddy and A.H. White, *Aust. J. Chem.*, 1987, **40**, 1545.
73. X. Hong, K.-K. Cheung, C.-X. Guo and C.-M. Che, *J. Chem. Soc., Dalton Trans.*, 1994, 1867.
74. M. Nakamoto, W. Hiller and H. Schmidbaur, *Chem. Ber.*, 1993, **126**, 605; J.P. Fackler, R.J. Staples, A. Elduque and T. Grant, *Acta Crystallogr. Sect. C*, 1994, **50**, 520.
75. U. Flärke, H.-J. Haupt and P.G. Jones, *Acta Crystallogr. Sect. C*, 1996, **52**, 609.

76. J.P. Fackler Jr, M.N.I. Khan, C. King, R.J. Staples and R.E.P. Winpenny, *Organometallics*, 1992, **10**, 2178.
77. G. Siasios and E.R.T. Tiekink, *Z. Krist.*, 1992, **198**, 139; A.M.M. Lanfredi, F. Ugozzoli, F. Asaro, G. Pellizer, N. Marsich and A. Camus, *Inorg. Chim. Acta*, 1992, **192**, 271.
78. J. Vicente, M.-T. Chicote, R. Guerrero and P.G. Jones, *J. Chem. Soc., Dalton Trans.*, 1995, 1251.
79. J.A. Muir, M.M. Muir, L.B. Pulgar, P.G. Jones and G.M. Sheldrick, *Acta Crystallogr. Sect. C*, 1985, **41**, 1174; H. Schmidbaur, G. Weidenhiller, A.A.M. Aly, O. Steigelmann and G. Müller, *Z. Naturforsch., Teil B*, 1989, **44**, 1503; H. Schmidbaur, G. Weidenhiller, O. Steigelmann and G. Müller, *Chem. Ber.*, 1990, **123**, 285; J.A. Muir, S.I. Cuadrado and M.M. Muir, *Acta Crystallogr. Sect. C*, 1991, **47**, 1072; P.G. Jones, *J. Cryst. Spect. Res.*, 1992, **22**, 397; K. Angermaier, E. Zeller and H. Schmidbaur, *J. Organomet. Chem.*, 1994, **472**, 371 and references therein; B. Weissbart, L.J. Larson, M.M. Olmstead, C.P. Nash and D.S. Tinti, *Inorg. Chem.*, 1995, **34**, 393 and references therein.
80. W. Fuss and M. Ruhe, *Z. Naturforsch., Teil B*, 1992, **47**, 591.
81. L.J. Baker, R.C. Bott, G.A. Bowmaker, P.C. Healy, B.W. Skelton, P. Schwerdtfeger and A.H. White, *J. Chem. Soc., Dalton Trans.*, 1995, 1341.
82. J.A. Muir, M.M. Muir and E. Lorca, *Acta Crystallogr. Sect. B*, 1980, **36**, 931.
83. R.J. Staples, C. King, M.N.I. Khan, R.E.P. Winpenny and J.P. Fackler, *Acta Crystallogr. Sect. C*, 1993, **49**, 472; J.-C. Wang and Y. Wang, *Acta Crystallogr. Sect. C*, 1993, **49**, 131; S. Ahrland, S. Balzamo and I. Persson, *Acta Chem. Scand*, 1992, **46**, 259 (in solution).
84. R.J. Staples, J.P. Fackler, M.N.I. Khan and R.E.P. Winpenny, *Acta Crystallogr. Sect. C*, 1994, **50**, 191.
85. P.G. Jones, *J. Chem. Soc., Chem. Commun.*, 1980, 1031; P.G. Jones, *Acta Crystallogr. Sect. B*, 1992, **48**, 1487; P.G. Jones, G.M. Sheldrick, J.A. Muir, M.M. Muir and L.B. Pulgar, *J. Chem. Soc., Dalton Trans.*, 1982, 2123; J.A. Muir, M.M. Muir, S. Arias, C.F. Campana and S.K. Dwight, *Acta Crystallogr. Sect. B*, 1982, **38**, 2047.
86. M. Khan, C. Oldham and D.G. Tuck, *Can. J. Chem.*, 1981, **59**, 2714; G.A. Bowmaker, J.C. Dyason, P.C. Healy, L.M. Engelhardt, C. Pakawatchai and A.H. White, *J. Chem. Soc., Dalton Trans.*, 1987, 1089; Z. Assefa, R.J. Staples and E.R.T. Tiekink, *Z. Krist.*, 1992, **198**, 139; Z. Assefa, R.J. Staples and J.P. Fackler, *Inorg. Chem.*, 1994, **33**, 2790; J.A. Muir, S.I. Cuadrado and M.M. Muir, *Acta Crystallogr. Sect. C*, 1992, **48**, 915; J.A. Muir, M.M. Muir and S. Arias, *Acta Crystallogr. Sect. B*, 1982, **38**, 1318. L.J. Guggenberger, *J. Organomet. Chem.*, 1974, **81**, 271; P.G. Jones, *Acta Crystallogr. Sect. B*, 1980, **36**, 3105.
87. W. Clegg, *Acta Crystallogr. Sect. B*, 1976, **32**, 2712.
88. C. King, M.N.I. Khan, R.J. Staples and J.P. Fackler, *Inorg. Chem.*, 1992, **31**, 3236; Z. Assefa, R.J. Staples and J.P. Fackler, *Inorg. Chem.*, 1994, **33**, 2790.
89. P.A. Bates and J.M. Waters, *Inorg. Chim. Acta*, 1985, **98**, 125; S.J. Berners-Price, M.A. Mazid and P.J. Sadler, *J. Chem. Soc., Dalton Trans.*, 1984, 969; H. Schmidbaur, G. Reber, A. Schier, F.E. Wagner and G. Muller, *Inorg. Chim. Acta*, 1988, **147**, 143; R. Usän, A. Laguna, M. Laguna, P.G. Jones and G.M. Sheldrick, *J. Chem. Soc., Dalton Trans.*, 1981, 366.
90. P. Braunstein and R.J.H. Clark, *J. Chem. Soc., Dalton Trans.*, 1973, 1845; P. Braunstein, A. Muller and H. Bogge, *Inorg. Chem.*, 1986, **25**, 2104.
91. R.J. Schubert and K.-J. Range, *Z. Naturforsch*, 1990, **45B**, 1118.
92. D.B. Dell'Amico, F. Calderazzo, P. Robino and A. Segre, *J. Chem. Soc., Dalton Trans.*, 1991, 3017.
93. (a) A.K.H. Al-Sa'ady, K. Moss, C.A. McAuliffe and R.V. Parish, *J. Chem. Soc., Dalton Trans.*, 1984, 1609; (b) I. Schröter and J. Strähle, *Chem. Ber.*, 1991, **124**, 2161; Y.Y. Tong, A.J.L. Pombeiro, D.L. Hughes and R.L. Richards, *Transit. Met. Chem.*, 1995, **20**, 372.
94. J. Vicente, M-T. Chicote, P. Gonzalez-Herrero, P.G. Jones and B. Ahrens, *Angew. Chem. Int. Ed. Engl.*, 1994, **33**, 1852.
95. P.A. Bates and J.M. Waters, *Acta Crystallogr. Sect. C*, 1985, **41**, 862.
96. P. Schwerdtfeger, P.D.W. Boyd, A.K. Burrell, W.T. Robinson and M.J. Taylor, *Inorg. Chem.*, 1990, **29**, 3593.
97. S. Ahrland, B. Noren and A. Oskarsson, *Inorg. Chem.*, 1985, **24**, 1330; S. Ahrland, K. Dreisch, B. Noren and A. Oskarsson, *Mat. Chem. Phys.*, 1993, **35**, 281.

98. L.C. Porter, J.P. Fackler, J. Costamagna and R. Schmidt, *Acta Crystallogr. Sect. C*, 1992, **48**, 1751.
99. R. Hesse and P. Jennische, *Acta Chem. Scand.*, 1972, **26**, 3855; P. Jennische, H. Anacker-Eickhoff and A. Wahlberg, *Acta Crystallogr. Sect A*, 1975, **31**, S 143; D.D. Heinrich, J.-C. Wang and J.P. Fackler, *Acta Crystallogr. Sect. C*, 1990, **46**, 1444, and references therein; M. Hong, X. Lei, Z. Huang, B. Kang, F. Jiang and H. Liu, *Chinese Sci. Bull.*, 1993, **38**, 912.
100. O. Piovanese and P.F. Zanelli, *Angew. Chem. Int. Ed. Engl.*, 1980, **19**, 561.
101. G.M. Bancroft, T. Chan, R.J. Puddephatt and J.S. Tse, *Inorg. Chem.*, 1982, **21**, 2946.
102. T. Vanngard and S. Akerstrom, *Nature*, 1959, **184**, 183; J.G.M. Van Rens, M.P.A. Viegers and E. De Boer, *Chem. Phys. Lett.*, 1974, **28**, 104; J.H. Waters and H.B. Gray, *J. Am. Chem. Soc.*, 1965, **87**, 3534; L.F. Warren and M.F. Hawthorne, *J. Am. Chem. Soc.*, 1968, **90**, 4823.
103. A.J. Holder, T.I. Hyde and M. Schroder, *J. Chem. Soc., Chem. Commun.*, 1989, 876; A.J. Blake, J.A. Greig, A.J. Holder, T.I. Hyde, A. Taylor and M. Schroder, *Angew. Chem. Int. Ed. Engl.*, 1990, **29**, 197.
104. M. Takeda, M. Takahashi, Y. Ho, T. Takano, M.A. Bennett and S.K. Bhargava, *Chem. Lett.*, 1990, 543.
105. F.G. Herring, G. Hwang, K.C. Lee, F. Mistry, P.S. Phillips, H. Willner and F. Aubke, *J. Am. Chem. Soc.*, 1992, **114**, 1271.
106. K. Takahashi and H. Tanino, *Chem. Lett.*, 1988, 641.
107. W. Denner, H. Schulz and H. D'Amour, *Acta Crystallogr. Sect. A*, 1979, **35**, 360.
108. J. Stanek, *J. Chem. Phys.*, 1982, **76**, 2315.
109. H. Kitigawa, N. Kojima, N. Matsushita, T. Ban and I. Tsujikawa, *J. Chem. Soc., Dalton Trans.*, 1991, 3115; H. Kitigawa, N. Kojima and T. Nakajima, *J. Chem. Soc., Dalton Trans.*, 1991, 3121; N. Kitigawa, N. Kojima and H. Sakai, *J. Chem. Soc., Dalton Trans.*, 1991, 3211; N. Kojima and H. Kitigawa, *J. Chem. Soc., Dalton Trans.*, 1994, 327.
110. P. Schwerdtfeger, *J. Am. Chem. Soc.*, 1989, **111**, 7261.
111. For vibrational data see: Y.M. Bosworth and R.J.H. Clark, *Inorg. Chem.*, 1975, **14** 170.
112. J.L. Ryan, *Inorg. Chem.*, 1969, **8**, 2058.
113. U. Engelmann and B.G. Muller, *Z. Anorg. Allgem. Chem.*, 1991, **598–599**, 103.
114. P.G. Jones and E. Bembenek, *J. Cryst. Spect. Res.*, 1992, **22**, 397; D.B. Dell'Amico, F. Calderazzo, A. Morvillo, G. Pelizzi and P. Robino, *J. Chem. Soc., Dalton Trans.*, 1991, 3009.
115. J.P. Johnson, H.B. Krause and E.G. Sherry, *Acta Crystallogr. Sect. A*, 1981, **37**, C 227.
116. C.D. Garner and S.C. Wallwork, *J. Chem. Soc. (A)*, 1970, 3093.
117. P.G. Jones and G.M. Sheldrick, *Acta Crystallogr. Sect. C*, 1984, **40**, 804, 1776.
118. J.J. Guy, P.G. Jones, M.J. Mays and G.M. Sheldrick, *J. Chem. Soc., Dalton Trans.*, 1977, 8; H.N. Adams and J. Strähle, *Z. Anorg. Allgem. Chem.*, 1982, **485**, 65.
119. M. Weishaupt and J. Strähle, *Z. Naturforsch., Teil B*, 1976, **31**, 554; J. Strähle, J. Gelinek and M. Kolmel, *Z. Anorg. Allgem. Chem.*, 1979, **456**, 241; K. Kaas and L.H. Skibsted, *Acta Chem. Scand.*, 1985, **39**, 1362 (structures). For synthesis see L.H. Skibsted and J. Bjerrum, *Acta Chem. Scand. A*, 1974, **28**, 740.
120. W. Beck and H. Näth, *Chem. Ber.*, 1984, **117**, 419; cyclization with RNC see W. Beck, K. Burger and W.P. Fehlhammer, *Chem. Ber.*, 1971, **104**, 1816.
121. (a) L.Kh. Minacheva, G.G. Sadikov, V.G. Sakharova, A.S. Gladkaya and M.A. Porai-Koshits, *Koord. Khim.*, 1983, **9**, 566; (b) G. Marangoni, B. Pitteri, V. Bertolasi, G. Gilli, and V. Ferretti, *J. Chem. Soc., Dalton Trans.*, 1986, 1941.
122. E.J.L. McInnes, A.J. Welch and L.J. Yellowlees, *Acta Crystallogr. Sect. C*, 1995, **51**, 2023.
123. J.-H. Kim and G.W. Everett, *Inorg. Chem.*, 1979, **18**, 3145; 1981, **20**, 853; C.H. Park, B. Lee and G.W. Everett, *Inorg. Chem.*, 1982, **21**, 1681.
124. L.S. Hollis and S.J. Lippard, *J. Am. Chem. Soc.*, 1983, **105**, 4293; V. Ferretti, P. Gilli, V. Bertolasi, G. Marangoni, B. Pitteri and G. Chessa, *Acta Crystallogr. Sect. C*, 1992, **48**, 814.
125. E. Kimura, Y. Kurogi and T. Takahashi, *Inorg. Chem.*, 1991, **30**, 4117; E. Kimura, Y. Kurogi, T. Koike, T. Takahashi and Y. IItaka, *J. Coord. Chem.*, 1993, **28**, 33.
126. R.J. Staples, T. Grant and J.P. Fackler, Jr, *Acta Crystallogr. Sect. C*, 1994, **50**, 39; D.S. Eggleston, D.F. Chodosh, D.T. Hill and G.R. Girard, *Acta Crystallogr. Sect. C*, 1984, **40**, 1357 .

127. L.F. Warren and M.A. Bennett, *Inorg. Chem.*, 1976, **15**, 3126; M.A. Bennett, K. Hoskins, W.R. Kneen, R.S. Nyholm, P.B. Hitchcock, R. Mason, G.B. Robertson and A.D.C. Towl, *J. Am. Chem. Soc.*, 1971, **93**, 4591.
128. P.G. Jones and J. Lautner, *Z. Krist.*, 1993, **208**, 130.
129. P.G. Jones and E.B. Bembenek, *Z. Krist.*, 1993, **208**, 126.
130. K. Takahashi and K. Kato, *Bull. Chem. Soc. Japan*, 1988, **61**, 991; K. Takahashi, *Bull. Chem. Soc. Japan*, 1991, **64**, 2572.
131. J.H. Noordik, *Cryst. Struct. Commun.*, 1973, **2**, 81.
132. M. Hong, Z. Huang, X. Lei, F. Jiang and H. Liu, *Acta Crystallogr. Sect C*, 1992, **48**, 1101; see also M. Nakamoto, H. Koijman, M. Paul, W. Hiller and H. Schmidbaur, *Z. Anorg. Allgem. Chem.*, 1993, **619**, 1341.
133. J.H. Noordik and P.T. Beurskens, *J. Cryst. Mol. Struct*, 1971, **1**, 339; J.H. Noordik, T.W. Hummelink and P.T. Beurskens, *J. Coord. Chem.*, 1973, **2**, 185.
134. C. Bertinotti and A. Bertinotti, *Acta Crystallogr. Sect. B*, 1970, **26**, 422; *C. R. Acad Sci. B*, 1971, **273**, 33.
135. R. Timkovich and A. Tulinsky, *Inorg. Chem.*, 1977, **16**, 962.
136. R.C. Elder and J.W. Watkins, *Inorg. Chem.*, 1986, **25**, 223.
137. W.T. Robinson and E. Sinn, *J. Chem. Soc., Dalton Trans.*, 1975, 726.
138. R.J. Charlton, C.M. Harris, H. Patil and N.C. Stephenson, *Inorg. Nucl. Chem Letters*, 1966, **2**, 409; S.M. Godfrey, N. Ho, C.A. McAucliffe and R.G. Pritchard, *Angew. Chem. Int. Ed. Engl.*, 1996, **35**, 2344.
139. V.F. Duckworth and N.C. Stephenson, *Inorg. Chem.*, 1969, **8**, 1661.
140. V. Ferretti, P. Gilli, V. Bertolasi, G. Marangoni, B. Pitteri, and G. Chessa, *Acta. Crystallogr. Sect. B*, 1992, **48**, 814.
141. L.H. Skibsted, *Acta Chem. Scand. A*, 1979, **33**, 113; 1983, **37**, 613.
142. G. Rindorf, N. Thorupo, T. Bjornholm and K. Bechgaard, *Acta Crystallogr. Sect C*, 1990, **46**, 1437; M. Nakamoto, H. Koijman, M. Paul, W. Hiller and H. Schmidbaur, *Z. Anorg. Allgem. Chem.*, 1993, **619**, 1341.
143. M.J. Vasile, T.J. Richardson, F.A. Stevie and W.E. Falconer, *J. Chem. Soc., Dalton Trans.*, 1976, 351; K. Leary, A. Zalkin and N. Bartlett, *J. Chem. Soc., Chem. Commun.*, 1973, 131; *Inorg. Chem.*, 1974, **14**, 775.
144. H.K. Hofstee, J. Boersma and G.J.M. van der Kerk, *J. Organomet. Chem.*, 1978, **168**, 241.
145. E.M. Meyer, S. Gambarotta, C. Floriani, A. Chiesi-Villa and C. Guastini, *Organometallics*, 1989, **8**, 1067.
146. R. Lingnau and J. Strähle, *Angew. Chem. Int. Ed. Engl.*, 1988, **27**, 436; A. Haaland, K. Rypdal, H.P. Verne, W. Scherer and W.R. Thiel, *Angew. Chem. Int. Ed. Engl.*, 1994, **33**, 2443.
147. C. Brasse, P.R. Raithby, M.-A. Rennie, C.A. Russell, A. Steiner and D.S. Wright, *Organometallics*, 1996, **15**, 639.
148. (a) P.K. Hurlbut, J.J. Rack, J.S. Luck, S.F. Dec, J.D. Webb, O.P. Anderson and S.H. Strauss, *J. Am. Chem. Soc.*, 1994, **116**, 10003; (b) J.J. Rack, B. Moasser, J.D. Gargulak, W.L. Gladfelter, H.D. Hochheimer and S.H. Strauss, *J. Chem. Soc., Chem. Commun.*, 1994, 685.
149. L. Weber, *Angew. Chem. Int. Ed. Engl.*, 1994, **33**, 1077.
150. H.V.R. Dias and W. Jin, *J. Am. Chem. Soc.*, 1995, **117**, 11381.
151. R.W. Turner and E.L. Amma, *J. Am. Chem. Soc.*, 1966, **88**, 3243.
152. L.A. Paquette, *Synthesis*, 1975, 347.
153. T.J. Wenzel and M.D. Russell, *J. Chem. Ed.*, 1987, **64**, 979 and references therein.
154. (a) G.K. Anderson, *Adv. Organomet. Chem.*, 1982, **20**, 39; (b) R. Uson and A. Laguna, *Coord. Chem. Rev.*, 1986, **70**, 1 (aryls); (c) K.I. Grandberg and V.P. Dyadchenko, *J. Organomet. Chem.*, 1994, **474**, 1 (substantially Russian work).
155. (a) e.g. J. Messelhauser, E.B. Flint and H. Suhr, *Appl. Surf. Sci.*, 1992, **54**, 64; J.L. Davidson, P. John, P.G. Roberts, M.G. Jubber and J.I.B. Wilson, *Chem. Mat.*, 1994, **6**, 1712; (b) R.J. Puddephatt and I. Treurnicht, *J. Organomet. Chem.*, 1987, **319**, 129; R.J. Puddephatt, *Polyhedron*, 1994, **13**, 1233; (c) M.M. Banaszak-Holl, P.F. Seidler, S.P. Kowalzyk and F.P. McFeely, *Inorg. Chem.*, 1994, **33**, 510.
156. A. Haaland, J. Hougen, H.V. Volden and R.J. Puddephatt, *J. Organomet. Chem.*, 1987, **325**, 311.

157. A. Sladek, S. Hofreiter, M. Paul and H. Schmidbaur, *J. Organomet. Chem.*, 1995, **501**, 47.
158. G.W. Rice and R.S. Tobias, *Inorg. Chem.*, 1976, **15**, 489; S. Komiya, T.A. Albright, R. Hoffmann and J.K. Kochi, *J. Am. Chem. Soc.*, 1977, **99**, 8440.
159. R. Uson, A. Laguna, J. Vicente, J. Garcia, P.G. Jones and G.M. Sheldrick, *J. Chem. Soc., Dalton Trans.*, 1981, 655; P.G. Jones, *Z. Kristallogr.*, 1993, **208**, 347.
160. R. Uson, A. Laguna, E.J. Fernandez, M.E. Ruiz-Romero, P.G. Jones and J. Lautner, *J. Chem. Soc., Dalton Trans.*, 1989, 2127.
161. R. Uson, A. Laguna and J. Vicente, *J. Organomet. Chem.*, 1977, **131**, 471; R. Uson, A. Laguna, J. Garcia and M. Laguna, *Inorg. Chim. Acta*, 1979, **37**, 201; J. Vicente, A. Arcas, P.G. Jones and J. Lautner, *J. Chem Soc., Dalton Trans.*, 1990, 451.
162. M.I. Bruce, E. Horn, J.G. Matisons and M.R. Snow, *Aust. J. Chem.*, 1984, **37**, 1163; P.W.R. Corfield and H.M.M. Shearer, *Acta Crystallogr.*, 1967, **23**, 156.
163. H. Werner, H. Otto, T. Ngo-Khac and C. Burschka, *J. Organomet. Chem.*, 1984, **262**, 123.
164. H. Willner and F. Aubke, *Inorg. Chem.*, 1990, **29**, 2915; H. Willner, J. Schaebs, G. Hwang, F. Mistry, R. Jones, J. Trotter and F. Aubke, *J. Am. Chem. Soc.*, 1992, **114**, 8972.
165. (a) S. Komiya, J.C. Huffman and J.K. Kochi, *Inorg. Chem.*, 1977, **16**, 1253; (b) M. Paul and H. Schmidbaur, *Z. Naturforsch., Teil B*, 1994, **49**, 647.
166. G.E. Glass, J.H. Konnert, M.G. Miles, D. Britton and R.S. Tobias, *J. Am. Chem. Soc.*, 1968, **90**, 1131; S. Komiya, J.C. Huffman and J.K. Kochi, *Inorg. Chem.*, 1977, **16**, 2138.
167. H.W. Chen, C. Paparizos and J.P. Fackler, *Inorg. Chim. Acta*, 1985, **96**, 137; U. Grassle and J. Strahle, *Z. Anorg. Allgem. Chem.*, 1985, **531**, 26; H.-N. Adams, U. Grassle, W. Hiller and J. Strahle, *Z. Anorg. Allgem. Chem.*, 1983, **504**, 7.
168. S. Shibata, K. Iijima and T.H. Baum, *J. Chem. Soc., Dalton Trans.*, 1990, 1519.
169. G.M. Bancroft, T. Chan and R.J. Puddephatt, *Inorg. Chem.*, 1983, **22**, 2133; J. Stein, J.P. Fackler, C. Paparizos and H.W. Chen, *J. Am. Chem. Soc.*, 1981, **103**, 2192.
170. S. Komiya, S. Ozaki, I. Endo, K. Inoue, N. Kasuga and Y. Ishizaki, *J. Organomet. Chem.*, 1992, **433**, 337; S. Komiya, S. Ochiai and Y. Ishizaki, *Inorg. Chem.*, 1992, **31**, 3168.
171. G.W. Rice and R.S. Tobias, *Inorg. Chem.*, 1976, **15**, 489; S. Komiya, S. Ochiai and Y. Ishizaki, *Inorg. Chem.*, 1992, **31**, 3168.
172. M.S. Kharasch and H.S. Isbell, *J. Am. Chem. Soc.*, 1931, **53**, 2701, 3053; P.W.J. de Graaf, J. Boersma and G.J.M. Van der Kerk, *J. Organomet. Chem.*, 1976, **105**, 399.
173. K.S. Liddle and C. Parkin, *J. Chem. Soc., Chem. Commun.*, 1972, 26; for structure see M. McPartlin and A.J. Markwell, *J. Organomet. Chem.*, 1973, **57**, C25.
174. P. Braunstein and R.J.H. Clark, *Inorg. Chem.*, 1974, **13**, 2224.
175. E. Ahmed, R.J.H. Clark, M.L. Tobe and L. Cattalini, *J. Chem. Soc., Dalton Trans.*, 1990, 2701.
176. See Refs 3(b), 9 and 154(b) in particular.
177. R. Usón, A. Laguna, M. Laguna, E. Fernandez, M.D. Villacampa, P.G. Jones and G.M. Sheldrick, *J. Chem. Soc., Dalton Trans.*, 1983, 1679.
178. R. Usón, A. Laguna, E. Fernandez, P.G. Jones and G.M. Sheldrick, *J. Chem. Soc., Dalton Trans.*, 1982, 1971.
179. P.G. Jones, *Z. Kristallogr.*, 1993, **208**, 362.
180. A.J. Markwell, *J. Organomet. Chem.*, 1985, **293**, 257; H.H. Murray, J.P. Fackler, L.C. Porter, D.A. Briggs, M.A. Guerra and R.J. Lagow, *Inorg. Chem.*, 1987, **26**, 357; see also Ref. 177.
181. J. Vicente, M.D. Bermudez and J. Escribano, *Organometallics*, 1991, **10**, 3380; J.K. Jawad, R.J. Puddephatt and M.A. Stalteri, *Inorg. Chem.*, 1982, **21**, 332; S. Komiya and A. Shibue, *Organometallics*, 1985, **4**, 684; S. Komiya, S. Ozaki and A. Shibue, *J. Chem. Soc., Chem. Commun.*, 1986, 1555.
182. J. Stein, J.P. Fackler, C. Paparizos and H-W. Chen, *J. Am. Chem. Soc.*, 1981, **103**, 2192; R.G. Raptis, H.H. Murray, R.J. Staples, L.C. Porter and J.P. Fackler, *Inorg. Chem.*, 1993, **32**, 5576 and references therein.
183. D.B. Dell'Amico, F. Calderazzo, R. Dantona, J. Strahle and H. Weiss, *Organometallics*, 1987, **6**, 1207.
184. For leading references see K.P. Hall and D.M.P. Mingos, *Prog. Inorg. Chem.*, 1984, **32**, 237; D.M.P. Mingos, *Gold Bull.*, 1984, **17**, 5; D.M.P. Mingos and D.J. Wales, *Introduction to Cluster Chemistry*, Prentice-Hall, New Jersey, 1990; G. González-Moraga, in *Cluster Chemistry*, Springer-Verlag, Berlin, 1993; D.M.P. Mingos, *J. Chem. Soc., Dalton Trans.*, 1996, 561.

185. E. Zeller, H. Beruda and H. Schmidbaur, *Inorg. Chem.*, 1993, **32**, 3203; R. Boca, *J. Chem. Soc., Dalton Trans.*, 1994, 2061.
186. C.E. Briant, K.P. Hall and D.M.P. Mingos, *J. Chem. Soc. Chem. Commun.*, 1984, 290.
187. B.K. Teo, X. Shi and H. Zhang, *J. Am. Chem. Soc.*, 1992, **114**, 2743.
188. G. Schmid, R. Pfeil, R. Boese, F. Bandermann, S. Meyer, G.H.M. Calis and J.W.A. van der Velden, *Chem. Ber.*, 1981, **114**, 3534; R.C. Thiel, R.E. Benfield, R. Zanoni, H.H.A. Smit and M.W. Dirken, *Struct. Bonding*, 1993, **81**, 1.
189. H. Schmidbaur, *Chem. Soc. Rev.*, 1995, 391; see also K. Angermeier and H. Schmidbaur, *Acta Crystallogr. Sect. C*, 1995, **51**, 1793; R.E. Bachman and H. Schmidbaur, *Inorg. Chem.*, 1996, **35**, 1399 and references therein.
190. Y. Yang and P.R. Sharp, *J. Am. Chem. Soc.*, 1994, **116**, 6983.
191. D.M.P. Mingos and R.P.F. Kanters, *J. Organomet. Chem.*, 1990, **384**, 405; for MO calculations on an all-gold cluster see D.M.P. Mingos, *J. Chem. Soc., Dalton Trans.*, 1976, 1163. Absorption and MCD spectra are discussed in: H.-R.C. Jaw and W.R. Mason, *Inorg. Chem.*, 1991, **30**, 3552; H.-R.C. Jaw and W.R. Mason, *Inorg. Chem.*, 1991, **30**, 275.
192. P. Pyykko, *Adv. Quantum Chem.*, 1978, **11**, 353; P. Pyykko and J.P. Desclaux, *Acct. Chem. Res.*, 1979, **12**, 276; P. Pyykko, *Chem. Rev.*, 1988, **88**, 563; L.R. Norrby, *J. Chem. Ed.*, 1991, **68**, 110.
193. See Refs 12, 13, 110 and P. Schwerdtfeger, M. Dolg, W.H.E. Schwarz, G.A. Bowmaker and P.D.W. Boyd, *J. Chem. Phys.*, 1989, **91**, 1762.
194. H. Schmidbaur, *Gold Bull.*, 1990, **23**, 11; H. Schmidbaur, *Interdisciplinary Science Rev.*, 1992, **17**, 213.
195. S.S. Pathaneni and G.R. Desiraju, *J. Chem. Soc., Dalton Trans.*, 1993, 319 (database).
196. P. Pyykko and Y. Zhao, *Angew. Chem. Int. Ed. Engl.*, 1991, **30**, 604 estimates Au–Au forces around 27 kJ mol^{-1}.
197. K. Dziwok, J. Lachmann, D.L. Wilkinson, G. Müller and H. Schmidbaur, *Chem. Ber.*, 1990, **123**, 423.
198. N.C. Baezinger and A.W. Struss, *Inorg. Chem.*, 1976, **15**, 1807.
199. G.J. Higby, *Gold Bull.*, 1982, **15**, 130; R.V. Parish and S.M. Cottrill, *Gold Bull.*, 1987, **20**, 3; E.R.T. Tiekink and M.W. Whitehouse, *Chem. Aust.*, 1990, 346; G.G. Graham, G.D. Champion and J.B. Ziegler, *Inflammopharmacology*, 1991, **1**, 99; R.V. Parish, *Interdisciplinary Sci. Rev.*, 1992, **17**, 221; *Gold Bull.*, 1994, **27**, 91; S.L. Best and P.J. Sadler, *Gold Bull.*, 1996, **29**, 87.
200. R.V. Parish, J. Mack, L. Hargreaves, J.P. Wright, R.G. Buckley, A.M. Elsome, S.P. Fricker and B.R.C. Theobald, *J. Chem. Soc., Dalton Trans.*, 1996, 69; R.V. Parish, B.P. Howe, J.P. Wright, J. Mack, R.G. Pritchard, R.G. Buckley, A.M. Elsome and S.P. Fricker, *Inorg. Chem.*, 1996, **35**, 1659.
201. R.V. Parish, *Gold Bull.*, 1982, **15**, 51; M. Melnik and R.V. Parish, *Coord. Chem. Rev.*, 1986, **70**, 157; R.V. Parish, in *NMR, NQR, EPR and Mössbauer Spectroscopy in Inorganic Chemistry*, Ellis Horwood, Chichester, 1990.

Index

This index is divided by element into eight parts. Each part is subdivided into sections devoted to each oxidation state, preceded by a general section. Thus if you want to find out about phosphine complexes of Rhodium, there is a general entry to phosphine complexes as well as separate references to phosphine complexes under the headings of Rhodium(0), (I), (II) and (III).

Index terms **Links**

Index terms **Links**

Index terms **Links**